Supporting Information

Ni(I)–X Complexes Bearing a Bulky α-Diimine Ligand: Synthesis, Structure and Superior Catalytic Performance in the Hydrogen Isotope Exchange in Pharmaceuticals

*Cayetana Zarate,[a] Haifeng Yang,[b] Máté J. Bezdek,[a] David Hesk[b†] and Paul J. Chirik[a]**

[a] Department of Chemistry, Frick Laboratory, Princeton University, Princeton, NJ 08544, USA

[b] MRL, Merck & Co, Inc., Rahway, New Jersey 07065, United States

pchirik@princeton.edu

Table of Contents

I. General Considerations

I.A. Materials

^{ipc}ADI was prepared according to literature procedures.[1] Anhydrous $NiCl_2$·DME, $NiBr_2$·DME, NiI_2 and $Ni(COD)_2$ were purchased from Strem Chemicals, Inc., stored in the glovebox and used as received. Sodium triethyl borohydride solution (1.0 M toluene) was purchased from Millipore Sigma, stored in the glovebox and used as received. Nicotine (Millipore Sigma), 2-pyridin-3-ylpiperidine ((*R*,*S*)-anabasine, Acros Organics), caffeine (Acros Organics), doxofylline (Alfa Aesar) and pentoxifylline (TCI America) were used without further purification. MK-6096 and MK-5395 were supplied by Merck and Co., Inc. and used directly. Papaverine (Millipore Sigma), paroxetine (Combi-blocks) and buspirone (Alfa Aesar) were purchased as HCl salt forms, and varenicline (Ontario Chemicals, Inc.) as tartrate salt. The free bases were obtained by reacting each salt in aqueous K_2CO_3 (or NaOH) followed by extraction with ethyl acetate. Etoricoxib (Alsachim), flumazenil (Natland International Corporation) and haloperidol (Alfa Aesar) were used without further purification. All other substrates were purchased from commercial sources (Millipore Sigma, Alfa Aesar, TCI or Acros Organics) and used directly. Anhydrous NMP and MeOH were purchased from Acros Organics and Millipore Sigma, respectively, stored in the glovebox and used as received. Deuterium gas was purchased from Cambridge Isotope Laboratories, Inc. and passed through a column containing manganese oxide supported on vermiculite and 4 Å molecular sieves before admission to a high vacuum line. Carrier free tritium gas was obtained from American Radiolabeled Chemicals, St Louis, MO.

I.B. Methods

All air- and moisture-sensitive manipulations were carried out using a high vacuum Schlenk line (1 mmHg) or in an MBraun inert atmosphere (nitrogen) glovebox. Glassware was stored in a pre-heated oven prior to use. The solvents used for air- and moisture-sensitive manipulations were dried and deoxygenated using literature procedures.[2] Celite was dried at 180 °C under high vacuum for 3 days prior to use. Deuterated solvents for NMR spectroscopy analysis of air sensitive nickel complexes (benzene-d_6 and THF-d_8) were distilled from sodium metal under high vacuum and stored in the glovebox. All liquid substrates used in catalytic labeling reactions were dried by stirring over CaH_2 under static vacuum at 23 °C for 12 hours and then distilled under high vacuum and stored in the glovebox. Solid substrates were dried under high vacuum for 12 hours at 23 °C and then stored in the glovebox with the exception of solid substrates used in H/T exchange reactions, which were dried in a vacuum oven for 16 h.

Catalytic H/D exchange reactions were carried out in a high vacuum Schlenk line attached to a deuterium gas tank. Catalytic H/T exchange reactions were performed at Merck and Co., Inc. Facility on a RC Tritech® manifold and the reaction vessel was sealed with a Swagelok S1.

Flash column chromatographic purification was performed with SiliaFlash® P60, Irregular Silica Gel (SiliCycle, 40 - 63 μm, 60 Å). Thin-layer chromatography (TLC) was carried out using Merck TLC Silica gel 60 F_{254} and visualized by short-wavelength ultraviolet light and by treatment with KMnO4 stain.

I.C. Instrumentation and Software

^{1}H NMR spectra were recorded at 23 °C on a Bruker NanoBay 300 MHz or Avance III 500 MHz spectrometers operating at 300.13 MHz or 500.46 MHz, respectively. Proton-decoupled conventional and quantitative ^{13}C{^{1}H} NMR spectra were recorded at 23 °C on Bruker NanoBay 300 MHz or Avance III 500 MHz spectrometers operating at 75.48 MHz or 125.85 MHz, respectively. ^{19}F NMR spectra were collected at 23 °C on a a Bruker 300 AVANCE spectrometer operating at 282 MHz. All the former experiments were performed at the Princeton University Nuclear Magnetic Resonance Facility. ^{3}H NMR spectra (proton decoupled or not) were recorded on Bruker AVANCE II 400 spectrometer operating at 426.6 MHz at Merck and Co., Inc. Facility. All ^{1}H and ^{13}C NMR chemical shifts are reported in part per million (ppm) relative to $SiMe_4$ using the ^{1}H ($CDCl_3$: 7.26 ppm; dimethyl sulfoxide-d_6: 2.50 ppm; acetonitrile-d_3: 1.94 ppm; benzene-d_6: 7.16 ppm; THF-d_8: 1.73 ppm) and ^{13}C{^{1}H} ($CDCl_3$: 77.16 ppm; dimethyl sulfoxide-d_6: 39.51 ppm; acetonitrile-d_3: 118.69 ppm; benzene-d_6: 128.06 ppm; THF- d_8: 25.38 ppm) chemical shifts of the solvent as a standard. NMR data for diamagnetic compounds are reported as follows: chemical shift (multiplicity, coupling constants in Hz, integration, assignment). NMR data for paramagnetic substances are reported as follows: chemical shift (integration, width at half height in Hz) where s = singlet, d = doublet, t = triplet, q = quartet, p = pentet, m = multiplet, and br = broad. NMR spectra were processed using the MestReNova software suite.[3]

An Agilent 6220 liquid chromatography/mass spectrometry (LC/MS) using electrospray ionization time-of-flight (ESI-TOF) was employed to analyze deuterium labeled compounds (**[^{2}H]11i**–**11k** and **[^{2}H]12a**–**12i**). All the former experiments were performed at the Princeton University Mass Spectrometry Facility.

Enantiomeric purity of **[^{2}H]11g** was determined by chiral gas chromatography performed on a Shimadzu GC-2010 gas chromatogram using a Supelco 30 m x 0.25 mm BETA DEX 120 capillary column.

Radioactivity measurements were performed at Merck and Co., Inc. Facility using either a PerkinElmer 3110TR or 4910TR liquid scintillation analyzer and PerkinElmer Ultra Gold liquid scintillation cocktail. Radiochemical purity was determined using RadioHPLC and HPLC-UV analysis, which was performed on Agilent 1100 series HPLC connected in series to a Perkinelmer Radiomatic 625 TR Flow Scintillation Analyzer. LC/MS analysis of tritium labeled compounds was performed on an Agilent 6130 quadruple LC/MS with an Agilent 1260 infinity HPLC operating in the ES^+ ionization mode. HPLC analyses were performed on a Waters 2695 Alliance HPLC with a Waters 2996 PDA Detector.

Continuous wave EPR spectra were recorded on an X-band Bruker EMXPlus spectrometer equipped with an EMX standard resonator and a Bruker PremiumX microwave bridge. The spectra were simulated using EasySpin for MATLAB.[4]

Elemental analyses of **2**–**10** were performed at Robinson Microlit Laboratories, Inc., in Ledgewood, NJ. Solid-state magnetic moments of **3**–**10** were determined using a Johnson Matthey Magnetic Susceptibility Balance that was calibrated with $HgCo(SCN)_4$.

Single crystals of **2** and **7**–**10** suitable for X-ray diffraction were coated with polyisobutylene oil in a glovebox, transferred to a nylon loop and then quickly transferred to the goniometer head of a Bruker VENTURE D8 PHOTON 100 diffractometer equipped with a molybdenum X-ray tube (λ = 0.71073 Å) and a Cu X-ray tube (λ = 1.54178 Å). Crystals of **2** were extremely sensitive to cooling and cracked under an N_2 stream, requiring room temperature collection protected by a N_2-purged

capillary. Preliminary data revealed the crystal system. The data collection strategy was optimized for completeness and redundancy using the Bruker COSMO software suite. The space group was identified, and the data were processed using the Bruker SAINT+ program and corrected for absorption using SADABS. The structures were solved using direct methods (SHELXS) completed by subsequent Fourier synthesis and refined by full-matrix least-squares procedures.

Cyclic Voltammetry (CV) of **8** was collected in THF solution (1 mM in compound) with $[^{n}Bu_4N][PF_6]$ (0.2 M) as electrolyte, using a 3 mm glassy carbon working electrode, platinum wire as the counter electrode, and silver wire as the reference in a glovebox equipped with electrochemical outlets. CV was collected at 23 °C with 100 mV/s scan rate. Data was collected using a BASi EC Epsilon electrochemical workstation and analyzed using the BASi Epsilon-EC software. Potentials are reported versus Cp_2Fe/Cp_2Fe^+ and were obtained using the in situ method.

All DFT calculations were performed with the ORCA program package in the gas phase.[5] Geometry optimizations of the complexes and single-point calculations on the optimized geometries were carried out at the B3LYP level of DFT.[6] This hybrid functional often outperforms pure gradient-corrected functionals in the accurate representation of transition metal complexes, especially those involving significant metal-ligand covalency.[7] The all-electron Gaussian basis sets were those developed by the Ahlrichs group.[8] Triple-ζ quality basis sets def2-TZVP with one set of polarization functions was used to describe metal atoms and all atoms directly coordinated to a metal center. For all the other atoms, slightly smaller polarized split-valence def2-SV(P) basis sets were used that were of double-ζ quality in the valence region and contained a polarizing set of d functions on the non-hydrogen atoms. Auxiliary basis sets to expand the electron density in the resolution-of-the-identity (RIJCOSX)[9] approach were chosen to match the orbital basis.[10]

II. Preparation of Nickel Complexes

II.A. General Synthesis of (^{ipc}ADI)Ni(I) Halides

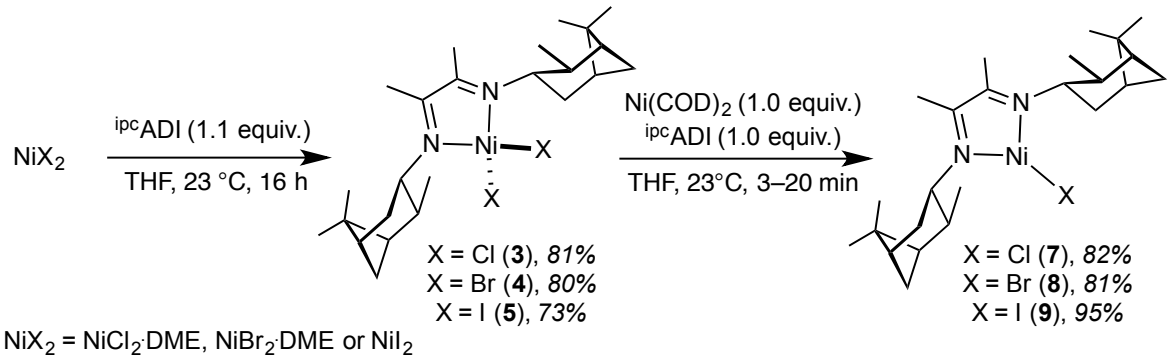

Scheme S1. General synthesis of [(^{ipc}ADI)NiX] (X = Cl, Br, I).

Preparation of [(^{ipc}ADI)NiCl$_2$] (2). 3 was prepared as depicted in Scheme S1. In a glovebox, to a 20 mL thick-walled glass vessel containing a magnetic stir bar and a solution of NiCl$_2$·DME (99 mg, 0.45 mmol) in THF (10 mL), ^{ipc}ADI (178 mg, 0.50 mmol) was added. The resulting suspension turned pink after a few minutes and was stirred at 23 °C for 16 hours. Then, the solvent was removed under vacuum and the solid residue was collected on a medium glass frit, rinsed with pentane (3 times × 10 mL) and dried under vacuum yielding 178 mg (81%) of **3** as a pale pink solid. **Anal. Calcd.** for $C_{24}H_{40}Cl_2N_2Ni$: C, 59.29; H, 8.29; N, 5.76; found: C, 58.84; H, 8.06; N, 5.45. **Magnetic Susceptibility (MSB, 23 ºC):** μeff = 3.4(1) μ_B. **^{1}H NMR (300 MHz, THF-d_8):** δ 15.86 (2H, Δν1/2 = 161 Hz), 12.84 (2H, Δν1/2 = 171 Hz), 10.19 (6H, Δν1/2 = 384 Hz), 8.44 (2H, Δν1/2 = 20 Hz), 7.28 (2H, Δν1/2 = 26 Hz), 5.94 (6H, Δν1/2 = 11 Hz), 5.08 (2H, Δν1/2 = 36 Hz), 4.15 (6H, Δν1/2 = 7 Hz), 2.42 (6H, Δν1/2 = 9 Hz), -29.8 (6H, Δν1/2 = 30 Hz, imine backbone CH_3) ppm.

Preparation of [(^{ipc}ADI)NiBr$_2$] (4). 4 was prepared as depicted in Scheme S1. In a glovebox, to a 20 mL thick-walled glass vessel containing a magnetic stir bar and a solution of NiBr$_2$·DME (350 mg, 1.14 mmol) in THF (10 mL), ^{ipc}ADI (446 mg, 1.25 mmol) was added. The resulting suspension turned pink after a few minutes and was stirred at 23 °C for 16 hours. Then, the solvent was

removed under vacuum and the solid residue was collected on a medium glass frit, rinsed with pentane (3 times × 10 mL) and dried under vacuum yielding 581 mg (80%) of **4** as a pale pink solid (this procedure is scalable to up to 3 g scale with similar efficiency). **Anal. Calcd.** for $C_{24}H_{40}Br_2N_2Ni$: C, 50.12; H, 7.01; N, 4.87; found: C, 50.60; H, 7.17; N, 5.01. **Magnetic Susceptibility (MSB, 23 ºC):** μeff = 3.0(1) μ_B. **^{1}H NMR (300 MHz, THF-*d*$_8$):** δ 12.47 (2H, Δv1/2 = 321 Hz), 8.70 (6H, Δv1/2 = 79 Hz), 7.36 (2H, Δv1/2 = 23 Hz), 7.06 (2H, Δv1/2 = 35 Hz), 5.11 (2H, Δv1/2 = 30 Hz), 4.56 (6H, Δv1/2 = 14 Hz), 4.26 (2H, Δv1/2 = 37 Hz), 3.12 (6H, Δv1/2 = 6 Hz), 1.29 (6H, Δv1/2 = 4 Hz), -29.69 (6H, Δv1/2 = 60 Hz, imine backbone C*H*$_3$) ppm.

Preparation of [(^{ipc}ADI)NiI$_2$] (5). 5 was prepared as depicted in Scheme S1. In a glovebox, to a 20 mL thick-walled glass vessel containing a magnetic stir bar and a solution of NiI_2 (156 mg, 0.50 mmol) in THF (10 mL), ^{ipc}ADI (196 mg, 0.55 mmol) was added. The resulting suspension turned dark red after a few minutes and was stirred at 23 °C for 16 hours. Then, the solvent was removed under vacuum and the solid residue was collected on a medium glass frit, rinsed with pentane (3 times × 10 mL) and dried under vacuum yielding 244 mg (73%) of **5** as a dark red solid. **Magnetic Susceptibility (MSB, 23 ºC):** μeff = 3.4(1) μ_B. **^{1}H NMR (300 MHz, THF-d$_8$, 23 ºC): δ** 13.19 (2H, Δv1/2 = 233 Hz), 5.81 (8H, Δv1/2 = 82 Hz), 2.53 (12H, Δv1/2 = 104 Hz), 1.63 (6H, Δv1/2 = 25 Hz), 1.28 (6H, Δv1/2 = 26 Hz), -29.75 (6H, Δv1/2 = 71 Hz, imine backbone C*H*$_3$) ppm.

Preparation of [(^{ipc}ADI)NiCl] (7). 7 was prepared as depicted in Scheme S1. In a glovebox, to a 20 mL thick-walled glass vessel, charged with a magnetic stir bar, **3** (102 mg, 0.21 mmol), ^{ipc}ADI (75 mg, 0.21 mmol) and THF (2.0 mL) were added. After stirring for 2 minutes at 23 °C, $Ni(COD)_2$ (58 mg, 0.21 mmol) was added as a solid and the reaction mixture turned dark green immediately. The mixture was stirred for 3 minutes at 23 °C and then filtered through Celite and the solvent was removed under vacuum. The resulting solid was collected on a medium glass frit, washed

with cold (-35 °C) pentane (3 times × 10 mL) and dried under vacuum yielding 155 mg (82%) of **7** as a dark green solid. Single crystals suitable for X-ray diffraction were obtained by slow diffusion from a concentrated diethyl ether solution to toluene at 23 °C. **Anal. Calcd.** for $C_{24}H_{40}ClN_2Ni$: C, 69.24; H, 8.95; N, 6.22; found: C, 68.79; H, 8.65; N, 5.80. **Magnetic Susceptibility (MSB, 23 ºC):** μeff = 1.8(1) μ_B. **^{1}H NMR (300 MHz, benzene-*d*$_6$):** δ 3.27 (8H, Δv1/2 = 230 Hz), 1.94 (6H, Δv1/2 = 187 Hz), 1.14 (8H, Δv1/2 = 68 Hz), 0.85 (12H, Δv1/2 = 101 Hz), -2.08 (6H, Δv1/2 = 599 Hz, imine backbone C*H*$_3$) ppm.

Preparation of [(^{ipc}ADI)NiBr] (8). 8 was prepared as depicted in Scheme S1. In a glovebox, to a 20 mL thick-walled glass vessel, charged with a magnetic stir bar, **4** (116 mg, 0.20 mmol), ^{ipc}ADI (72 mg, 0.20 mmol) and THF (2.5 mL) were added. After stirring for 2 minutes at 23 °C, $Ni(COD)_2$ (56 mg, 0.20 mmol) was added as a solid and the reaction mixture turned dark green immediately. The mixture was stirred for 3 minutes at 23 °C and then filtered through Celite and the solvent was removed under vacuum. The resulting solid was collected on a medium glass frit, washed with cold (-35 °C) pentane (3 times × 10 mL) and dried under vacuum yielding 162 mg (81%) of **8** as a dark green solid (this procedure is scalable to up to 1 g scale with similar efficiency). Single crystals suitable for X-ray diffraction were obtained by recrystallization from a concentrated THF solution layered with pentane stored at -35 °C overnight. **Anal. Calcd.** for $C_{24}H_{40}BrN_2Ni$: C, 58.21; H, 8.14; N, 5.66; found: C, 58.32; H, 8.32; N, 5.48. **Magnetic Susceptibility (MSB, 23 ºC):** μeff = 1.8(1) μ_B. **^{1}H NMR (300 MHz, benzene-*d*$_6$):** δ 3.18 (8H, Δv1/2 = 223 Hz), 1.86 (6H, Δv1/2 = 223 Hz), 1.08 (8H, Δv1/2 = 79 Hz), 0.76 (12H, Δv1/2 = 107 Hz), -2.08 (6H, Δv1/2 = 348 Hz, imine backbone C*H*$_3$) ppm. ***Note:*** **8** is air sensitive but stable under inert atmosphere at -35 ºC in solid state for at least 6 months.

Preparation of [(^{ipc}ADI)NiI] (9). 9 was prepared as depicted in Scheme S1. In a glovebox, to a 20 mL thick-walled glass vessel, charged with a magnetic stir bar, **5** (170 mg, 0.25 mmol), ^{ipc}ADI (89 mg, 0.25 mmol) and THF (2.0 mL) were added. After stirring for 2 minutes at 23 °C, $Ni(COD)_2$ (69 mg, 0.25 mmol) was added as a solid and the reaction mixture turned dark green immediately. The mixture was stirred for 20 minutes at 23 °C and then filtered through Celite and the solvent was removed under vacuum. The solid was collected on a medium glass frit, washed with cold (-35 °C) pentane (3 times × 10 mL) and dried under vacuum yielding 129 mg (95%) of **9** as a dark green solid. Single crystals suitable for X-ray diffraction were obtained by recrystallization from a concentrated pentane solution at -35 °C. **Anal. Calcd.** for $C_{24}H_{40}IN_2Ni$: C, 53.17; H, 7.44; N, 5.17; found: C, 52.80; H, 7.25; N, 5.16. **Magnetic Susceptibility (MSB, 23 ºC):** μeff = 2.2(1) μ_B. **^{1}H NMR (300 MHz, benzene-d_6):** δ 3.26 (8H, Δv1/2 = 227 Hz), 2.01 (m, 6H), 1.02 (8H, Δv1/2 = 411 Hz), 0.82 (12H, Δv1/2 = 281 Hz), -1.94 (6H, Δv1/2 = 452 Hz, imine backbone CH_3) ppm.

II.B. Synthesis of [(^{ipc}ADAI)NiBr]$_2$

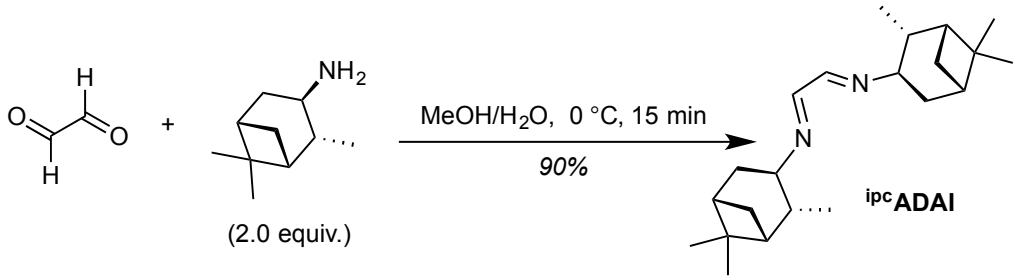

Scheme S2. Synthesis of ^{ipc}ADAI.

Preparation of *N*,*N*'-bis(1*R*,2*R*,3*R*,5*S*)-(−)-isopinocampheyl-1,2-ethanediimine (^{ipc}ADAI). ^{ipc}ADAI was prepared as depicted in Scheme S2 according to a modified procedure from that used previously for the synthesis of *N*,*N*'-bis(cyclohexyl)-1,2-ethanediimine (^{Cy}ADAI).[11] A 100 mL round bottom flask containing a magnetic stir bar and (1*R*,2*R*,3*R*,5*S*)-(-)-isopinocampheylamine (4.4 mL, 26 mmol) in 20 mL MeOH/H_2O (1:1) was placed in an ice-bath. Then, a 40% wt aqueous glyoxal solution (1,9 mL, 13 mmol) was slowly added and formation of a white precipitate was immediately observed. After stirring the reaction mixture at 0 °C for 15 minutes, the resulting white solid residue was collected on a medium glass frit, washed with a chilled (-35 °C) 1:1 EtOH/H_2O mixture (3 times × 25 mL) and dried under reduced pressure to yield 3.8 g (90%) of ^{ipc}ADAI as a white solid. **^{1}H NMR (500 MHz, benzene-*d*$_6$):** δ 7.99 (s, 2H, aldimine backbone C*H*), 3.32 (dd, *J* = 10, 5 Hz, 2H, N–C*H*), 2.35 (dtd, *J* = 10, 6, 2 Hz, 2H, β-amino methine C*H*CH$_3$), 2.27 (qdd, *J* = 7, 5, 2 Hz, 2H, 1 × bridge methylene C*H*$_2$), 2.19 (dddd, *J* = 13, 10, 3, 2 Hz, 2H, 1 × β-amino methylene N–C*H*CH$_2$), 2.07 (ddd, *J* = 14, 5, 3 Hz, 2H, 1 × bridgehead C–*H*), 1.90 (tt, *J* = 6, 3 Hz, 2H, 1 × bridgehead C–*H*), 1.77 (ddd, *J* = 7, 5, 2 Hz, 2H, 1 × β-amino methylene N–C*H*CH$_2$), 1.42 (d, *J* = 10 Hz, 2H, 1 × bridge methylene C*H*$_2$), 1.16 (s, 6H, 1 × bridge C(C*H*$_3$)$_2$), 0.91(m, 12H, 1 bridge C(C*H*$_3$)$_2$ + methyl of CHC*H*$_3$) ppm. **^{13}C{^{1}H} NMR (126 MHz, benzene-*d*$_6$):** δ 159.4 (CH$_1$, imine *C*=N), 70.2 (CH$_1$, imine N–*C*H), 47.8 (CH$_1$, bridgehead C–H), 43.9 (CH$_1$, methine CHCH$_3$),

42.0 (CH_1, bridgehead C–H), 38.9 (CH_0, bridge $C(CH_3)_2$), 36.1 (CH_2, β-amino methylene CH_2), 33.9 (CH_2, bridge methylene CH_2), 28.0 (CH_3, 1 × $C(CH_3)_2$), 23.6 (CH_3, $CHCH_3$), 20.0 (CH_3, 1 × $C(CH_3)_2$) ppm.

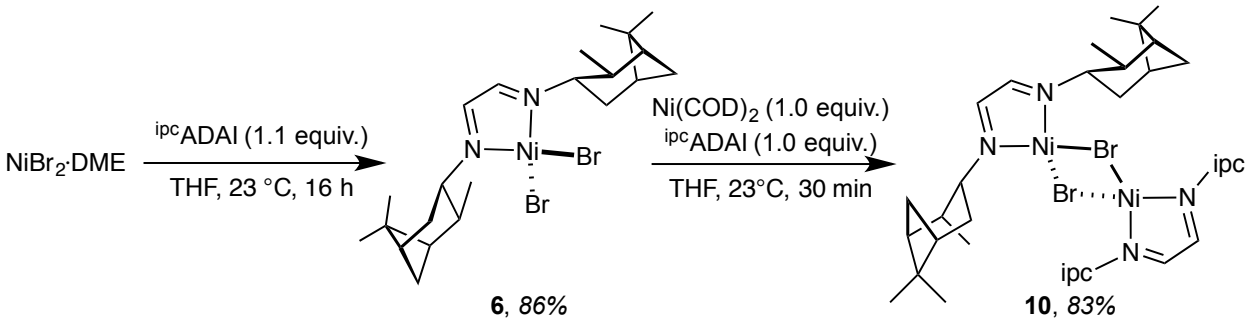

Scheme S3. Synthesis of [(^{ipc}ADAl)NiBr]$_2$.

Preparation of [(^{ipc}ADAl)NiBr]$_2$ (6). 6 was prepared as reflected in Scheme S3. In a glovebox, to a 100 mL round-bottom flask containing a magnetic stir bar and a solution of $NiBr_2$·DME (1.005 g, 3.26 mmol) in THF (30 mL), ^{ipc}ADAl (1.178 g, 3.59 mmol) was added. The resulting suspension turned pink after a few minutes and was stirred at 23 °C for 16 hours. Then, the solvent was removed under vacuum and the solid residue was collected on a medium glass frit, rinsed with pentane (3 times × 10 mL) and dried under vacuum yielding 1.534 g (86%) of **6** as a pale pink solid. **Anal. Calcd.** for $C_{22}H_{36}Br_2N_2Ni$: C, 48.30; H, 6.63; N, 5.12; found: C, 48.07; H, 6.50; N, 5.07. **Magnetic Susceptibility (MSB, 23 ºC):** μeff = 2.9(1) μ_B. **^{1}H NMR (300 MHz, THF-*d*$_8$):** δ 5.54 (m, 8H, Δv1/2 = 182 Hz), 3.95 (10H, Δv1/2 = 75 Hz), 2.31 (12H, Δv1/2 = 17 Hz), 1.07 (m, 6H, Δv1/2 = 134 Hz) ppm.

Preparation of [(^{ipc}ADAl)NiBr]$_2$ (10). 10 was prepared as depicted in Scheme S3. In a glovebox, a 20 mL thick-walled glass vessel, containing a magnetic stir bar, was charged with **6** (940 mg, 1.72 mmol), ^{ipc}ADAl (565 mg, 1.72 mmol) and THF (10 mL). After stirring for 2 minutes at 23 °C,

$Ni(COD)_2$ (473 mg, 1.72 mmol) was added as a solid and the reaction mixture turned purple immediately. The mixture was stirred for 30 minutes at 23 °C and then filtered through Celite and the solvent was removed under vacuum. The resulting solid was collected on a medium glass frit, washed with cold (-35 °C) pentane (3 times × 10 mL) and dried under vacuum yielding 1.334 g (83%) of **10** as a purple solid. Single crystals suitable for X-ray diffraction were obtained by recrystallization from a concentrated THF solution layered with pentane stored at -35 °C overnight. **Anal. Calcd.** for $C_{44}H_{72}Br_2N_4Ni_2$: C, 56.57; H, 7.77; N, 6.00; found: C, 56.33; H, 8.05; N, 5.82. **Magnetic Susceptibility (MSB, 23 ºC):** μeff = 2.8(1) μ_B. **^{1}H NMR (300 MHz, benzene-*d*$_6$):** δ 9.03 (2H, Δv1/2 = 30 Hz), 5.58 (2H, Δv1/2 = 31 Hz), 3.99 (2H, Δv1/2 = 47 Hz), 3.43 (2H, Δv1/2 = 43 Hz), 3.12 (3H, Δv1/2 = 50 Hz), 2.78 (3H, Δv1/2 = 43 Hz), 2.43 (2H, Δv1/2 = 40 Hz), 2.21(4H, Δv1/2 = 31 Hz), 2.03 (4H, Δv1/2 = 33 Hz), 1.84 (4H, Δv1/2 = 63 Hz), 1.29 (38H, Δv1/2 = 95 Hz), 0.91 (6H, Δv1/2 = 60 Hz) ppm.

II.C. Synthesis of [(^{ipc}ADI)Ni(μ$_2$-H)]$_2$

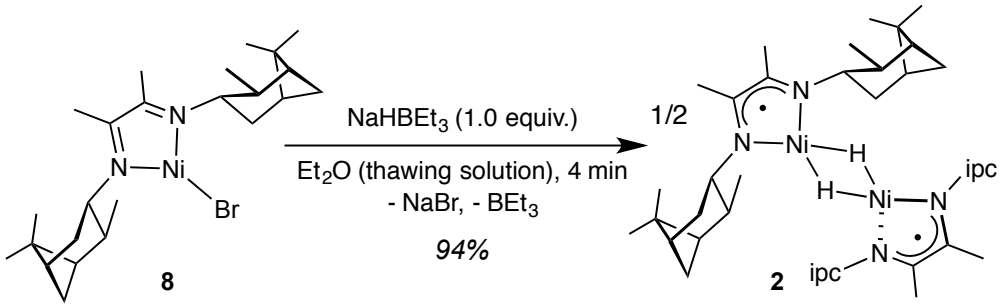

Scheme S4. Synthesis of [(^{ipc}ADI)Ni(μ$_2$-H)]$_2$.

Preparation of [(^{ipc}ADI)Ni(μ$_2$-H)]$_2$ (2). 2 was prepared as depicted in Scheme S4. In a glovebox, a 20 mL thick-walled glass vessel was charged with a magnetic stir bar, **8** (74 mg, 0.15 mmol), and Et_2O (7 mL). The resulting mixture was frozen in a cold well containing liquid nitrogen. A vial filled with Et_2O, a filtration flask and a glass frit with Celite were also cooled in the cold well. In

other 20 mL thick-walled glass vessel. a 1.0 M solution of $NaHBEt_3$ in toluene (149 µL, 0.15 mmol) was diluted with additional Et_2O (3 mL), and the resulting solution was cooled in a freezer at -35 °C. Once cooled, this solution was added dropwise to the frozen solution of **8** and the mixture, which immediately turned dark blue, was stirred outside of the cold well for 2 minutes, placed again in the cold well for 1 minute and stirred outside for 2 additional minutes. While still cold, the mixture was filtered using the previously cooled filter flask and glass frit with Celite and the solvent was evaporated at 23 °C under vacuum (during filtration the blue solution turned dark brown tentatively due to dimerization of the nickel hydride monomer). The resulting brown solid residue was dissolved in cold (-35 °C) pentane (5 mL) and filterred through a plug of Celite on a medium glass frit rinsing with additional cold pentane (15 mL total). The filtrate was concentrated under vacuum yielding 58 mg (94%) of **2** as a dark brown solid. Single crystals suitable for X-ray diffraction were obtained by recrystallization from a concentrated pentane solution at -35 °C for two days. **Anal. Calcd.** for $C_{24}H_{40}ClN_2Ni$: C, 69.24; H, 9.93; N, 6.73; found: C, 68.96; H, 10.15; N, 6.81. **^{1}H NMR (300 MHz, benzene-d_6):** δ 4.24 (m, 8H, 4 x imine N–C*H* + 4 x β-amino methine C*H*CH_3), 4.12 (d, *J* = 9 Hz, 4H, 2 x bridge methylene CH_2), 3.47 (m, 4H, 2 x β-amino methylene N–CHCH_2), 2.80 (m, 4H, 4 x bridgehead C–*H*), 2.48 (m, 4H, 4 x bridgehead C–*H*), 2.20 (m, 4H, 2 x β-amino methylene N–CHCH_2), 2.12 (m, 4H, 2 x bridge methylene CH_2), 1.38 (s, 12H, 2 x bridge C(CH_3)$_2$), 1.24 (d, *J* = 7 Hz, 12H, 4 x methyl of CHCH_3), 1.19 (s, 12H, 2 x bridge C(CH_3)$_2$), -1.58 (s, 12H, 4 x imine backbone CH_3), -29.30 (s, 2H, 2 x Ni–*H*) ppm. **^{13}C{^{1}H} NMR (75 MHz, benzene-d_6):** δ 144.7 (CH_0, imine *C*=N), 66.2 (CH_1, imine N–*C*H), 49.1 (CH_2, bridge methylene *C*H_2), 44.1 (CH_1, β-amino methine *C*HCH_3), 42.8 (CH_2, β-amino methylene N–CH*C*H_2), 41.0 (CH_0, bridge C(*C*H_3)$_2$), 33.3 (CH_2, bridge methylene *C*H_2, CH bridgehead C–*H*), 29.1 (CH_2, β-amino methylene N–CH*C*H_2 + CH_1, bridgehead *C*–H + CH_3, bridge C(*C*H_3)$_2$), 23.6 (CH_3, bridge C(*C*H_3)$_2$), 22.5 (CH_3, imine *C*H_3), 21.6 (CH_3, methyl of CH*C*H_3) ppm. ***Note 1:*** **2** is air sensitive but is stable under inert atmosphere at -35 ºC either in solid state or in THF solution for at least 6 months. ***Note 2:*** It is important to keep the reaction mixture cold in order to minimize the formation of what

is likely $Ni_n(^{ipc}ADI)_2$ (n = 1 or 2) with a diagnostic ^{1}H NMR (300 MHz, benzene-d_6) peak at -2.05 ppm (>100: 1 **2**/$Ni_n(^{ipc}ADI)_2$). ***Note 3:*** **2** can be synthesized in higher scale, although the amount of presumed $Ni_n(^{ipc}ADI)_2$ (n = 1 or 2) increased (1.50 mmol **8** scale yielded 543 mg (87%) of **2** as a 12: 1 **2**/$Ni_n(^{ipc}ADI)_2$ mixture). ***Note 4:*** $Ni_n(^{ipc}ADI)_2$ was independently synthesized by reduction of **4** with Na (2.0 equiv.) in Et_2O at 23 °C for 4 h; ^{1}H NMR (300 MHz, benzene-d_6): δ 4.44 (t, J = 6.8 Hz, 2nH), 3.34 (m, 4nH), 2.88 (m, 2nH), 2.42 (m, 2nH), 1.92 (m, 6nH), 1.30 (m, 18nH), -2.06 (s, 6nH, imine backbone CH_3) ppm. The ^{1}H NMR spectrum of $Ni_n(^{ipc}ADI)_2$ supports formulation of this complex and containing only the diimine and no hydride ligands. The connectivity of this ^{ipc}ADI-supported Ni(0) compound has yet be elucidated largely in part due to the inability to obtain single crystals suitable for X-ray diffraction. $Ni_n(^{ipc}ADI)_2$ could potentially be a bimetallic compound (n = 2) as the analogous Ni(0) complex supported by ^{ipr}DI, $Ni_2(^{iPr}DI)_2$;[12] or monometallic (n = 1) as for $Ni(^{Cy}ADI)_2$.[13]

II.D. Synthesis of $[(^{ipc}ADI\text{-}d_{12})Ni(\mu_2\text{-}H)]_2$

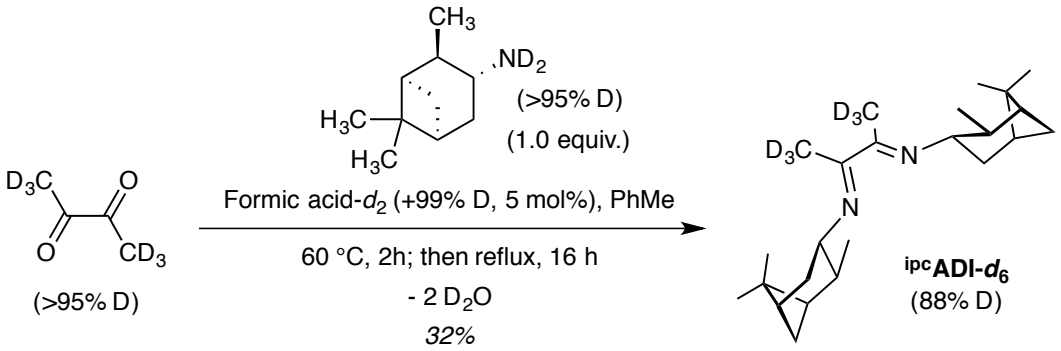

Scheme S5. Synthesis of ^{ipc}ADI-d_{12}.

Preparation of ^{ipc}ADI-d_6. ^{ipc}**ADI-d_6** was synthesized as depicted in Scheme S5. 2,3-butanedione-d_6 (>95% D) was prepared following a reported protocol.[14] ND_2-(1R,2R,3R,5S)-(-)-isopinocampheylamine (>95% D) was synthesized by H/D exchange in -(1R,2R,3R,5S)-(-)-isopinocampheylamine with methanol-d_4 (99.8 %D) as solvent after three cycles consisting of 6 h

stirring at 23 °C followed by methanol removal under reduced pressure. Condensation of deuterated 2,3-butanedione (559 mg, 6.07 mmol) and amine (2.1 mL, 12.14 mmol) was carried out as for the synthesis of natural abundance ^{ipc}ADI,[1] using formic acid-d_2 instead of p-toluenesulfonic acid as catalyst, to yield 702 mg (32%) of ^{ipc}ADI-d_6 (88% D) as an off-white solid. **^{1}H NMR (500 MHz, benzene-d_6):** δ 3.92 (ddd, *J* = 10, 6, 4 Hz, 2H, N–C*H*), 2.52 (m, 2H, β-amino methine of C*H*CH$_3$), 2.39 (m, 2H, one of bridge methylene C*H*2), 2.28 (m, 2H, one of β-amino methylene N-CHC*H*$_2$), 2.19 (m, labeled, 0.75H, imine backbone C*H*$_3$), 1.93 (m, 2H, one of bridgehead C–*H*), 1.87 (m, 2H, one of bridgehead C–*H*), 1.74 (ddd, *J* = 14, 5, 3 Hz, 2H, one of β-amino methylene N–CHC*H*$_2$), 1.47 (d, *J* = 10 Hz, 2H, one of bridge methylene C*H*$_2$), 1.23 (s, 6H, one of bridge C(C*H*$_3$)$_2$), 1.04 (d, *J* = 7 Hz, 6H, methyl of CHC*H*$_3$), 1.03 (s, 6H, one of bridge C(C*H*$_3$)$_2$) ppm. **Quantitative ^{13}C{^{1}H} NMR (126 MHz, benzene-d_6):** δ 165.0 (CH$_0$, imine *C*=N), 60 (CH$_1$, imine C=N-*C*H), 48.4 (CH1, bridgehead *C*–H), 45.7 (CH$_1$, methine *C*HCH$_3$), 42.0 (CH$_1$, bridgehead *C*–H), 38.9 (CH$_0$, bridge *C*(CH$_3$)$_2$), 35.9 (CH$_2$, β-amino methylene *C*H$_2$), 33.8 (CH$_2$, bridge methylene *C*H$_2$), 28.1 (*C*H$_3$, one of C(*C*H$_3$)$_2$), 23.8 (CH$_3$, CH*C*H$_3$), 21.4 (CH$_3$, one of C(*C*H$_3$)$_2$), 12.8, 12.7, 12.6, 12.6, 12.5, 12.4, 12.3, 12.2, 12.2, 12.1, 12.0, 11.9, 11.7 (CH$_3$, imine *C*H$_3$, labeled 88%) ppm. **^{2}H NMR (77 MHz, None):** δ -1.60 ppm.

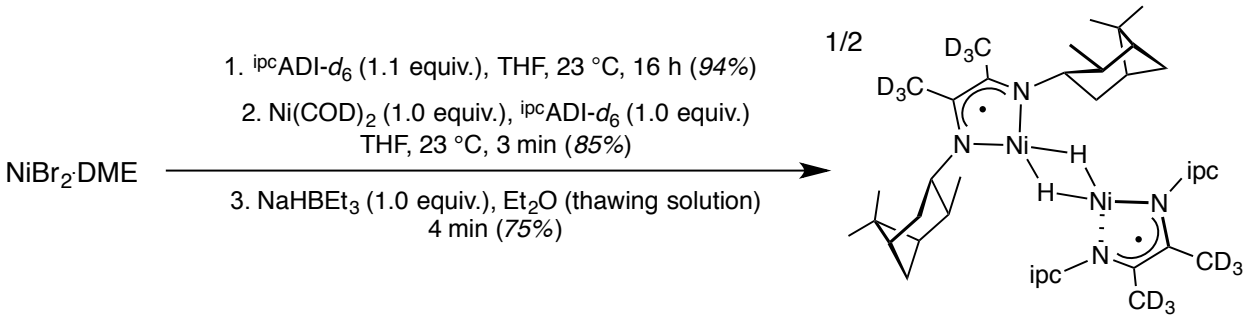

2-d_{12} (88% D)

Scheme S6. Synthesis of [(^{ipc}ADI-d_{12})Ni(μ$_2$-H)]$_2$.

Preparation of [(^{ipc}ADI-d_{12})Ni(μ_2-H)]$_2$ (2-d_{12}). 2-d_{12} was prepared as depicted in Scheme S6 following the same synthetic procedure of **2** (vide supra) to yield **2-d_{12}** (88% D) as a dark brown solid. **^{1}H NMR (300 MHz, benzene-d_6):** δ 4.22 (m, 8H, 4 x imine N–C*H* + 4 x β-amino methine C*H*CH$_3$), 4.09 (d, *J* = 9 Hz, 4H, 2 x bridge methylene C*H*$_2$), 3.45 (m, 4H, 2 x β-amino methylene N–CHC*H*$_2$), 2.77 (m, 4H, 4 x bridgehead C–*H*), 2.46 (m, 4H, 4 x bridgehead C–*H*), 2.20 (m, 4H, 2 x β-amino methylene N–CHC*H*$_2$), 2.11 (m, 4H, 2 x bridge methylene C*H*$_2$), 1.37 (s, 12H, 2 x bridge C(C*H*$_3$)$_2$), 1.21 (d, *J* = 7 Hz, 12H, 4 x methyl of CHC*H*$_3$), 1.18 (s, 12H, 2 x bridge C(C*H*$_3$)$_2$), -1.68 (m, labeled, 1.40H, 4 x imine backbone CH$_3$), -29.36 (s, 2H, 2 x Ni–*H*) ppm. **^{13}C{^{1}H} NMR (75 MHz, benzene-d_6):** δ 144.7 (CH$_0$, imine *C*=N), 66.3 (CH$_1$, imine N–*C*H), 49.1 (CH$_2$, bridge methylene *C*H$_2$), 44.0 (CH$_1$, β-amino methine *C*HCH$_3$), 42.8 (CH$_2$, β-amino methylene N–CH*C*H$_2$), 41.0, (CH$_0$, bridge C(*C*H$_3$)$_2$), 33.3 (CH$_2$, bridge methylene *C*H$_2$, CH bridgehead C–*H*), 28.9 (CH$_2$ β-amino methylene N–CH*C*H$_2$ + CH bridgehead *C*–H + CH$_3$ bridge C(*C*H$_3$)$_2$), 23.6 (CH$_3$, bridge C(*C*H$_3$)$_2$), 21.6 (CH$_3$, methyl of CH*C*H$_3$) ppm. ***Note:*** septet corresponding to imine *C*D$_3$ is undesignable due to the low intensity of the signals.

III. Additional Reactivity of [(^{ipc}ADI)Ni(μ_2-H)]$_2$

III.A. Reactivity with CCl$_4$

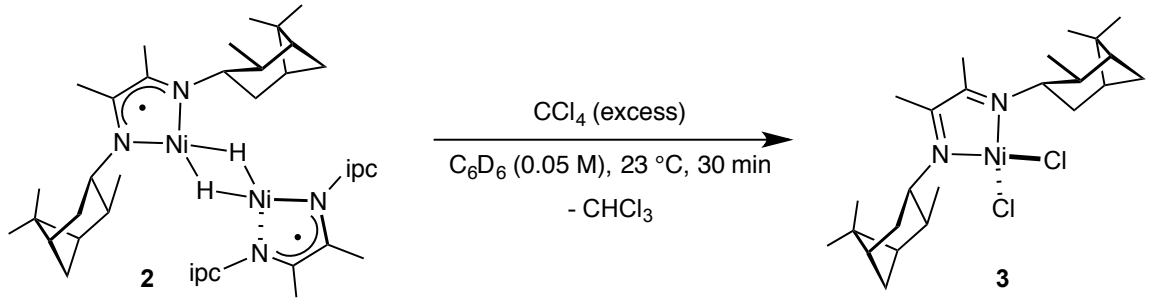

Scheme S7. Reaction of [(^{ipc}ADI-d_{12})Ni(μ_2-H)]$_2$ with CCl$_4$.

In a glovebox, a J. Young NMR tube was charged with **2** (15 mg, 18 μmol) and benzene-d_6 (0.4 mL). The sealed tube was taken out of the glovebox and the solution was frozen by submersion in liquid nitrogen (- 196 °C). While frozen, the headspace of the tube was evacuated on a high vacuum Schlenk line and an excess of CCl_4, contained in a Schlenk flask under vacuum attached to the line, was then transferred under vacuum to the frozen tube. The tube was sealed, allowed to thaw and rotated (inverting and mixing the containing solution) at 23 °C for 30 minutes. The reaction mixture changed color from dark brown to orange immediately. Next, the tube was attached to a high vacuum line and the volatiles were collected under static vacuum in other J. Young tube previously attached to the line, submitted to vacuum and frozen by submersion in liquid nitrogen (-196 °C). Analysis of the volatiles by ^{1}H NMR in benzene-d_6 revealed formation of C*H*Cl_3 (6.41 ppm) from reacting Ni–*H* (**2**) with CCl_4.[15] The tube containing the solid residue was brought to a glovebox and the residue was dissolved in dried THF-d_8 and analyzed by ^{1}H NMR spectroscopy indicating formation of **3** (Scheme S7).

III.B. Reactivity with 1-hexene

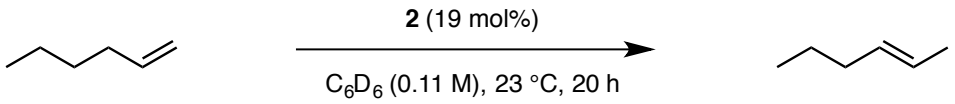

Scheme S8. Reaction of [(^{ipc}ADI-d_{12})Ni(μ_2-H)]$_2$ with 1-hexene.

In a glovebox, a J. Young NMR tube was charged with **2** (5 mg, 6 μmol), 1-hexene (4 μL, 0.032 mmol) and benzene-d_6 (0.3 mL). The sealed tube was taken out of the glovebox and rotated (inverting and mixing the containing solution) at 23 °C for 20 hours (no significant color change of the reaction mixture was observed during this time). Then, the reaction mixture was directly analyzed by ^{1}H NMR spectroscopy revealing full conversion of 1-hexene to 2-hexene and presence of **2** (Scheme S8).

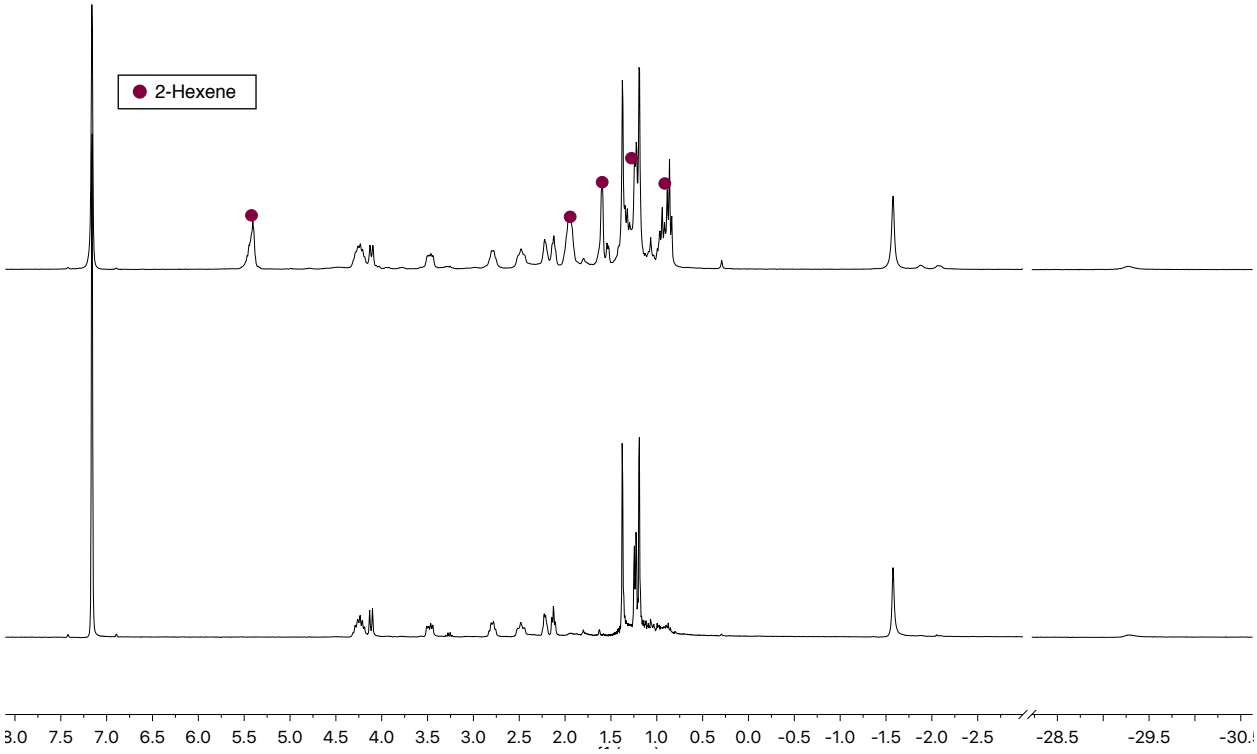

Figure S1. Stacked ^{1}H NMR spectra (300 MHz, benzene-d_6): reacting **2** and 1-hexene indicating formation of **2** and 2-hexene (first) and isolated **2** (second).

III.C. Reactivity with N_2

In a nitrogen-filled glovebox, a 20 mL thick-walled glass vessel containing a magnetic stir bar was charged with **2** (6 mg, 7.2 μmol) and benzene-d_6 (0.4 mL). The resulting mixture was stirred at 23 °C for 20 hours without sealing the vessel to ensure a continuous contact with the nitrogen atmosphere. Then, the reaction mixture was analyzed by ^{1}H NMR spectroscopy that indicated the presence of unreacted **2**.

IV. Solution Behavior of $[(^{ipc}ADI)Ni(\mu_2\text{-}H)]_2$

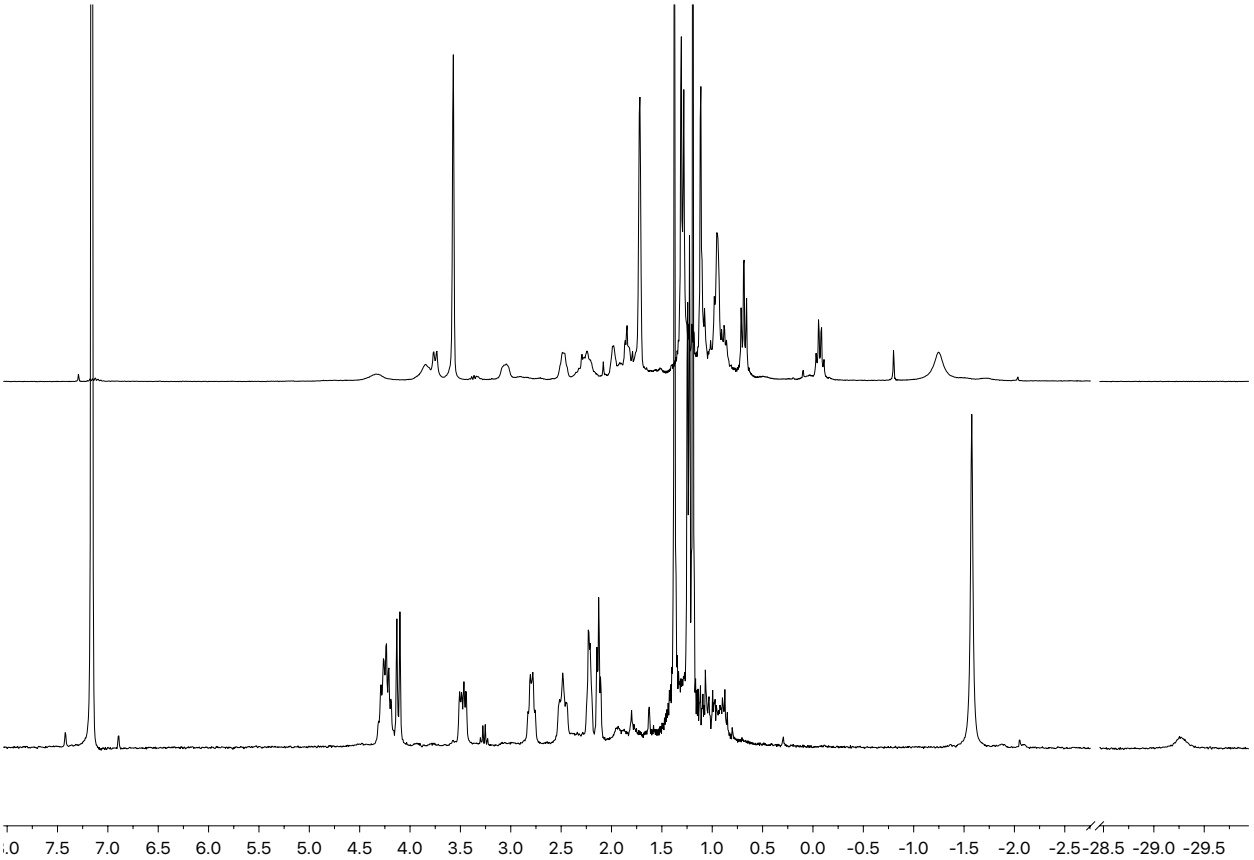

Figure S2. Stacked ^{1}H NMR spectra (300 MHz) of **2**: in THF-d_8 (first) and in benzene-d_6 (second).

As reflected in Figure S2, the ^{1}H NMR spectrum of **2** in THF-d_8 exhibits significantly broadened signals as compared to the corresponding spectrum of **2** in benzene-d_6. After THF-d_8 evaporation and reconstitution of the sample in benzene-d_6, the spectrum featured identical sharpen signals as that shown in Figure S2 (second spectrum), indicating that irreversible decomposition does not occur.

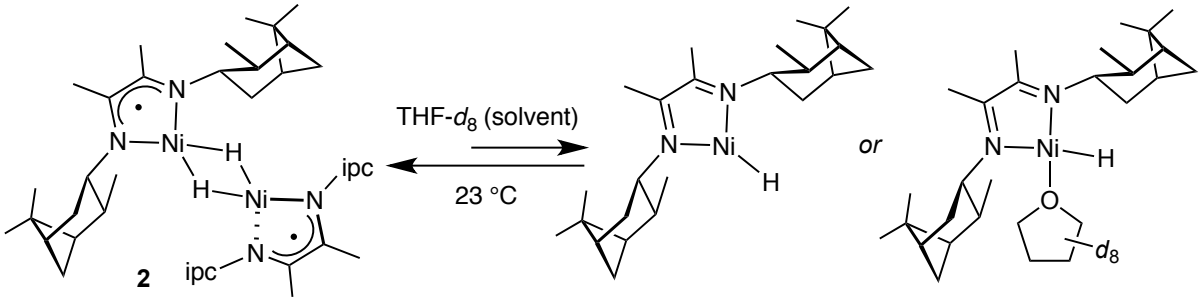

Scheme S9. THF-promoted nickel hydride dimer dissociation.

The magnetic moment of a solution of **2** in both benzene-d_6 and THF-d_8 was determined at 23 °C using ferrocene as an internal standard according to the Evans procedure modified for the use with NMR spectrometer with superconducting.[16] The solution of **2** in benzene-d_6 is diamagnetic as indicated by the unperturbed ferrocene chemical shift (Figure S3). In THF-d_8, however, **2** gave rise to two observable ferrocene proton resonances (4.11 ppm and 3.66 ppm; $\Delta\delta$ = 0.45 ppm) (Figure S4), consistent with the generation of a paramagnetic species in solution. The presence of a paramagnetic compound is likely responsible for the broadening of peaks in the THF-d_8 spectrum and supports the reversible, THF-promoted dimer dissociation to generate a monomeric nickel hydride complex. The nickel center in the monomer may contain THF-d_8 as a ligand and, therefore, two potential structures can be drawn for such monometallic complex: [(^{ipc}ADI)NiH] or [(^{ipc}ADI)NiH(THF-d_8)] (Scheme S9).

Attempts to observe the monomeric species by EPR spectroscopic in THF at 298K failed due to the high dielectric constant of THF (4.33 vs 2.27 (benzene) and 2.38 (toluene)) that results in the absorption of microwaves and precludes the observation of an EPR signal at room temperature using this solvent. The UV-Vis spectra of **2** were collected in benzene and THF solvent and exhibit very similar features. It is likely that the concentration of the monomeric nickel complex responsible for the catalytic activity in THF is not sufficient to significantly alter the absorbance profile of the mixture (Figure S5).

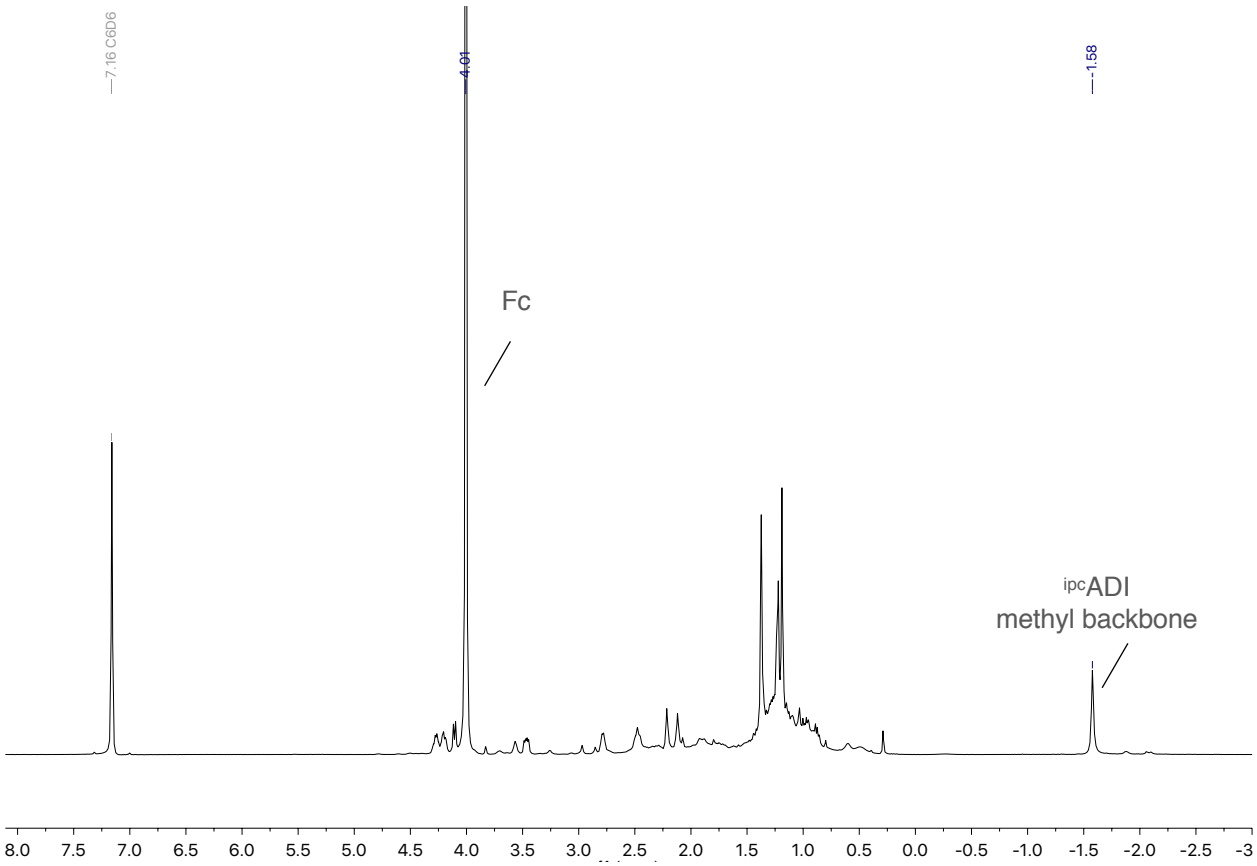

Figure S3. ^{1}H NMR spectra (300 MHz, benzene-d_6) of **2** and ferrocene (dissolved in the solution and contained in a capillary with benzene-d_6).

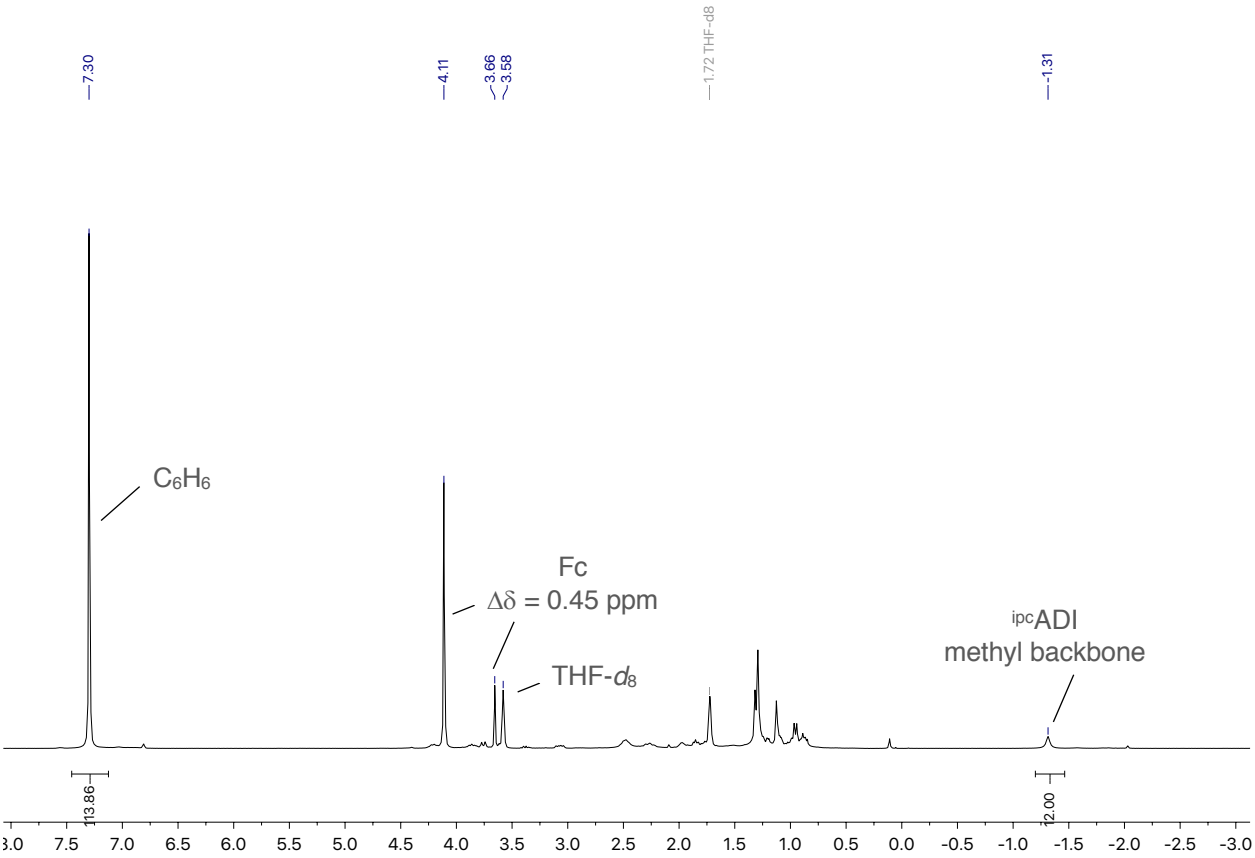

Figure S4. ^{1}H NMR spectra (300 MHz, THF-d_8) of **2**, ferrocene (dissolved in the solution and contained in a capillary with THF-d_8), and benzene as internal standard.

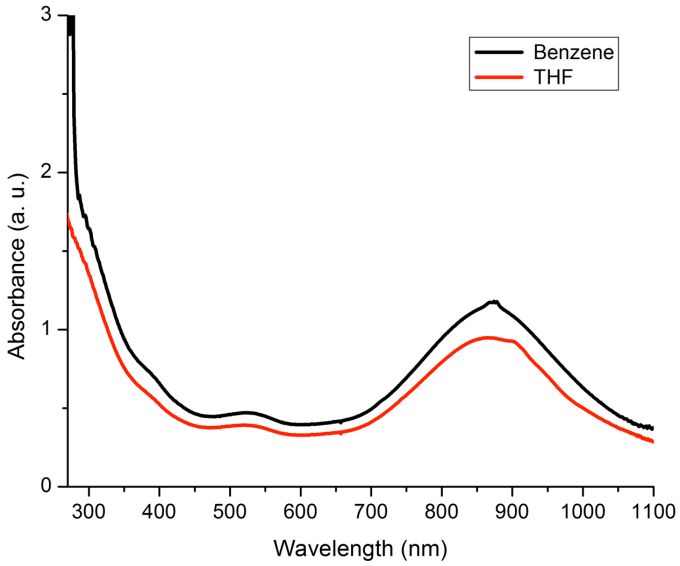

Figure S5. UV-Vis spectra of **2** in benzene (black) and THF (red).

V. General Procedure for H/D Exchange in Arenes

Unless otherwise specified, all H/D exchange reactions in arenes were performed as follows. In a glovebox, a thick-walled glass vessel containing a magnetic stir bar was charged with **2** (5 mg, 6 μmol), the corresponding arene substrate (**11a**–**11p**) (0.60 mmol) and THF (1 mL).The vessel was sealed, taken out of the glovebox and attached to a high vacuum Schlenk line. The solution was then frozen by submersion of the entire vessel in liquid nitrogen (-196 °C). After evacuating the headspace, D_2 (~1 atm) was added. The reaction vessel was sealed, and the reaction mixture was thawed (when 23 °C is reached, the pressure of D_2 in the headspace is ~4 atm) and stirred at 45 °C for 24 hours. At the end of the reaction, the vessel was opened to air and the reaction mixture was worked-up as indicated for each arene substrate. Unless otherwise specified, degree of deuterium incorporation at each specific site was determined by the decrease of the corresponding ^{1}H NMR signal intensities relative to an unlabeled site. Degree of deuterium incorporation was further confirmed by integration of the corresponding quantitative ^{13}C{^{1}H} NMR spectrum. HRMS (GC/MS) was used to corroborate the deuterium incorporation in specific arenes.

VI. General Procedure for H/D Exchange in Pharmaceuticals

VI.A. H/D Exchange with [(^{ipc}ADI)Ni(μ_2-H)]$_2$

Unless otherwise specified, all H/D exchange reactions in pharmaceutical compounds using [(^{ipc}ADI)Ni(μ_2-H)]$_2$ (**2**) as nickel precatalyst were performed following Method A as described below.

Method A: In a glovebox, a thick-walled glass vessel containing a magnetic stir bar was charged with **2** (15 mg, 18 μmol), the corresponding pharmaceutical compound (**12a**–**12i**) (0.14 mmol) and THF (1 mL). The vessel was sealed, taken out of the glovebox and attached to a high vacuum Schlenk line. The solution was then frozen by submersion of the bottom of the vessel (only the portion containing the reaction mixture) in liquid nitrogen (-196 °C). After evacuating the

headspace, D_2 (~1 atm) was added. The reaction vessel was sealed, and the reaction mixture was thawed (when 23 °C is reached, the pressure of D_2 in the headspace is ~1 atm) and stirred at 45 °C for 24 hours. At the end of the reaction, the vessel was opened to air and the reaction mixture was diluted with methanol (~10 mL) (deuterated flumazenil was diluted with DCM to avoid transesterification) and the product was purified by column chromatography as specified for each drug substrate. Degree of deuterium incorporation at each site was determined by the decrease of the corresponding ^{1}H NMR signal intensities relative to an unlabeled site. Degree of deuterium incorporation was further confirmed by integration of the corresponding quantitative ^{13}C{^{1}H} NMR spectrum and High Resolution Mass Spectrometry (HRMS), LC/MS, in combination with IsoPat[2] analysis.[17]

VI.B. H/D Exchange with [(^{ipc}ADI)NiBr$_2$]

Unless otherwise specified, all H/D exchange reactions in pharmaceutical compounds using [(^{ipc}ADI)NiBr$_2$] (**4**) as nickel precatalyst were performed following Method B as described below.

Method B*:* In a glovebox, a thick-walled glass vessel containing a magnetic stir bar was charged with **4** (20 mg, 0.035 mmol) and THF (0.5 mL). While stirring at 23 °C, a 1.0 M solution of NaHBEt$_3$ in toluene (70 µL, 0.07 mmol) was added to the pink solution, which immediately turned dark brown due to formation of **2**.[18] The resulting mixture was then stirred at 23°C for 2 additional minutes and, subsequently, the corresponding pharmaceutical compound (**12a**–**12d**) (0.14 mmol) and additional THF (0.5 mL) were added. The vessel was sealed, taken out of the glovebox and attached to a high vacuum Schlenk line. The solution was then frozen by submersion of the bottom of the vessel (only the portion containing the reaction mixture) in liquid nitrogen (-196 °C). After evacuating the headspace, D_2 (~1 atm) was added. The reaction vessel was sealed, and the reaction mixture was thawed (when 23 °C is reached, the pressure of D_2 in the headspace is ~1 atm) and stirred at 45 °C for 24 hours. At the end of the reaction, the vessel was opened to air and the reaction mixture was diluted with methanol (~10 mL) and the product was purified by column chromatography as specified for each drug substrate. Degree of deuterium incorporation

at each site was determined by the decrease of the corresponding ^{1}H NMR signal intensities relative to an unlabeled site. Degree of deuterium incorporation was further corroborated by integration of the corresponding quantitative $^{13}C\{^{1}H\}$ NMR spectrum and HRMS, LC/MS, in combination with IsoPat[2] analysis.[17]

VI.C. H/D Exchange with $[(^{iPr}DI)Ni(\mu_2\text{-}H)]_2$

H/D exchange reactions in **12a**–**12c**, **12e** and **12f** using $[(^{iPr}DI)Ni(\mu_2\text{-}H)]_2$ (**1**) as nickel precatalyst were reported in our previous work.[19] H/D exchange reactions in **12d**, **12g**, **12h** and **12i** using $[(^{iPr}DI)Ni(\mu_2\text{-}H)]_2$ (**1**) as nickel precatalyst were performed following Method A using **1** (17 mg, 18 μmol) instead of **2**.

VII. General Procedure for H/T Exchange in Pharmaceuticals

Unless otherwise specified, all H/T exchange in pharmaceuticals were performed as follows. In a glovebox, a 4 mL glass vessel containing a magnetic stir bar was charged with **4** (8.1 mg, 14 μmol) and CPME (800 μL). While stirring the resulting mixture at 23 °C, 1.0 M solution of $NaHBEt_3$ in toluene (28 μL, 28 μmol) was added. After $NaHBEt_3$ addition, the reaction mixture changed color from pink to dark brown due to formation of **2**[18] and was stirred at 23 °C for 5 minutes. In a second 4 mL vial charged with a magnetic stir, MK-6096 or varenicline (21 μmol) was dissolved in CPME (300 μL). MK-5395 and papaverine, both insoluble in neat CPME, were dissolved in a solvent mixture containing CPME (450 μL) and NMP (60 μL). A 1 mL round bottom flask containing a magnetic stir bar was charged with 100 μL of the MK-6096/varenicline solution, or 170 μL of the MK-5395/papaverine solution (7 μmol of the corresponding drug compound). Then, 100 μL of the previously prepared nickel precatalyst solution (~1.75 μmol of [Ni]) were also added to the round bottom flask. The flask was attached to a Swagelok, sealed and carefully taken out of the glovebox. The Swagelok was attached to the Tritech® manifold and the reaction mixture was degassed via freeze-pump-thaw (3 cycles). After the third freeze-pump-thaw cycle and keeping the bottom of the reaction flask submersed in liquid nitrogen (-196 °C), T_2 (1.0 Ci, 0.15

atm) was added. The reaction mixture, sealed under the Swagelok, was stirred at 45 °C for 20 hours. After this time, the reaction flask was opened, the tritium-containing volatiles and the unstable tritium labels were removed by three successive evaporations from ethanol (10 mL per iteration). The crude product was analyzed by scintillation counting and radio-HPLC, and subsequently purified by semipreparative reverse phase HPLC using the indicated column and solvent system for each drug substrate. Specific activity of each tritium labeled compound was determined by LC/MS in combination with IsoPat[2] analysis,[17] while HPLC analysis and liquid scintillation counting were used to determine the radiochemical purity and total activity. Degrees of tritium incorporation were determined by ^{3}H NMR spectroscopy and correspond to relative numbers normalized to 100%. ^{1}H and ^{13}H NMR spectra were recorded from a mixture of the isolated tritium labeled compound and the corresponding unlabeled compound (2 mg).

VIII. Analysis of Deuterium Labeled Arenes

H/D exchange in pyridine

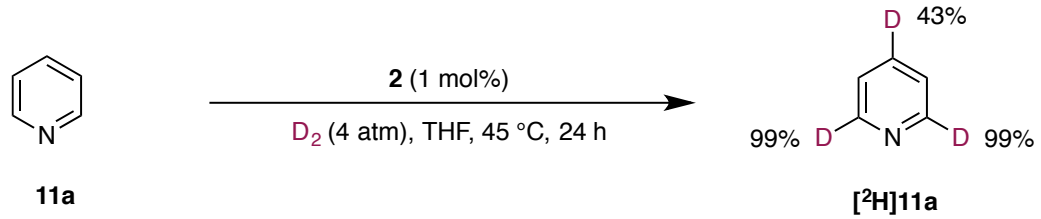

Scheme S10. H/D exchange in pyridine.

Reaction was carried out following the general procedure described in section V, using pyridine, **11a** (0.6 mmol, 48 μL) as substrate. At the end of the reaction, the product mixture was diluted with $CDCl_3$ (0.5 mL), filtered through a thin pad of alumina and analyzed without further purification. **^{1}H NMR (500 MHz, $CDCl_3$):** δ 8.54 (m, labeled, 0.02H), 7.61 (t, *J* = 8 Hz, labeled, 0.57H), 7.22 (m, 2H) ppm. **Quantitative ^{13}C{^{1}H} NMR (126 MHz, $CDCl_3$):** δ 149.7, 149.4, 149.2 (2 carbons, labeled, 99% D), 135.9, 135.8, 135.7, 135.5 (labeled, 43% D), 123.6, 123.5 ppm.

H/D exchange in 2-methylpyrimidine

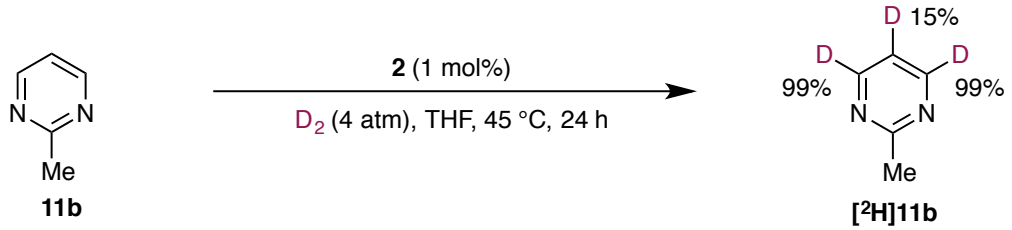

Scheme S11. H/D exchange in 2-methylpyrimidine.

Reaction was carried out following the general procedure described in section V, using 2-methylpyridine, **11b** (0.6 mmol, 56 μL) as substrate. At the end of the reaction, the product mixture was diluted with $CDCl_3$ (0.5 mL), filtered through a thin pad of alumina and analyzed without further purification. **^{1}H NMR (500 MHz, $CDCl_3$):** δ 8.57 (labeled, 0.03H), 7.05 (s, labeled, 0.85H), 2.66 (s, 3H) ppm. **Quantitative ^{13}C{^{1}H} NMR (126 MHz, $CDCl_3$):** δ 168.3, 156.8, 156.8, 156.6, 156.5, 156.34, 156.3 (2 carbons, labeled, 99% D), 118.0, 117.9, 117.7, 117.5 (labeled, 15% D), 26.1 ppm.

H/D exchange in 3,5-lutidine

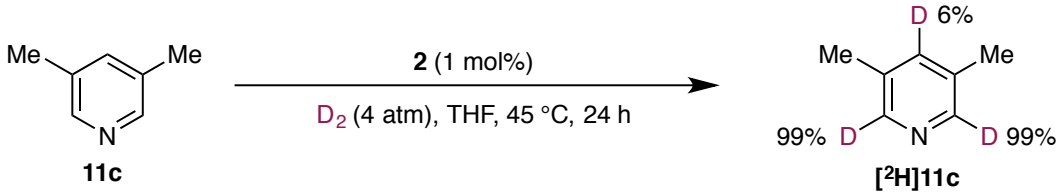

Scheme S12. H/D exchange in 3,5-lutidine.

Reaction was carried out following the general procedure described in section V, using 3,5-lutidine, **11c** (0.6 mmol, 68 μL) as substrate. At the end of the reaction the product mixture was diluted with $CDCl_3$ (0.5 mL), filtered through a thin pad of alumina and analyzed without further purification. **^{1}H NMR (500 MHz, $CDCl_3$):** δ 8.18 (s, labeled, 0.02H), 7.25 (s, labeled, 0.94H), 2.24

(s, 6H) ppm. **Quantitative $^{13}C\{^1H\}$ NMR (126 MHz, $CDCl_3$):** δ 146.8, 146.6, 146.4 (2 carbons, labeled, 99% D), 136.7 (labeled, 6%), 132.0, 17.7 ppm.

H/D exchange in pyrazine

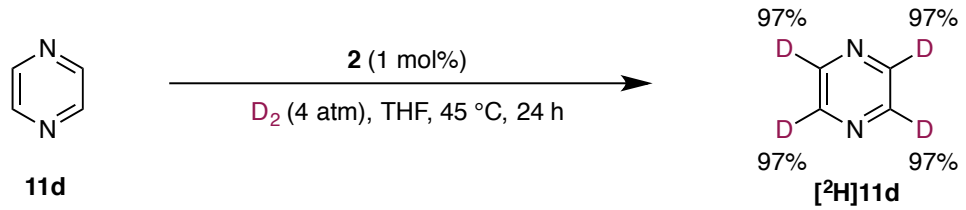

Scheme S13. H/D exchange in pyrazine.

Reaction was carried out following the general procedure described in section V, using pyrazine, **11d** (0.6 mmol, 48 mg) as substrate. At the end of the reaction, the product mixture was diluted with $CDCl_3$ (0.5 mL), filtered through a thin pad of alumina and analyzed without further purification. Isotopic incorporation was determined by quantitative $^{13}C\{^1H\}$ NMR due to the lack of a reference signal in the ^1H NMR spectrum. **^1H NMR (500 MHz, $CDCl_3$):** δ 8.43 (s, labeled) ppm. **Quantitative $^{13}C\{^1H\}$ NMR (126 MHz, $CDCl_3$):** δ 144.9, 144.7, 144.5, 144.3 (4 carbons, labeled, 97%) ppm.

H/D exchange in 1,2,4,5-tetrafluorobenzene

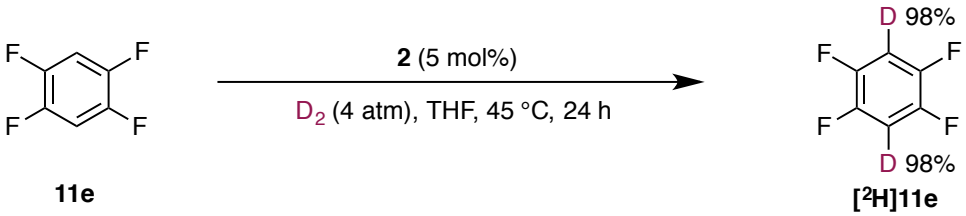

Scheme S14. H/D exchange in 1,2,4,5-tetrafluorobenzene.

Reaction was carried out following the general procedure described in section V, using 1,2,4,5-tetrafluorobenzene, **11e** (0.6 mmol, 67 μL) as substrate and **2** (0.03 mmol, 25 mg). At the end of

the reaction, the product mixture was diluted with DMSO-d_6 (0.5 mL) and 1,1,2,2-tetrachloroethane (0.6 mmol, 63 μL) was added as internal standard for determining the isotopic incorporation. The mixture was then filtered through a thin pad of alumina and analyzed without further purification. **^{1}H NMR (500 MHz, DMSO-d_6):** δ 7.75 (m, labeled, 0.05H) ppm. **Quantitative ^{13}C{^{1}H} NMR (126 MHz, DMSO-d_6):** δ 145.6 (m), 107.2 (m, labeled, 98% D) ppm. **^{19}F NMR (282 MHz, DMSO-d_6)**: δ -140.2 (br s) ppm. **^{2}H NMR (77 MHz, THF-d_0):** δ 8.01 ppm.

H/D exchange in 2-phenylpyridine

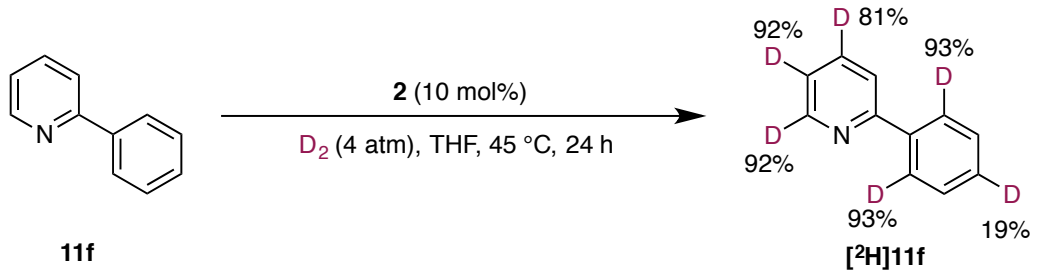

Scheme S15. H/D exchange in 2-phenylpyridine.

Reaction was carried out following the general procedure described in section V, using 2-phenylpyridine, **11f** (0.6 mmol, 86 μL) as substrate and **2** (0.06 mmol, 50 mg). At the end of the reaction, the product mixture was diluted with hexanes (10 mL), filtered through a thin pad of alumina, dried under vacuum and analyzed without further purification. **^{1}H NMR (500 MHz, $CDCl_3$):** δ 8.70 (s, labeled, 0.08H), 8.00 (m, labeled, 0.14H), 7.72 (br s, labeled, 1.23H), 7.48 (m, 2H), 7.42 (m, labeled, 0.83H), 7.21 (s, labeled, 0.08H) ppm. **Quantitative ^{13}C{^{1}H} NMR (126 MHz, $CDCl_3$):** δ 157.5, 149.7, 149.56, 149.3, 149.1 (labeled, 92% D), 139.4, 139.3, 136.7, 136.6, 136.5, 136.4, 136.3, 136.2, 136.1 (labeled, 77% D), 129.0, 128.9, 128.8, 128.8, 128.7, 128.6, 128.5, 128.4, 128.3, 128.2, 128.1 (labeled, 17% D), 127.0, 126.9, 126.7, 126.7, 126.6, 126.5, 126.4 (2 carbons, labeled, 93% D), 121.9, 121.8, 121.6, 121.4 (labeled, 92% D), 120.6, 120.5 ppm.

H/D exchange in nicotine

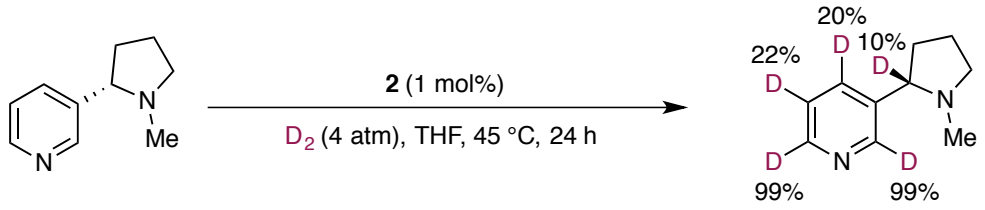

11g **[^{2}H]11g**

Scheme S16. H/D exchange in nicotine.
Reaction was carried out following the general procedure described in section V, using nicotine, **11g** (0.6 mmol, 96 μL) as substrate. At the end of the reaction, the product mixture was diluted with methanol (10 mL) and dried under reduced pressure. The product was then purified by column chromatography using 95:5 hexanes/EtOAc as eluent followed by flushing with EtOAc with 1% NEt_3 to give 86 mg (89% yield) **[^{2}H]11g** as a colorless oil. **^{1}H NMR (500 MHz, $CDCl_3$):** δ 8.50 (d, *J* = 2 Hz, labeled, 0.01H), 8.45 (dd, *J* = 5, 2 Hz, labeled, 0.01H), 7.66 (d, *J* = 8 Hz, labeled, 0.80H), 7.22 (d, *J* = 8 Hz, labeled, 0.78H), 3.20 (ddd, *J* = 10, 8, 2 Hz, 1H), 3.04 (dd, *J* = 9, 8 Hz, labeled, 0.90H), 2.27 (td, *J* = 9, 8 Hz, 1H), 2.14 (m, 4H), 1.93 (m, 1H), 1.78 (m, 1H), 1.69 (dddd, *J* = 13, 11, 9, 6 Hz, 1H) ppm. **Quantitative ^{13}C{^{1}H} NMR (126 MHz, $CDCl_3$):** δ 149.5, 149.3, 149.0 (labeled, 99% D), 148.6, 148.4, 148.1 (labeled, 99% D), 138.7, 138.6, 134.9, 134.8, 134.6, 134.4 (labeled, 20% D), 123.5, 123.4 (labeled, 22% D), 68.9, 68.9 (labeled, 10% D), 57.1, 40.5, 35.3, 22.7 ppm. Enantiomeric retention in **[^{2}H]11g** was determined by chiral gas chromatography (Figure S6).

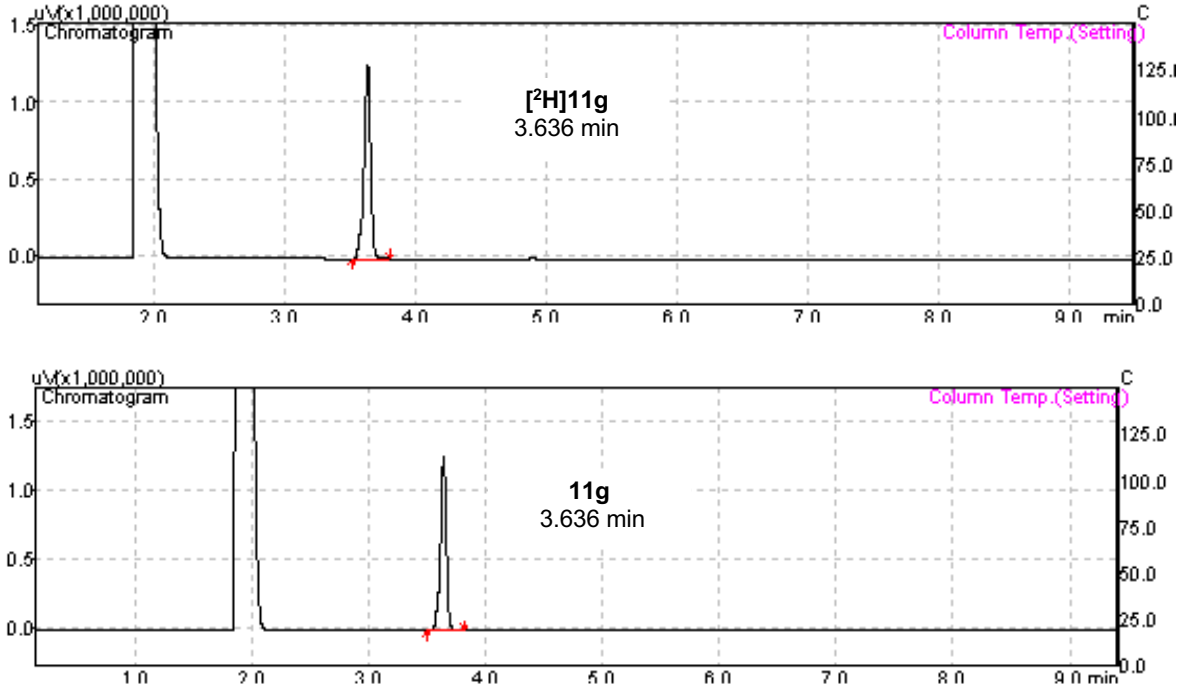

Figure S6. Stacked chiral gas chromatogram of **nicotine**: D-labeled, **[^{2}H]11g** (first) and unlabeled, **11g** (second).

H/D exchange in (*R*,*S*)-anabasine

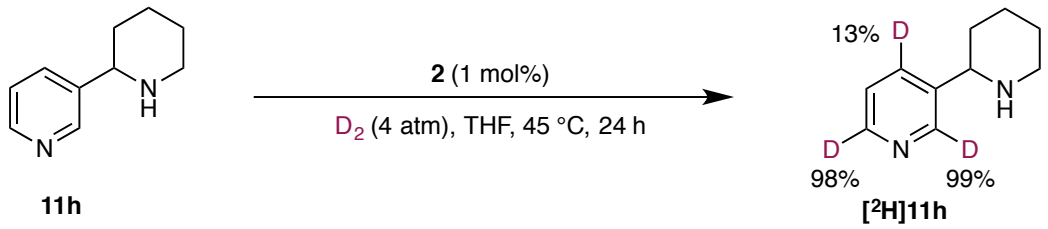

Scheme S17. H/D exchange in (*R*,*S*)-anabasine.

Reaction was carried out following the general procedure described in section V, using (*R*,*S*)-anabasine, **11h** (0.6 mmol, 93 μL) as substrate. At the end of the reaction, the product mixture was diluted with methanol (10 mL) and dried under reduced pressure. The product was then purified by column chromatography using 6:4 hexanes/EtOAc as eluent followed by flushing with EtOAc with 10% NEt_3 to give 80 mg (82% yield) **[^{2}H]11h** as a colorless oil. **^{1}H NMR (500 MHz, $CDCl_3$):** δ 8.51 (d, *J* = 2 Hz, labeled, 0.01H), 8.41 (dd, *J* = 5, 2 Hz, labeled, 0.02H), 7.64 (d, *J* = 8

Hz, labeled, 0.87H), 7.16 (d, J = 8 Hz, 1H), 3.56 (m, 1H), 3.12 (m, 1H), 2.73 (td, J = 12, 3 Hz, 1H), 1.82 (m, 1H), 1.65 (m, 3H), 1.44 (m, 3H) ppm. **Quantitative $^{13}C\{^1H\}$ NMR (126 MHz, $CDCl_3$):** δ 147.5, 147.4, 147.3, 147.2, 147.1, 147.0 (2 carbons, labeled, 99% and 98% D), 139.6, 133.2 (labeled, 13% D), 122.3, 58.7, 46.6, 33.8, 24.7, 24.2 ppm.

H/D exchange in caffeine

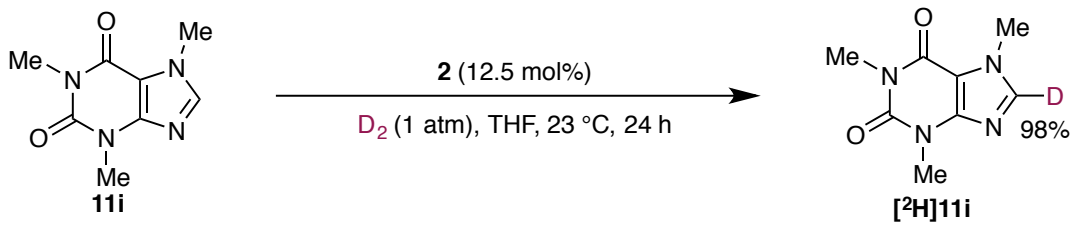

Scheme S18. H/D exchange in caffeine.

Reaction was carried out following Method A, described in section VI.A, using caffeine, **11i** (0.14 mmol, 27 mg) as substrate. At the end of the reaction, the product mixture was diluted with methanol (10 mL) and dried under reduced pressure. The product was then purified by column chromatography using 100:10:1 DCM/MeOH/NH_4OH as eluent to give 27 mg (100% yield) **[^{2}H]11i** as a white solid. **^{1}H NMR (500 MHz, $CDCl_3$):** δ 7.50 (s, labeled, 0.02H), 3.97 (s, 3H), 3.56 (s, 3H), 3.38 (s, 3H) ppm. **Quantitative $^{13}C\{^1H\}$ NMR (126 MHz, $CDCl_3$):** δ 155.5, 151.8, 148.8, 141.5, 141.3, 141.0 (labeled, 98% D), 107.6, 33.7, 29.8, 29.8, 28.0 ppm. **Deuterium incorporation**: 0.98 D/molecule (^{1}H NMR), 1.00 D/molecule (HRMS/IsoPat^2), 0.00% unlabeled compound.

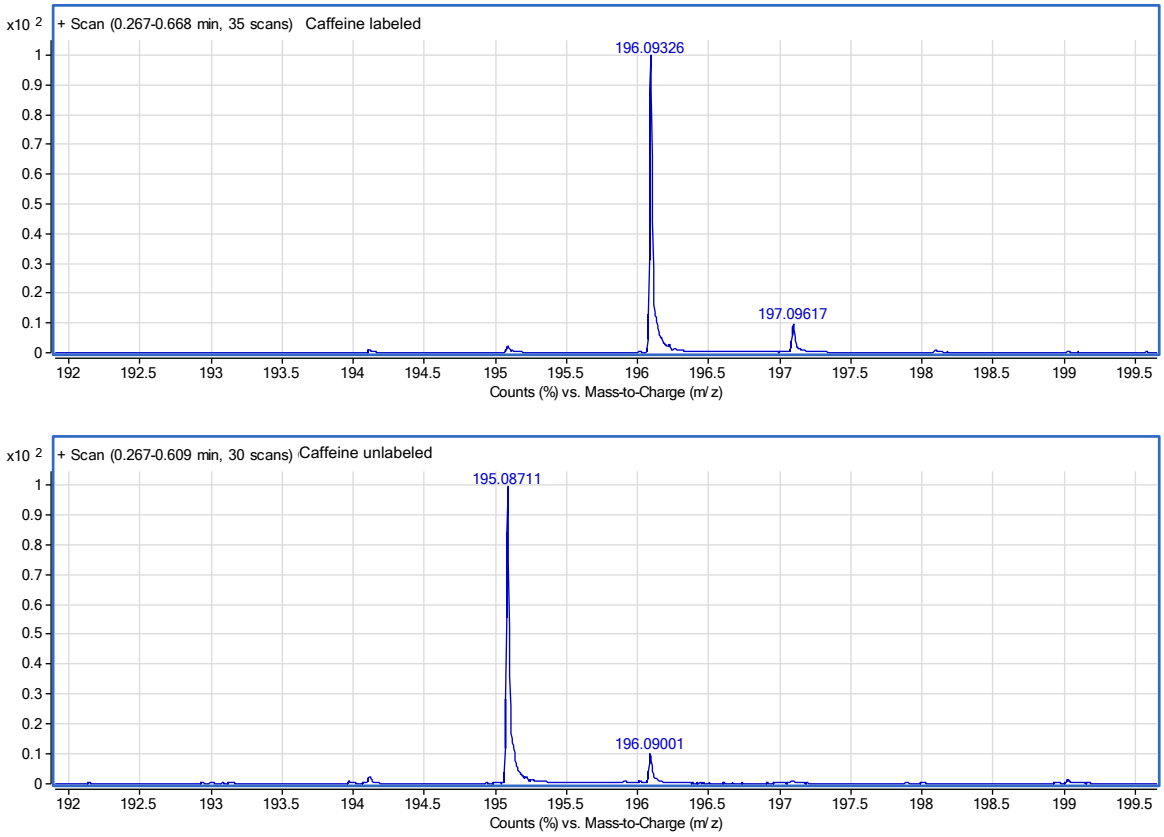

Figure S7. Stacked mass spectra of caffeine: D-labeled, **[^{2}H]11i** (first) and unlabeled, **11i** (second).

H/D exchange in doxofylline

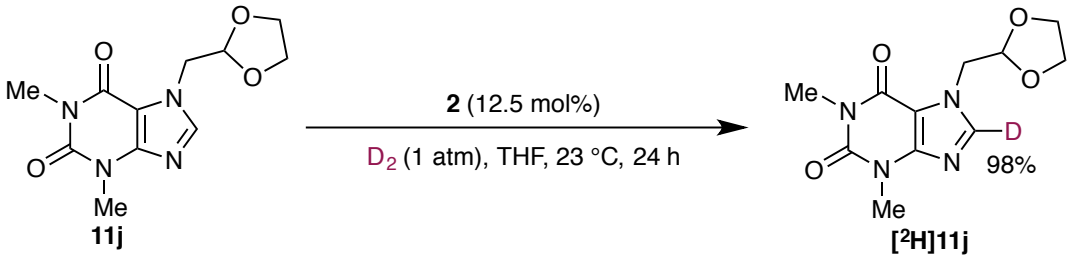

Scheme S19. H/D exchange in doxofylline.

Reaction was carried out following Method A, described in section VI.A, using doxofylline, **11j** (0.14 mmol, 37 mg) as substrate. At the end of the reaction, the product mixture was diluted with methanol (10 mL) and dried under reduced pressure. The product was then purified by column chromatography using 2:8 hexanes/EtOAc as eluent to give 32 mg (86% yield) **[^{2}H]11j** as a white solid. **^{1}H NMR (500 MHz, $CDCl_3$):** δ 7.62 (s, labeled, 0.02H), 5.20 (t, *J* = 3 Hz, 1H), 4.56 (d, *J* = 3 Hz, 2H), 3.83 (m, 4H), 3.56 (s, 3H), 3.38 (s, 3H) ppm. **Quantitative ^{13}C{^{1}H} NMR (126 MHz, $CDCl_3$):** δ 155.4, 151.8, 148.4, 142.3, 142.1, 141.8 (labeled, 98% D), 107.4, 100.9, 65.5, 48.0, 29.9, 29.8, 28.1 ppm. **Deuterium incorporation**: 0.98 D/molecule (^{1}H NMR), 1.01 D/molecule (HRMS/IsoPat[2]), 0.00% unlabeled compound.

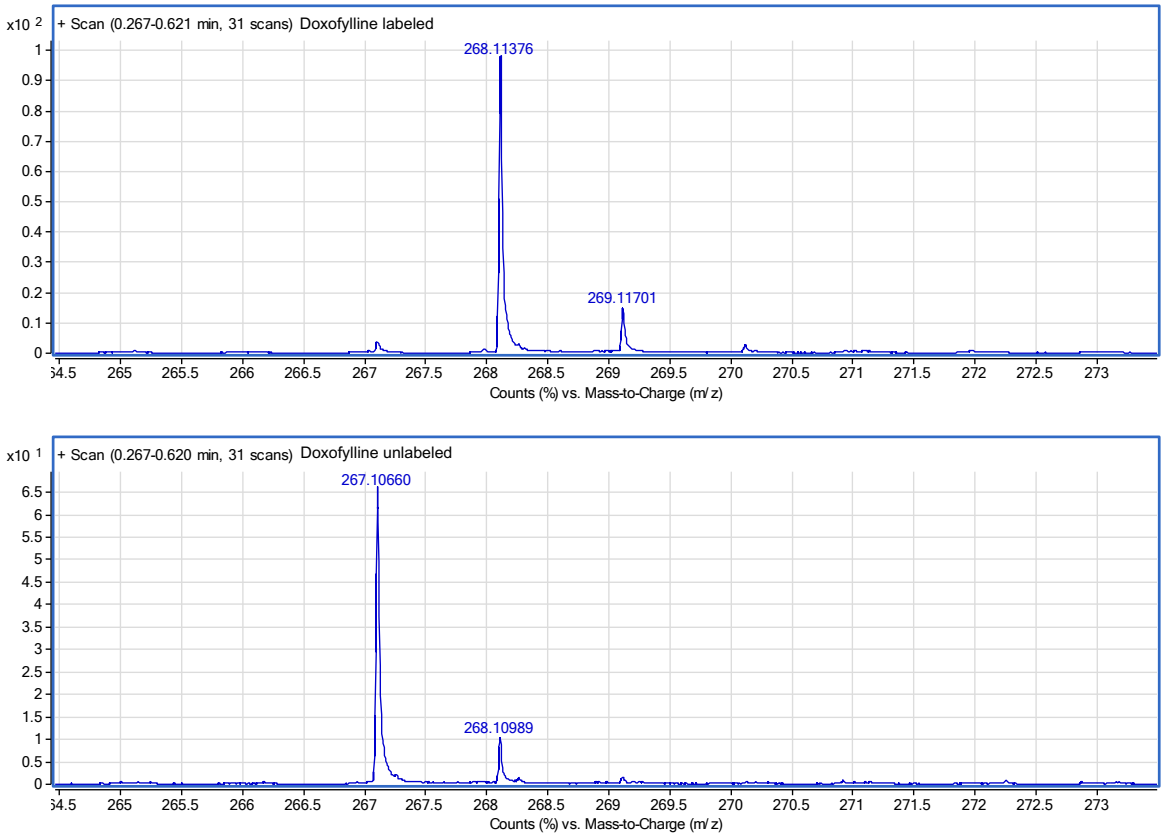

Figure S8. Stacked mass spectra of doxofylline: D-labeled, **[^{2}H]11j** (first) and unlabeled, **11j** (second).

H/D exchange in pentoxifylline

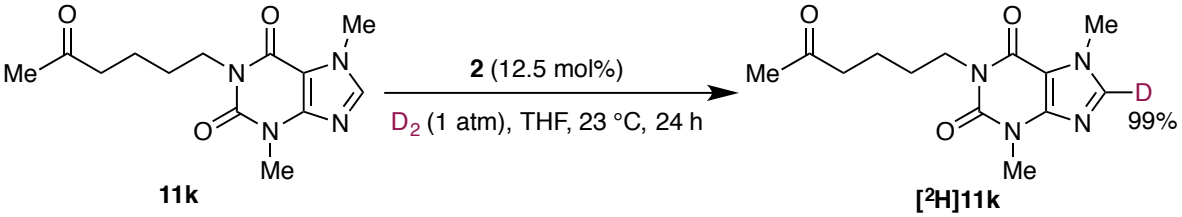

Scheme S20. H/D exchange in pentoxifylline.

Reaction was carried out following Method A, described in section VI.A, using pentoxifylline, **11k** (0.14 mmol, 39 mg) as substrate. At the end of the reaction, the product mixture was diluted with methanol (10 mL) and dried under reduced pressure. The product was then purified by column

chromatography using 2:8 hexanes/EtOAc as eluent to give 37 mg (93% yield) **[^{2}H]11k** as a white solid. **^{1}H NMR (500 MHz, $CDCl_3$):** δ 7.48 (s, labeled, 0.01H), 3.96 (d, *J* = 11 Hz, 5H), 3.53 (s, 3H), 2.47 (t, *J* = 7Hz, 2H), 2.10 (s, 3H), 1.62 (dqd, *J* = 12, 7, 6, 4 Hz, 4H) ppm. Quantitative **^{13}C{^{1}H} NMR (126 MHz, $CDCl_3$):** δ 208.8, 155.3, 151.5, 148.8, 141.5, 141.3, 141.0 (labeled, 99% D), 107.7, 43.2, 40.9, 33.6, 30.0, 29.8, 27.5, 21.0 ppm. **Deuterium incorporation**: 0.99 D/molecule (^{1}H NMR), 1.02 D/molecule (HRMS/IsoPat[2]), 0.00% unlabeled compound.

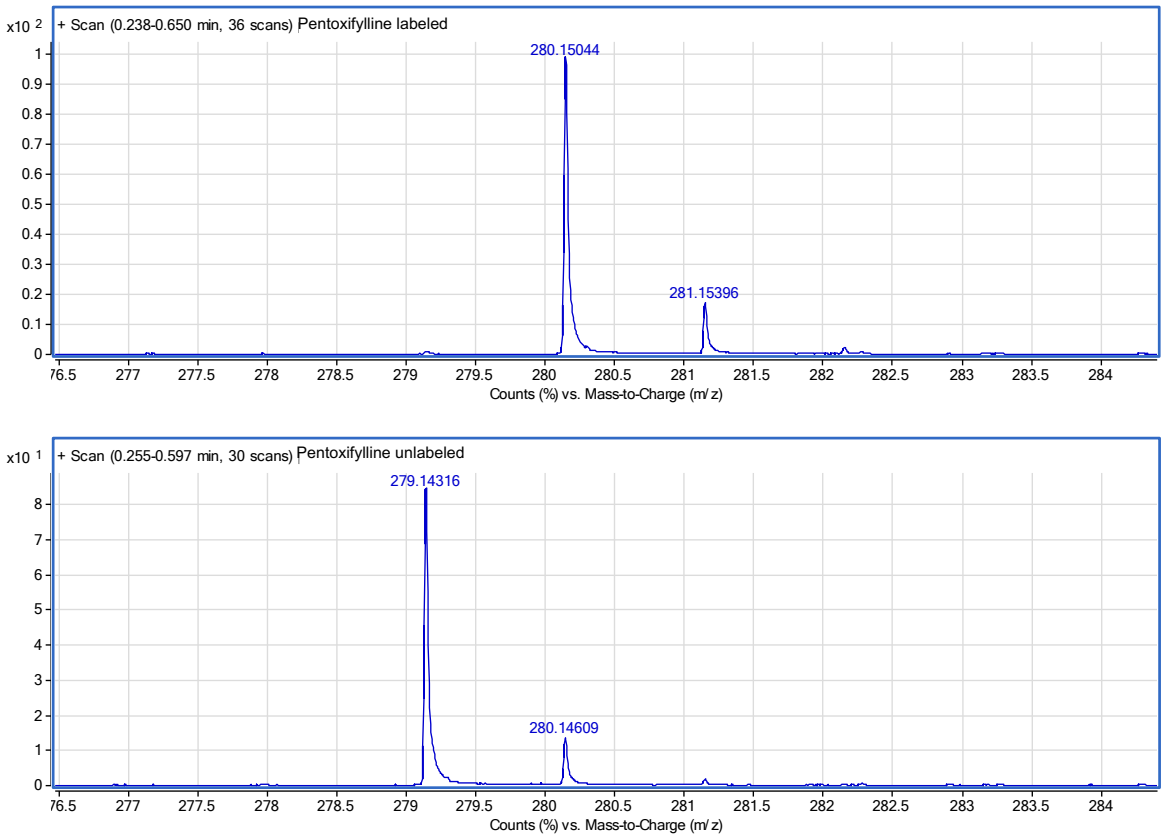

Figure S9. Stacked mass spectra of pentoxifylline: D-labeled, **[^{2}H]11k** (first) and unlabeled, **11k** (second).

H/D exchange in oxazole

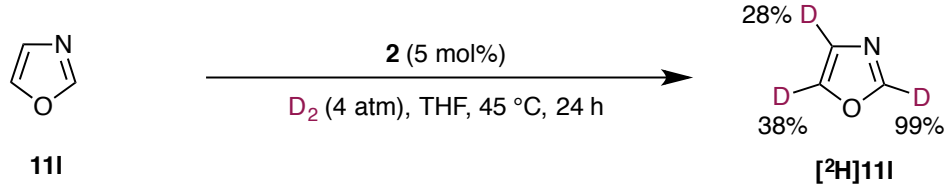

Scheme S21. H/D exchange in oxazole.

Reaction was carried out following the general procedure described in section V, using oxazole, **11l** (0.6 mmol, 39 μL) as substrate and **2** (0.03 mmol, 25 mg). At the end of the reaction, the product mixture was diluted with DMSO-d_6 (0.5 mL) and 1,1,2,2-tetrachloroethane (0.6 mmol, 63 μL) was added as internal standard for determining the isotopic incorporation. The mixture was then filtered through a thin pad of alumina and analyzed without further purification. **^{1}H NMR (500 MHz, DMSO-d_6):** δ 8.34 (s, labeled, 0.99H), 8.08 (s, labeled, 0.72H), 7.22 (s, labeled, 0.62H) ppm. **Quantitative ^{13}C{^{1}H} NMR (126 MHz, DMSO-d_6):** δ 152.4, 152.1, 151.8 (labeled, 99% D), 139.8, 139.8 (labeled, 38% D), 126.6, 126.4, 126.2 (labeled, 28% D) ppm.

H/D exchange in thiazole

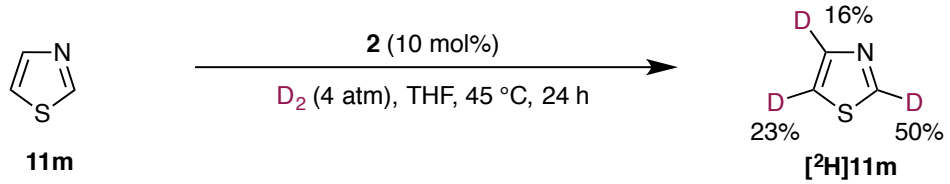

Scheme S22. H/D exchange in thiazole.

Reaction was carried out following the general procedure described in section V, using thiazole, **11m** (0.6 mmol, 43 μL) as substrate and **2** (0.06 mmol, 50 mg). At the end of the reaction, the product mixture was diluted with CD_3CN (0.5 mL) and 1,1,2,2-tetrachloroethane (0.6 mmol, 63 μL) was added as internal standard for determining the isotopic incorporation. The mixture was then filtered through a thin pad of alumina and analyzed without further purification. **^{1}H NMR (500**

MHz, CD_3CN): δ 8.93 (s, labeled, 0.50H), 7.92 (s, labeled, 0.84H), 7.56 (s, labeled, 0.77H) ppm. **Quantitative $^{13}C\{^1H\}$ NMR (126 MHz, CD_3CN):** δ 154.4, 154.2, 153.9 (labeled, 50% D), 144.4 (labeled, 16%D), 120.3 (labeled, 23%D) ppm.

H/D exchange *N*-methylpyrrole

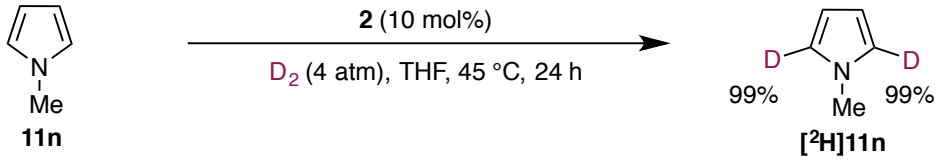

Scheme S23. H/D exchange in *N*-methylpyrrole.

Reaction was carried out following the general procedure described in section V, using 1-methylpyrrole, **11n** (0.6 mmol, 53 μL) as substrate and **2** (0.06 mmol, 50 mg). At the end of the reaction, the product mixture was diluted with $CDCl_3$ (0.5 mL) and filtered through a thin pad of alumina and analyzed without further purification. **^1H NMR (500 MHz, $CDCl_3$):** δ 6.49 (m, labeled, 0.03H), 6.00 (s, 2H), 3.56 (s, 3H) ppm. **Quantitative $^{13}C\{^1H\}$ NMR (126 MHz, $CDCl_3$):** δ 121.4, 121.1, 120.9 (labeled, 99% D), 107.8, 35.7 ppm.

H/D exchange in 1-methylindole

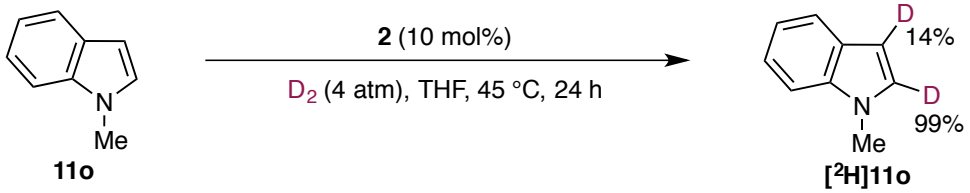

Scheme S24. H/D exchange in *N*-methylindole.

Reaction was carried out following the general procedure described in section V, using 1-methylindole, **11o** (0.6 mmol, 75 μL) as substrate and **2** (0.03 mmol, 50 mg). At the end of the reaction the product mixture was diluted with methanol and dried under reduced pressure. The product was then purified by column chromatography using 9:1 hexanes/EtOAc to give 66 mg

(84% yield) **[^{2}H]11o** as a yellow oil. **^{1}H NMR (500 MHz, $CDCl_3$):** δ 7.73 (d, *J* = 8 Hz, 1H), 7.40 (m, 1H), 7.32 (ddd, *J* = 8, 7, 1 Hz, 1H), 7.21 (td, *J* = 7, 1 Hz, 1H), 7.11 (d, *J* = 3 Hz, labeled, 0.01H), 6.58 (s, labeled, 0.86H), 3.83 (s, 3H) ppm. **Quantitative ^{13}C{^{1}H} NMR (126 MHz, $CDCl_3$):** δ 136.7, 128.9, 128.6, 128.6, 128.5, 128.41 (labeled, 99% D), 121.5, 120.9, 120.9, 119.3, 109.3, 100.8 (labeled, 14% D), 32.79 ppm.

H/D exchange in furan

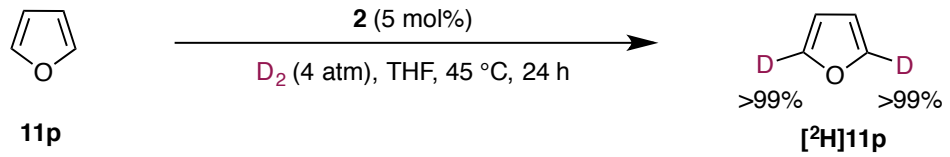

Scheme S25. H/D exchange in furan.

Reaction was carried out following the general procedure described in section V, using furan, **11p** (0.6 mmol, 43 μL) as substrate and **2** (0.06 mmol, 25 mg). At the end of the reaction, the product mixture was diluted with $CDCl_3$ (0.5 mL) and filtered through a thin pad of alumina and analyzed without further purification. Isotopic incorporation was determined by quantitative ^{13}C{^{1}H} NMR due to the lack of a reference signal in the ^{1}H NMR spectrum. **^{1}H NMR (500 MHz, $CDCl_3$):** δ 6.21 (s, 2H) ppm. **Quantitative ^{13}C{^{1}H} NMR (126 MHz, $CDCl_3$):** δ 142.2, 141.9, 141.7 (labeled, >99% D), 109.1, 108.9 ppm.

IX. Analysis of Deuterium Labeled Pharmaceuticals

H/D exchange in MK-6096 with Method A

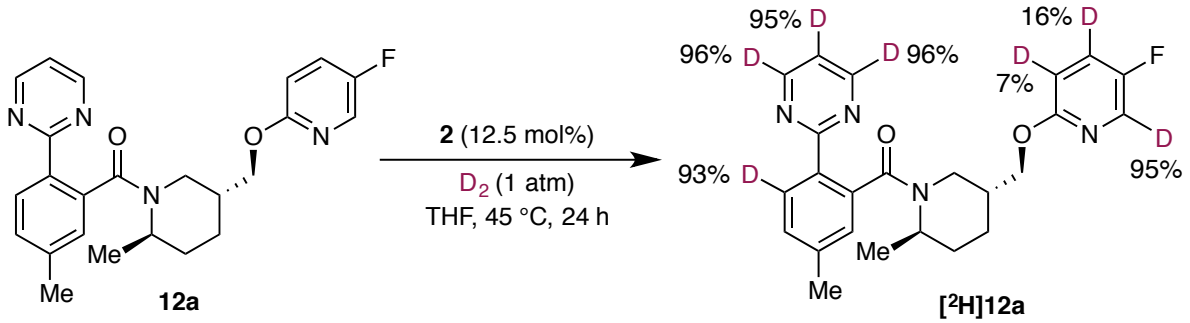

Scheme S26. H/D exchange in MK-6096 with Method A.

Reaction was carried out following Method A, described in section VI.A, using MK-6096, **12a** (59 mg, 0.14 mmol) as substrate. The product was purified by column chromatography using 100:10 DCM/MeOH as eluent to give 58 mg (99% chemical recovery yield) **[^{2}H]12a** as a white solid. In solution (DMSO-d_6) at room temperature MK-6096 exists as a mixture of 4 rotamers (58:26:8:5),[20] the most dominant isomer is following reported. **^{1}H NMR (500 MHz, DMSO-d_6):** δ 8.86 (m, labeled, 0.09H), 8.17 (m, labeled, 0.05H), 8.10 (m, labeled, 0.07), 7.65 (m, labeled, 0.84H), 7.49 (m, labeled, 0.05H), 7.21 (s, 1H), 6.79 (s, 1H), 6.55 (m, labeled, 0.93H), 4.73 (quintet, J = 6 Hz, 1H), 4.43 (m, 1H), 4.35 (t, J = 10 Hz, 1H), 4.03 (m, 1H), 3.29 (d, J = 13 Hz, 1H), 3.08 (dd, J = 14, 3 Hz, 1H), 1.92 (m, 2H), 1.88 (s, 3H), 1.53 (m, J = 12 Hz, 1H), 1.41 (m, 1H), 1.24 (d, J = 7 Hz, 3H) ppm. **Quantitative ^{13}C{^{1}H} NMR (126 MHz, DMSO-d$_6$):** δ 170.9, 163.4, 159.6, 157.0, 156.8, 156.6 (2 carbons, labeled, 96% D), 156.0 (J_{CF} = 245 Hz), 140.0, 137.9, 132.9, 132.7, 132.5 (J_{CF} = 26 Hz, labeled, 95% D), 132.4, 129.0 (labeled, 93% D), 128.6, 127.6, 127.2 (J_{CF} = 21 Hz, labeled, 16%), 119.0 (labeled, 95% D), 111.4 (J_{CF} = 5 Hz, labeled, 7% D), 66.3, 65.5, 43.6, 41.3, 36.3, 32.0, 25.1, 20.3, 20.2, 13.6 ppm. **Deuterium incorporation**: 4.98 D/molecule (^{1}H NMR), 4.96 D/molecule (HRMS/IsoPat[2]), 0.00% unlabeled compound.

H/D exchange in MK-6096 with Method B

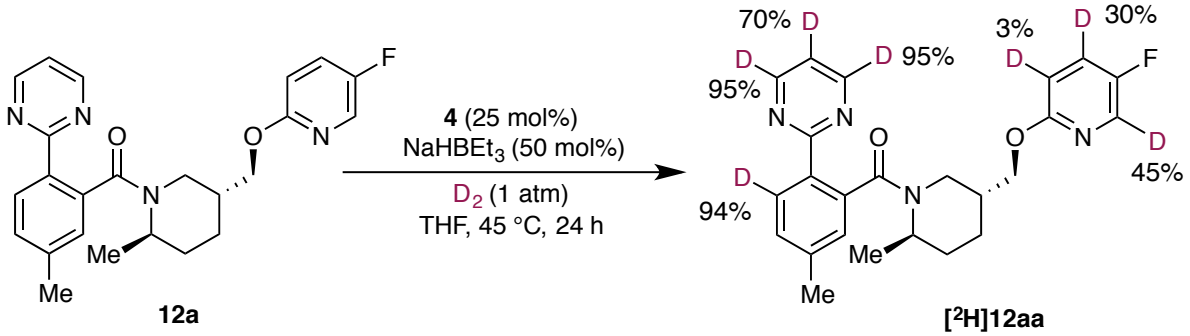

Scheme S27. H/D exchange in MK-6096 with Method B.

Reaction was carried out following Method B, described in section VI.A, using MK-6096, **12a** (59 mg, 0.14 mmol) as substrate. The product was purified by column chromatography using 100:10 DCM/MeOH as eluent to give 56 mg (95% chemical recovery yield) **[^{2}H]12aa** as a white solid. In

solution (DMSO-d_6) at room temperature MK-6096 exists as a mixture of 4 rotamers (58:26:8:5),[20] the most dominant isomer is following reported. **^{1}H NMR (500 MHz, DMSO-d_6):** δ 8.86 (m, labeled, 0.11H), 8.18 (m, labeled, 0.55H), 8.09 (m, labeled, 0.06H), 7.65 (m, labeled, 0.70H), 7.40 (m, labeled, 0.30H), 7.21 (s, 1H), 6.79 (s, 1H), 6.54 (m, labeled, 0.97), 4.73 (quintet, J = 6 Hz, 1H), 4.43 (m, 1H), 4.35 (t, J = 10 Hz, 1H), 4.03 (m, 1H), 3.28 (d, J = 13 Hz, 1H), 3.08 (dd, J = 14, 3 Hz, 1H), 1.98 (m, 2H), 1.88 (s, 3H), 1.53 (d, J = 12 Hz, 1H), 1.42 (d, J = 12 Hz, 1H), 1.23 (d, J = 7 Hz, 3H) ppm. **Quantitative ^{13}C{^{1}H} NMR (126 MHz, DMSO-d$_6$):** δ 170.9, 163.4, 159.6, 157.0, 156.8, 156.6 (2 carbons, labeled, 95% D), 156.0 (J_{CF} = 245 Hz), 140.0, 137.9, 133.0, 132.9, 132.8 (J_{CF} = 26 Hz, labeled, 45% D), 132.0, 129.0 (labeled, 94% D), 128.7, 127.6, 127.2 (J_{CF} = 21 Hz, labeled, 30%), 119.0 (labeled, 70% D), 111.4 (J_{CF} = 5 Hz, labeled, 3% D), 66.3, 65.5, 43.6, 41.3, 36.3, 32.0, 25.1, 20.3, 20.2, 13.6 ppm. **Deuterium incorporation**: 4.32 D/molecule (^{1}H NMR), 4.01 D/molecule (HRMS/IsoPat[2]), 0.00% unlabeled compound.

H/D Exchange in MK-6096 in Methanol

Reaction was carried out following both modified Method A and Method B.

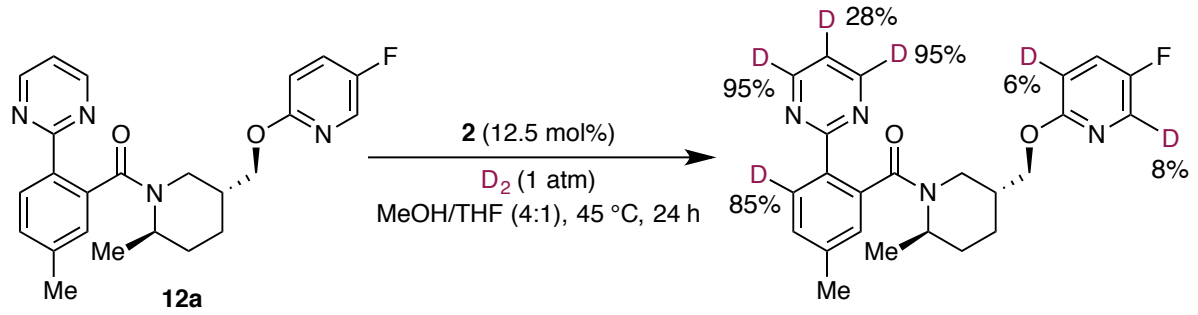

Scheme S28. H/D exchange in MK-6096 with Method A in MeOH/THF (4:1).

Method A, described in section VI.A, was followed using MK-6096, **12a** (59 mg, 0.14 mmol) as substrate and 0.8 mL methanol and 0.2 mL THF as solvent mixture (instead of using 1 mL THF). The product was purified by column chromatography using 100:10 DCM/MeOH as eluent to give 58 mg (99% chemical recovery yield) of deuterated MK-6096 as a white solid. In solution (DMSO-

d_6) at room temperature MK-6096 exists as a mixture of 4 rotamers (58:26:8:5),[20] the most dominant isomer is following reported. **^{1}H NMR (500 MHz, DMSO-d_6):** δ 8.86 (m, labeled, 0.10H), 8.18 (m, labeled, 092), 8.09 (m, labeled, 0.15), 7.65 (m, 1H), 7.49 (s, labeled, 0.72H), 7.22 (s, 1H), 6.79 (s, 1H), 6.56 (m, labeled, 0.94H), 4.73 (quintet, J = 6 Hz, 1H), 4.43 (m, 1H), 4.35 (t, J = 10 Hz, 1H), 4.03 (m, 1H), 3.28 (d, J = 13 Hz, 1H), 3.08 (dd, J = 14, 3 Hz, 1H), 1.92 (m, 2H), 1.88 (s, 3H), 1.54 (m, J = 12 Hz, 1H), 1.42 (m, 1H), 1.24 (d, J = 7 Hz, 3H) ppm**. Quantitative ^{13}C{^{1}H} NMR (126 MHz, DMSO-d$_6$):** δ 170.9, 163.4, 159.6, 157.1, 156.9, 156.6 (2 carbons, labeled, 95 %D), 156.0 (J_{CF} = 245 Hz), 140.0, 137.9, 133.1 (J_{CF} = 26 Hz, labeled, 6% D), 132.0, 129.1 (labeled, 85% D), 128.7, 127.6, 127.2 (J_{CF} = 21 Hz), 119.3 (labeled, 28% D), 111.5 (J_{CF} = 5 Hz, labeled, 8% D), 66.3, 65.5, 43.6, 41.3, 36.3, 32.0, 25.1, 20.3, 20.2, 13.6 ppm. **Deuterium incorporation**: 3.17 D/molecule (^{1}H NMR), 3.37 D/molecule (HRMS/IsoPat[2]), 0.00% unlabeled compound.

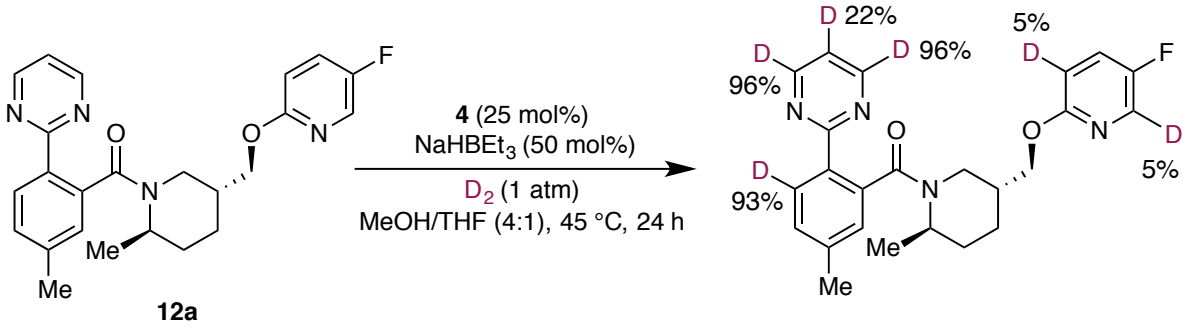

Scheme S29. H/D exchange in MK-6096 with Method B in MeOH/THF (4:1).

Method B, described in section VI.B, was followed using MK-6096, **12a** (59 mg, 0.14 mmol) as substrate with the following modifications: (a) **4** was first dissolved in 0.2 mL THF prior to $NaHBEt_3$ addition instead of dissolving it in 0.5 mL THF; (b) after stirring **4**/ $NaHBEt_3$ solution in THF at 23 °C for 2 minutes and adding MK-6096, 0.8 mL methanol were added instead of adding 0.5 mL THF. The product was purified by column chromatography using 100:10 DCM/MeOH as eluent to give 58 mg (99% chemical recovery yield) of deuterated MK-6096 as a white solid. In solution (DMSO-d_6) at room temperature MK-6096 exists as a mixture of 4 rotamers (58:26:8:5),[20] the

most dominant isomer is following reported. **^{1}H NMR (500 MHz, DMSO-d_6):** δ 8.86 (m, labeled, 0.08H), 8.18 (m, labeled, 0.95H), 8.09 (m, labeled, 0.07H), 7.65 (m, 1H), 7.40 (s, labeled, 0.78H), 7.22 (s, 1H), 6.79 (s, 1H), 6.56 (dd, *J* = 9 Hz, 4 Hz, labeled, 0.95), 4.73 (quintet, *J* = 6 Hz, 1H), 4.43 (m, 1H), 4.35 (t, *J* = 10 Hz, 1H), 4.03 (m, 1H), 3.28 (d, *J* = 13 Hz, 1H), 3.08 (dd, *J* = 14, 3 Hz, 1H), 1.98 (m, 2H), 1.88 (s, 3H), 1.54 (d, *J* = 12 Hz, 1H), 1.42 (d, *J* = 12 Hz, 1H), 1.24 (d, *J* = 7 Hz, 3H) ppm. **Quantitative ^{13}C{^{1}H} NMR (126 MHz, DMSO-d$_6$):** δ 170.9, 163.4, 159.6, 157.1, 156.9, 156.6 (2 carbons, labeled, 96% D), 156.0 (J_{CF} = 245 Hz), 140.0, 137.9, 133.0 (J_{CF} = 26 Hz, labeled, 5% D), 132.0, 129.0 (labeled, 93% D), 128.7, 127.6, 127.2 (J_{CF} = 21 Hz), 119.3 (labeled, 22% D), 111.5 (J_{CF} = 5 Hz, labeled, 5% D), 66.3, 65.5, 43.6, 41.3, 36.3, 32.0, 25.1, 20.3, 20.2, 13.6 ppm. **Deuterium incorporation**: 3.17 D/molecule (^{1}H NMR), 3.44 D/molecule (HRMS/IsoPat[2]), 0.00% unlabeled compound.

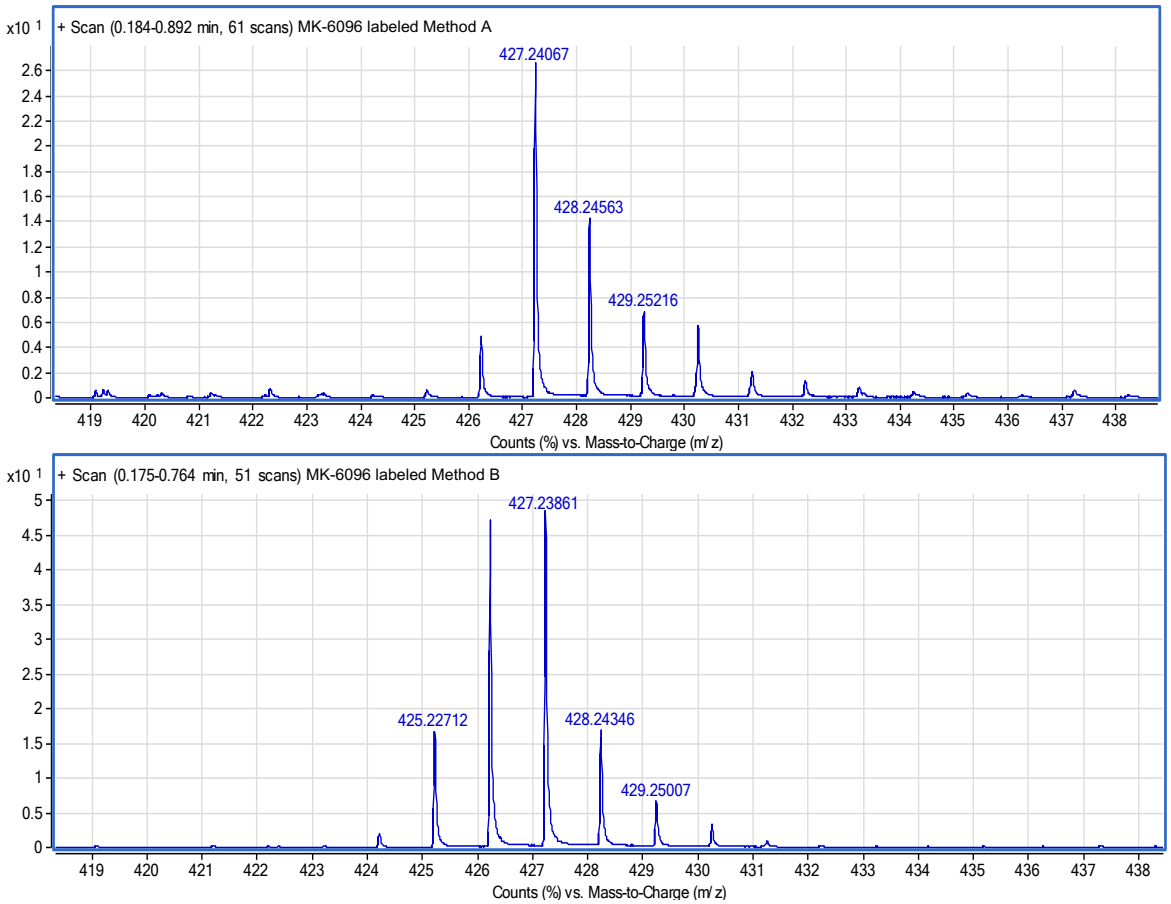

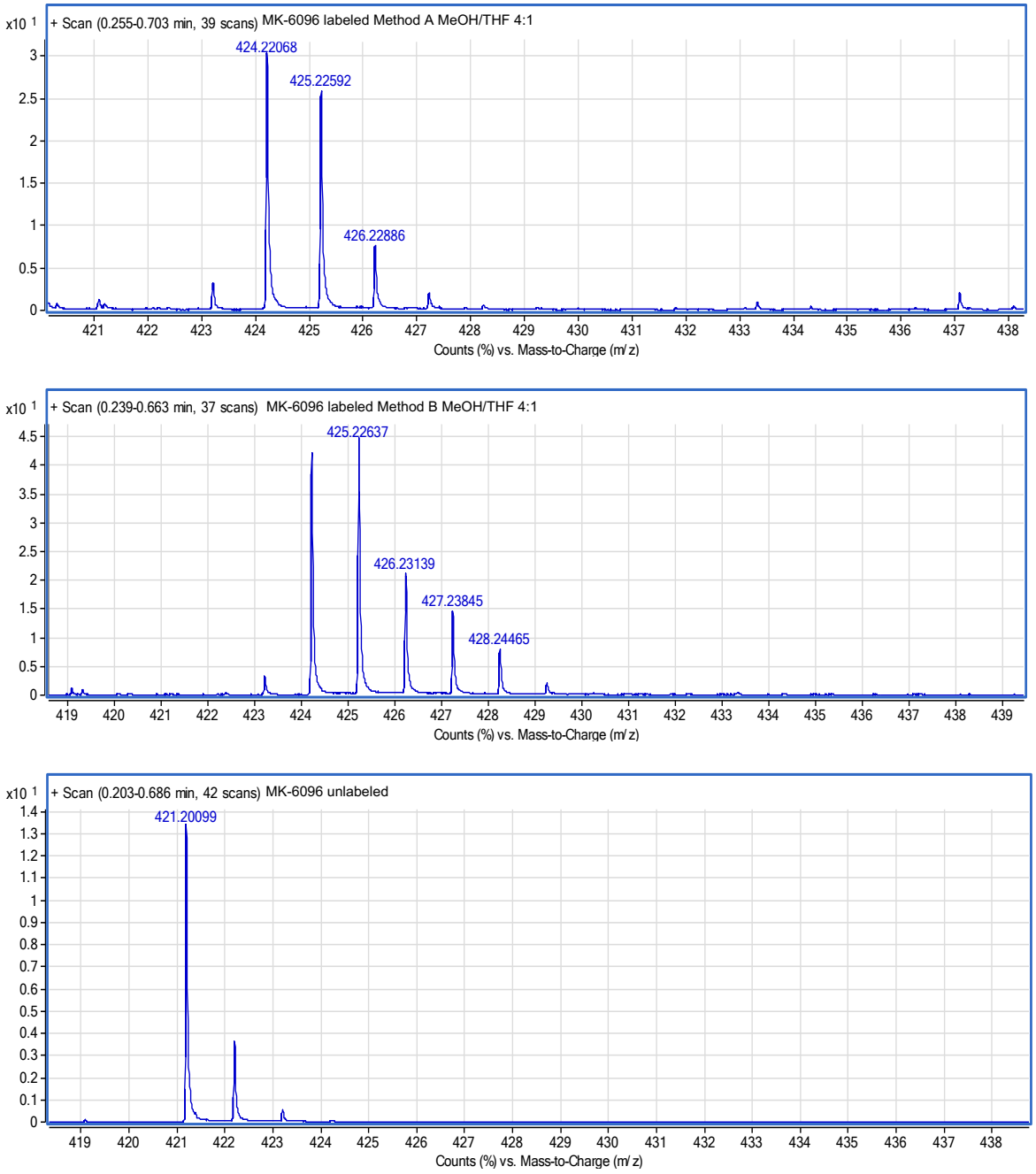

Figure S10. Stacked mass spectra of MK-6096: D-labeled with Method A, **[^{2}H]12a** (first); D-labeled with Method B, **[^{2}H]12aa** (second); D-labeled with Method A in MeOH/THF 4:1 (third); D-labeled with Method B in MeOH/THF 4:1 (fourth); and unlabeled, **12a** (fifth).

H/D exchange in MK-5395 with Method A

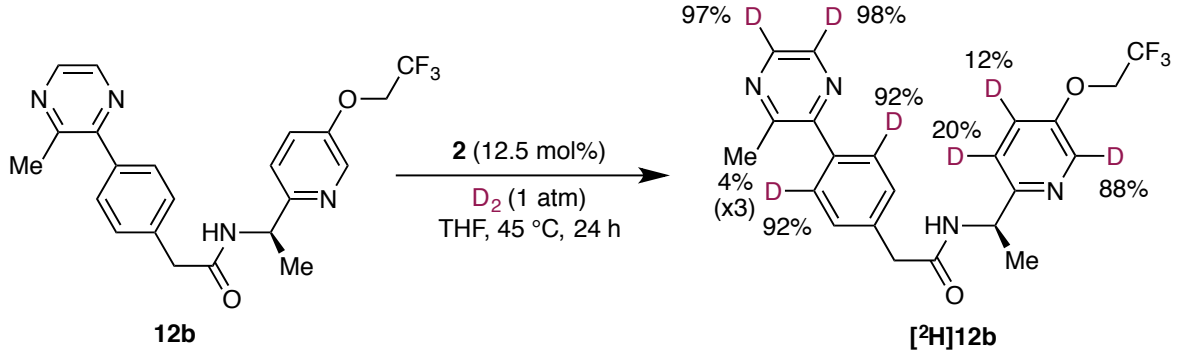

12b **[^{2}H]12b**

Scheme S30. H/D exchange in MK-5395 with Method A.

Reaction was carried out following Method A, described in section VI.A, using MK-5395, **12b** (60 mg, 0.14 mmol) as substrate. The product was purified by column chromatography using 100:10 DCM/MeOH as eluent to give 50 mg (83% chemical recovery yield) **[^{2}H]12b** as a white solid. **^{1}H NMR (500 MHz, DMSO-*d*$_6$):** δ 8.61 (d, *J* = 8 Hz, 1H), 8.54 (s, labeled, 0.03H), 8.50 (s, labeled, 0.02H), 8.34 (m, labeled, 0.12H), 7.57 (d, *J* = 8 Hz, labeled, 0.16H), 7.48 (d, *J* = 9 Hz, labeled, 0.80H), 7.40 (t, *J* = 4 Hz, 2H), 7.31 (m, *J* = 8 Hz, labeled, 0.88H), 4.96 (p, *J* = 7 Hz, 1H), 4.85 (q, *J* = 9 Hz, 2H), 3.57 (s, 2H), 2.56 (s, labeled, 2.89H), 1.38 (d, *J* = 7 Hz, 3H) ppm. **Quantitative ^{13}C{^{1}H} NMR (126 MHz, DMSO-d$_6$):** 169.2, 156.2, 156.2, 152.9, 152.9, 152.9, 152.2, 152.2, 152.1, 152.1, 151.2, 151.2, 142.0, 141.8, 141.6 (labeled, 98% D), 141.5, 141.3, 141.1 (labeled, 97% D), 137.1, 136.9, 136.8 (labeled, 88% D), 136.5, 136.4, 136.3, 128.9, 128.9, 128.8, 128.6, 128.4 (2 carbons, labeled, 92% D), 122.8, 122.6, 122.6, 122.6 (labeled, 20%), 121.0, 120.9, 120.6 (labeled 12% D), 64.9 (q, *J* = 34 Hz), 49.1, 42.0, 23.0, 22.9, 22.8, 22.6 (3 carbons, labeled, 9% D), 21.2 ppm. **Deuterium incorporation**: 5.11 D/molecule (^{1}H NMR), 5.00 D/molecule (HRMS/IsoPat[2]), 0.00% unlabeled compound.

H/D exchange in MK-5395 with Method B

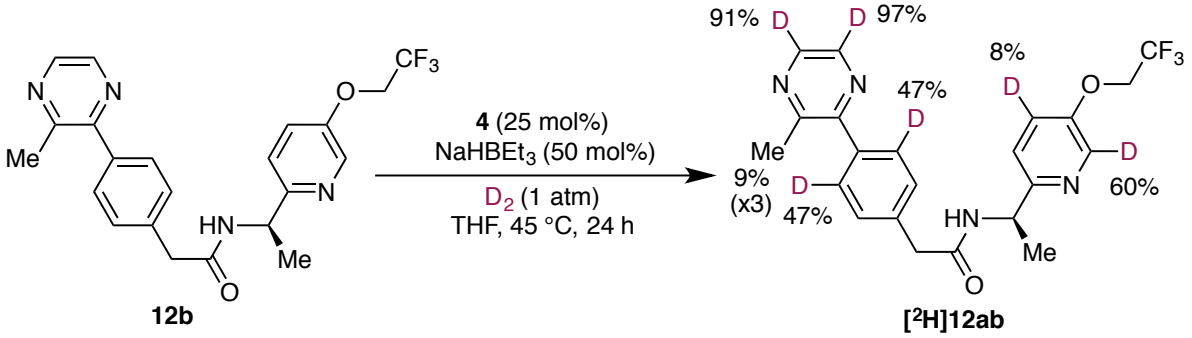

Scheme S31. H/D exchange in MK-5395 with Method B.

Reaction was carried out following Method B, described in section VI.B, using MK-5395, **12b** (60 mg, 0.14 mmol) as substrate. The product was purified by column chromatography using 100:10 DCM/MeOH as eluent to give 57 mg (95% chemical recovery yield) **[^{2}H]12ab** as a white solid. **^{1}H NMR (500 MHz, DMSO-d_6):** δ 8.60 (d, *J* = 8 Hz, 1H), 8.54 (s, labeled, 0.09H), 8.50 (s, labeled, 0.03H), 8.34 (d, *J* = 3 Hz, labeled, 0.40H), 7.57 (d, *J* = 8 Hz, labeled, 1.06H), 7.48 (d, *J* = 9 Hz, 1H), 7.39 (t, *J* = 4 Hz, 2H), 7.31 (d, *J* = 8 Hz, labeled, 0.92H), 4.96 (p, *J* = 7 Hz, 1H), 4.85 (q, *J* = 9 Hz, 2H), 3.57 (s, 2H), 2.56 (s, labeled, 2.73H), 1.38 (d, *J* = 7 Hz, 3H) ppm. **Quantitative ^{13}C{^{1}H} NMR (126 MHz, DMSO-d_6):** 169.2, 156.2, 156.2, 152.9, 152.9, 152.9, 152.9, 152.2, 152.2, 152.1, 152.1, 151.2, 151.2, 142.0, 141.8, 141.6 (labeled, 97% D), 141.5, 141.3, 141.1 (labeled, 91% D), 137.1, 136.9, 136.8 (labeled, 60% D), 136.5, 136.4, 136.3, 128.9, 128.9, 128.8, 128.6, 128.4 (2 carbons, labeled, 47% D), 122.8, 122.6, 122.6, 121.0, 120.9, 120.6 (labeled 8% D), 64.9 (q, *J* = 34 Hz), 49.1, 42.0, 23.0, 23.0, 22.8, 22.6 (3 carbons, labeled, 9% D), 21.2 ppm. **Deuterium incorporation**: 3.77 D/molecule (^{1}H NMR), 3.49 D/molecule (HRMS/IsoPat[2]), 0.00% unlabeled compound.

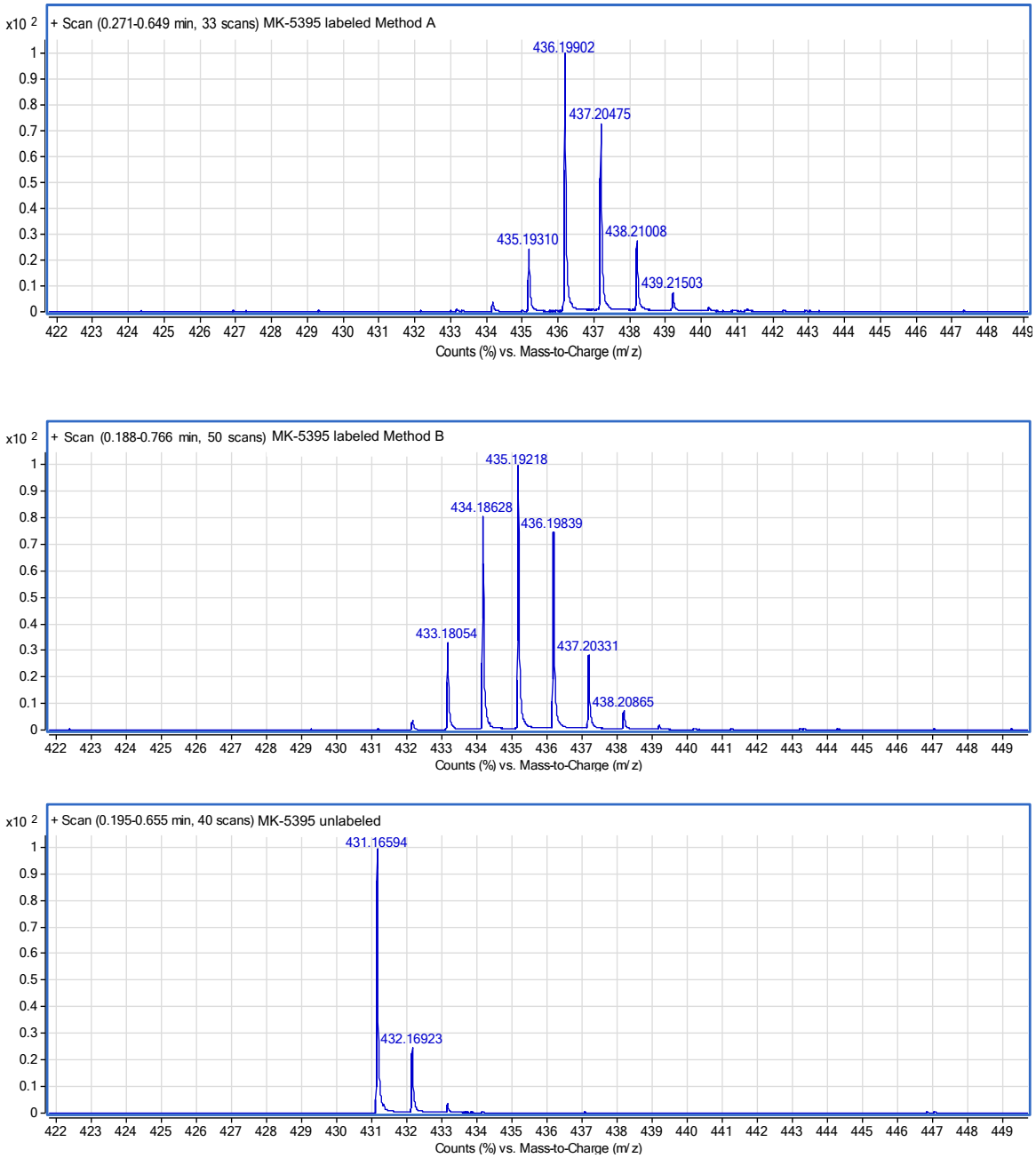

Figure S11. Stacked mass spectra of MK-5395: D-labeled with Method A, **[^{2}H]12b** (first); D-labeled with Method B, **[^{2}H]12ab** (second); and unlabeled, **12b** (third).

H/D exchange in varenicline with Method A

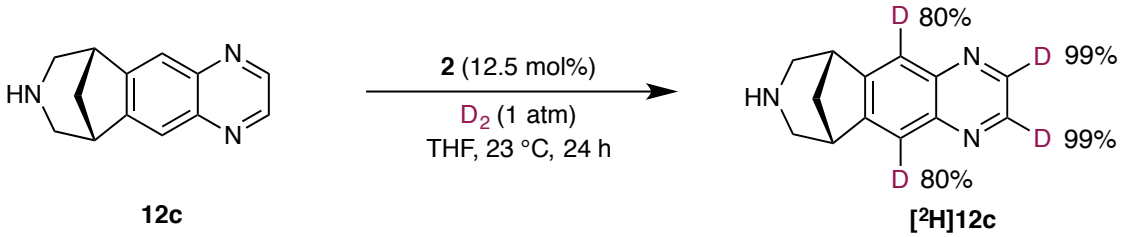

Scheme S32. H/D exchange in varenicline with Method A.

Reaction was carried out following Method A, described in section VI.A, using varenicline, **12c** (30 mg, 0.14 mmol) as substrate and at 23 °C. The product was purified by column chromatography using 100:10:1 DCM/MeOH/NH_4OH as eluent to give 27 mg (90% chemical recovery yield) **[^{2}H]12c** as a yellow solid. **^{1}H NMR (500 MHz, $CDCl_3$):** δ 8.76 (s, labeled, 0.02H), 7.84 (s, labeled, 0.41H), 3.27 (t, *J* = 4 Hz, 2H), 3.17 (d, *J* = 13 Hz, 2H), 2.94 (dt, *J* = 13, 3 Hz, 2H), 2.50 (ddt, *J* = 11, 5, 3 Hz, 1H), 2.10 (d, *J* = 11 Hz, 1H) ppm. **Quantitative ^{13}C NMR (126 MHz, $CDCl_3$):** δ 149.7, 149.6, 143.7, 143.6, 143.6, 143.5, 143.5, 143.3 (2 carbons, labeled, 80% D), 122.1, 122.1, 122.0, 121.8, 121.6 (2 carbons labeled, 99% D), 50.6, 43.3, 42.4, 42.4 ppm. **Deuterium incorporation**: 3.58 D/molecule (^{1}H NMR), 3.52 D/molecule (HRMS/IsoPat[2]), 0.00% unlabeled compound.

H/D exchange in varenicline with Method B

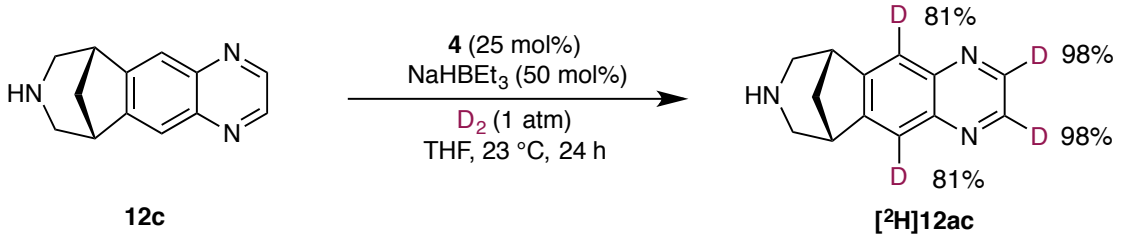

Scheme S33. H/D exchange in varenicline with Method B.

Reaction was carried out following Method B, described in section VI.B, using varenicline, **12c** (30 mg, 0.14 mmol) as substrate and at 23 °C. The product was purified by column chromatography using 100:10:1 DCM/MeOH/NH_4OH as eluent to give 28 mg (93% chemical recovery yield) **[^{2}H]12ac** as a yellow solid. **^{1}H NMR (500 MHz, $CDCl_3$):** 8.74 (s, labeled, 0.04H),

7.84 (s, labeled, 0.39H), 3.28 (t, *J* = 4 Hz, 2H), 3.17 (d, *J* = 13 Hz, 2H), 2.95 (dt, *J* = 13, 3 Hz, 2H), 2.48 (ddt, *J* = 11, 5, 3 Hz, 1H), 2.09 (d, *J* = 11 Hz, 1H) ppm. **Quantitative ^{13}C NMR (126 MHz, $CDCl_3$):** δ 149.3, 149.2, 143.7, 143.6, 143.6, 143.5, 143.3 (2 carbons, labeled, 81% D), 122.3, 122.2, 122.1, 121.9, 121.7 (2 carbons, labeled, 98% D), 50.3, 43.1, 42.1, 42.1 ppm. **Deuterium incorporation**: 3.58 D/molecule (^{1}H NMR), 3.56 D/molecule (HRMS/IsoPat[2]), 0.00% unlabeled compound.

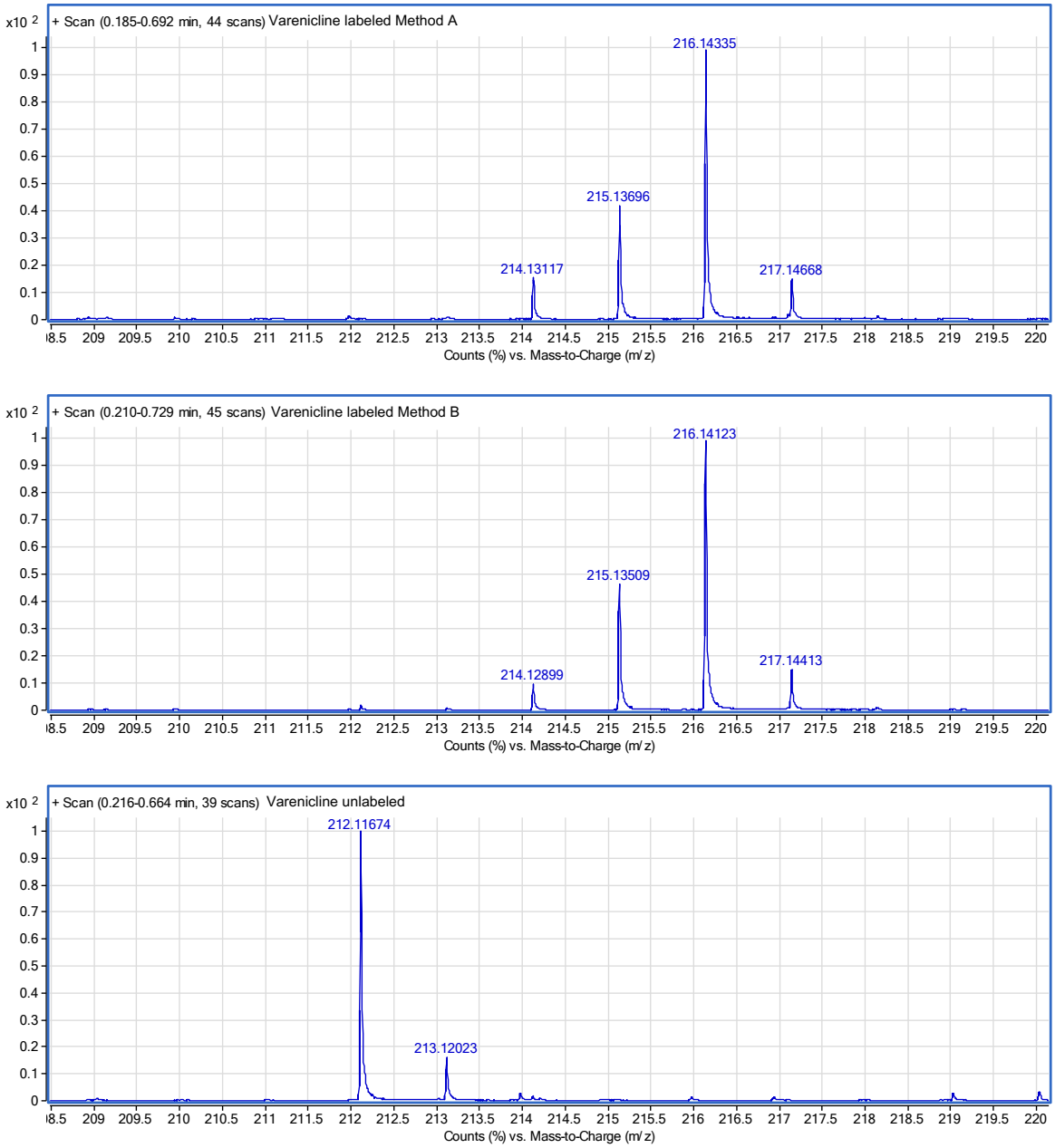

Figure S12. Stacked mass spectra of varenicline: D-labeled with Method A, **[^{2}H]12c** (first); D-labeled with Method B, **[^{2}H]12ac** (second); and unlabeled, **12c** (third).

H/D exchange in buspirone with Method A

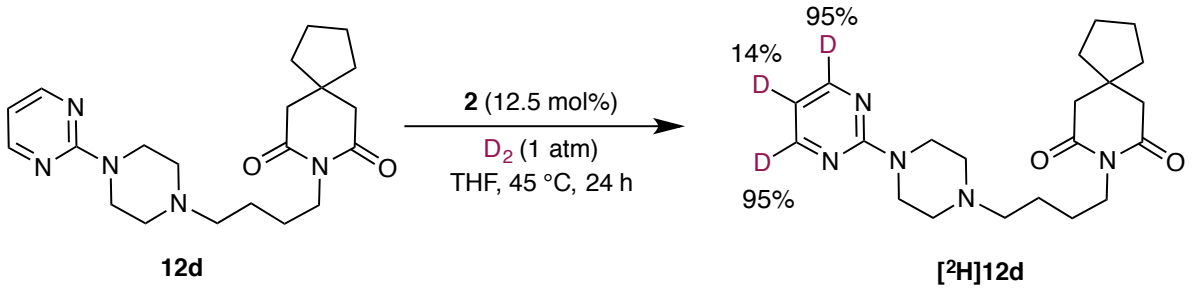

Scheme S34. H/D exchange in buspirone with Method A.

Reaction was carried out following Method A, described in section VI.A, using buspirone, **12d** (54 mg, 0.14 mmol) as substrate. The product was purified by column chromatography using 50:1 DCM/MeOH as eluent to give 53 mg (98% chemical recovery yield) **[^{2}H]12d** as a white solid. **^{1}H NMR (500 MHz, $CDCl_3$):** δ 8.26 (d, *J* = 5 Hz, labeled, 0.10H), 6.44 (br s, labeled, 0.86H), 3.78 (m, 6H), 2.55 (s, 4H), 2.51 (t, *J* = 5 Hz, 4H), 2.41 (m, 2H), 1.66 (m, 4H), 1.51 (p, *J* = 4 Hz, 4H), 1.45 (td, *J* = 7, 6, 3 Hz, 4H) ppm. **Quantitative ^{13}C{^{1}H} NMR (126 MHz, $CDCl_3$):** δ 172.3, 161.6, 157.8, 157.7, 157.4, 157.2 (2 carbons, labeled, 95% D), 109.8, 109.7 (labeled, 14% D), 58.2, 52.9, 45.0, 43.4, 39.5, 39.3, 37.6, 26.0, 24.2, 23.9 ppm. **Deuterium incorporation**: 2.04 D/molecule (^{1}H NMR), 2.03 D/molecule (HRMS/IsoPat[2]), 0.00% unlabeled compound.

H/D exchange in buspirone with Method B

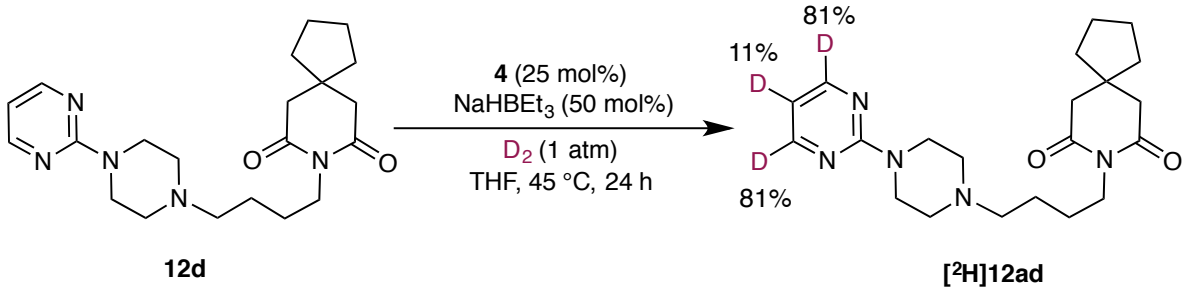

Scheme S35. H/D exchange in buspirone with Method B.

Reaction was carried out following Method B, described in section VI.B, using buspirone, **12d** (54 mg, 0.14 mmol) as substrate. The product was purified by column chromatography using 50:1 DCM/MeOH as eluent to give 53 mg (98% chemical recovery yield) **[^{2}H]12ad** as a white solid. **^{1}H**

NMR (500 MHz, $CDCl_3$): δ 8.25 (d, *J* = 5 Hz, labeled, 0.39H), 6.43 (m, labeled, 0.89H), 3.78 (m, 6H), 2.54 (s, 4H), 2.45 (t, *J* = 5 Hz, 4H), 2.35 (m, 2H), 1.66 (m, 4H), 1.50 (p, *J* = 4 Hz, 4H), 1.45 (m, 4H) ppm. **Quantitative ^{13}C NMR (126 MHz, $CDCl_3$):** δ 172.3, 161.7, 157.8, 157.7, 157.6, 157.4, 157.2 (2 carbons, labeled, 81% D), 109.8, 109.7, 109.6 (labeled, 11% D), 58.3, 53.1, 45.0, 43.6, 39.5, 39.4, 37.6, 26.1, 24.2, 24.2 ppm. **Deuterium incorporation**: 1.73 D/molecule (^1H NMR), 1.73 D/molecule (HRMS/IsoPat[2]), 0.00% unlabeled compound.

H/D exchange in buspirone with $[(^{iPr}DI)Ni(\mu_2\text{-}H)]_2$

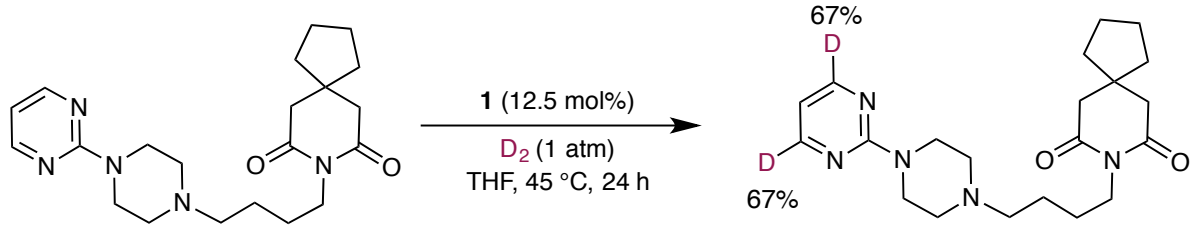

12d

Scheme S36. H/D exchange in buspirone with $[(^{iPr}DI)Ni(\mu_2\text{-}H)]_2$.

Reaction was carried out following Method A, described in section VI.A, using buspirone, **12d** (54 mg, 0.14 mmol) as substrate and **1** (17 mg, 18 μmol) instead of **2**. The product was purified by column chromatography using 50:10 DCM/MeOH as eluent to give 53 mg (98% chemical recovery yield) deuterated buspirone as a white solid. **^1H NMR (500 MHz, $CDCl_3$):** δ 8.28 (dd, *J* = 5, 1.1 Hz, labeled, 0.67H), 6.46 (m, 1H), 3.80 (m, 6H), 2.57 (s, 4H), 2.49 (t, *J* = 5 Hz, 4H), 2.40 (m, 2H), 1.69 (m, 4H), 1.53 (p, *J* = 4 Hz, 4H), 1.48 (m, 4H) ppm. **Quantitative ^{13}C NMR (126 MHz, $CDCl_3$):** δ 172.3, 161.7, 157.8, 157.8, 157.7, 157.5, 157.3 (2 carbons, labeled, 67% D), 109.9, 109.8, 109.7, 58.4, 53.1, 45.0, 43.6, 39.6, 39.4, 37.7, 26.1, 24.3, 24.2 ppm. **Deuterium incorporation**: 1.34 D/molecule (^1H NMR), 1.40 D/molecule (HRMS/IsoPat[2]), 12.17% unlabeled compound.

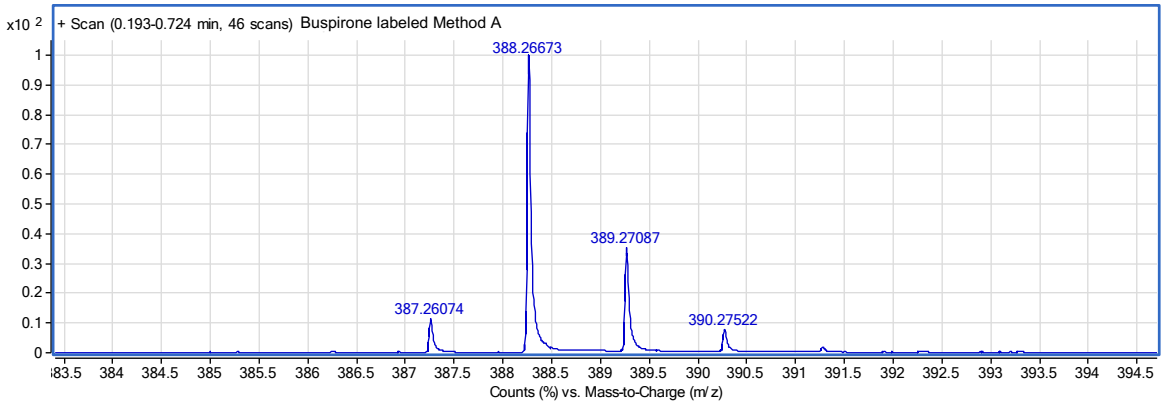
x10 2
+ Scan (0.193-0.724 min, 46 scans) Buspirone labeled Method A
388.26673
389.27087
387.26074
390.27522
Counts (%) vs. Mass-to-Charge (m/z)

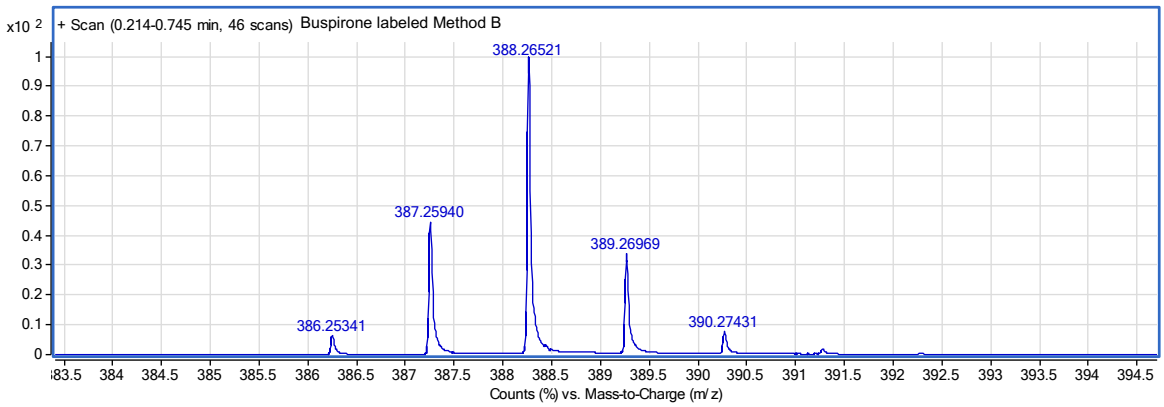
x10 2
+ Scan (0.214-0.745 min, 46 scans) Buspirone labeled Method B
388.26521
387.25940
389.26969
386.25341
390.27431
Counts (%) vs. Mass-to-Charge (m/z)

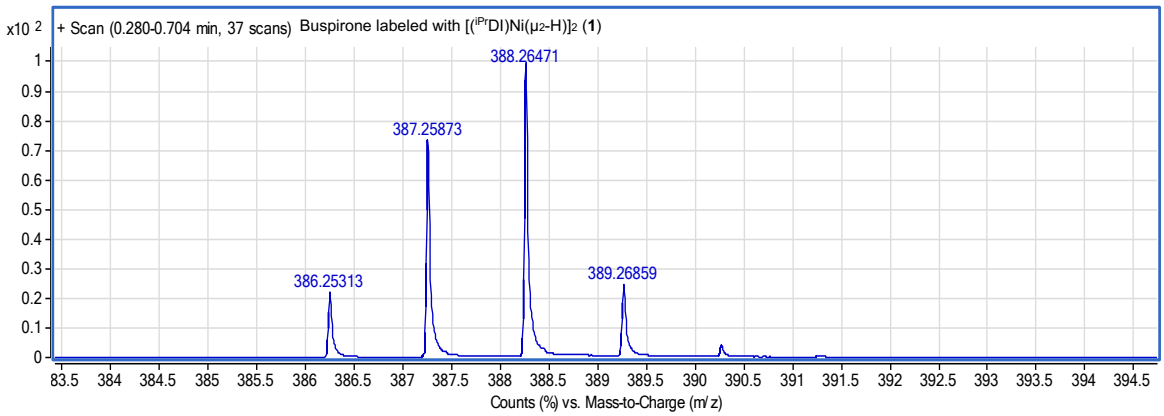
x10 2
+ Scan (0.280-0.704 min, 37 scans) Buspirone labeled with [(iPrDI)Ni(μ2-H)]2 (1)
388.26471
387.25873
386.25313
389.26859
Counts (%) vs. Mass-to-Charge (m/z)

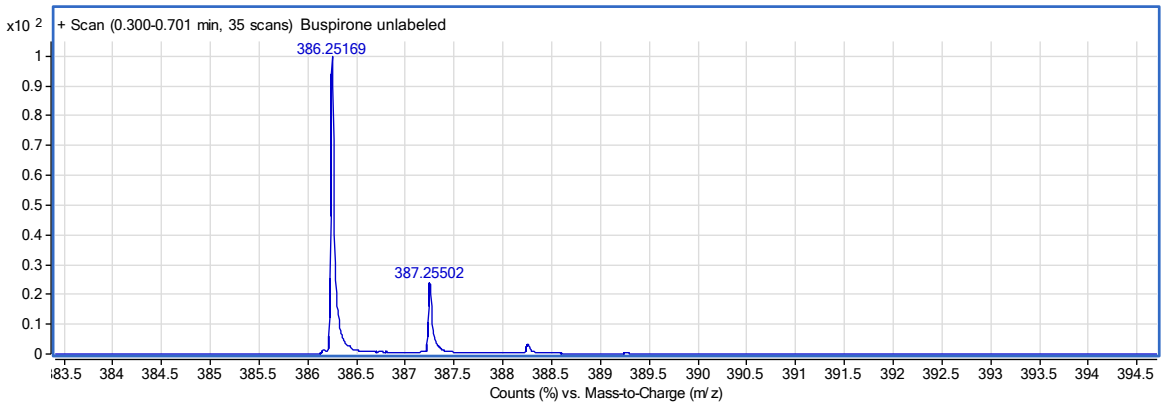
x10 2
+ Scan (0.300-0.701 min, 35 scans) Buspirone unlabeled
386.25169
387.25502
Counts (%) vs. Mass-to-Charge (m/z)

Figure S13. Stacked mass spectra of buspirone: D-labeled with Method A, **[^{2}H]12d** (first); D-labeled with Method B, **[^{2}H]12ad** (second); D-labeled with [(^{iPr}DI)Ni(μ_2-H)]$_2$ (**1**)*;* and unlabeled, **12d** (fourth).

H/D exchange in etoricoxib with Method A

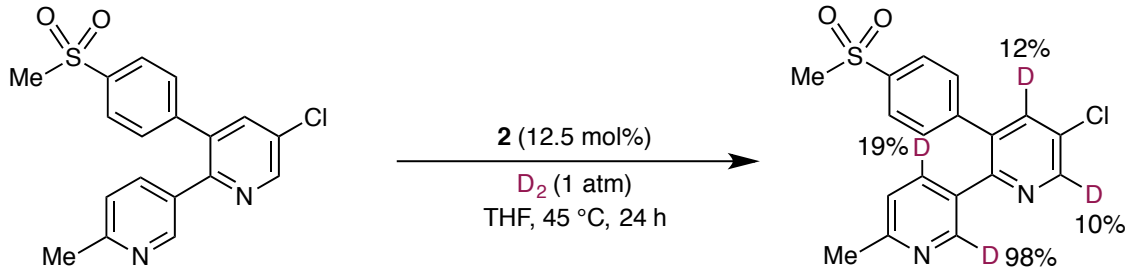

12e **[^{2}H]12e**

Scheme S37. H/D exchange in etoricoxib with Method A.

Reaction was carried out following Method A, described in section VI.A, using etoricoxib, **12e** (50 mg, 0.14 mmol) as substrate. The product was purified by column chromatography using 100:10 DCM/MeOH as eluent to give 41 mg (82% chemical recovery yield) **[^{2}H]12e** as a white solid. **^{1}H NMR (500 MHz, CD_3CN):** δ 8.70 (s, labeled, 0.88H), 8.32 (s, labeled, 0.02H), 7.87 (m, labeled, 2.90H), 7.48 (dd, *J* = 22, 8 Hz, labeled, 2.81H), 7.09 (d, *J* = 8 Hz, 1H), 3.07 (s, 3H), 2.45 (s, 3H) ppm. **Quantitative ^{13}C NMR (126 MHz, CD_3CN):** δ 159.2, 153.7, 150.5, 150.3, 150.1 (labeled, 98% D), 148.8 (labeled, 12% D), 144.6, 141.3, 138.9 (labeled, 10% D), 138.3 (labeled, 19%D), 136.6, 132.4, 131.6, 131.5, 128.4, 123.2, 44.4, 24.3 ppm. **Deuterium incorporation**: 1.39 D/molecule (^{1}H NMR), 1.30 D/molecule (HRMS/IsoPat[2]), 1.07% unlabeled compound.

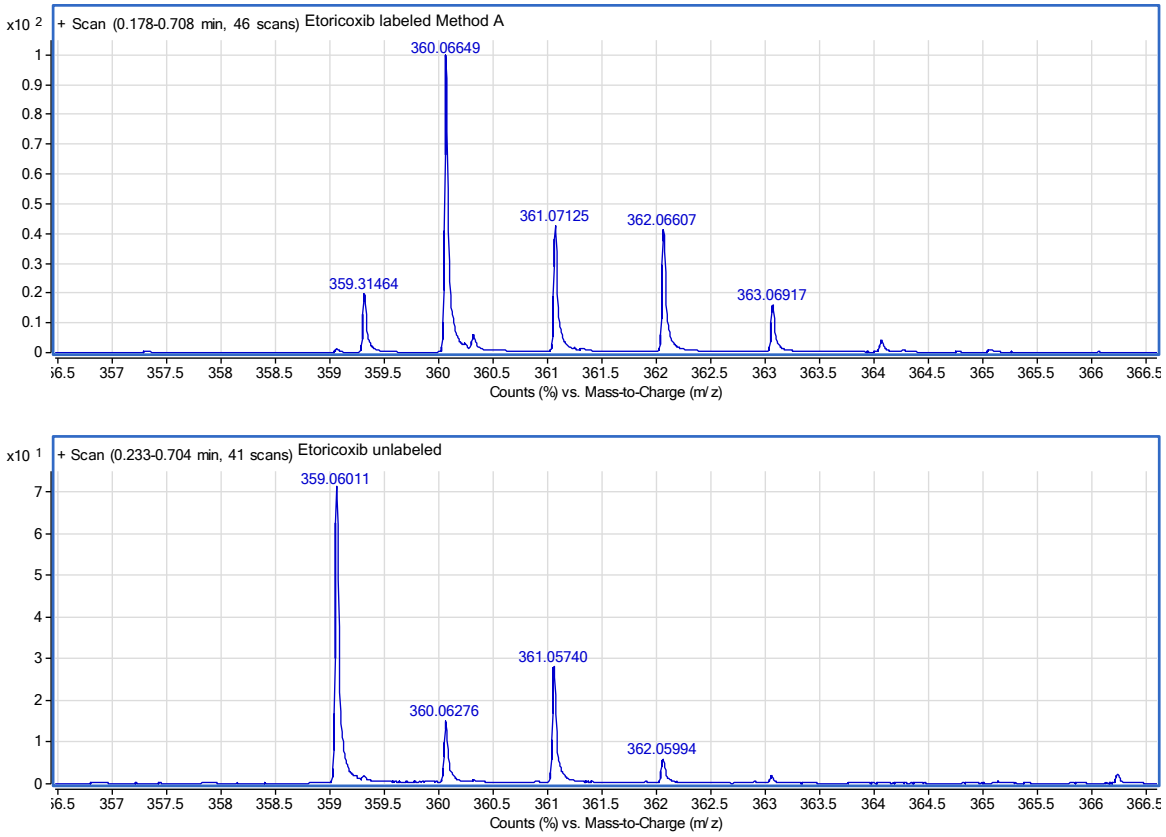

Figure S14. Stacked mass spectra of etoricoxib: D-labeled with Method A, **[^{2}H]12e** (first) and unlabeled, **12e** (second).

H/D exchange in papaverine with Method A

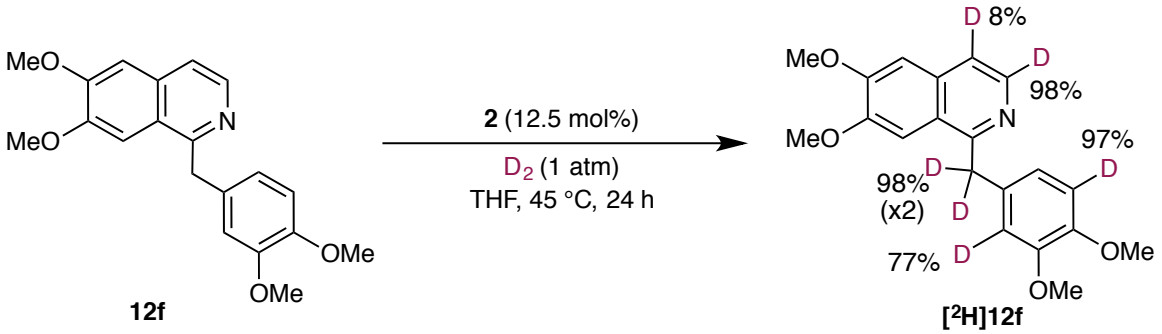

Scheme S38. H/D exchange in papaverine with Method A.

Reaction was carried out following Method A, described in section VI.A, using papaverine, **12f** (48 mg, 0.14 mmol) as substrate. The product was purified by column chromatography using 100:10 DCM/MeOH as eluent to give 40 mg (85% chemical recovery yield) **[^{2}H]12f** as a white solid. **^{1}H NMR (500 MHz, DMSO-d_6):** δ 8.26 (d, *J* = 6 Hz, labeled, 0.02H), 7.52 (2 s, labeled,

1.92H), 7.30 (s, 1H), 7.02 (s, labeled, 0.23H), 6.80 (s, labeled, 1.03H), 4.48 (2 s, labeled, 0.05H), 3.89 (s, 3H), 3.88 (s, 3H), 3.67 (s, 3H), 3.66 (s, 3H) ppm. **Quantitative ^{13}C NMR (126 MHz, $CDCl_3$):** δ 157.9, 152.2, 149.6, 148.5, 148.5, 147.1, 147.1, 140.6, 140.5, 140.3, 140.1 (labeled, 98% D), 132.8, 132.8, 132.1, 132.0, 122.1, 120.6, 120.5, 120.3, 120.1 (labeled, 97% D), 118.5, 118.4, 118.3 (labeled, 8% D), 112.6, 112.5, 112.3, 112.2 (labeled, 77% D), 111.8, 111.8, 111.7, 105.6, 105.5, 104.3, 55.7, 55.6, 55.4, 55.4, 40.8 (2 carbons, labeled, 98%, overlapped with DMSO-d6 signal) ppm. **Deuterium incorporation**: 4.76 D/molecule (^{1}H NMR), 4.40 D/molecule (HRMS/IsoPat[2]), 0.00% unlabeled compound.

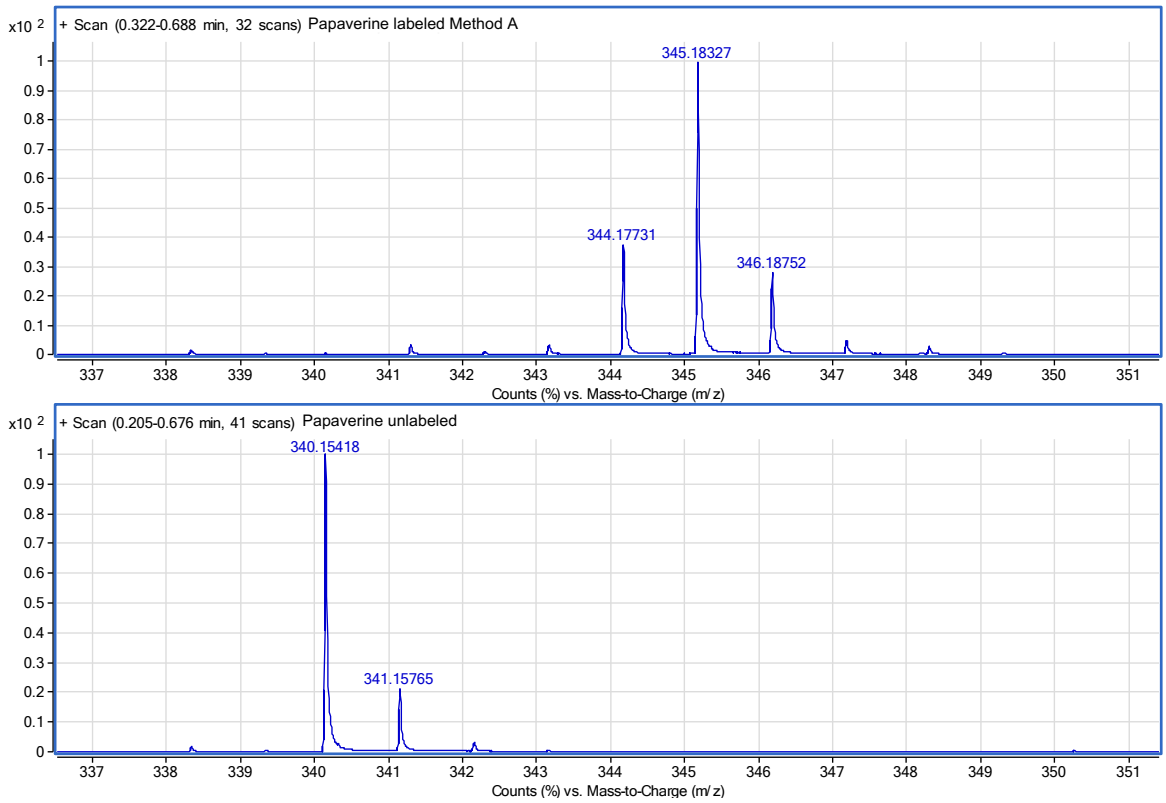

Figure S15. Stacked mass spectra of papaverine: D-labeled with Method A, **[^{2}H]12f** (first) and unlabeled, **12f** (second).

H/D exchange in flumazenil with Method A

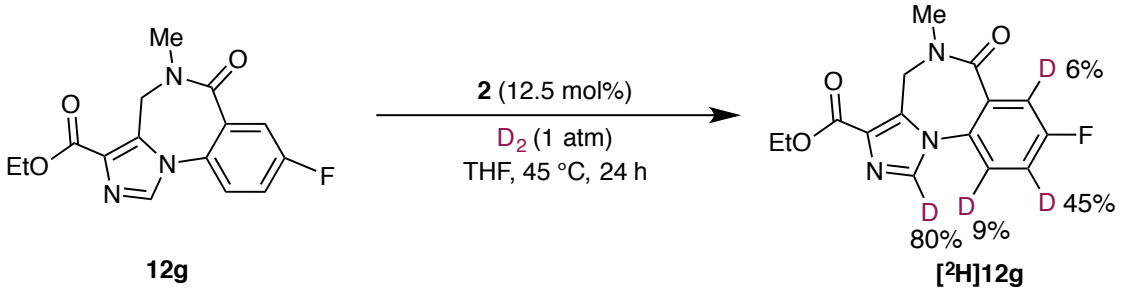

12g **[^{2}H]12g**

Scheme S39. H/D exchange in flumazenil with Method A.

Reaction was carried out following Method A, described in section VI.A, using flumazenil, **12g** (42 mg, 0.14 mmol) as substrate. The product mixture was diluted with DCM and purified by column chromatography using 100:10 DCM/MeOH as eluent to give 41 mg (98% chemical recovery yield) **[^{2}H]12g** as a white solid. **^{1}H NMR (500 MHz, $CDCl_3$):** δ 7.86 (s, labeled, 0.20H), 7.75 (dt, *J* = 9, 2 Hz, labeled, 0.94H), 7.43 (m, labeled, 0.91H), 7.33 (ddd, *J* = 9, 7, 3 Hz, labeled, 0.55H), 5.19 (br s, 1H), 4.41 (m, 3H), 3.22 (s, 3H), 1.42 (t, *J* = 7 Hz, 3H) ppm. **Quantitative ^{13}C NMR (126 MHz, CD_3CN):** δ 165.3, 165.3, 163.0, 161.8 (d, J_{CF} = 251 Hz), 135.4, 135.4, 135.0, 134.8, 134.5 (labeled, 80% D), 131.3 (d, J_{CF} = 8 Hz), 128.9, 128.9, 128.4 (d, J_{CF} = 3 Hz), 124.0 (d, J_{CF} = 8 Hz, labeled, 9% D), 120.1 (d, J_{CF} = 23 Hz, labeled, 45% D), 119.5 (2 d, J_{CF} = 25 Hz, labeled, 6% D), 61.1, 42.4, 36.0, 14.5 ppm. **Deuterium incorporation**: 1.40 D/molecule (^{1}H NMR), 1,38 D/molecule (HRMS/IsoPat[2]), 17.01% unlabeled compound.

H/D exchange in flumazenil with [(^{iPr}DI)Ni(μ$_2$-H)]$_2$

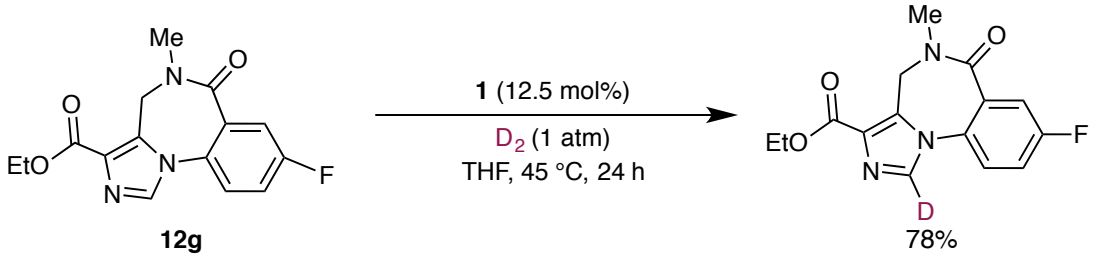

12g

Scheme S40. H/D exchange in flumazenil with **[(^{iPr}DI)Ni(μ$_2$-H)]$_2$**.

Reaction was carried out following Method A, described in section VI.A, using flumazenil, **12g** (42 mg, 0.14 mmol) as substrate and **1** (17 mg, 18 μmol) instead of **2**. The product was diluted with

DCM and purified by column chromatography using 100:10 DCM/MeOH as eluent to give 42 mg (100% chemical recovery yield) **[^{2}H]12g** as a white solid. **^{1}H NMR (500 MHz, $CDCl_3$):** δ 7.81 (s, labeled, 0.22H), 7.69 (dd, *J* = 9, 3 Hz, 1H), 7.39 (m, 1), 7.28 (ddd, *J* = 9, 7, 3 Hz, 1H), 5.14 (m, 1H), 4.36 (m, 3H), 3.17 (s, 3H), 1.37 (t, *J* = 7 Hz, 3H) ppm. **Quantitative ^{13}C NMR (126 MHz, CD_3CN):** δ 165.3, 165.2, 163.0, 161.8 (d, J_{CF} = 251 Hz), 135.4, 135.3, 135.0, 134.8, 134.5 (labeled, 78% D), 131.2 (d, J_{CF} = 8 Hz), 128.8, 128.8, 128.4 (d, J_{CF} = 3 Hz), 124.0 (2 d, J_{CF} = 8 Hz), 120.1 (d, J_{CF} = 23 Hz), 119.4 (d, J_{CF} = 25 Hz), 61.1, 42.4, 36.0, 14.4 ppm. **Deuterium incorporation**: 0.78 D/molecule (^{1}H NMR), 0.84 D/molecule (HRMS/IsoPat[2]), 21.57% unlabeled compound.

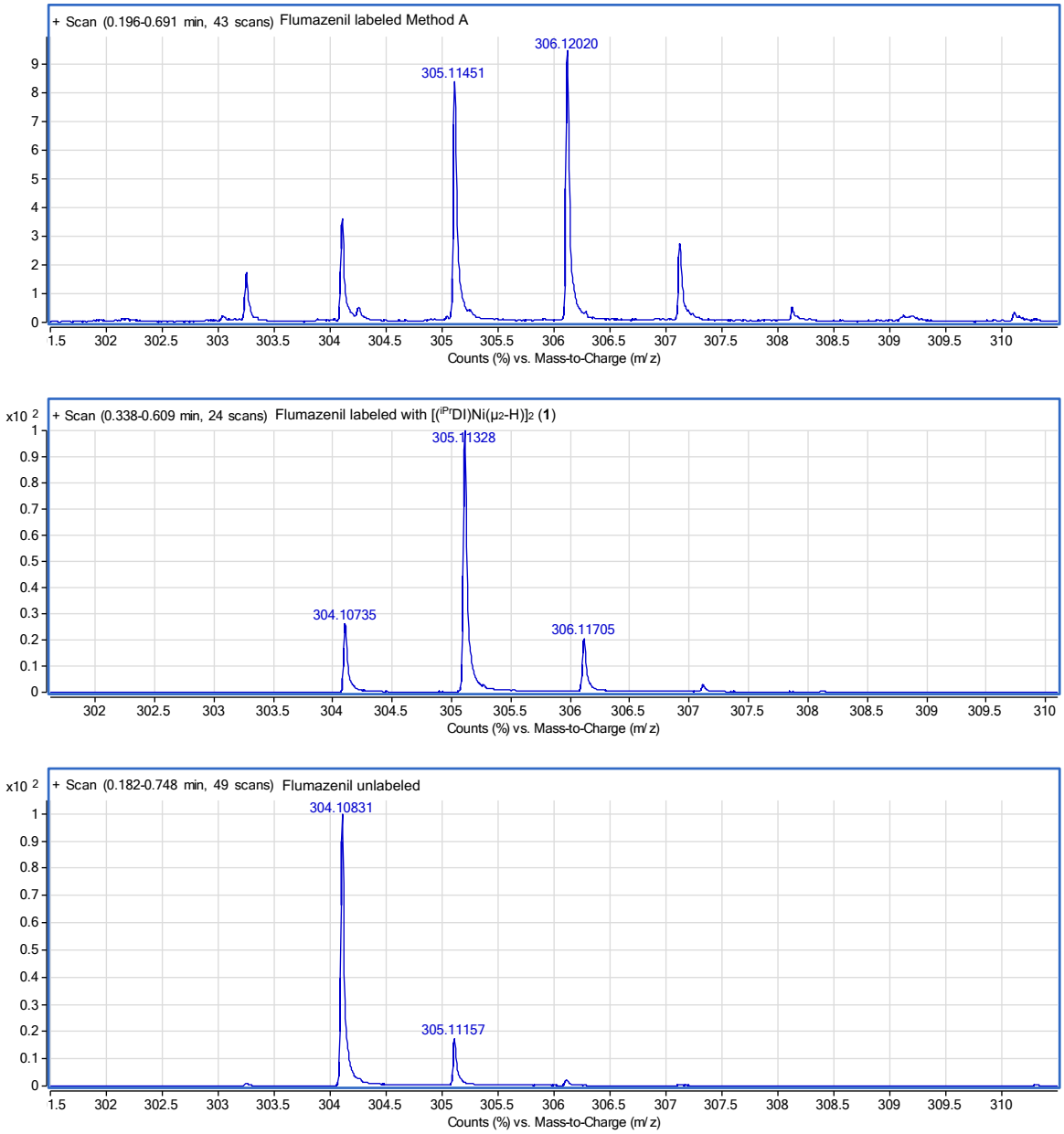

Figure S16. Stacked mass spectra of flumazenil: D-labeled with Method A, **[^{2}H]12g** (first); D-labeled with [(^{iPr}DI)Ni(μ_2-H)]$_2$ (**1**) (second); and unlabeled, **12g** (third).

H/D exchange in haloperidol with Method A

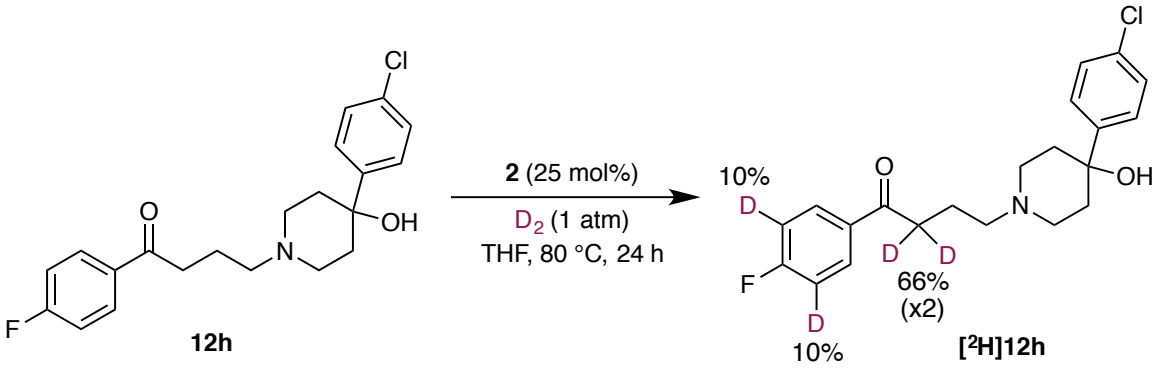

Scheme S41. H/D exchange in haloperidol with Method A.

Reaction was carried out following Method A, described in section VI.A, using haloperidol, **12h** (53 mg, 0.14 mmol) as substrate, **2** (29 mg, 35 μmol), in CPME (1 mL) solvent at 80 °C. The product was purified by column chromatography using 100:10:1 DCM/MeOH/NH_4OH as eluent to give 47 mg (89% chemical recovery yield) **[^{2}H]12h** as a white solid. **^{1}H NMR (500 MHz, $CDCl_3$):** δ 8.00 (m, 2H), 7.37 (m, labeled, 1.80H), 7.29 (m, 2H), 7.13 (m, 2H), 2.96 (m, labeled, 0.68H), 2.80 (d, *J* = 11 Hz, 2H), 2.48 (m, 4H), 2.00 (m, 4H), 1.68 (d, *J* = 14 Hz, 2H) ppm. **Quantitative ^{13}C NMR (126 MHz, $CDCl_3$):** δ 198.6, 198.5, 198.5, 166.8, 164.8, 147.0, 133.8, 133.7, 132.9, 130.9, 130.8, 128.5, 128.4, 126.2 (2 carbons, labeled, 10% D), 115.8, 115.7, 71.3, 71.1, 57.9, 57.9, 49.5, 49.4, 38.3, 38.3, 36.4, 36.3, 36.2, 36.0, 35.8, 35.7, 35.5 (labeled, 66% D), 21.8, 21.8 ppm. **Deuterium incorporation**: 1.52 D/molecule (^{1}H NMR), 1.48 D/molecule (HRMS/IsoPat[2]), 11.54% unlabeled compound.

H/D exchange in haloperidol with [(^{iPr}DI)Ni(μ$_2$-H)]$_2$

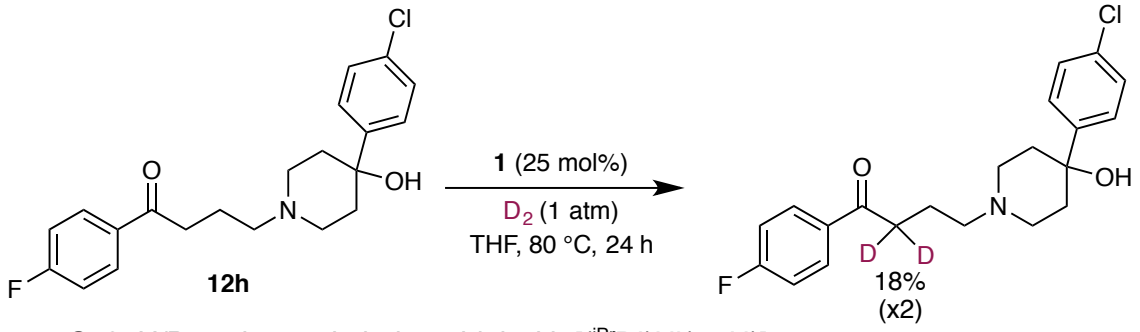

Scheme S42. H/D exchange in haloperidol with [(^{iPr}DI)Ni(μ$_2$-H)]$_2$.

Reaction was carried out following Method A, described in section VI.A, using haloperidol, **12h** (53 mg, 0.14 mmol) as substrate, **1** (32 mg, 35 μmol) instead of **2**, in CPME (1 mL) solvent at 80 °C. The product was purified by column chromatography using 100:10:1 DCM/MeOH/NH_4OH as eluent to give 47 mg (89% chemical recovery yield) **[^{2}H]12h** as a white solid. **^{1}H NMR (500 MHz, $CDCl_3$):** δ 8.00 (m, 2H), 7.37 (m, 2H), 7.27 (m, 2H), 7.12 (m, 2H), 2.98 (m, labeled, 1.65H), 2.83 (d, *J* = 11 Hz, 2H), 2.50 (m, 4H), 2.02 (m, 4H), 1.68 (d, *J* = 14 Hz, 2H) ppm. **Quantitative ^{13}C NMR (126 MHz, $CDCl_3$):** δ 198.4, 198.4, 166.8, 164.8, 146.8, 133.7, 133.6, 132.9, 130.8, 130.8, 128.5, 128.4, 126.2 (2 carbons, labeled, 10% D), 115.8, 115.7, 71.1, 71.0, 57.8, 57.8, 49.5, 49.4, 38.2, 38.1, 38.0, 36.3, 36.1, 36.0, 35.8 (labeled, 18% D), 21.6, 21.5 ppm. **Deuterium incorporation**: 0.36 D/molecule (^{1}H NMR), 0.42 D/molecule (HRMS/IsoPat[2]), 59.46% unlabeled compound.

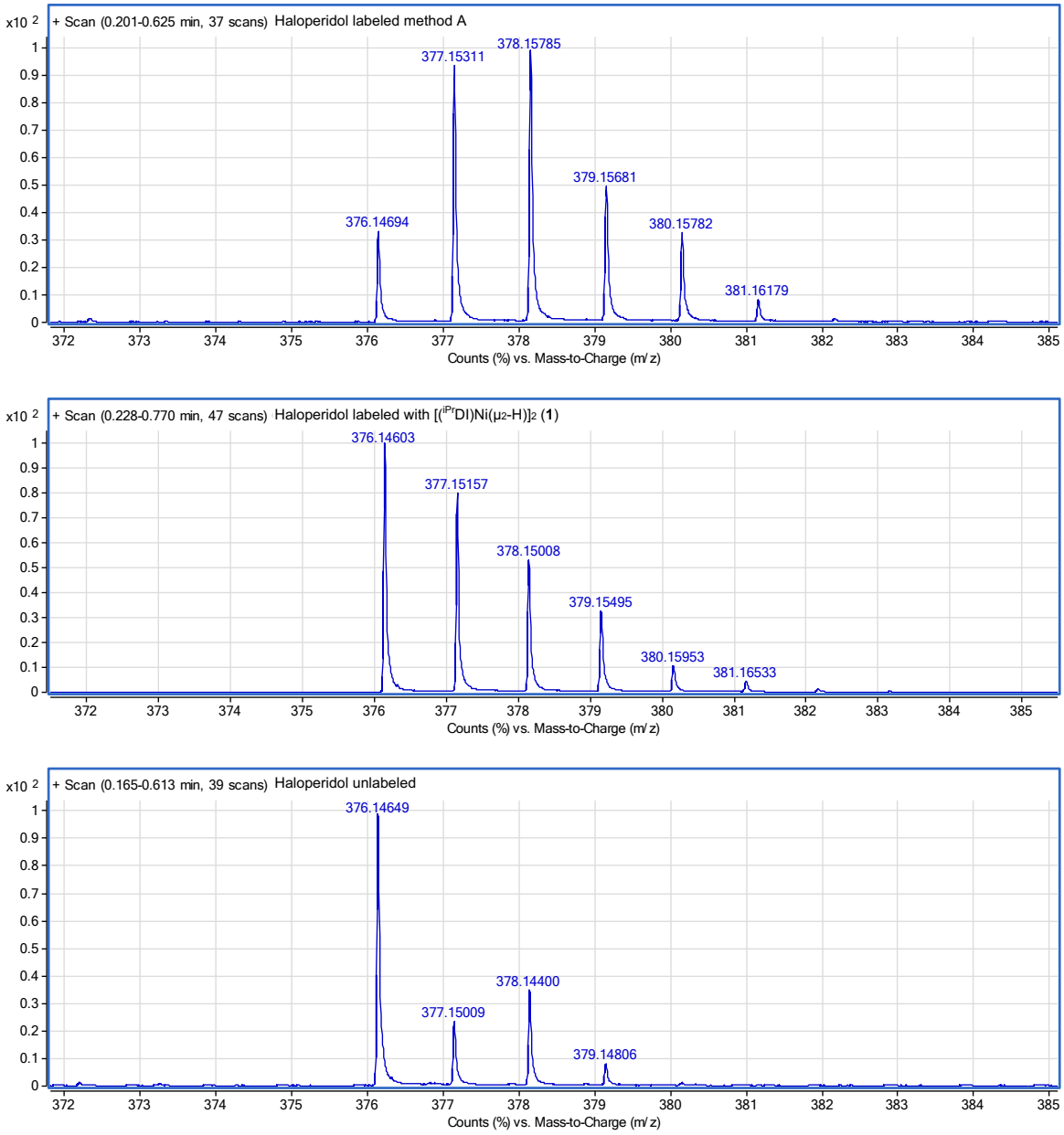

Figure S17. Stacked mass spectra of haloperidol: D-labeled with Method A, **[^{2}H]12h** (first); D-labeled with [(^{iPr}DI)Ni(μ_2-H)]$_2$ (**1**) (second); and unlabeled, **12h** (third).

H/D exchange in paroxetine with Method A

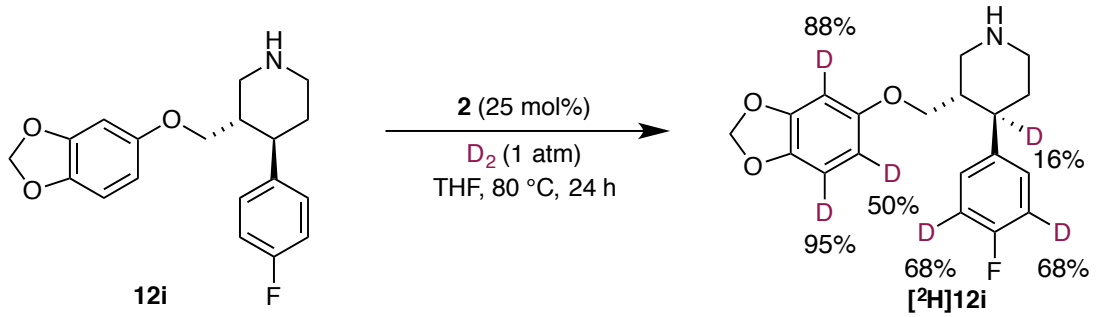

Scheme S43. H/D exchange in paroxetine with Method A.

Reaction was carried out following Method A, described in section VI.A, using paroxetine, **12i** (46 mg, 0.14 mmol) as substrate, **2** (29 mg, 35 μmol), in CPME (1 mL) solvent at 80 °C. The product was purified by column chromatography using 100:10:1 DCM/MeOH/NH_4OH as eluent to give 37 mg (81% chemical recovery yield) **[^{2}H]12i** as a pale yellow solid. **^{1}H NMR (500 MHz, DMSO-*d*$_6$):** δ 7.26 (m, 2H), 7.10 (t, *J* = 9 Hz, labeled, 0.65H), 6.71 (m, labeled, 0.05H), 6.41 (s, labeled, 0.12H), 6.13 (s, labeled, 0.50H), 5.91 (s, 2H), 3.45 (m, 2H), 3.21 (dd, *J* = 12, 4 Hz, 1H), 2.98 (m, 1H), 2.55 (m, 1H), 2.44 (m, labeled, 0.84H), 1.97 (m, 1H), 1.60 (m, 2H) ppm. **Quantitative ^{13}C NMR (126 MHz, DMSO-*d*$_6$):** δ 160.7 (three d, J_{CF} = 242 Hz), 154.1, 154.0, 154.0, 147.9, 147.8, 147.8, 147.78, 141.0, 141.0, 140.9, 129.0 (2 d, J_{CF} = 7.8 Hz), 115.11 (d, J_{CF} = 21 Hz), 115.0, 114.8, 114.6 (2 carbons, labeled, 68% D), 107.9, 107.8, 107.7, 107.6 (labeled, 95% D), 105.3, 105.2, 105.2, 105.0, 104.8 (labeled, 50% D), 100.9, 97.7, 97.4, 97.2 (labeled, 88% D), 69.4, 50.0, 48.6, 46.5, 44., 44.0, 42.2, 42.1, 42.0, 35.1, 35.0, 34.9 (labeled, 16% D) ppm. **^{19}F NMR (282 MHz, DMSO-*d*$_6$):** δ -116.9 (tt, *J* = 10, 5 Hz), -117.2 (dt, *J* = 10, 6 Hz), -117.48 (t, *J* = 6 Hz) ppm. **Deuterium incorporation**: 3.85 D/molecule (^{1}H NMR), 3.44 D/molecule (HRMS/IsoPat[2]), 0.00% unlabeled compound.

H/D exchange in paroxetine with [(^{iPr}DI)Ni(μ_2-H)]$_2$

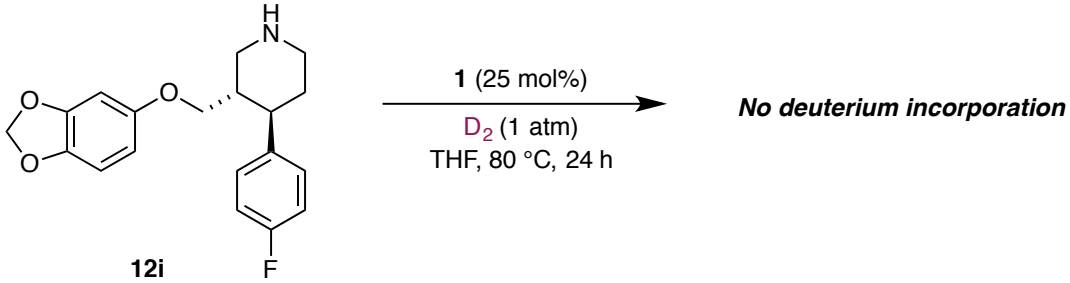

Scheme S44. H/D exchange in paroxetine with [(^{iPr}DI)Ni(μ_2-H)]$_2$.

Reaction was carried out following Method A, described in section VI.A, using paroxetine, **12i** (46 mg, 0.14 mmol) as substrate, **1** (32 mg, 35 µmol) instead of **2**, in CPME (1 mL) solvent at 80 °C. The vessel was then opened to air and the reaction mixture was diluted with methanol (10 mL) and analyzed by HRMS without further purification. **Deuterium incorporation**: 0.00 D/molecule (HRMS/IsoPat[2]), 100% unlabeled compound.

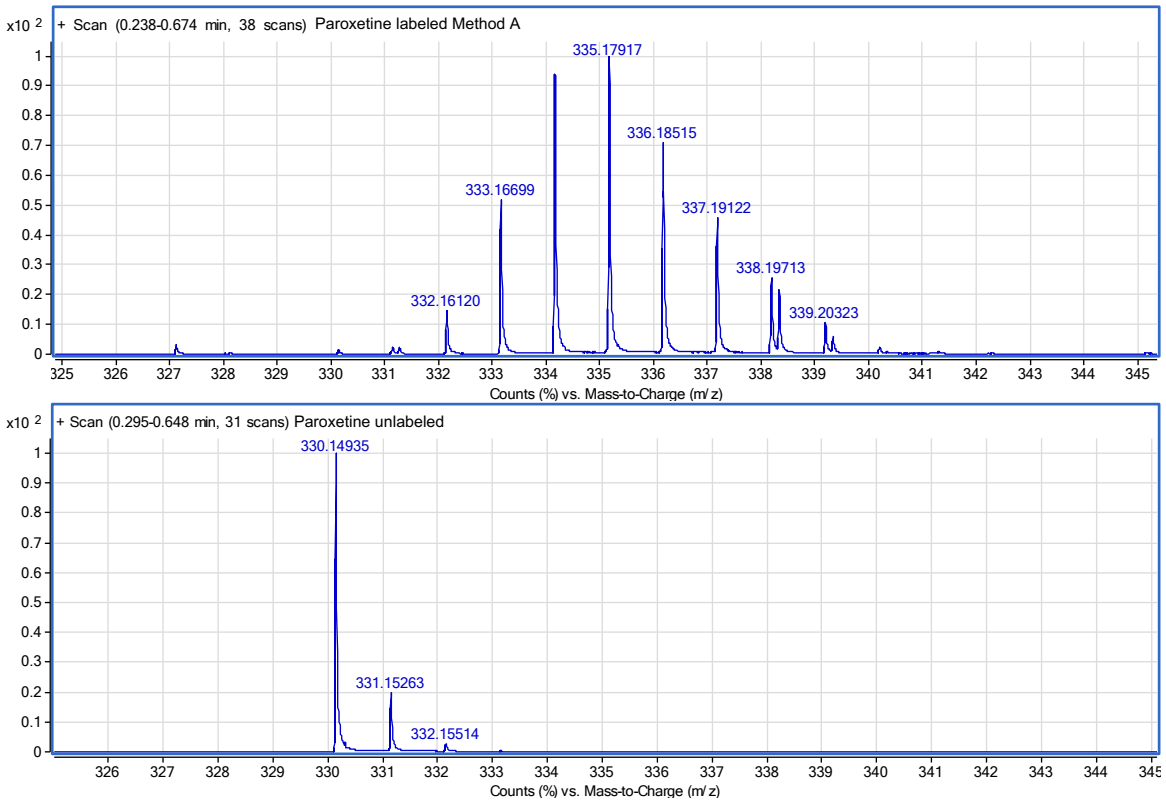

Figure S18. Stacked mass spectra of haloperidol: D-labeled with Method A, **[^{2}H]12i** (first) and unlabeled, **12i** (second).

X. Analysis of Tritium Labeled Pharmaceuticals

H/T Exchange in MK-6096

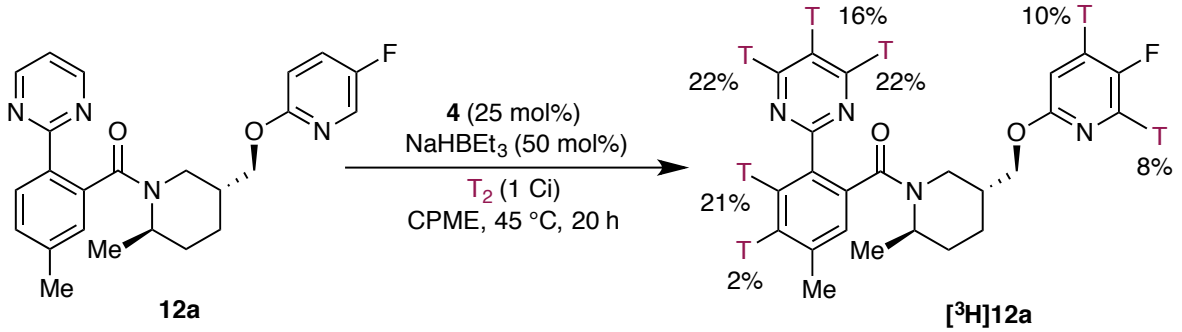

Scheme S45. H/T exchange in MK-6096.

Reaction was performed according to the general procedure for H/T exchange in pharmaceuticals, described in section VII. Following the three successive evaporation steps from ethanol, the crude product was dissolved in ethanol and a total radioactivity of 707.1 mCi at 85.3% radiochemical purity was measured. Ethanol was then removed under vacuum and the crude mixture was dissolved in DMSO (0.5 mL) and **[^{3}H]12a** was purified via semipreparative reverse phase HPLC (Column: 10 x 250 mm Gemini NX C18. Mobile phase: 50 mM TEAA/acetonitrile (50:50). Flow rate: 5 mL/min. Detection: 254 nm). Fractions containing the purified compound were collected and diluted with water, concentrated on a pair of C18 cartridges and eluted with ethanol (40 mL). **Specific Activity:** 99.2 Ci/mmol. **Radiochemical yield:** 562.1 mCi. **Radiochemical purity:** 99.9%.

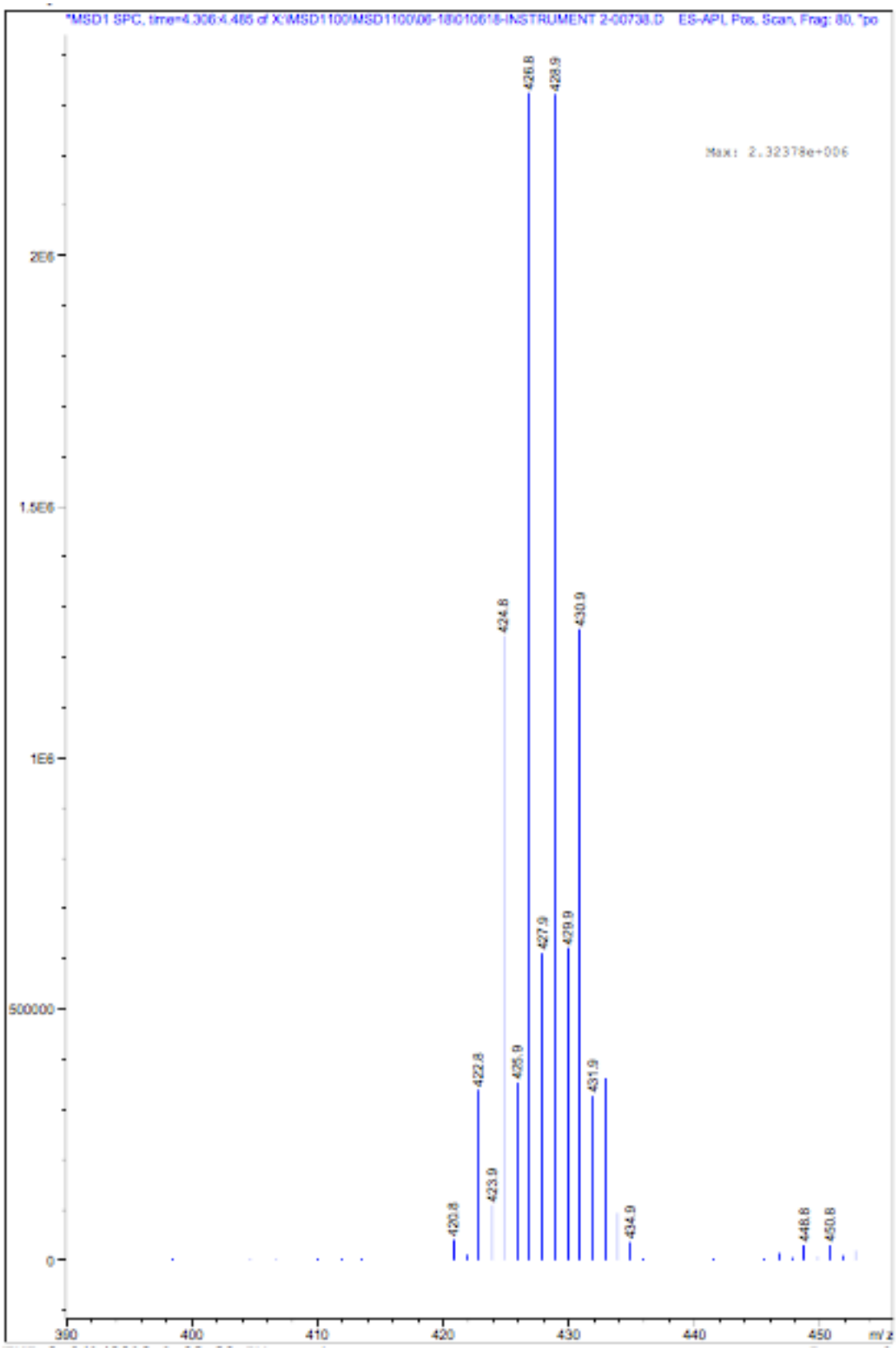

Figure S19. Mass spectrum of tritium labeled MK-6096, **[^{3}H]12a**.

H/T Exchange in MK-5395

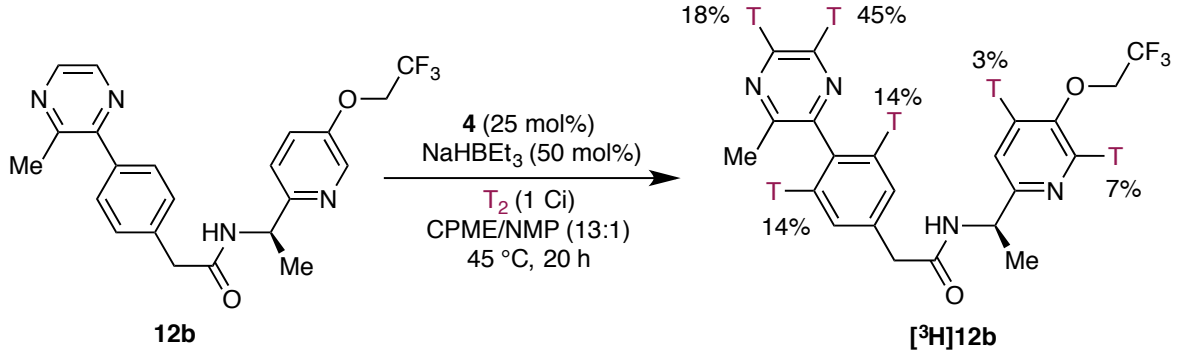

Scheme S46. H/T exchange in MK-5395.

Reaction was performed according to the general procedure for H/T exchange in pharmaceuticals, described in section VII. Following the three successive evaporation steps from ethanol, the crude product was dissolved in ethanol (10 mL) and a total radioactivity of 254.6 mCi at 93.6% radiochemical purity was measured. Ethanol was then removed under vacuum and the crude mixture was dissolved in DMSO (0.4 mL) and **[^{3}H]12b** was purified via semipreparative reverse phase HPLC (Column: 10 x 250 mm Gemini NX C18. Mobile phase: 50 mM TEAA/acetonitrile (65:35). Flow rate: 5 mL/min. Detection: 254 nm). Fractions containing the purified compound were collected and diluted with water, concentrated on a pair of C18 cartridges and eluted with ethanol (40 mL). **Specific Activity:** 53.6 Ci/mmol. **Radiochemical yield:** 219.7 mCi. **Radiochemical purity:** 98.7%.

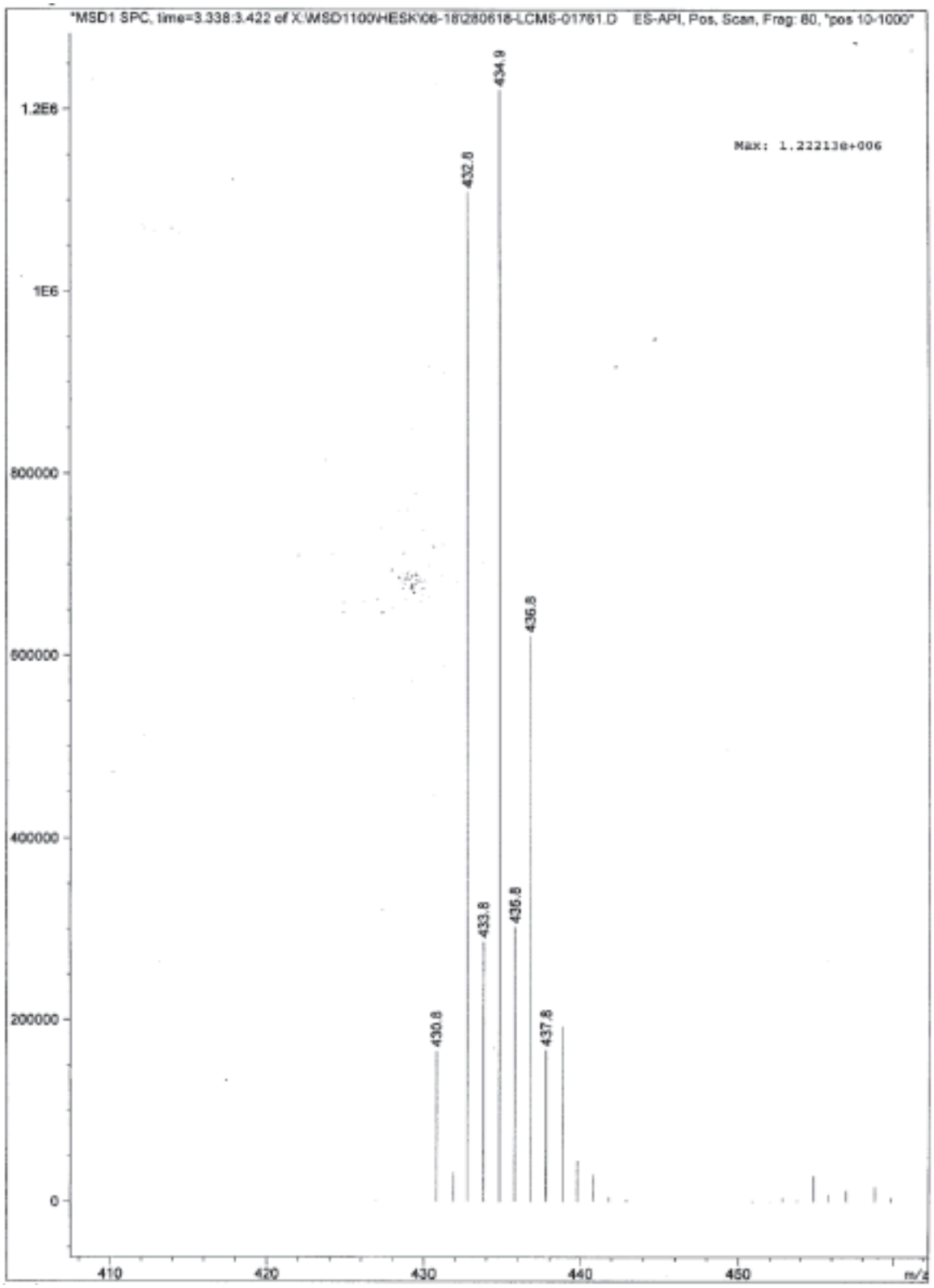

Figure S20. Mass spectrum of tritium labeled MK-5395, **[^{3}H]12b**.

H/T Exchange in varenicline

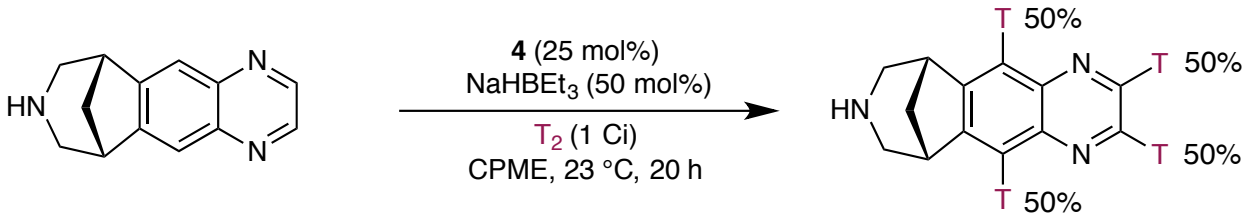

12c **[^{3}H]12c**

Scheme S47. H/T exchange in varenicline.

Reaction was performed according to the general procedure for H/T exchange in pharmaceuticals, described in section VII, at 23 °C. Following the three successive evaporation steps from ethanol, the crude product was dissolved in ethanol (10 mL) and a total radioactivity of 504 mCi at 19.6% radiochemical purity was measured. Ethanol was then removed under vacuum and the crude mixture was dissolved in DMSO (0.4 mL) and **[^{3}H]12c** was purified via semipreparative reverse phase HPLC (Column: 10 x 250 mm Gemini NX C18. Mobile phase: 50 mM TEA in water/acetonitrile (85:15). Flow rate: 5 mL/min. Detection: 340 nm). Fractions containing the purified compound were collected and diluted with water, concentrated on a pair of C18 cartridges and eluted with ethanol (20 mL). **Specific Activity:** 76.1 Ci/mmol. **Radiochemical yield:** 67.0 mCi. **Radiochemical purity:** 98.8%.

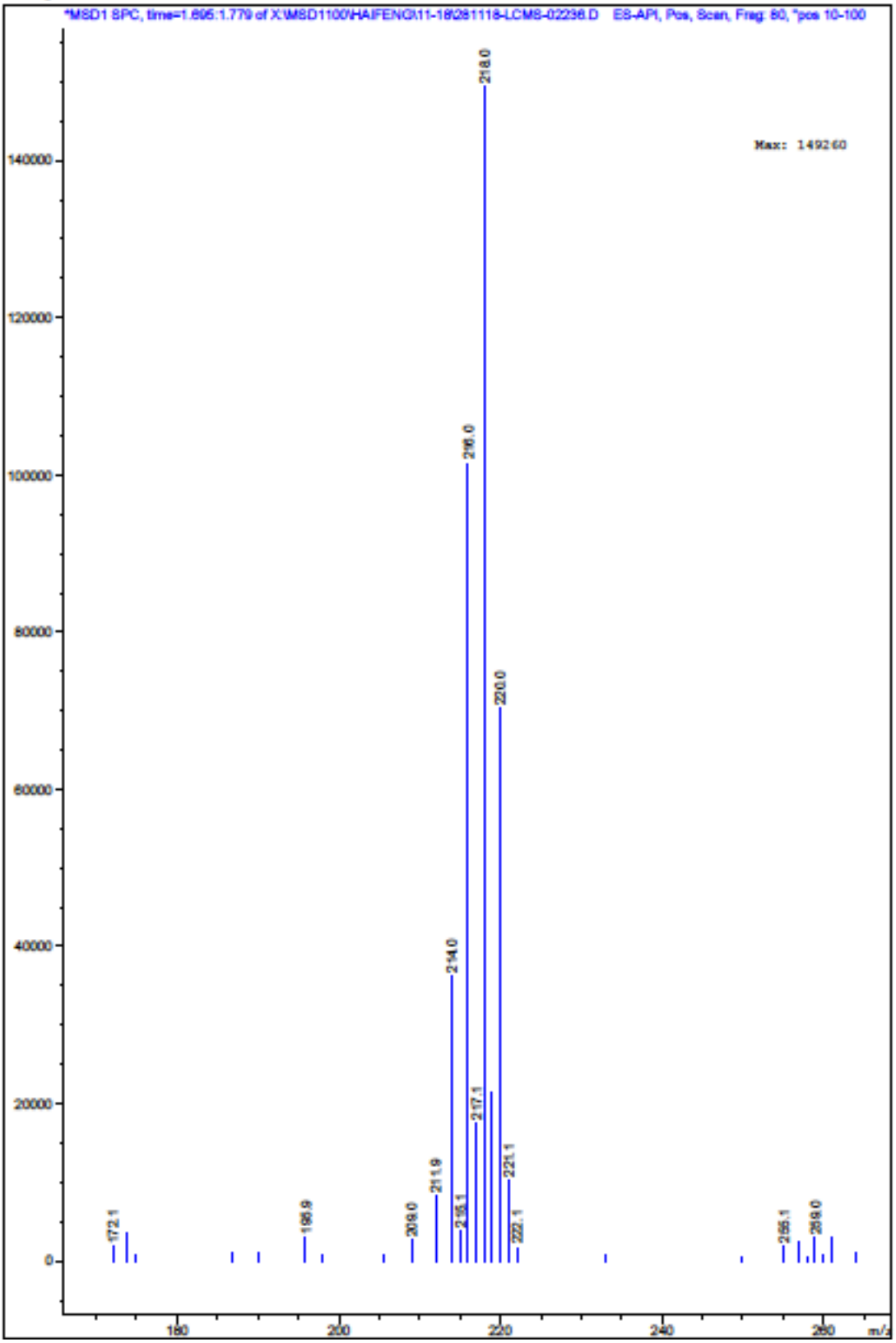

Figure S21. Mass spectrum of tritium labeled varenicline, **[^{3}H]12c**.

H/T Exchange in papaverine

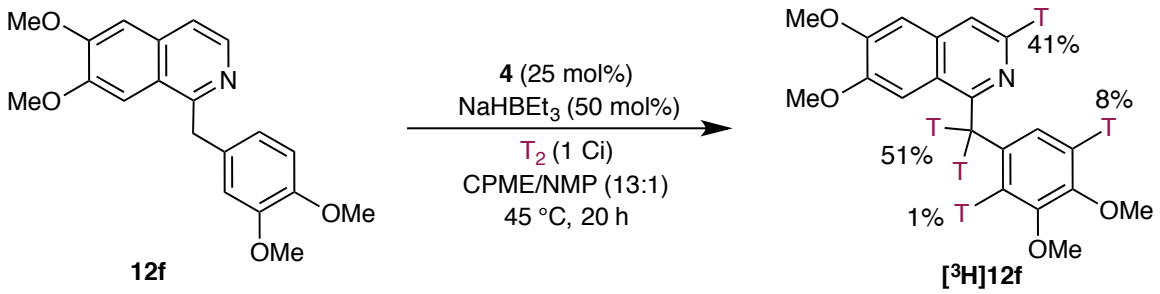

Scheme S48. H/T exchange in papaverine.

Reaction was performed according to the general procedure for H/T exchange in pharmaceuticals, described in section VII. Following the three successive evaporation steps from ethanol, the crude product was dissolved in ethanol (10 mL) and a total radioactivity of 389.6 mCi at 87.98% radiochemical purity was measured. Ethanol was then removed under vacuum and the crude mixture was dissolved in DMSO (0.7 mL) and **[^{3}H]12d** was purified via semipreparative reverse phase HPLC (Column: 10 x 250 mm Gemini NX C18. Mobile phase: 50 mM TEAA/acetonitrile (78:22). Flow rate: 5 mL/min. Detection: 254 nm). Fractions containing the purified compound were collected and diluted with water, concentrated on a pair of C18 cartridges and eluted with ethanol (20 mL). **Specific Activity:** 49.5 Ci/mmol. **Radiochemical yield:** 215.7 mCi. **Radiochemical purity:** 99.2%.

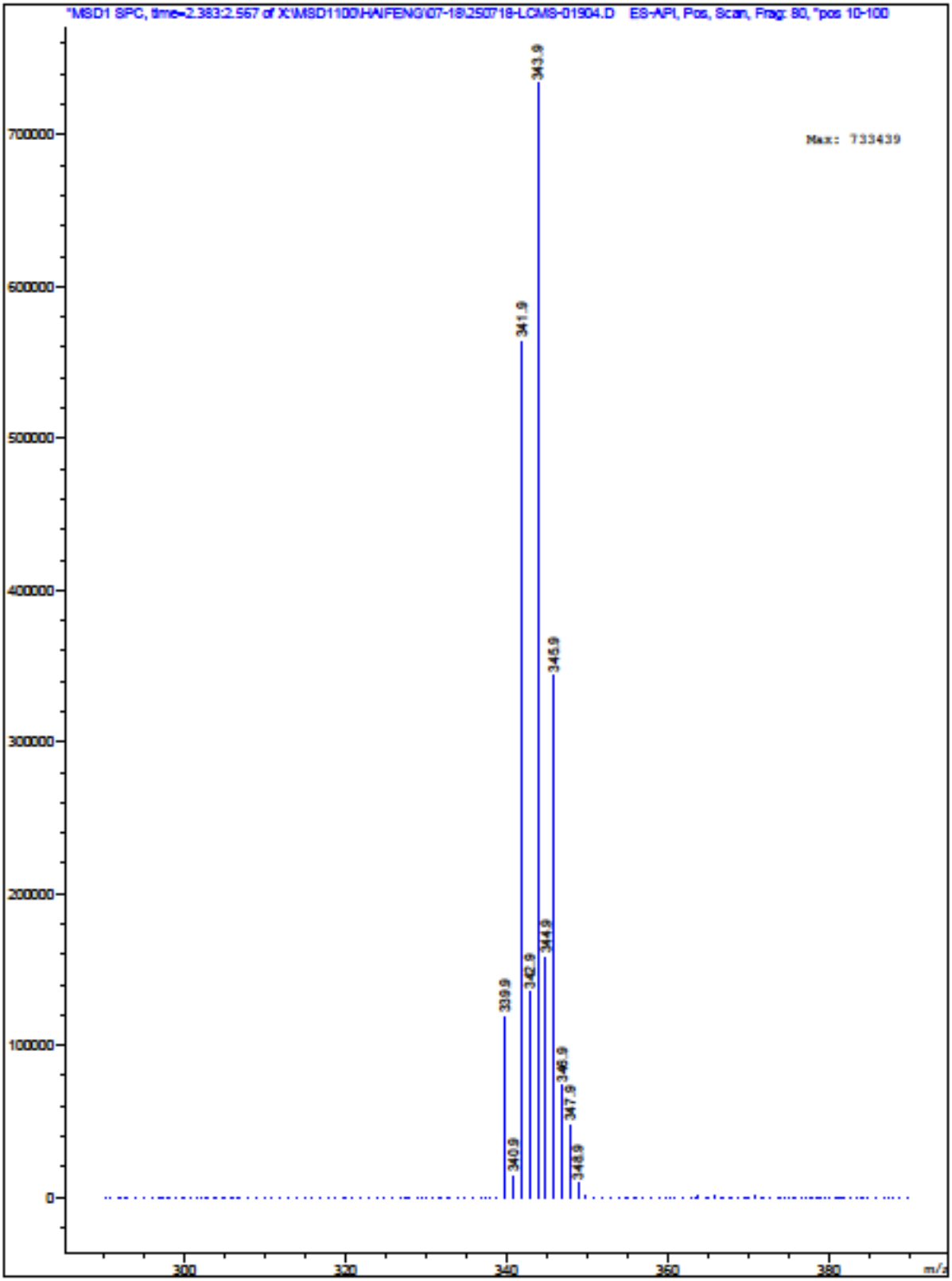

Figure S22. Mass spectrum of tritium labeled papaverine, **[^{3}H]12f**.

XI. Heterogeneous Test

The significantly higher catalytic activity of [(^{ipc}ADI)Ni(μ_2-H)]$_2$ (**2**) as compared to [(^{iPr}DI)Ni(μ_2-H)]$_2$ (**1**) could be alternatively attributed to a favored dissociation of the sterically demanding ^{ipc}ADI chelate and generation of heterogeneous catalytic species. In order to support the homogeneity of our catalytic system, H/D exchange of a representative substrate (2-phenylpyridine) was performed in the absence of ^{ipc}ADI ligand, using $NiBr_2$·DME catalytic precursor and $NaHBEt_3$ activator as described below.

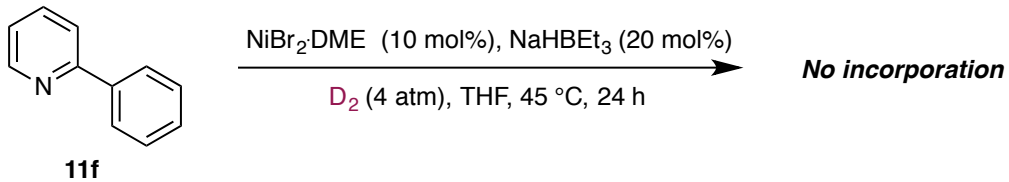

Scheme S49. H/D exchange in 2-phenylpyridine in the absence of ^{ipc}ADI.

In a glovebox, a thick-walled glass vessel containing a magnetic stir bar was charged with $NiBr_2$·DME (34 mg, 0.06 mmol) and THF (0.5 mL). While stirring at 23 °C, a 1.0 M solution of $NaHBEt_3$ in toluene (120 μL, 0.12 mmol) was added to the solution, which immediately turned black. The resulting mixture was then stirred at 23°C for 2 additional minutes and, subsequently, 2-phenylpyridine (86 μL, 0.6 mmol) and additional THF (0.5 mL) were added. The vessel was sealed, taken out of the glovebox and attached to a high vacuum line. The solution was then frozen by submersion of the entire vessel in liquid nitrogen (-196 °C). After evacuating the headspace, D_2 (~1 atm) was added. The vessel was then sealed, and the reaction mixture was thawed (when 23 °C is reached, the pressure of D_2 in the headspace is ~4 atm) and stirred at 45 °C for 24 hours. At the end of the reaction, the vessel was opened to air and the reaction mixture was diluted with hexanes (~10 mL) and analyzed by HRMS without further purification. **Deuterium incorporation**: 0.00 D/molecule (HRMS/IsoPat[2]), 100% unlabeled compound.

Although more detailed investigations are currently ongoing in our laboratories, the lack of reactivity in the absence of supporting ^{ipc}ADI ligand preliminarily supports the homogeneity of our novel nickel-catalyzed HIE methodology.

XII. Electrochemical Data

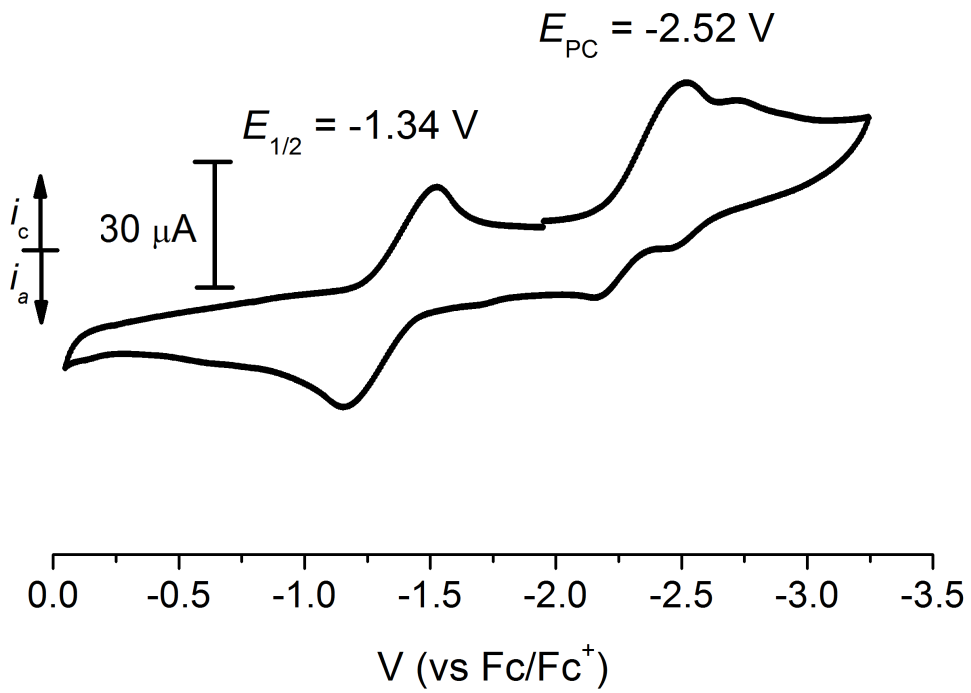

Figure S23. Cyclic voltammogram of [(^{ipc}ADI)NiBr] at 100 mV/sec scan rate.

Cyclic Voltammetry (CV) of [(^{ipc}ADI)NiBr] (**8**) was collected as indicated in section I.C. and exhibits a reversible anodic wave at $E_{1/2}$ = -1.34 V (vs Fc/Fc$^+$) assigned as the formal Ni(I)/Ni(II) redox couple (Figure S23). The CV of **8** also exhibits an irreversible cathodic peak with E_{PC} = -2.52 V that likely corresponds to a reduction event leading to a formally Ni(0) complex that is unstable on the timescale of the electrochemical experiment, presumably due to dissociation of the bromide ligand as proposed for related diimine nickel complexes.[21]

XIII. X-Ray Structural Data

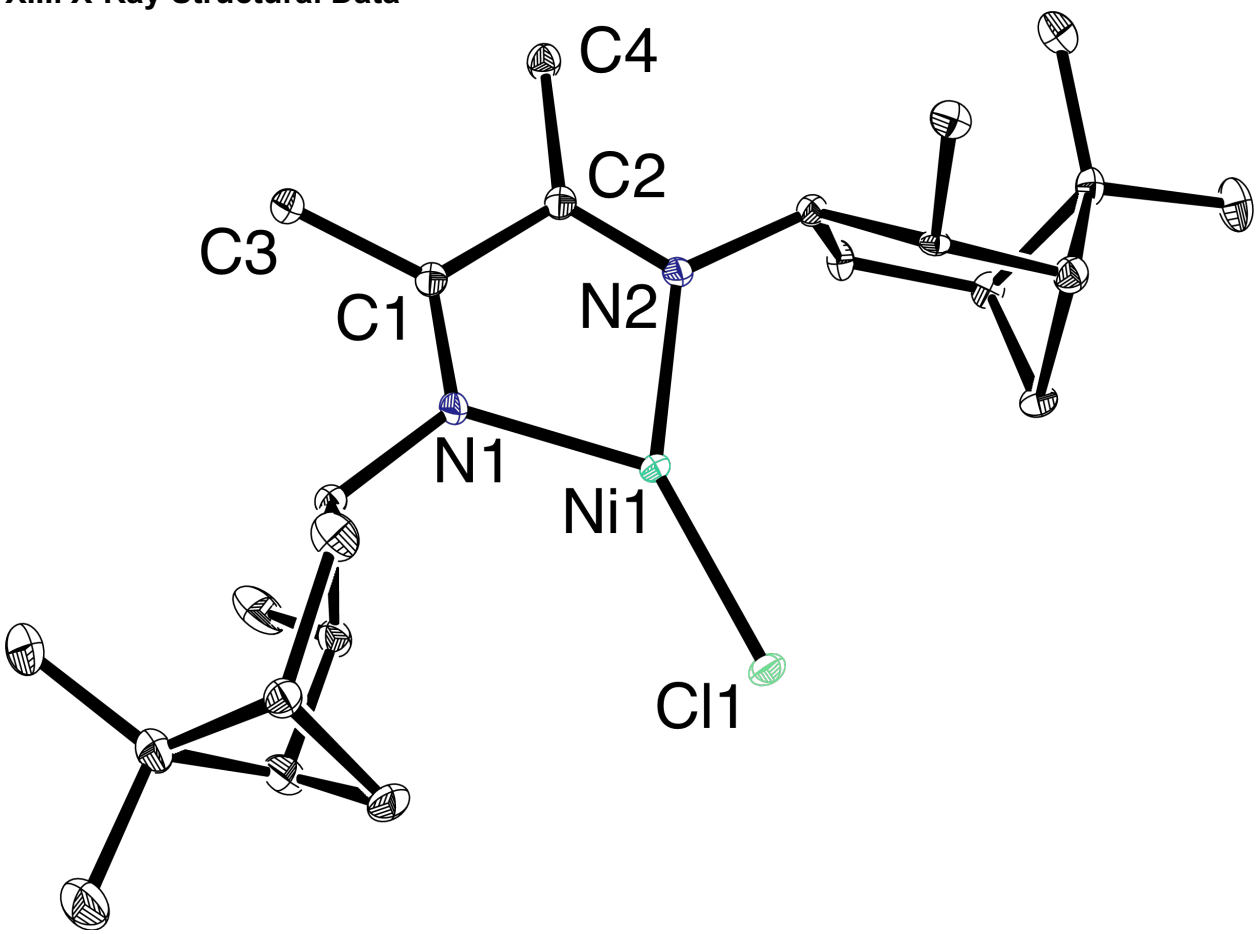

Figure S24. Solid-state structure of **7** at 30% probability ellipsoids. Hydrogen atoms have been omitted for clarity.

Table S1. Selected bond lengths (Å) and angles (deg) for **7**.

Ni1–Cl1	2.147 (2)
Ni1–N1	1.950 (6)
Ni1–N2	1.947 (6)
N1–C1	1.285 (10)
C1–C3	1.510 (10)
C1–C2	1.485 (10)
C2–C4	1.494 (10)
C2–N2	1.295 (9)
N2—Ni1—N1	81.9 (3)
N2—Ni1—Cl1	143.64 (19)
N1—Ni1—Cl1	134.23 (19)
C1—N1—Ni1	114.4 (5)
C2—N2—Ni1	114.5 (5)

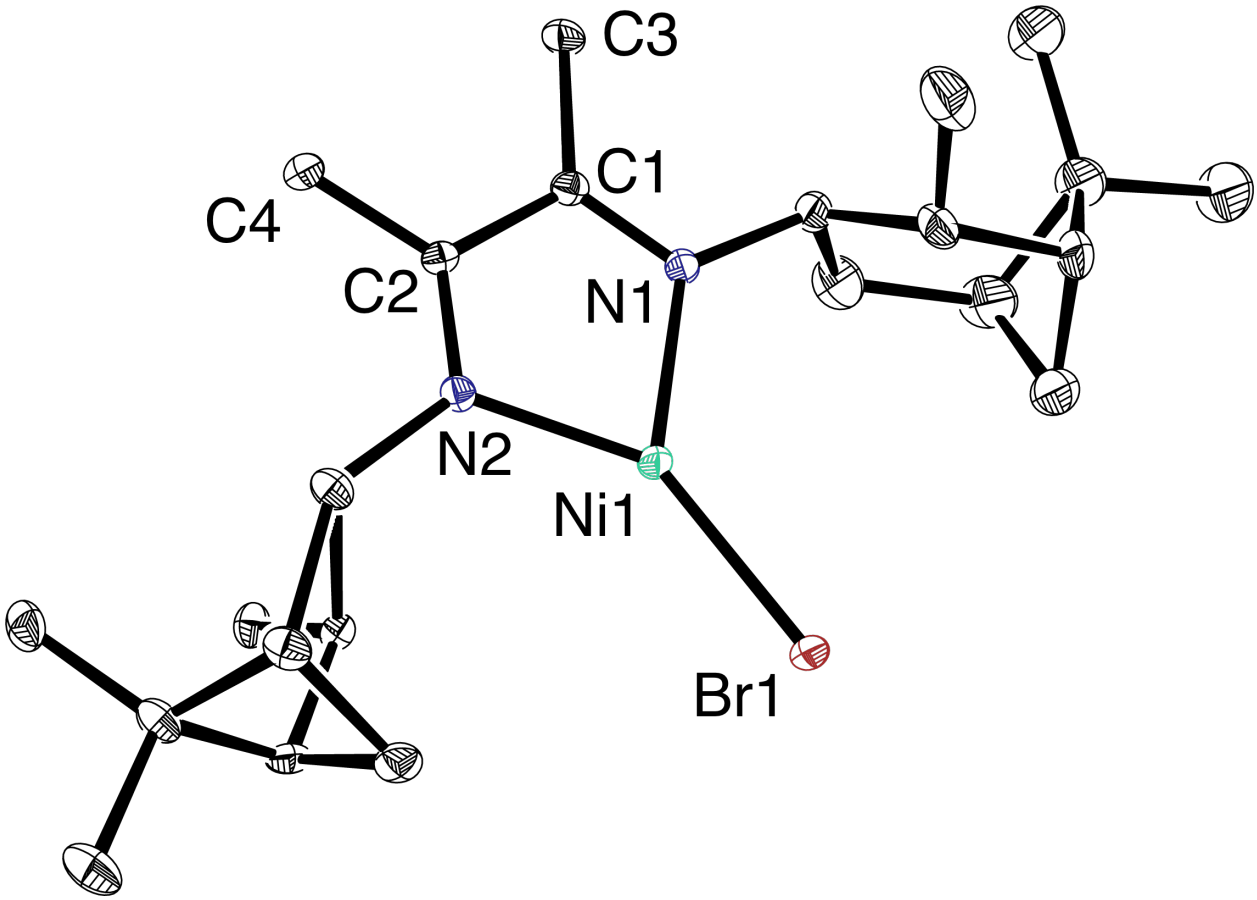

Figure S25. Solid-state structure of **8** at 30% probability ellipsoids. Hydrogen atoms have been omitted for clarity.

Table S2. Selected bond lengths (Å) and angles (deg) for **8**.

Ni1–Br1	2.2813 (9)
Ni1–N1	1.955 (4)
Ni1–N2	1.943 (4)
N1–C1	1.289 (7)
C1–C3	1.511 (7)
C1–C2	1.480 (7)
C2–C4	1.495 (7)
C2–N2	1.299 (6)
N2—Ni1—N1	81.93 (17)
N2—Ni1—Br1	144.66 (12)
N1—Ni1—Br1	133.17 (13)
C1—N1—Ni1	114.2 (3)
C2—N2—Ni1	114.6 (3)

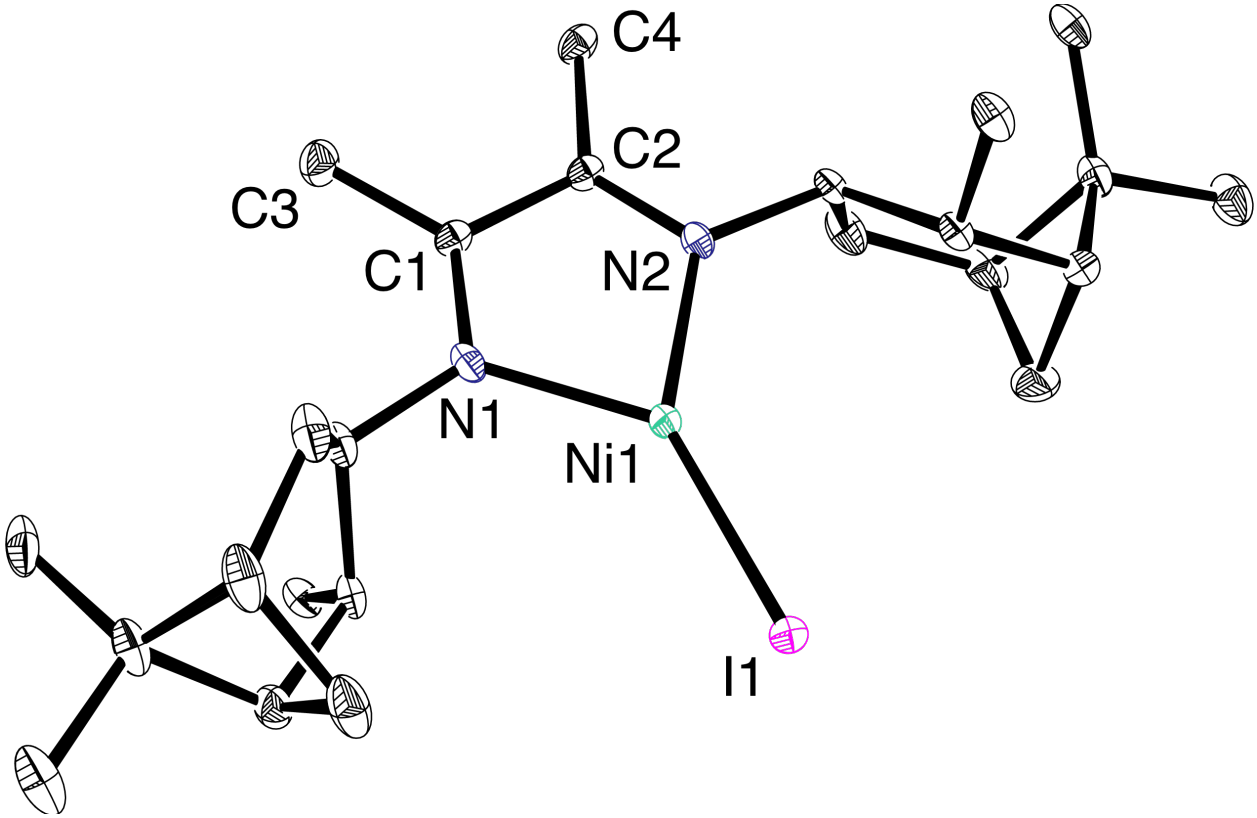

Figure S26. Solid-state structure of **9** at 30% probability ellipsoids. Hydrogen atoms have been omitted for clarity.

Table S3. Selected bond lengths (Å) and angles (deg) for **9**.

Ni1–I1	2.4565 (12)
Ni1–N1	1.946 (6)
Ni1–N2	1.946 (6)
N1–C1	1.302 (9)
C1–C3	1.493 (10)
C1–C2	1.478 (9)
C2–C4	1.501 (10)
C2–N2	1.301 (9)
N2—Ni1—N1	82.1 (2)
N2—Ni1—I1	143.15 (17)
N1—Ni1—I1	134.68 (18)
C1—N1—Ni1	114.4 (5)
C2—N2—Ni1	114.3 (4)

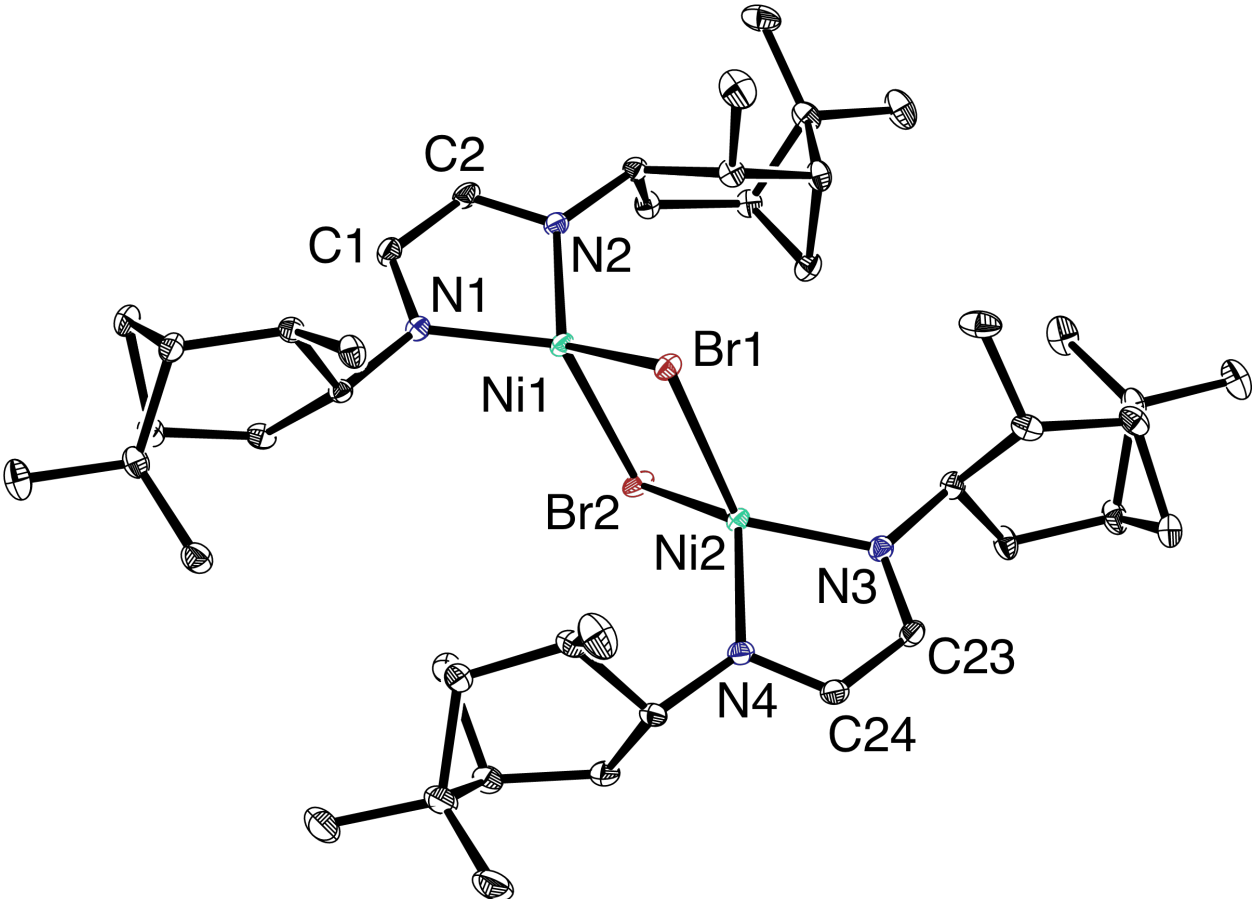

Figure S27. Solid-state structure of **10** at 30% probability ellipsoids. Hydrogen atoms have been omitted for clarity.

Table S4. Selected bond lengths (Å) for **10**.

Ni1–Br1	2.4752 (5)
Ni1–Br2	2.4209 (5)
Ni1–N1	1.933 (2)
Ni1–N2	1.944 (2)
N1–C1	1.304 (4)
C1–C2	1.419 (4)
C2–N2	1.304 (4)
Ni2–Br1	2.4447 (5)
Ni2–Br2	2.4305 (5)
Ni2–N3	1.931 (2)
Ni2–N4	1.938 (2)
N3–C23	1.309 (4)
C23–C24	1.423 (4)
C24–N4	1.310 (4)

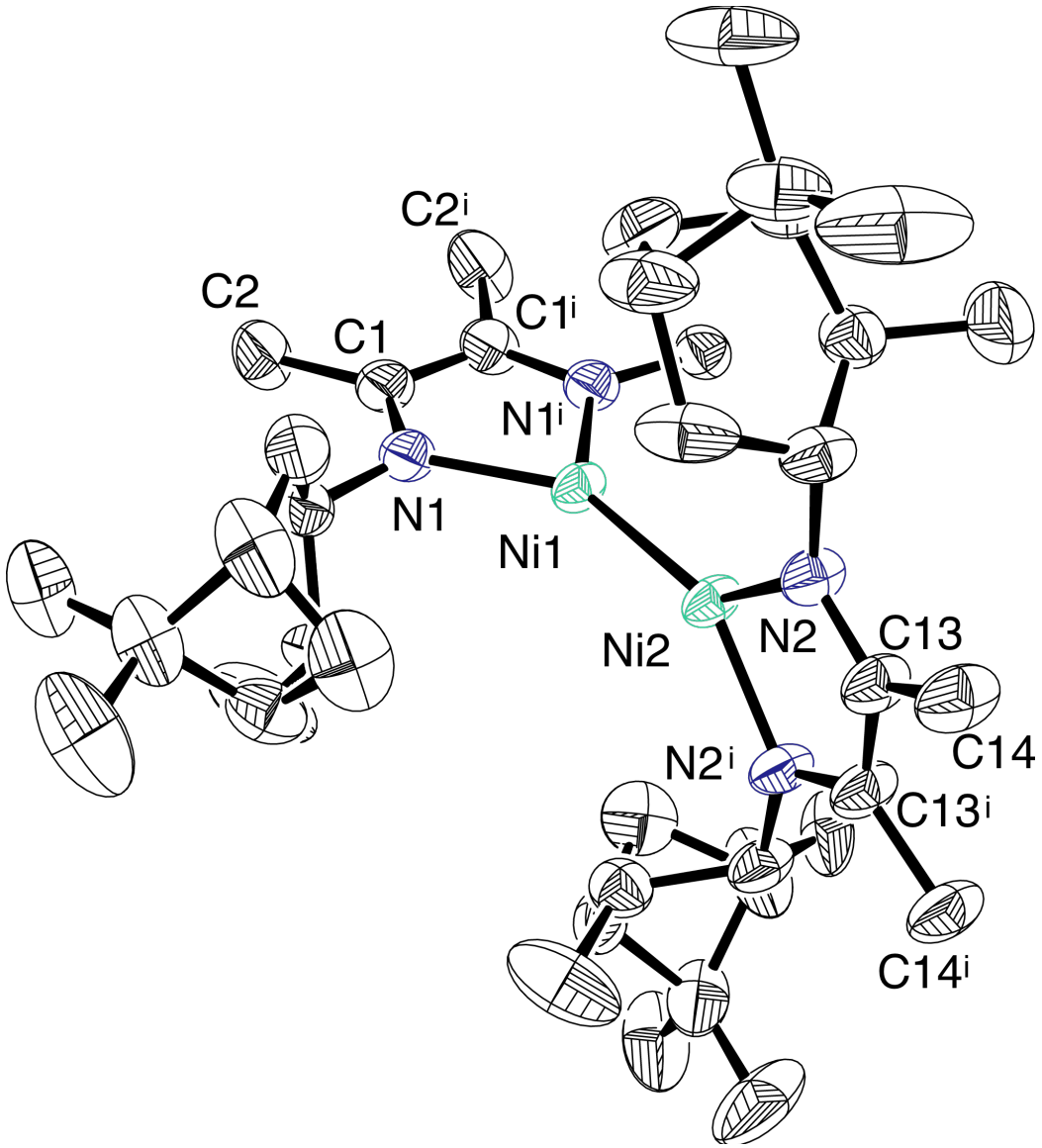

Figure S28. Solid-state structure of **2** at 30% probability ellipsoids. Hydrogen atoms have been omitted for clarity. Superscript "i" refers to atoms generated by symmetry.

Table S5. Selected bond lengths (Å) for **2**.

Ni1–Ni2	2.3391 (9)
Ni1–N1	1.916 (4)
N1–C1	1.313 (6)
C1–C2	1.502 (7)
C1–C1^{i}	1.428 (11)
Ni2–N2	1.916 (4)
N2–C13	1.313 (6)
C13–C14	1.498 (7)
C13–C13^{i}	1.440 (12)

XIV. Computational Analysis of [(^{ipc}ADI)NiBr] and [(^{ipc}ADI)Ni(μ_2-H)]$_2$

XIV.A. Sample Geometry Optimization Input File

```
#Filename
! UKS B3LYP RIJCOSX def2-SVP def2/J Normalprint SlowConv TightSCF Opt Pal8 UCO

%basis NewGTO 35 "def2-TZVP(-f)" end
        NewGTO 28 "def2-TZVP(-f)" end
        NewGTO 7 "def2-TZVP(-f)" end
        NewAuxGTO 35 "def2/J" end
        NewAuxGTO 28 "def2/J" end
        NewAuxGTO 7 "def2/J" end
       end

%SCF MaxIter 500
   TolE 1e-7
   TolErr 1e-6
  end

* xyz 0 2

XYZ Coordinates from crystal structure.

*
```

XIV.B. Optimized Coordinates

[(^{ipc}ADI)NiBr]

Br	2.45539369044389	-0.05227606933777	-0.02844368207942
Ni	0.13757427558254	-0.05865238131983	-0.00157867405253
N	-1.25056716374299	-0.13514079391346	1.44138683186580
N	-1.48607590311707	-0.09421805550145	-1.15942463327304
C	-1.48087024167044	-0.08579770673040	-2.63984644481465
H	-2.40659545240940	0.40631804141617	-2.96188180878365
C	-0.31888383128045	0.78376433359966	-3.21147867885074
H	0.51412091798268	0.73838235275728	-2.48718550009282
C	-1.51357982831066	-1.54462696354403	-3.20121267648263
H	-1.09808944300167	-2.23306930425808	-2.44748498562574
H	-2.56355342862893	-1.84740060199681	-3.35438330805102
C	-0.73114343541863	2.25546039395553	-3.34915579810604
H	-1.08680725905122	2.66257159079810	-2.38822717451366
H	-1.53666791129916	2.39252632591423	-4.08900502057220
H	0.12284902957116	2.87139351098769	-3.67456542124761
C	-2.21993305707331	0.13695672852504	-5.71349345638786
H	-2.77838106474427	0.38485069556581	-4.80318810842333
H	-2.84420936807498	-0.55977382040982	-6.29923986612905
H	-2.13445412214124	1.06437954243576	-6.30426583821888
C	-1.00975944585458	-0.08616785823415	2.89789151379661
H	-1.87800743455547	-0.54026012394514	3.38857180526667

C	-2.46381920072898	-0.18297359164533	0.98661009835072
C	-3.98032813021651	-0.32906071523701	-1.09158795733578
H	-3.96937063309445	-0.42934095921761	-2.18190460035987
H	-4.61345672606498	0.53777021164437	-0.83624333066514
H	-4.48432632595580	-1.21996719899230	-0.68264974699821
C	0.74223819788419	-1.25514355043836	-4.20570839379833
H	1.47800582232194	-1.63102925574026	-4.92709843448707
H	1.13146750130246	-1.43348326930496	-3.19067728634501
C	-2.59844960160456	-0.19246099764432	-0.49580983156772
C	-0.23720550712444	-0.78516856710636	-6.85610117041765
H	0.74368478716259	-1.27946136645954	-6.81417690250311
H	-0.11050178425425	0.15031353902029	-7.42630808214019
H	-0.90959779534043	-1.43818609982537	-7.43803026642808
C	-3.69469045312755	-0.22183834787575	1.86491208645979
H	-3.65713677291289	0.55578379160583	2.64104450232866
H	-3.78023389785809	-1.19302232330116	2.38232983589210
H	-4.61611989697260	-0.07256313015853	1.29313106983563
C	-0.70664349007568	-1.71430531525323	-4.49794992043763
H	-0.87487803448087	-2.71772513574415	-4.92699660070086
C	-0.83896766825913	-0.48711711528947	-5.46809533986137
C	-0.93999582496618	1.40158041169837	3.37445630526735
H	-0.64535646809605	2.04113466171302	2.52678220803403
H	-1.94908422535773	1.72890114832016	3.67933076966521
C	0.97587308883087	-0.28677515386562	4.49997985074814
H	1.73649572990719	-0.97927349132920	4.89957046382948
C	0.21914150213569	-0.94718365528897	3.32379771929633
H	0.92716606296542	-0.95089285836006	2.47777341533228
C	0.23689541485487	0.17838518053386	-4.52105234779189
H	0.94126365554120	0.88184751492108	-4.99685447160230
C	1.44633782041666	1.11641956338823	4.03052326065807
H	1.68366777653564	1.22937877659487	2.96094132033614
H	2.28493512049805	1.51609265877733	4.61440308842853
C	0.06568804499571	0.45072681978694	5.55929082736734
C	-1.26608453994372	-0.13574997471311	6.04829074940547
H	-1.96317909903160	-0.42436610565753	5.25244806968764
H	-1.78695912716058	0.60142805512616	6.68386126865269
H	-1.09384251437901	-1.03059247719051	6.66947105246378
C	0.87337336928619	0.81900678394849	6.81890305472787
H	1.83363539042377	1.30506886194153	6.59698528761730
H	1.08921657110628	-0.08262530636335	7.41684536018766
H	0.29501073340713	1.50907856896782	7.45640994476249
C	-0.18112755881215	-2.40423138346432	3.59436245845169
H	0.70276889710687	-3.01042192278360	3.85173216557308
H	-0.64441140853016	-2.85997550253409	2.70358041071576
H	-0.89707386974995	-2.49460283462738	4.42851083023375
C	0.06422185812844	1.62070656644779	4.51332325491849
H	-0.01960631391859	2.64852465421099	4.90746487898851

[(^{ipc}ADI)Ni(μ_2-H)]$_2$

C	-0.25785555903168	4.71947740728357	0.21041918343345
C	-0.16793047299667	6.11236302744492	0.79861751340264
C	-0.67838603292569	3.78018347360408	2.37772926411525
C	-1.79769945753440	2.81970027330142	2.87924694841009
C	-1.55733796768645	2.40629847558891	4.34964070945380
C	-0.92975479710725	3.52832298468551	5.26714244392392
C	0.42744589646970	3.09458582352452	4.60424338551817
C	0.63966856941686	3.69442661551876	3.20391296165515
C	-3.19271150698853	3.40954687772859	2.63841021709114
C	-0.18698374563996	1.68362904368359	4.41689486524015
C	-0.99119327029083	3.12331470560203	6.75141584363305
C	-1.38137077101108	4.99341486056349	5.20344680702345
C	0.18536524183659	-3.18565409275774	-0.02638375414022
C	-0.09230320074373	-4.65062949875646	-0.29589790369722
C	-2.10573745159218	-2.54077946812685	-0.39096141002336
C	-3.08659418270054	-1.60670636655628	0.37512327594118
C	-4.39995607220630	-1.41562315308613	-0.42075585878815
C	-4.89277903679068	-2.68221816474696	-1.23090426303334
C	-3.82489094206047	-2.22732062134325	-2.28908942587769
C	-2.38672873471028	-2.63333963748025	-1.91930468257140
C	-3.30520732143784	-2.09223045583099	1.81403093778456
C	-4.03334275772415	-0.77632157448447	-1.78713920958176
C	-6.33086863873899	-2.47894081958835	-1.74866606170267
C	-4.84842506675622	-4.10562002016412	-0.65825545785965
N	-0.44648659155429	3.63229675409246	0.92796551425079
N	-0.69420654706564	-2.21371232333637	-0.10372929081743
Ni	-0.21377112124547	1.95925103182109	-0.09911634207953
Ni	0.10428554327505	-0.40638311043868	0.14064408953527
C	-0.13772370687097	4.49727652805636	-1.22544362947811
C	-0.13918263482416	5.66578240412715	-2.18859900012668
C	0.02038239083658	2.93907324106031	-3.03987123203935
C	1.02928250655423	1.80240452886396	-3.37578188031129
C	0.57949463112334	1.02720029161833	-4.63733140264365
C	-0.14565931504576	1.88574913602228	-5.74932927834726
C	-1.40622257087086	1.73330028388612	-4.82369038698368
C	-1.40205520635832	2.71025452758293	-3.63764657551572
C	2.46859554067403	2.32424959119705	-3.46893008977141
C	-0.80325648759326	0.39732190474180	-4.32545040829538
C	-0.29951542388176	1.07562693878260	-7.05168556971644
C	0.34320511404023	3.28135044426642	-6.16419039579934
N	-0.05862597196874	3.23597826794670	-1.59627912551920
C	1.53086941334834	-2.77809208792293	0.38392081379095
C	2.61663800632220	-3.81851980853369	0.56789347076776
C	3.00087885594863	-0.99634782321456	1.05616265549394
C	3.72738125770050	-0.12506333994098	-0.01670651478819
C	4.60289355377197	0.95519653782313	0.65775163611654
C	5.27928340896407	0.53770521350407	2.02479648714797
C	3.86558406685274	0.85016512496201	2.63745217347914
C	2.86958518875210	-0.30419449553079	2.44536772840297

C	4.49930655753760	-0.99234848599771	-1.01843064686593
C	3.65689432749912	1.86366932698017	1.48527450013412
C	6.33404148444647	1.57964892406221	2.43912415709604
C	5.92531224531070	-0.83873137917206	2.24504837566063
N	1.69575958150479	-1.49037266023264	0.58020138851119
H	0.47012830811554	6.12887529636220	1.69269031187069
H	-1.15574581414099	6.50579773639960	1.10175934957326
H	0.26360701702749	6.82624154123620	0.08722095075621
H	-1.07524421192788	4.79018762652450	2.53028807876201
H	-1.71406879424015	1.89966814806030	2.27728971949870
H	-2.44052012610222	1.87793973556275	4.74995974617497
H	1.34054036384886	3.19915070818951	5.21667713682983
H	1.08784086682758	4.70088677847261	3.27245266163797
H	1.36435511474469	3.06730890785508	2.66369111944367
H	-3.32688584959841	3.69429402089882	1.58165766717579
H	-3.97646475895864	2.67580383365482	2.88778214240930
H	-3.37331620081957	4.30573643704755	3.25352869375912
H	0.11106536258204	1.12829194360805	3.51642170441732
H	-0.06944477116695	1.03020612196019	5.29115578196815
H	-0.67749931389449	2.08606021618029	6.93461039768781
H	-0.34099242441600	3.77555663175239	7.35786323639830
H	-2.01894286168123	3.23614500457417	7.13676522866006
H	-0.72705127068586	5.61178954180057	5.84123027679943
H	-1.36639502848137	5.43966602825423	4.20245088974434
H	-2.40652210657447	5.10400703539934	5.59700916791135
H	0.04913208866702	-5.26421565612225	0.60996088182887
H	0.59821593281162	-5.04642178146648	-1.05736857558912
H	-1.10562573487776	-4.83420156387477	-0.66607219993892
H	-2.28718028253980	-3.53791108698743	0.02509077965337
H	-2.60734229240707	-0.61502884822498	0.42985429372730
H	5.15442058017237	-0.90546929119345	0.20284761419239
H	-4.03851814422339	-2.46231970906701	-3.34690047283527
H	-1.69185847524636	-1.96787845217850	-2.45519591623975
H	-2.15972701808502	-3.65723190817797	-2.26534767732042
H	-2.34329452353127	-2.21032853627661	2.33914559702331
H	-3.90893319287996	-1.36911819571739	2.38618891528417
H	-3.83175467498858	-3.06063398104801	1.84884440833177
H	-4.86491645351204	-0.25328464770772	-2.27687051043463
H	-3.14924691133835	-0.12122419565186	-1.79775612459598
H	-6.51688480288592	-1.47596756655999	-2.15846005456978
H	-6.55961309100952	-3.20804710071794	-2.54412162047631
H	-7.05528452097237	-2.64644713767376	-0.93325959068962
H	-5.53659854322101	-4.20406941765743	0.19847372535595
H	-5.18910963806726	-4.82296896687420	-1.42545541838169
H	-3.86018120581292	-4.43818553232315	-0.32116462404395
H	-0.77770657337159	5.47125067457996	-3.06097245870455
H	0.87347968901115	5.89326032785283	-2.56887040994909
H	-0.52213061102370	6.57744391166471	-1.71628389900830
H	0.42735717877256	3.83148257802431	-3.52574485060840
H	0.98942248319991	1.08372993346702	-2.53965036096442
H	1.38562305467303	0.35674916867834	-4.98206469682522

H	-2.39426303609081	1.71779979599486	-5.31607009710921
H	-1.82865173323810	3.68423061730618	-3.93470236413394
H	-2.05967046342281	2.30956600556405	-2.84953792023869
H	2.77478043321409	2.81584337285316	-2.53119603595134
H	3.17153962914222	1.49464369003518	-3.65241031256518
H	2.59758772991009	3.05239849804796	-4.28721103126930
H	-0.98924216806117	0.13234376693690	-3.27461666474308
H	-1.05312506061582	-0.46545120355116	-4.95663720696402
H	-0.71561827040592	0.06986621419653	-6.89813387512804
H	-0.96532664417492	1.60373542267054	-7.75508521280029
H	0.67859600797949	0.95845106252198	-7.54826027811548
H	-0.36626449077601	3.72860195714711	-6.88162323118570
H	0.46069061440788	3.99200790027734	-5.33779318632090
H	1.31801221673975	3.21739560727007	-6.67764416110670
H	3.48690987480245	-3.61588371654379	-0.07429715447218
H	2.25854375832038	-4.82400073279262	0.32294843003326
H	2.98513135889467	-3.84985575168400	1.60703832655689
H	3.65160031608206	-1.86172226776338	1.20681628571580
H	2.94664894821488	0.41830885046057	-0.57654558781780
H	5.26179920165899	1.43421170419432	-0.08743524699013
H	3.83495916875037	1.22556493425085	3.67533358206388
H	1.84960519009545	0.09204079642177	2.55647249751611
H	3.00059341898137	-1.06784004246523	3.23159805571538
H	3.82631954217286	-1.68460078991354	-1.55086391694473
H	4.99211681933997	-0.36584937669870	-1.77957479428721
H	5.28214699445049	-1.59060565548029	-0.52395463757891
H	4.06908496253289	2.85765916014191	1.70239829318738
H	2.63357629903714	1.97786937639196	1.09695464134399
H	5.99746544031290	2.61727371145975	2.30629836735702
H	6.60973860259077	1.45193696684718	3.50002940165217
H	7.25261934258676	1.45029088116896	1.84246079516953
H	6.77291946902158	-0.98695084705444	1.55503494025739
H	6.33699157690306	-0.89733289862060	3.26741817264390
H	5.24831916618580	-1.69323891987246	2.12575911429156
H	-0.70999942882627	0.58103331200129	-0.79955202748512
H	0.22852773662377	0.95837711003606	1.01803547536433

XIV.C. DFT-Computed Qualitative Molecular Orbital Diagram for [(^{ipc}ADI)Ni(μ$_2$-H)]$_2$

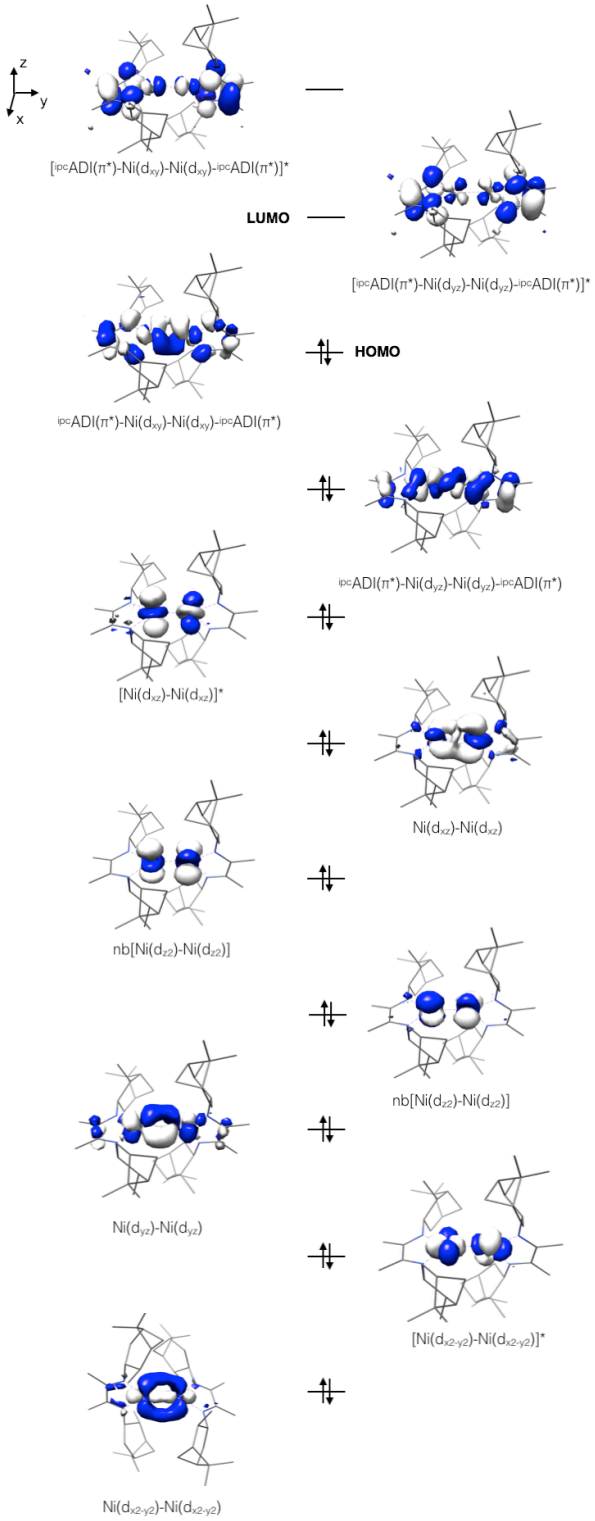

Figure S29. Qualitative frontier molecular orbital diagram of **2** obtained from a spin-restricted B3LYP−DFT calculation. The y axis is defined as the Ni–Ni vector. nb = non-bonding.

As shown in Figure S29, the results of the DFT computations establish the population of two orbitals with significant ^{ipc}ADI π^* character, consistent with mono-reduced chelates. Additionally, the coordination geometry at both nickel centers in the geometry-optimized structure of **2** appears to be slightly distorted square planar, which is in agreement with a low-spin Ni(II) assignment. Overall, these results together with the perturbations to the bond distances of the ^{ipc}ADI chelate with respect to its neutral form support an electronic structure assignment for **2** as containing two nickel(II) centers each ligated to one-electron reduced α-diimine chelate.

XV. EPR Spectra of Nickel Complexes

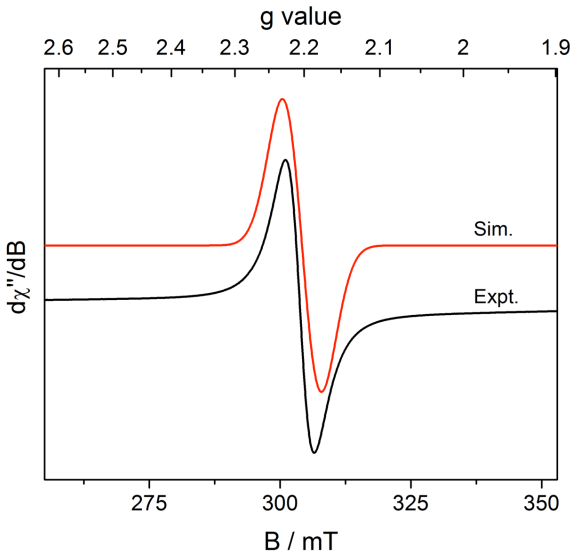

Figure S30. X-Band EPR spectrum of [(^{ipc}ADI)NiCl] (**7**) recorded at 298 K in toluene (g = 2.203, Gaussian Broadening = 7.5).

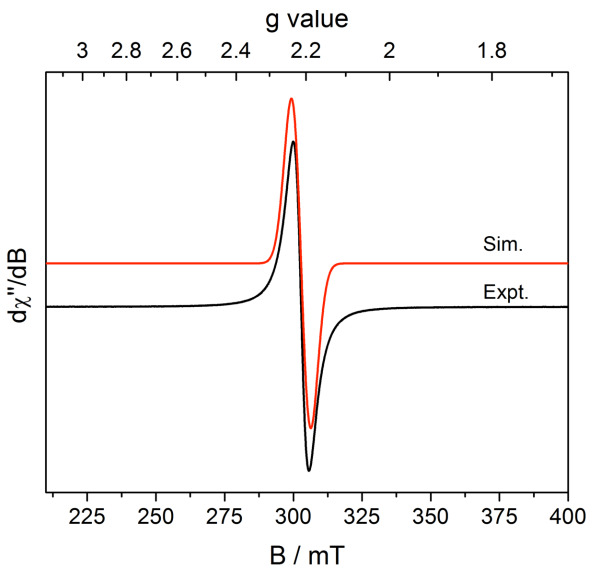

Figure S31. X-Band EPR spectrum of [(^{ipc}ADI)NiBr] (**8**) recorded at 298 K in toluene (g = 2.212, Gaussian Broadening = 3.5).

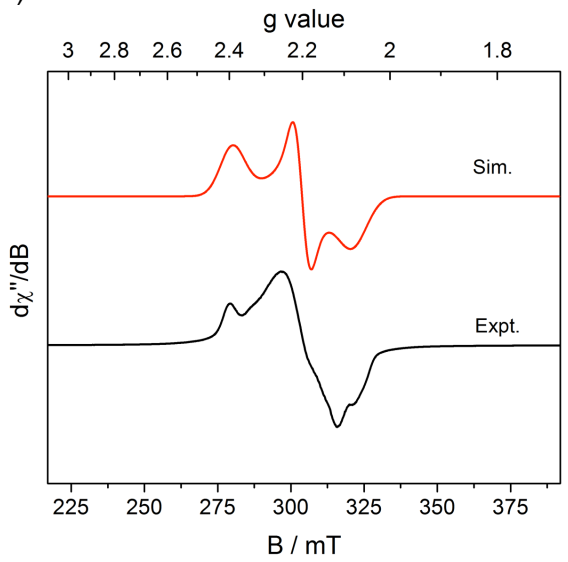

Figure S32. X-Band EPR spectrum of [(^{ipc}ADI)NiBr] (**8**) recorded at 10 K in toluene (g_x = 2.310, g_y = 2.205, g_z = 2.135; $g_{strain}(x)$ = 0.044, $g_{strain}(y)$ = 0.023, $g_{strain}(z)$ = 0.022).

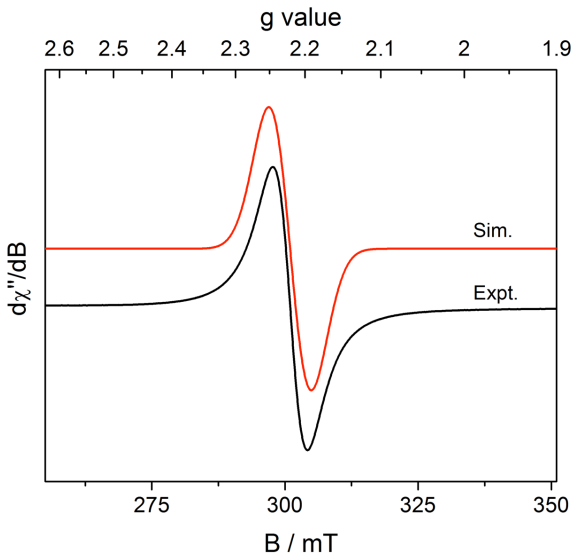

Figure S33. X-Band EPR spectrum of [(^{ipc}ADI)NiI] (**9**) recorded at 298 K in toluene (g = 2.205, Gaussian Broadening = 8.0).

XVI. NMR Spectra

XVI.A. NMR Spectra of Nickel Compounds

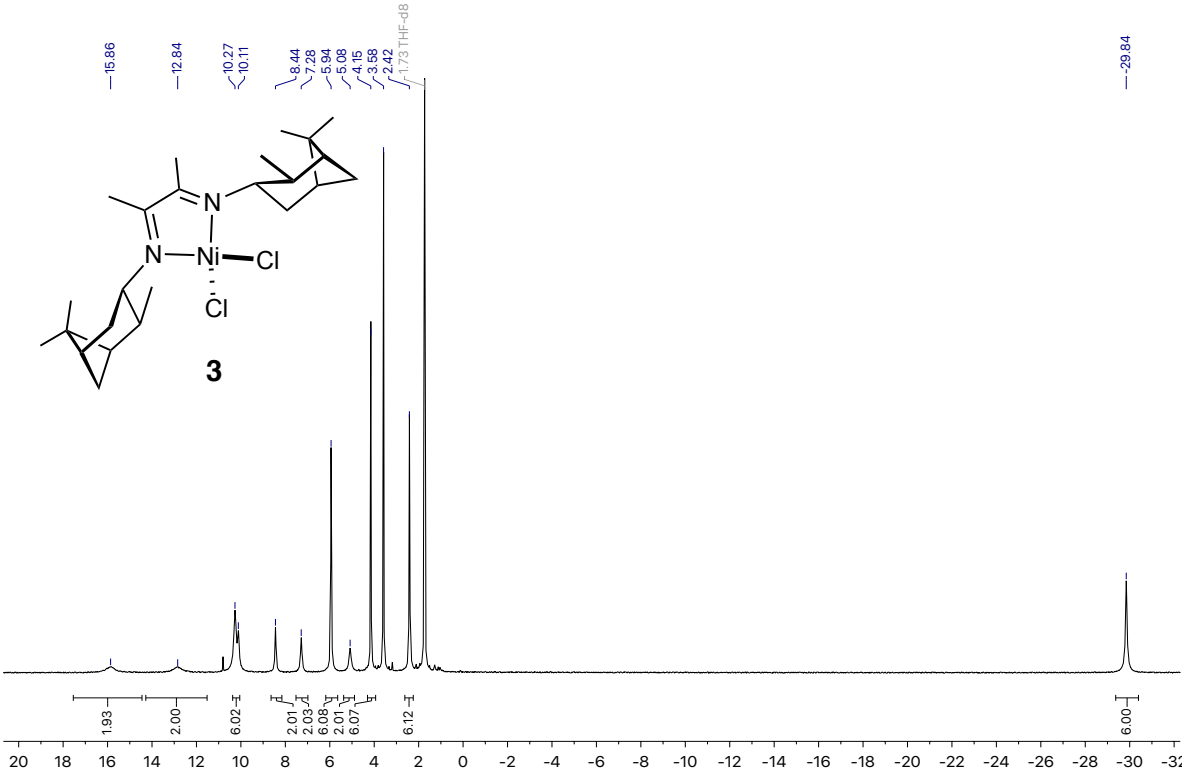

Figure S34. ^{1}H NMR (300 MHz, THF-d_8) of **3**.

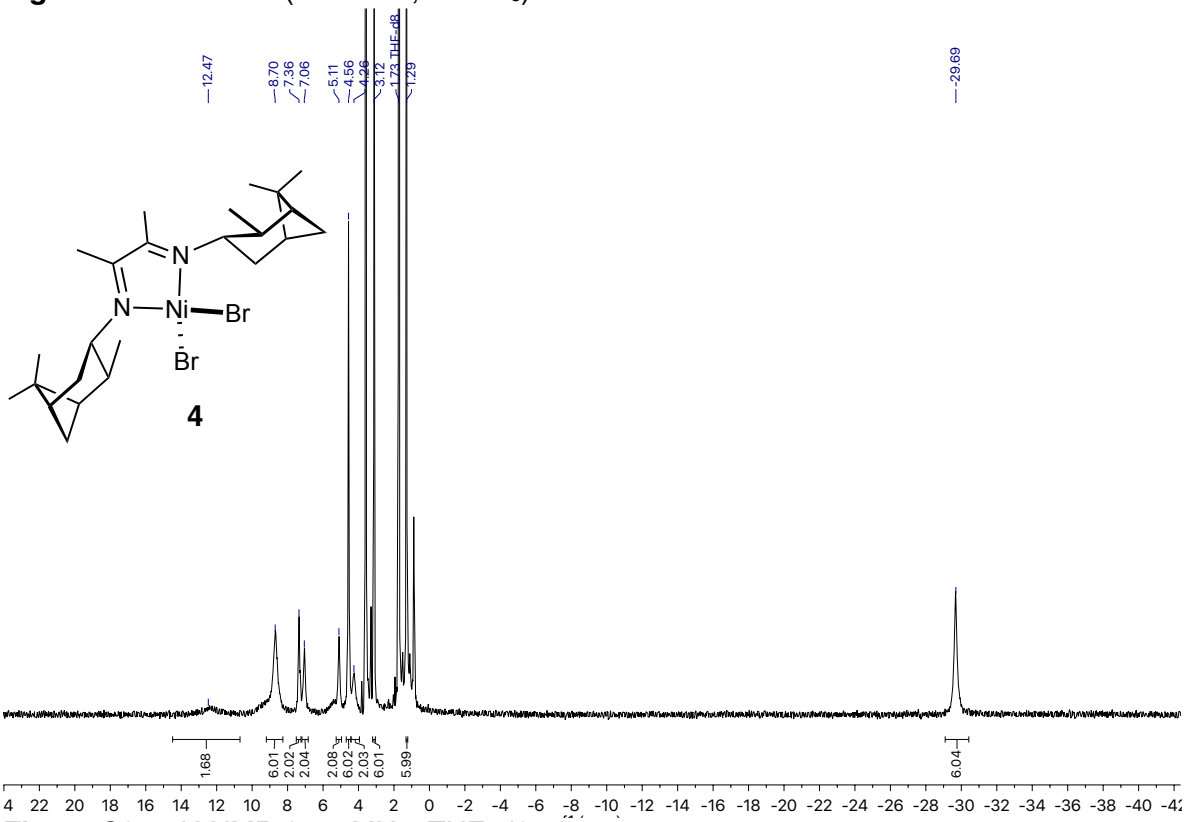

Figure S35. ^{1}H NMR (300 MHz, THF-d_8) of **4**.

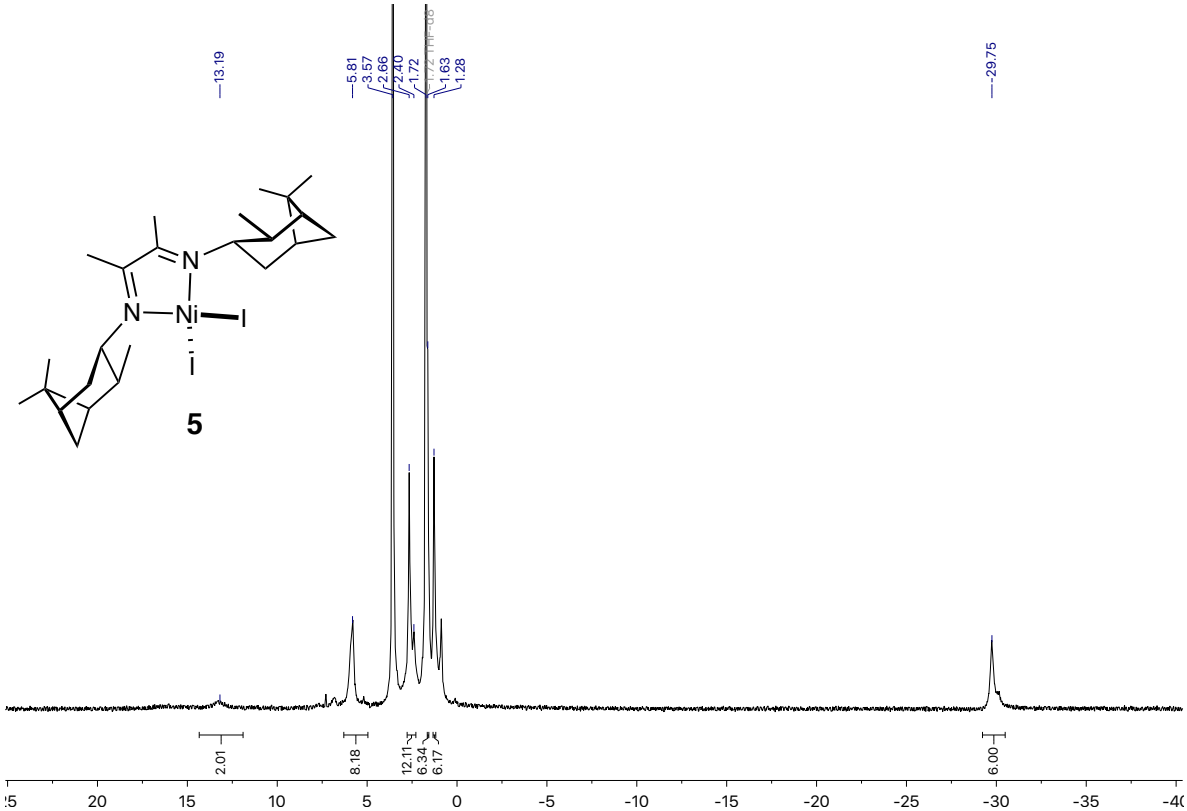

Figure S36. ^{1}H NMR (300 MHz, THF-d_8) of **5**.

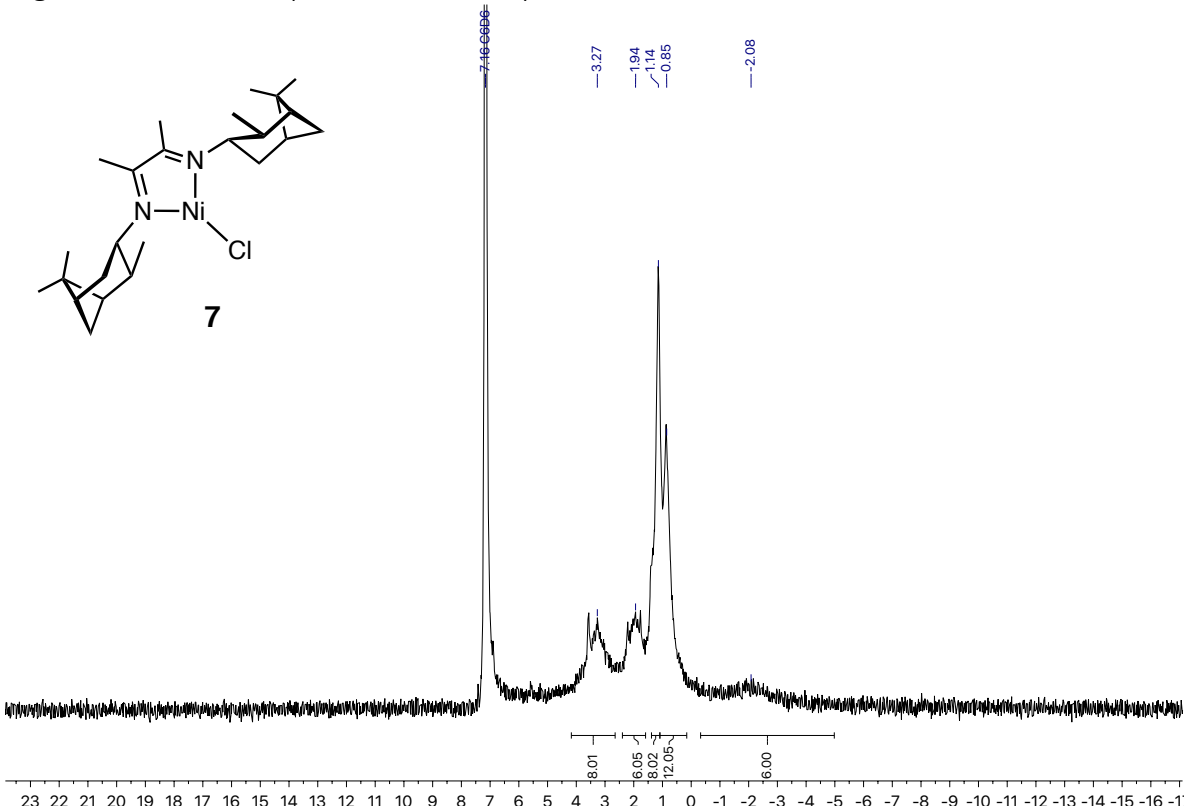

Figure S37. ^{1}H NMR (300 MHz, benzene-d_6) of **7**.

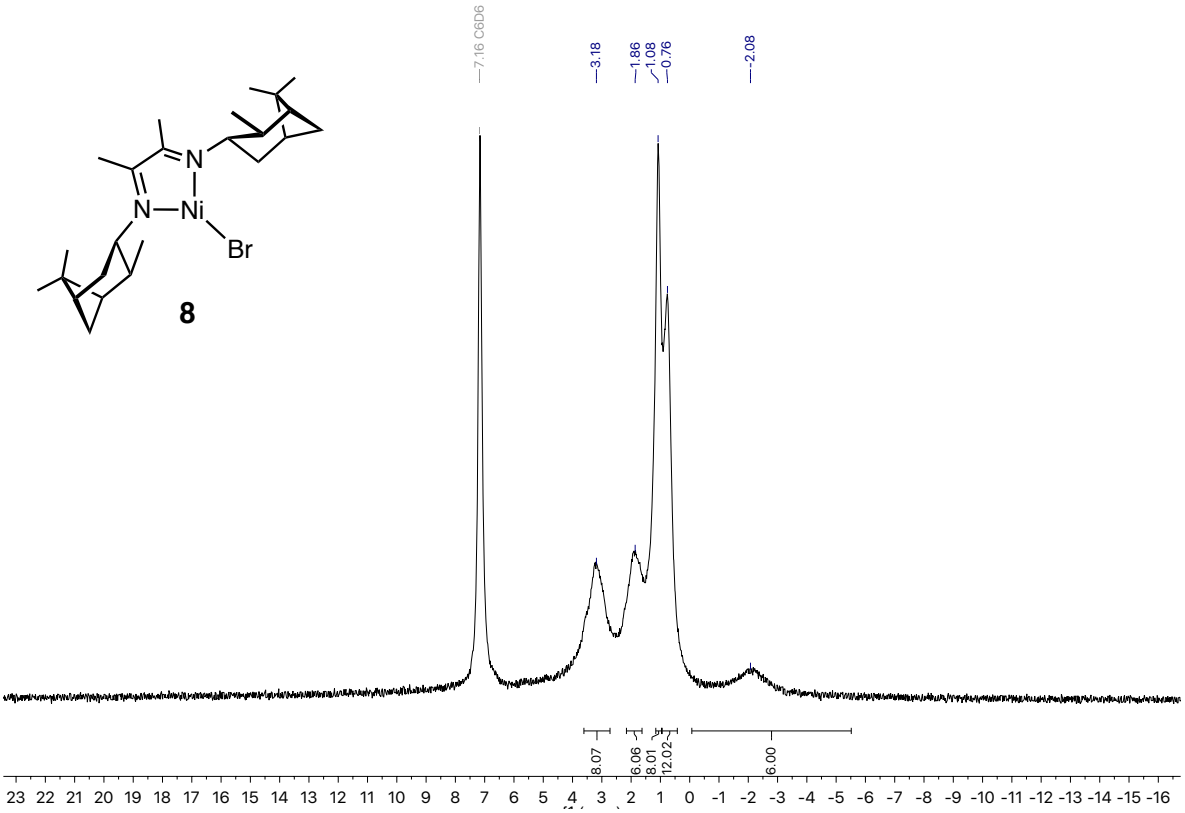

Figure S38. ^{1}H NMR (300 MHz, benzene-d_6) of **8**.

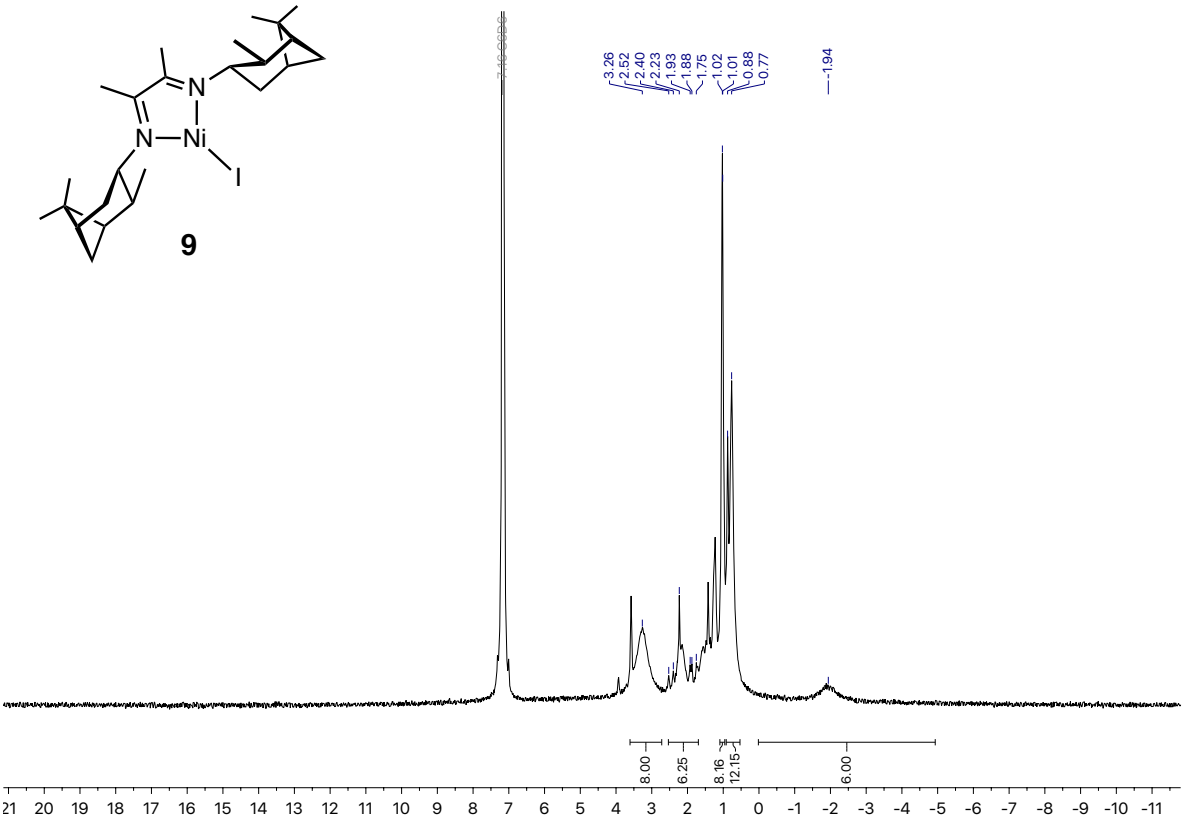

Figure S39. ^{1}H NMR (300 MHz, benzene-d_6) of **9**.

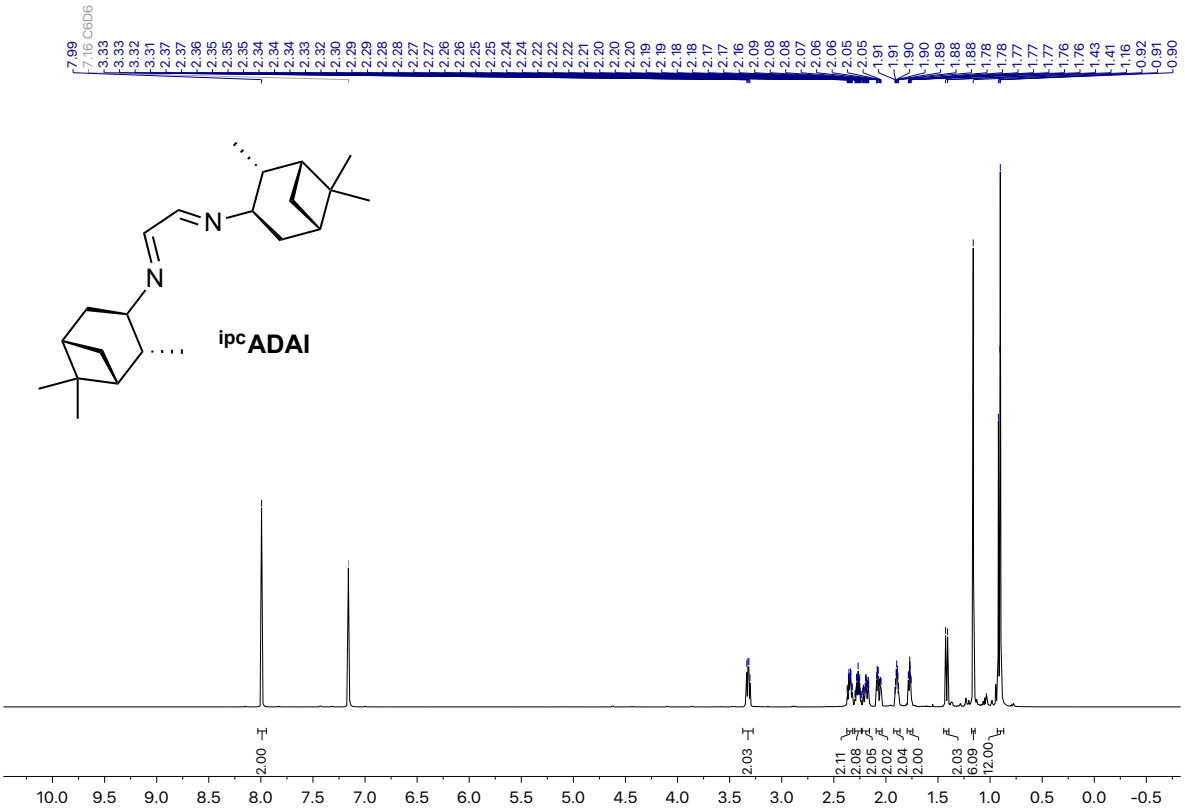

Figure S40. ^{1}H NMR (500 MHz, benzene-d_6) of ^{ipc}**ADAI**.

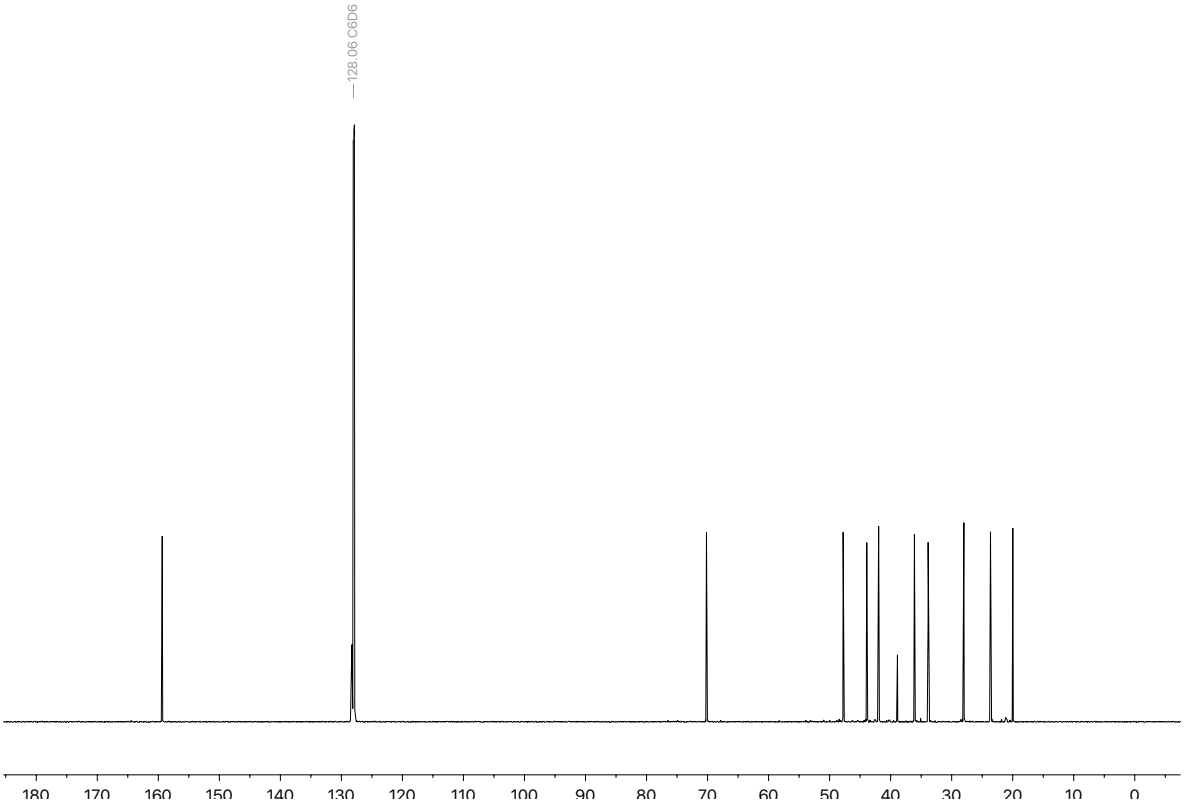

Figure S41. ^{13}C{^{1}H} NMR (126 MHz, benzene-d_6) of ^{ipc}**ADAI**.

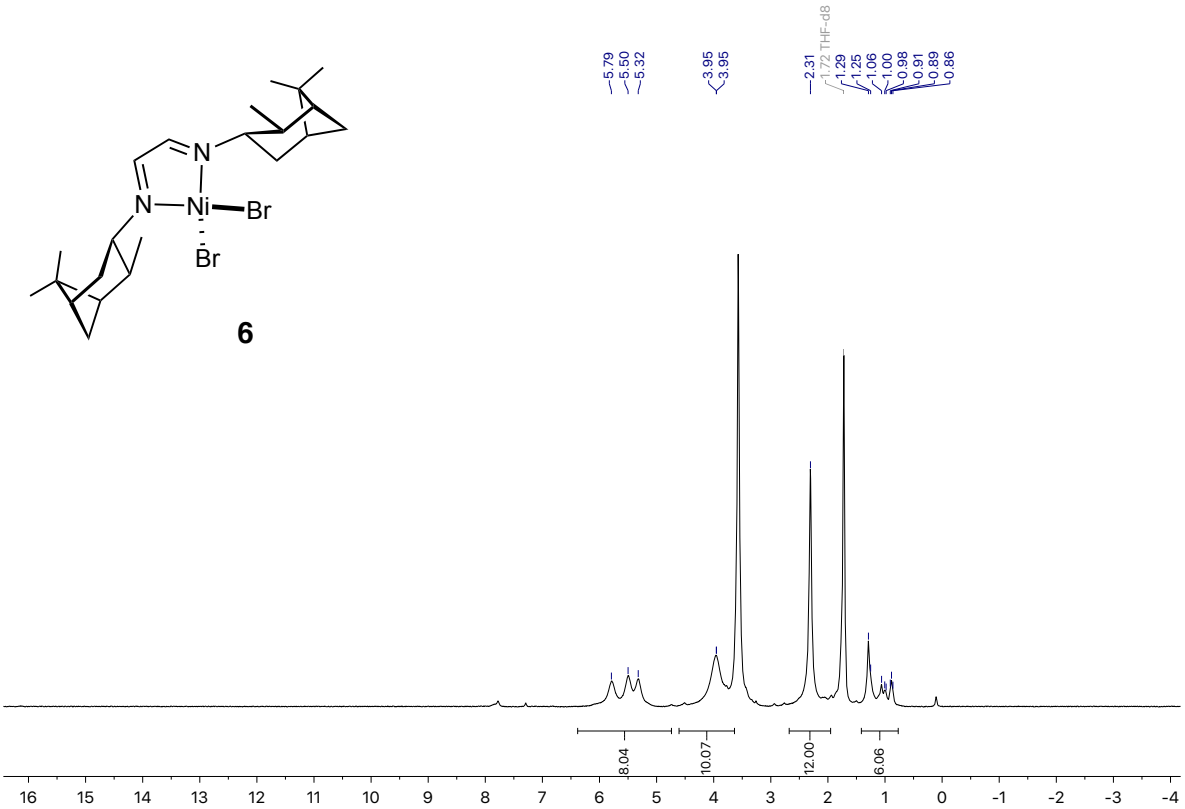

Figure S42. ^{1}H NMR (300 MHz, THF-d_8) of **6**.

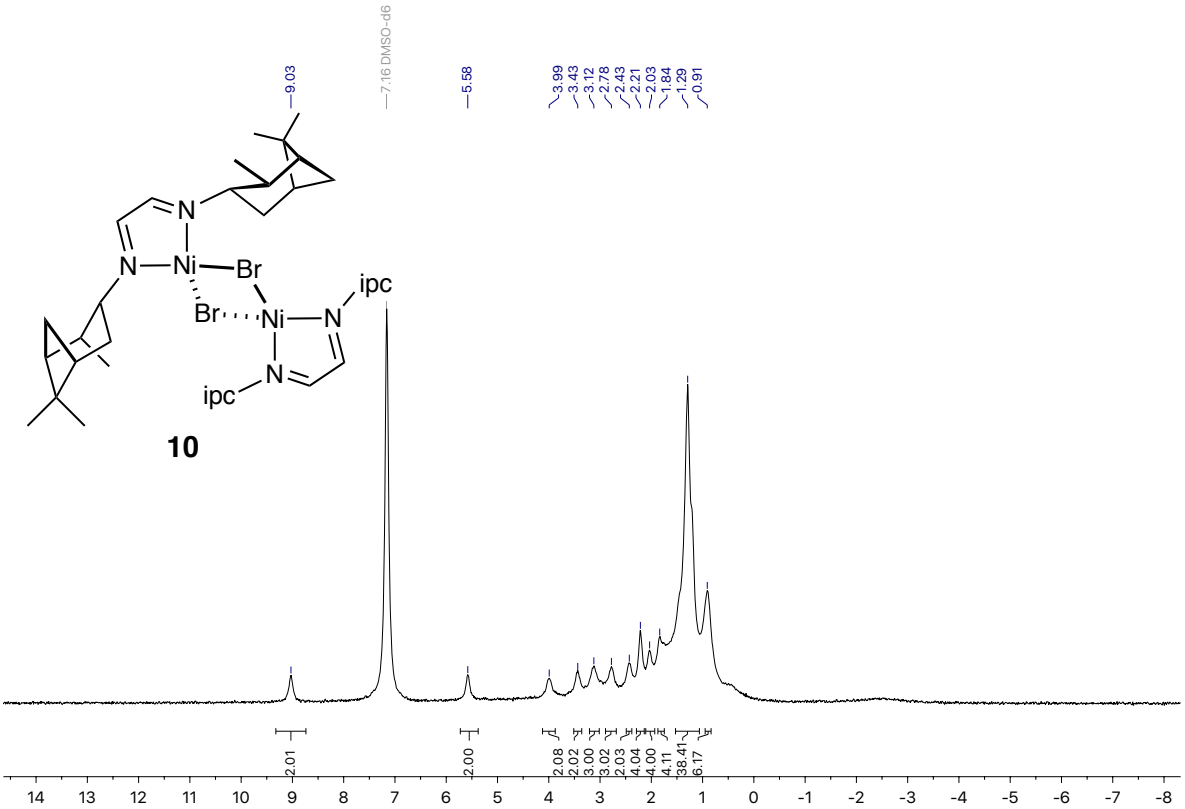

Figure S43. ^{1}H NMR (300 MHz, benzene-d_6) of **10**.

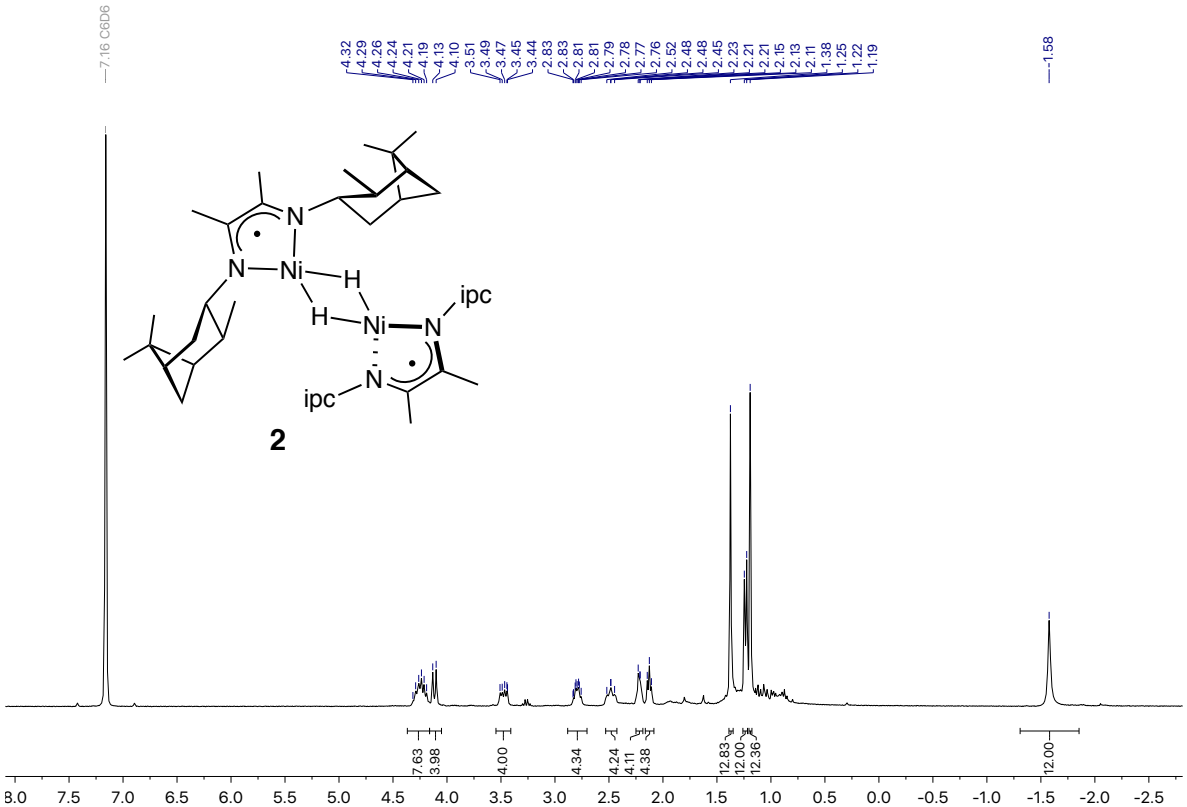

Figure S44. ^{1}H NMR (300 MHz, benzene-d_6) of **2**.

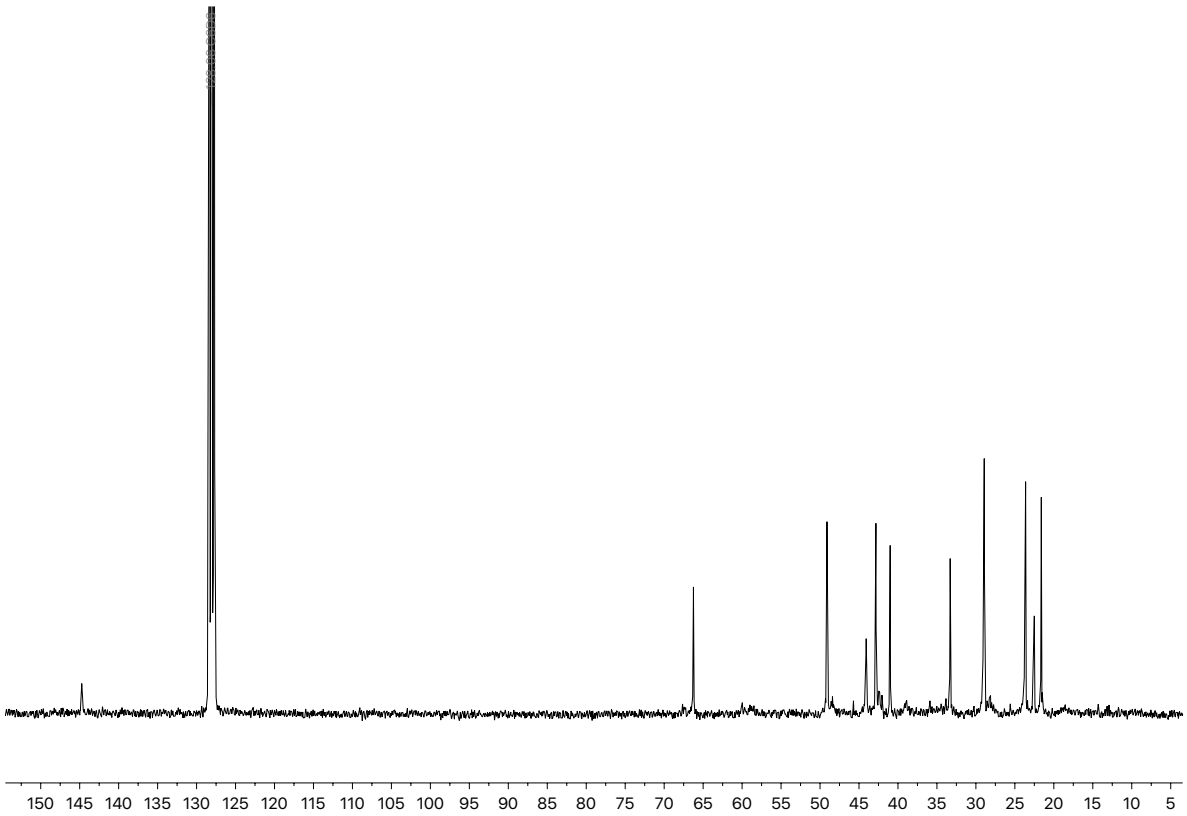

Figure S45. ^{13}C{^{1}H} NMR (75 MHz, benzene-d_6) of **2**.

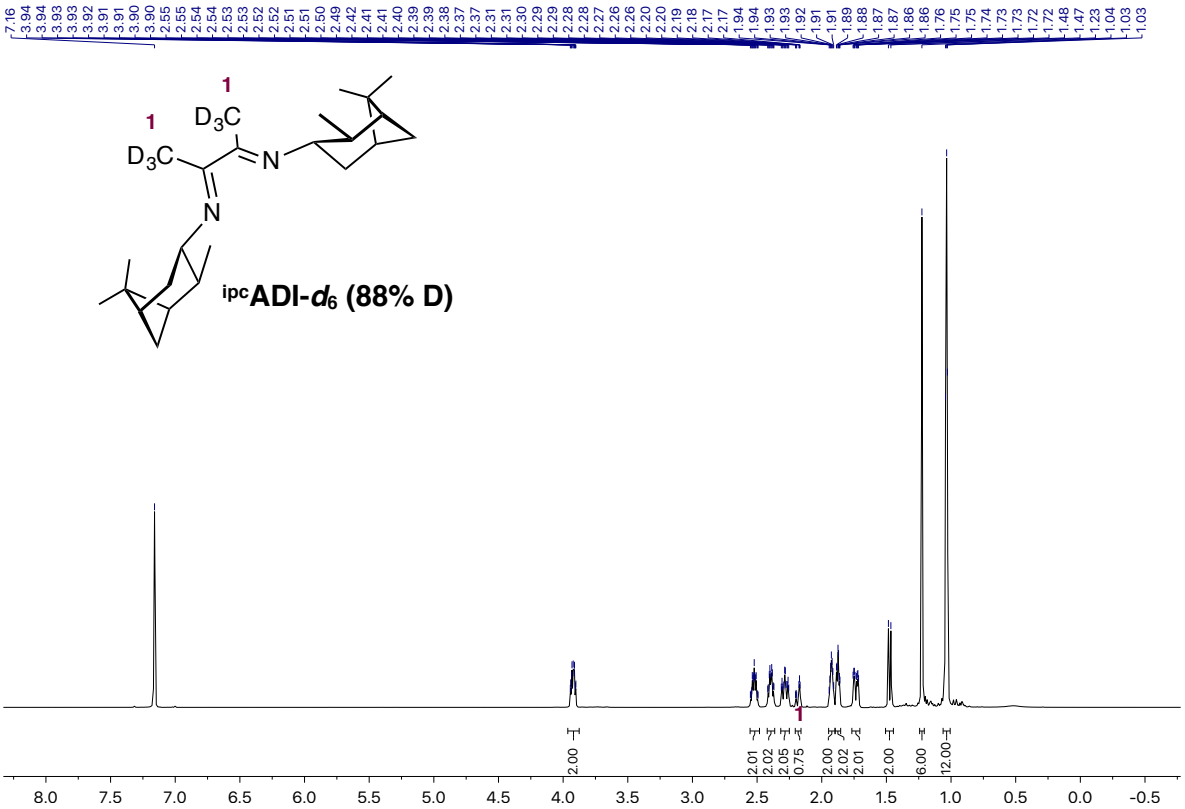

Figure S46. ^{1}H NMR (500 MHz, benzene-d_6) of **^{ipc}ADI-d_6** (88% D).

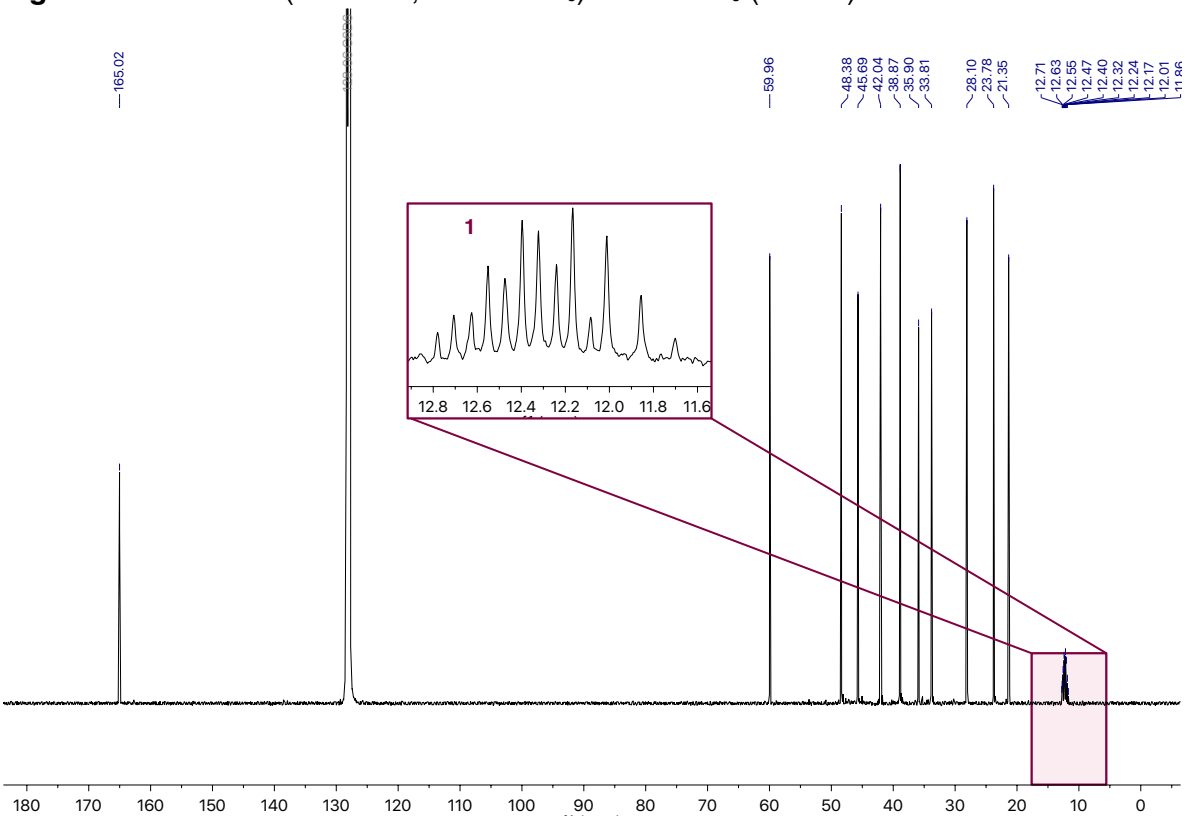

Figure S47. Quantitative ^{13}C{^{1}H} NMR (126 MHz, benzene-d_6) of **^{ipc}ADI-d_6 (88% D)**.

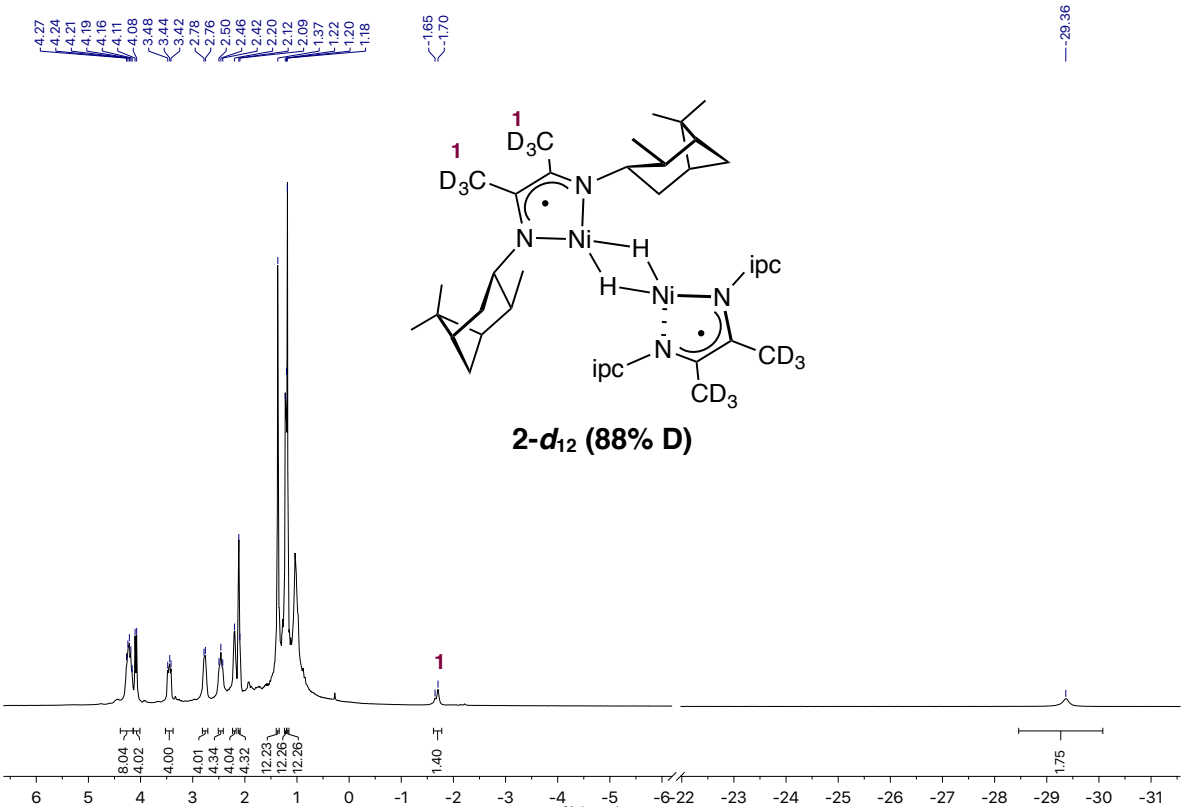

Figure S48. ^{1}H NMR (300 MHz, benzene-d_6) of **2-d_{12}** (88% D).

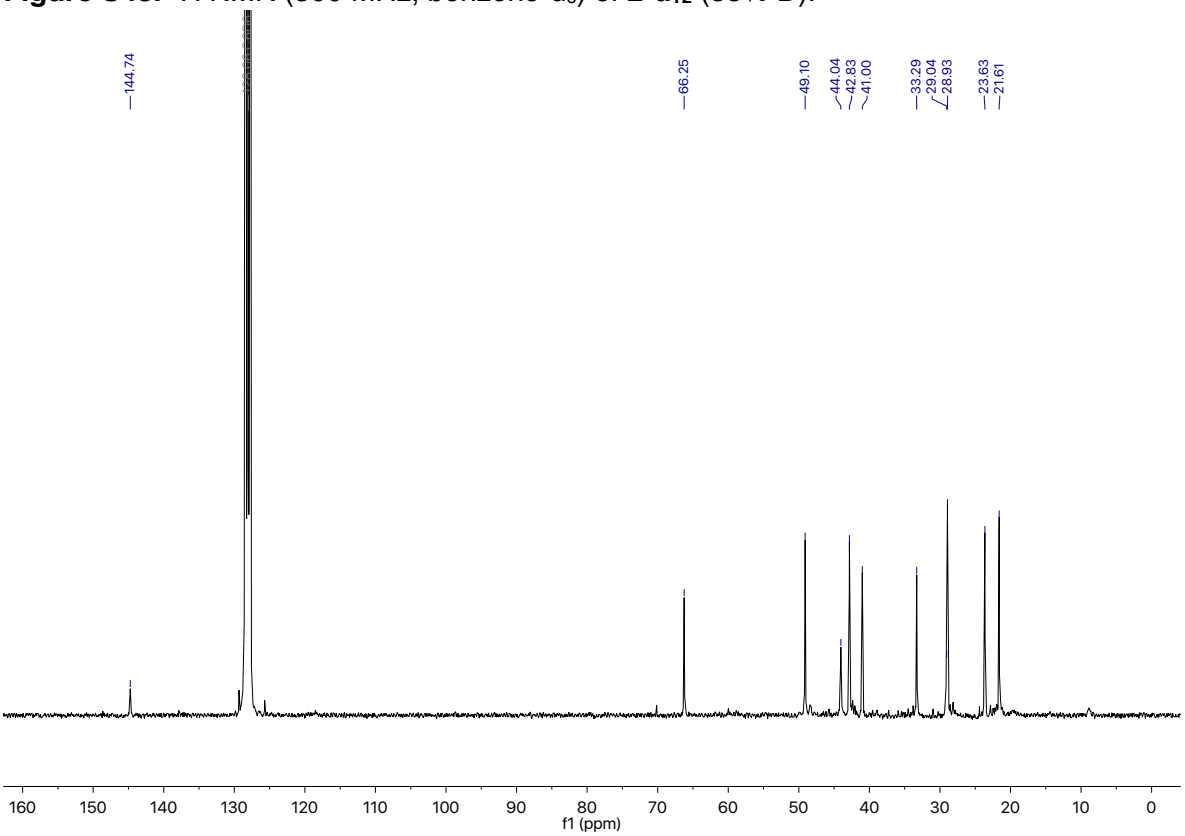

Figure S49. ^{13}C{^{1}H} NMR (75 MHz, benzene-d_6) of **2-d_{12}** (88% D).

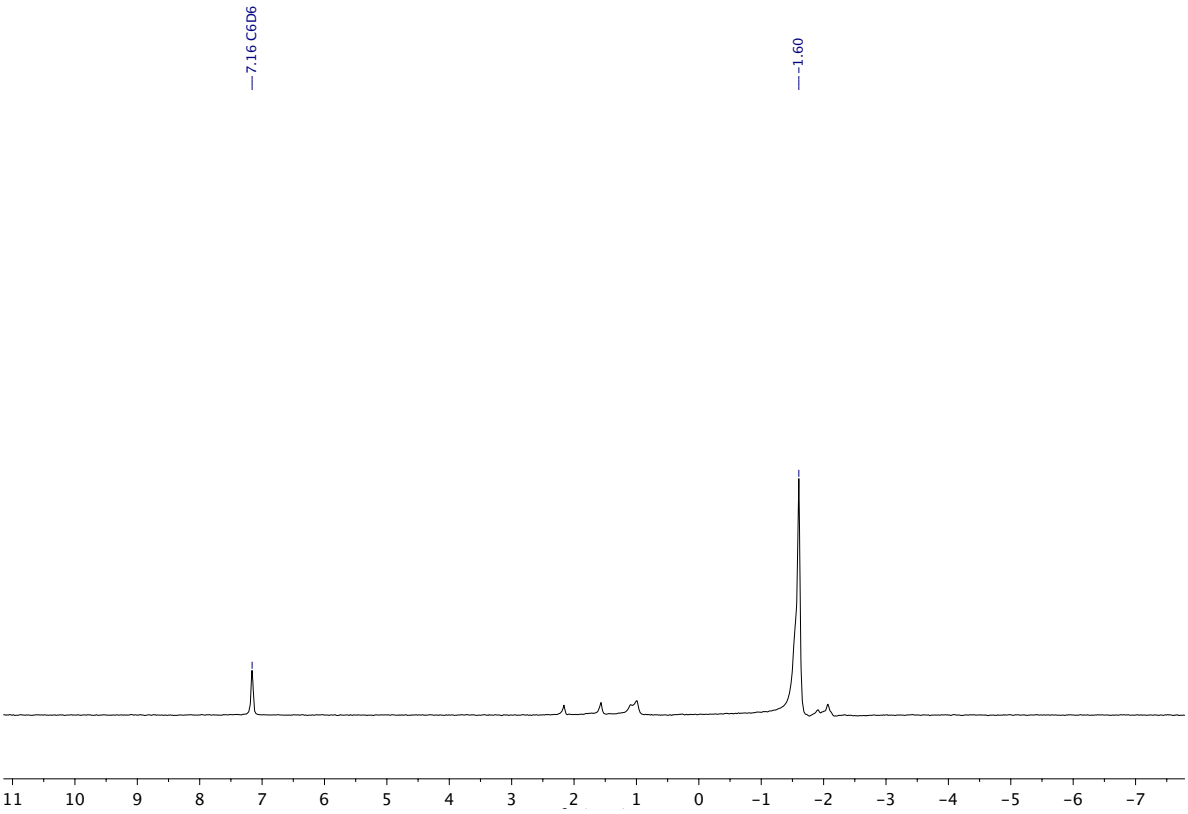

Figure S50. ^{2}H NMR (77 MHz, benzene-d_6) of **2-d_{12}** (88% D).

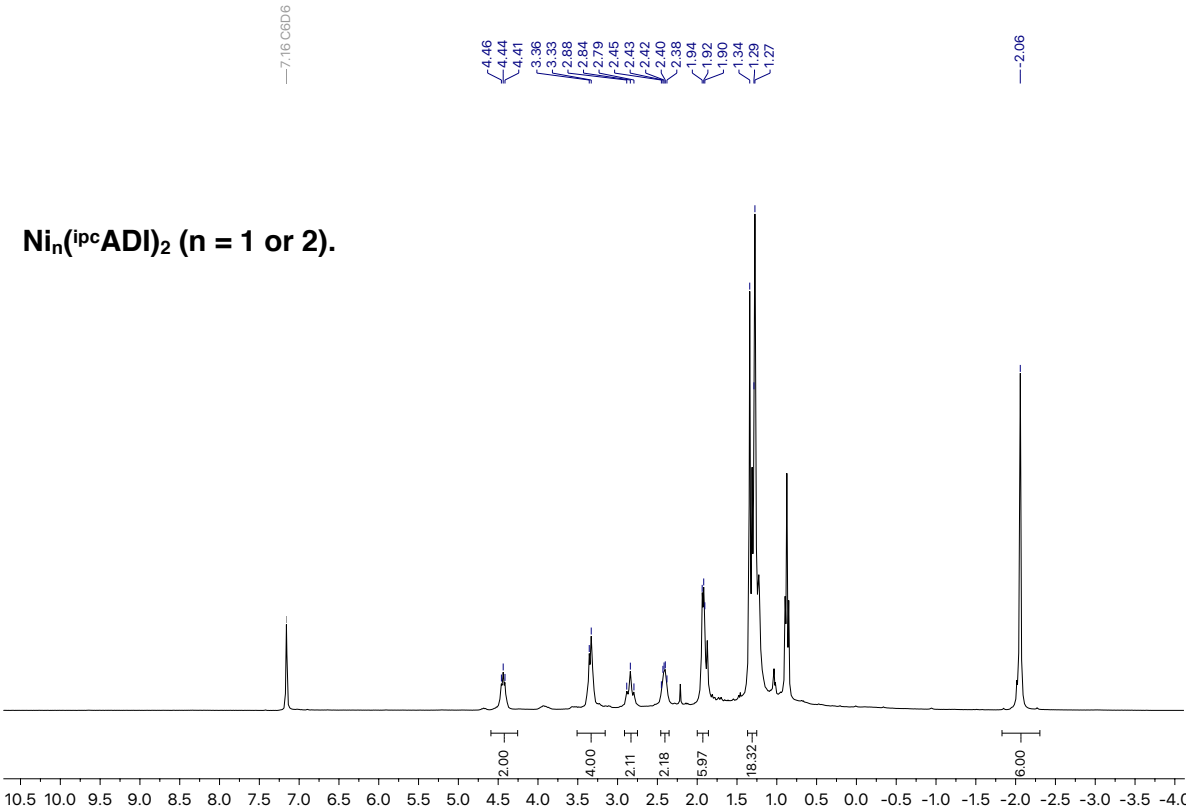

$Ni_n(^{ipc}ADI)_2$ (n = 1 or 2).

Figure S51. ^{1}H NMR (300 MHz, benzene-d_6) of $Ni_n(^{ipc}ADI)_2$ (n = 1 or 2).

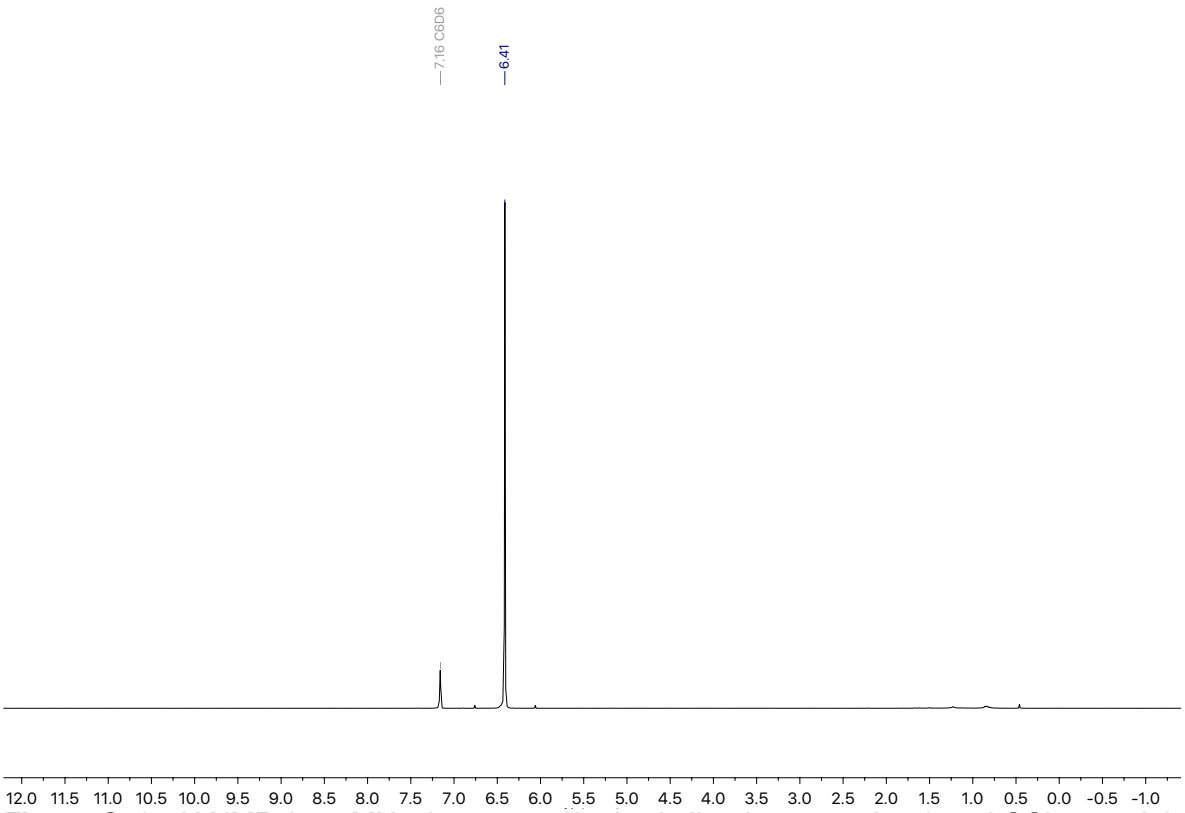

Figure S52. ^{1}H NMR (300 MHz, benzene-d_6) of volatiles from reacting **2** and CCl_4 containing $CHCl_3$.

XVI.B. NMR Spectra of Deuterium Labeled Compounds

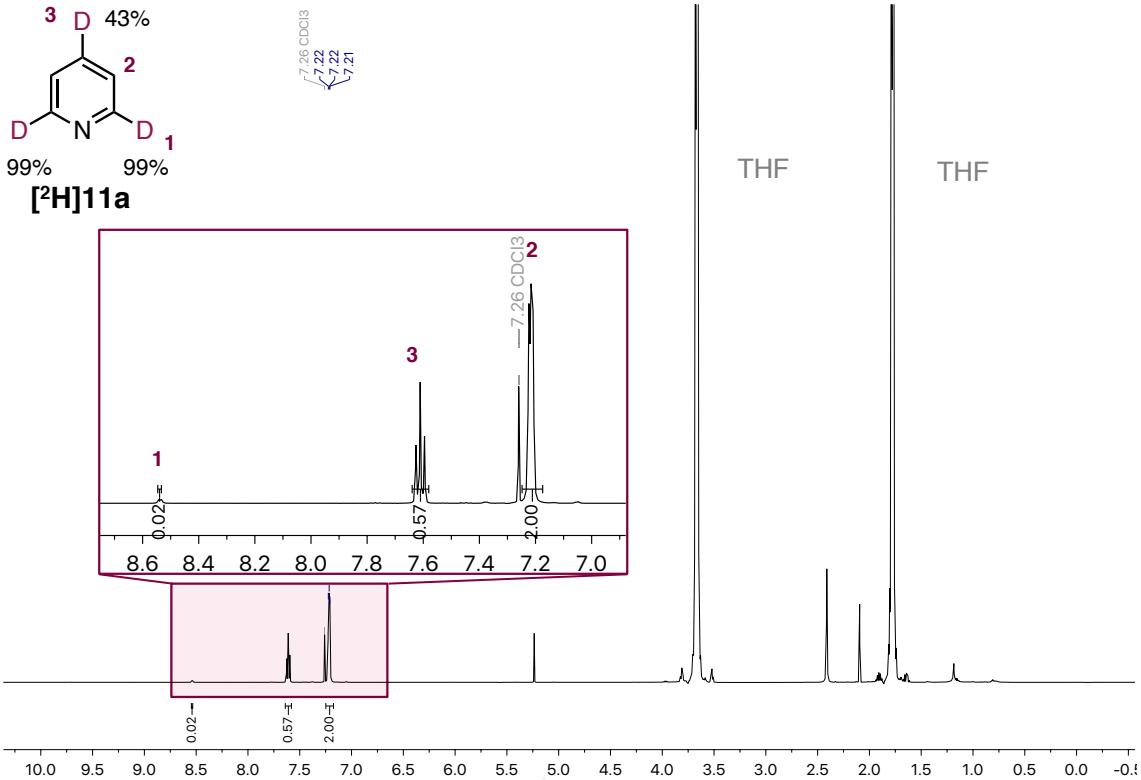

Figure S53. ^{1}H NMR (500 MHz, $CDCl_3$) of labeled pyridine, **[^{2}H]11a**.

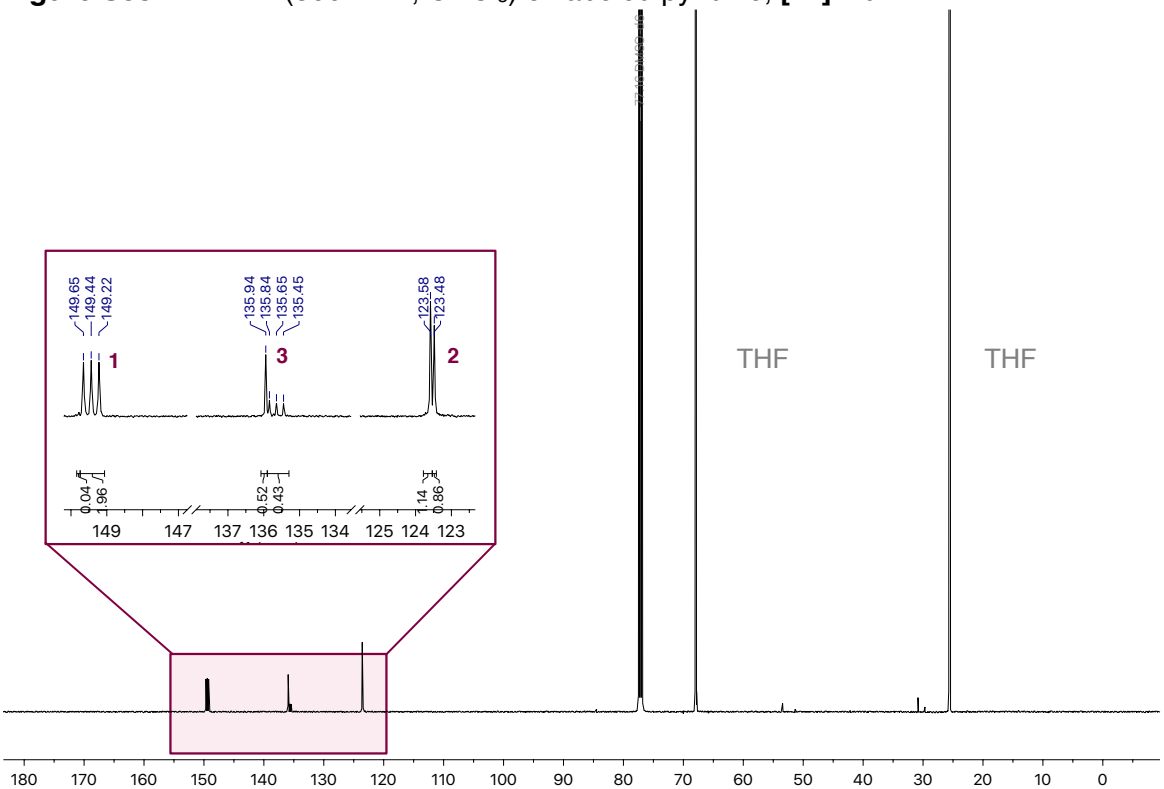

Figure S54. Quantitative ^{13}C{^{1}H} NMR (126 MHz, $CDCl_3$) of **[^{2}H]11a**.

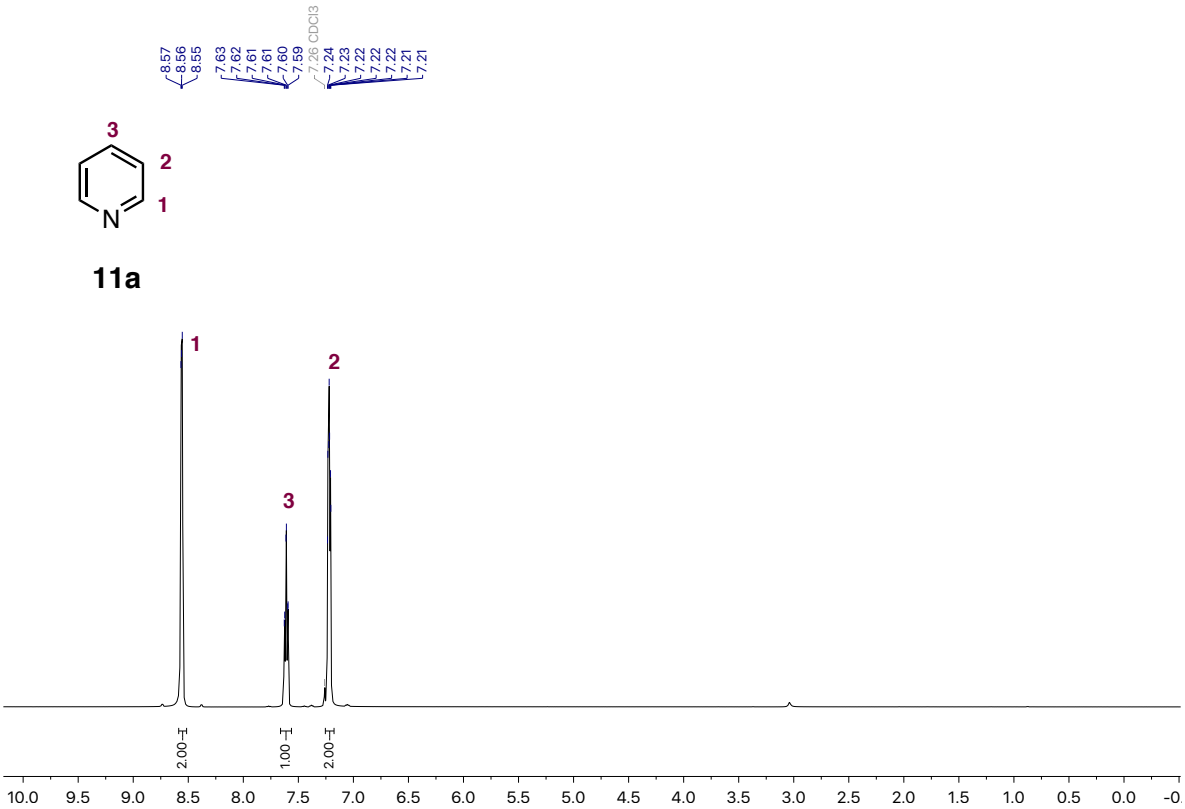

Figure S55. ^{1}H NMR (500 MHz, $CDCl_3$) of unlabeled pyridine, **11a**.

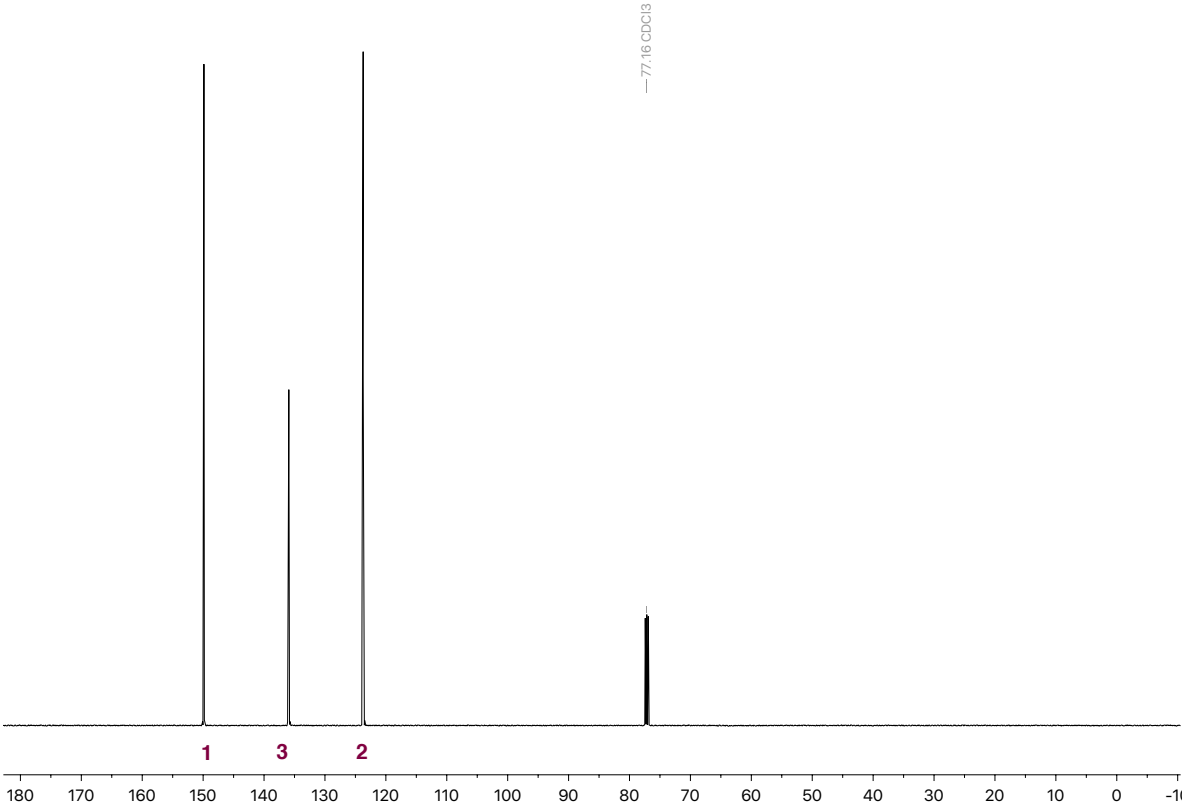

Figure S56. ^{13}C{^{1}H} NMR (126 MHz, $CDCl_3$) of **11a**.

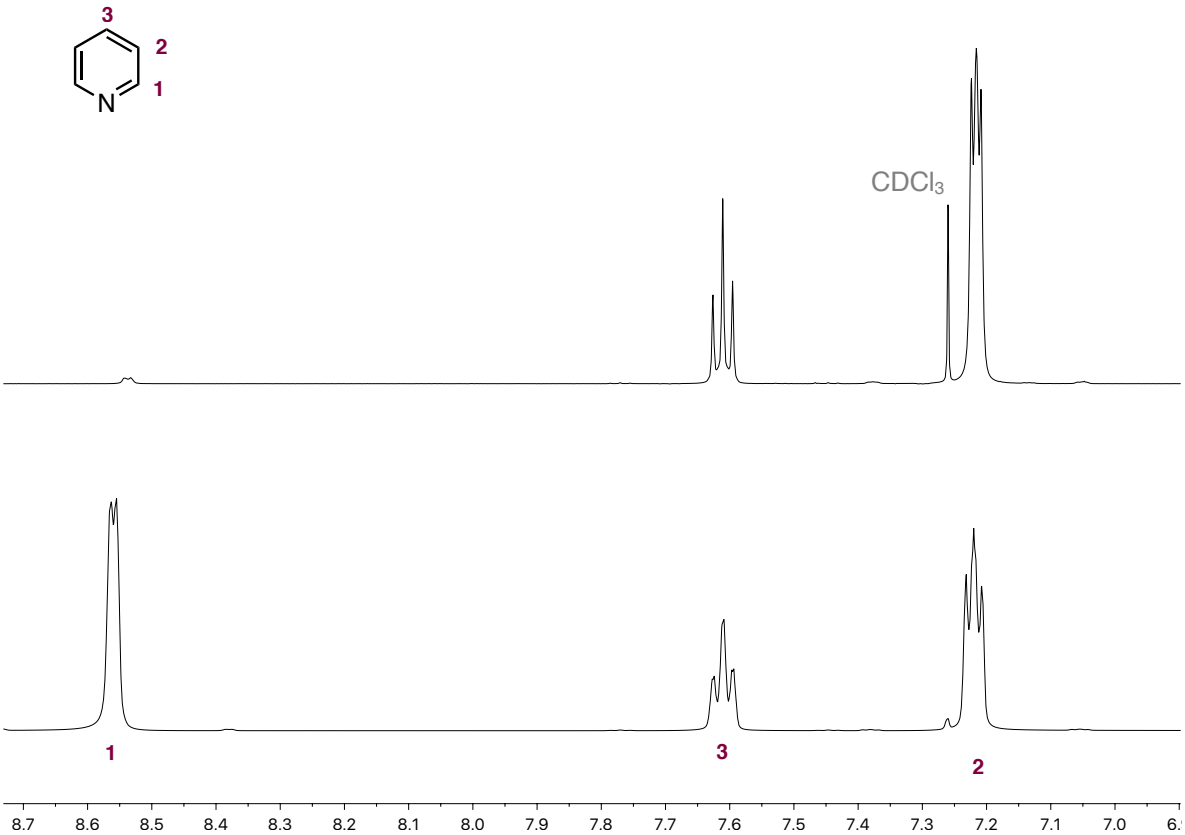

Figure S57. Stacked ^{1}H NMR spectra of pyridine: labeled, **[^{2}H]11a** (first) and unlabeled, **11a** (second).

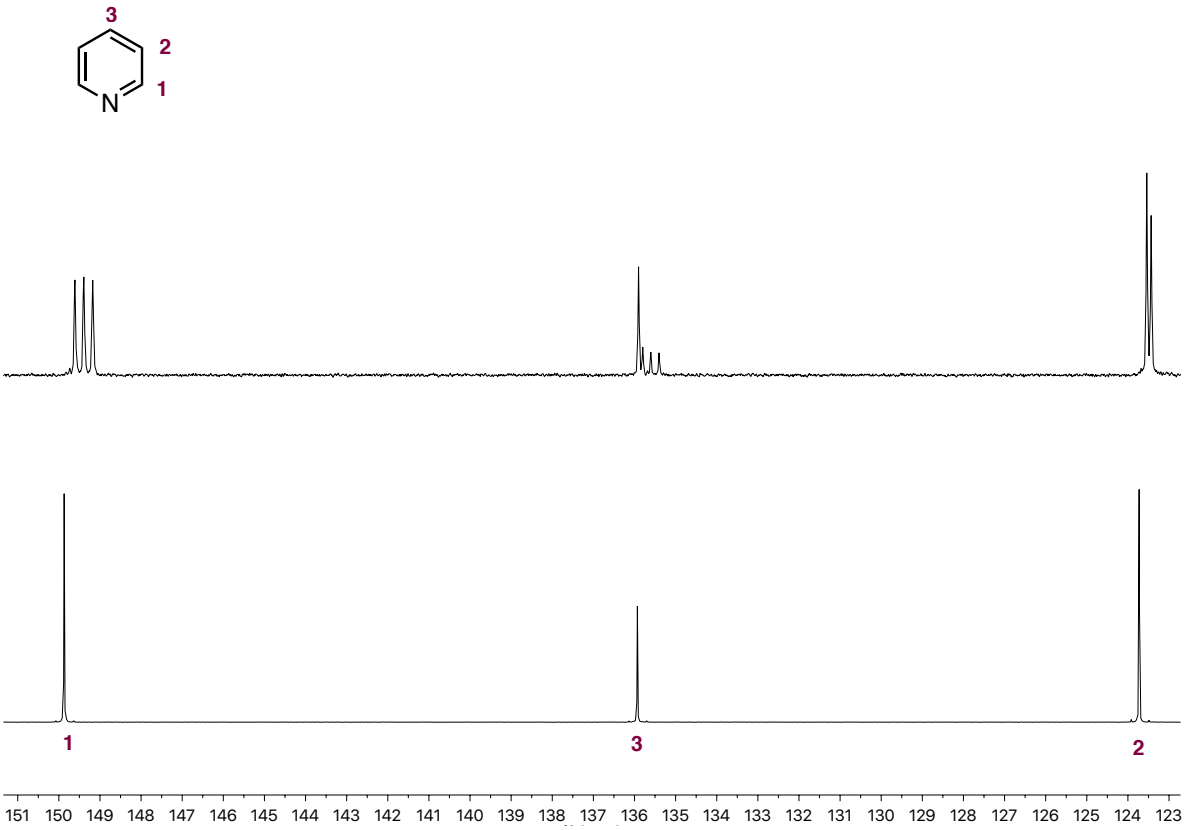

Figure S58. Stacked $^{13}C\{^{1}H\}$ NMR spectra of pyridine: labeled, **[^{2}H]11a** (first, quantitative) and unlabeled, **11a** (second).

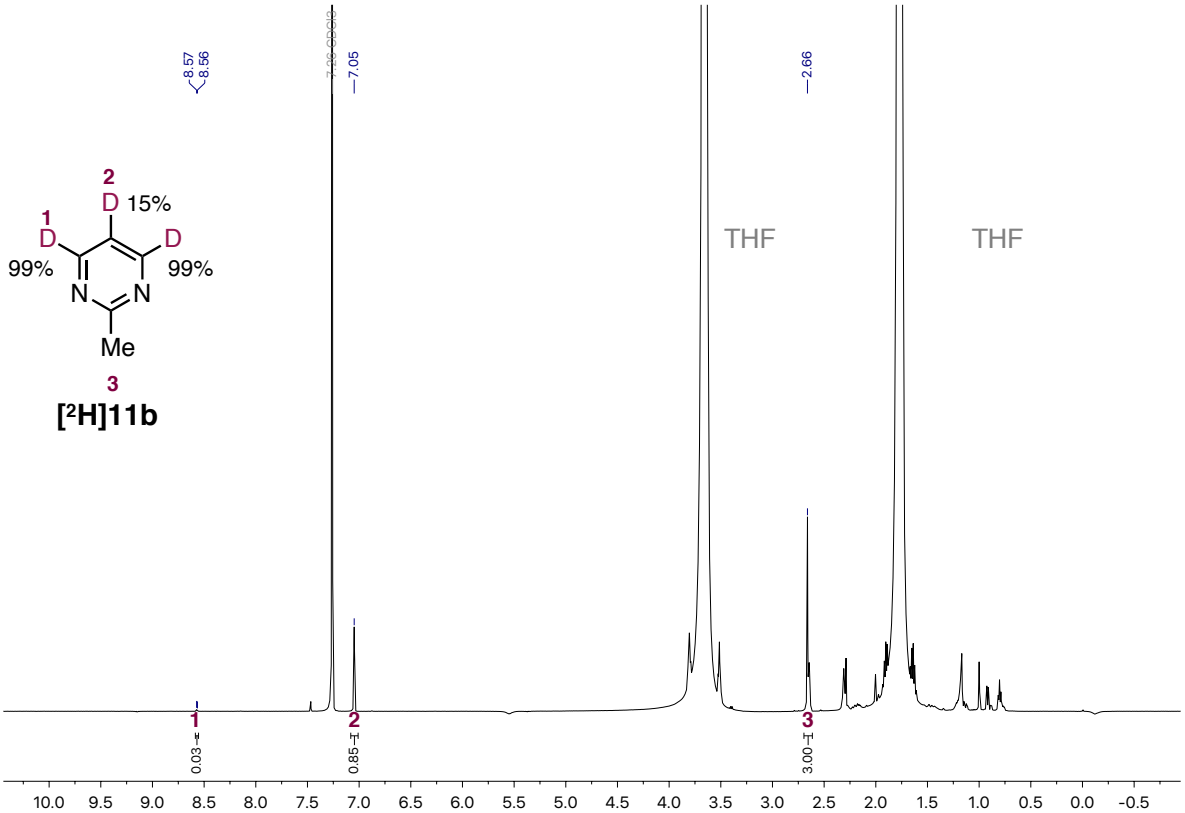

Figure S59. ^{1}H NMR (500 MHz, $CDCl_3$) of labeled 2-methylpyrimidine, **[^{2}H]11b**.

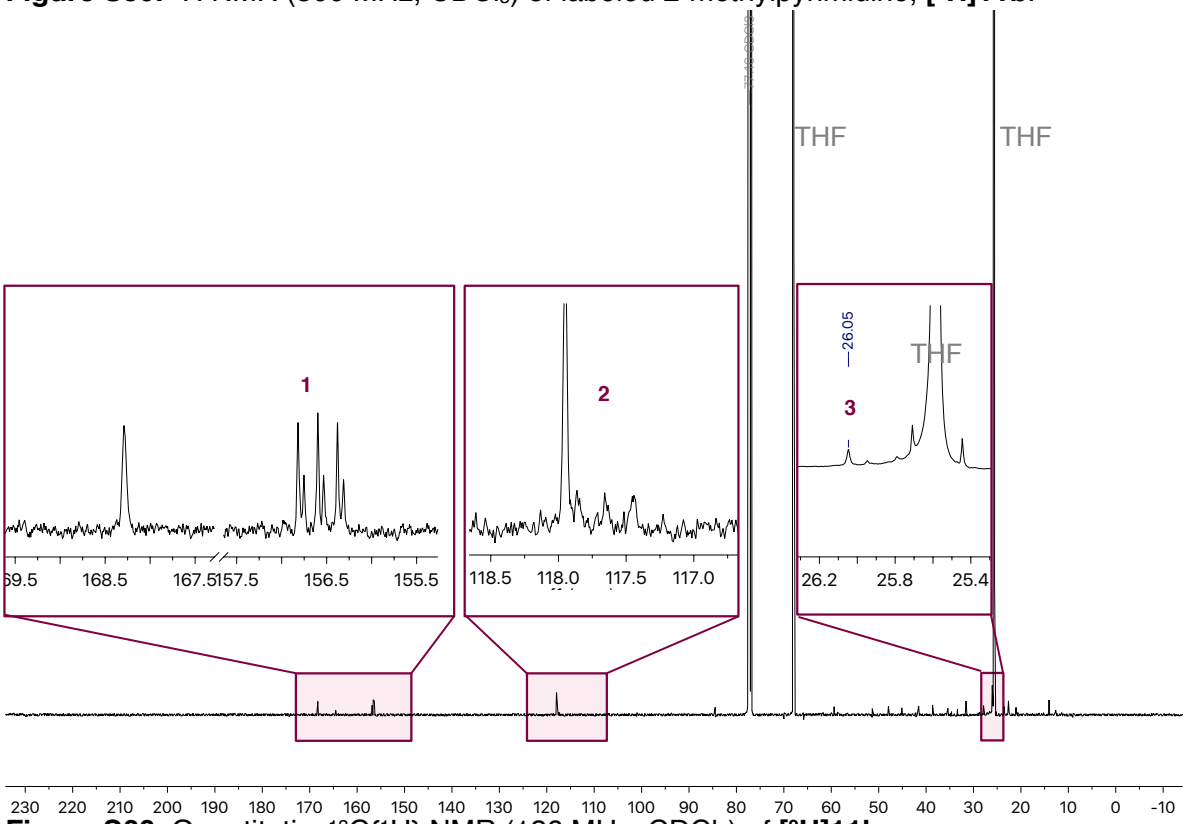

Figure S60. Quantitative ^{13}C{^{1}H} NMR (126 MHz, $CDCl_3$) of **[^{2}H]11b**.

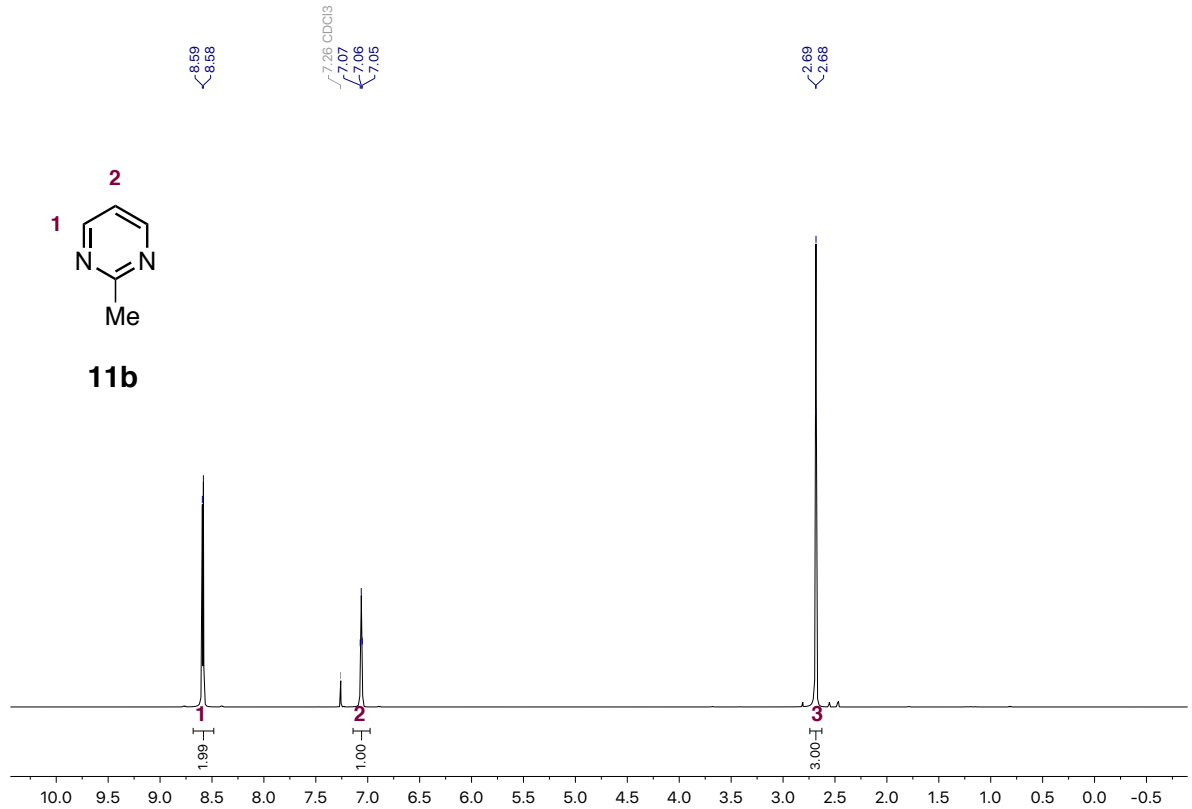

Figure S61. ^{1}H NMR (500 MHz, $CDCl_3$) of unlabeled 2-Methylpyrimidine, **11b**.

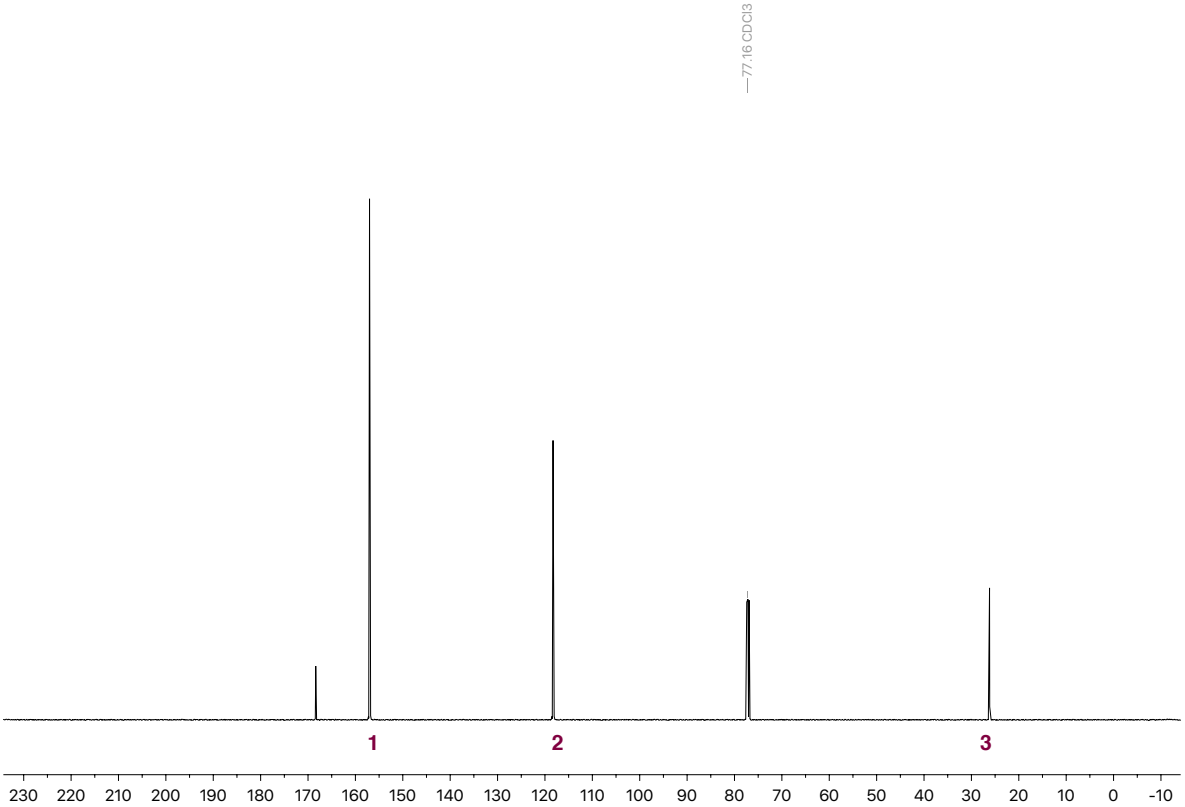

Figure S62. ^{13}C{^{1}H} NMR (126 MHz, $CDCl_3$) of **11b**.

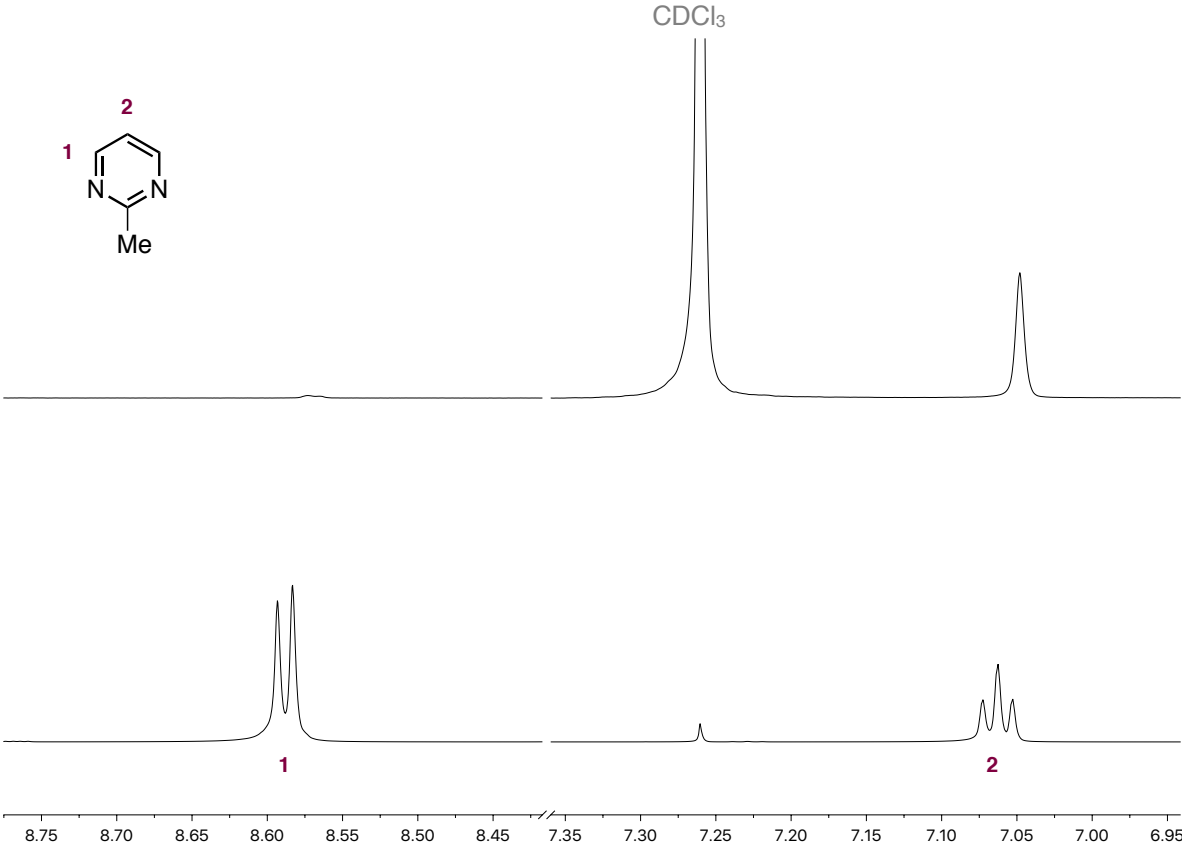

Figure S63. Stacked ^{1}H NMR spectra of 2-methylpyrimidine: labeled, **[^{2}H]11b** (first) and unlabeled, **11b** (second).

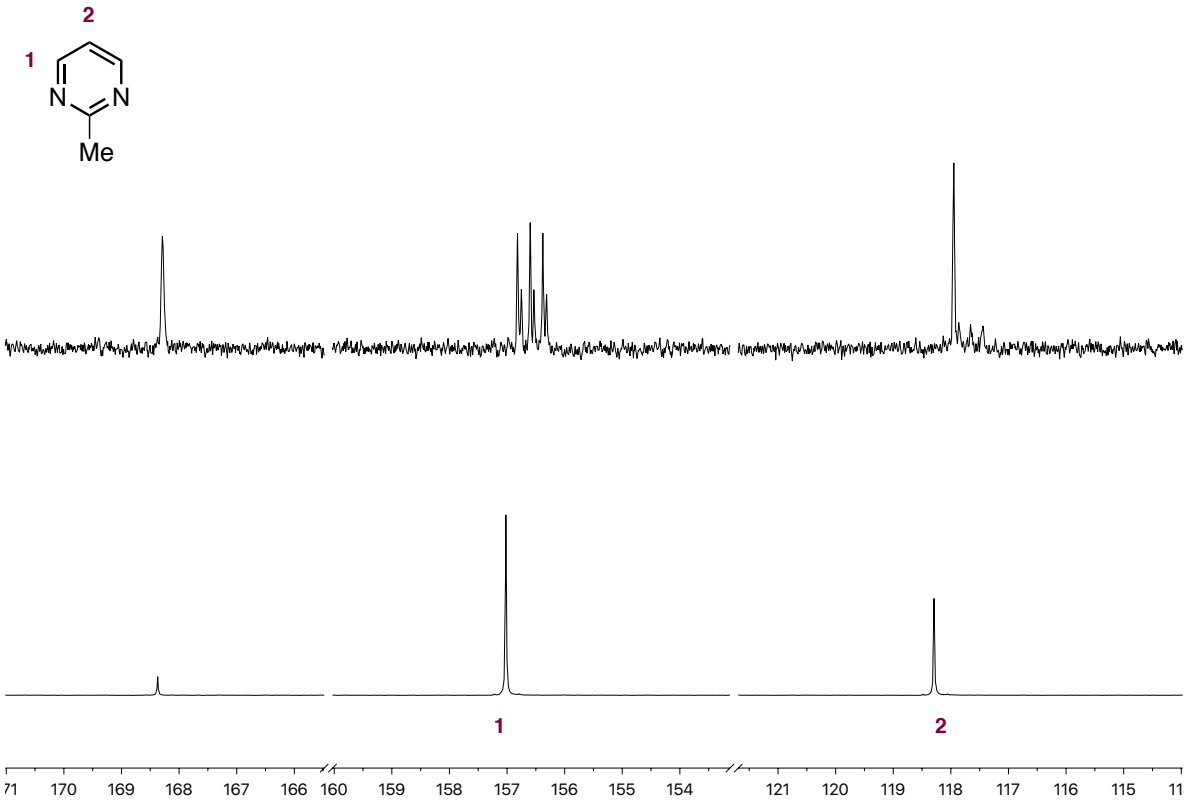

Figure S64. Stacked $^{13}C\{^{1}H\}$ NMR spectra of 2-methylpyrimidine: labeled, **[^{2}H]11b** (first, quantitative) and unlabeled, **11b** (second).

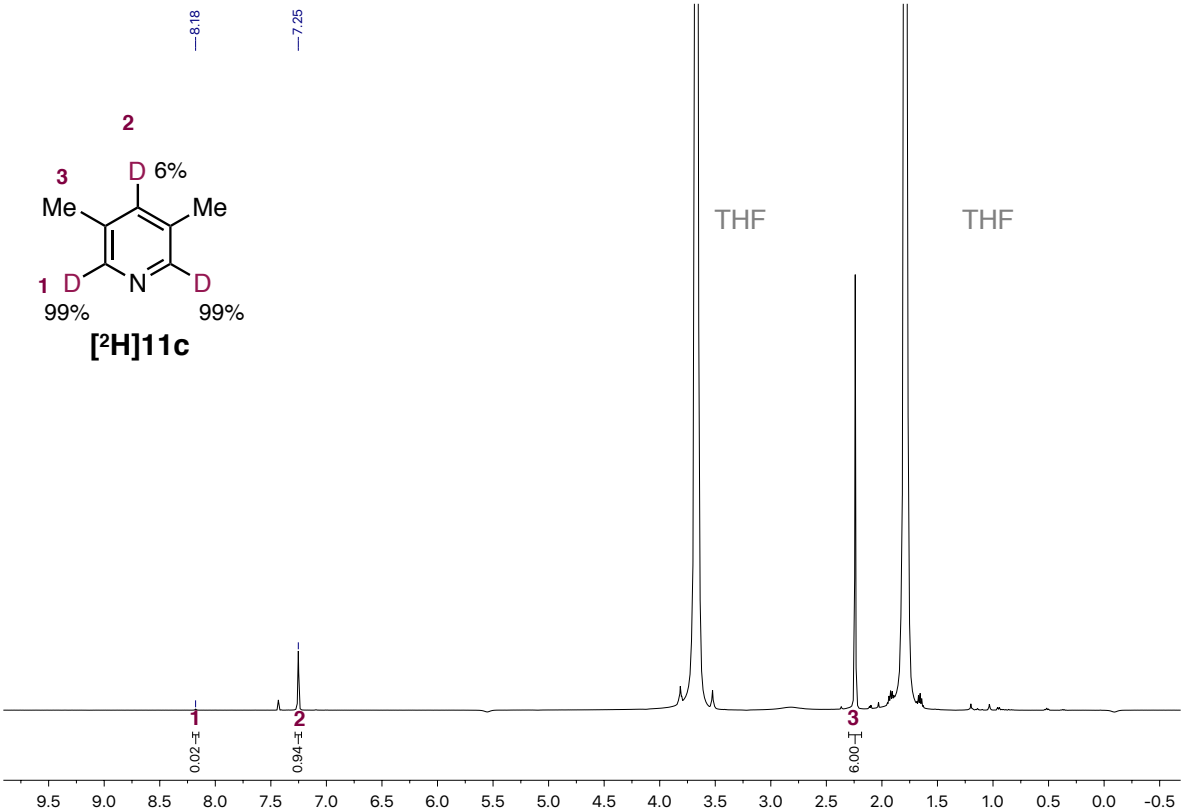

Figure S65. ^{1}H NMR (500 MHz, $CDCl_3$) of labeled 3,5-lutidine, **[^{2}H]11c**.

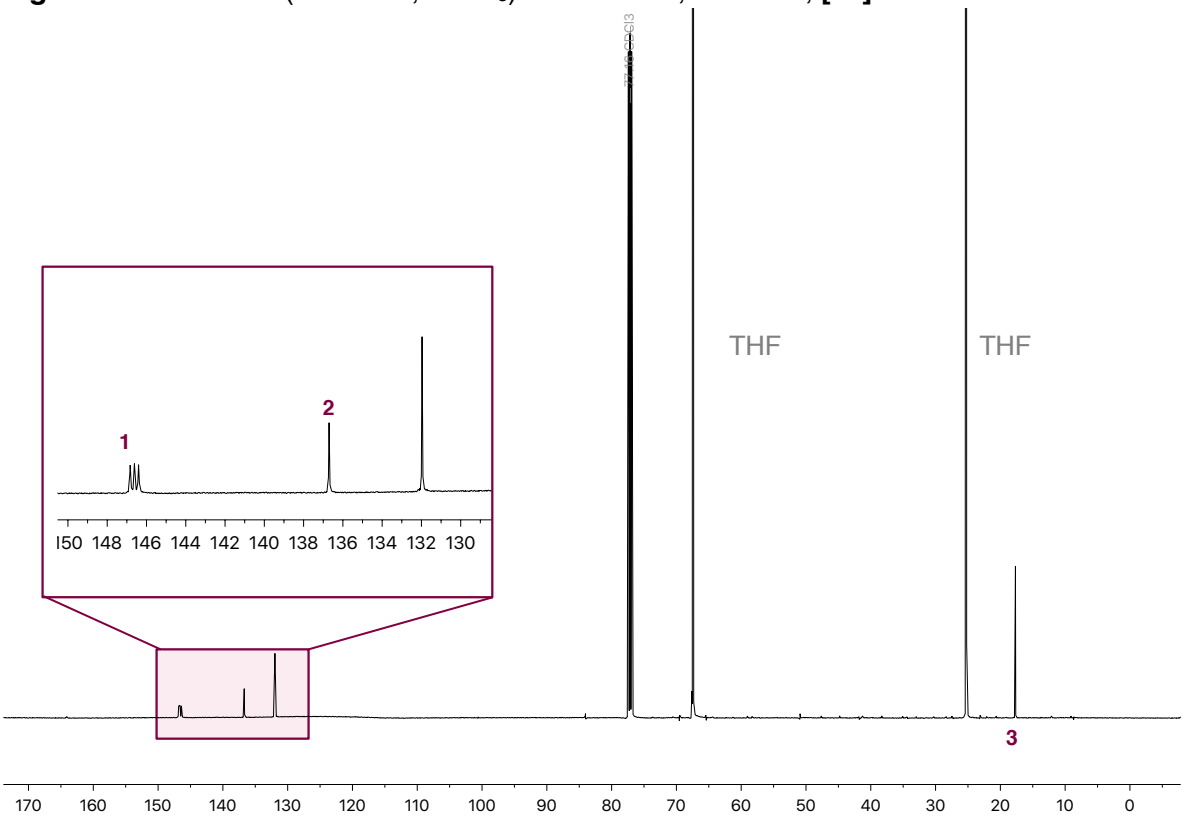

Figure S66. Quantitative ^{13}C{^{1}H} NMR (126 MHz, $CDCl_3$) of **[^{2}H]11c**.

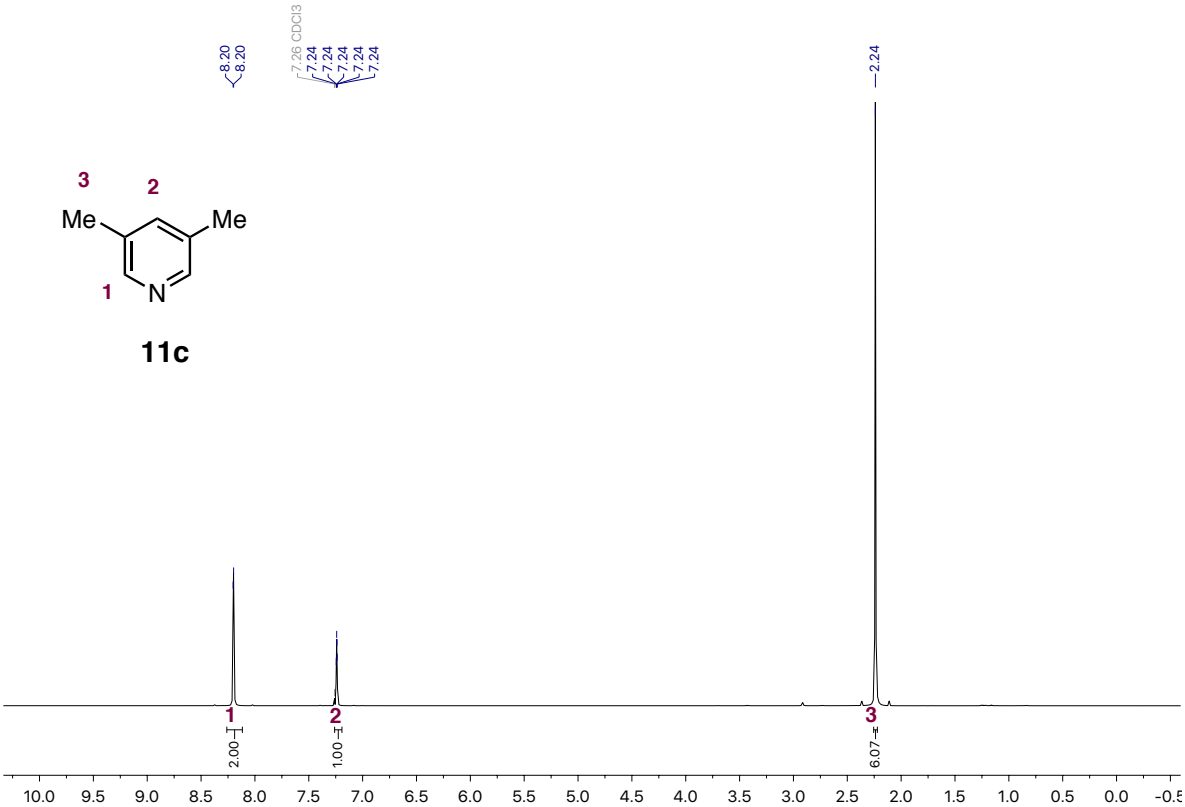

Figure S67. ^{1}H NMR (500 MHz, $CDCl_3$) of unlabeled 3,5-lutidine, **11c**.

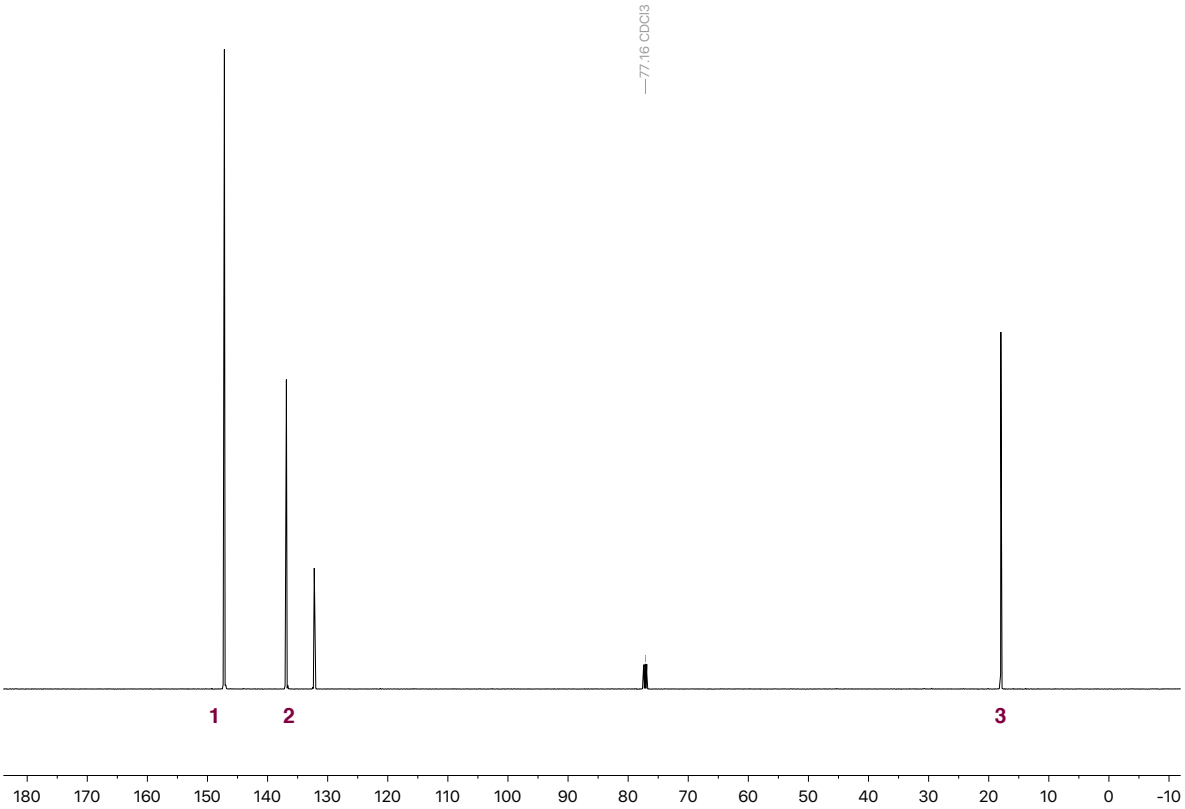

Figure S68. ^{13}C{^{1}H} NMR (126 MHz, $CDCl_3$) of **11c**.

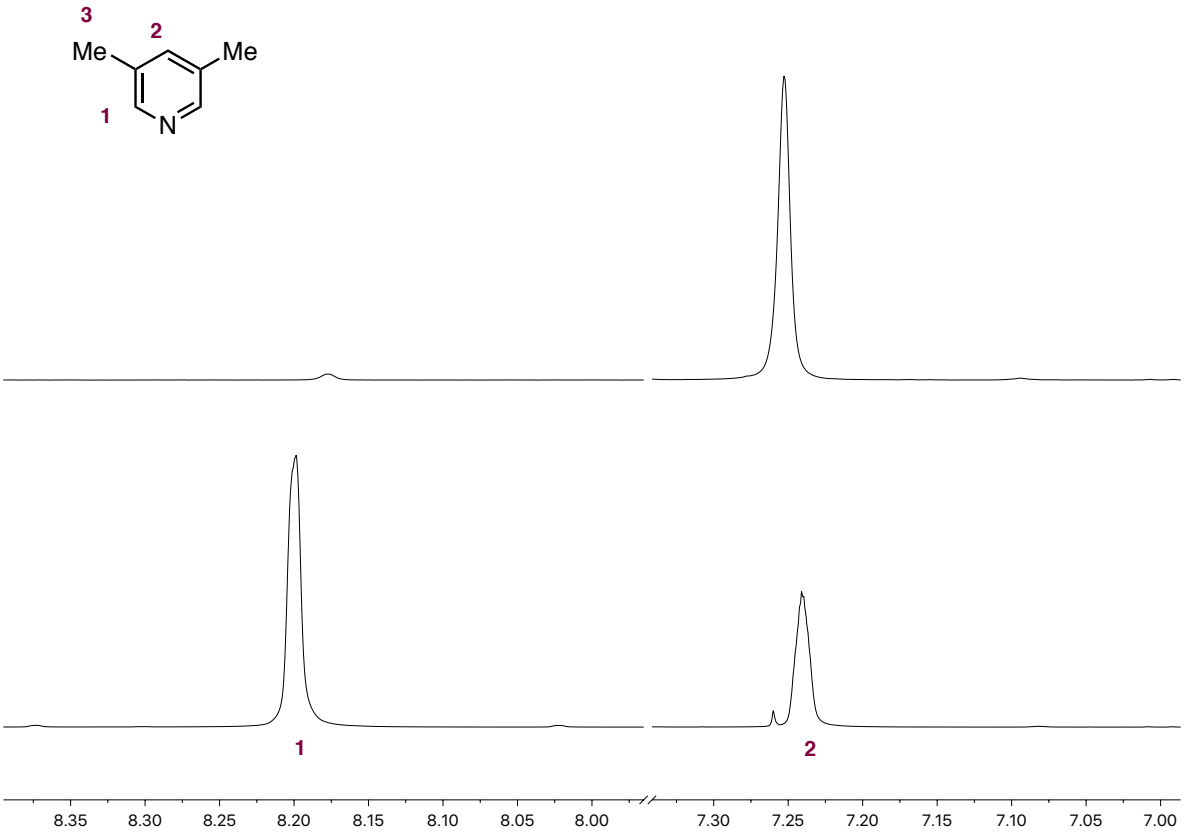

Figure S69. Stacked ^{1}H NMR spectra of 3,5-lutidine: labeled, **[^{2}H]11c** (first) and unlabeled, **11c** (second).

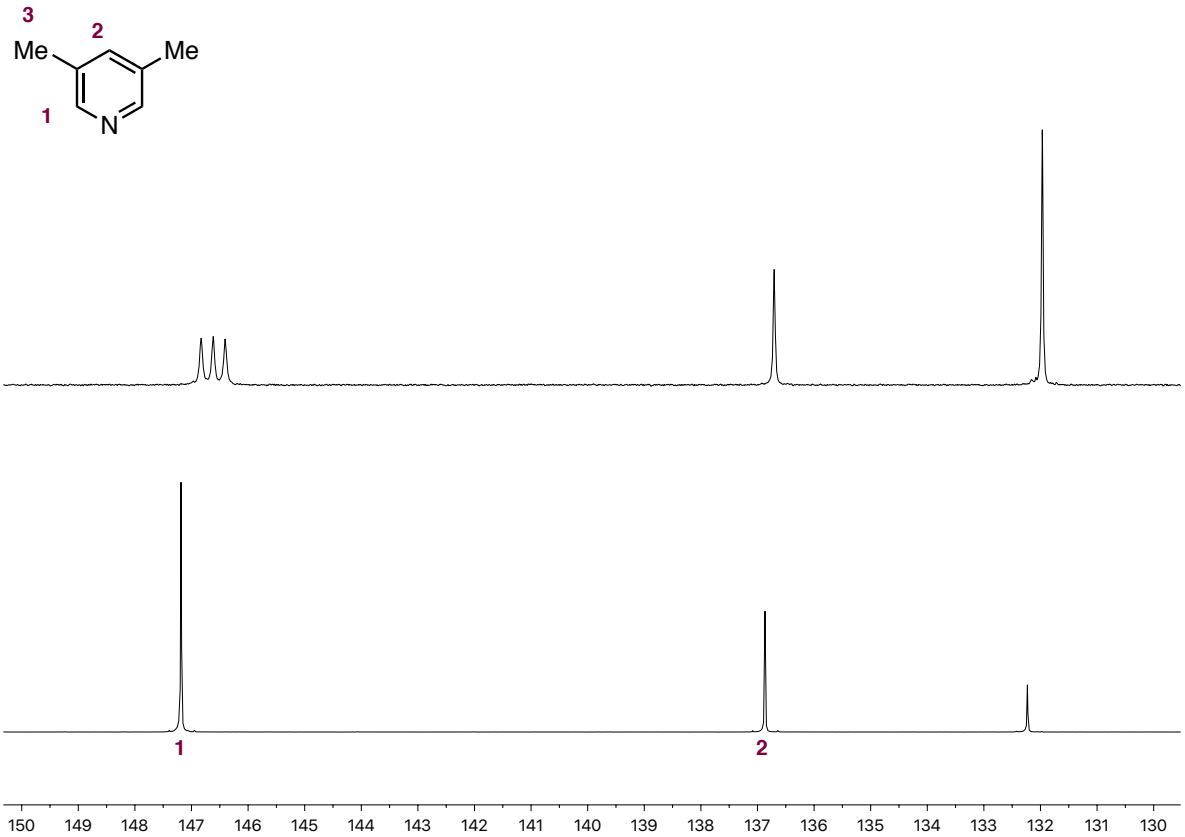

Figure S70. Stacked $^{13}C\{^{1}H\}$ NMR spectra of 3,5-lutidine: labeled, **[^{2}H]11c** (first, quantitative) and unlabeled, **11c** (second).

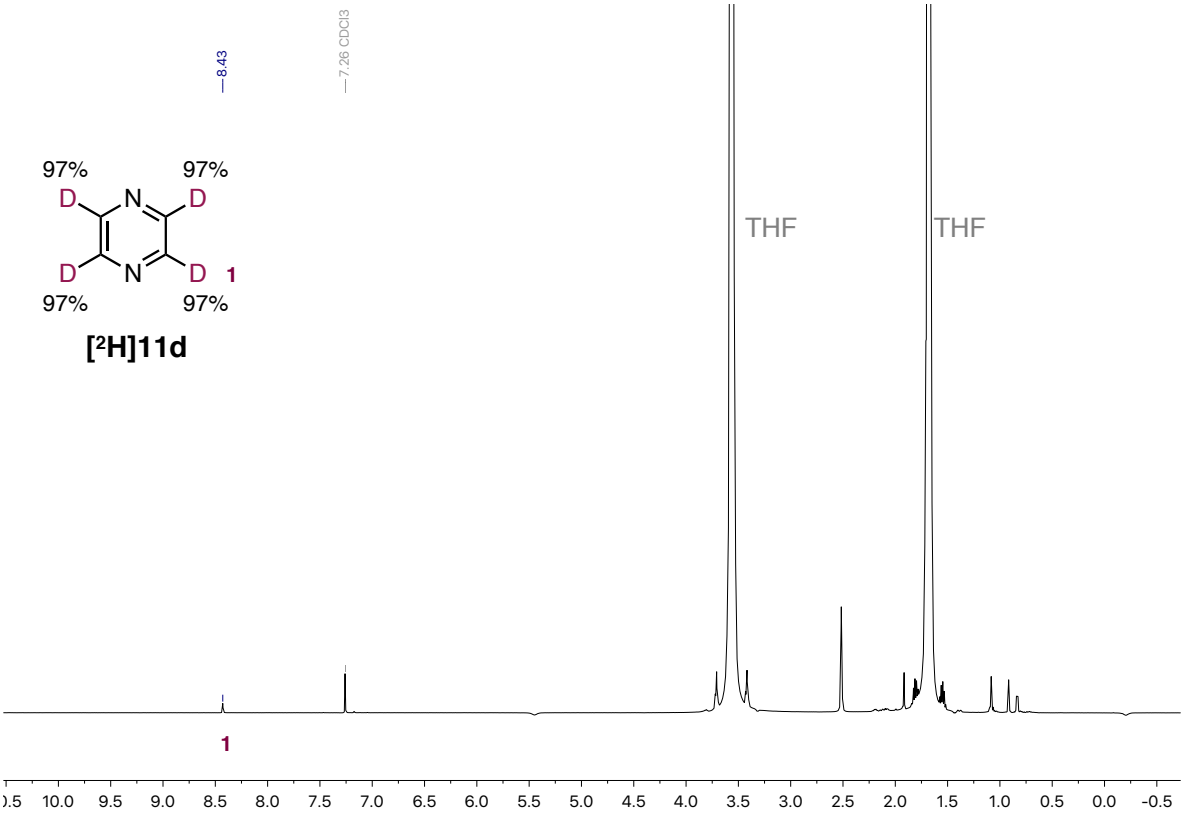

Figure S71. ^{1}H NMR (500 MHz, $CDCl_3$) of labeled pyrazine, **[^{2}H]11d**.

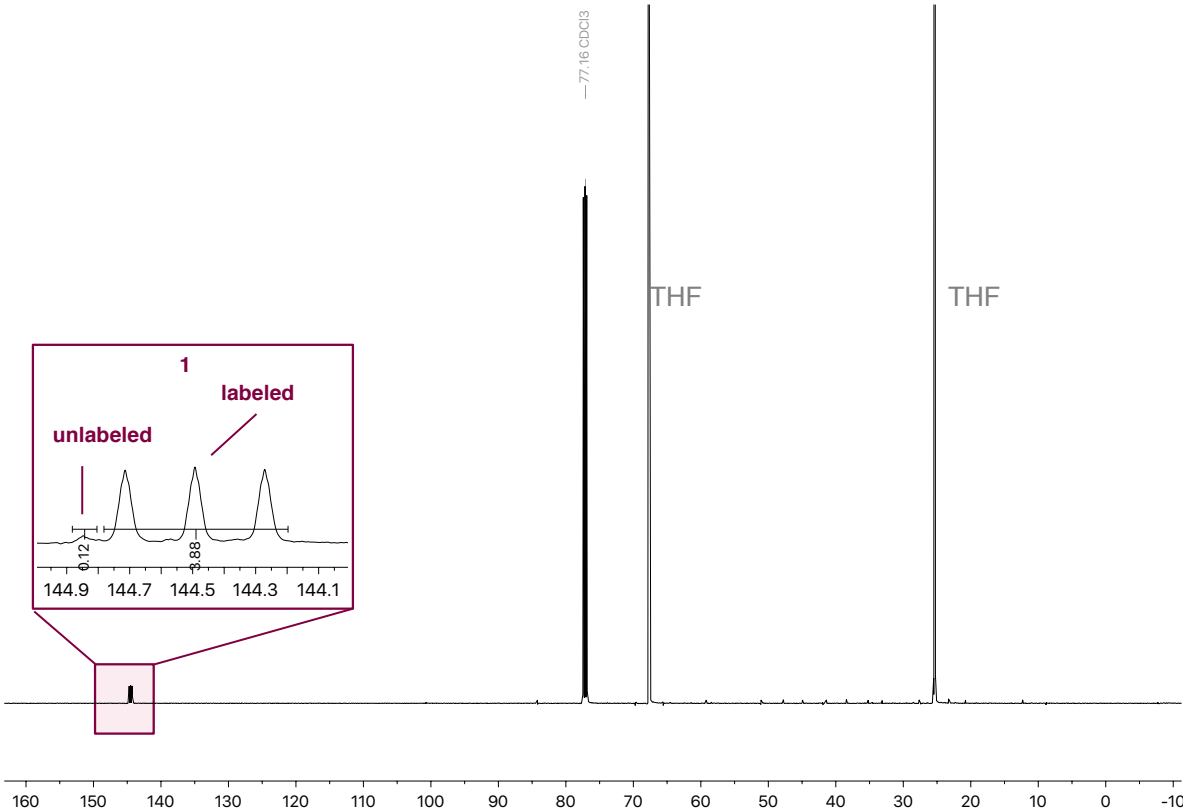

Figure S72. Quantitative ^{13}C{^{1}H} NMR (126 MHz, $CDCl_3$) of **[^{2}H]11d**.

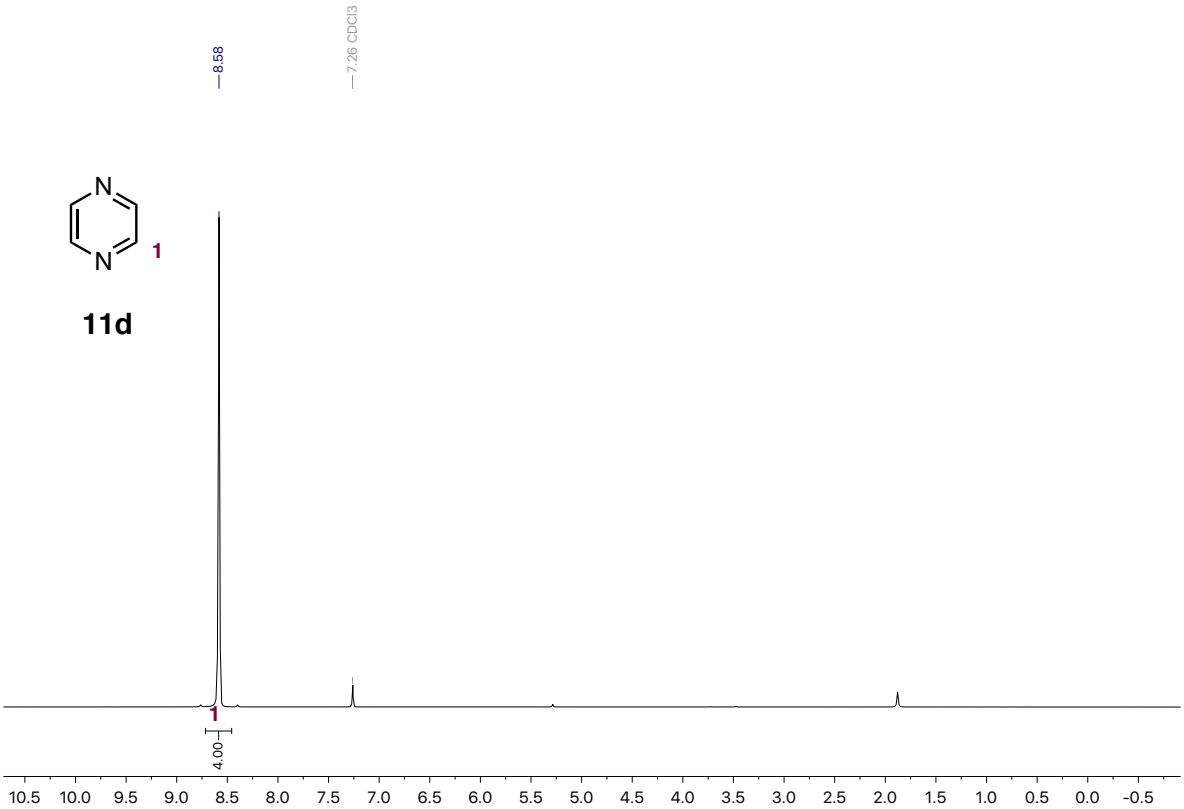

Figure S73. ^{1}H NMR (500 MHz, $CDCl_3$) of unlabeled pyrazine, **11d**.

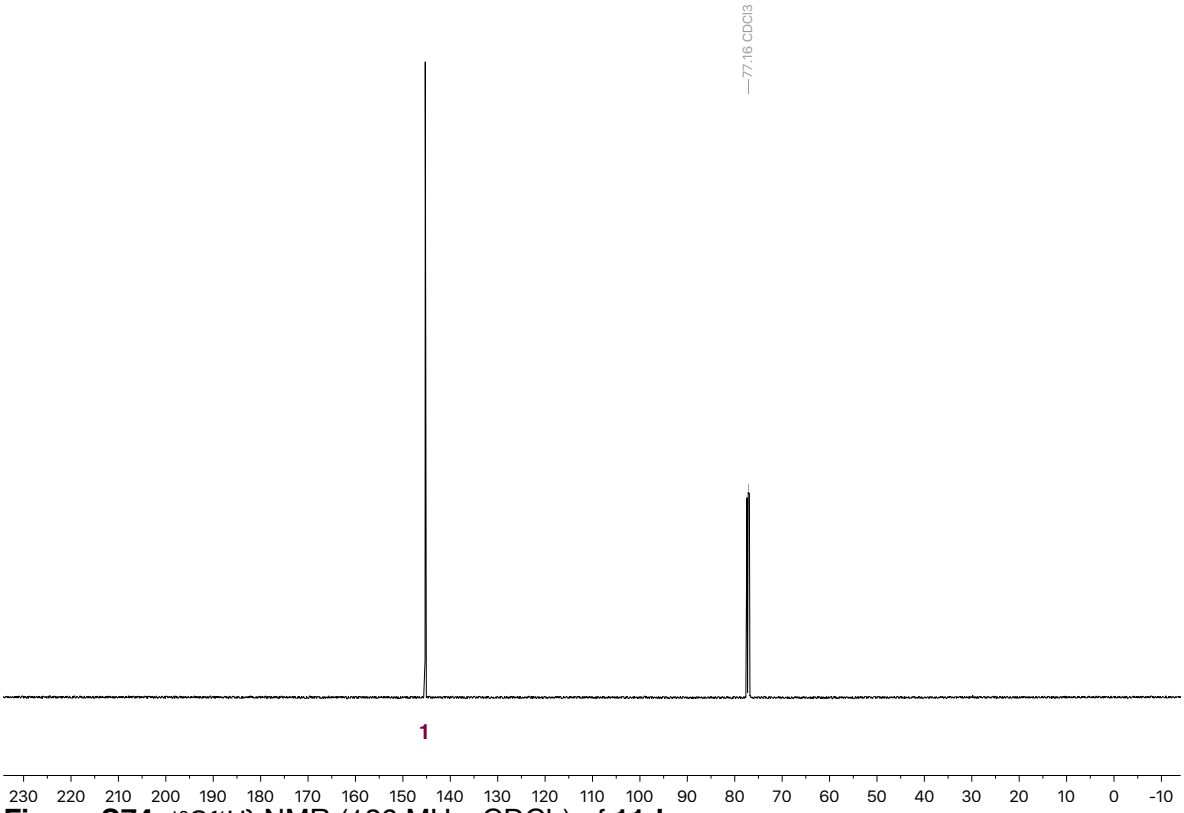

Figure S74. ^{13}C{^{1}H} NMR (126 MHz, $CDCl_3$) of **11d**.

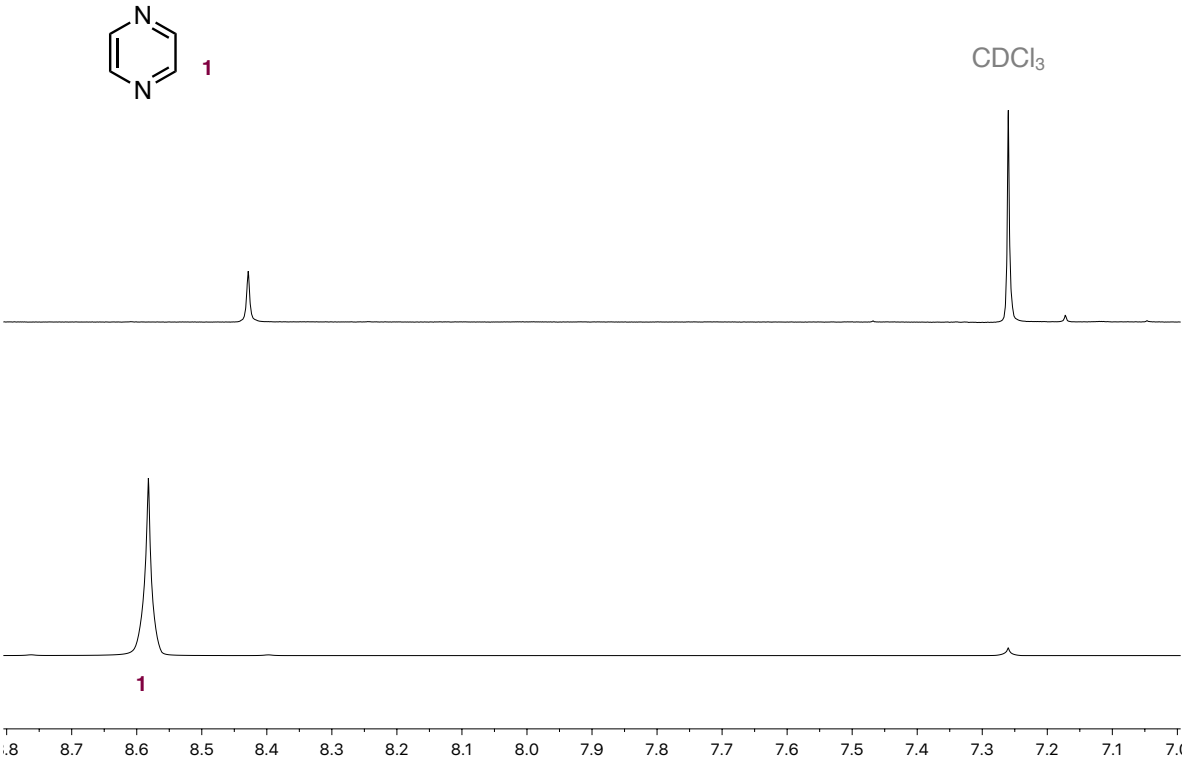

Figure S75. Stacked ^{1}H NMR spectra of pyrazine: labeled, **[^{2}H]11d** (first) and unlabeled, **11d** (second).

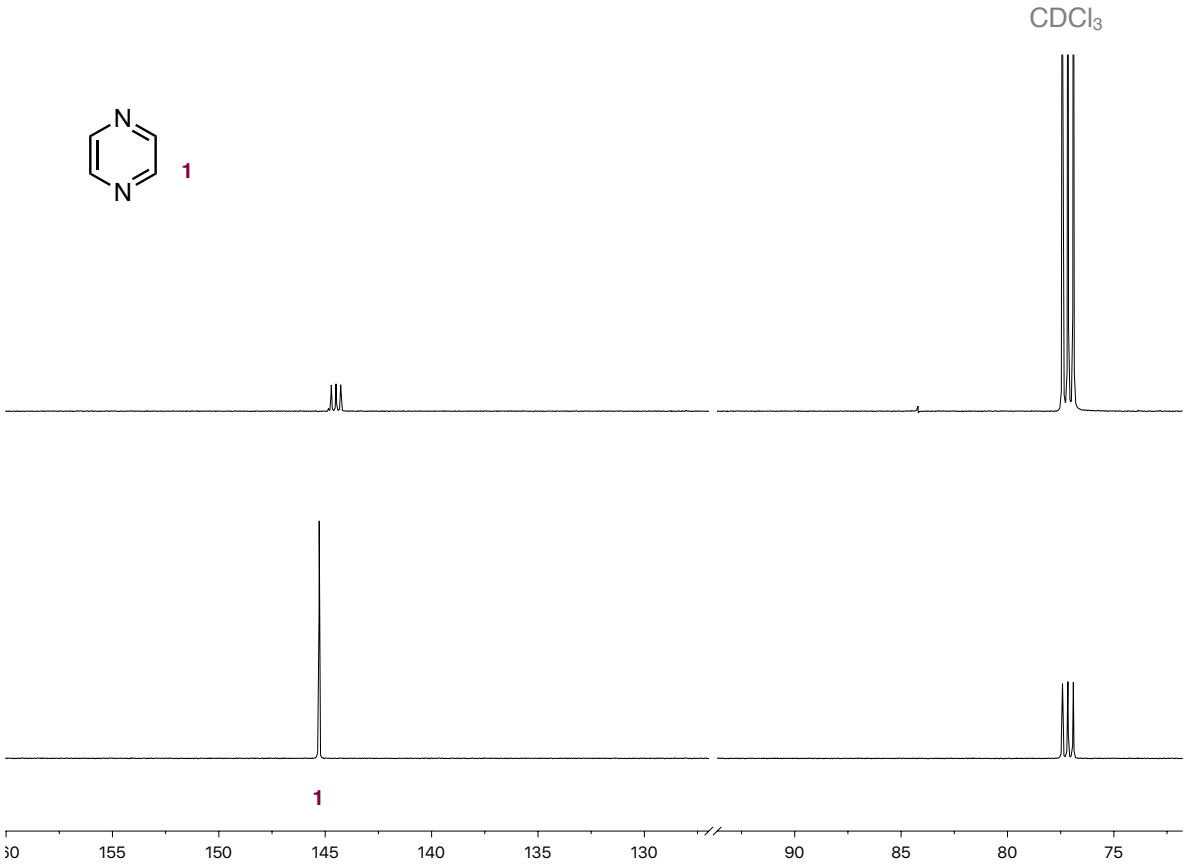

Figure S76. Stacked $^{13}C\{^{1}H\}$ NMR spectra of pyrazine: labeled, **[^{2}H]11d** (first, quantitative) and unlabeled, **11d** (second).

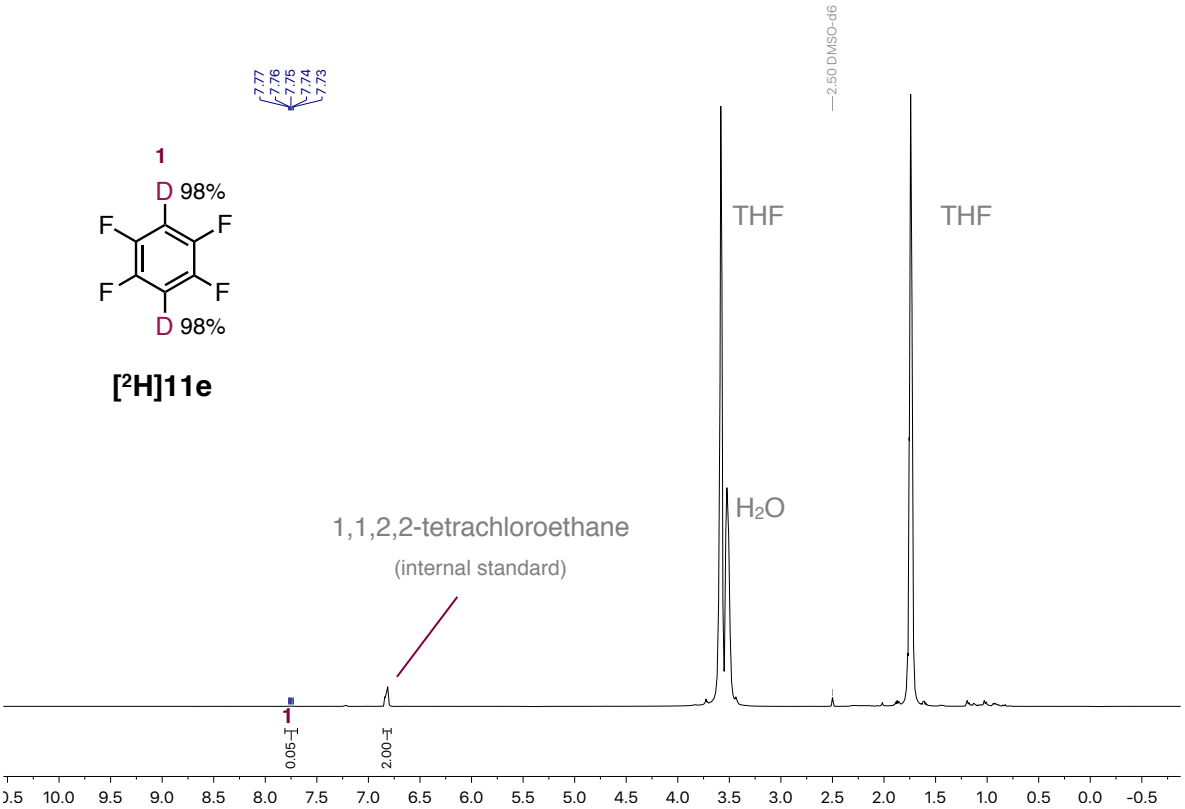

Figure S77. ^{1}H NMR (500 MHz, DMSO-d_6) of labeled 1,2,4,5-tetrafluorobenzene, **[^{2}H]11e**.

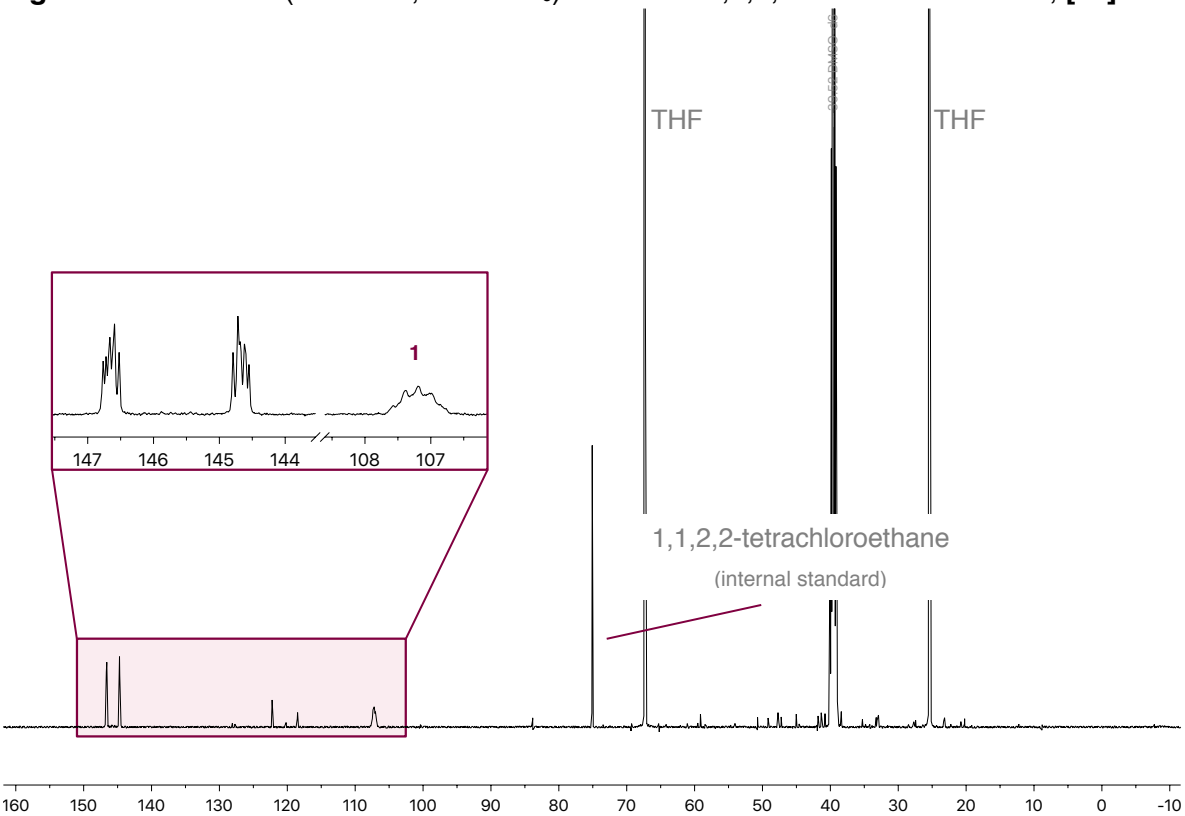

Figure S78. Quantitative ^{13}C{^{1}H} NMR (126 MHz, DMSO-d_6) of **[^{2}H]11e**.

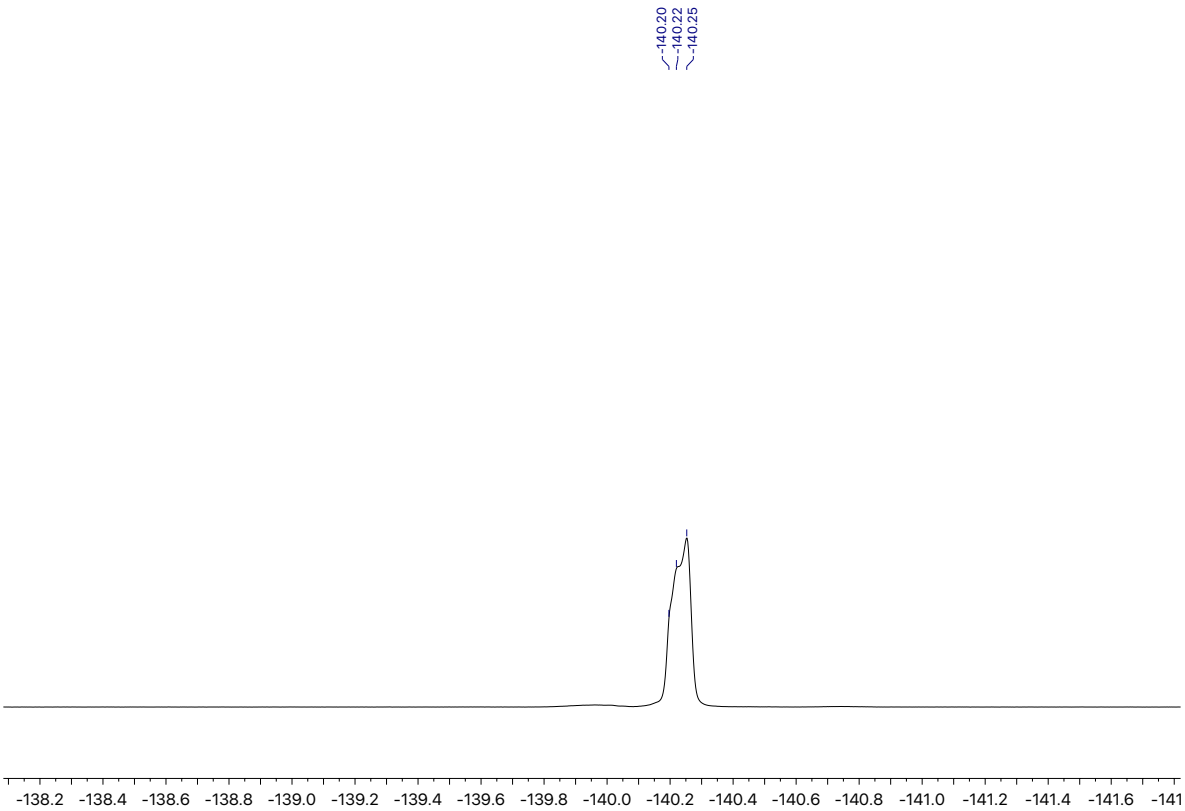

Figure S79. ^{19}F NMR (282 MHz, DMSO-d_6) of **[^{2}H]11e**.

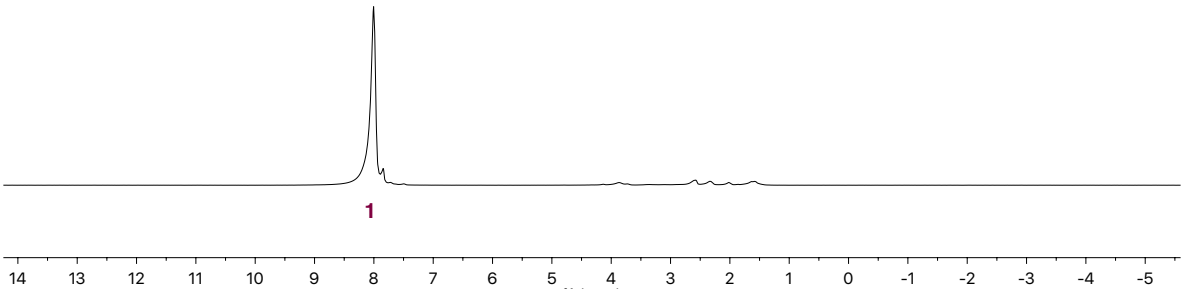

Figure S80. ^{2}H NMR (77 MHz, THF-d_0) of **[^{2}H]11e**.

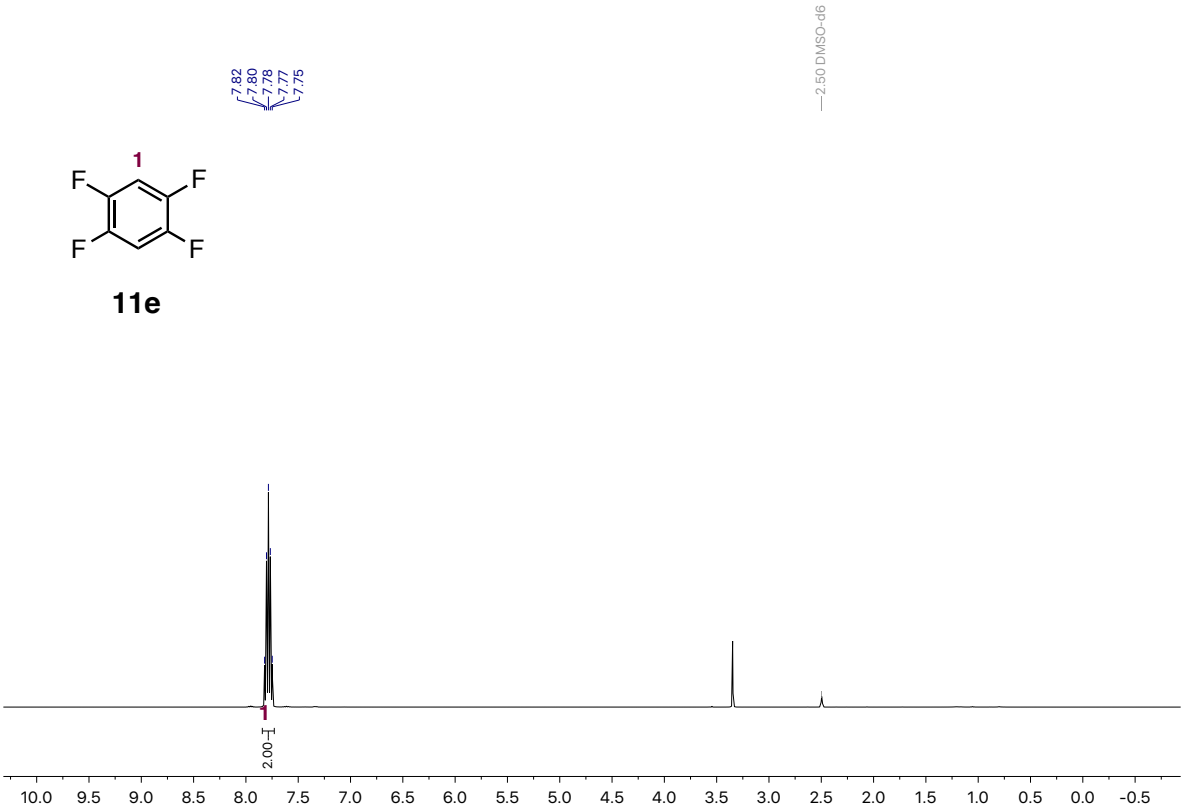

Figure S81. ^{1}H NMR (500 MHz, DMSO-d_6) of unlabeled 1,2,4,5-tetrafluorobenzene, **11e**.

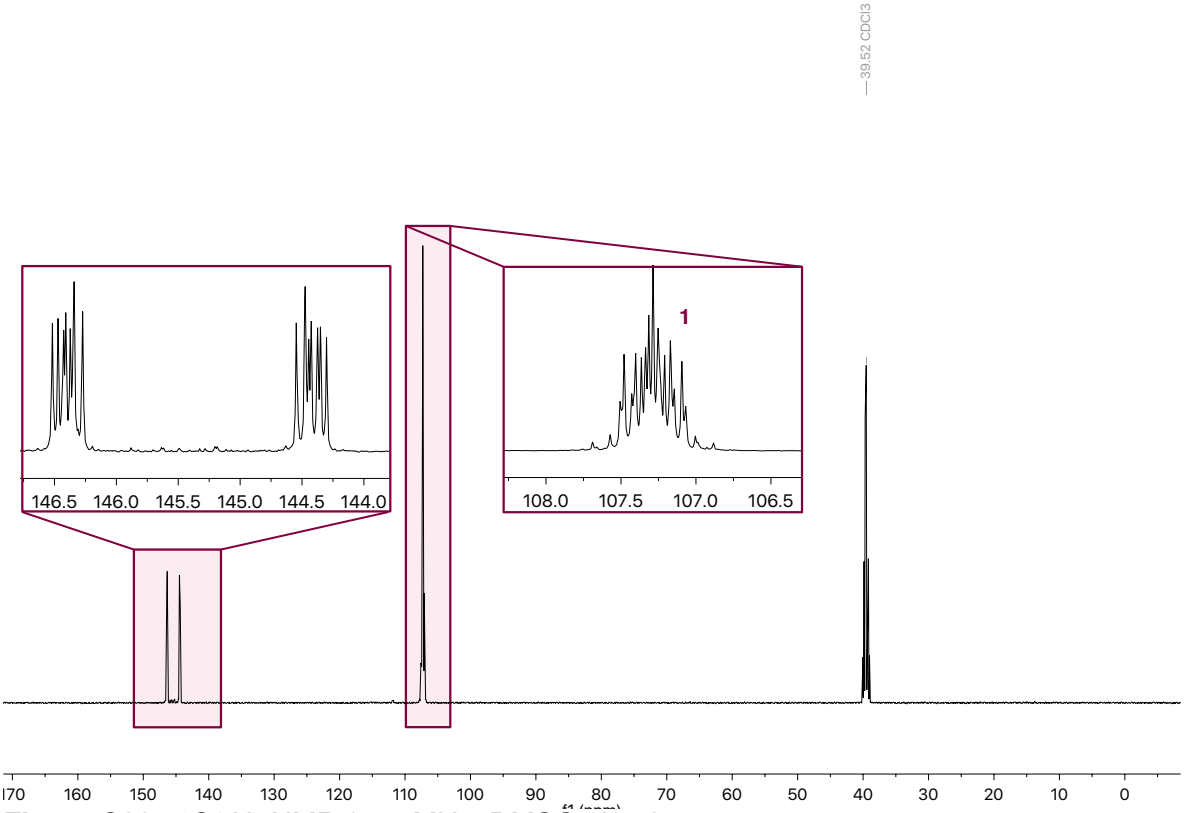

Figure S82. ^{13}C{^{1}H} NMR (126 MHz, DMSO-d_6) of **11e**.

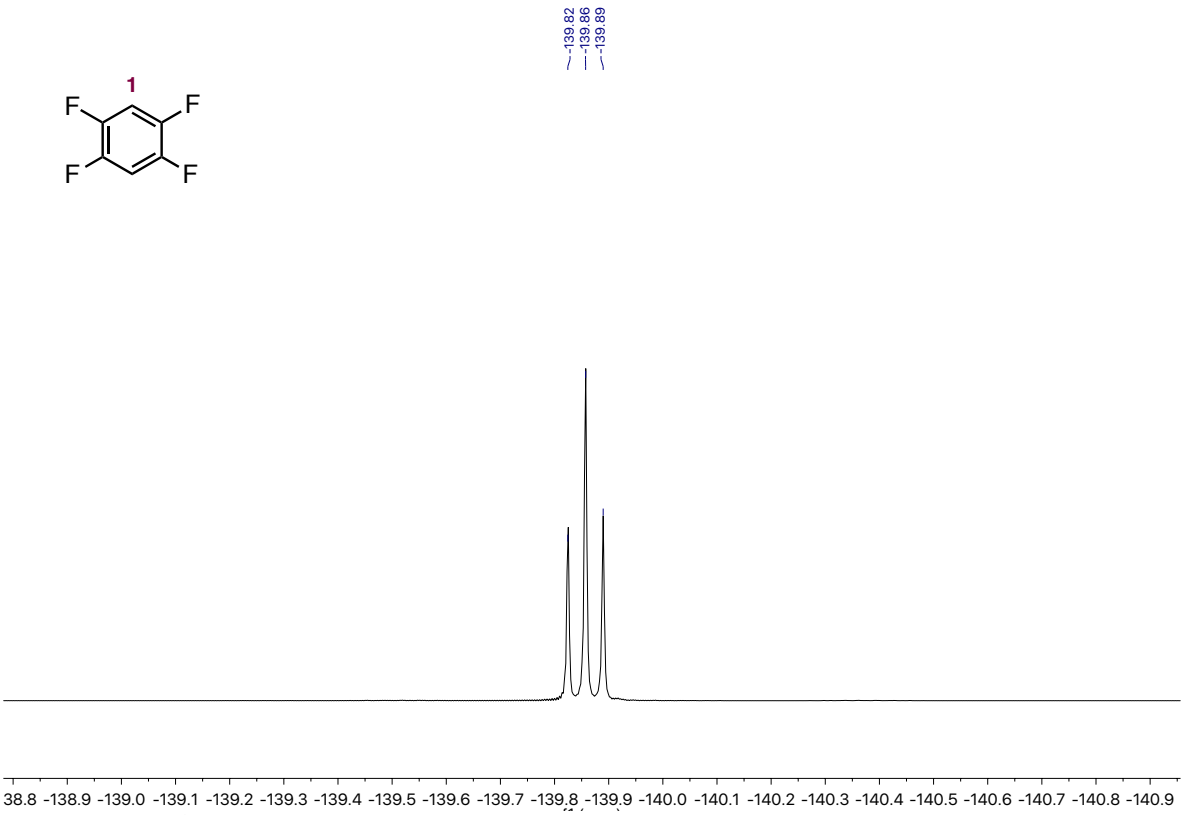

Figure S83. ^{19}F NMR (282 MHz, DMSO-d_6) of **11e**.

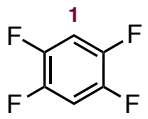

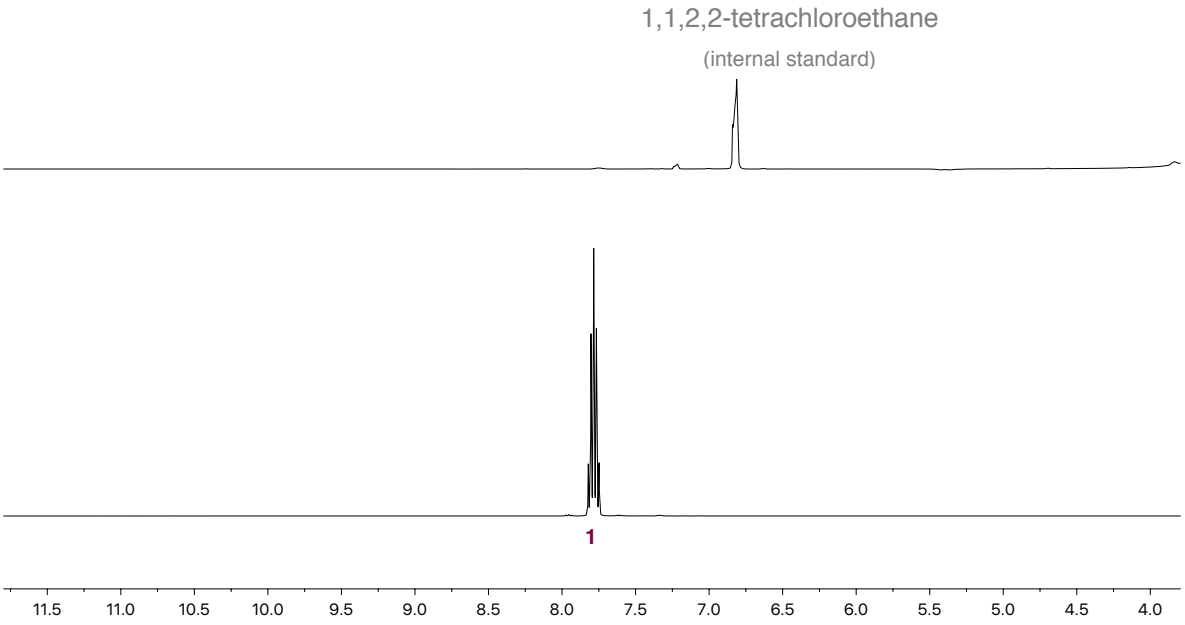

Figure S84. Stacked ^{1}H NMR spectra of 1,2,4,5-tetrafluorobenzene: labeled, **[^{2}H]11e** (first) and unlabeled, **11e** (second).

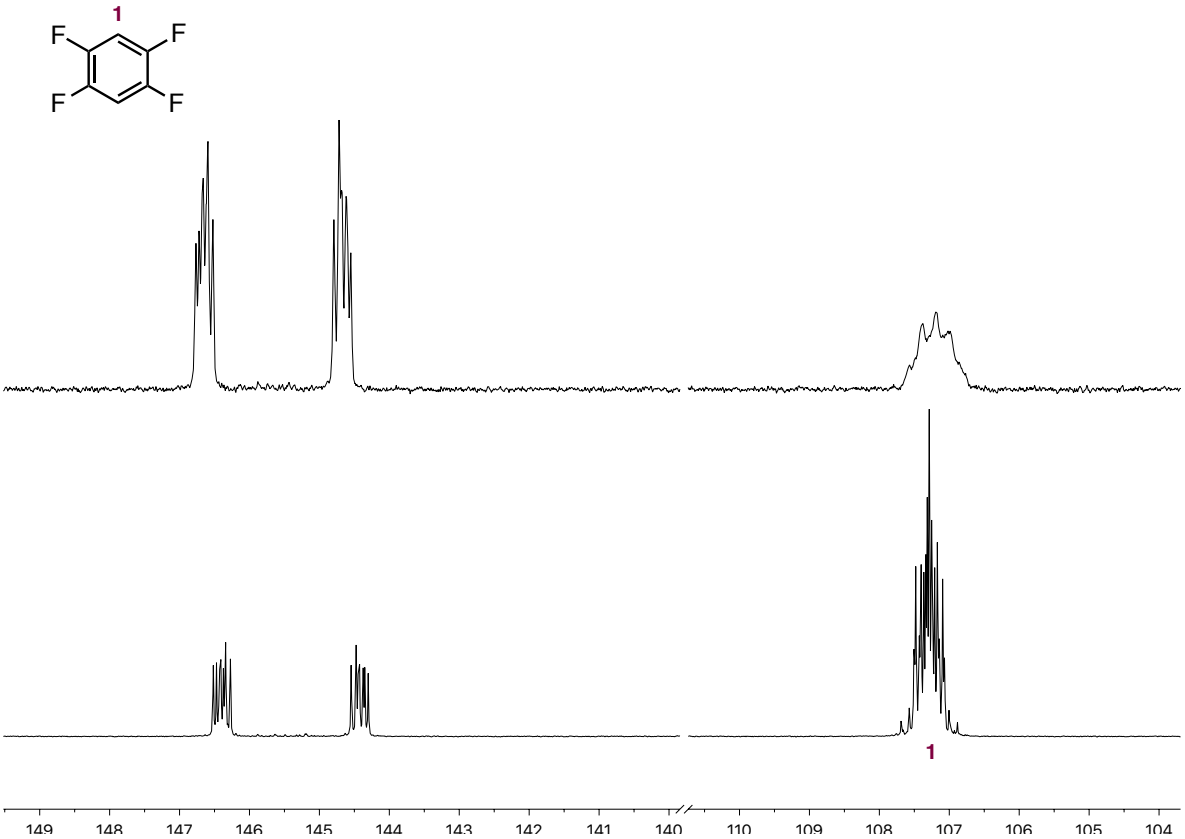

Figure S85. Stacked $^{13}C\{^{1}H\}$ NMR spectra of 1,2,4,5-tetrafluorobenzene: labeled, **[^{2}H]11e** (first, quantitative) and unlabeled, **11e** (second).

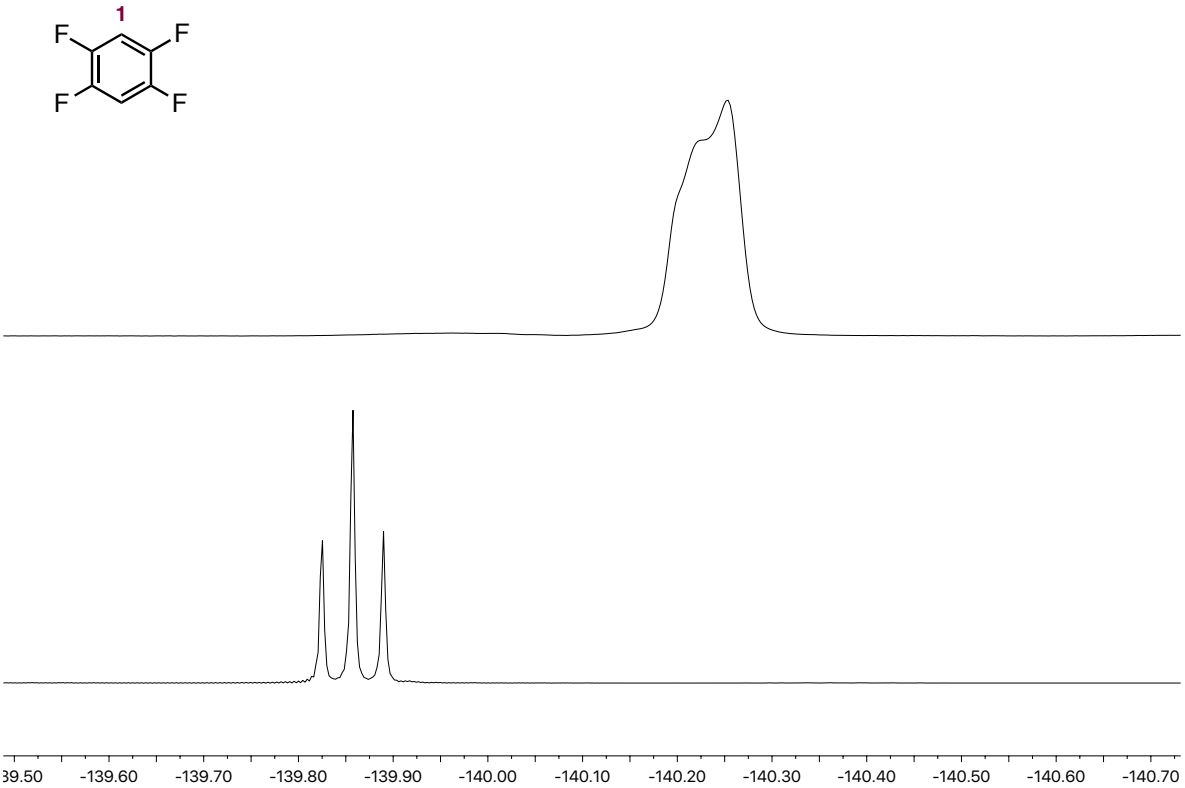

Figure S86. Stacked ^{19}F NMR spectra of 1,2,4,5-tetrafluorobenzene: labeled, **[^{2}H]11e** (first, quantitative) and unlabeled, **11e** (second).

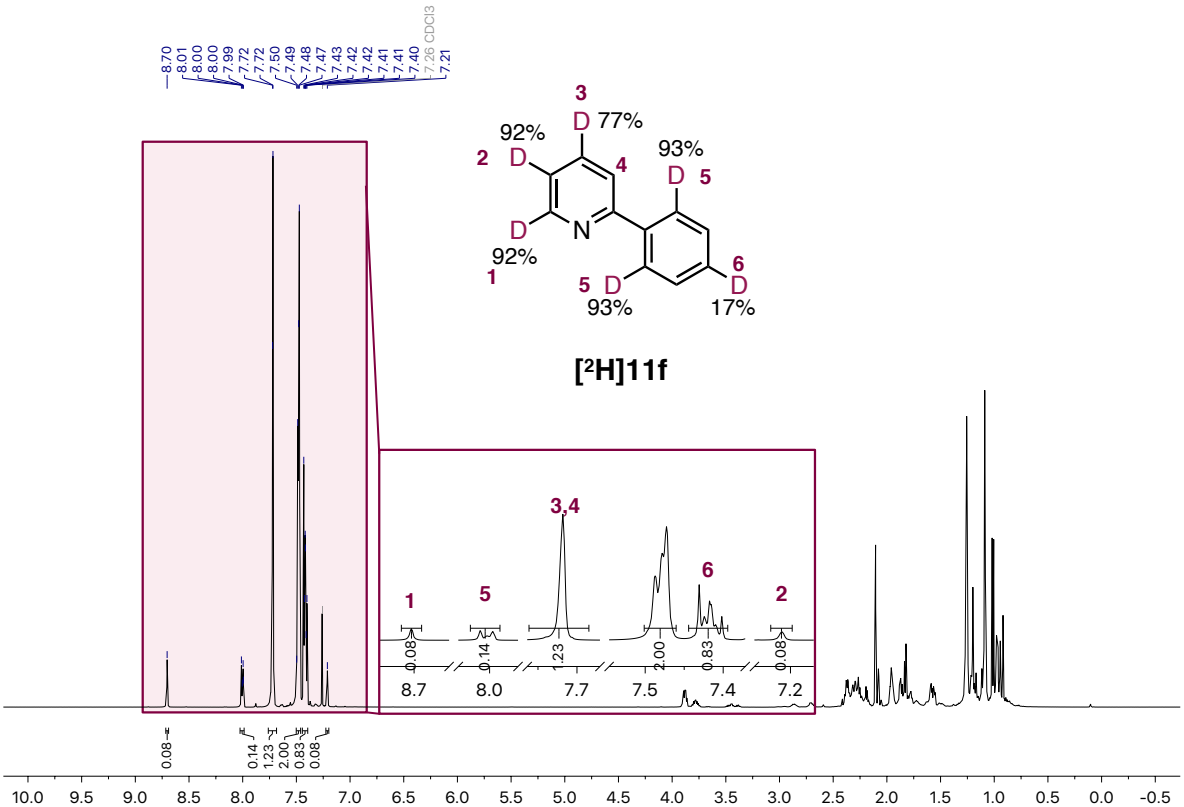

Figure S87. ^{1}H NMR (500 MHz, $CDCl_3$) of labeled 2-phenylpyridine, **[^{2}H]11f**.

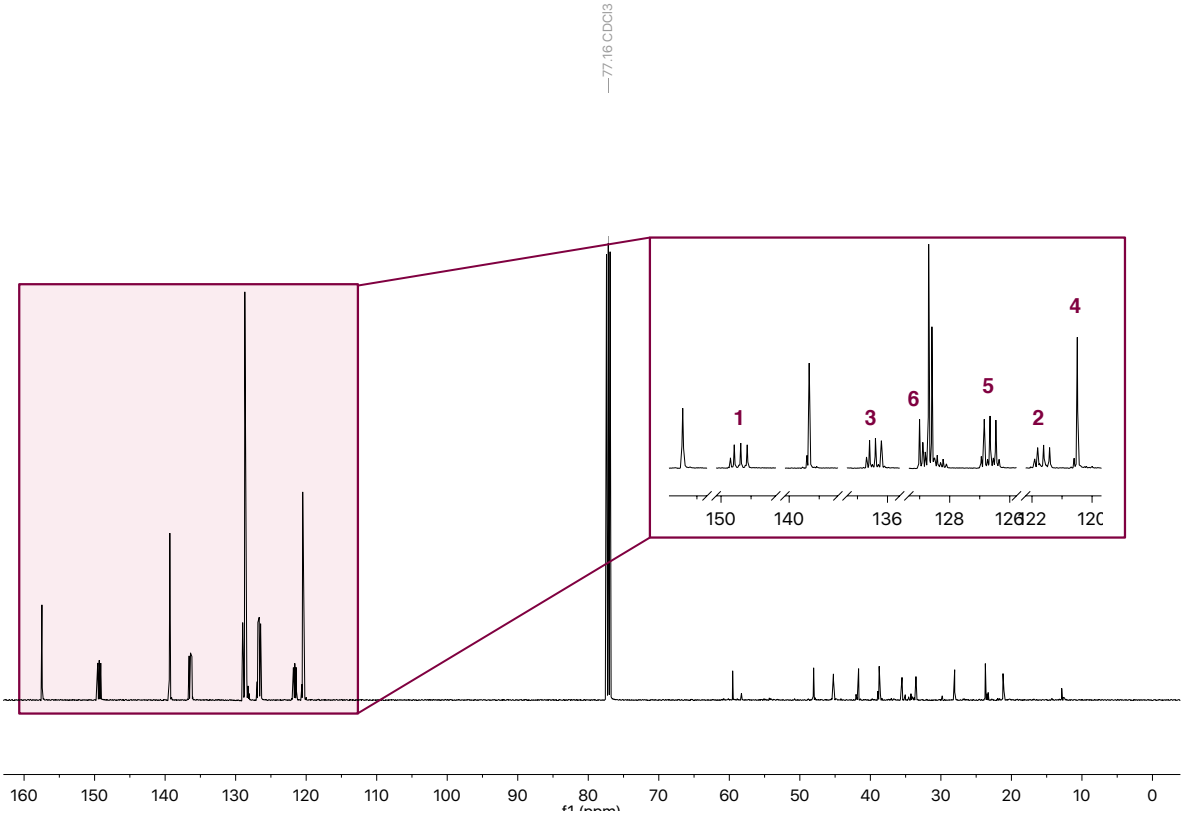

Figure S88. Quantitative ^{13}C{^{1}H} NMR (126 MHz, $CDCl_3$) of **[^{2}H]11f**.

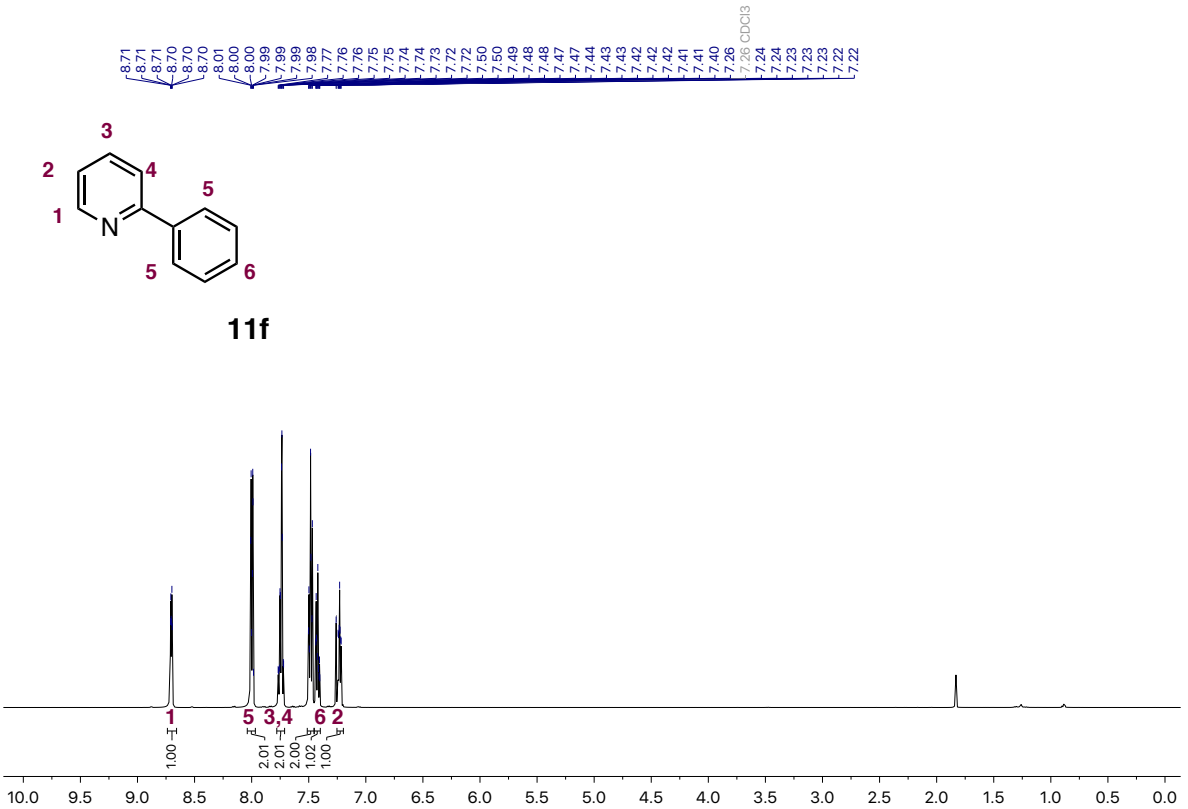

Figure S89. ^{1}H NMR (500 MHz, $CDCl_3$) of unlabeled 2-phenylpyridine, **11f**.

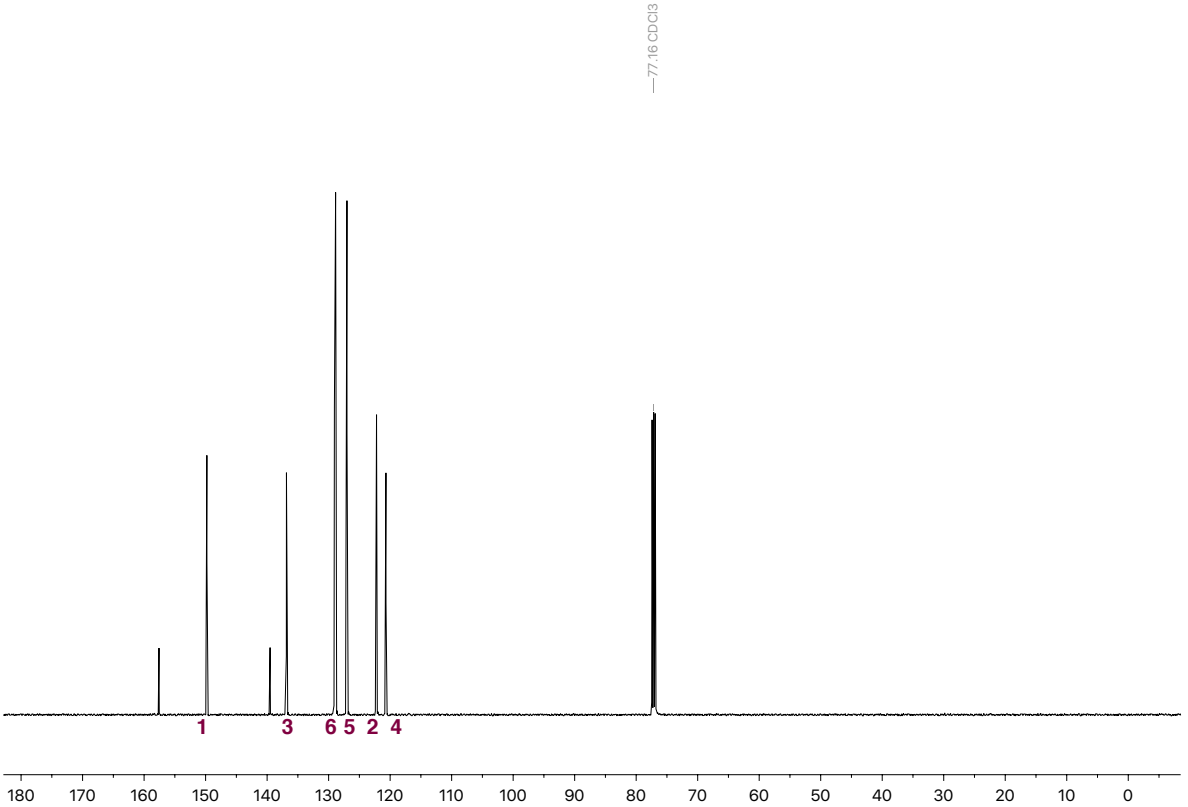

Figure S90. ^{13}C{^{1}H} NMR (126 MHz, $CDCl_3$) of **11f**.

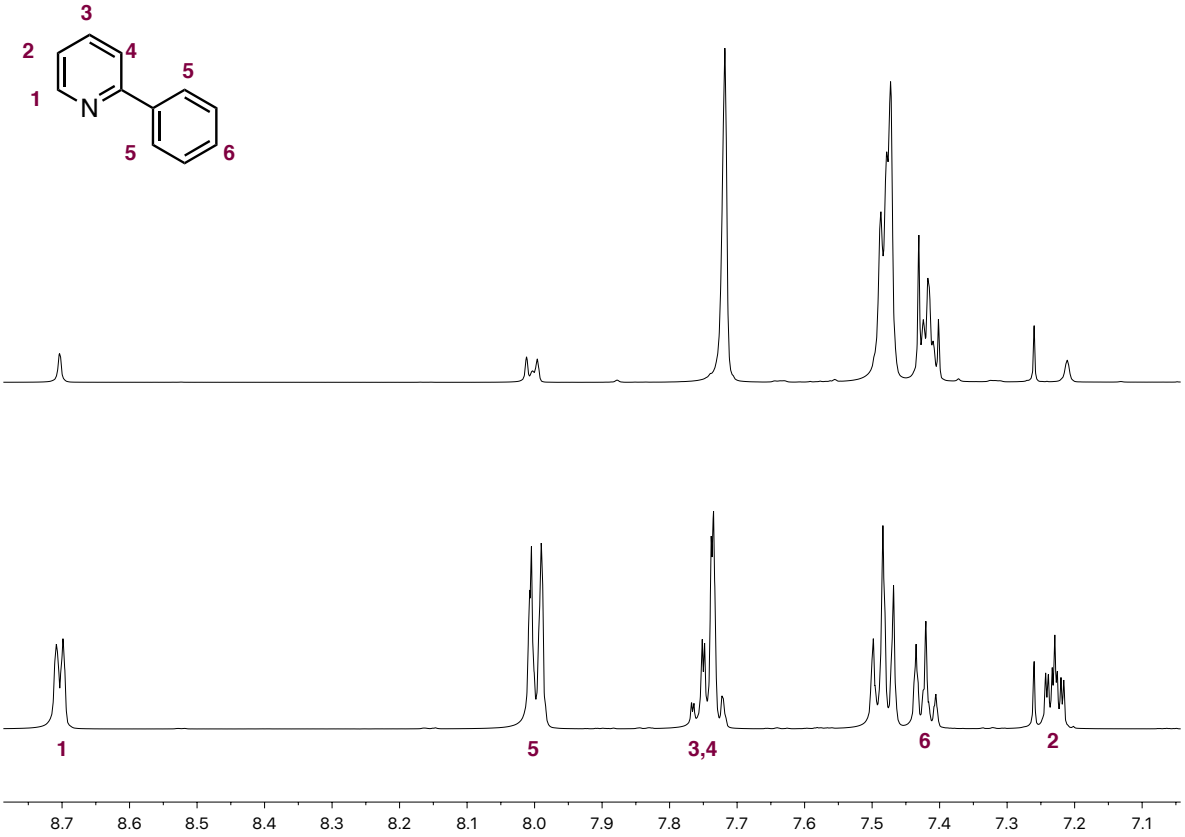

Figure S91. Stacked ^{1}H NMR spectra of 2-phenylpyridine: labeled, **[^{2}H]11f** (first) and unlabeled, **11f** (second).

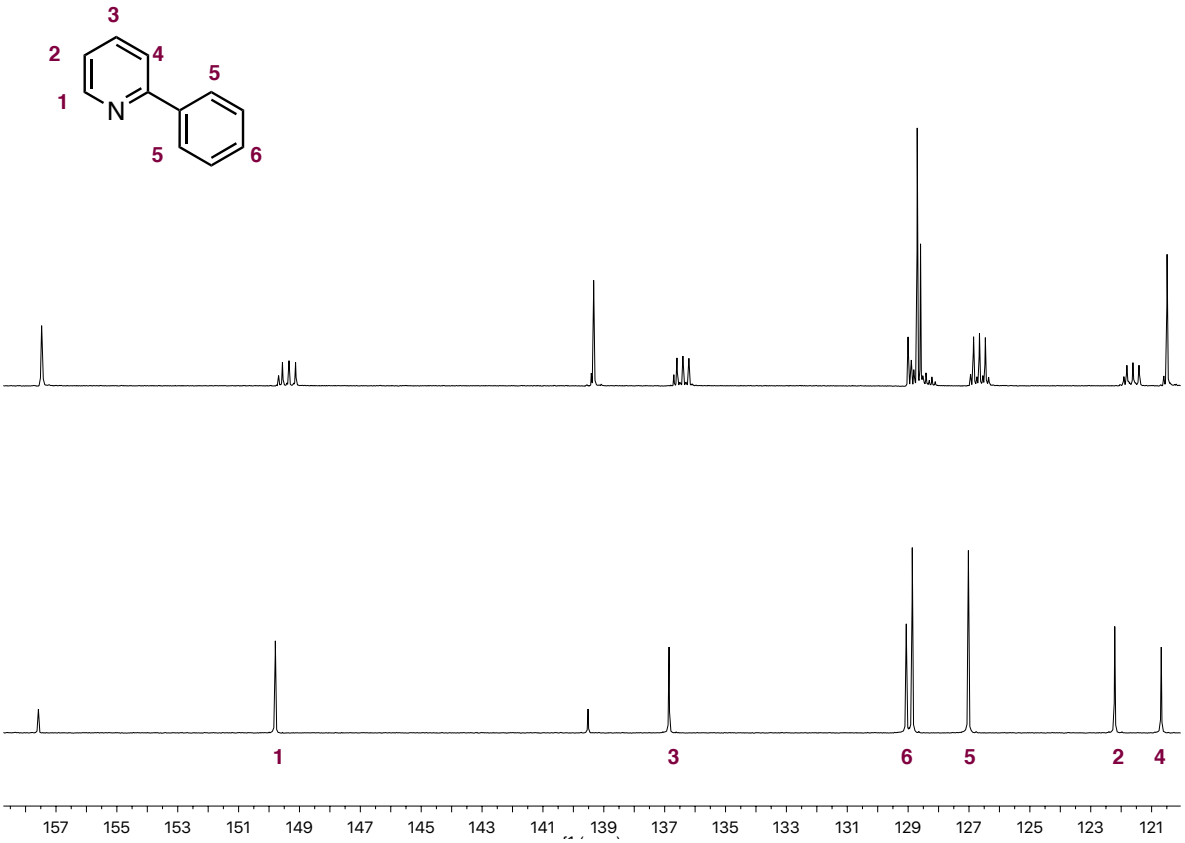

Figure S92. Stacked $^{13}C\{^{1}H\}$ NMR spectra of 2-phenylpyridine: labeled, **[^{2}H]11f** (first, quantitative) and unlabeled, **11f** (second).

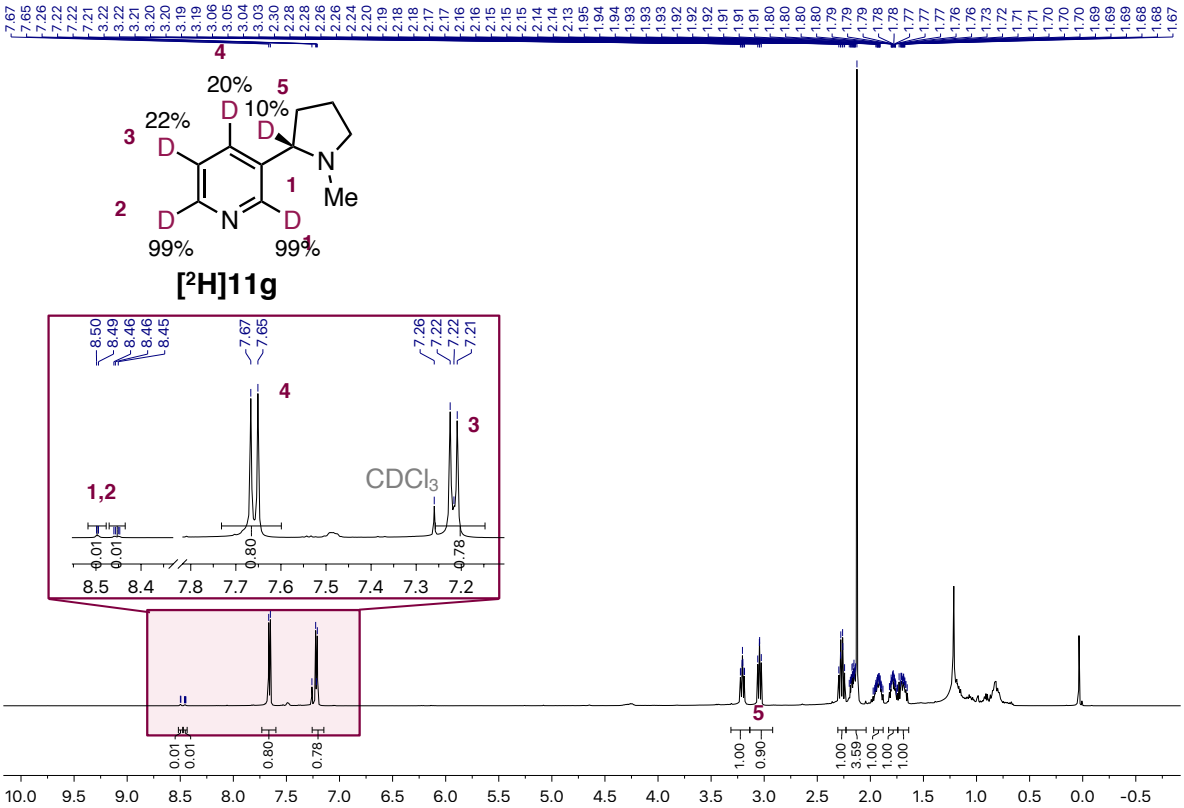

Figure S93. ^{1}H NMR (500 MHz, $CDCl_3$) of labeled nicotine, **[^{2}H]11g**.

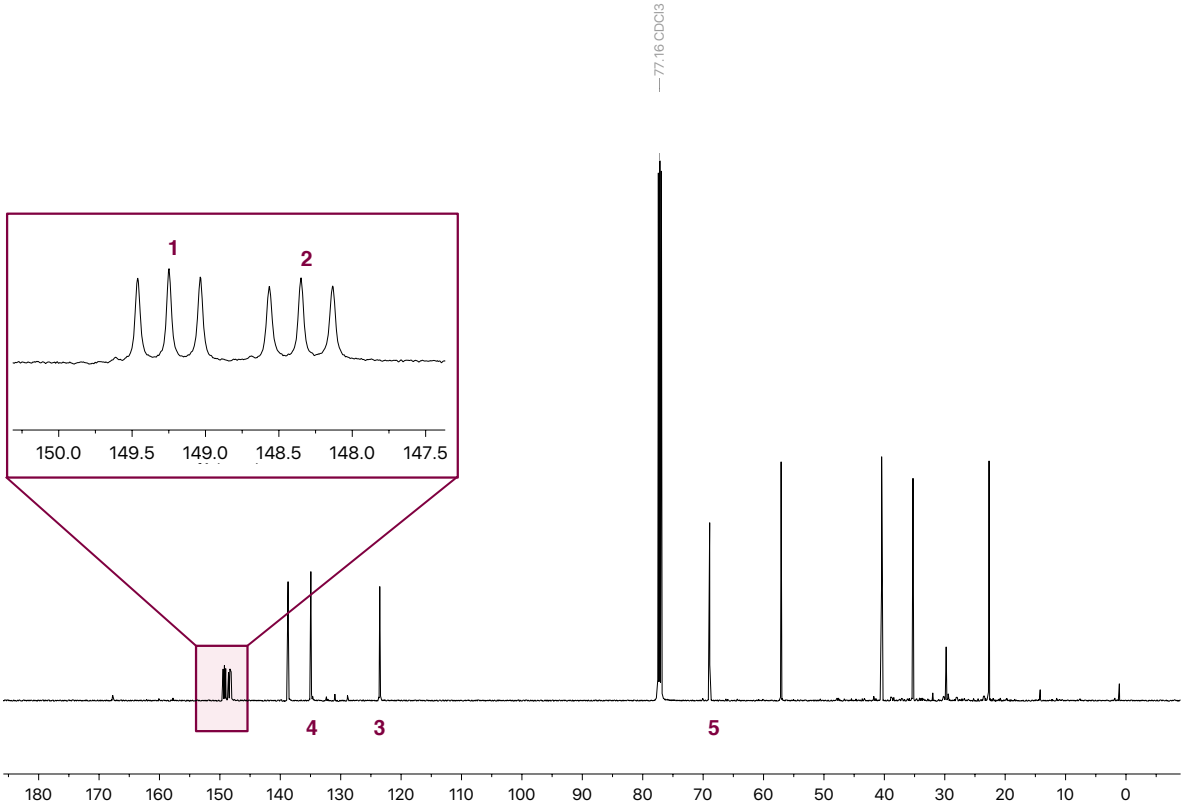

Figure S94. Quantitative ^{13}C{^{1}H} NMR (126 MHz, $CDCl_3$) of **[^{2}H]11g**.

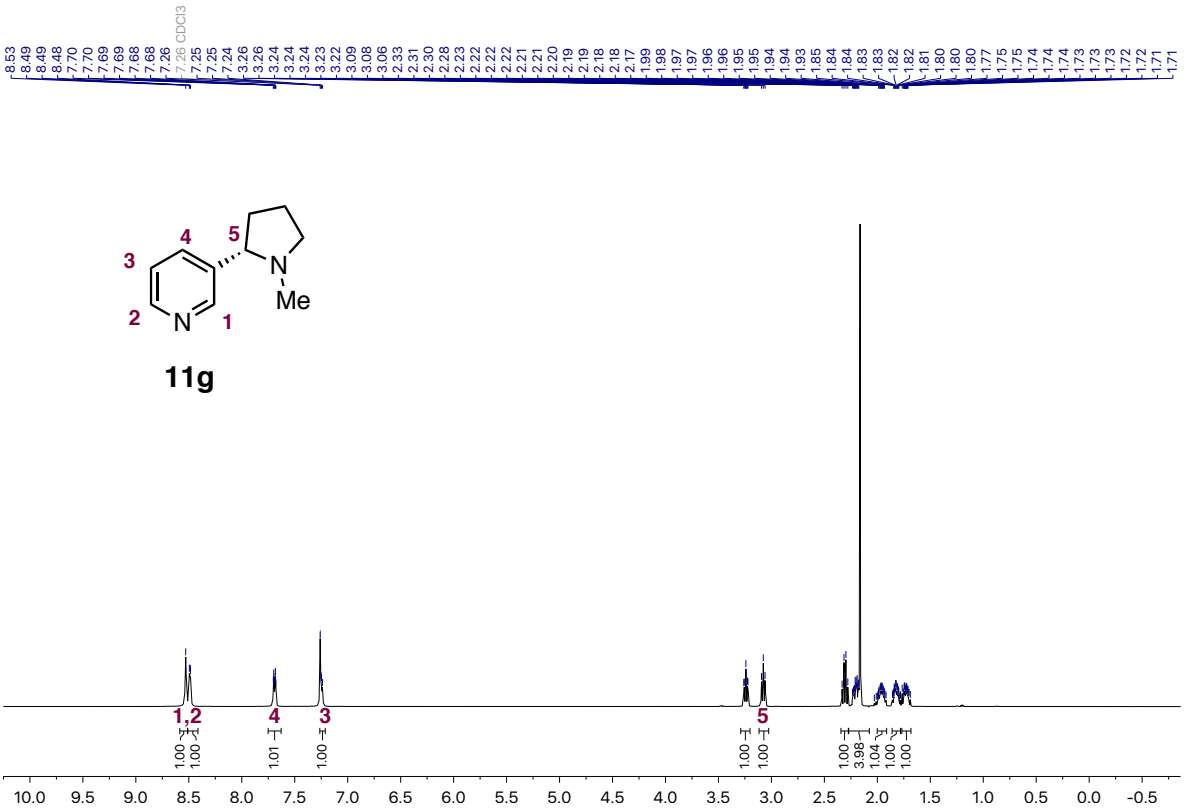

Figure S95. ^{1}H NMR (500 MHz, $CDCl_3$) of unlabeled nicotine, **11g**.

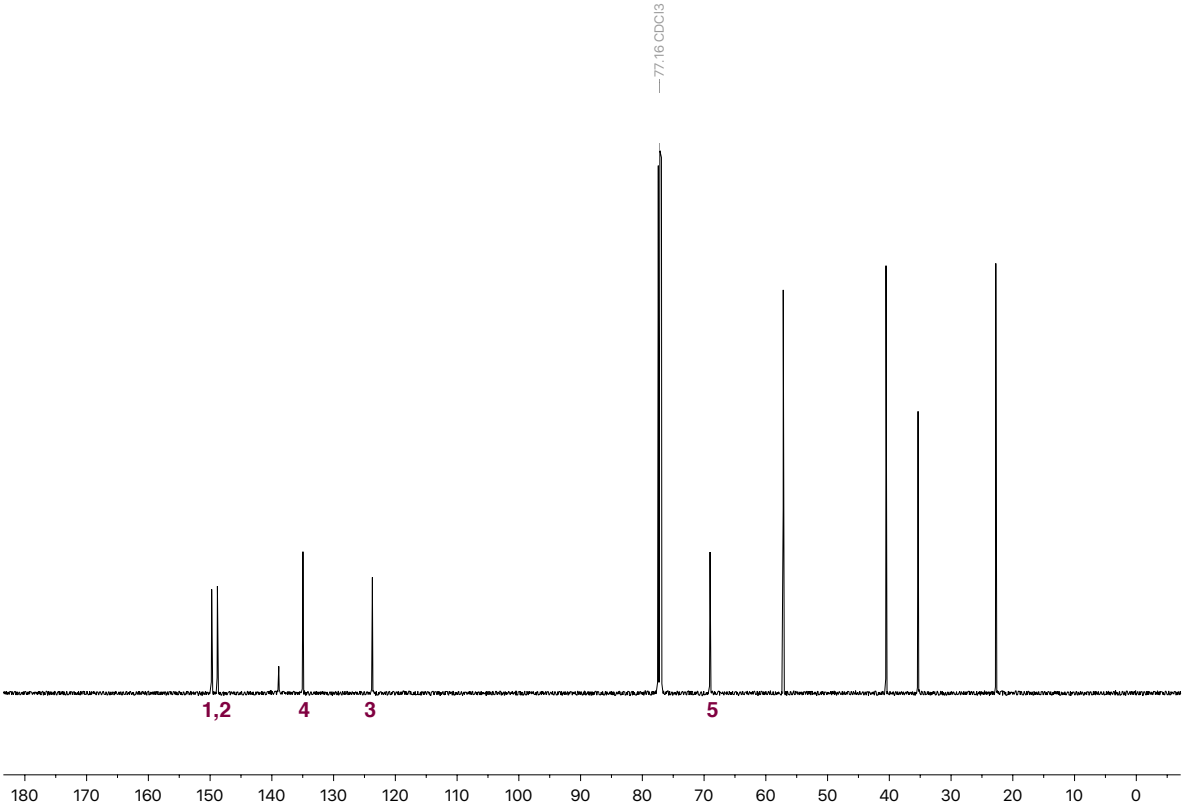

Figure S96. ^{13}C{^{1}H} NMR (126 MHz, $CDCl_3$) of **11g**.

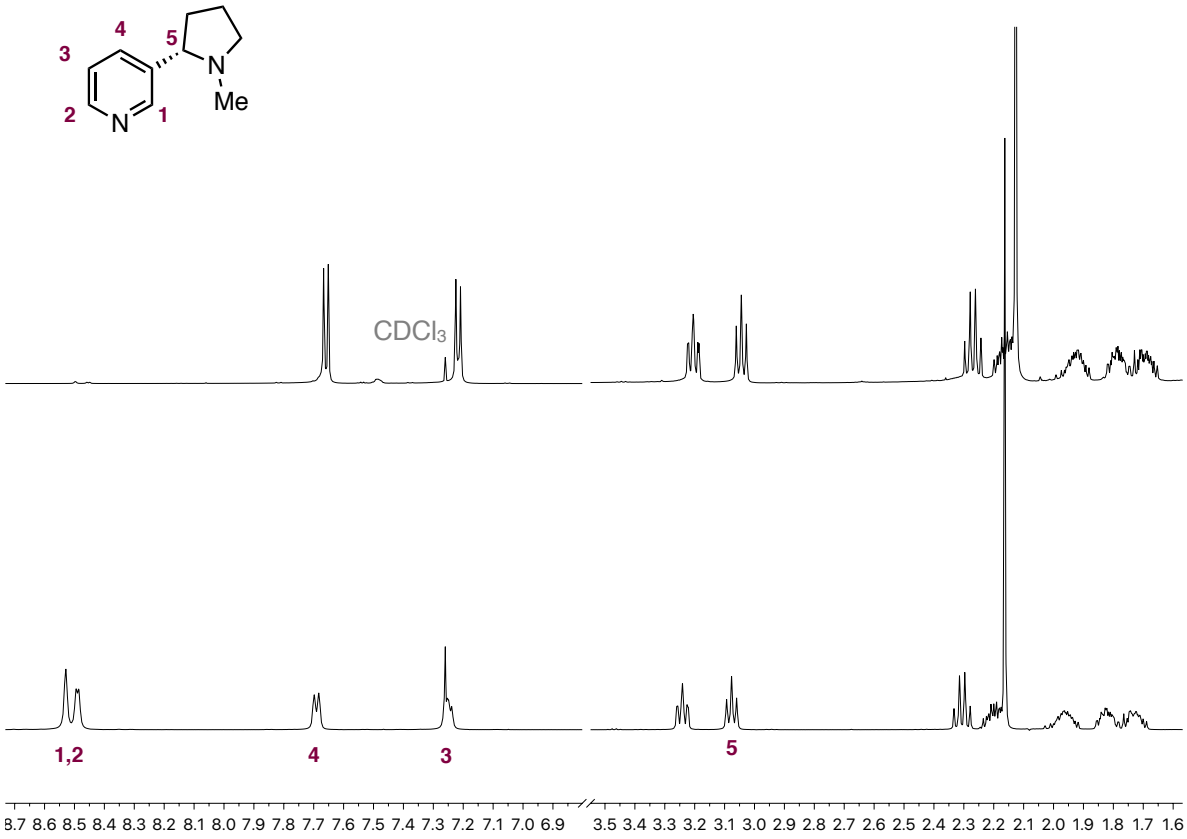

Figure S97. Stacked ^{1}H NMR spectra of nicotine: labeled, **[^{2}H]11g** (first) and unlabeled, **11g** (second).

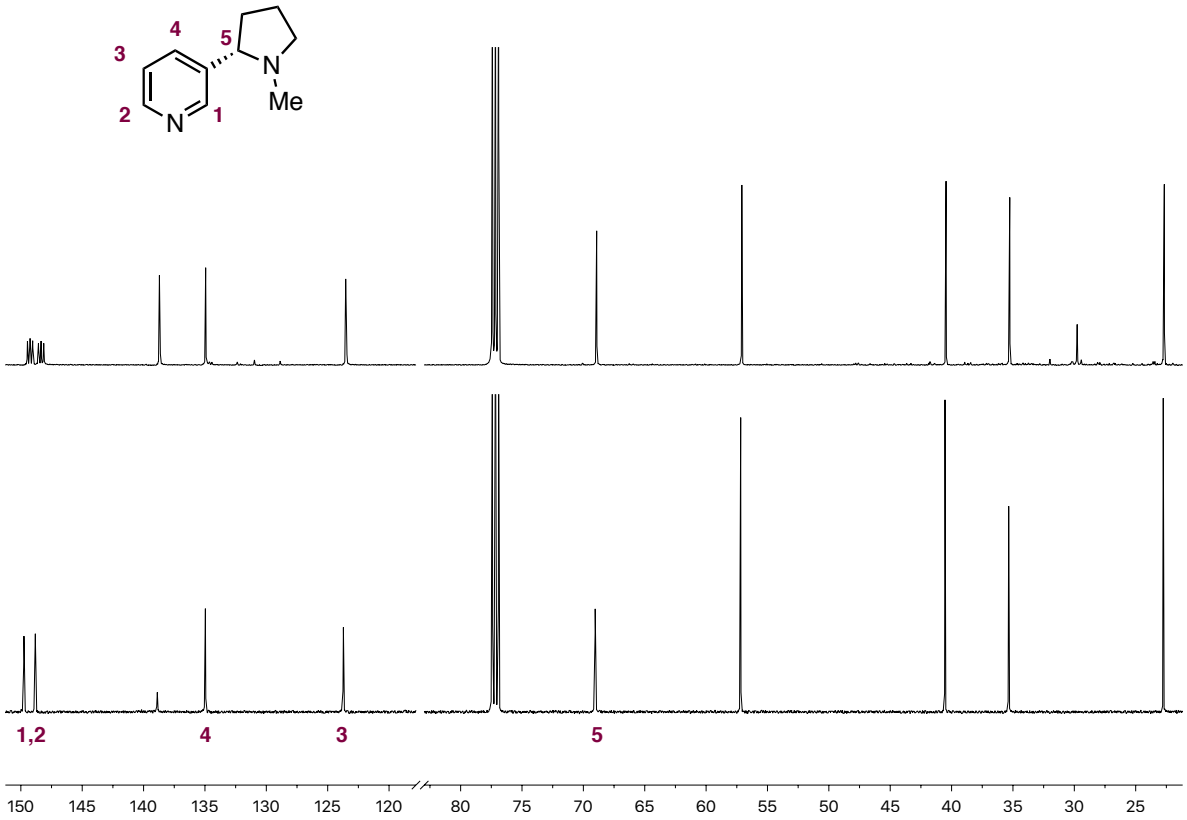

Figure S98. Stacked $^{13}C\{^{1}H\}$ NMR spectra of nicotine: labeled, **[^{2}H]11g** (first, quantitative) and unlabeled, **11g** (second).

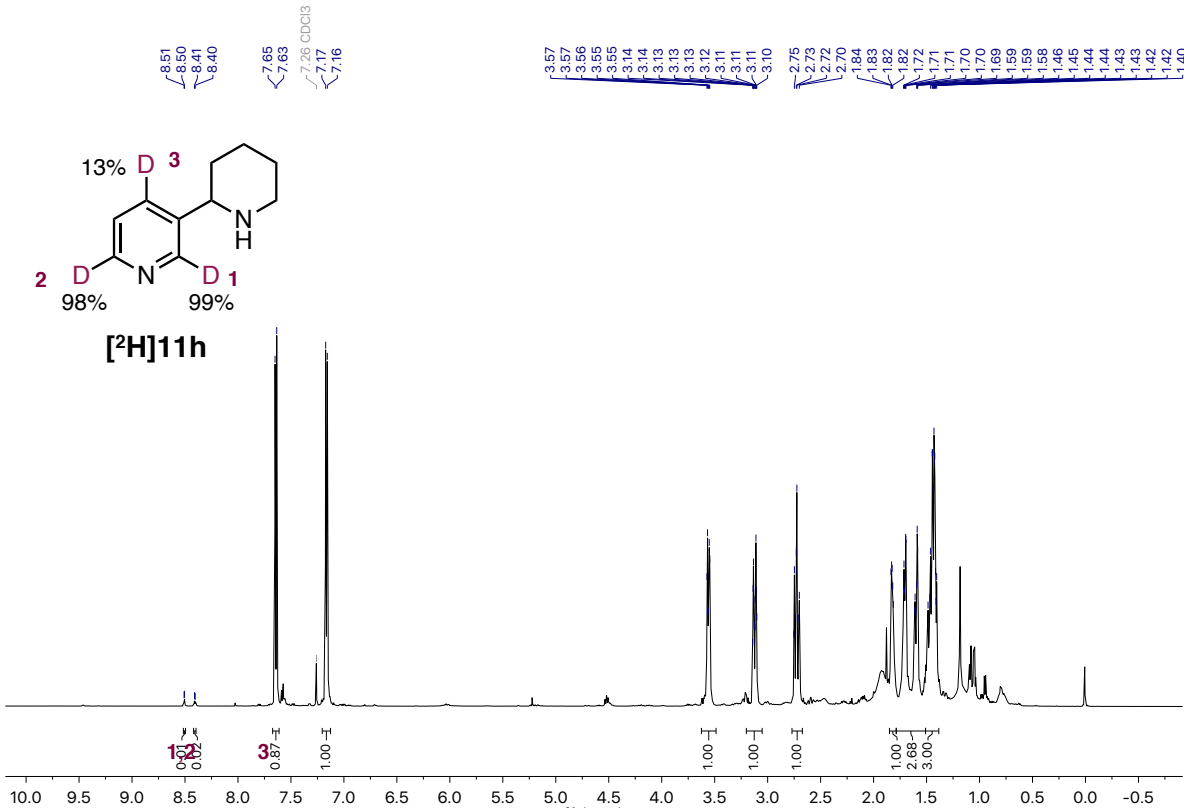

Figure S99. ^{1}H NMR (500 MHz, $CDCl_3$) of labeled (*R*,*S*)-anabasine, **[^{2}H]11h**.

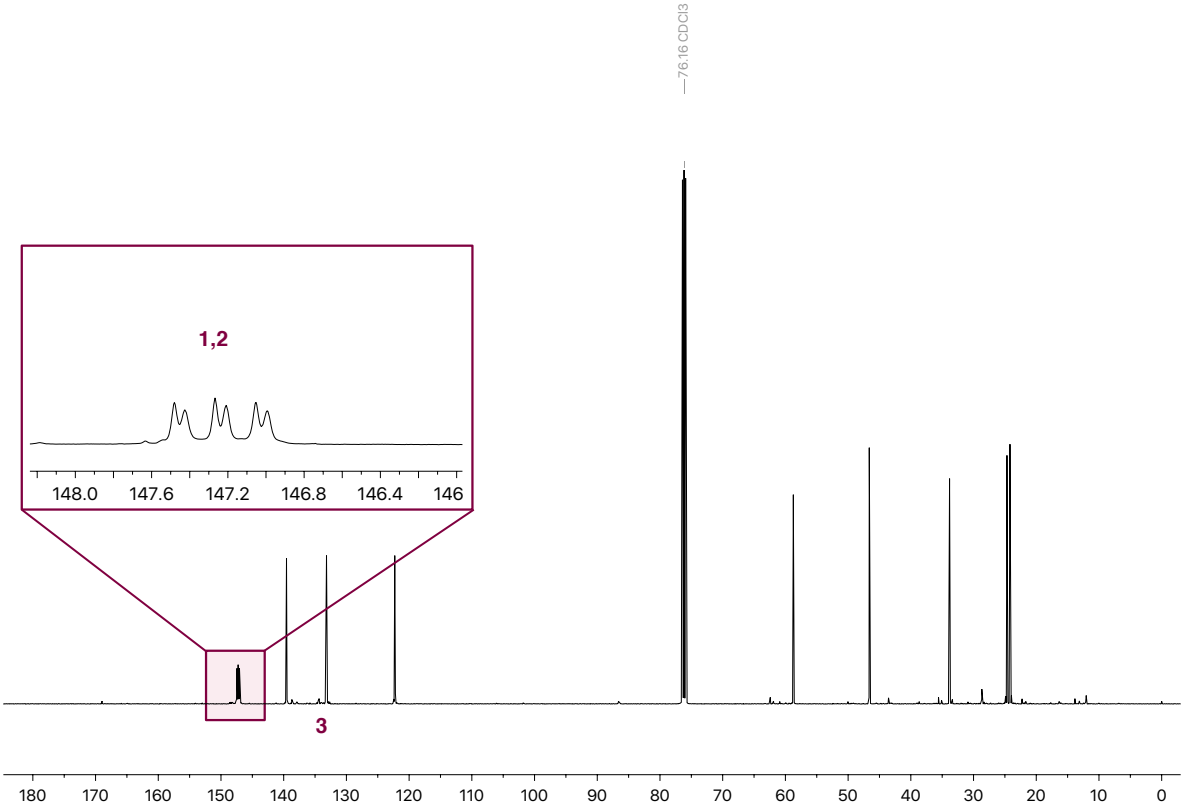

Figure S100. Quantitative ^{13}C{^{1}H} NMR (126 MHz, $CDCl_3$) of **[^{2}H]11h**.

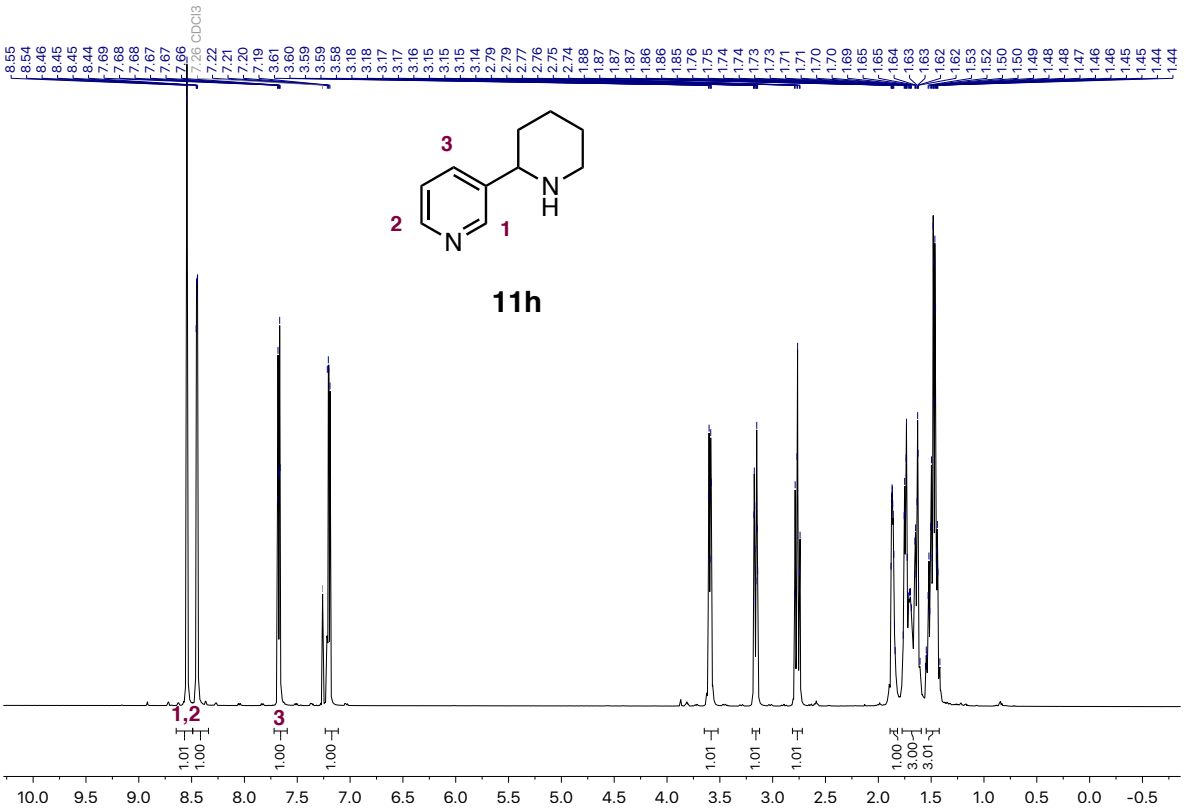

Figure S101. ^{1}H NMR (500 MHz, $CDCl_3$) of unlabeled (*R*,*S*)-anabasine, **11h**.

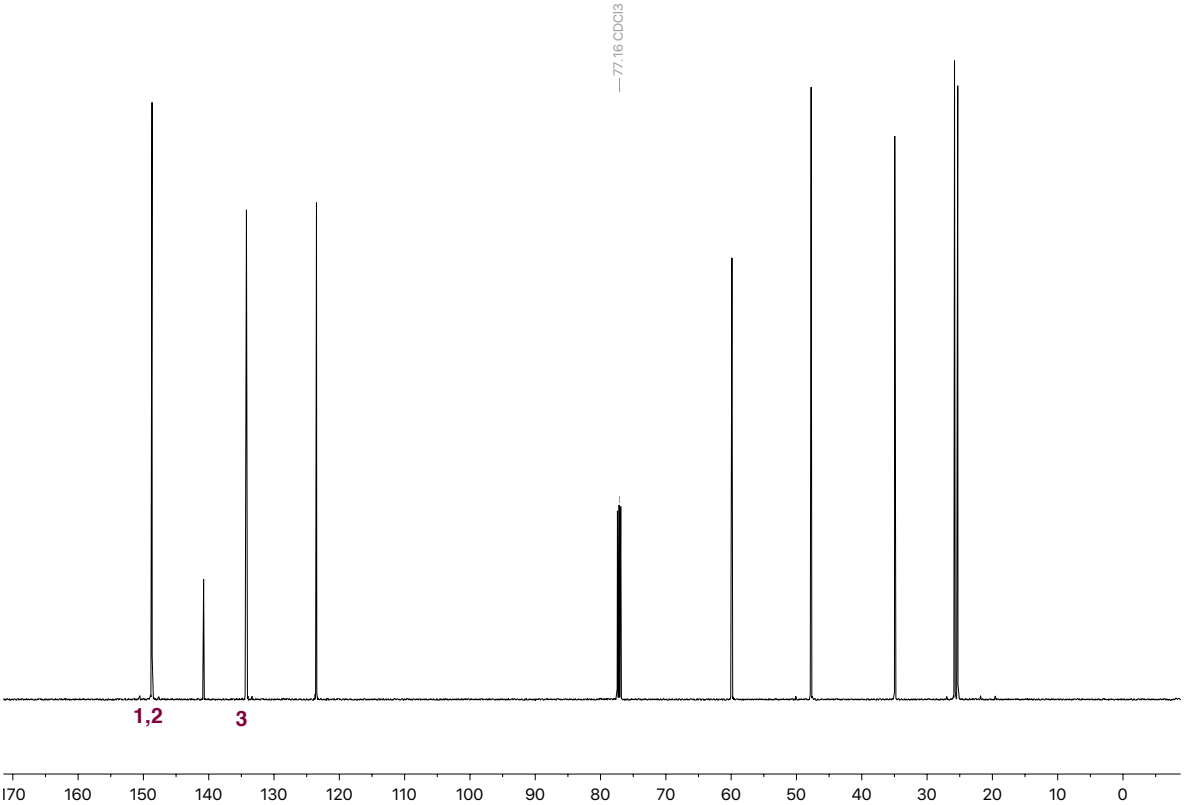

Figure S102. ^{13}C{^{1}H} NMR (126 MHz, $CDCl_3$) of **11h**.

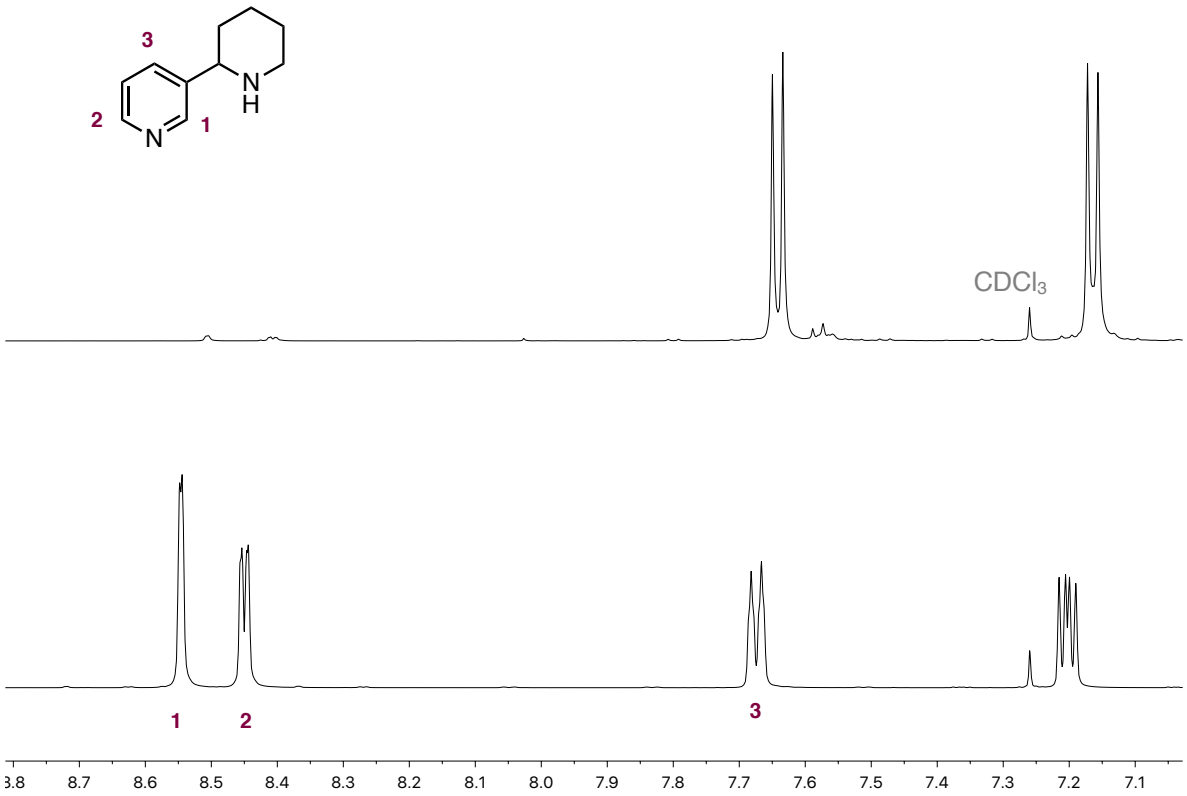

Figure S103. Stacked ^{1}H NMR spectra of (*R*,*S*)-anabasine: labeled, **[^{2}H]11h** (first) and unlabeled, **11h** (second).

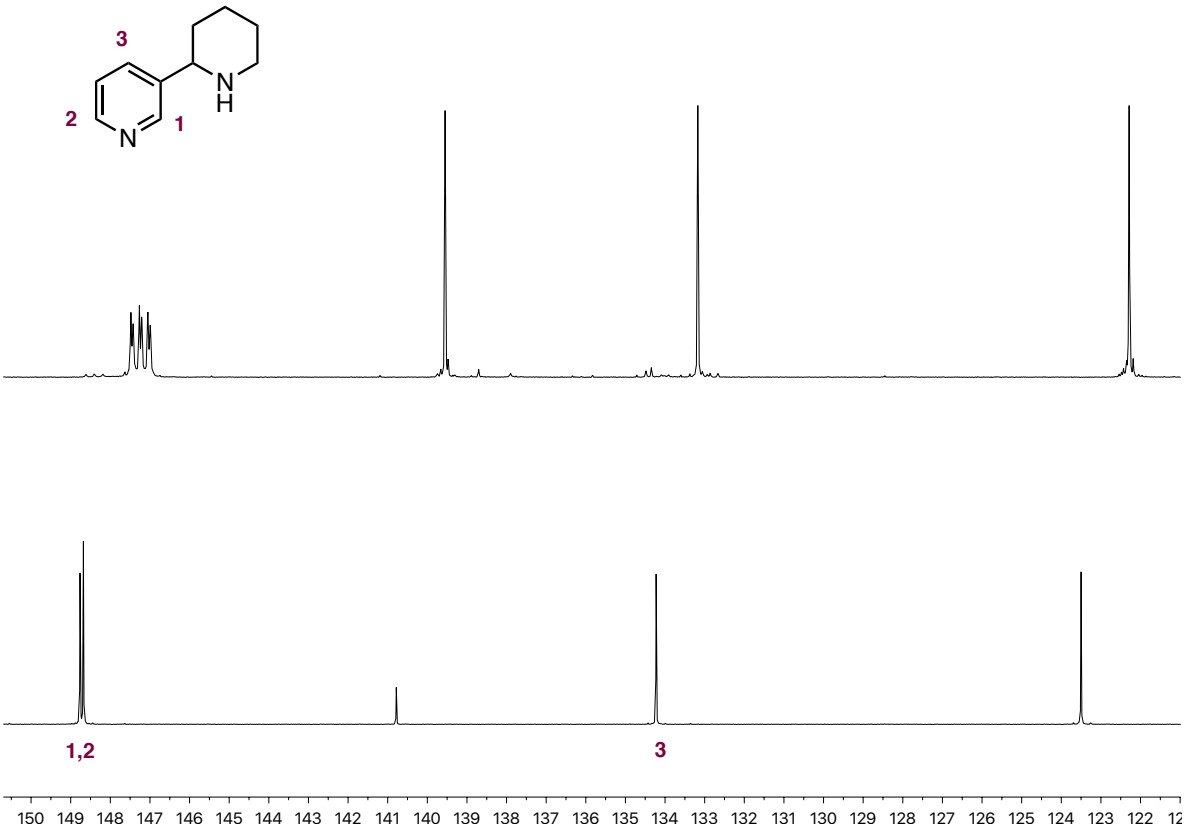

Figure S104. Stacked $^{13}C\{^{1}H\}$ NMR spectra of (*R*,*S*)-anabasine: labeled, **[^{2}H]11h** (first, quantitative) and unlabeled, **11h** (second).

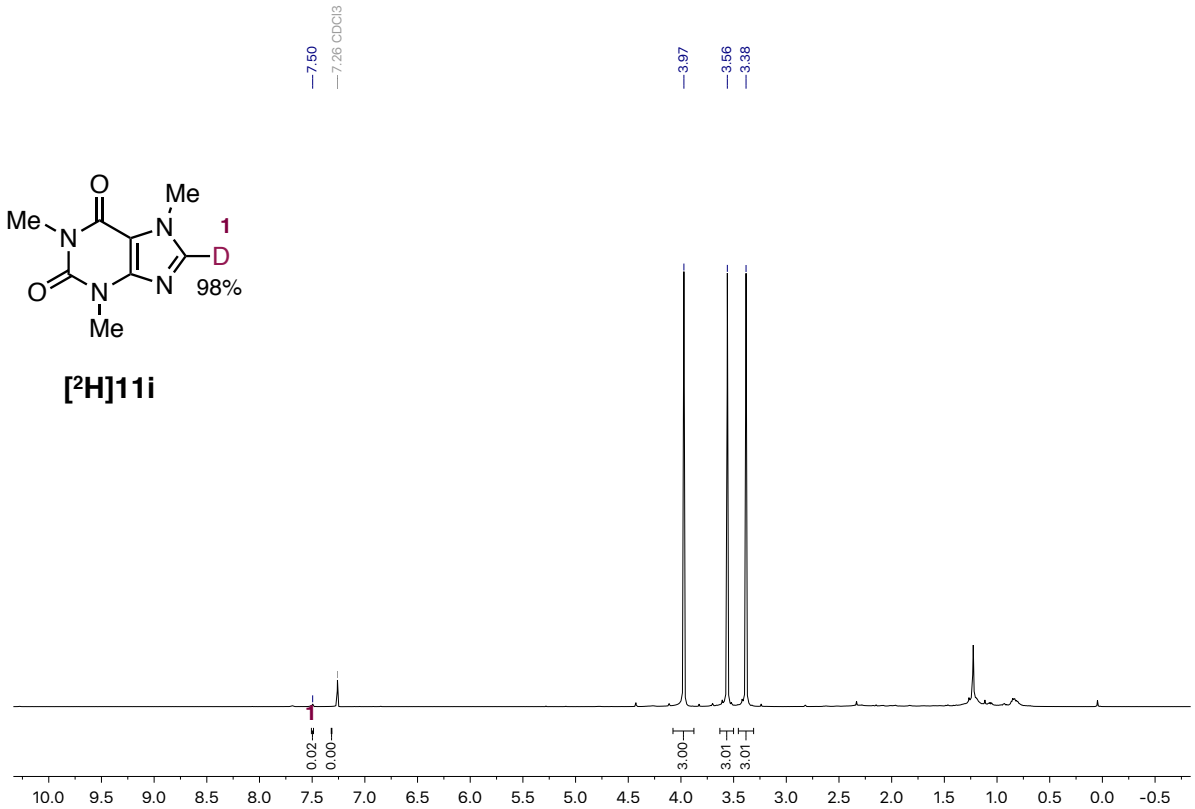

Figure S105. ^{1}H NMR (500 MHz, $CDCl_3$) of labeled caffeine, **[^{2}H]11i**.

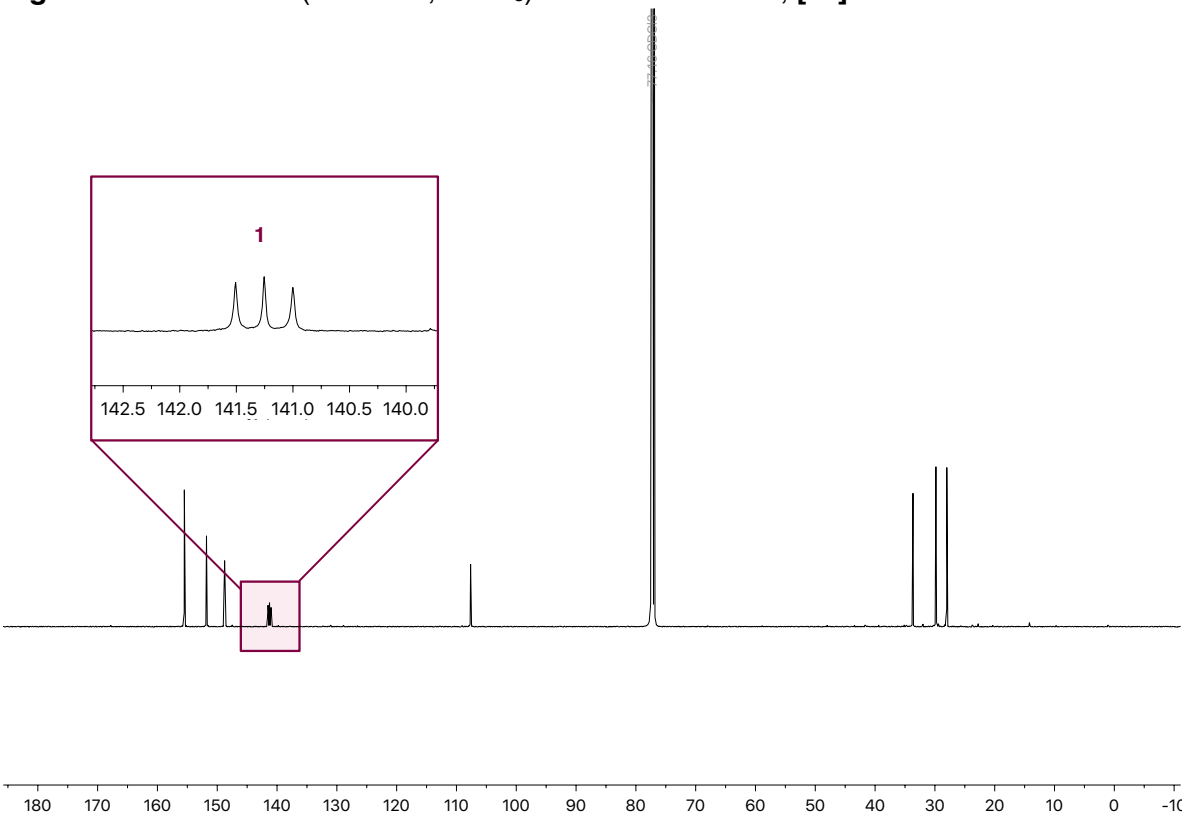

Figure S106. Quantitative ^{13}C{^{1}H} NMR (126 MHz, $CDCl_3$) of **[^{2}H]11i**.

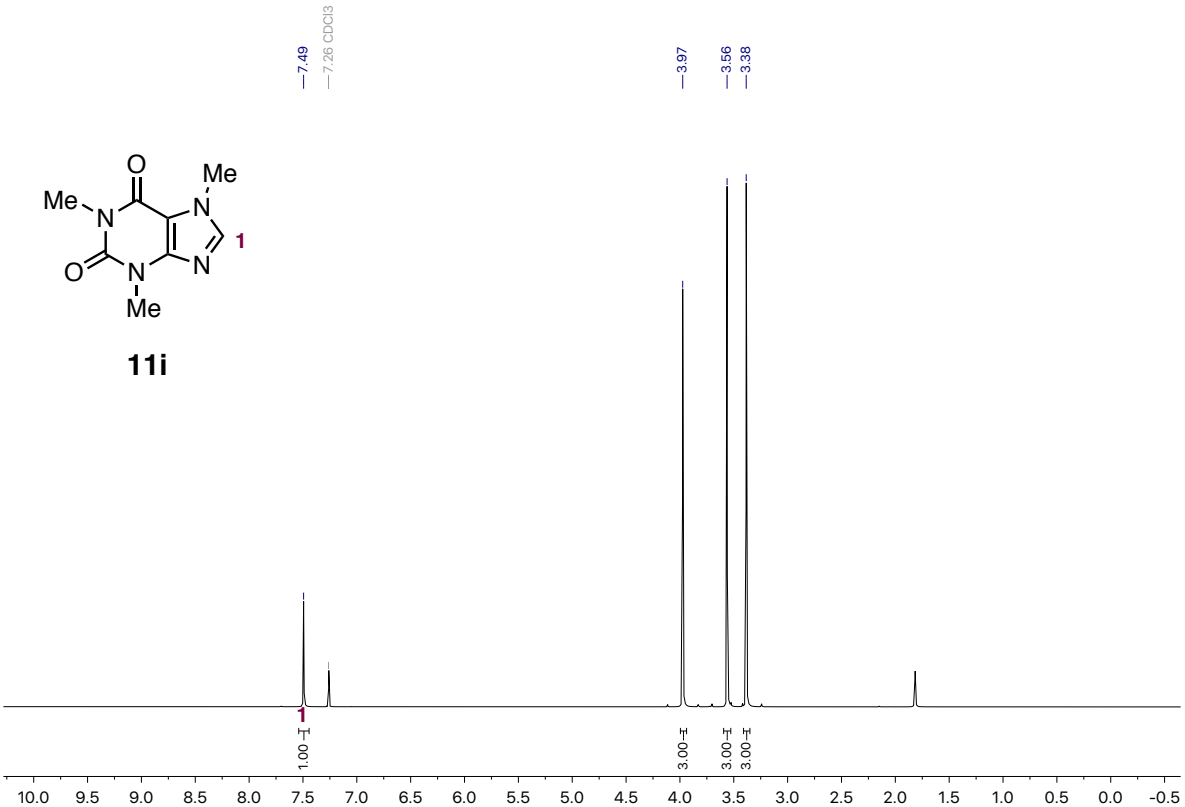

Figure S107. ^{1}H NMR (500 MHz, $CDCl_3$) of unlabeled caffeine, **11i**.

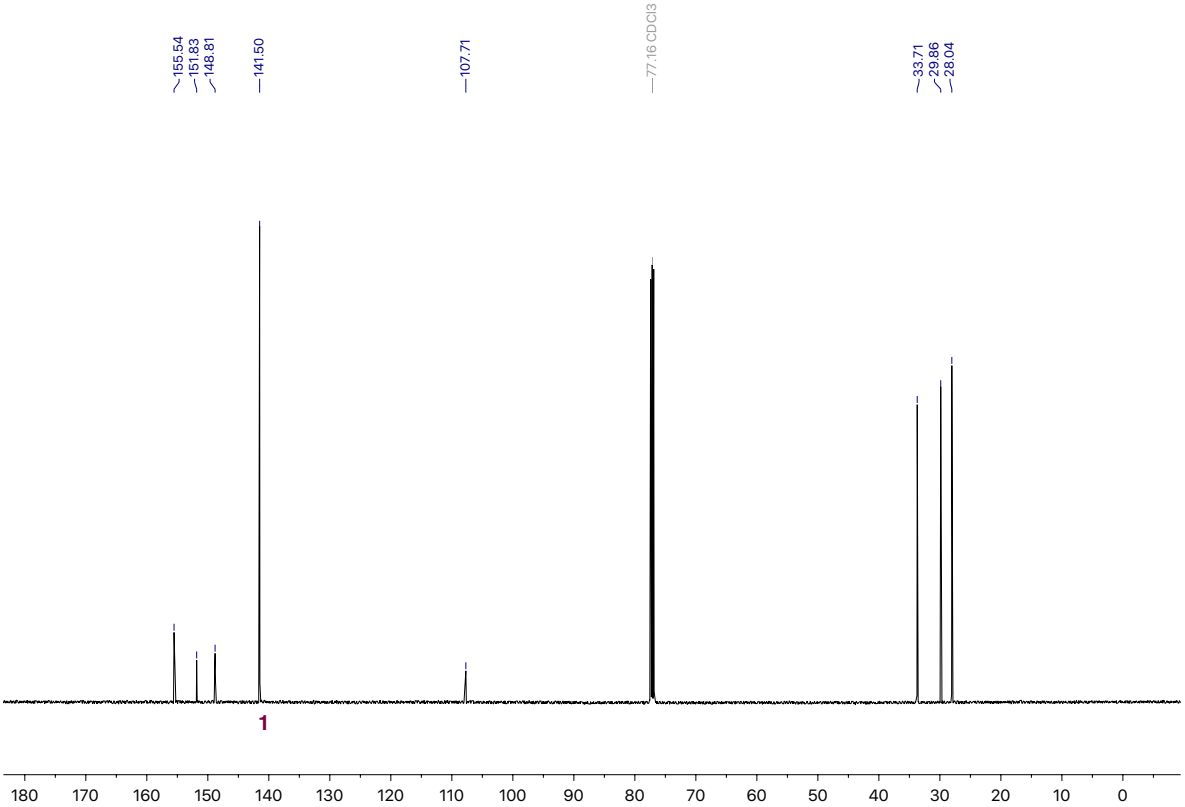

Figure S108. ^{13}C{^{1}H} NMR (126 MHz, $CDCl_3$) of **11i**.

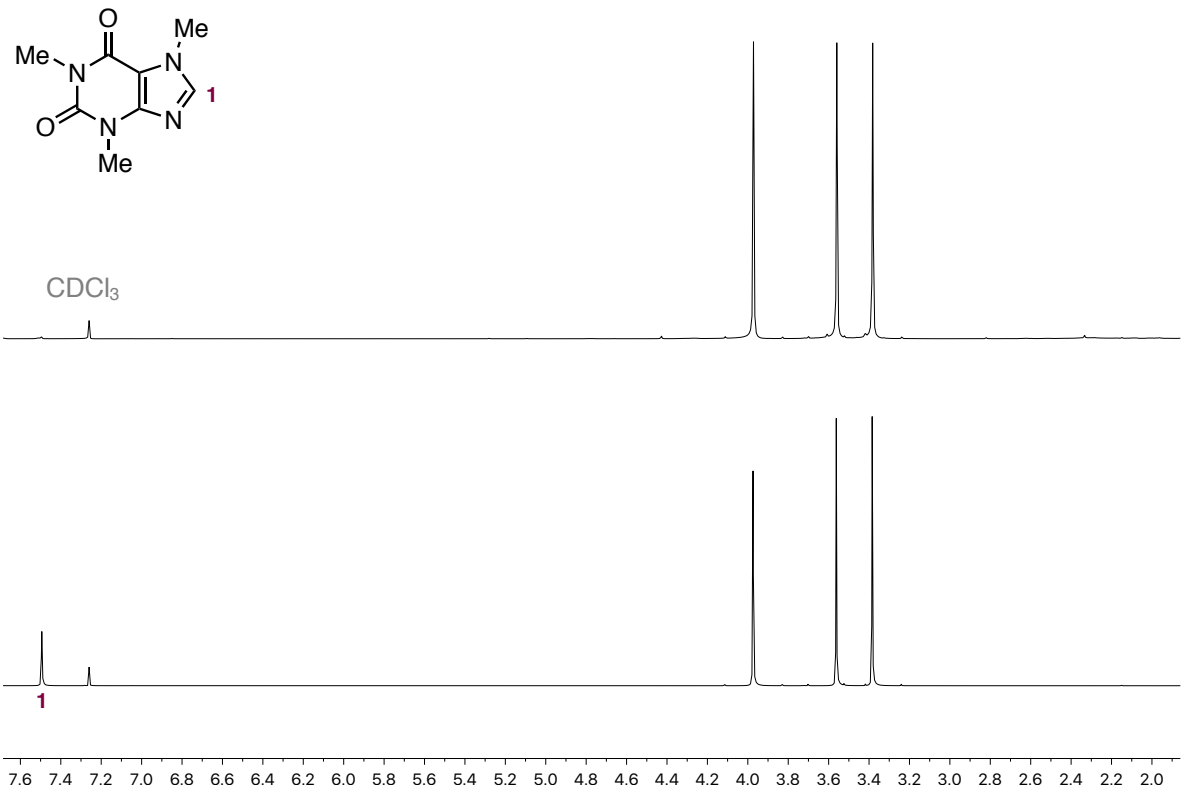

Figure S109. Stacked ^{1}H NMR spectra of caffeine: labeled, **[^{2}H]11i** (first) and unlabeled, **11i** (second).

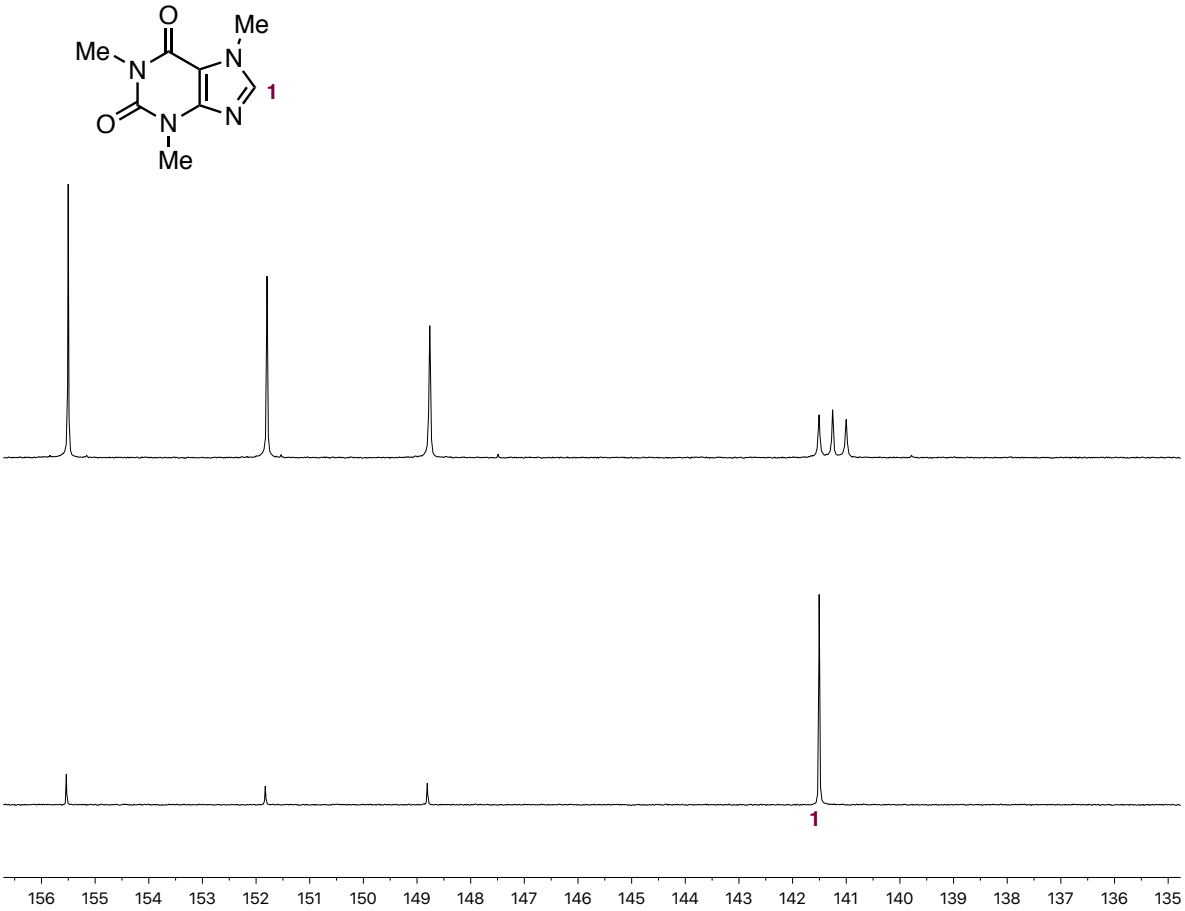

Figure S110. Stacked $^{13}C\{^{1}H\}$ NMR spectra of caffeine: labeled, **[^{2}H]11i** (first, quantitative) and unlabeled, **11i** (second).

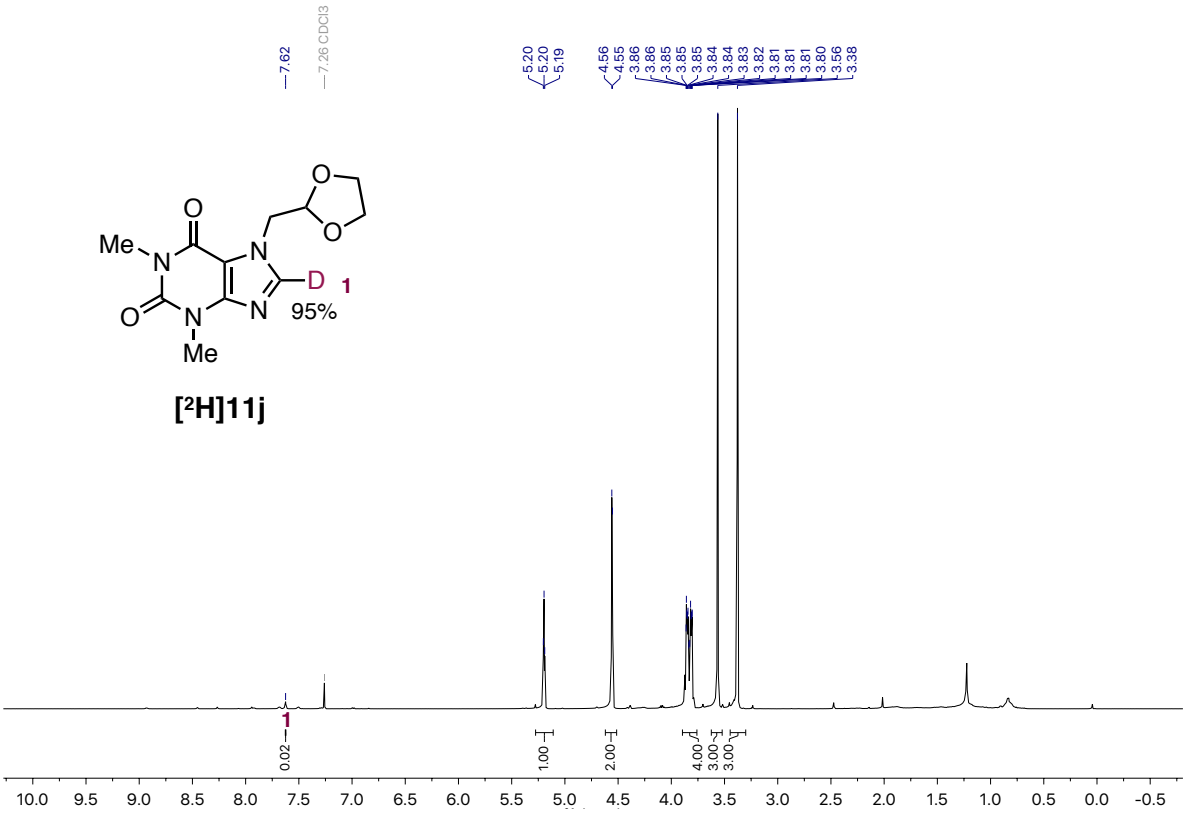

Figure S111. ^{1}H NMR (500 MHz, $CDCl_3$) of labeled doxofylline, **[^{2}H]11j.**

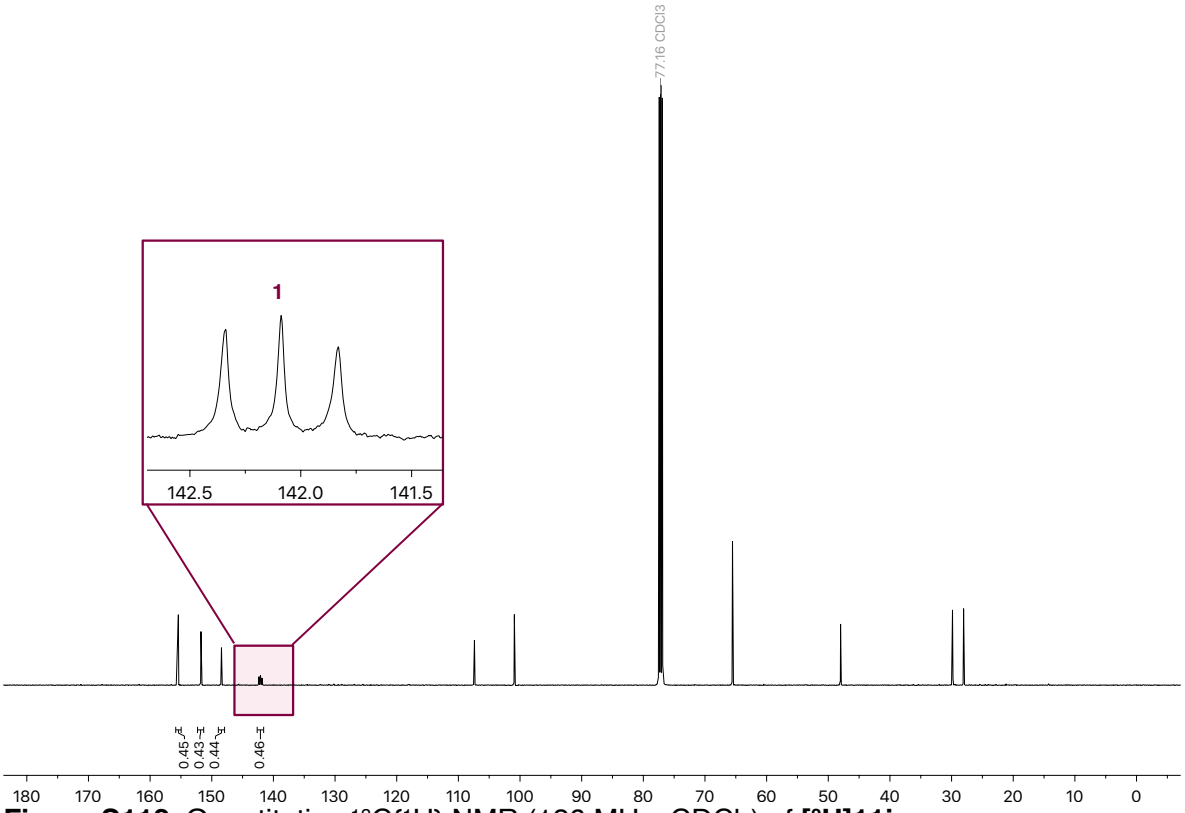

Figure S112. Quantitative ^{13}C{^{1}H} NMR (126 MHz, $CDCl_3$) of **[^{2}H]11j.**

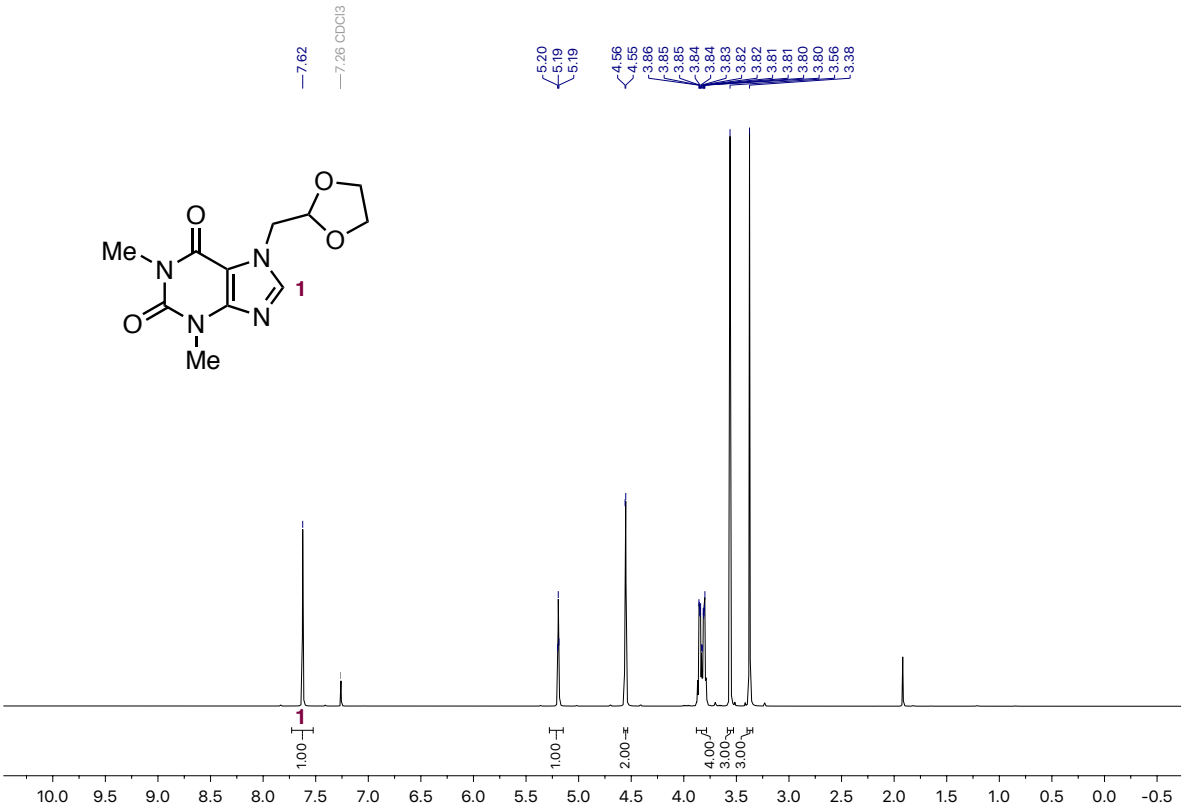

Figure S113. ^{1}H NMR (500 MHz, $CDCl_3$) of unlabeled doxofylline, **11j.**

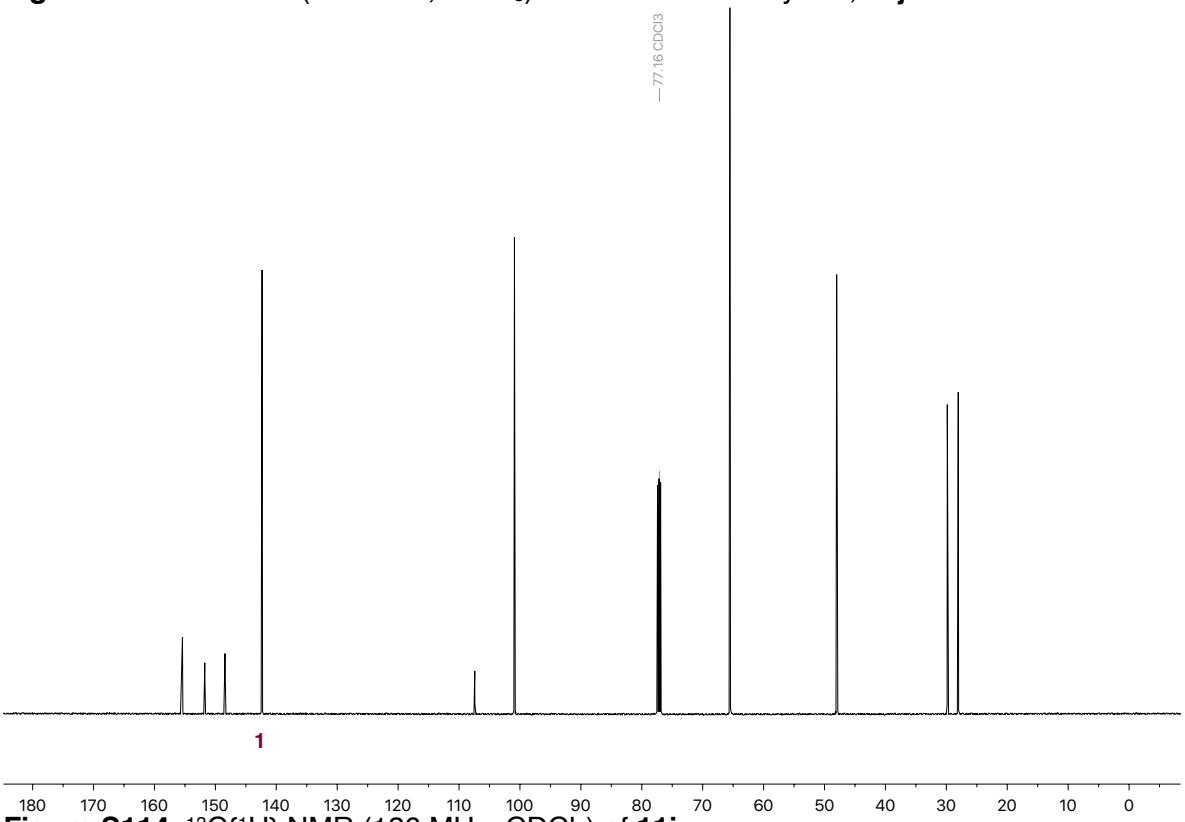

Figure S114. ^{13}C{^{1}H} NMR (126 MHz, $CDCl_3$) of **11j.**

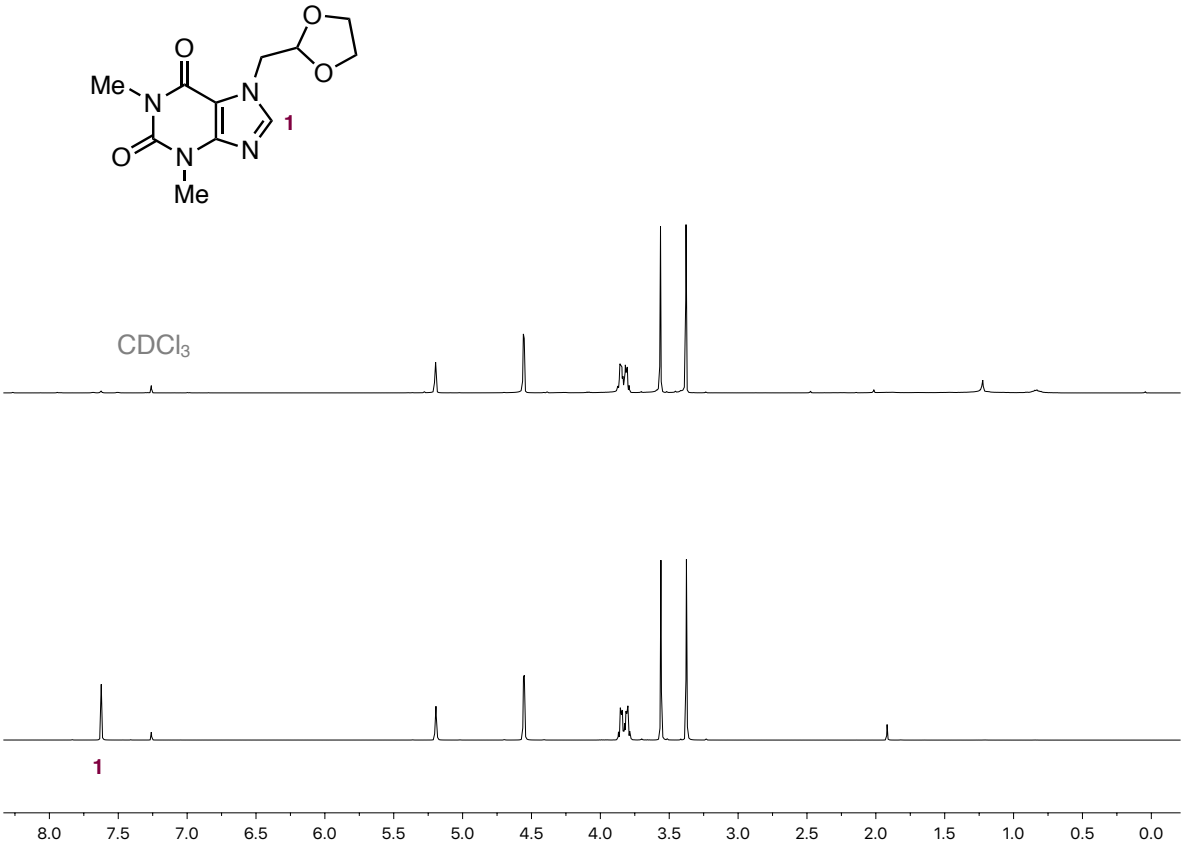

Figure S115. Stacked ^{1}H NMR spectra of doxofylline: labeled, **[^{2}H]11j** (first) and unlabeled, **11j** (second).

Figure S116. Stacked $^{13}C\{^{1}H\}$ NMR spectra of doxofylline (aromatic region): labeled, **[^{2}H]11j** (first, quantitative) and unlabeled, **11j** (second).

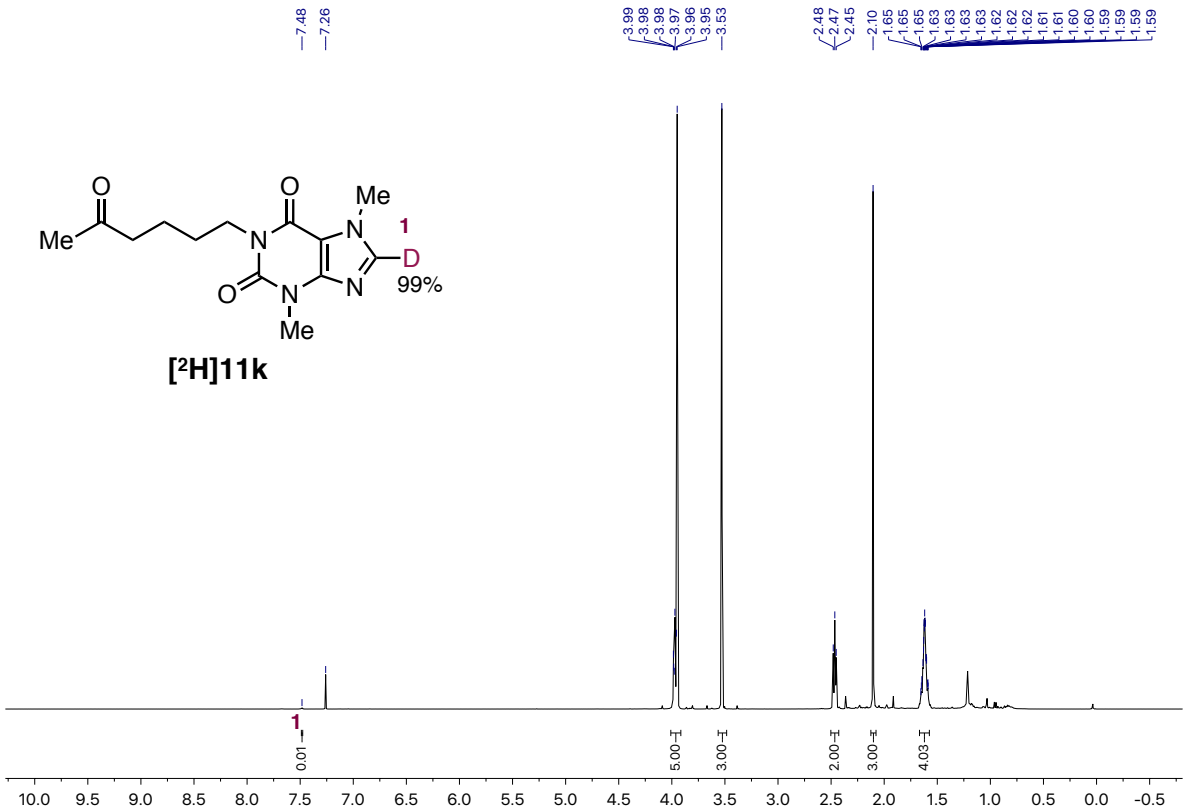

Figure S117. ^{1}H NMR (500 MHz, $CDCl_3$) of labeled pentoxifylline, **[^{2}H]11k.**

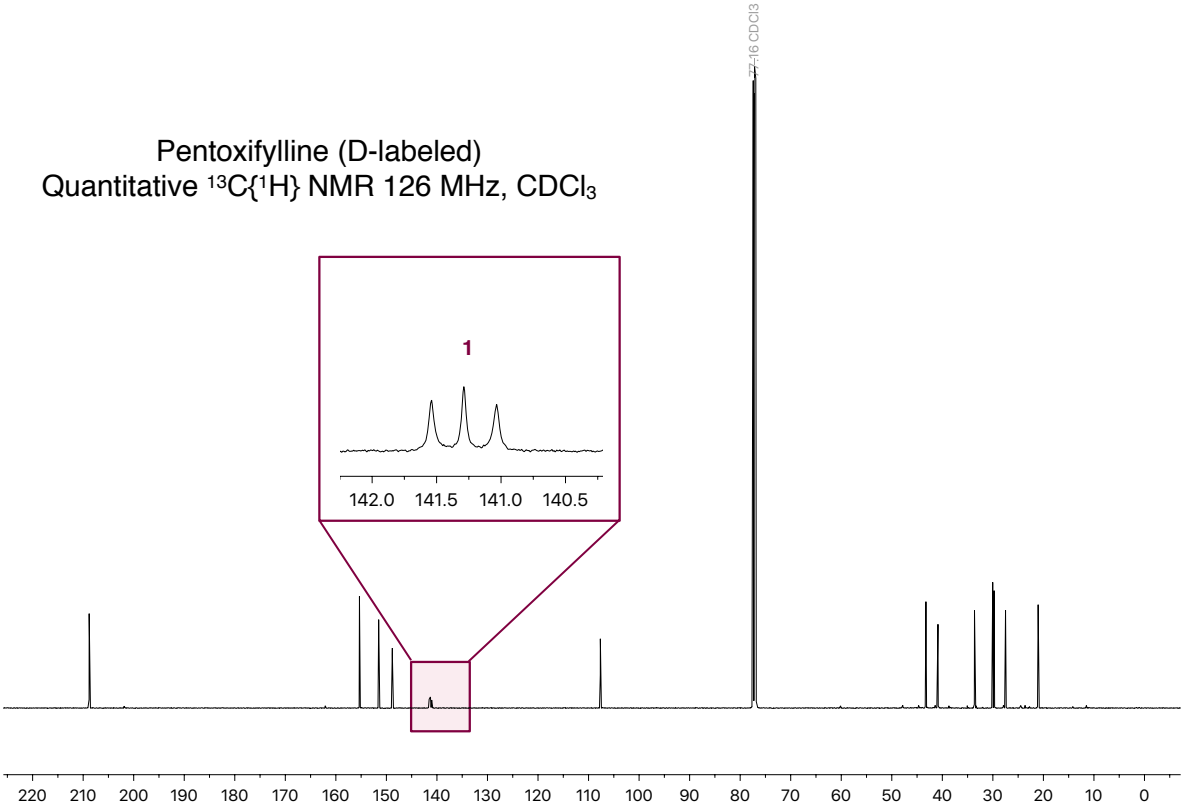

Figure S118. Quantitative ^{13}C{^{1}H} NMR (126 MHz, $CDCl_3$) of **[^{2}H]11k.**

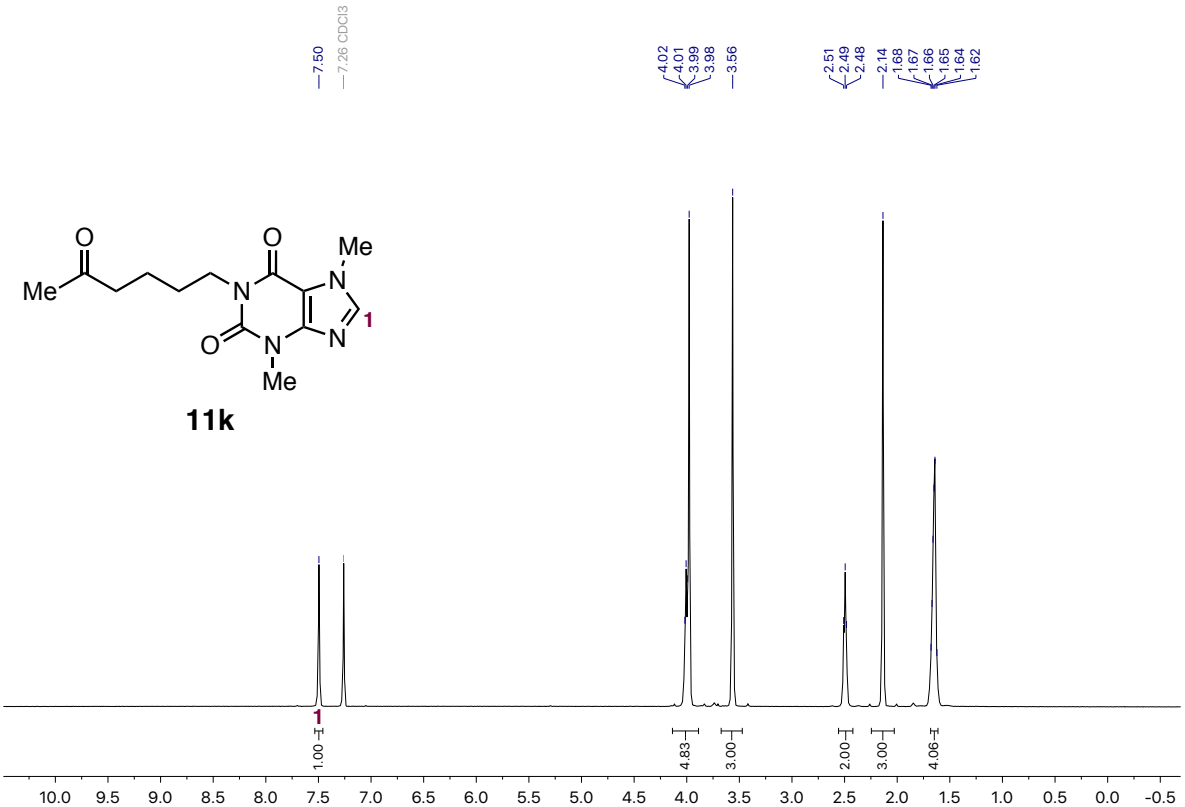

Figure S119. ^{1}H NMR (500 MHz, $CDCl_3$) of unlabeled pentoxifylline, **11k.**

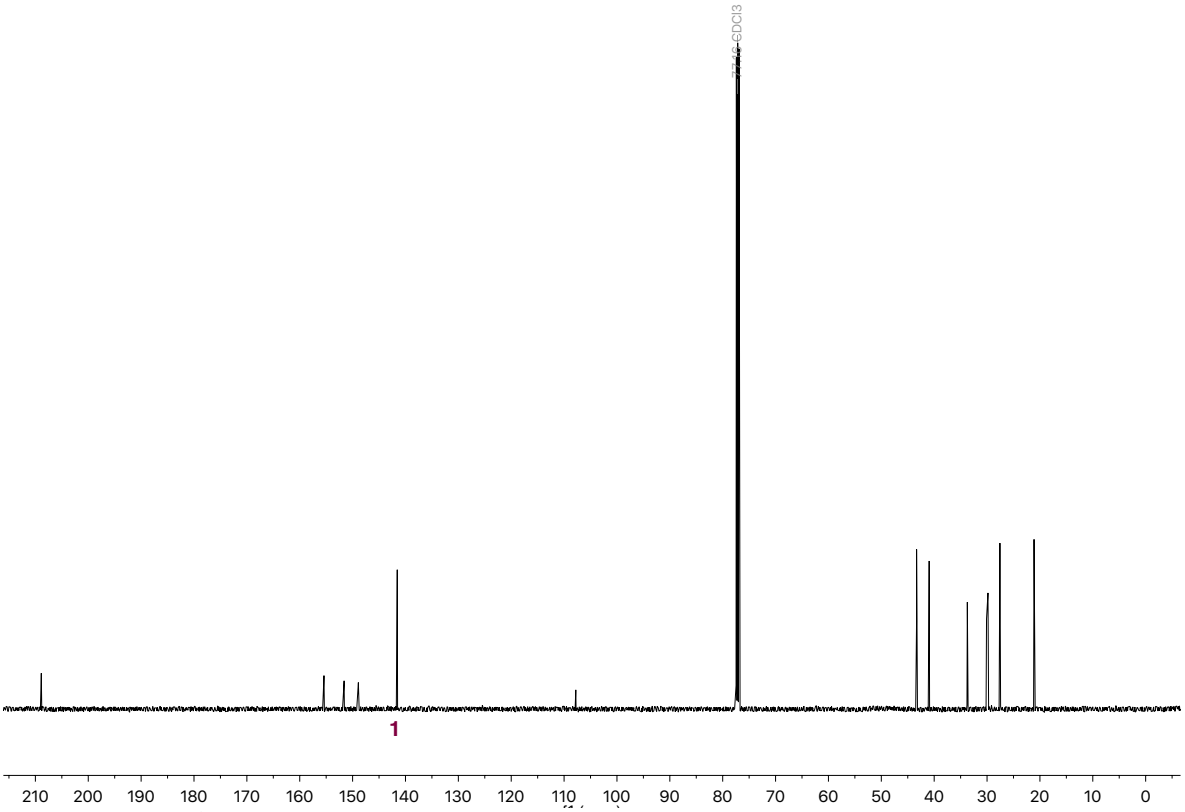

Figure S120. ^{13}C{^{1}H} NMR (126 MHz, $CDCl_3$) of **11k.**

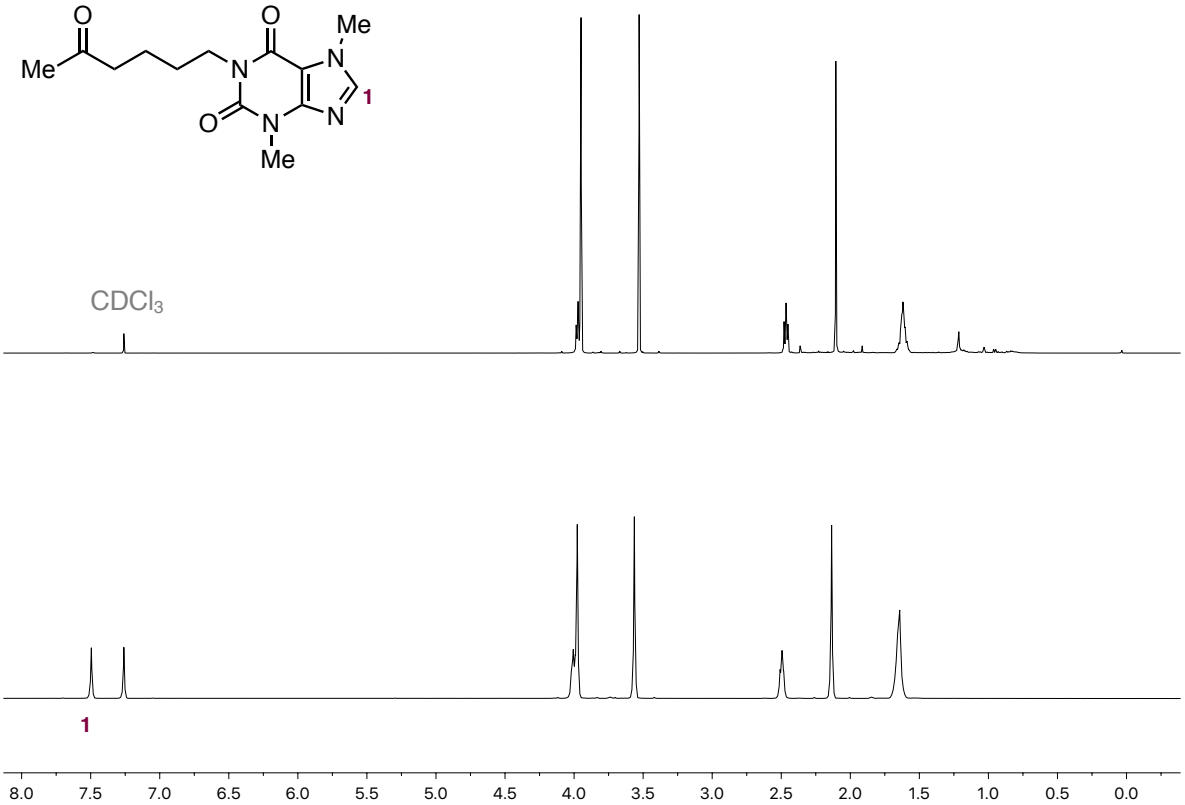

Figure S121. Stacked ^{1}H NMR spectra of pentoxifylline: labeled, **[^{2}H]11k** (first) and unlabeled, **11k** (second).

Figure S122. Stacked $^{13}C\{^{1}H\}$ NMR spectra of pentoxifylline (aromatic region): labeled, **[^{2}H]11k** (first, quantitative) and unlabeled, **11k** (second).

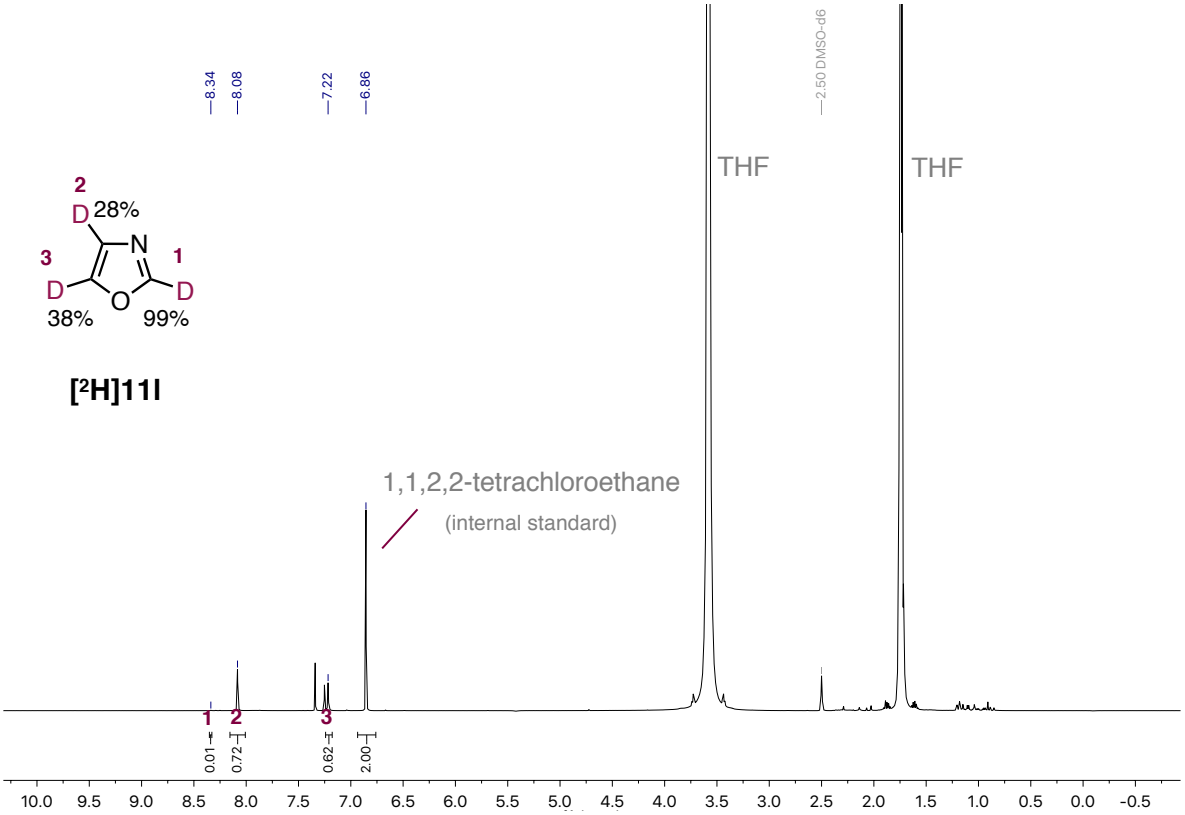

Figure S123. ^{1}H NMR (500 MHz, DMSO-d_6) of labeled oxazole, **[^{2}H]11I.**

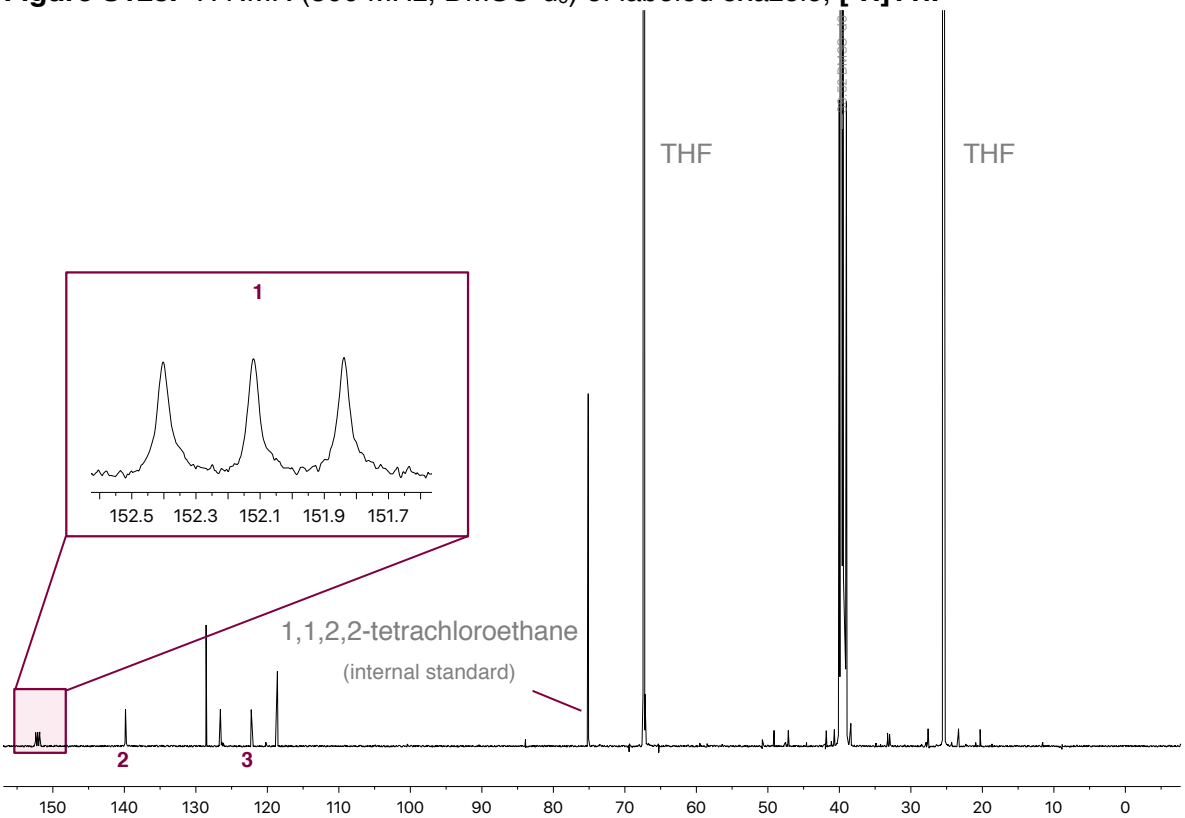

Figure S124. Quantitative ^{13}C{^{1}H} NMR (126 MHz, DMSO-d_6) of **[^{2}H]11I.**

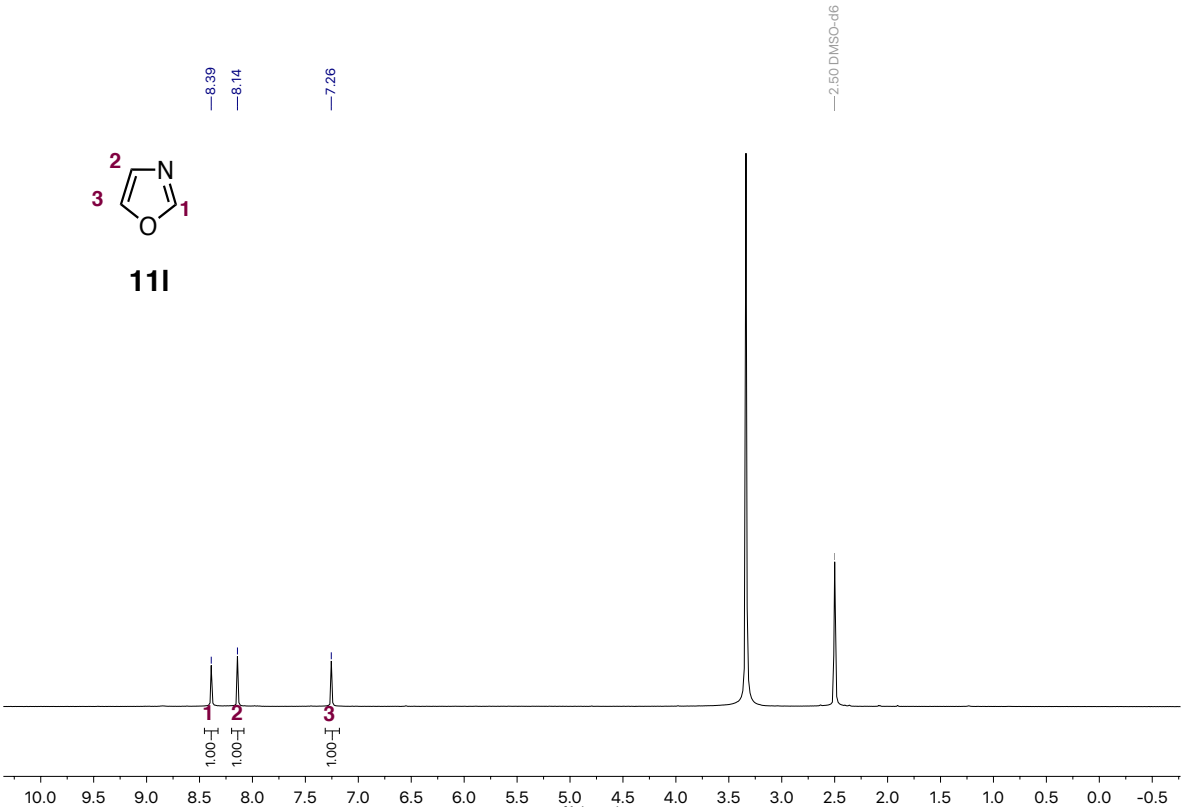

Figure S125. ^{1}H NMR (500 MHz, DMSO-d_6) of unlabeled oxazole, **11l.**

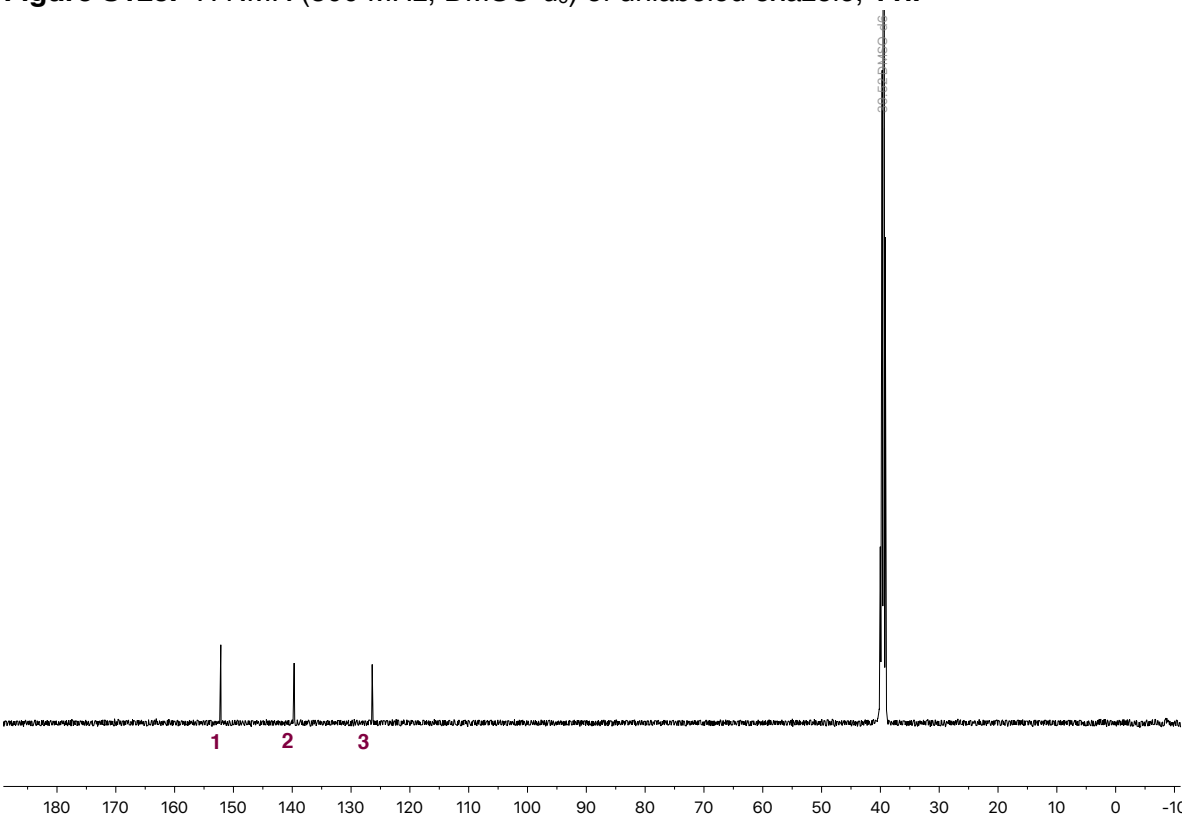

Figure S126. ^{13}C{^{1}H} NMR (126 MHz, DMSO-d_6) of **11l.**

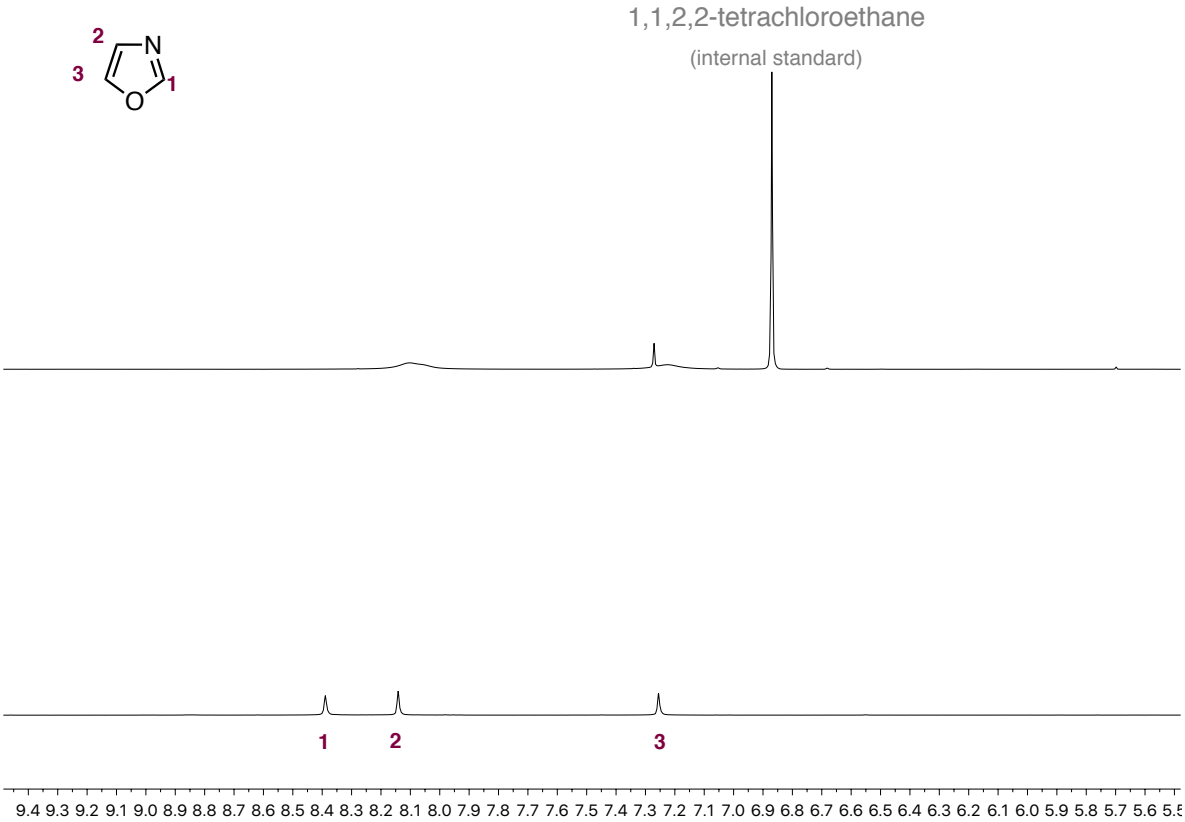

Figure S127. Stacked ^{1}H NMR spectra of oxazole: labeled, **[^{2}H]11l** (first) and unlabeled, **11l** (second).

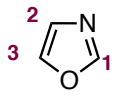

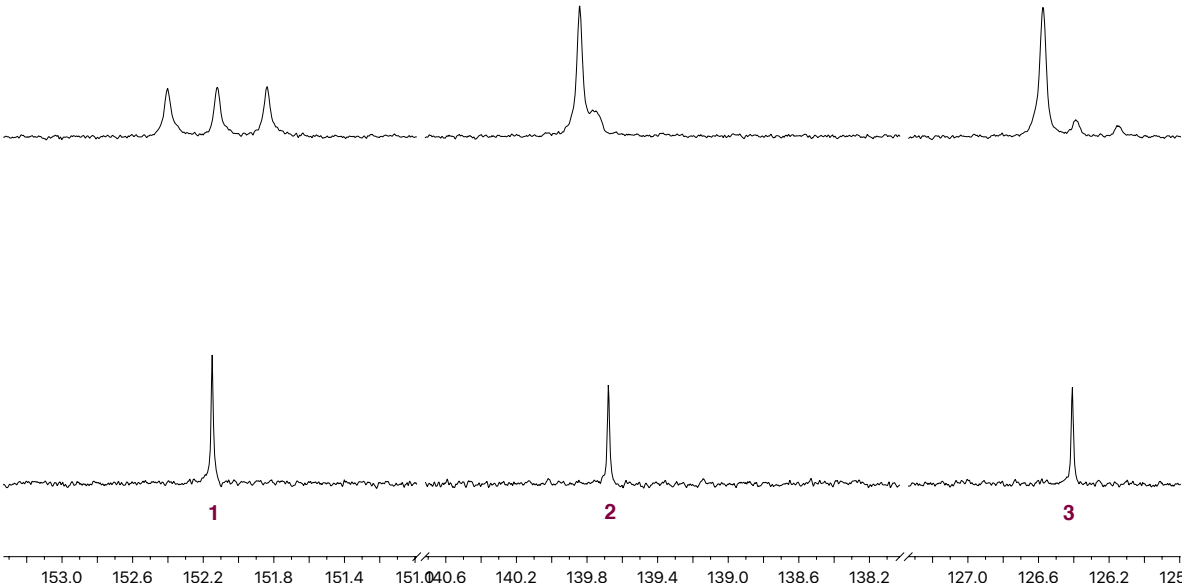

Figure S128. Stacked $^{13}C\{^{1}H\}$ NMR spectra of oxazole: labeled, **[^{2}H]11l** (first, quantitative) and unlabeled, **11l** (second, conventional).

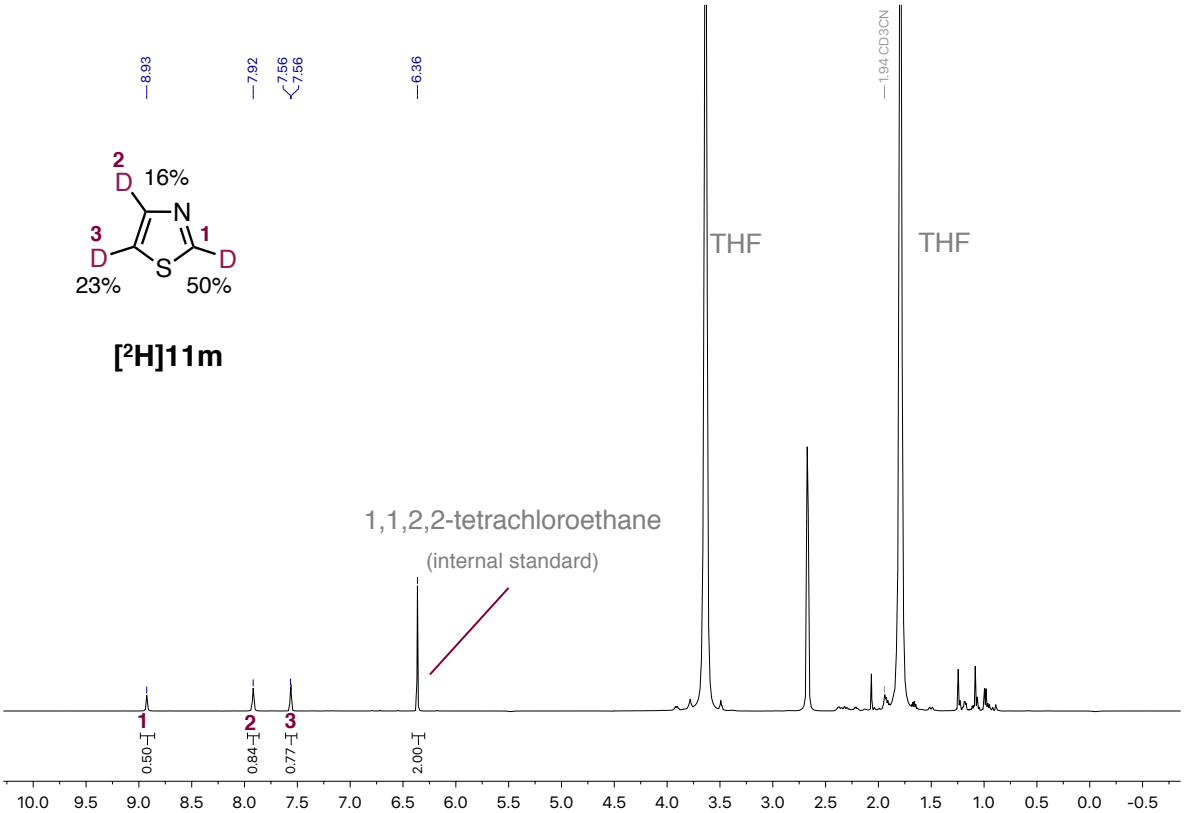

Figure S129. ^{1}H NMR (500 MHz, CD_3CN) of labeled thiazole, **[^{2}H]11m.**

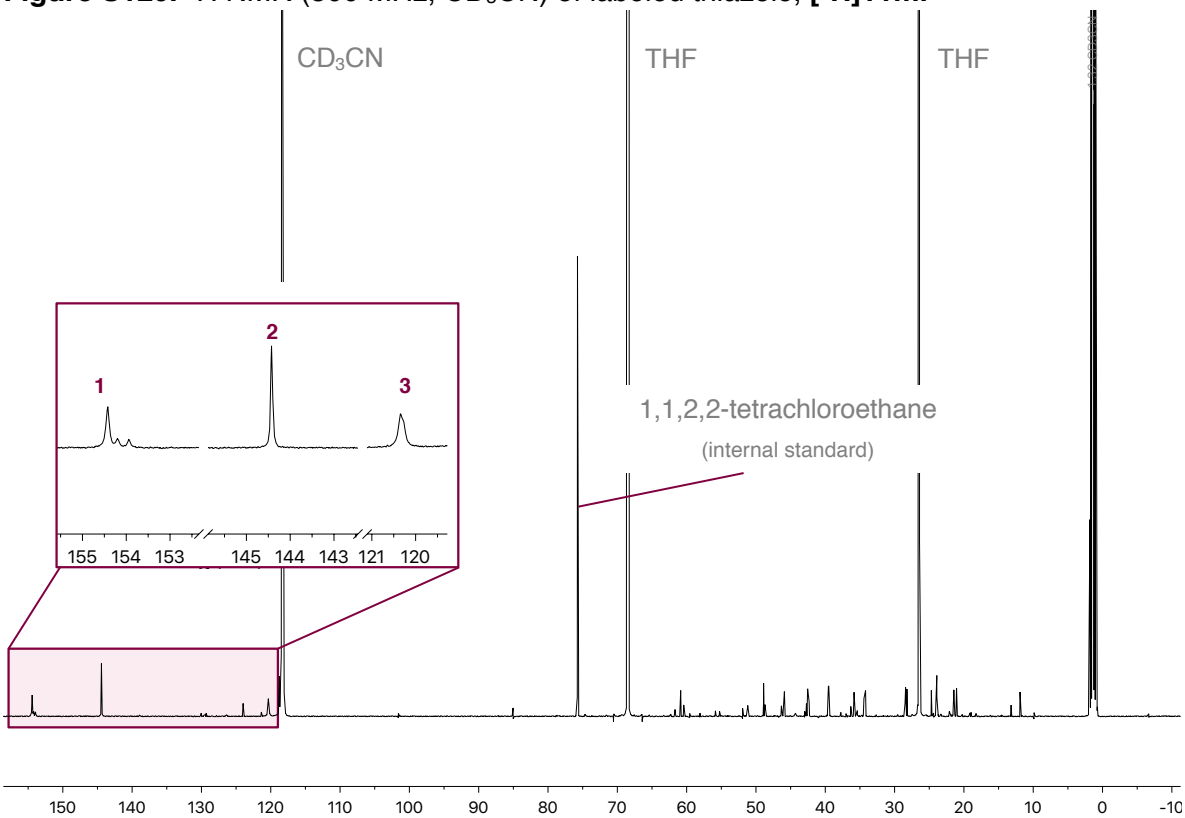

Figure S130. Quantitative ^{13}C{^{1}H} NMR (126 MHz, CD_3CN) of **[^{2}H]11m.**

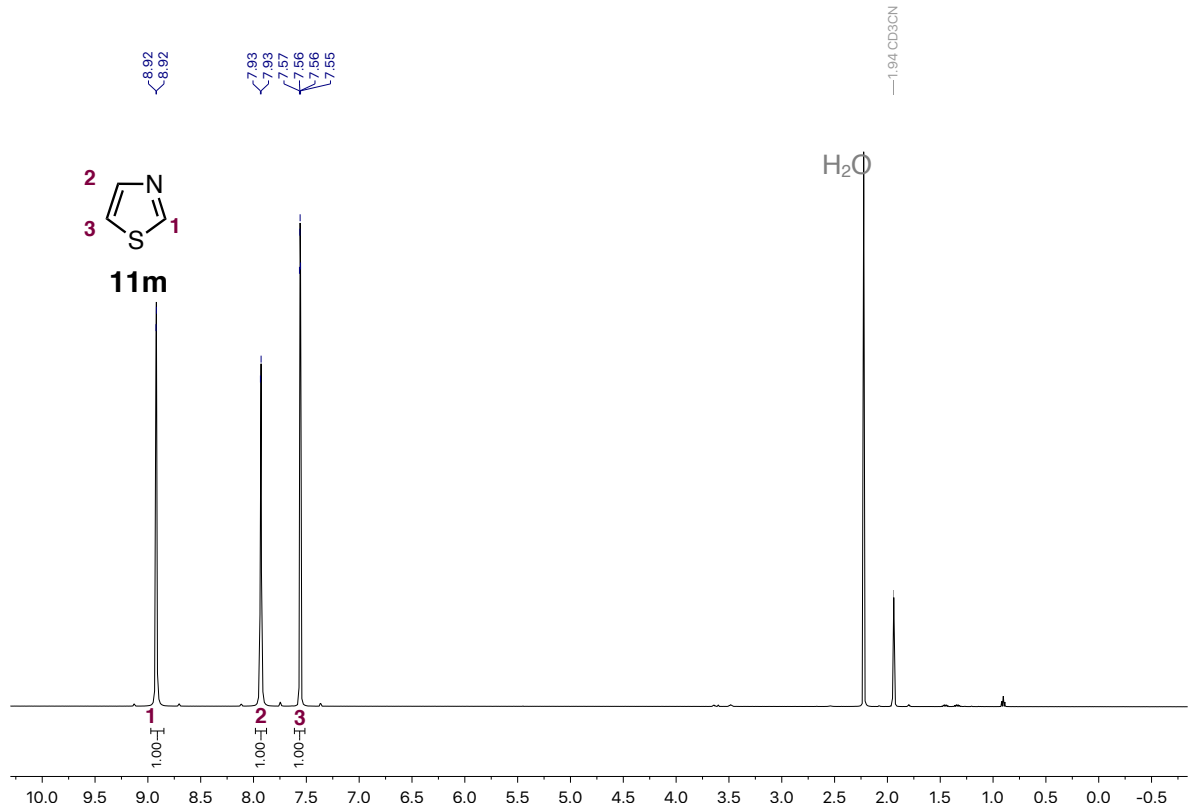

Figure S131. ^{1}H NMR (500 MHz, CD_3CN) of unlabeled thiazole, **11m.**

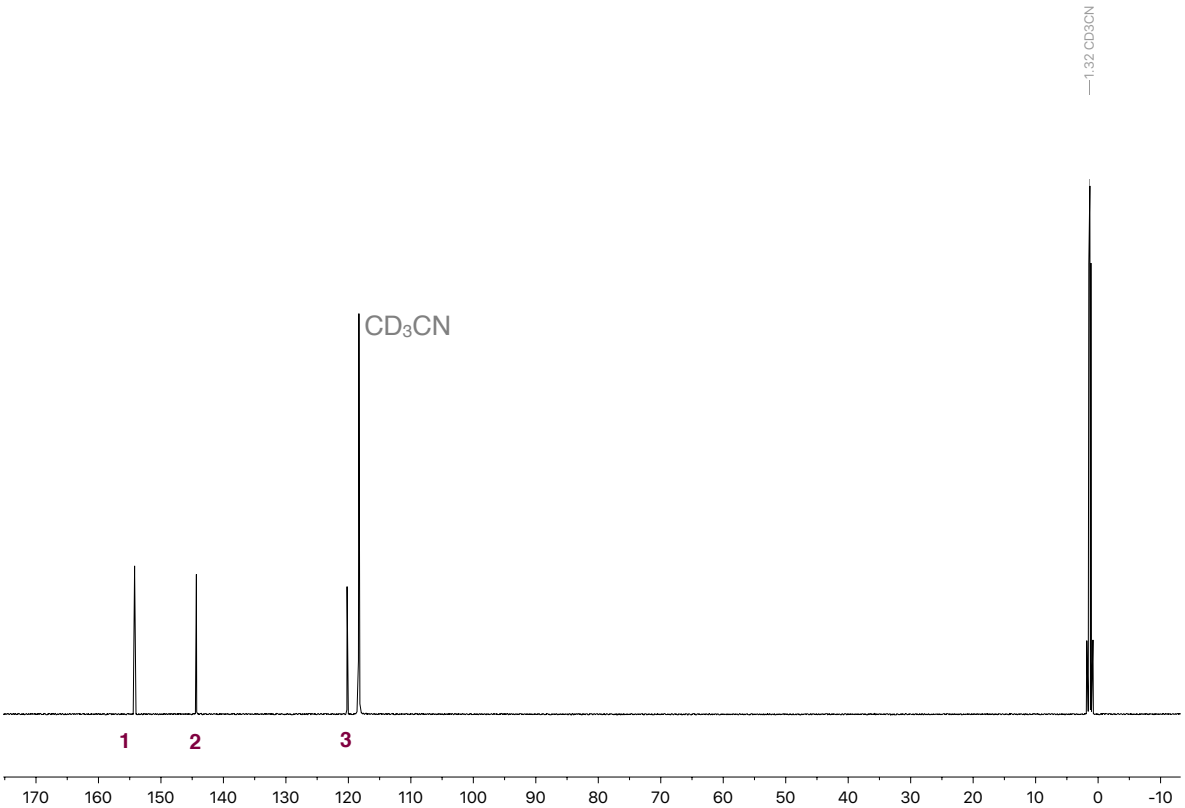

Figure S132. ^{13}C{^{1}H} NMR (126 MHz, CD_3CN) of **11m.**

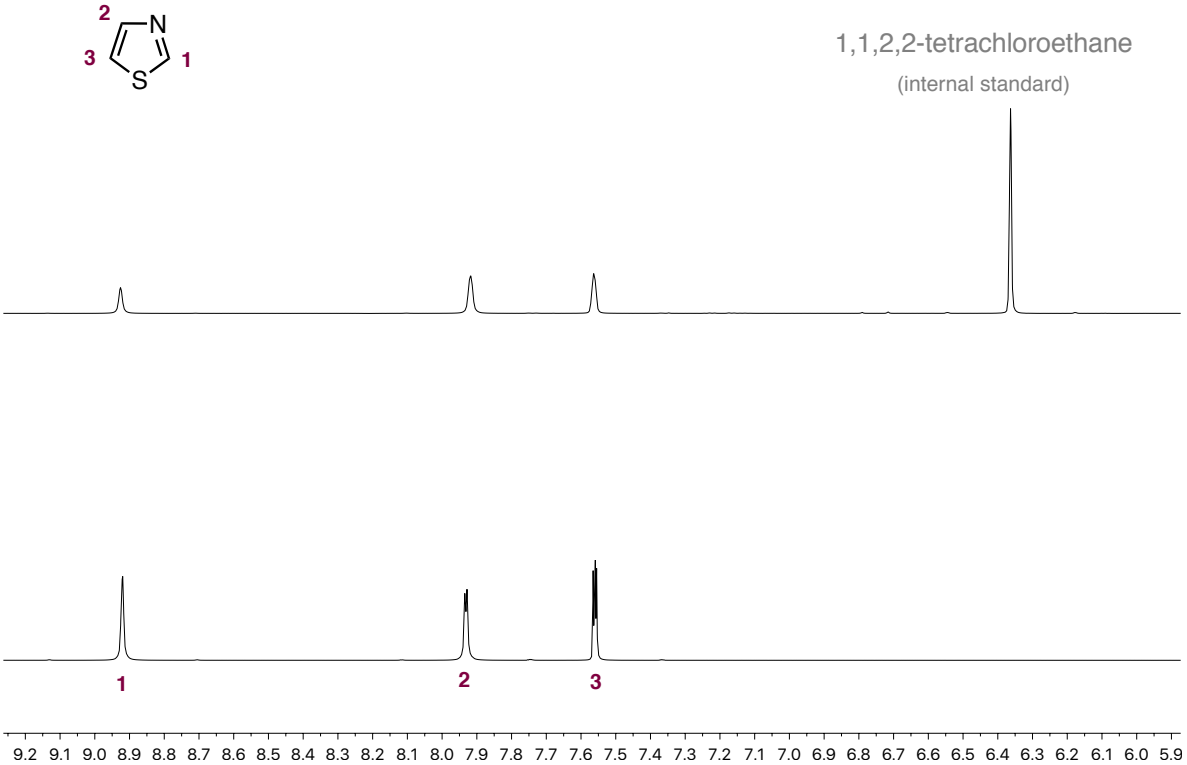

Figure S133. Stacked ^{1}H NMR spectra of thiazole: labeled, **[^{2}H]11m** (first) and unlabeled, **11m** (second).

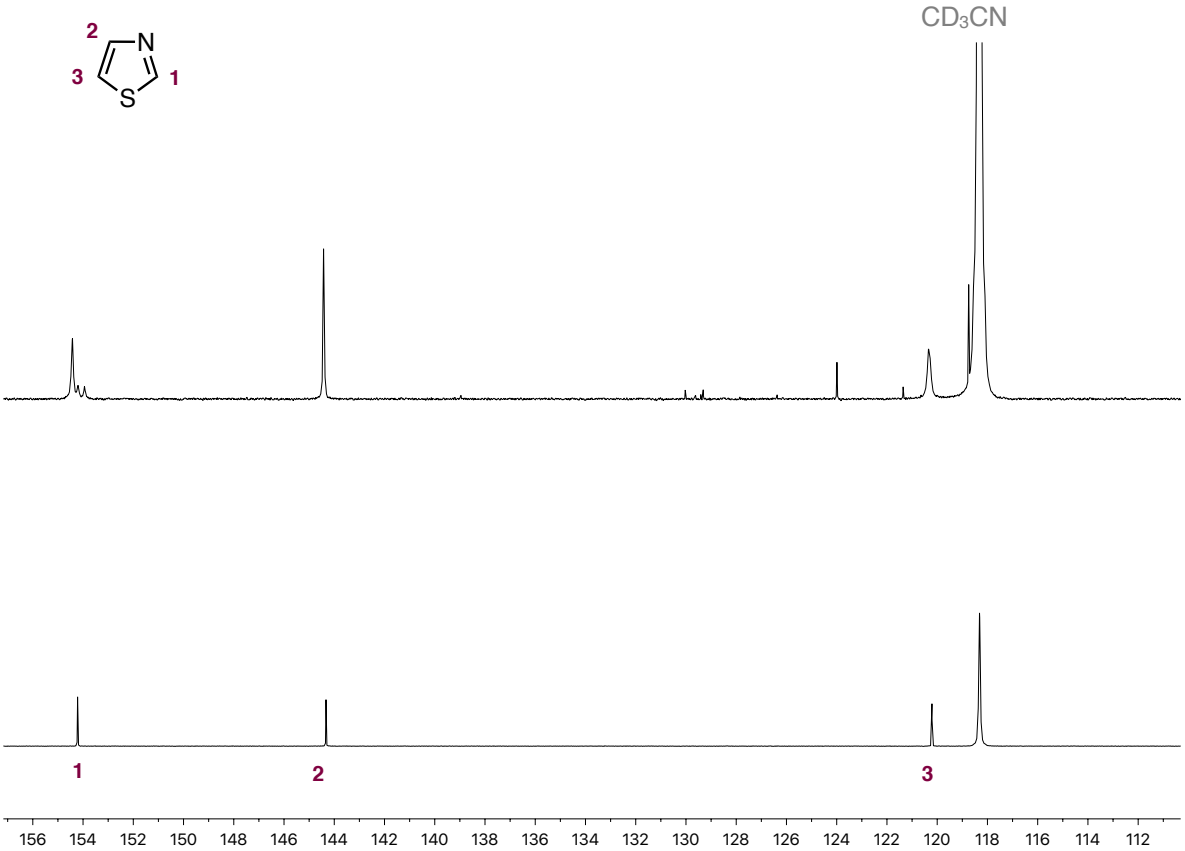

Figure S134. Stacked $^{13}C\{^{1}H\}$ NMR spectra of thiazole: labeled, **[^{2}H]11m** (first, quantitative) and unlabeled, **11m** (second, conventional).

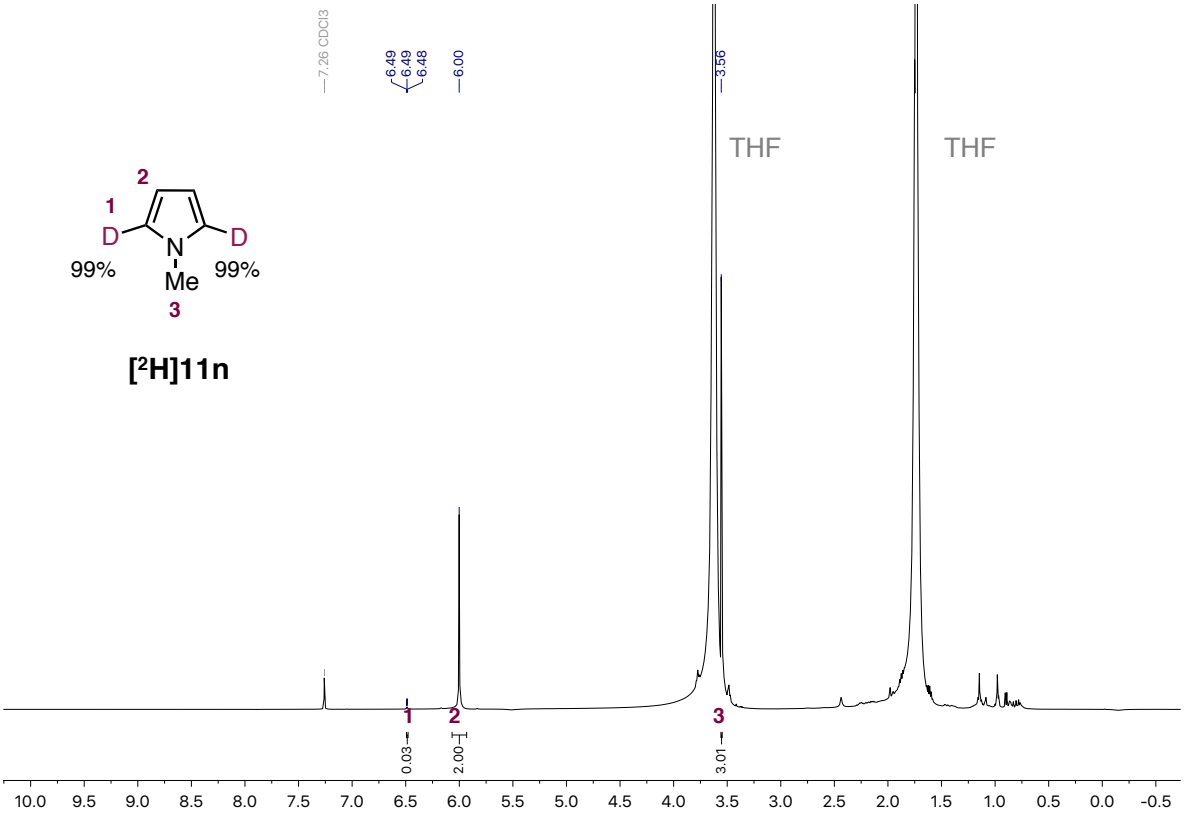

Figure S135. ^{1}H NMR (500 MHz, $CDCl_3$) of labeled *N*-methylpyrrole, **[^{2}H]11n.**

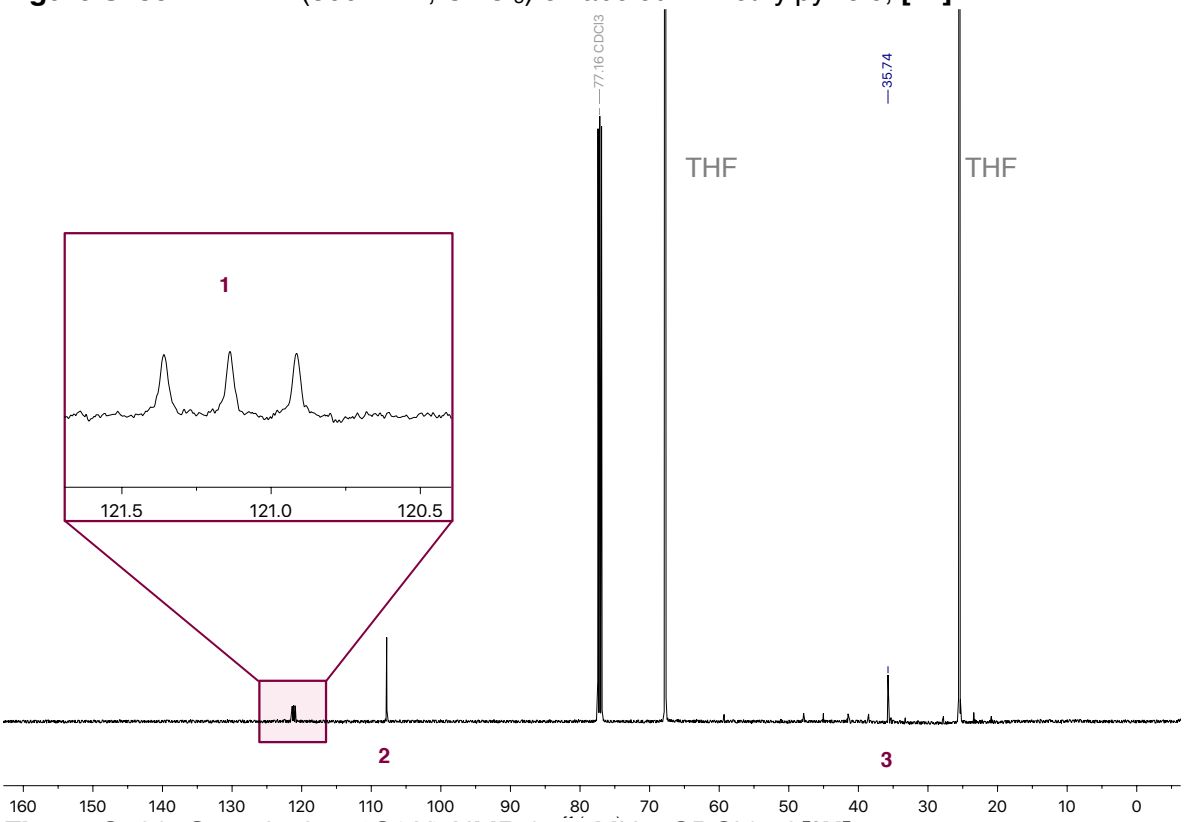

Figure S136. Quantitative ^{13}C{^{1}H} NMR (126 MHz, $CDCl_3$) of **[^{2}H]11n.**

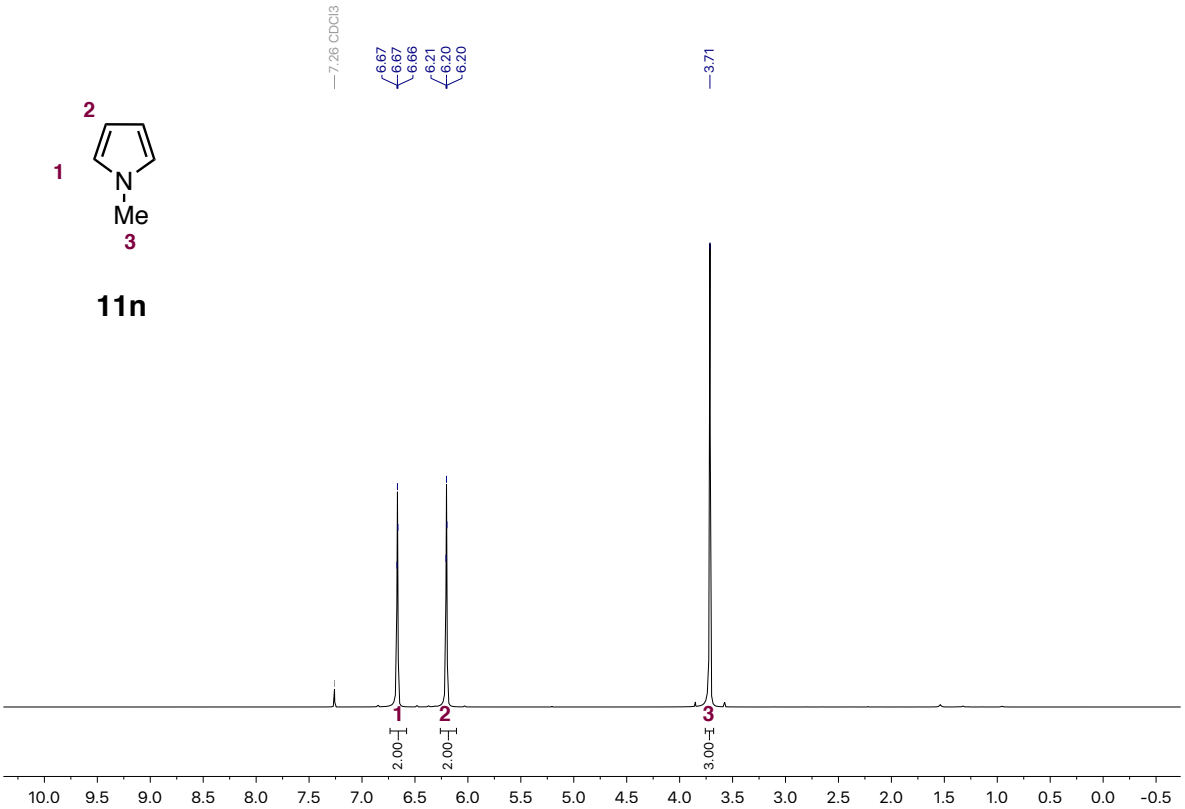

Figure S137. ^{1}H NMR (500 MHz, $CDCl_3$) of unlabeled *N*-methylpyrrole, **11n.**

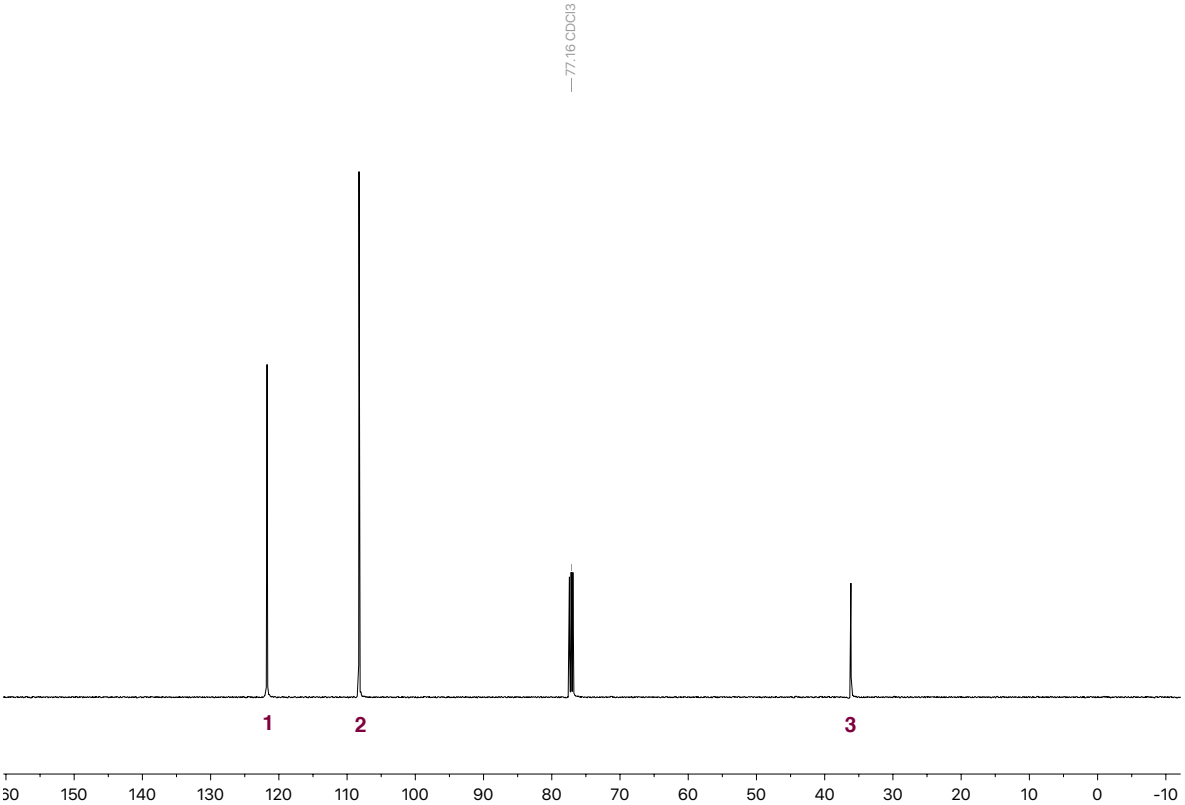

Figure S138. ^{13}C{^{1}H} NMR (126 MHz, $CDCl_3$) of **11n.**

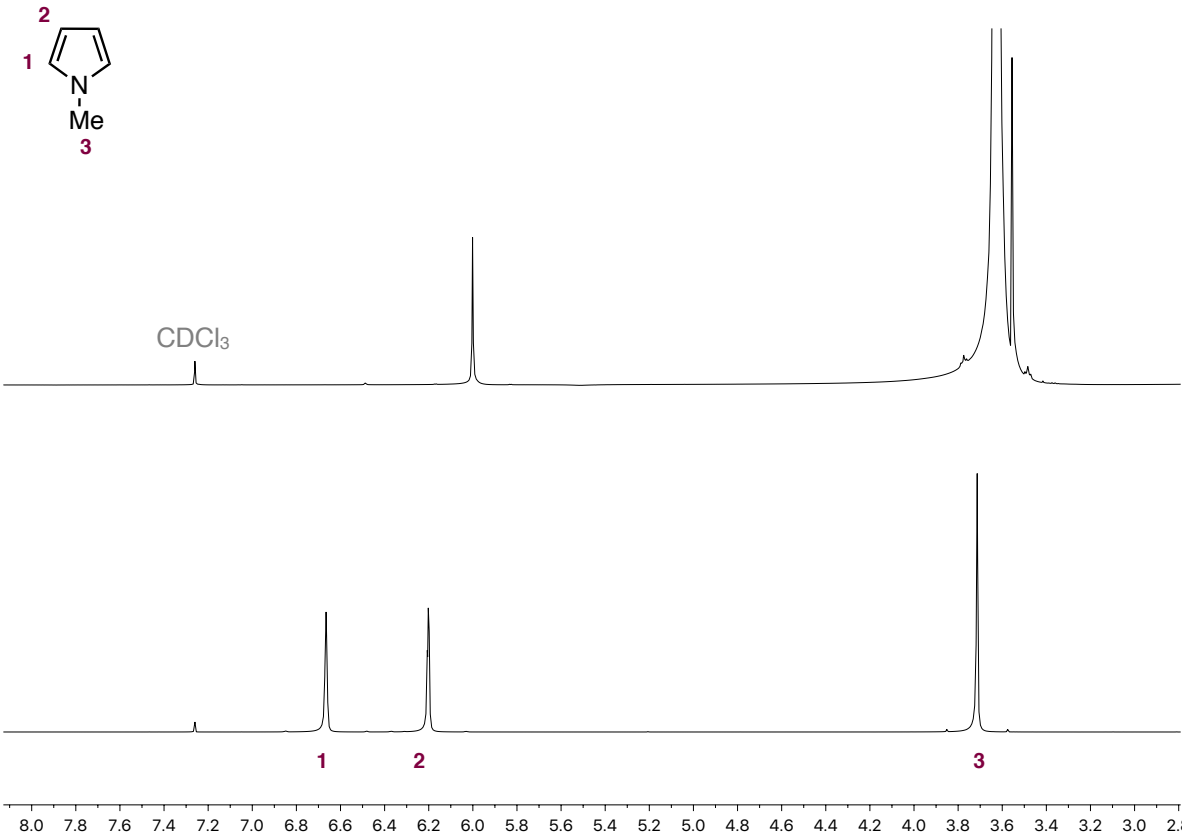

Figure S139. Stacked ^{1}H NMR spectra of *N*-methylpyrrole: labeled, **[^{2}H]11n** (first) and unlabeled, **11n** (second).

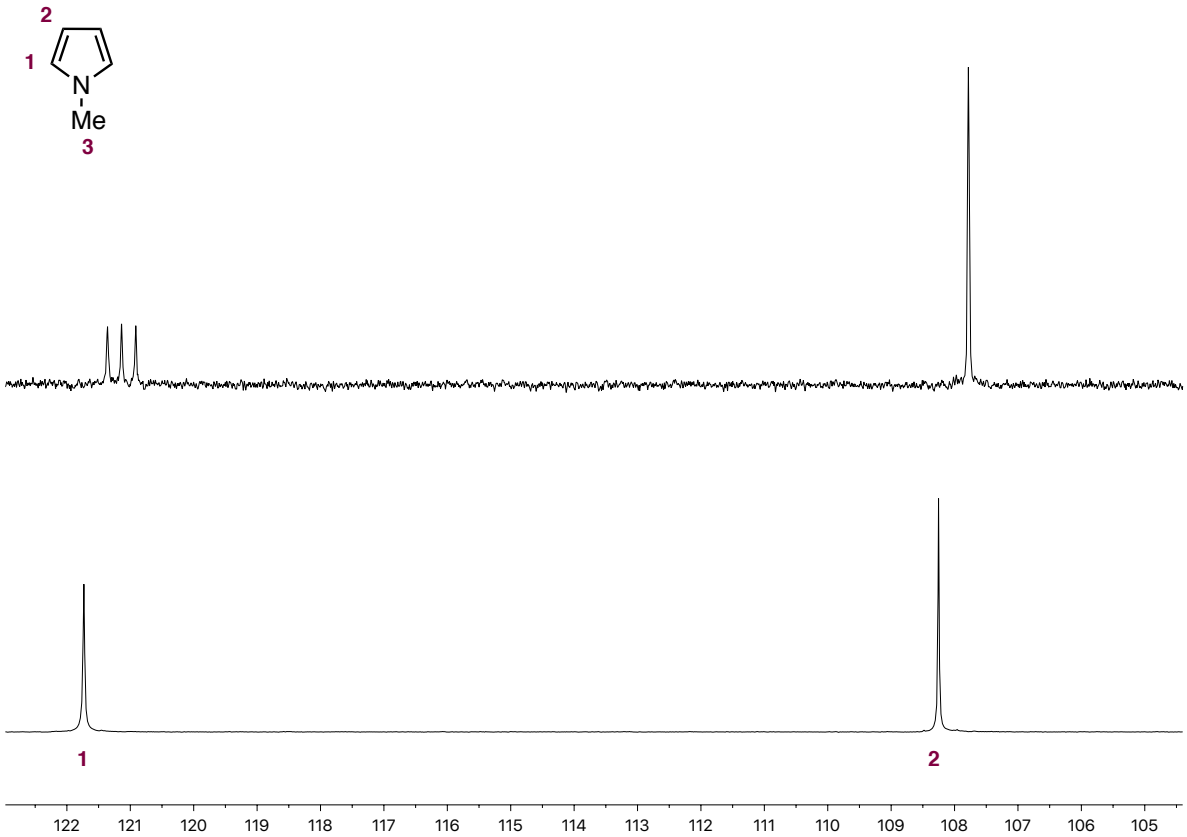

Figure S140. Stacked $^{13}C\{^{1}H\}$ NMR spectra of *N*-methylpyrrole: labeled, **[^{2}H]11n** (first, quantitative) and unlabeled, **11n** (second, conventional).

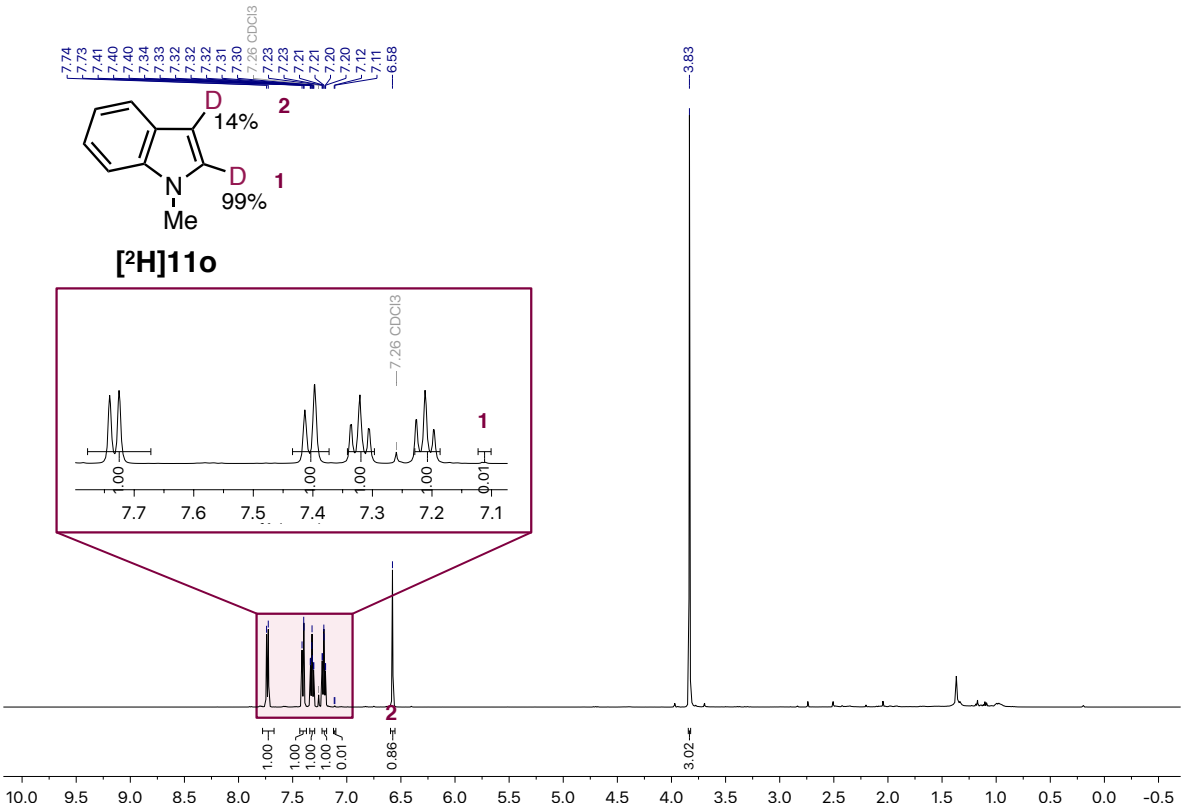

Figure S141. ^{1}H NMR (500 MHz, $CDCl_3$) of labeled *N*-methylindole, **[^{2}H]11o.**

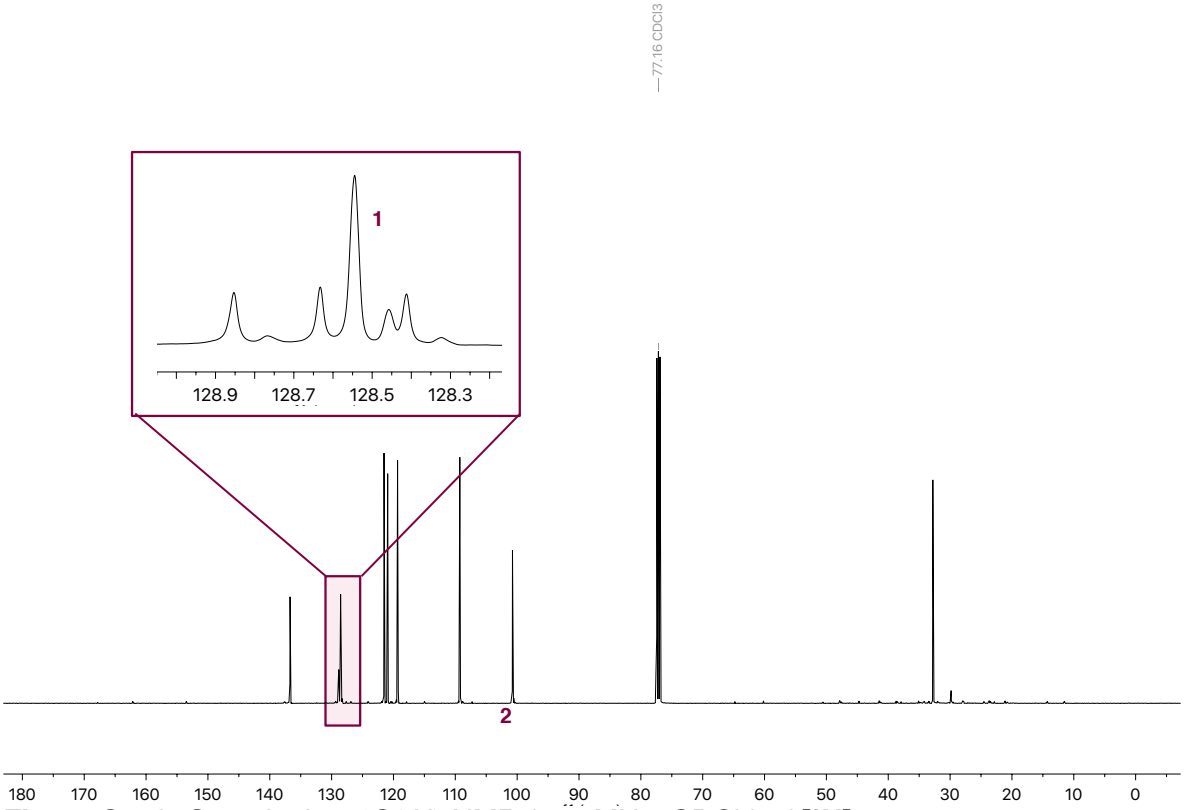

Figure S142. Quantitative ^{13}C{^{1}H} NMR (126 MHz, $CDCl_3$) of **[^{2}H]11o.**

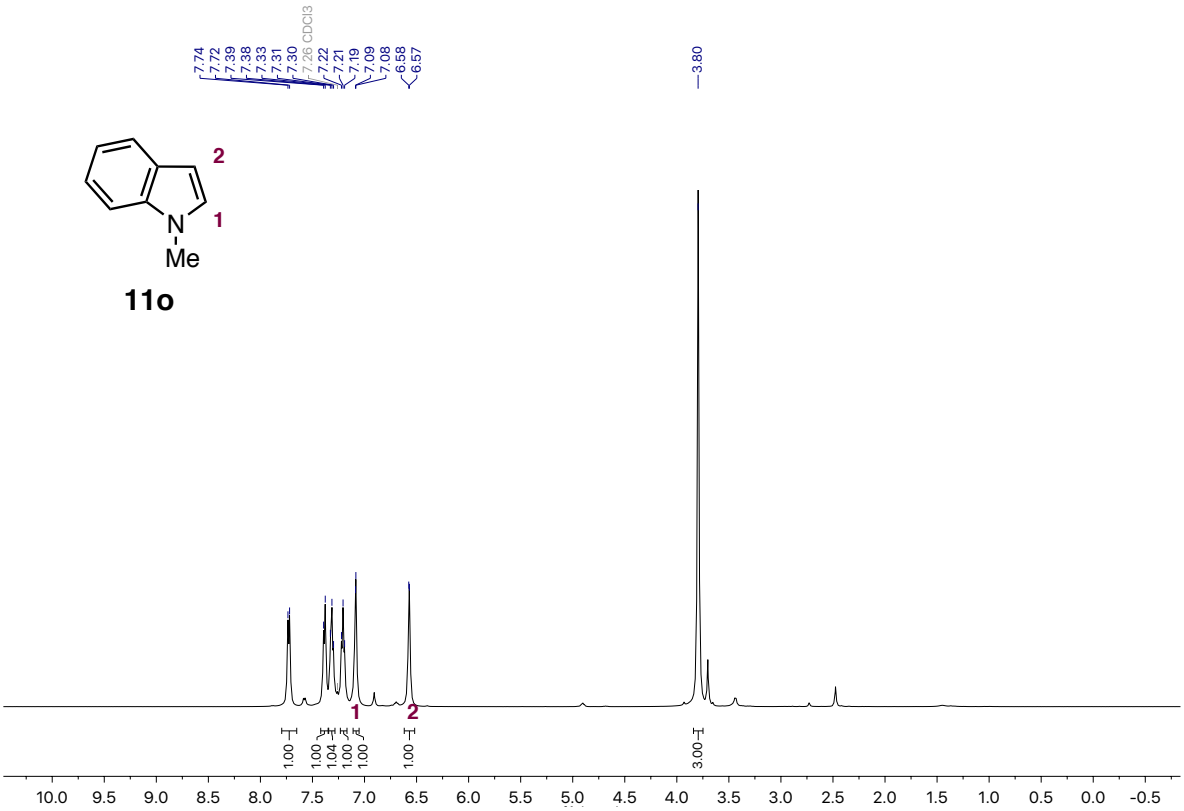

Figure S143. ^{1}H NMR (500 MHz, $CDCl_3$) of unlabeled *N*-methylindole **11o.**

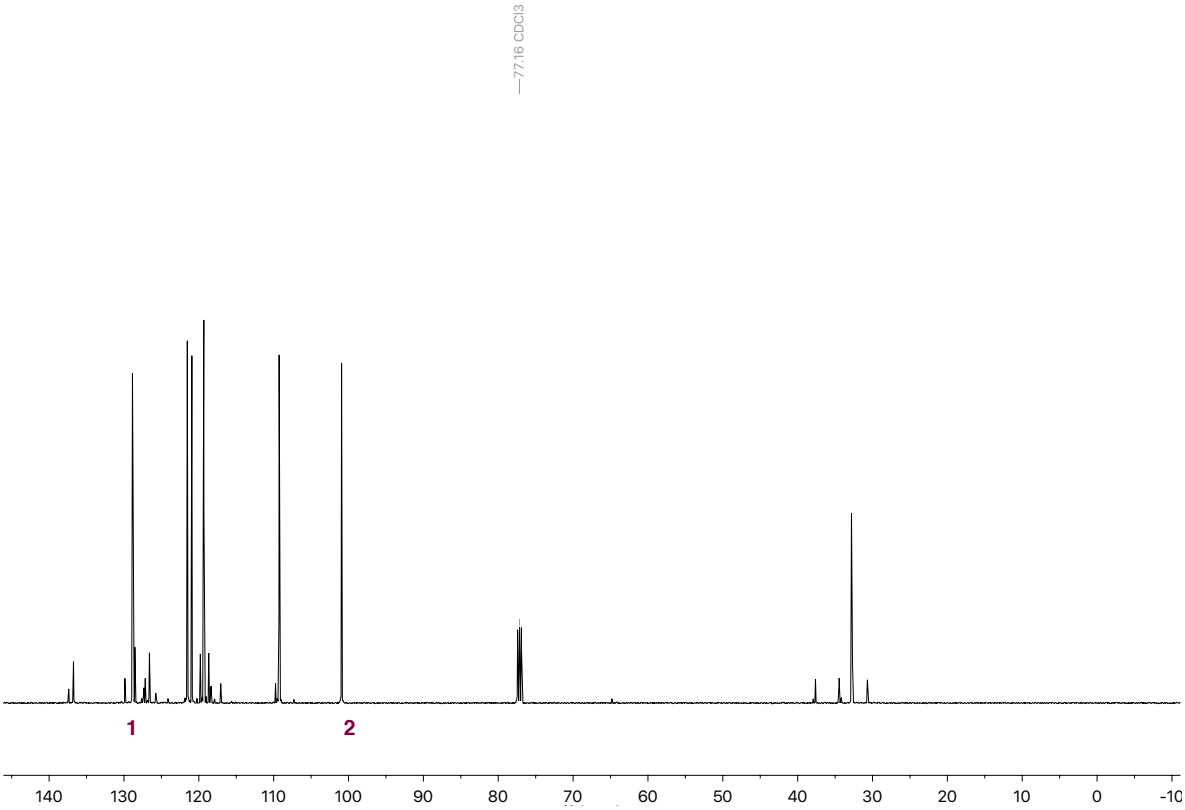

Figure S144. ^{13}C{^{1}H} NMR (126 MHz, $CDCl_3$) of **11o.**

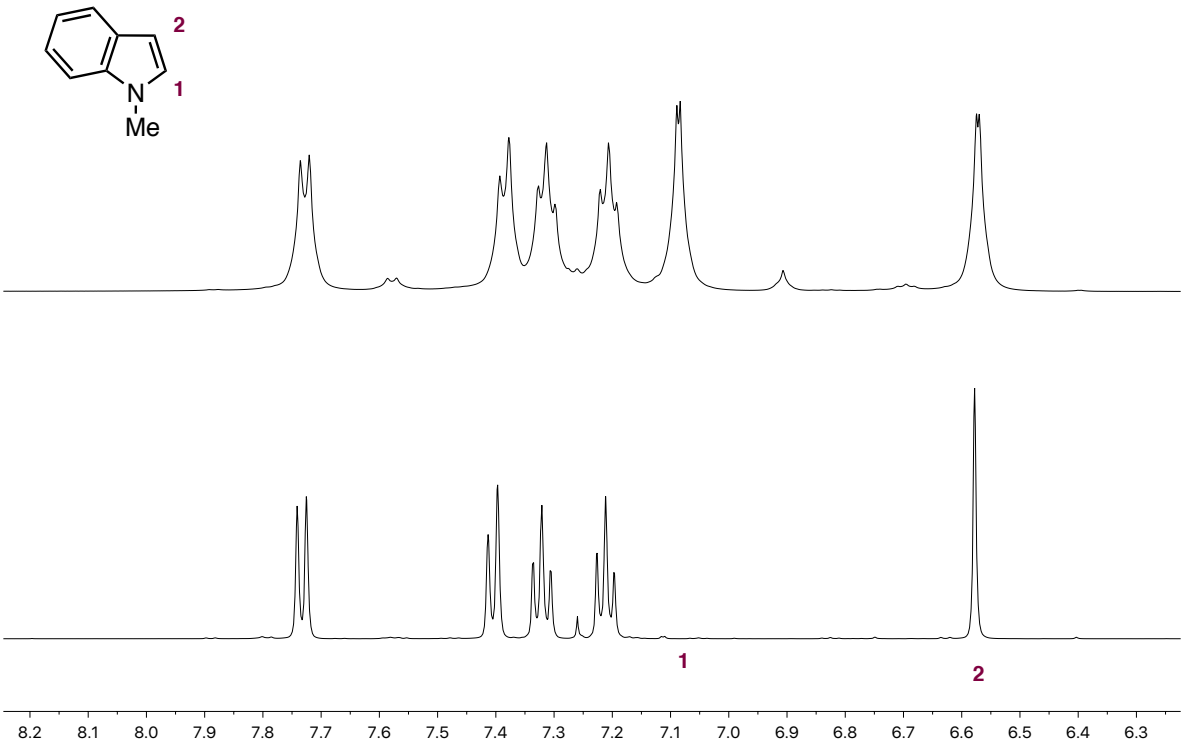

Figure S145. Stacked ^{1}H NMR spectra of *N*-methylindole: labeled, **[^{2}H]11o** (first) and unlabeled, **11o** (second).

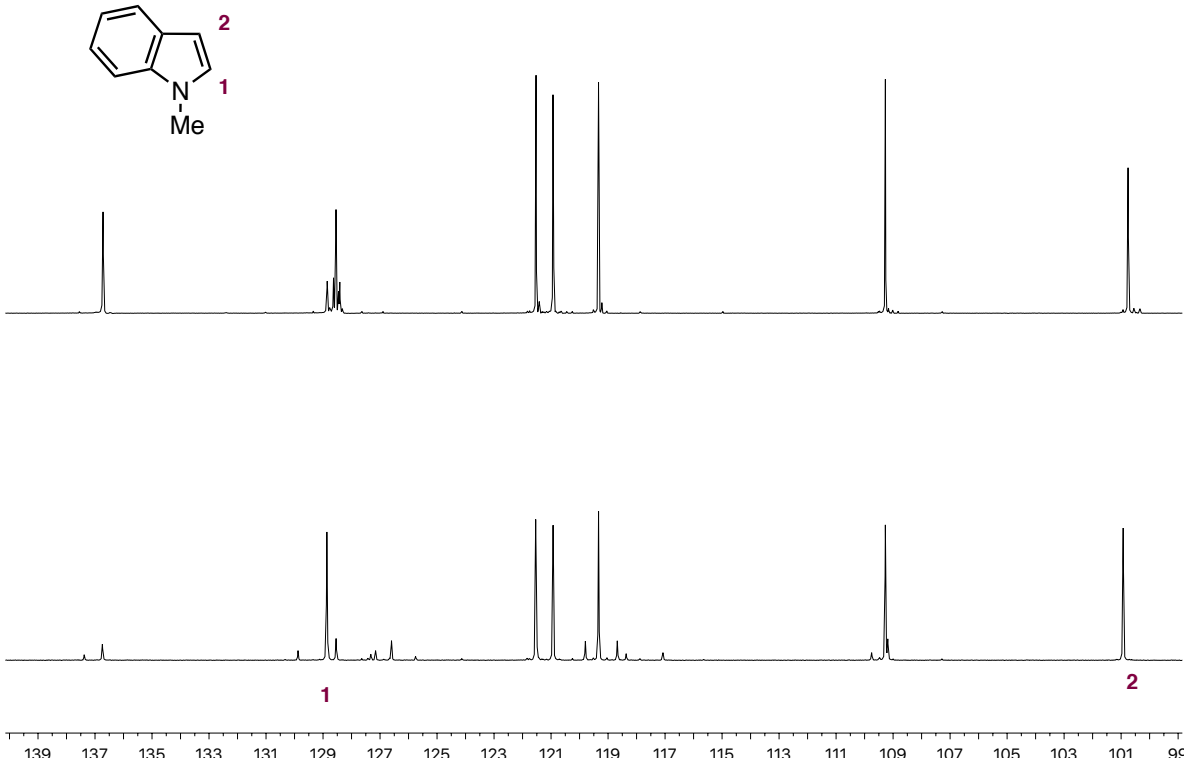

Figure S146. Stacked $^{13}C\{^{1}H\}$ NMR spectra of *N*-methylindole: labeled, **[^{2}H]11o** (first, quantitative) and unlabeled, **11o** (second, conventional).

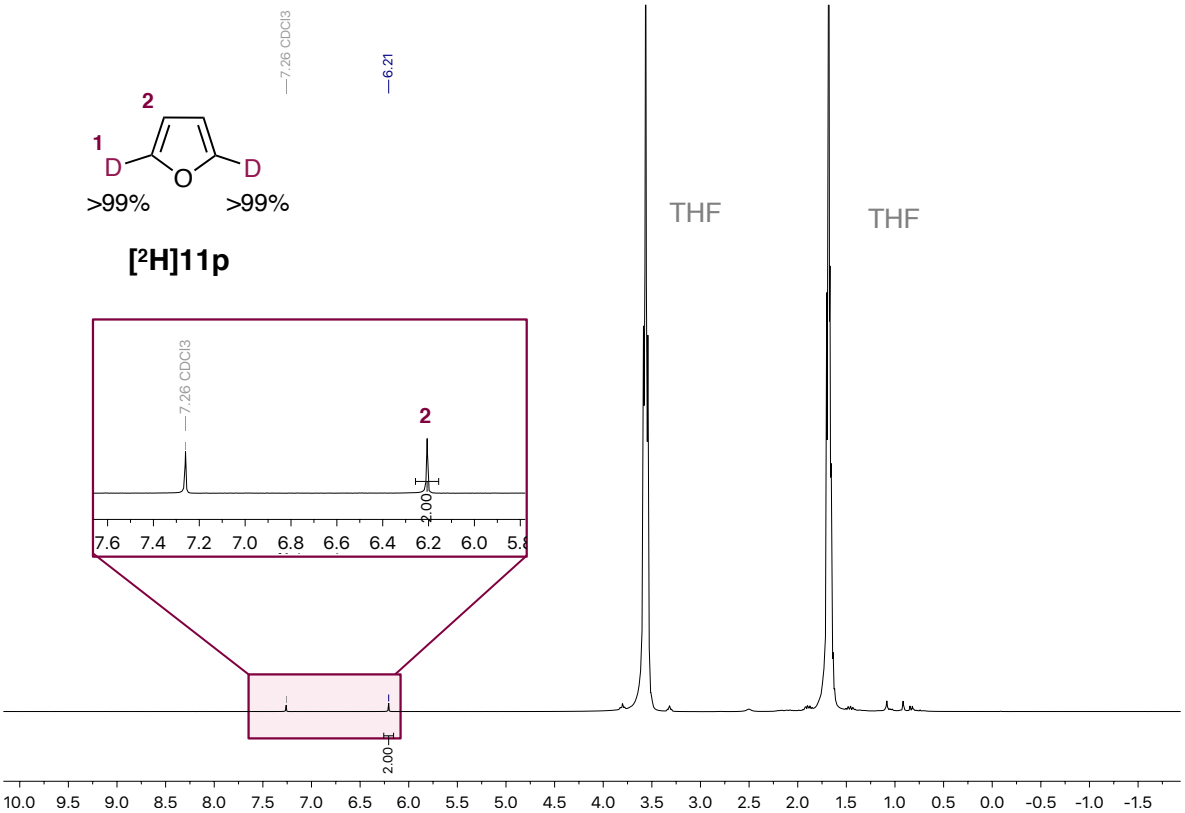

Figure S147. ^{1}H NMR (500 MHz, $CDCl_3$) of labeled furan, **[^{2}H]11p.**

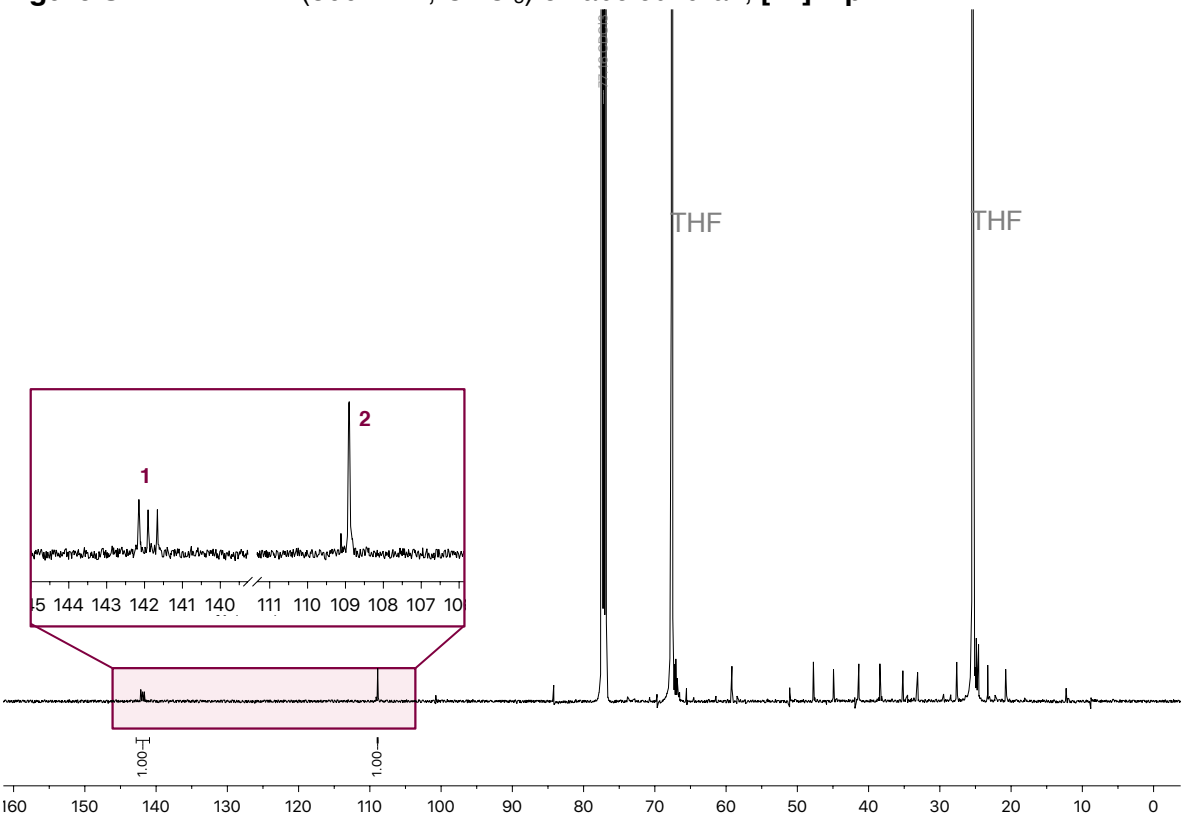

Figure S148. Quantitative ^{13}C{^{1}H} NMR (126 MHz, $CDCl_3$) of **[^{2}H]11p.**

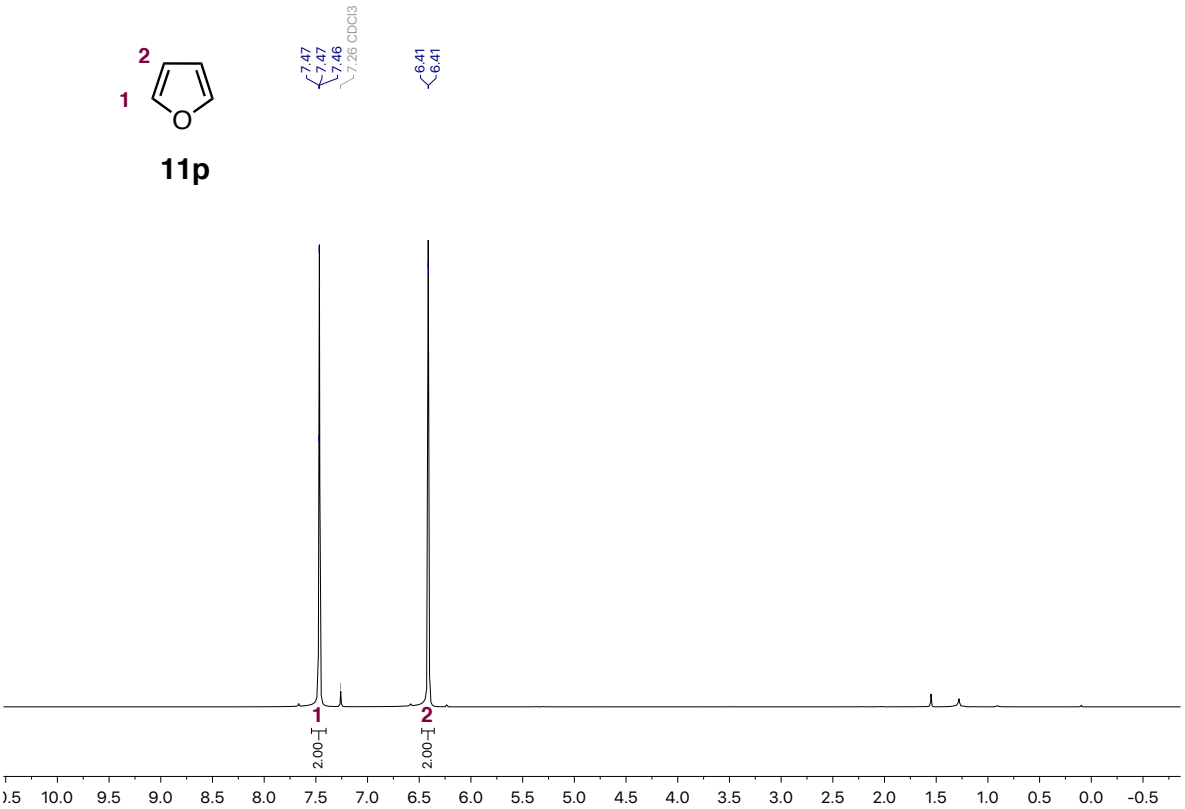

Figure S149. ^{1}H NMR (500 MHz, $CDCl_3$) of D-unlabeled furan, **11p.**

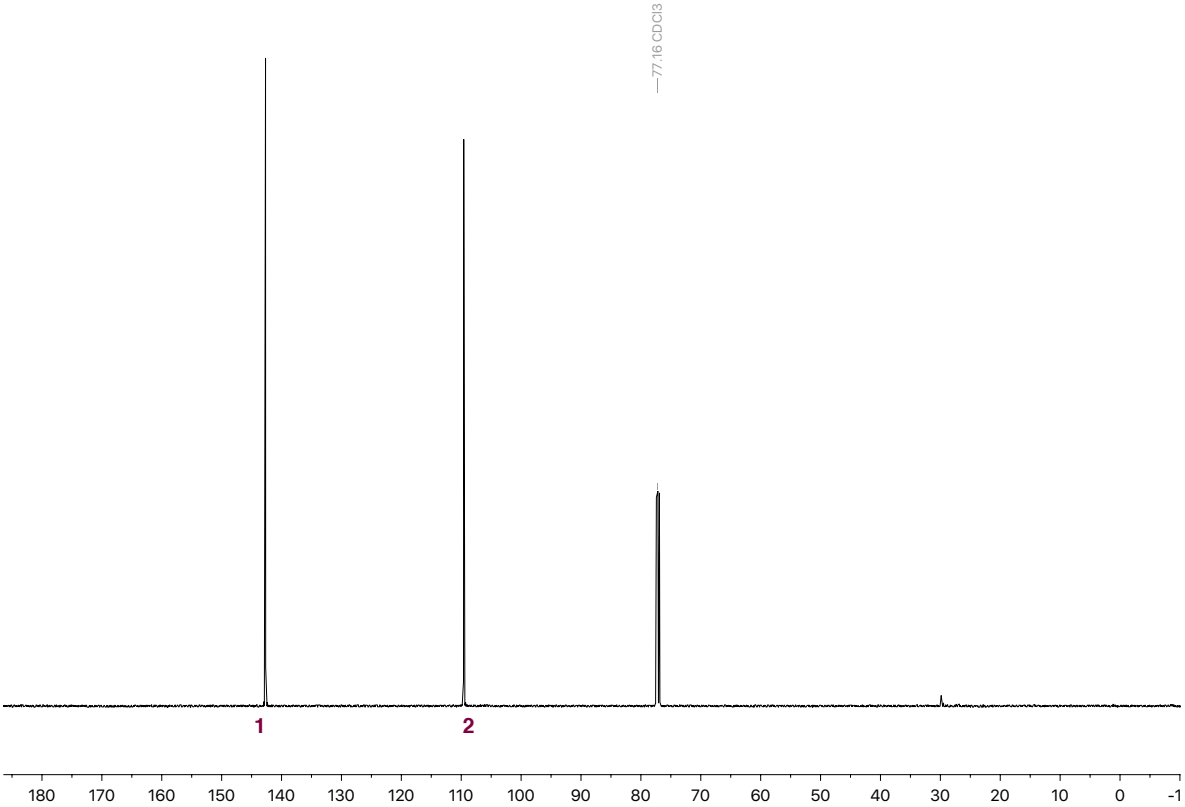

Figure S150. ^{13}C{^{1}H} NMR (126 MHz, $CDCl_3$) of **11p.**

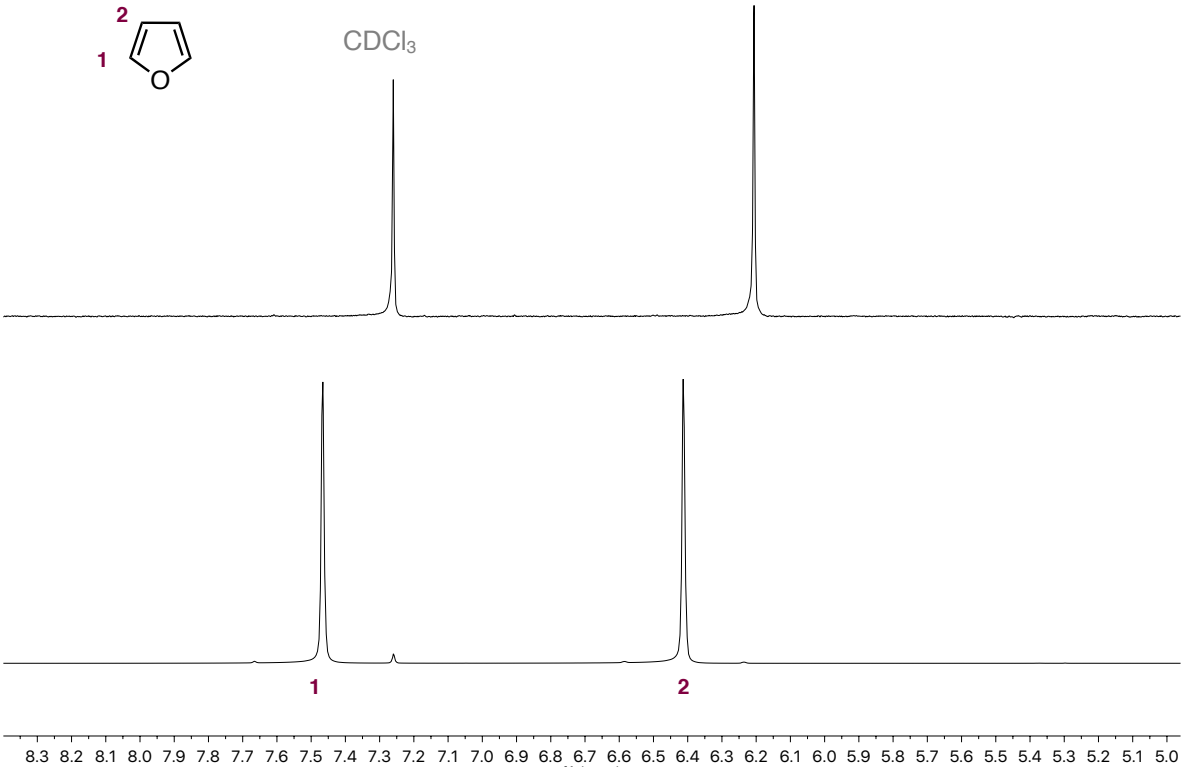

Figure S151. Stacked ^{1}H NMR spectra of furan: labeled, **[^{2}H]11p** (first) and unlabeled, **11p** (second).

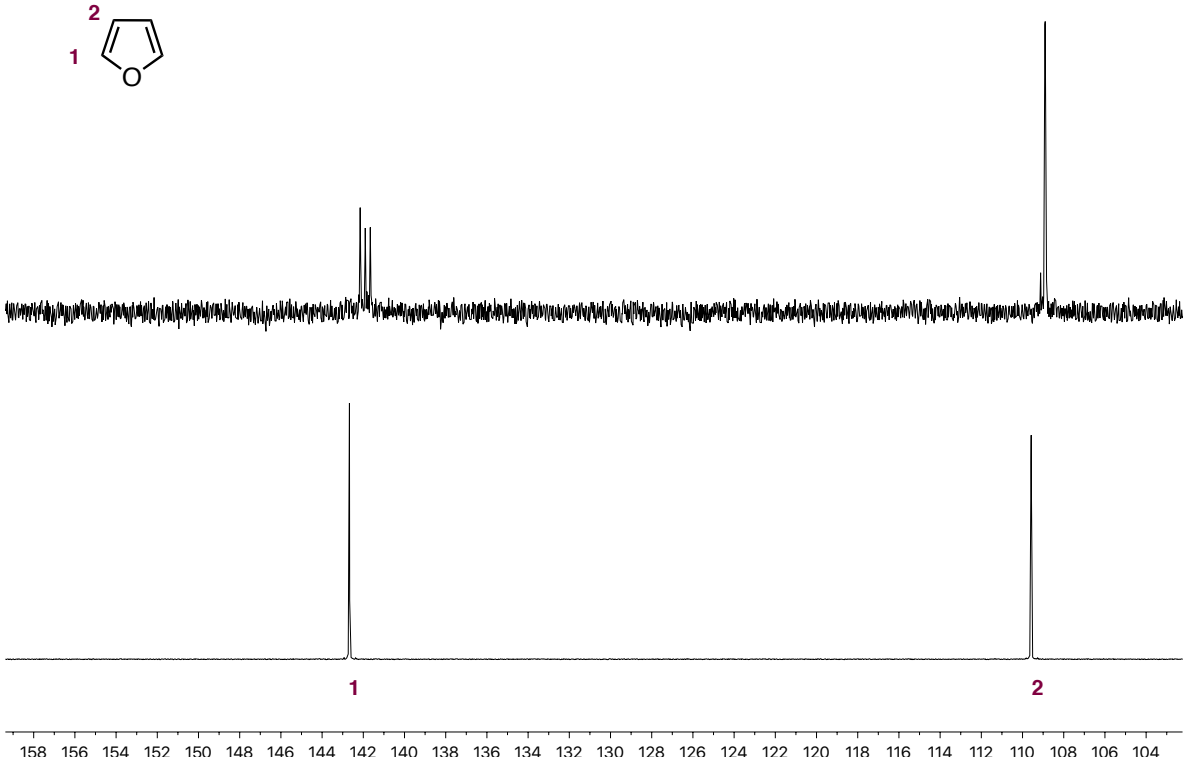

Figure S152. Stacked $^{13}C\{^{1}H\}$ NMR spectra of furan: labeled, **[^{2}H]11p** (first, quantitative) and unlabeled, **11p** (second, conventional).

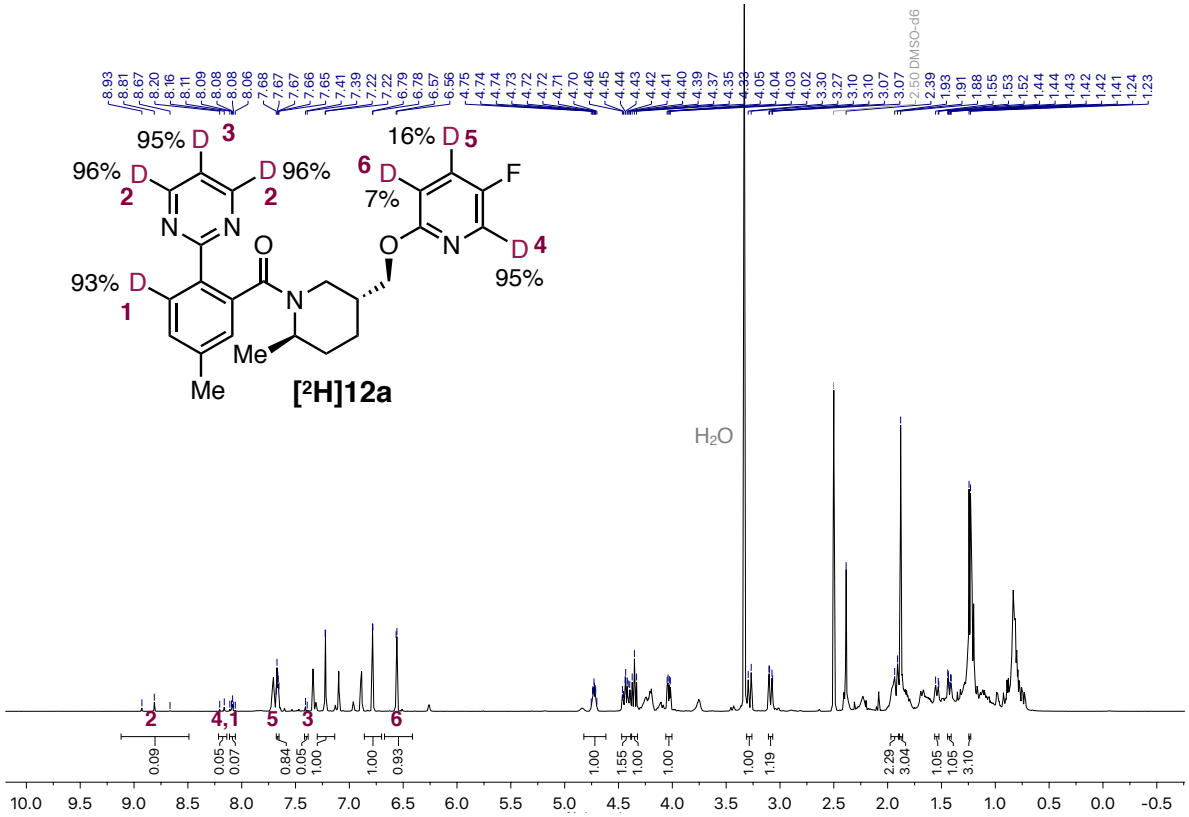

Figure S153. ^{1}H NMR (500 MHz, DMSO-d_6) of labeled MK-6096 with Method A, **[^{2}H]12a**.

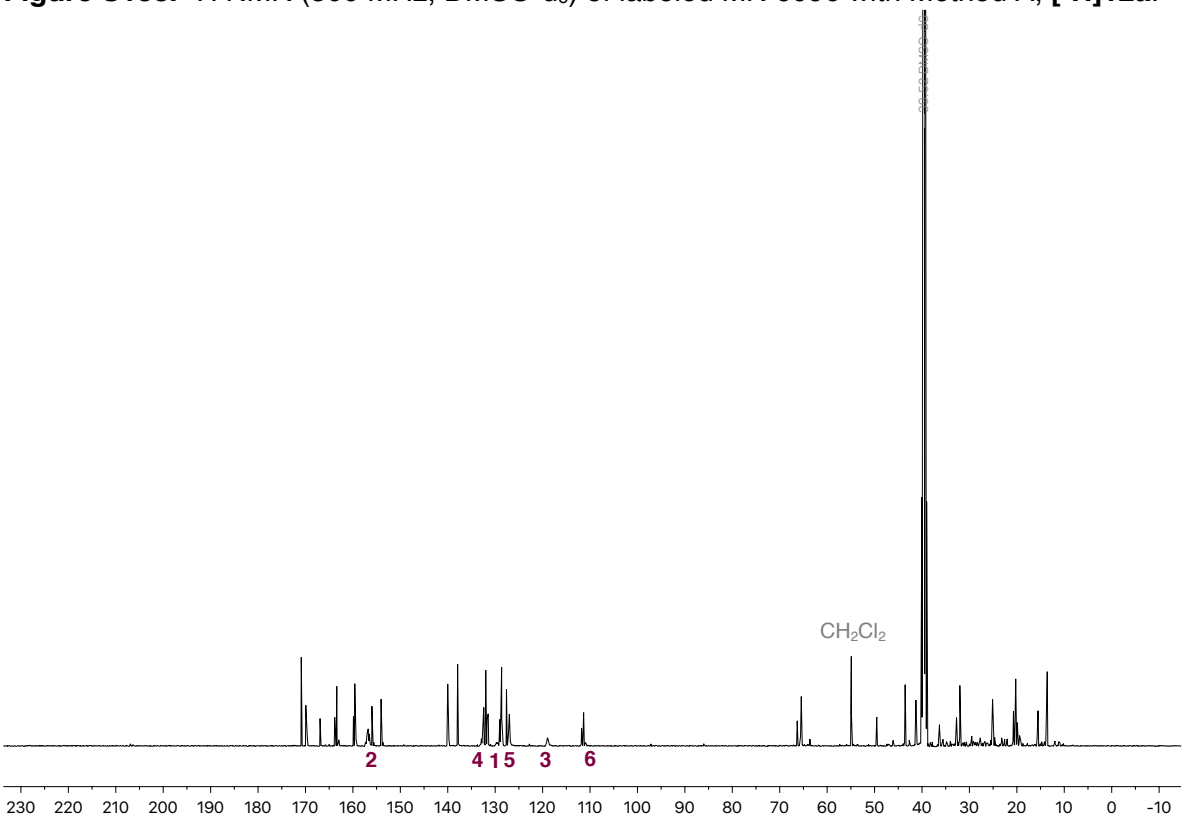

Figure S154. Quantitative ^{13}C{^{1}H} NMR (126 MHz, DMSO-d_6) of **[^{2}H]12a**.

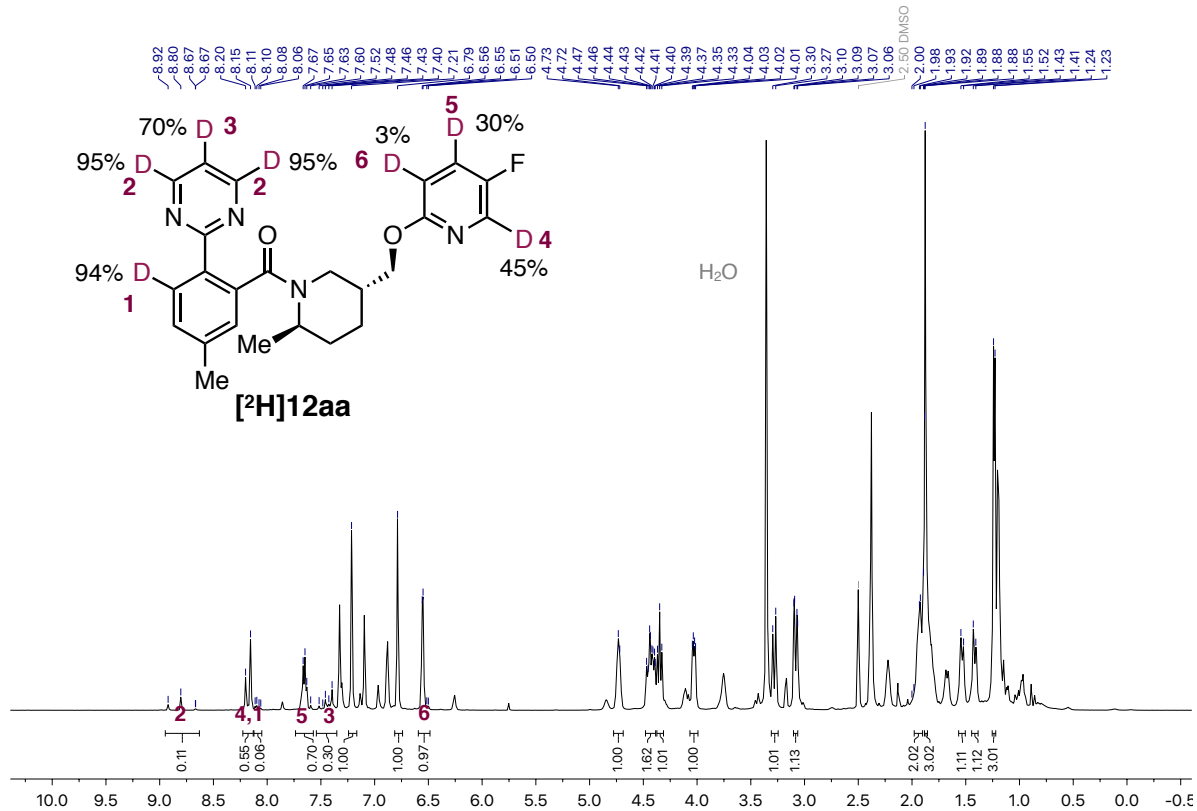

Figure S155. ^{1}H NMR (500 MHz, DMSO-d_6) of labeled MK-6096 with Method B, **[^{2}H]12aa**.

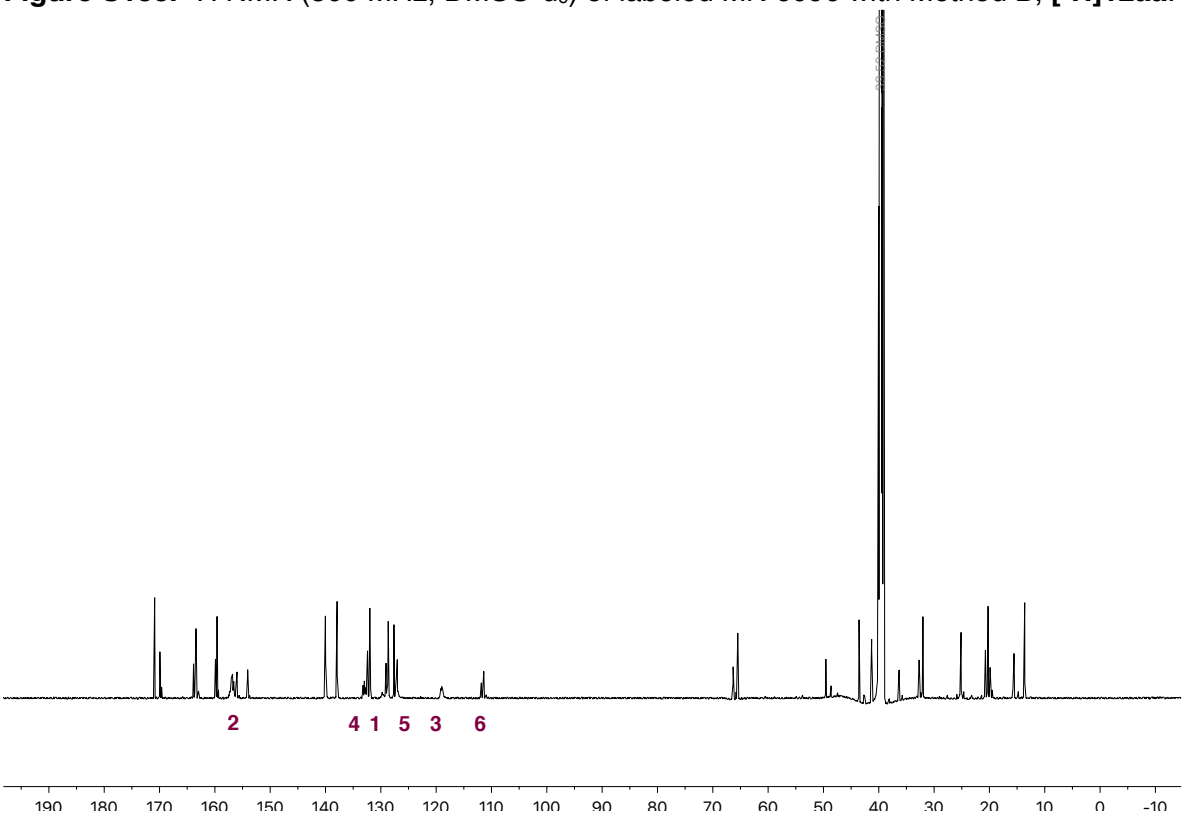

Figure S156. Quantitative ^{13}C{^{1}H} NMR (126 MHz, DMSO-d_6) of **[^{2}H]12aa**.

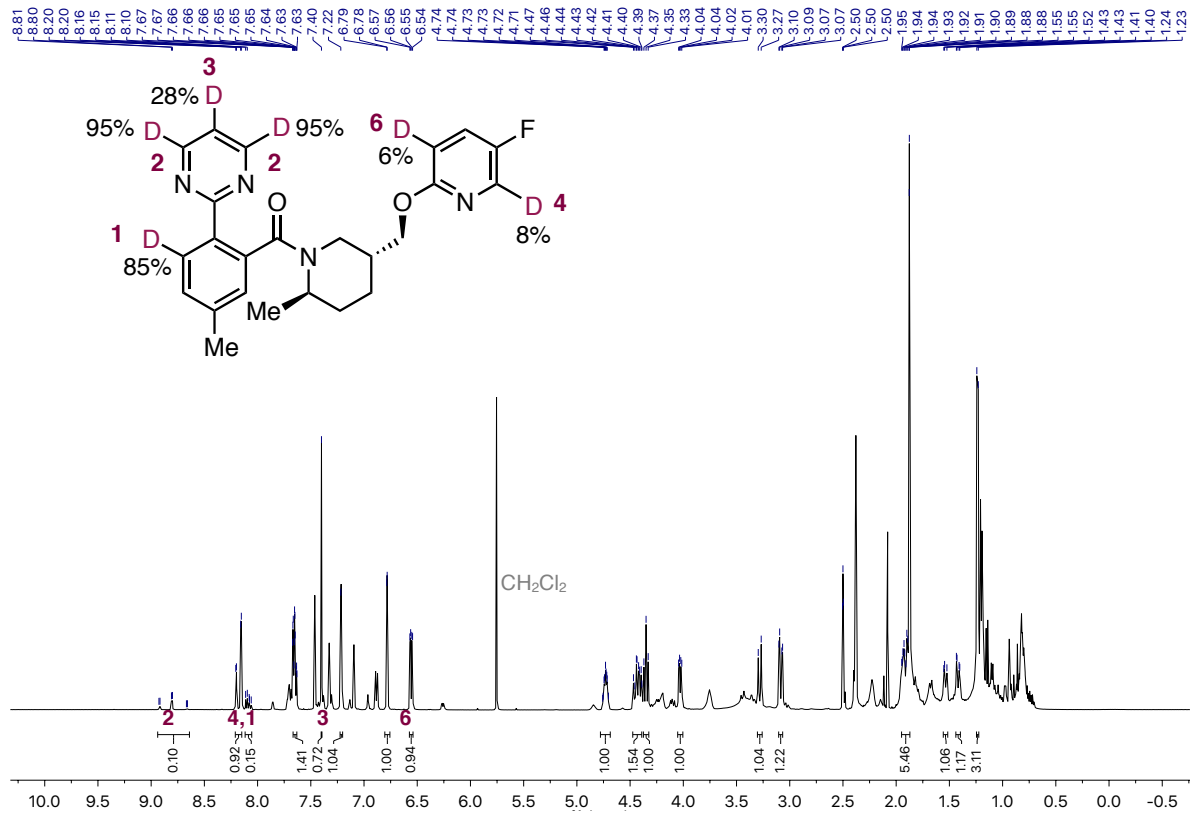

Figure S157. ^{1}H NMR (500 MHz, DMSO-d_6) of labeled MK-6096 with Method A in MeOH.

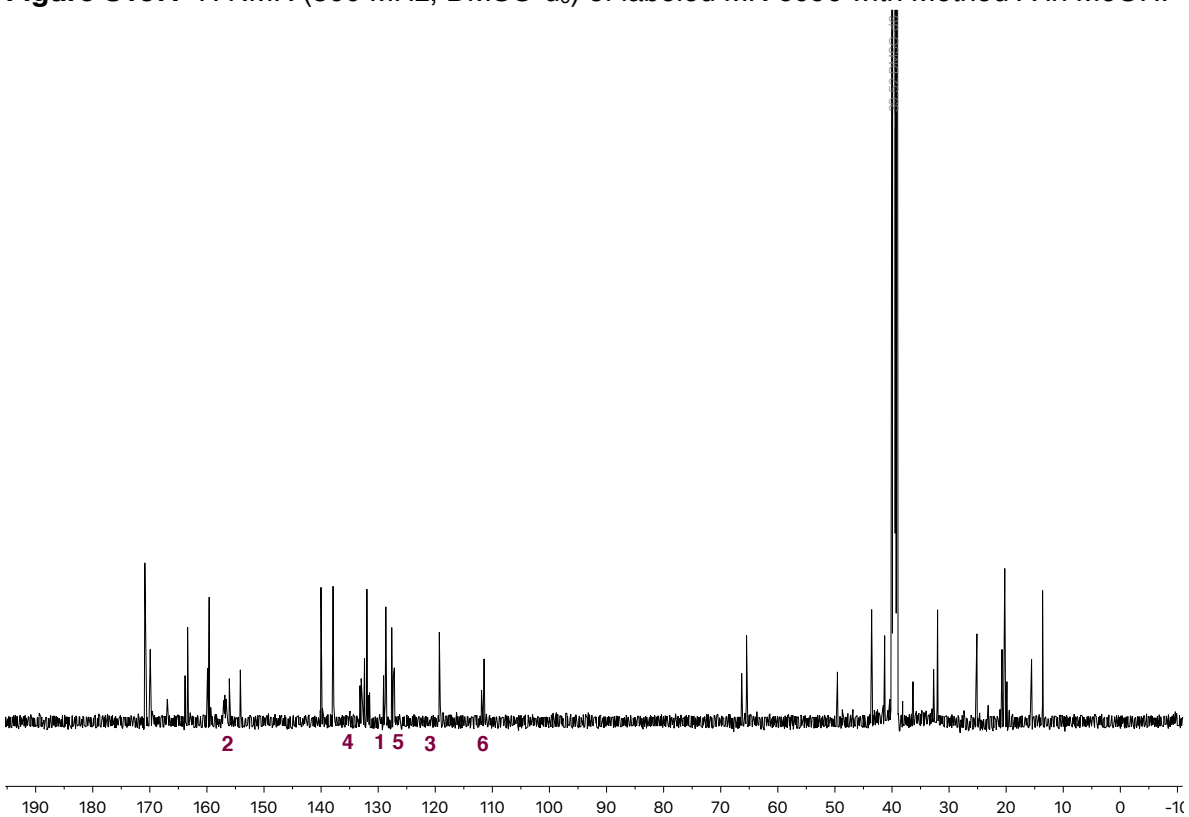

Figure S158. Quantitative ^{13}C{^{1}H} NMR (126 MHz, DMSO-d_6) of labeled MK-6096 with Method A in MeOH.

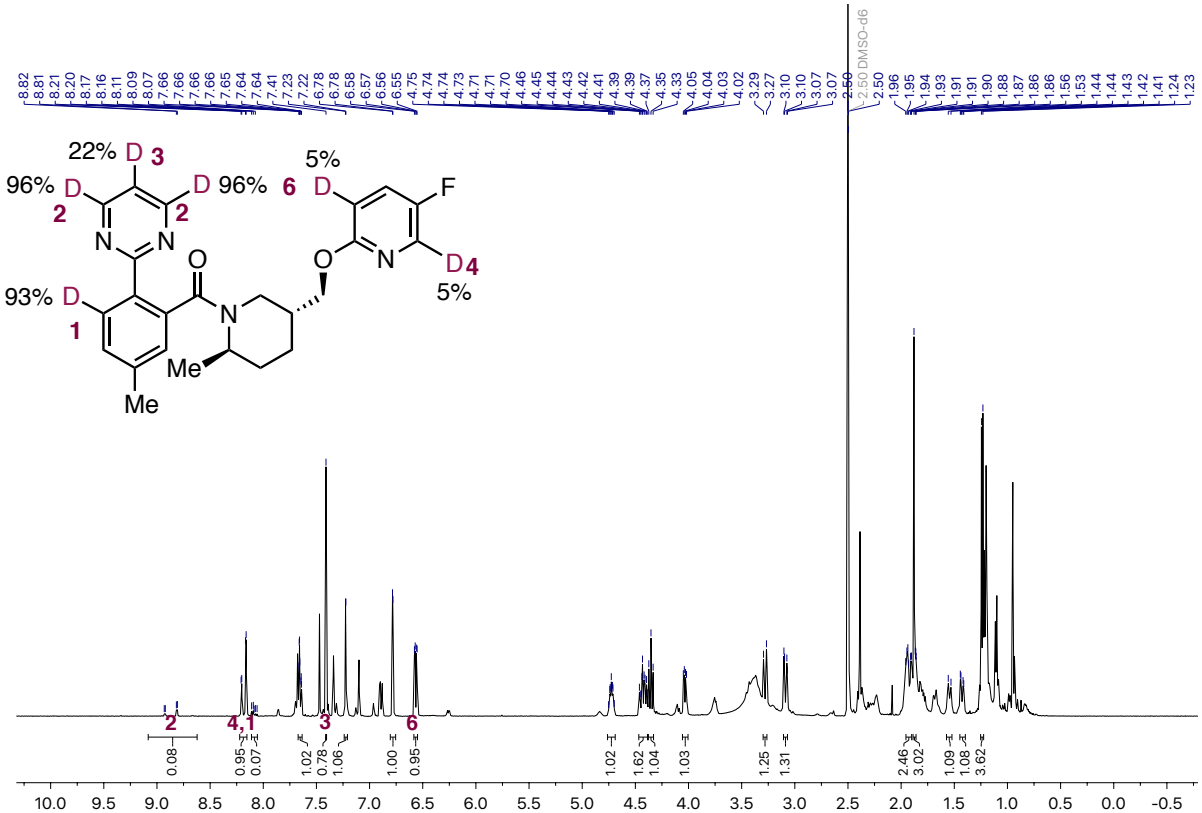

Figure S159. ^{1}H NMR (500 MHz, DMSO-d_6) of labeled MK-6096 with Method B in MeOH.

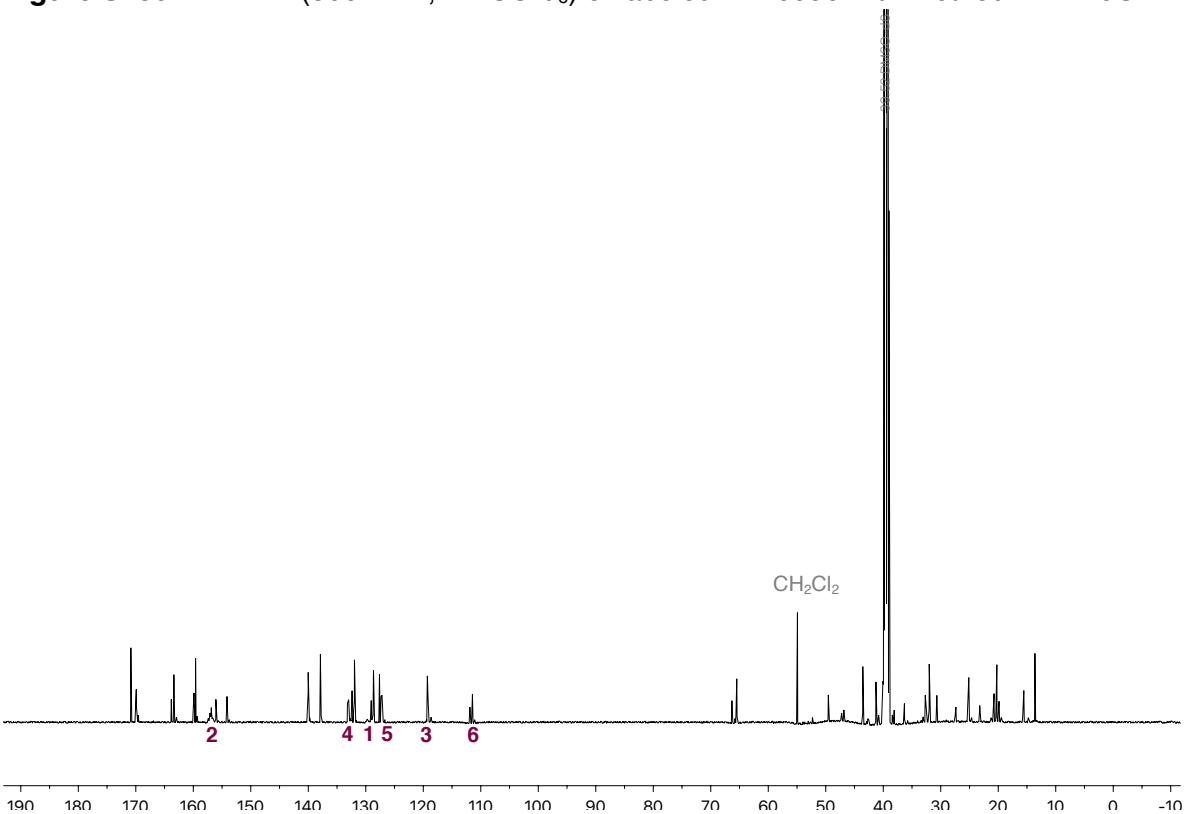

Figure S160. Quantitative ^{13}C{^{1}H} NMR (126 MHz, DMSO-d_6) of labeled MK-6096 with Method B in MeOH.

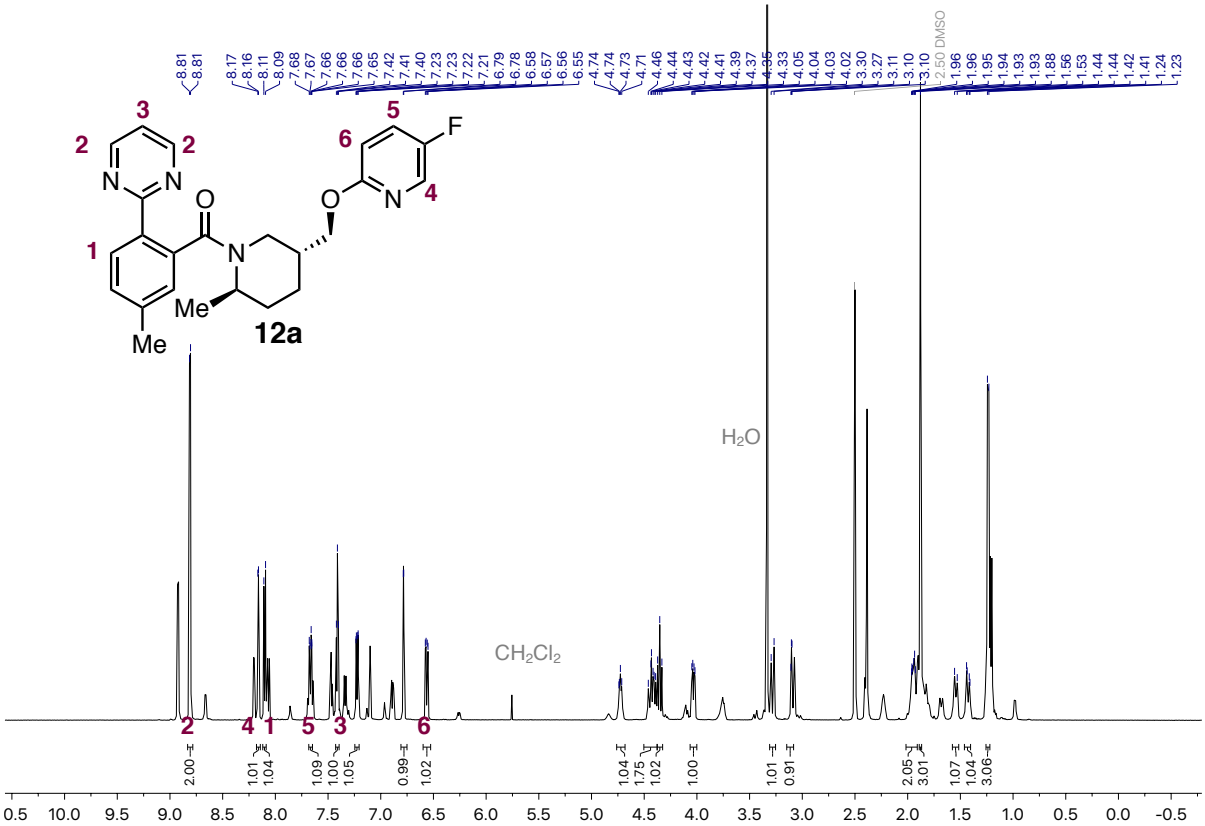

Figure S161. ^{1}H NMR (500 MHz, DMSO-d_6) of unlabeled MK-6096, **12a**.

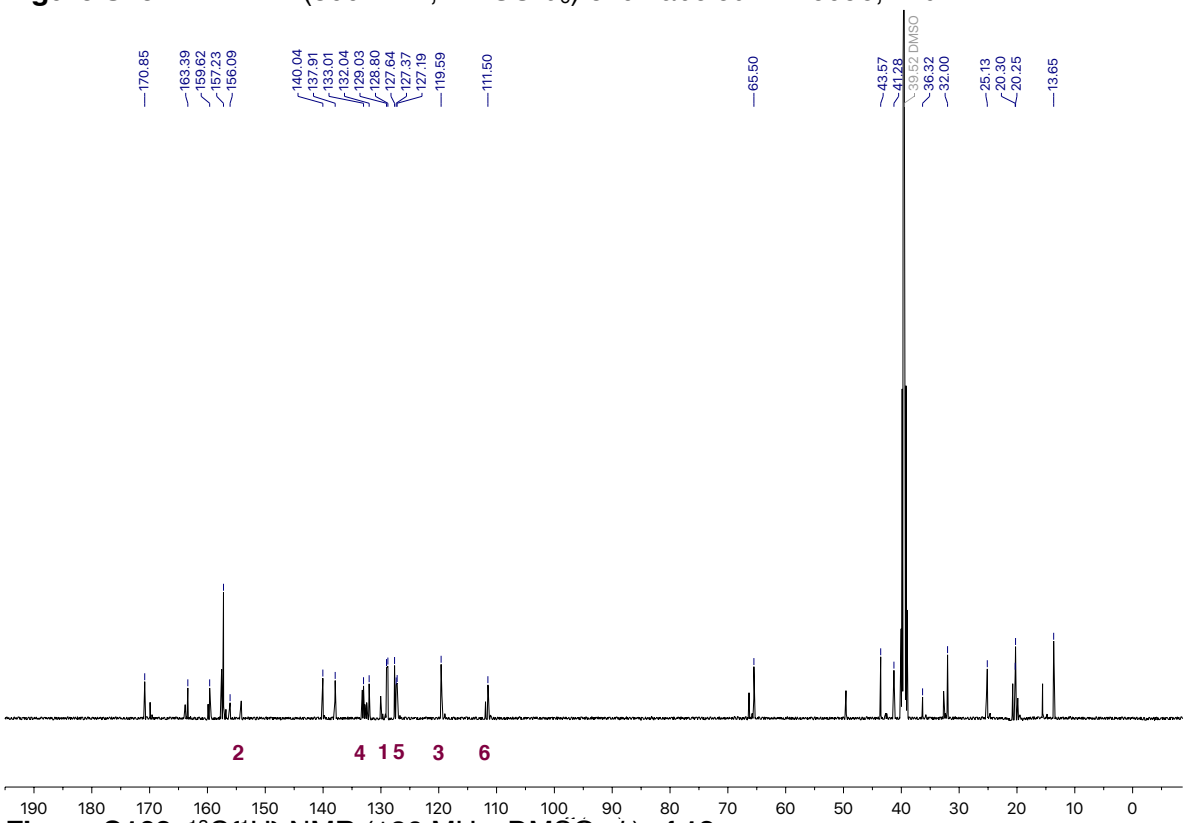

Figure S162. ^{13}C{^{1}H} NMR (126 MHz, DMSO-d_6) of **12a**.

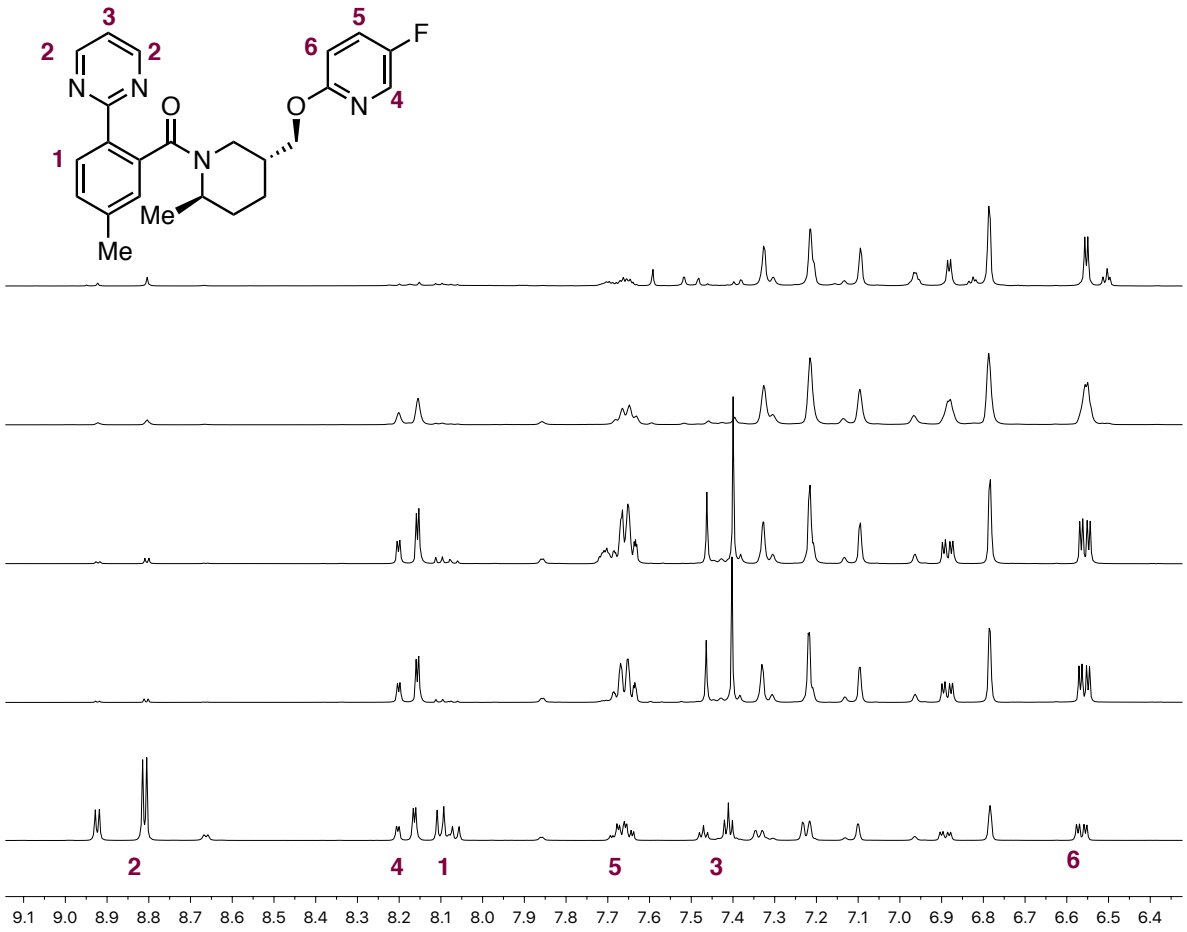

Figure S163. Stacked ^{1}H NMR spectra of MK-6096 (aromatic region): labeled with Method A, **[^{2}H]12a** (first); labeled with Method B, **[^{2}H]12aa** (second); labeled with Method A in MeOH (third); labeled with Method B in MeOH (fourth); and unlabeled, **12a** (fifth).

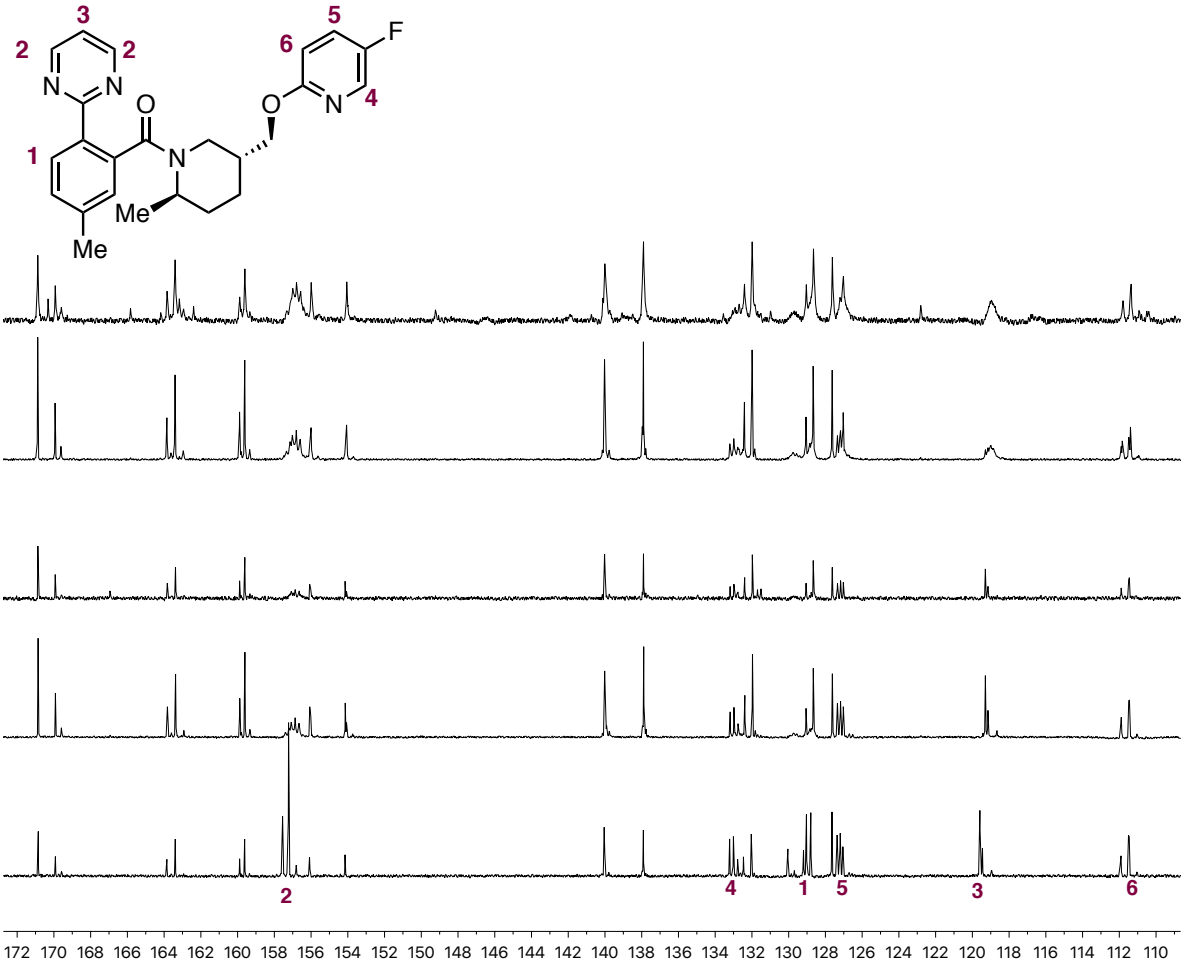

Figure S164. Stacked $^{13}C\{^{1}H\}$ NMR spectra of MK-6096 (aromatic region): labeled with Method A, **[^{2}H]12a** (first, quantitative); labeled with Method B, **[^{2}H]12aa** (second, quantitative); labeled with Method A in MeOH (third, quantitative); labeled with Method B in MeOH (fourth, quantitative); and unlabeled, **12a** (fifth, conventional).

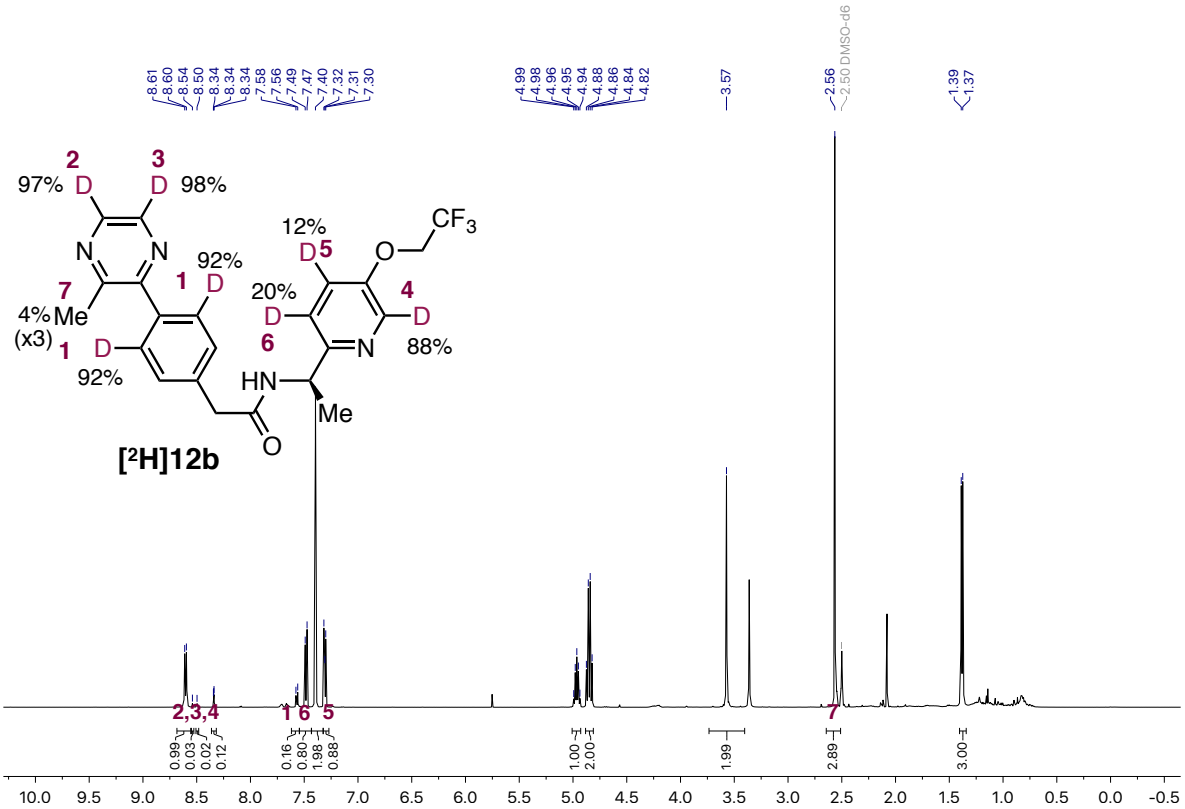

Figure S165. ^{1}H NMR (500 MHz, DMSO-d_6) of labeled MK-5395 with Method A, **[^{2}H]12b**.

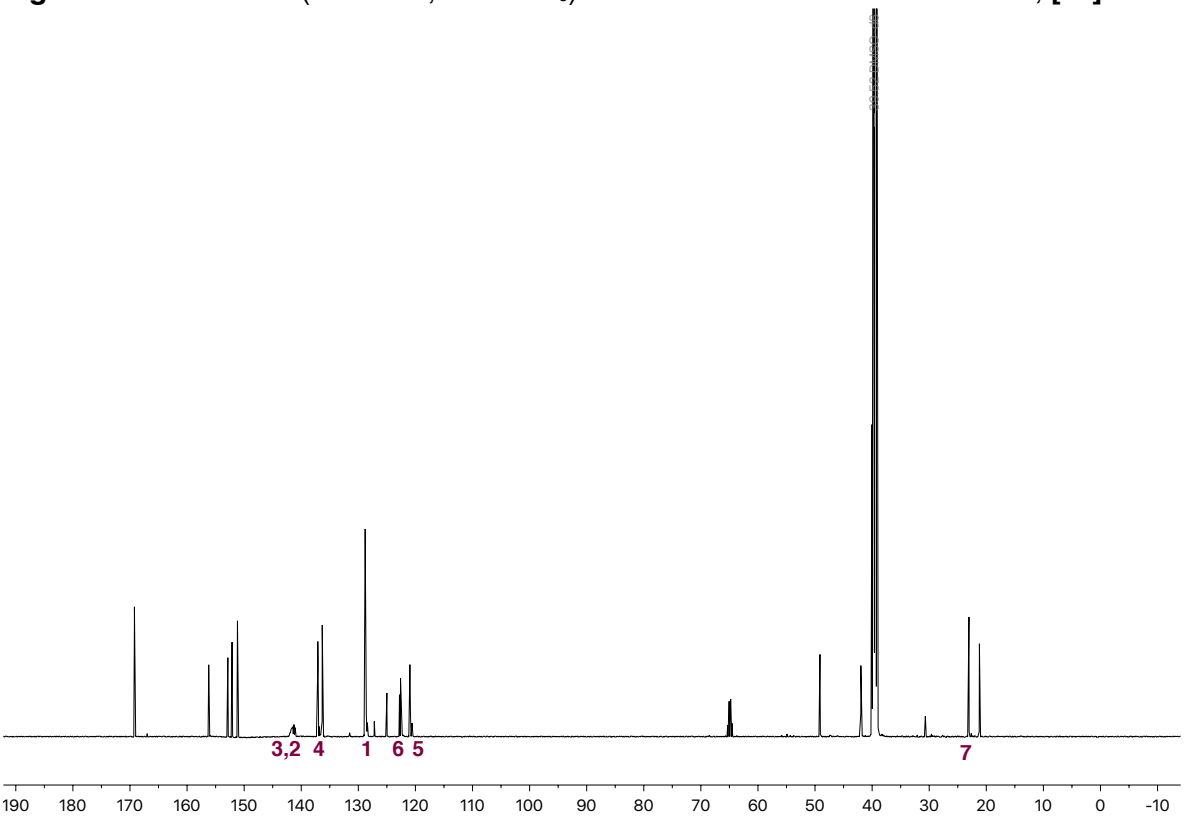

Figure S166. Quantitative ^{13}C{^{1}H} NMR (126 MHz, DMSO-d_6) of **[^{2}H]12b**.

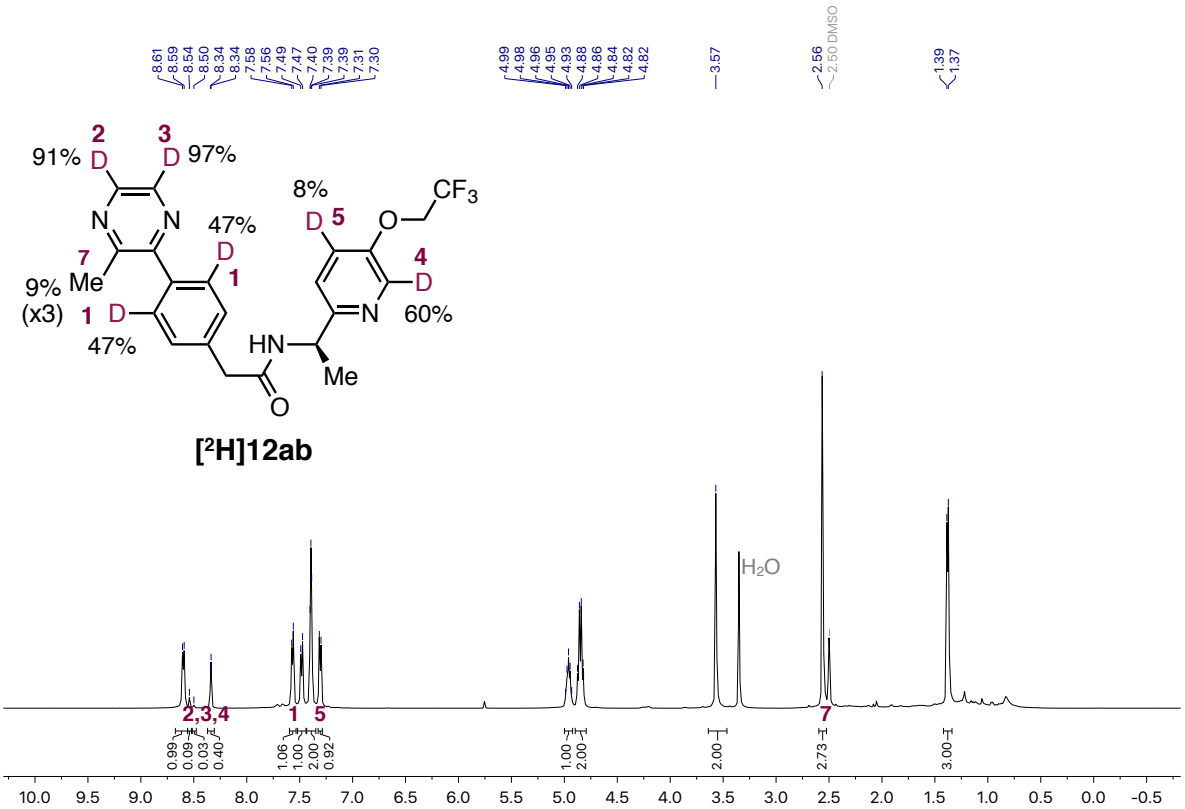

Figure S167. ^{1}H NMR (500 MHz, DMSO-d_6) of labeled MK-5395 with Method B, **[^{2}H]12ab**.

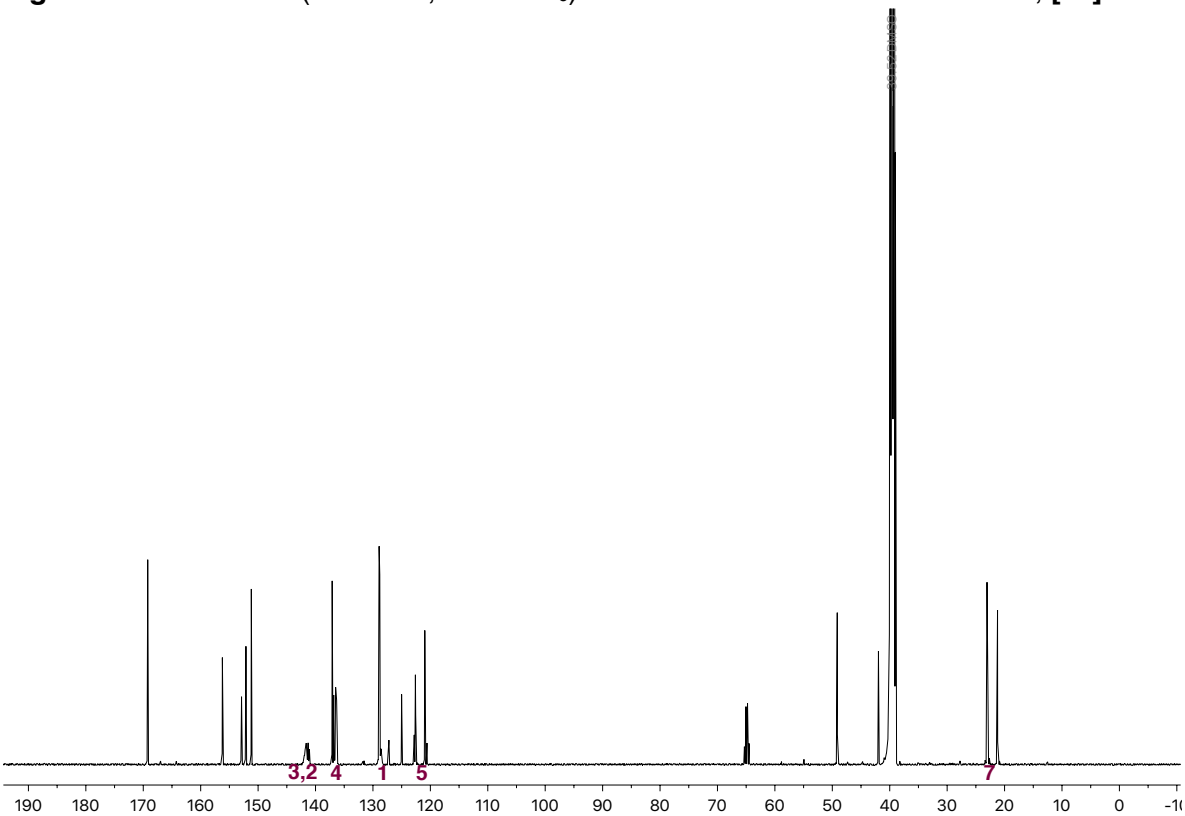

Figure S168. Quantitative ^{13}C{^{1}H} NMR (126 MHz, DMSO-d_6) of **[^{2}H]12ab**.

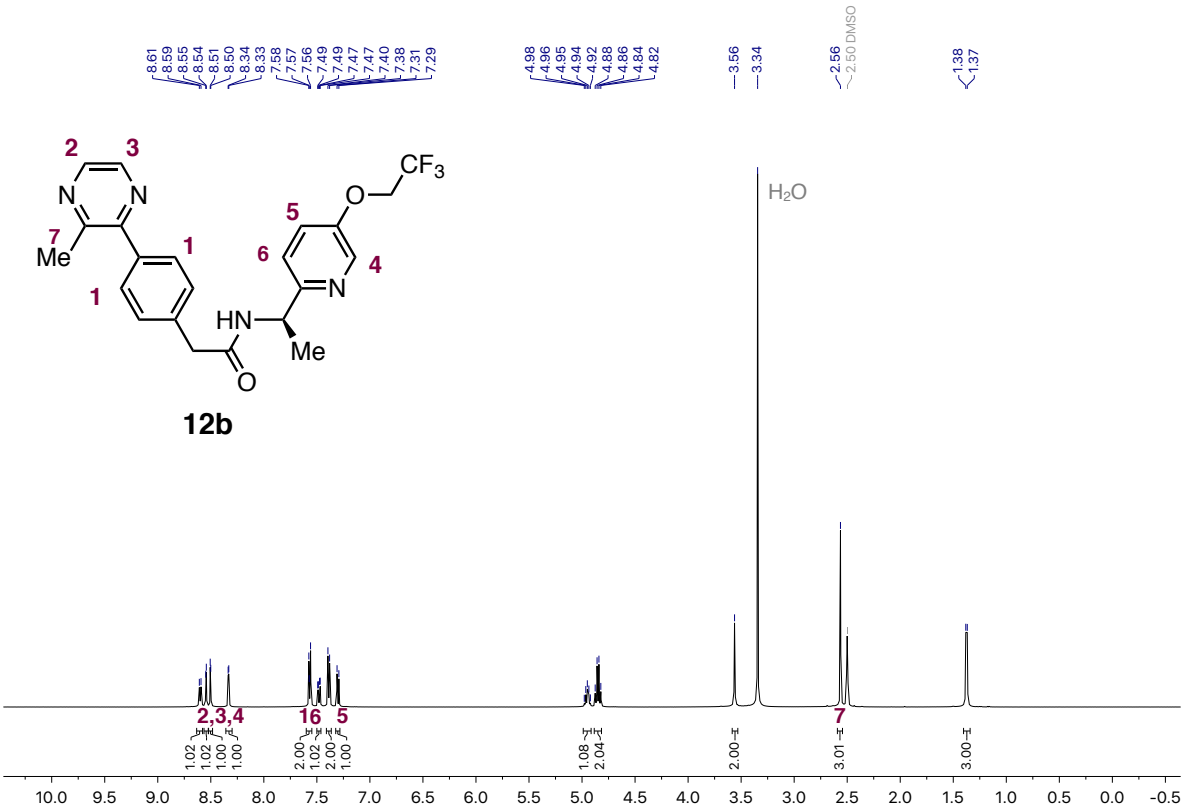

Figure S169. ^{1}H NMR (500 MHz, DMSO-d_6) of unlabeled MK-5395, **12b.**

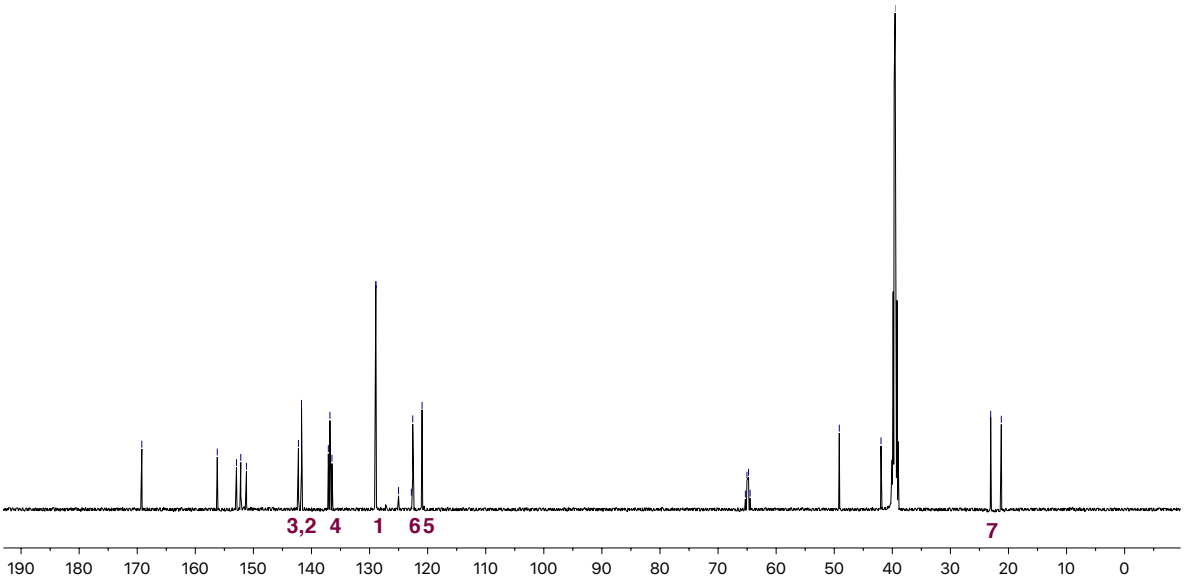

Figure S170. ^{13}C{^{1}H} NMR (126 MHz, DMSO-d_6) of **12b**.

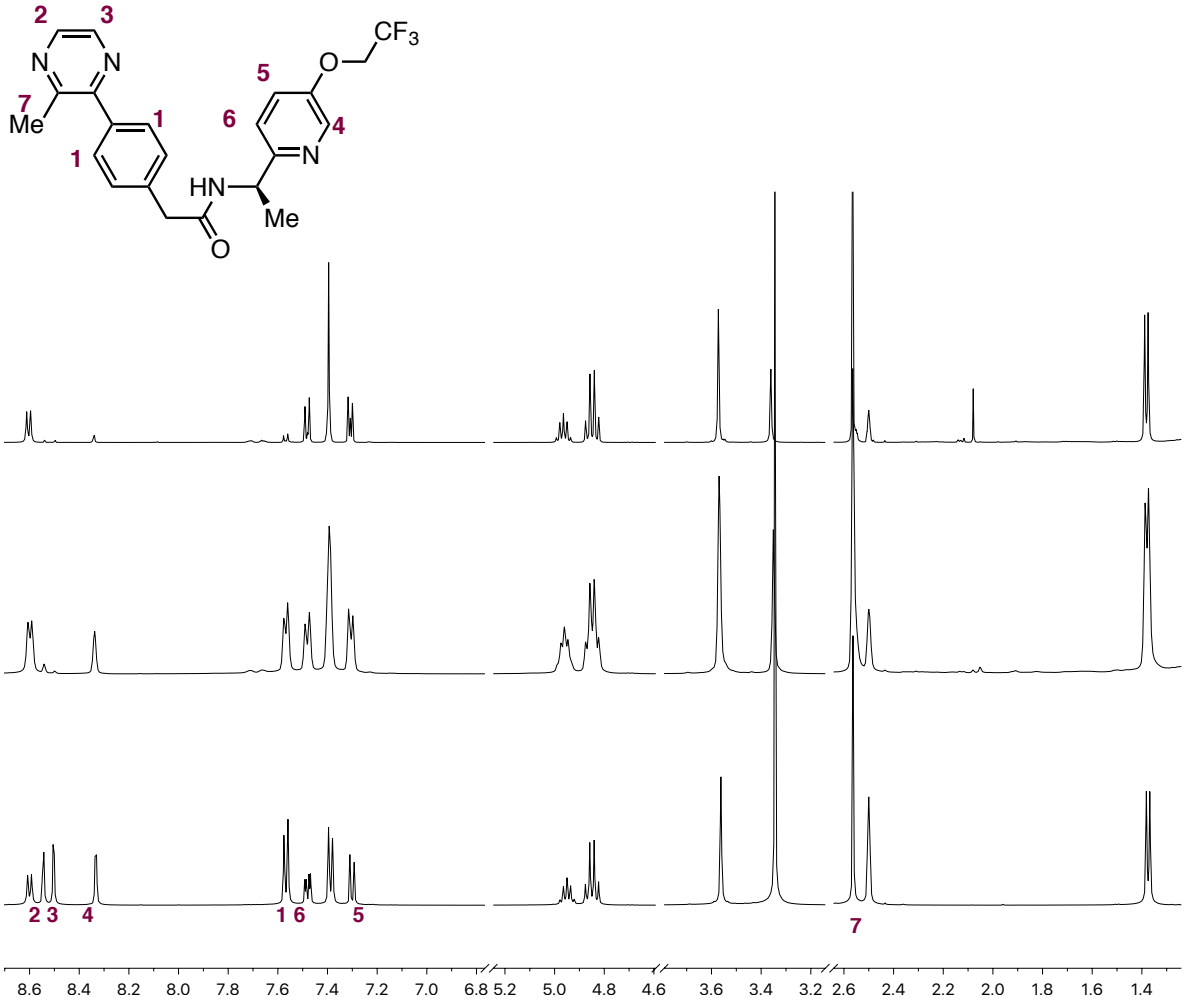

Figure S171. Stacked ^{1}H NMR spectra of MK-5395: labeled with Method A, **[^{2}H]12b** (first); labeled with Method B, **[^{2}H]12ab** (second); and unlabeled, **12b** (third).

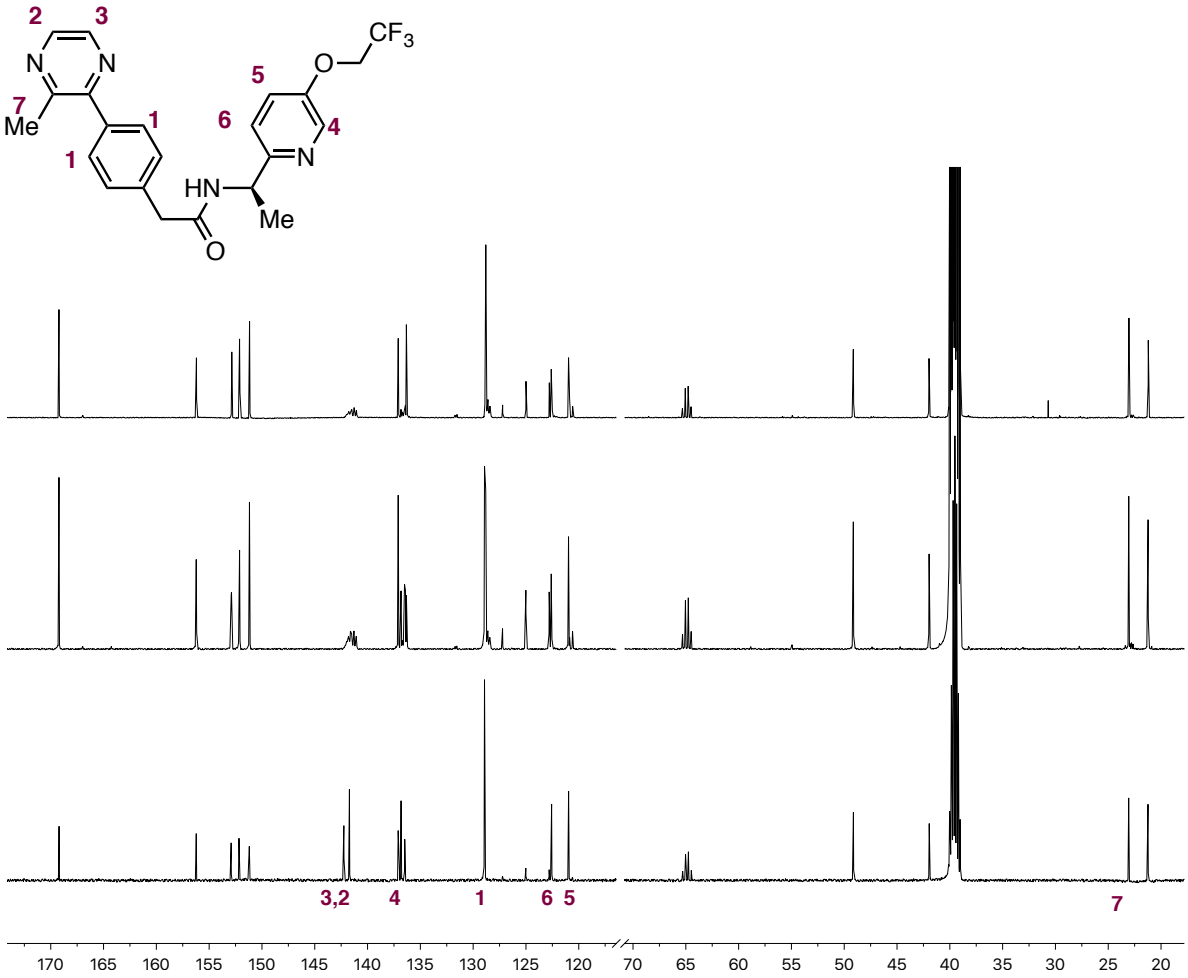

Figure S172. Stacked $^{13}C\{^{1}H\}$ NMR spectra of MK-5395: labeled with Method A, **[^{2}H]12b** (first, quantitative); labeled with Method B, **[^{2}H]12ab** (second, quantitative); unlabeled, **12b** (third).

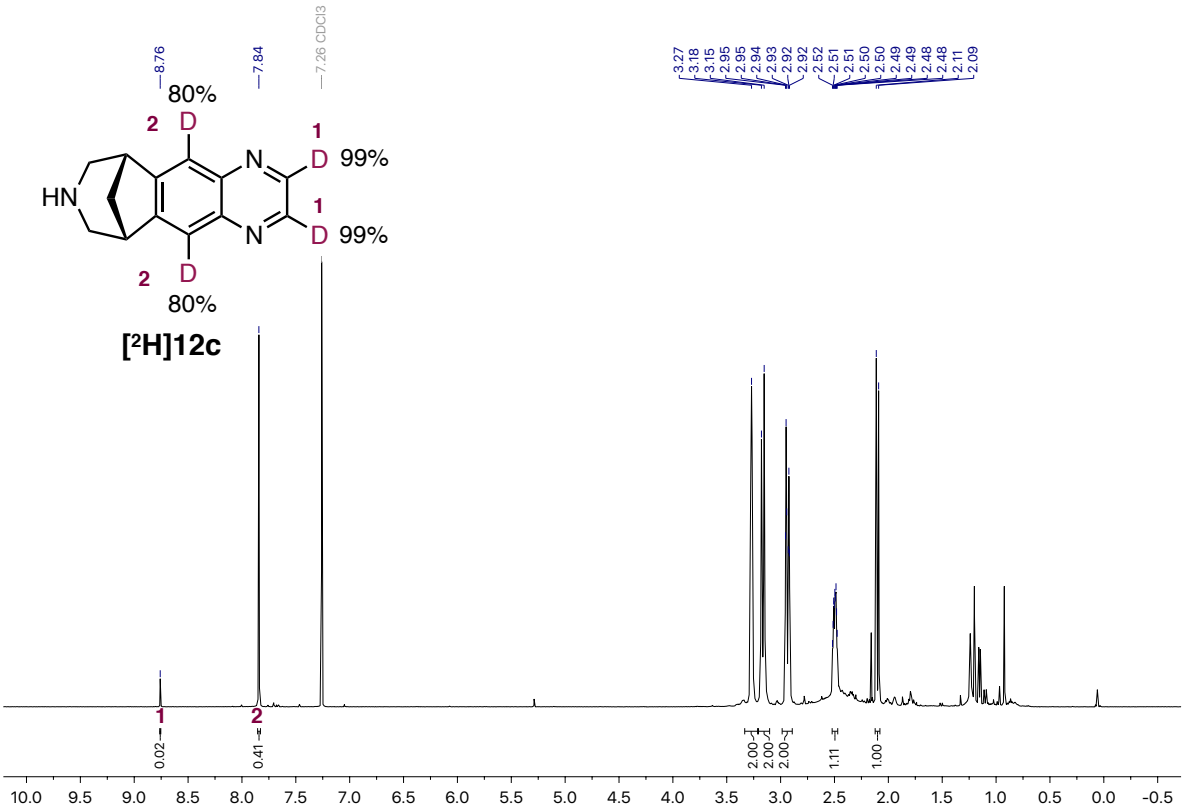

Figure S173. ^{1}H NMR (500 MHz, $CDCl_3$) of labeled varenicline with Method A, **[^{2}H]12c**.

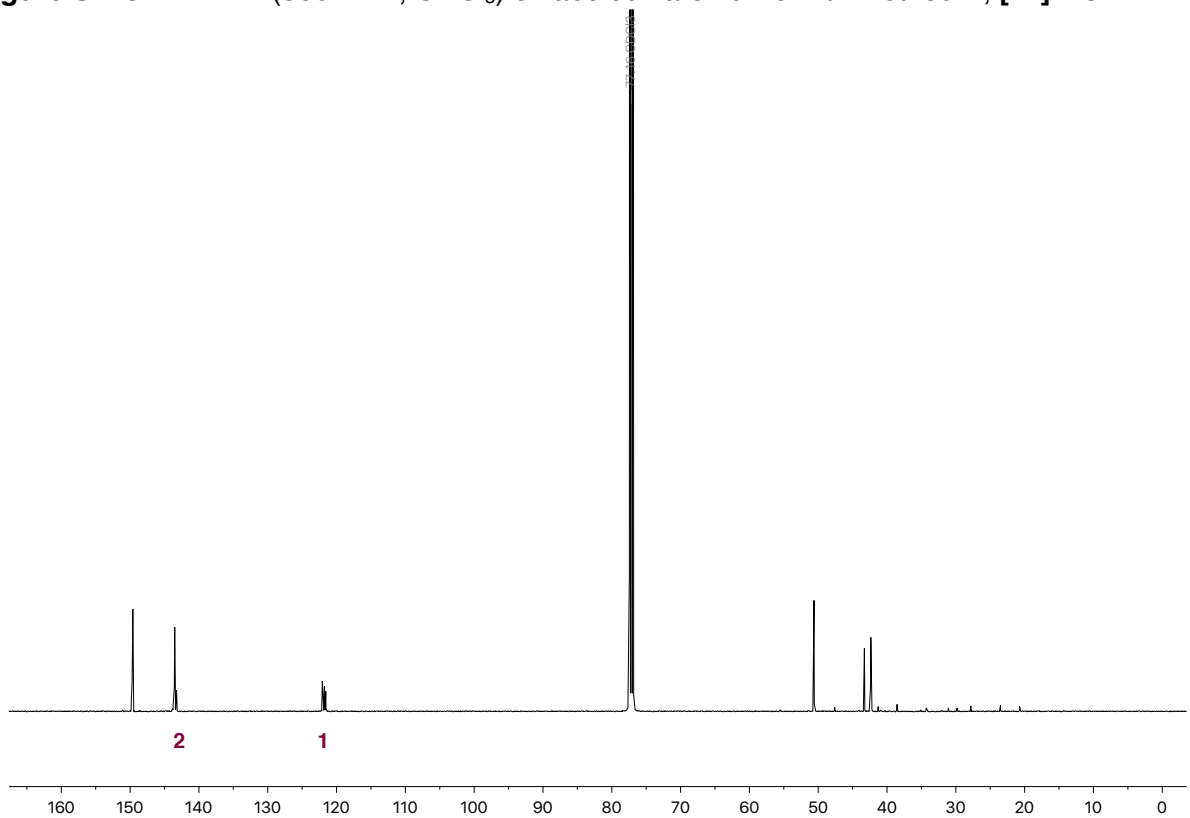

Figure S174. Quantitative ^{13}C{^{1}H} NMR (126 MHz, $CDCl_3$) of **[^{2}H]12c**.

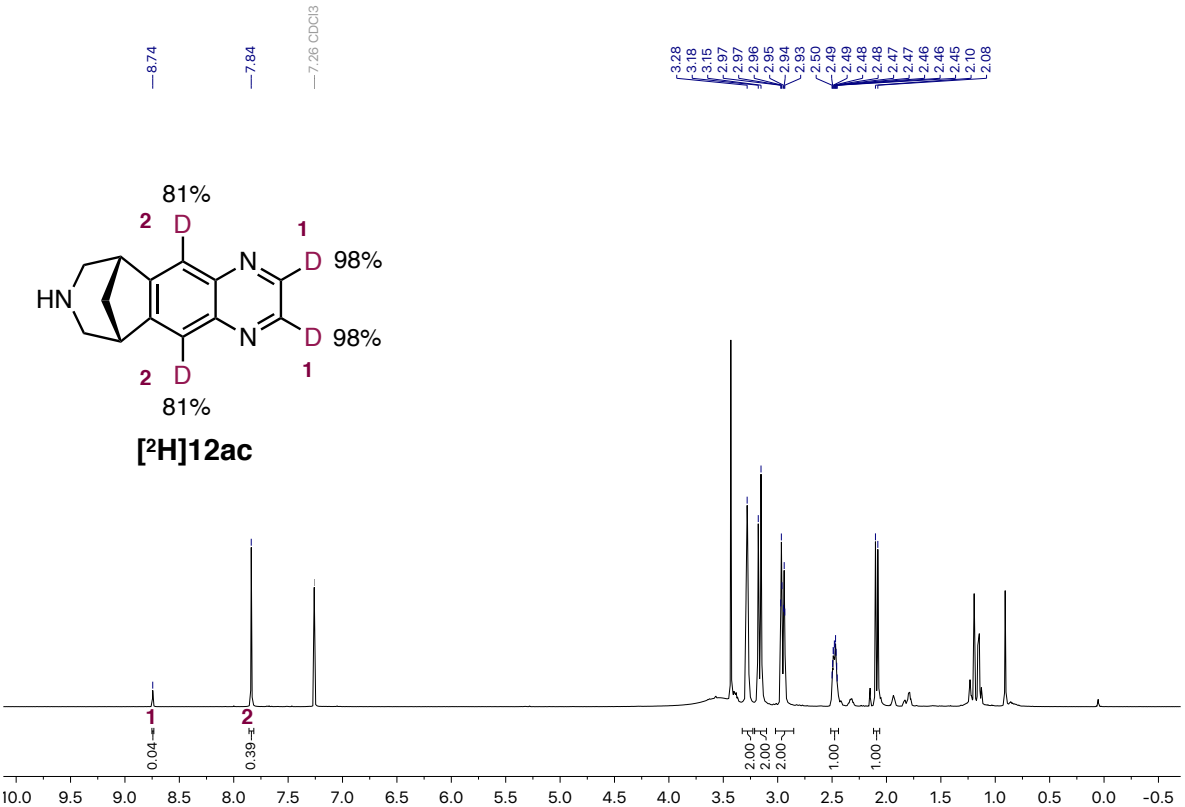

Figure S175. ^{1}H NMR (500 MHz, $CDCl_3$) of labeled varenicline with Method B, **[^{2}H]12ac**.

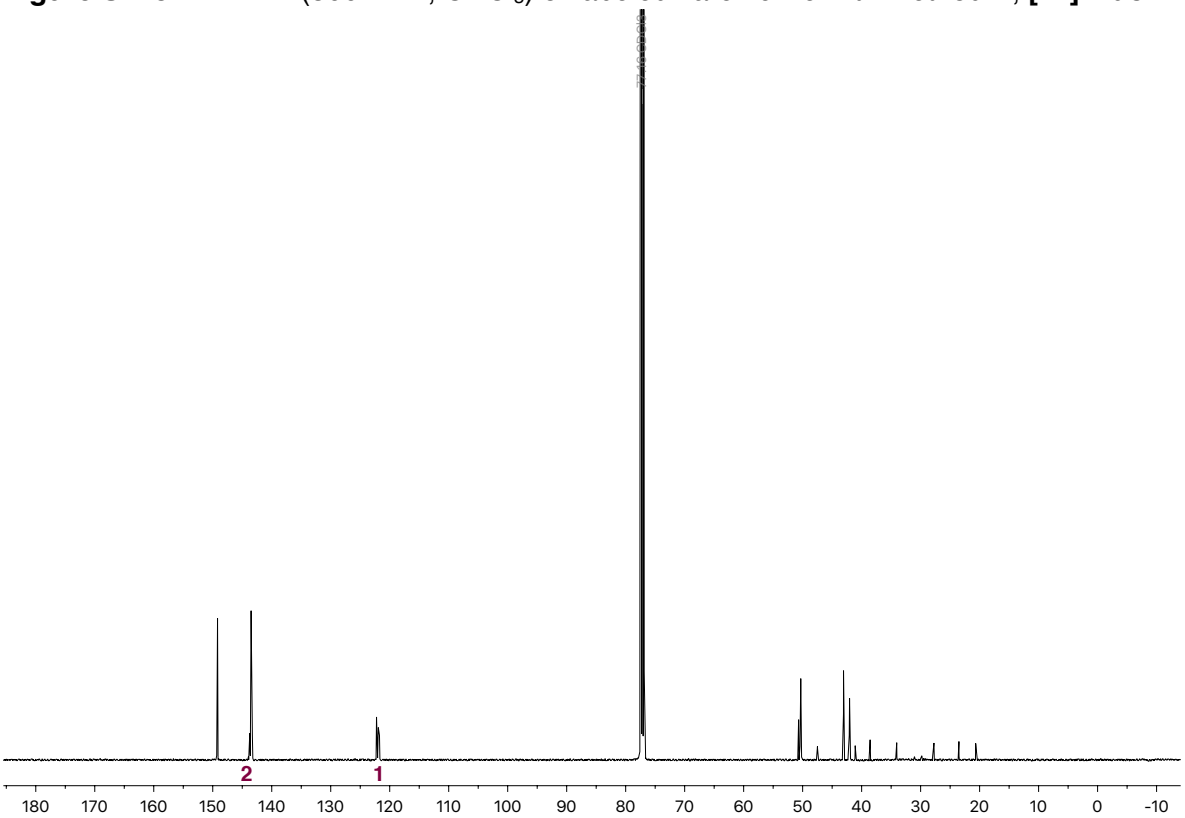

Figure S176. Quantitative ^{13}C{^{1}H} NMR (126 MHz, $CDCl_3$) of **[^{2}H]12ac**.

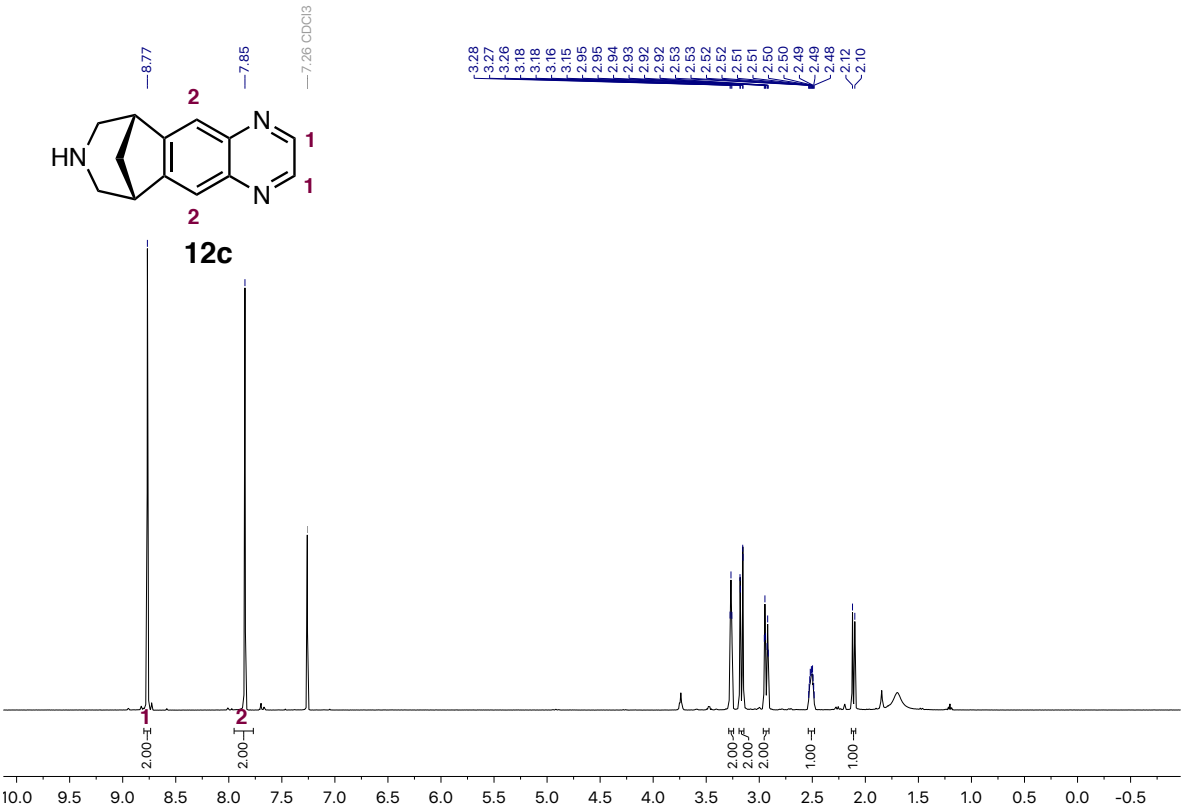

Figure S177. ^{1}H NMR (500 MHz, $CDCl_3$) of unlabeled varenicline,**12c**.

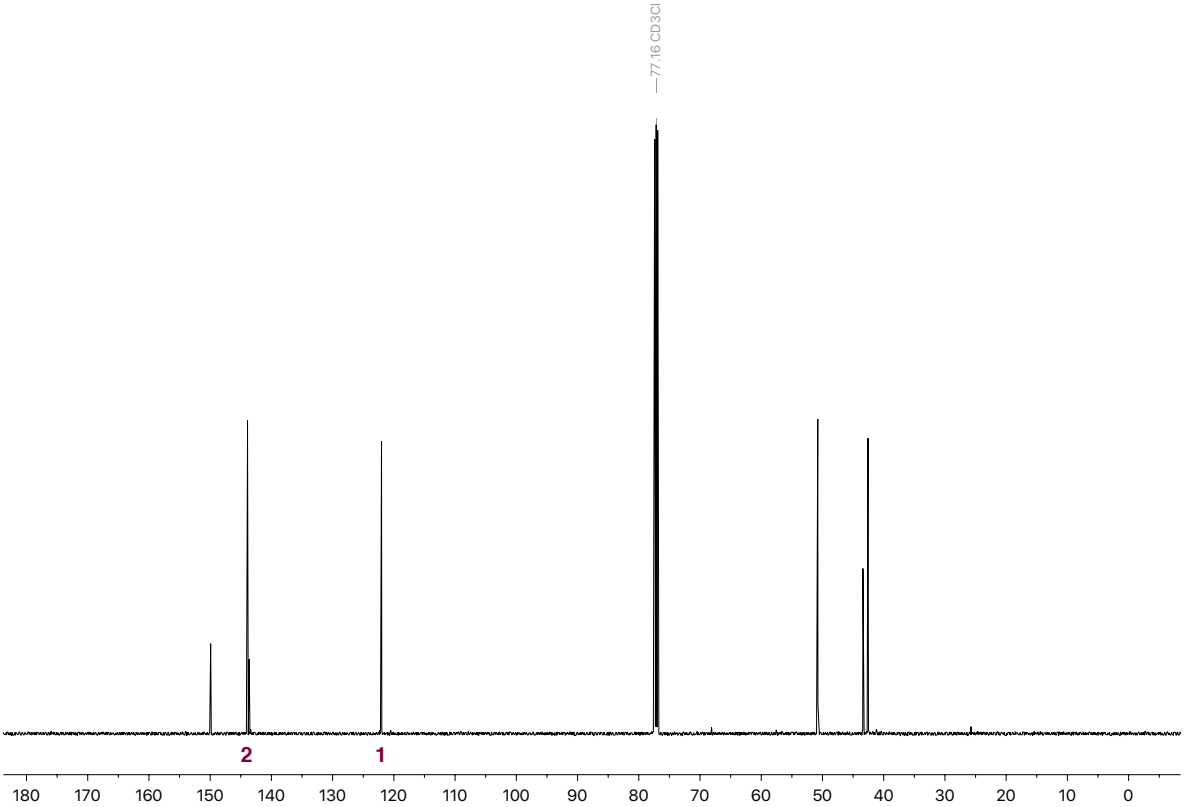

Figure S178. ^{13}C{^{1}H} NMR (126 MHz, $CDCl_3$) of **12c**.

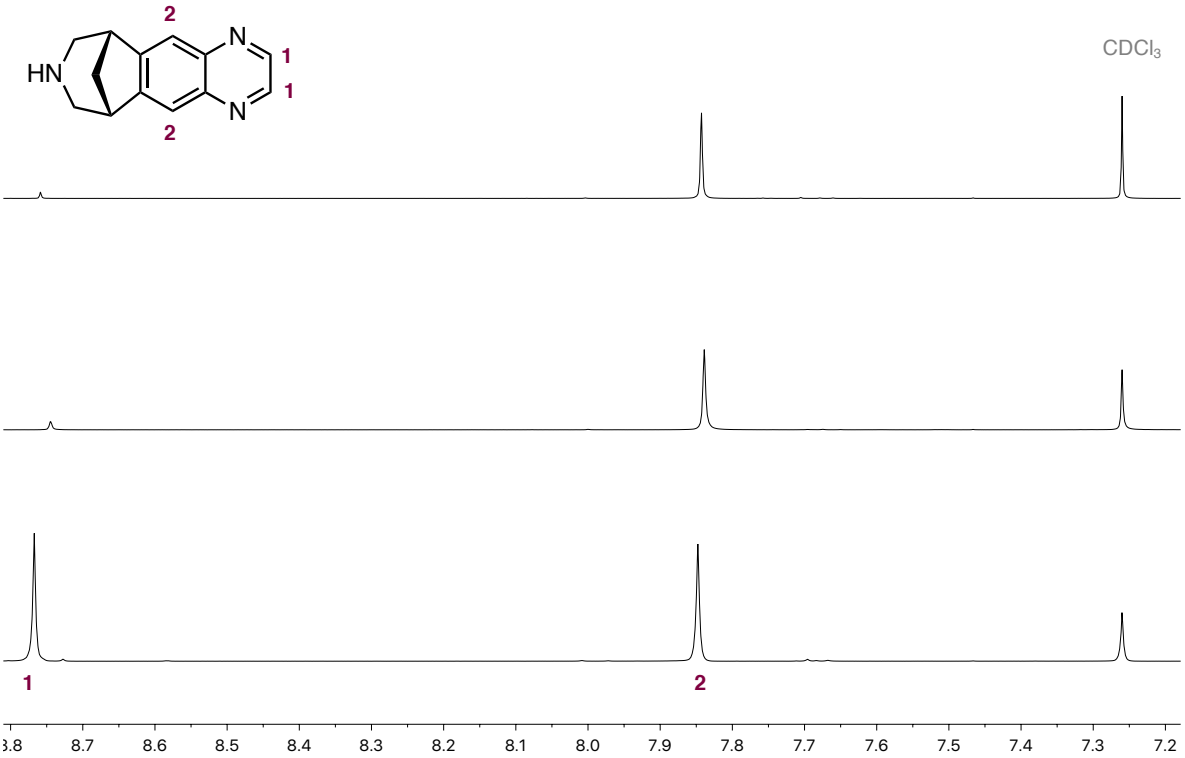

Figure S179. Stacked ^{1}H NMR spectra of varenicline (aromatic region): labeled with Method A, **[^{2}H]12c** (first); labeled with Method B, **[^{2}H]12ac** (second); and unlabeled, **12c** (third).

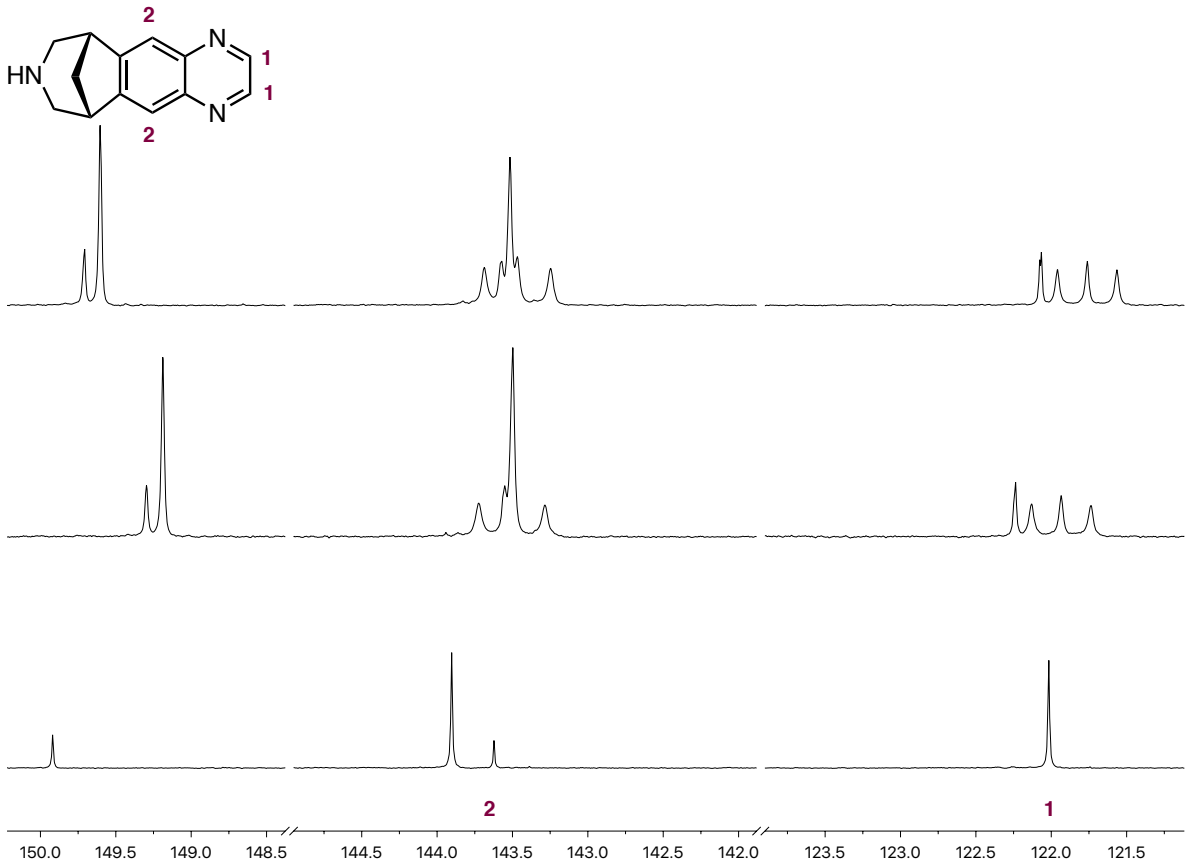

Figure S180. Stacked $^{13}C\{^{1}H\}$ NMR spectra of varenicline (aromatic region): labeled with Method A, **[^{2}H]12c** (first, quantitative); labeled with Method B, **[^{2}H]12ac** (second, quantitative); unlabeled, **12c** (third).

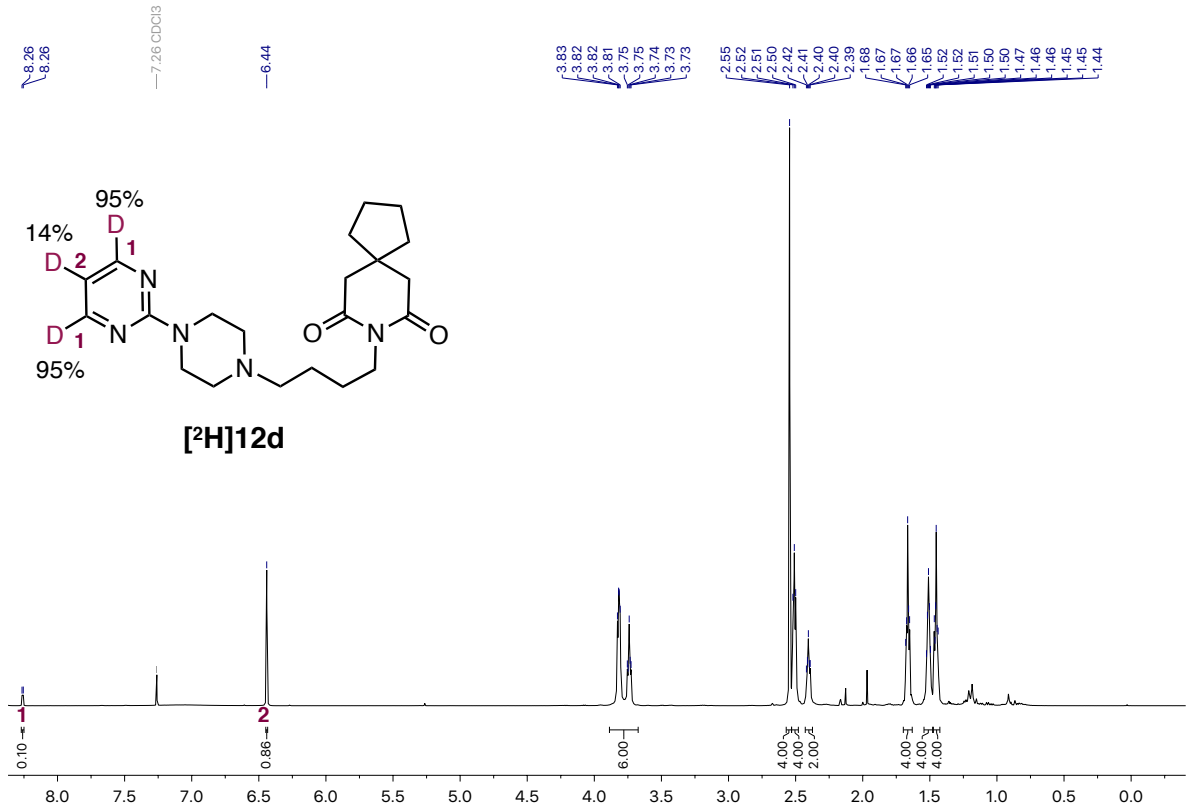

Figure S181. ^{1}H NMR (500 MHz, $CDCl_3$) of labeled buspirone with Method A, **[^{2}H]12d**.

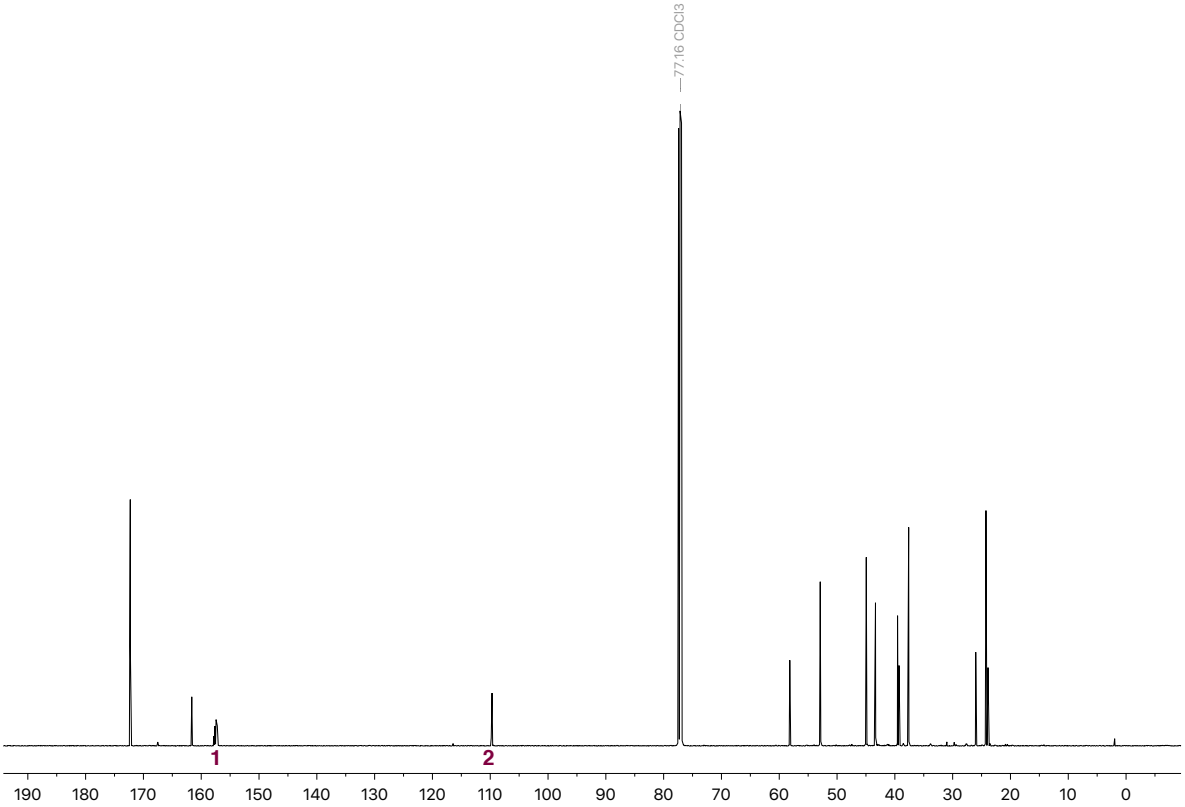

Figure S182. Quantitative ^{13}C{^{1}H} NMR (126 MHz, $CDCl_3$) of **[^{2}H]12d**.

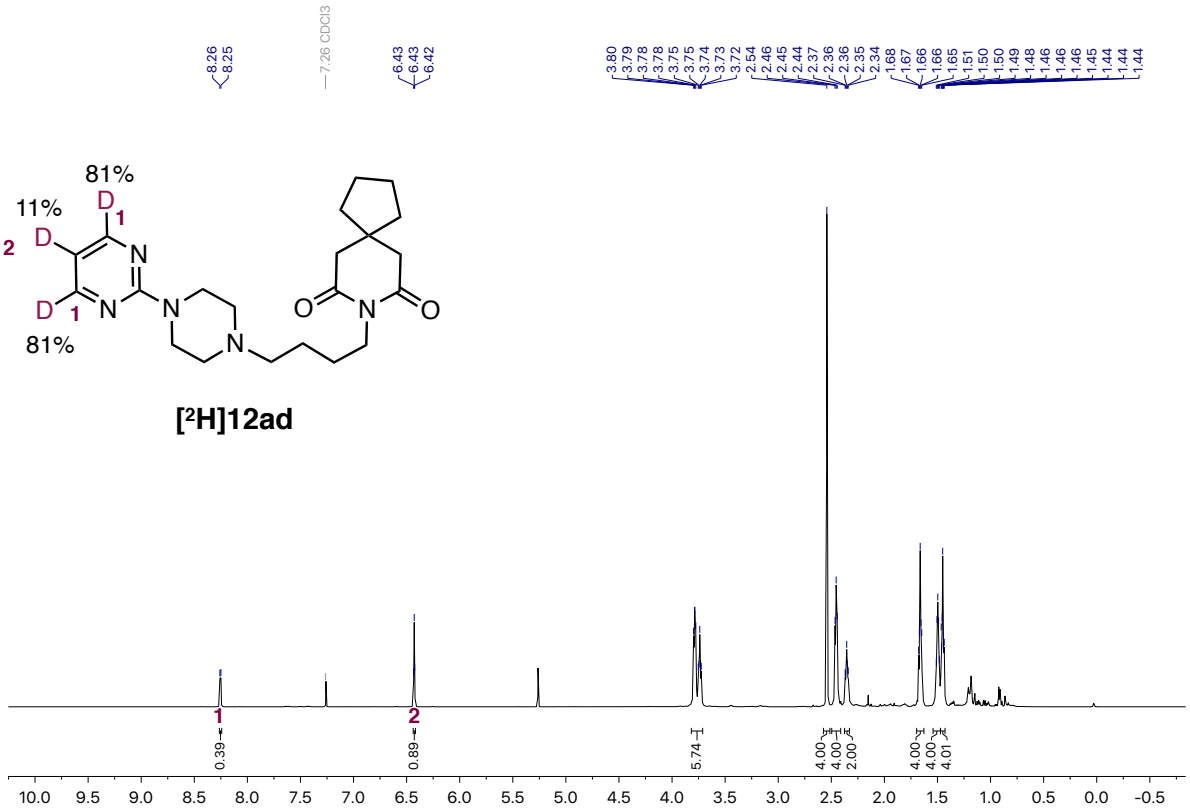

Figure S183. ^{1}H NMR (500 MHz, $CDCl_3$) of labeled buspirone with Method B, **[^{2}H]12ad**.

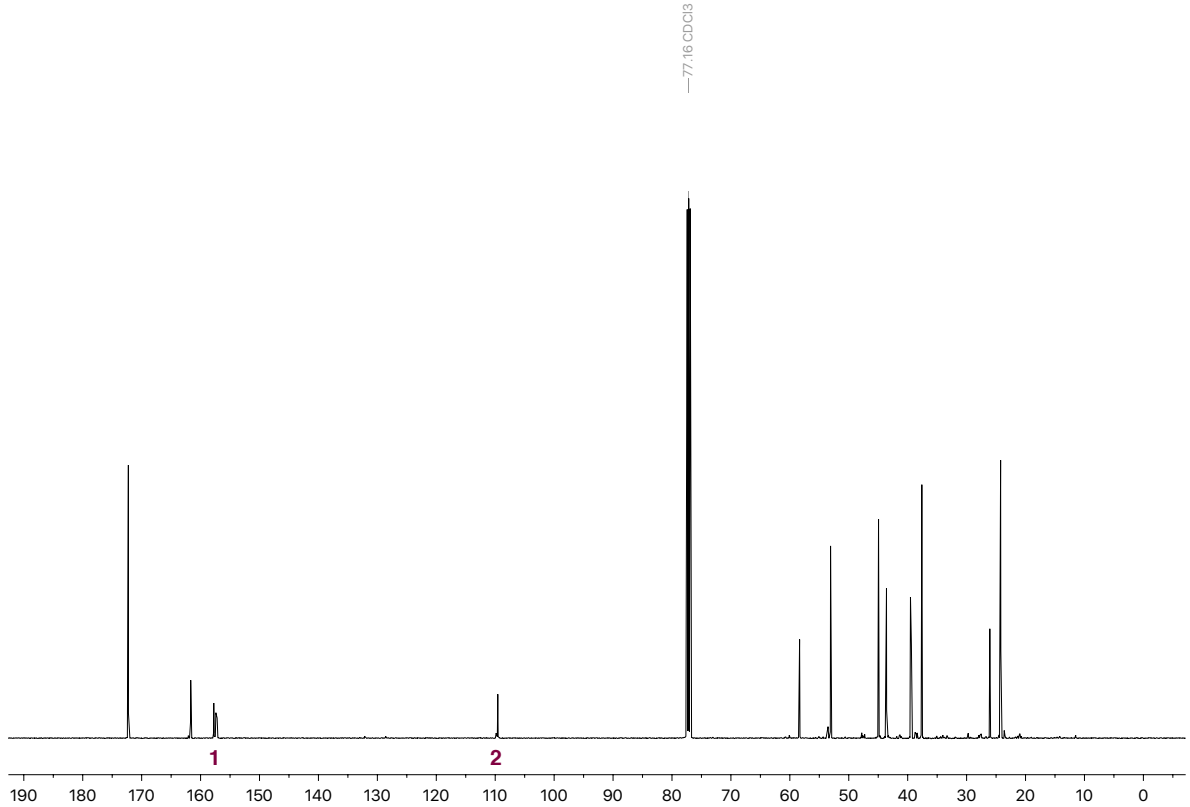

Figure S184. Quantitative ^{13}C{^{1}H} NMR (126 MHz, DMSO-d_6) of **[^{2}H]12ad**.

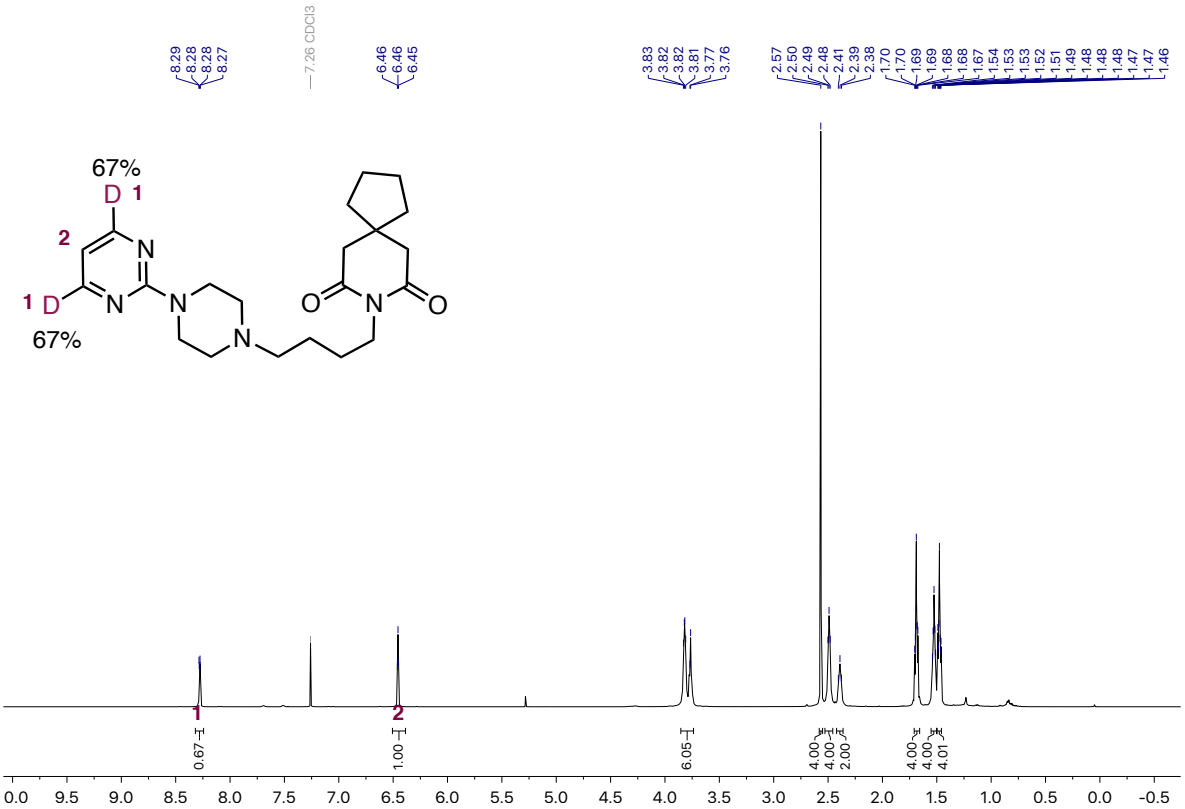

Figure S185. ^{1}H NMR (500 MHz, $CDCl_3$) of labeled buspirone with $[(^{iPr}DI)Ni(\mu_2\text{-}H)]_2$.

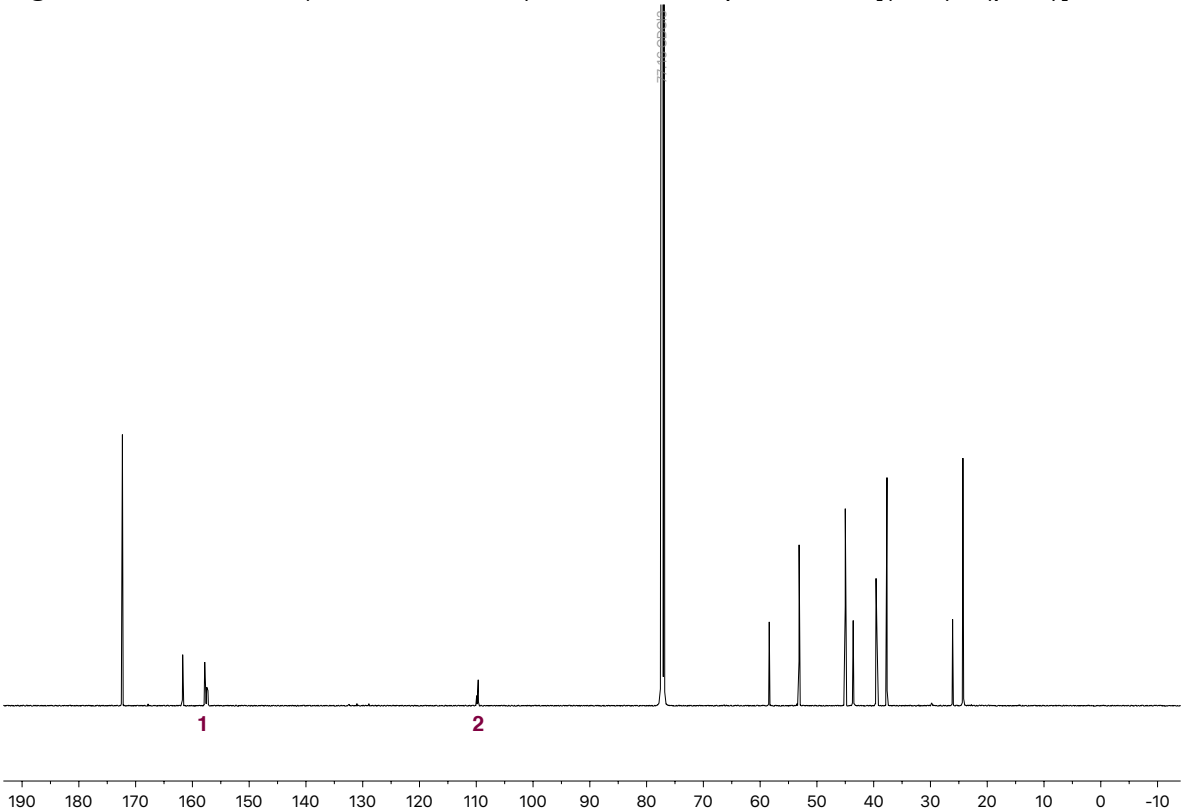

Figure S186. Quantitative $^{13}C\{^{1}H\}$ NMR (126 MHz, $CDCl_3$) of labeled buspirone with $[(^{iPr}DI)Ni(\mu_2\text{-}H)]_2$.

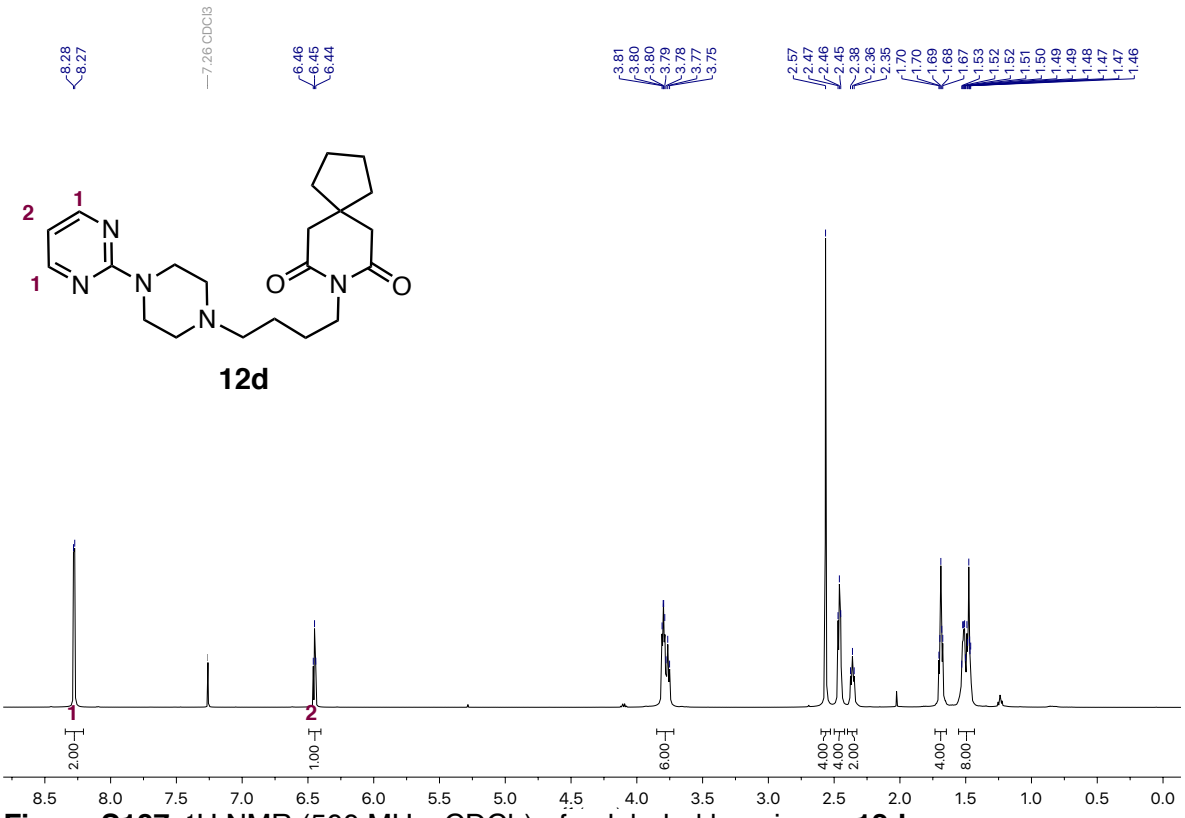

Figure S187. ^{1}H NMR (500 MHz, $CDCl_3$) of unlabeled buspirone, **12d**.

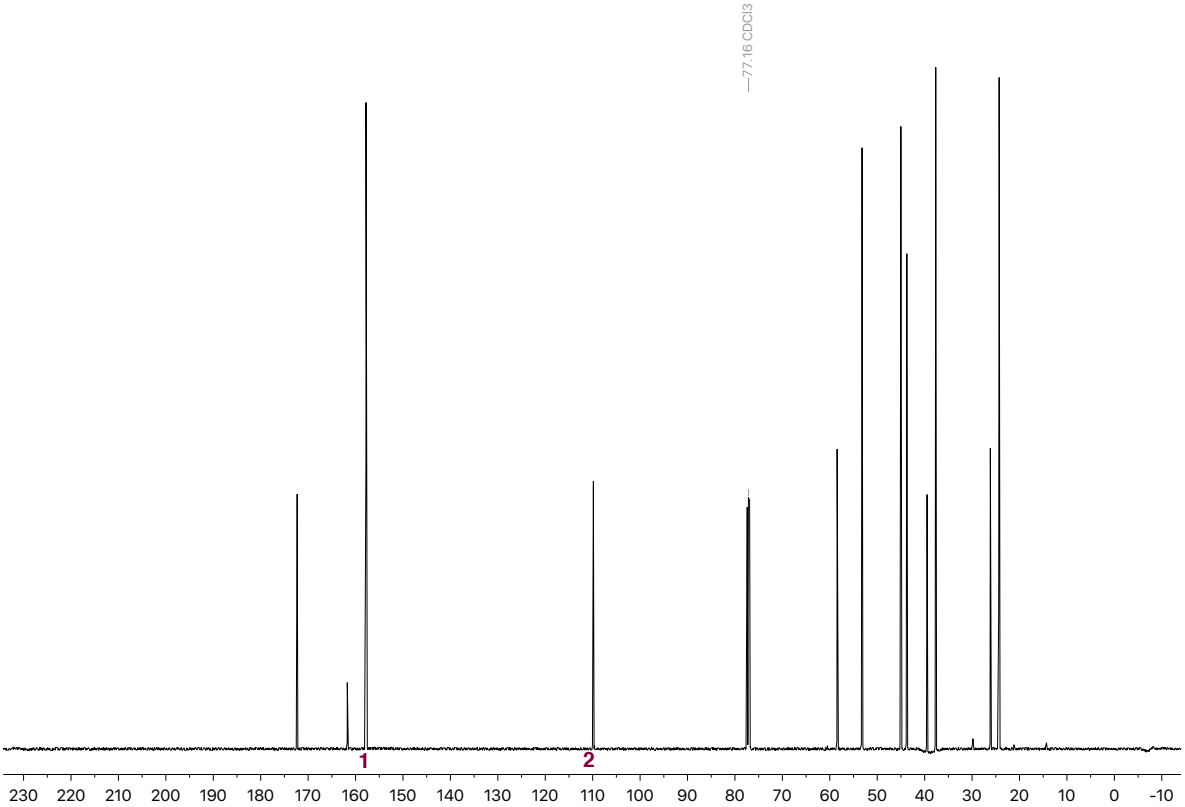

Figure S188. ^{13}C{^{1}H} NMR (126 MHz, $CDCl_3$) of **12d**.

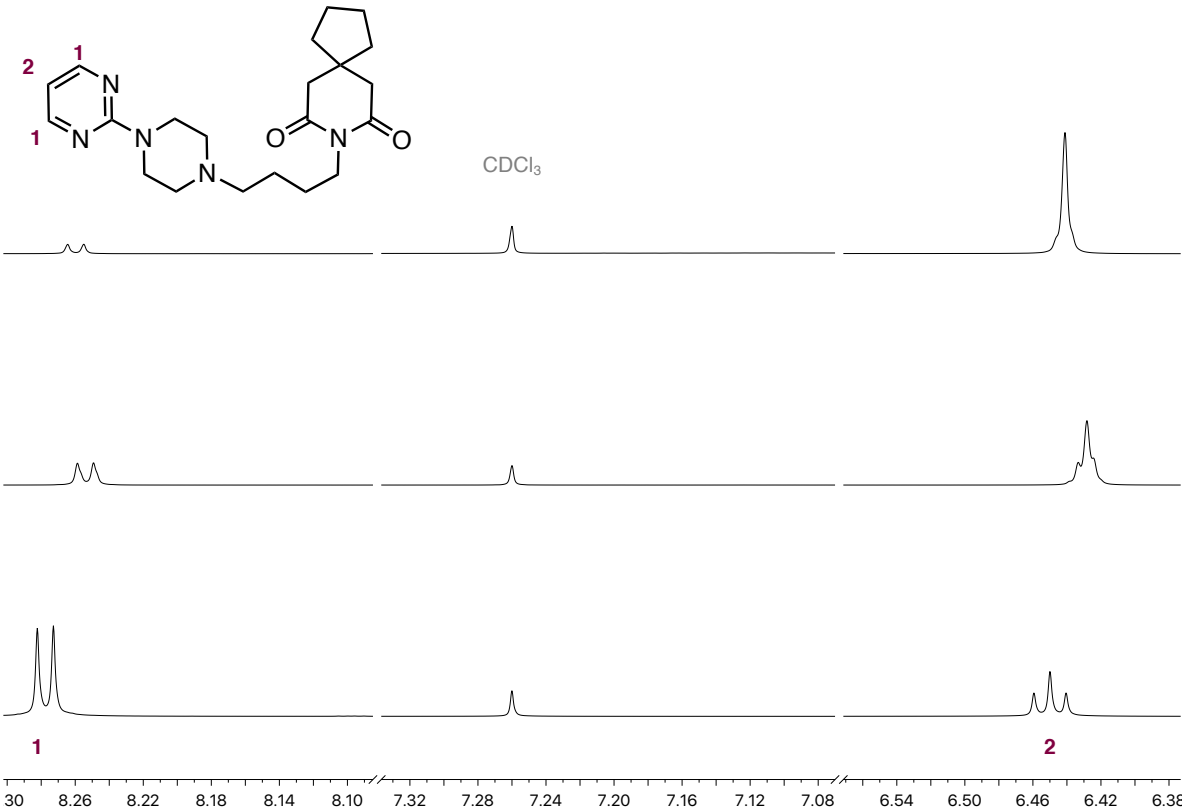

Figure S189. Stacked ^{1}H NMR spectra of buspirone (aromatic region): labeled with Method A, **[^{2}H]12d** (first); labeled with Method B, **[^{2}H]12ad** (second); and unlabeled, **12d** (third).

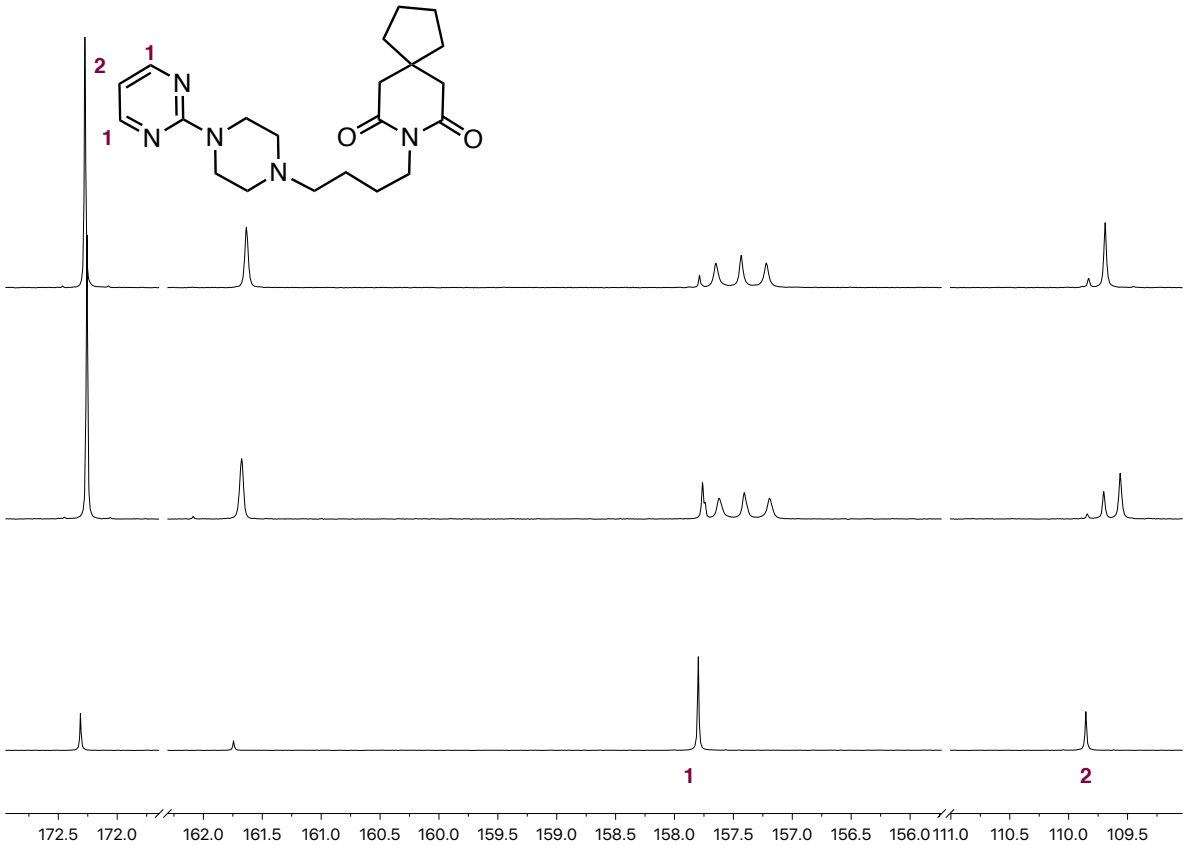

Figure S190. Stacked $^{13}C\{^{1}H\}$ NMR spectra of buspirone (aromatic region): labeled with Method A, **[^{2}H]12d** (first, quantitative); labeled with Method B, **[^{2}H]12ad** (second, quantitative); and unlabeled, **12d** (third).

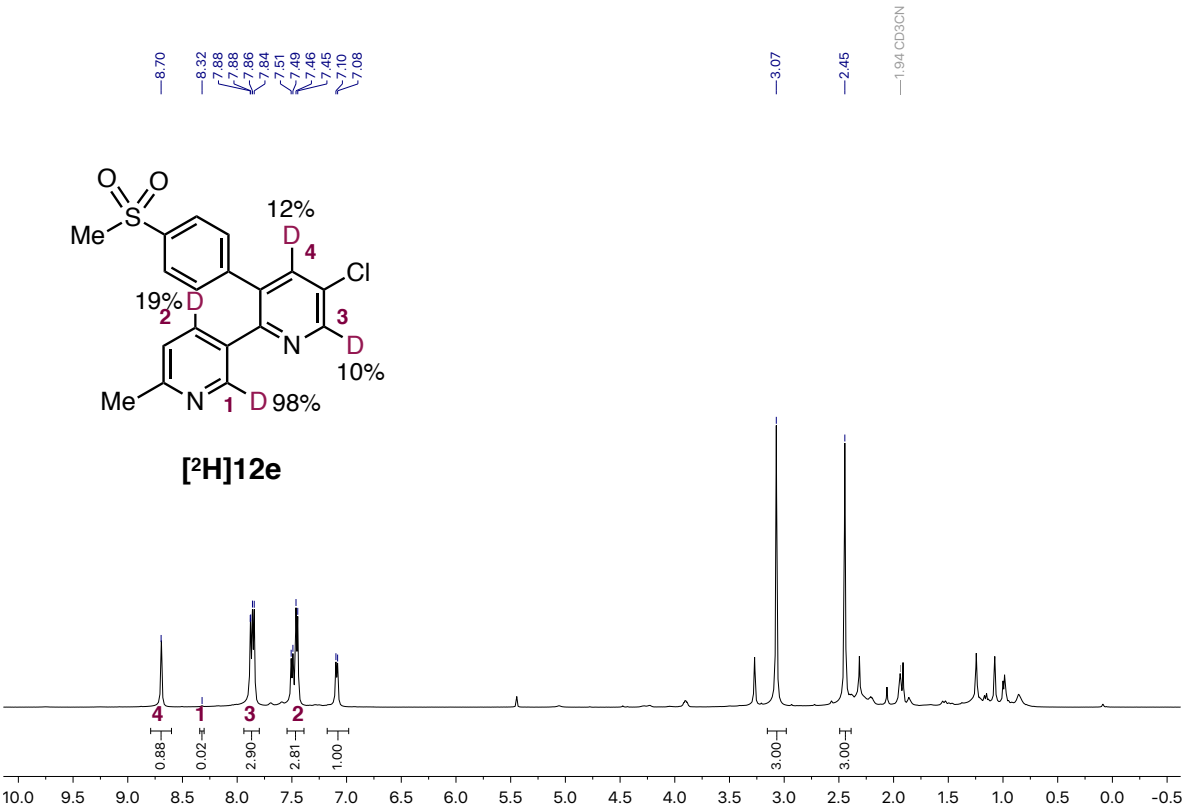

Figure S191. ^{1}H NMR (500 MHz, CD_3CN) of labeled etoricoxib with Method A, **[^{2}H]12e**.

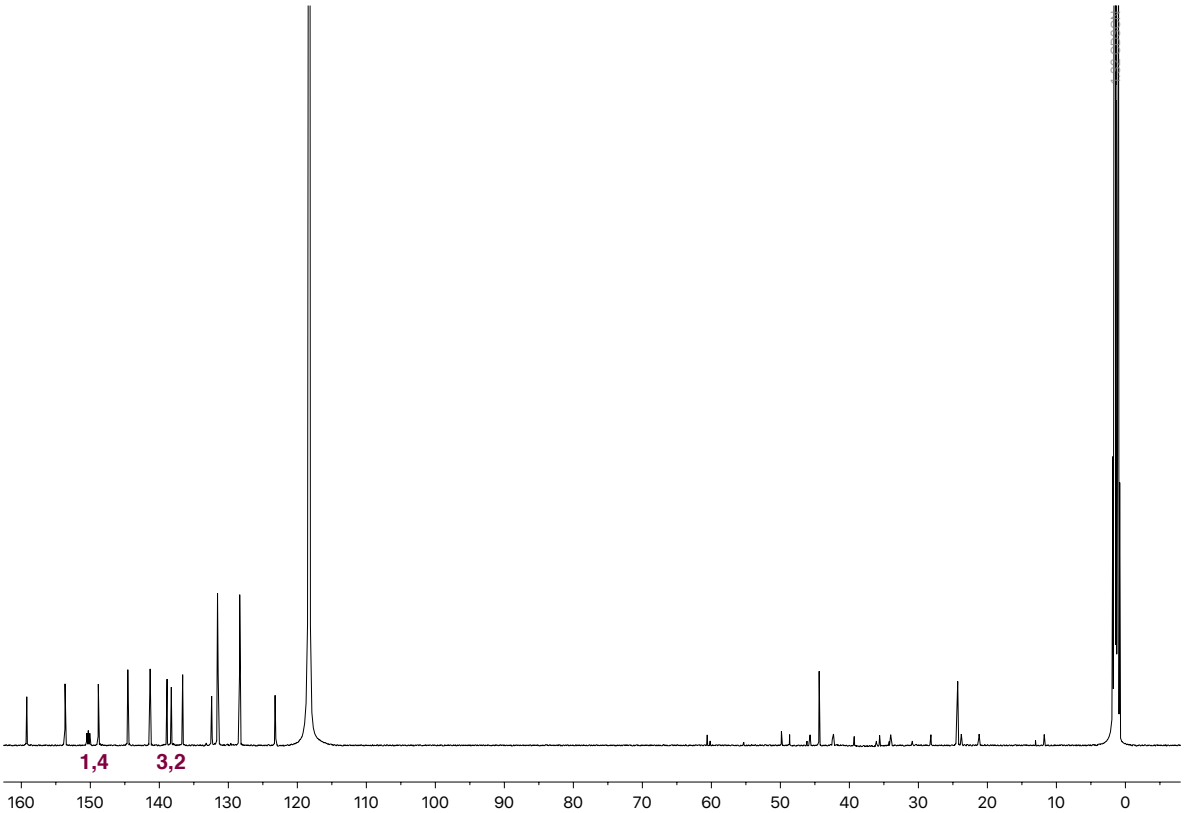

Figure S192. Quantitative ^{13}C{^{1}H} NMR (126 MHz, CD_3CN) of **[^{2}H]12e**.

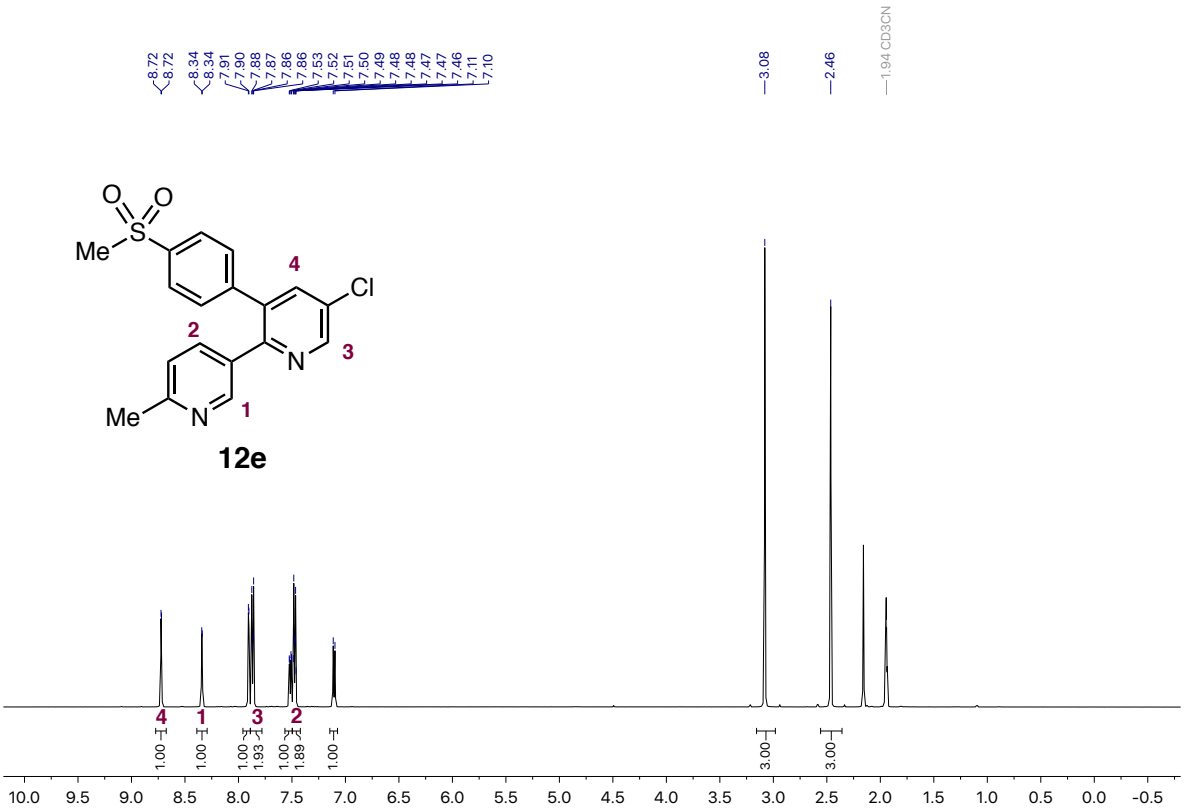

Figure S193. ^{1}H NMR (500 MHz, CD_3CN) of unlabeled etoricoxib, **12e**.

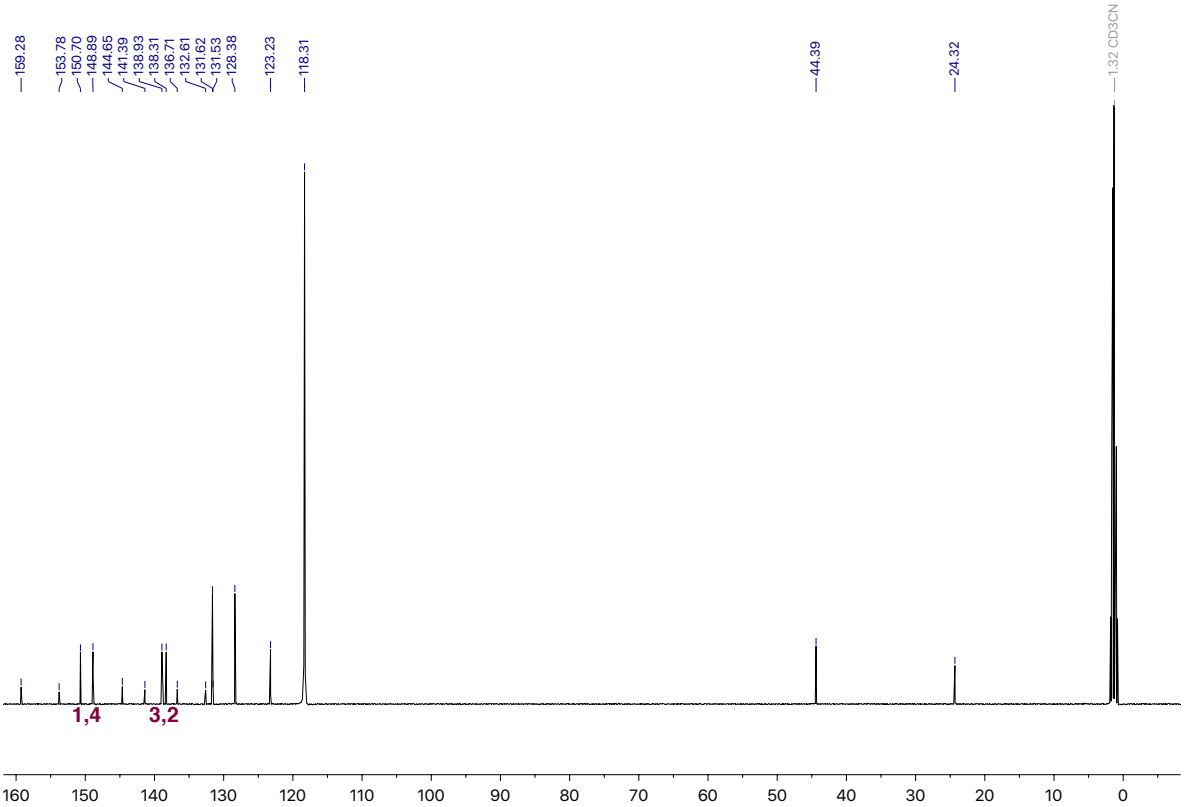

Figure S194. ^{13}C{^{1}H} NMR (126 MHz, CD_3CN) of **12e**.

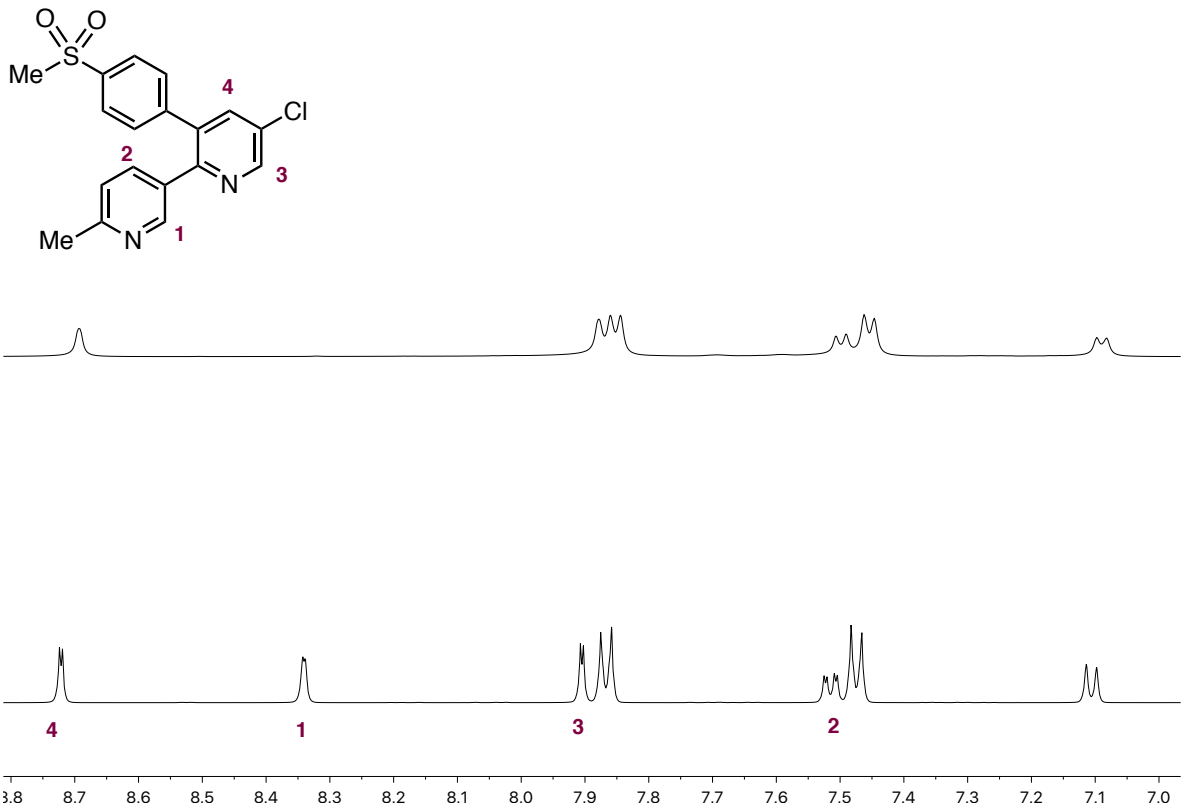

Figure S195. Stacked ^{1}H NMR spectra of etoricoxib (aromatic region): labeled with Method A, **[^{2}H]12e** (first) and unlabeled, **12e** (second).

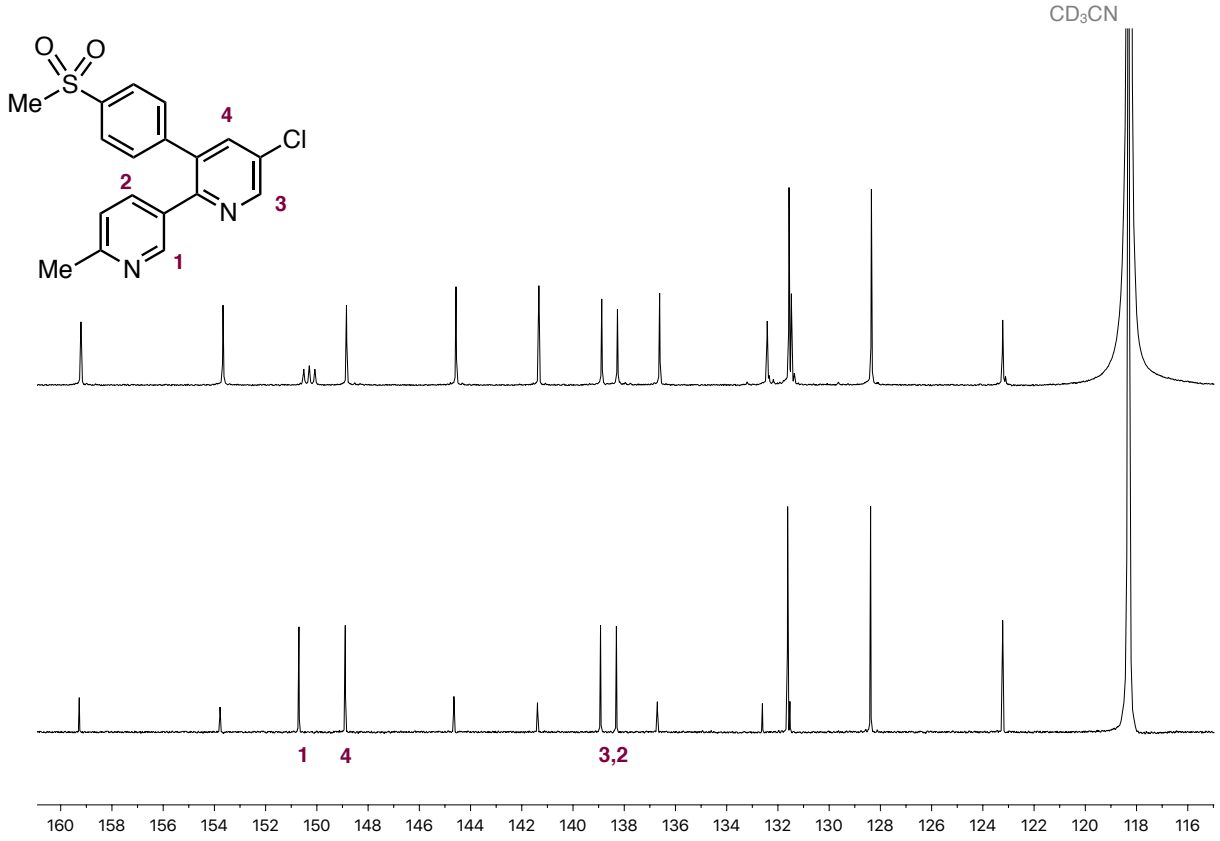

Figure S196. Stacked $^{13}C\{^{1}H\}$ NMR spectra of etoricoxib: labeled with Method A, **[^{2}H]12e** (first, quantitative) unlabeled, **12e** (second,).

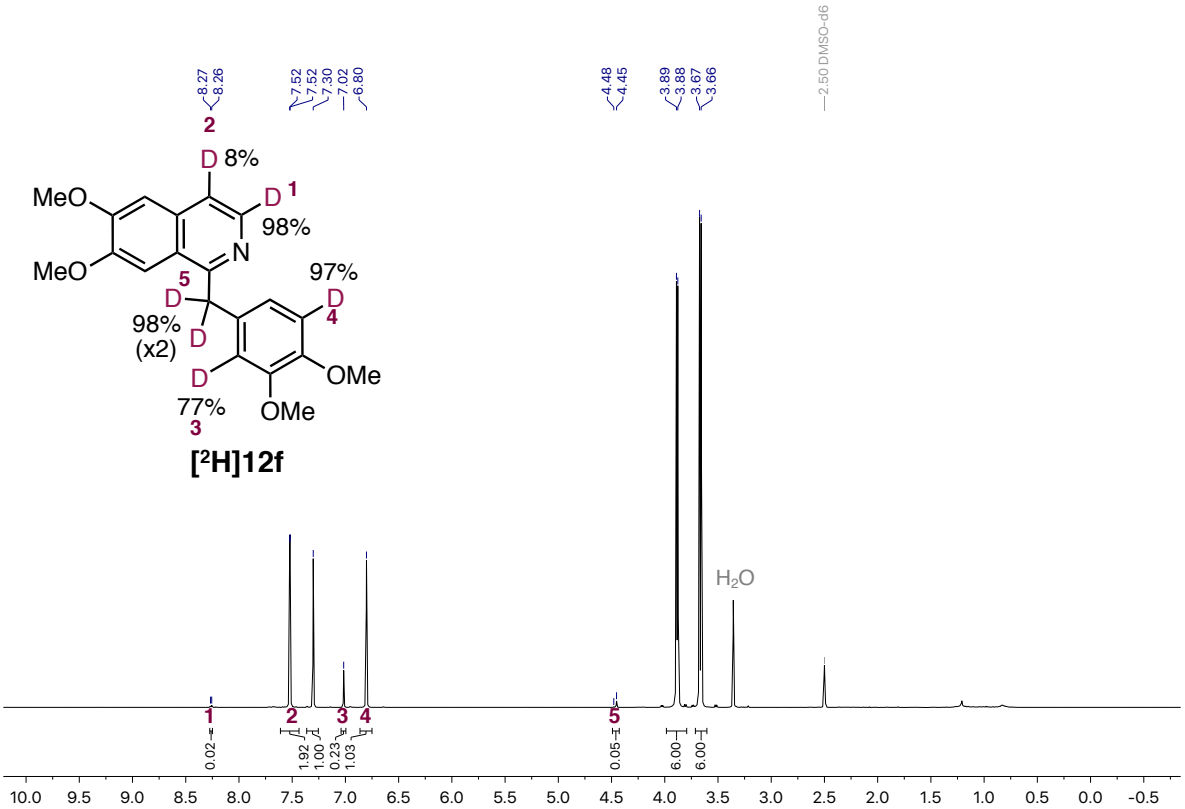

Figure S197. ^{1}H NMR (500 MHz, DMSO-d_6) of labeled papaverine with Method A, **[^{2}H]12f**.

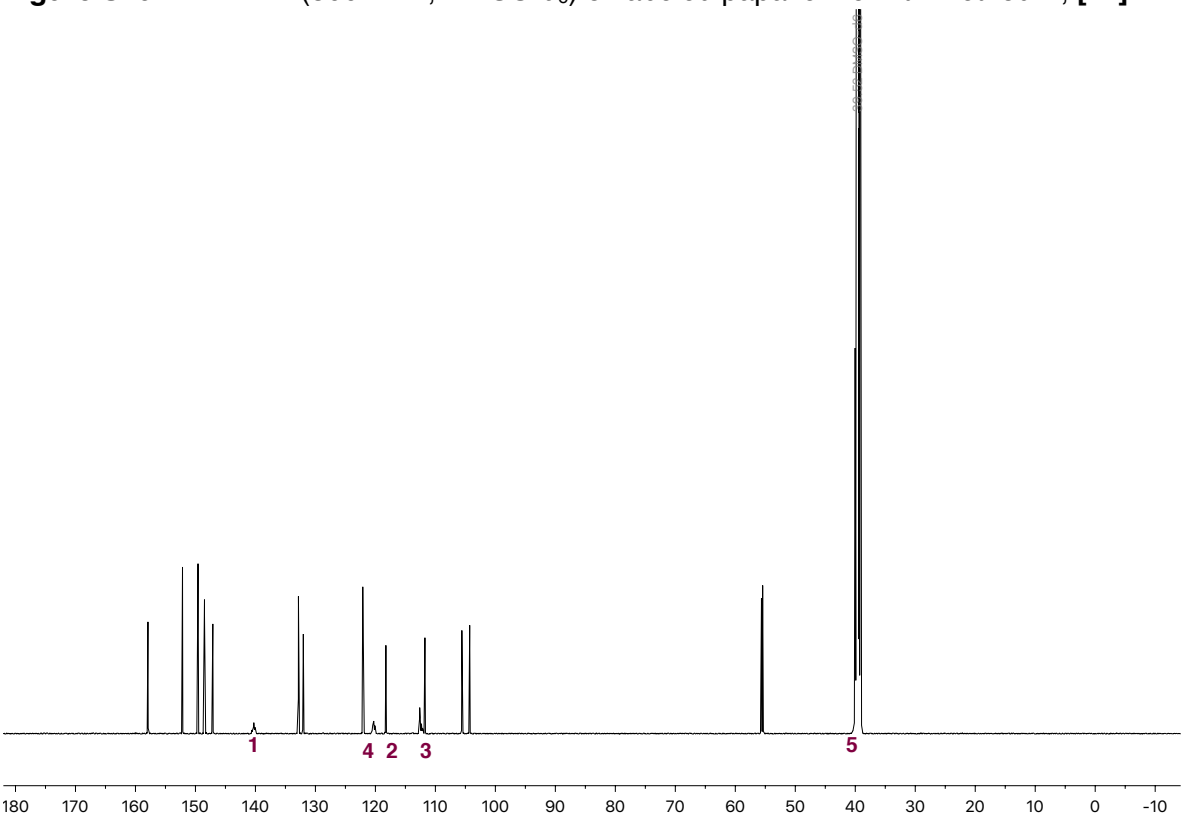

Figure S198. Quantitative ^{13}C{^{1}H} NMR (126 MHz, DMSO-d_6) of **[^{2}H]12f**.

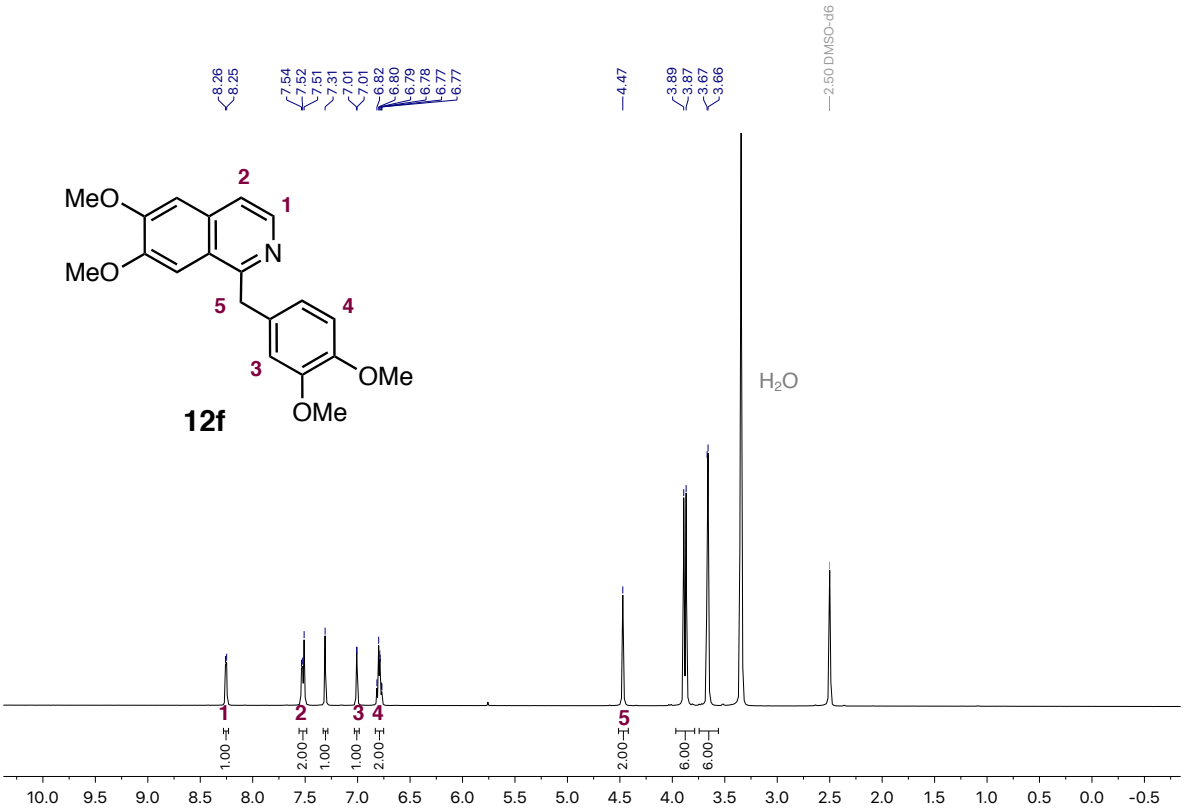

Figure S199. ^{1}H NMR (500 MHz, DMSO-d_6) of unlabeled papaverine, **12f**.

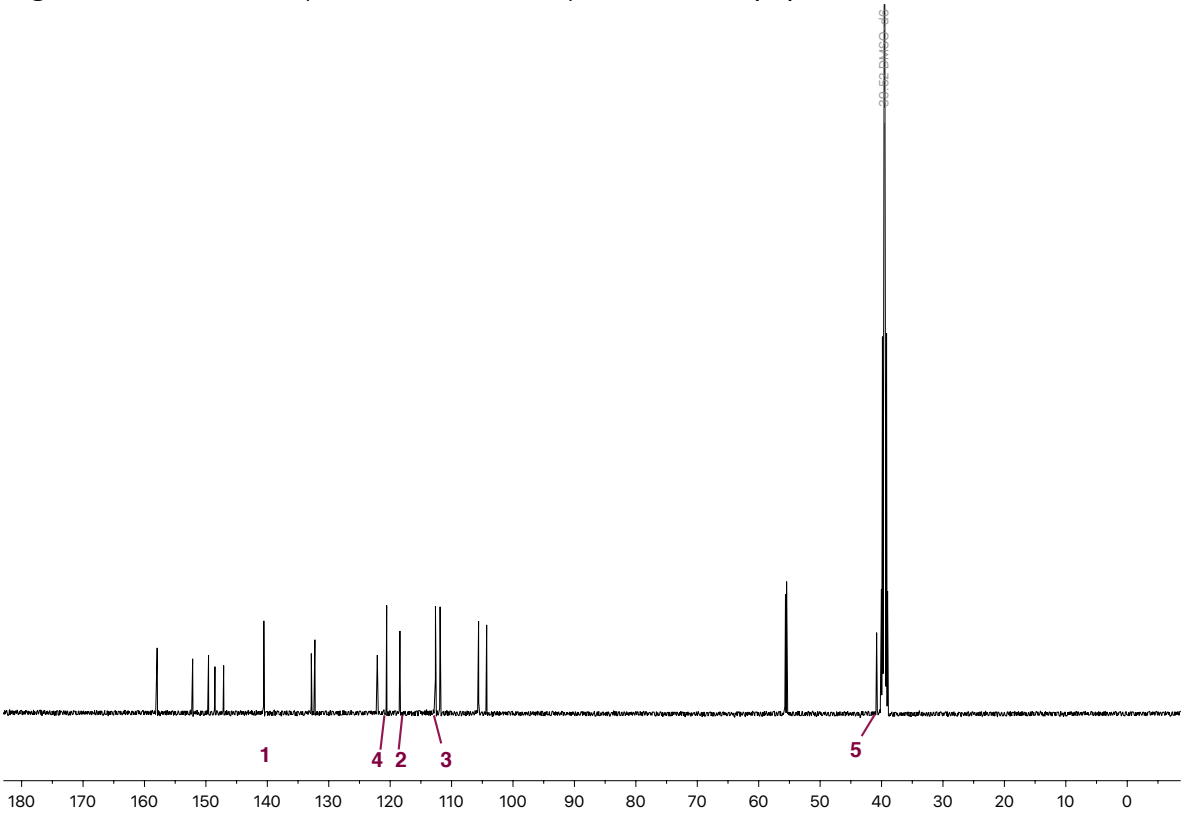

Figure S200. ^{13}C{^{1}H} NMR (126 MHz, DMSO-d_6) of **12f**.

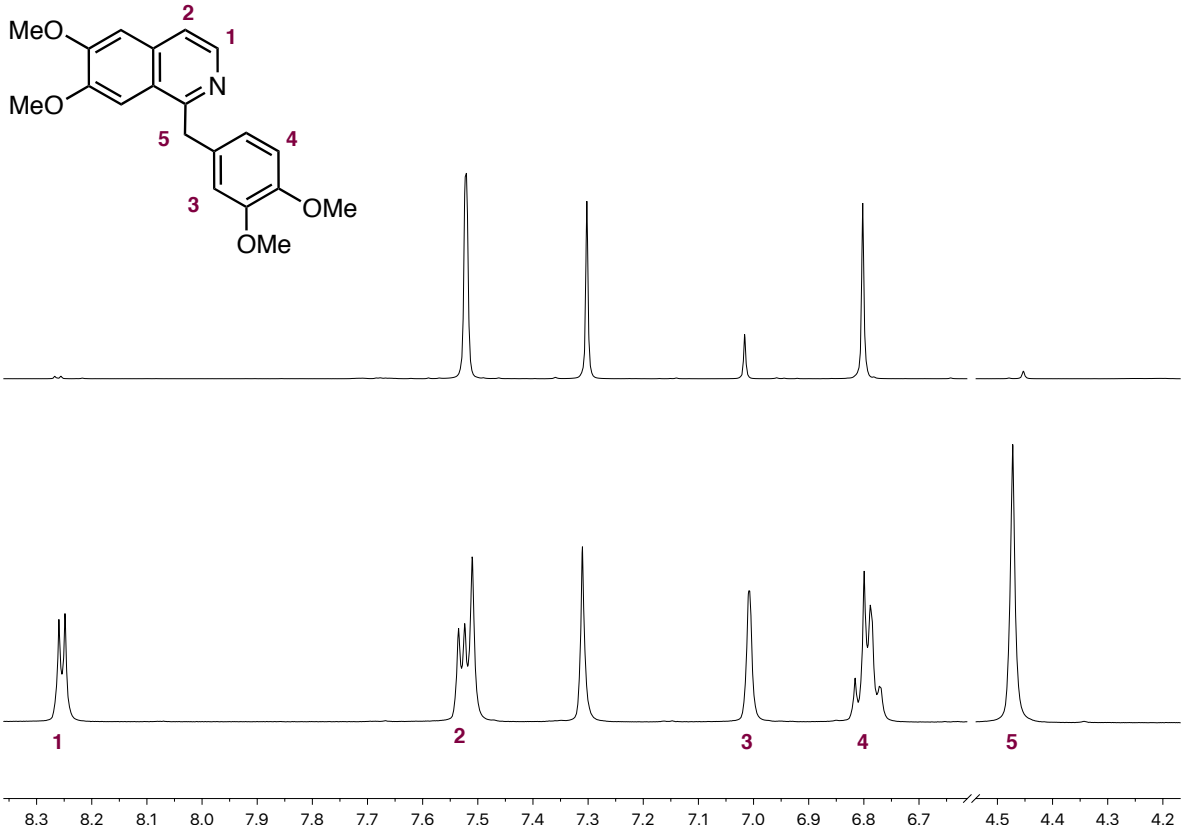

Figure S201. Stacked ^{1}H NMR spectra of papaverine (aromatic region): labeled with Method A, **[^{2}H]12f** (first) and unlabeled, **12f** (second).

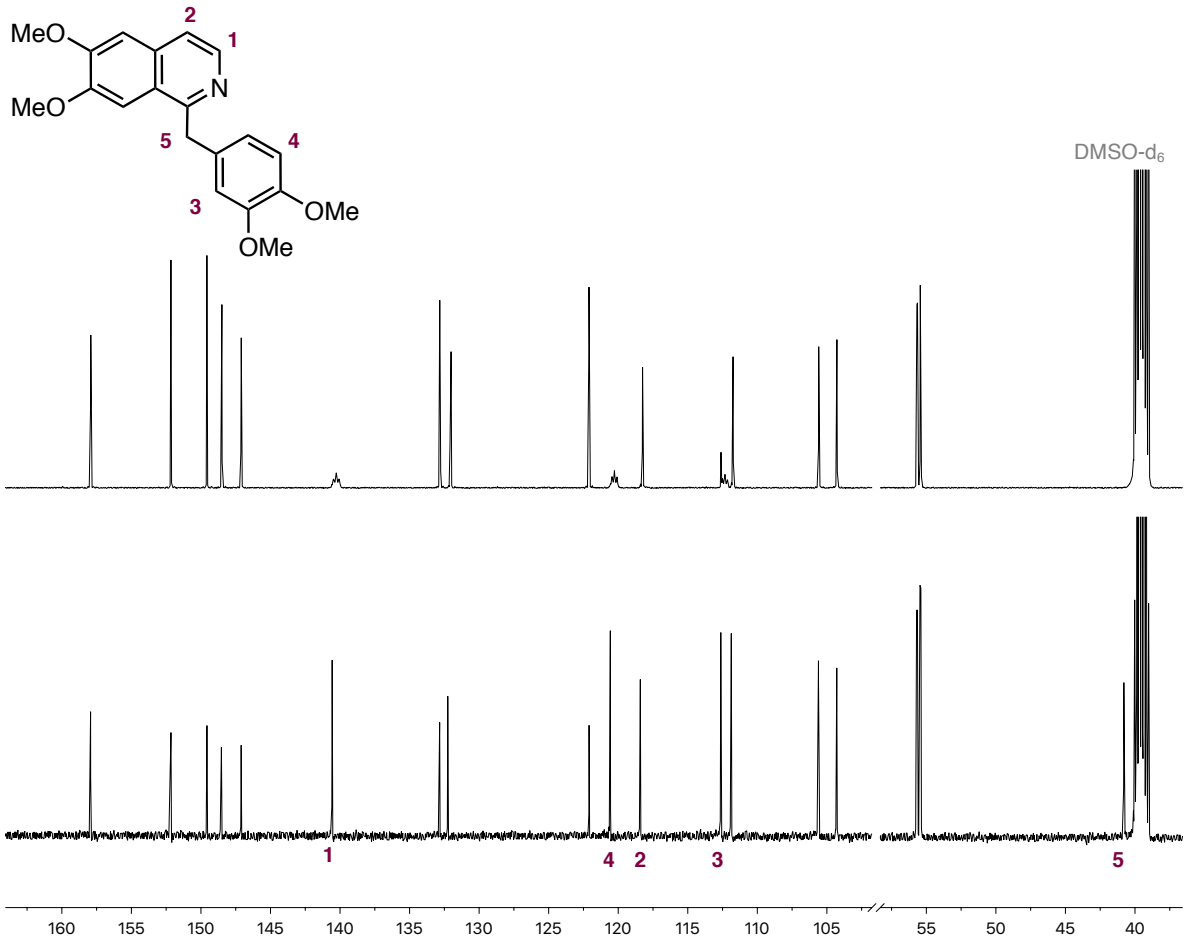

Figure S202. Stacked $^{13}C\{^{1}H\}$ NMR spectra of papaverine: labeled with Method A, **[^{2}H]12f** (first, quantitative) and unlabeled, **12f** (second).

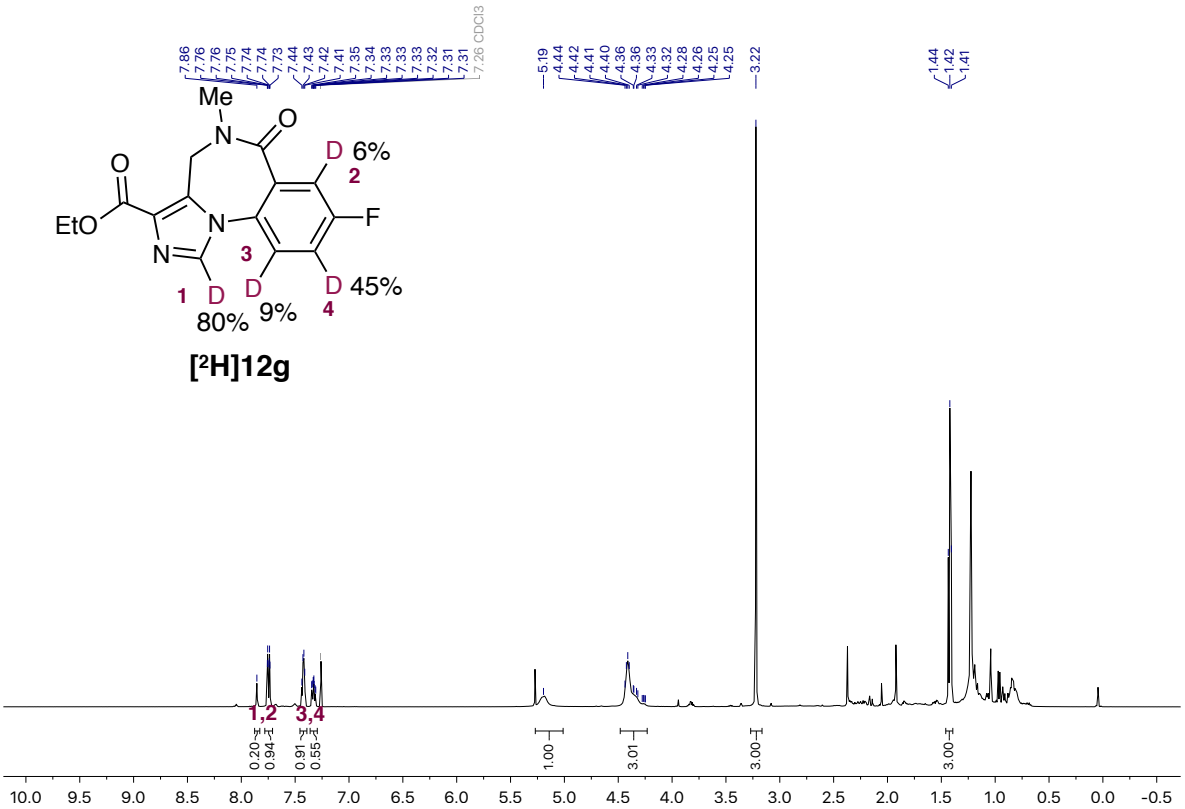

Figure S203. ^{1}H NMR (500 MHz, $CDCl_3$) of labeled flumazenil with Method A, **[^{2}H]12g**.

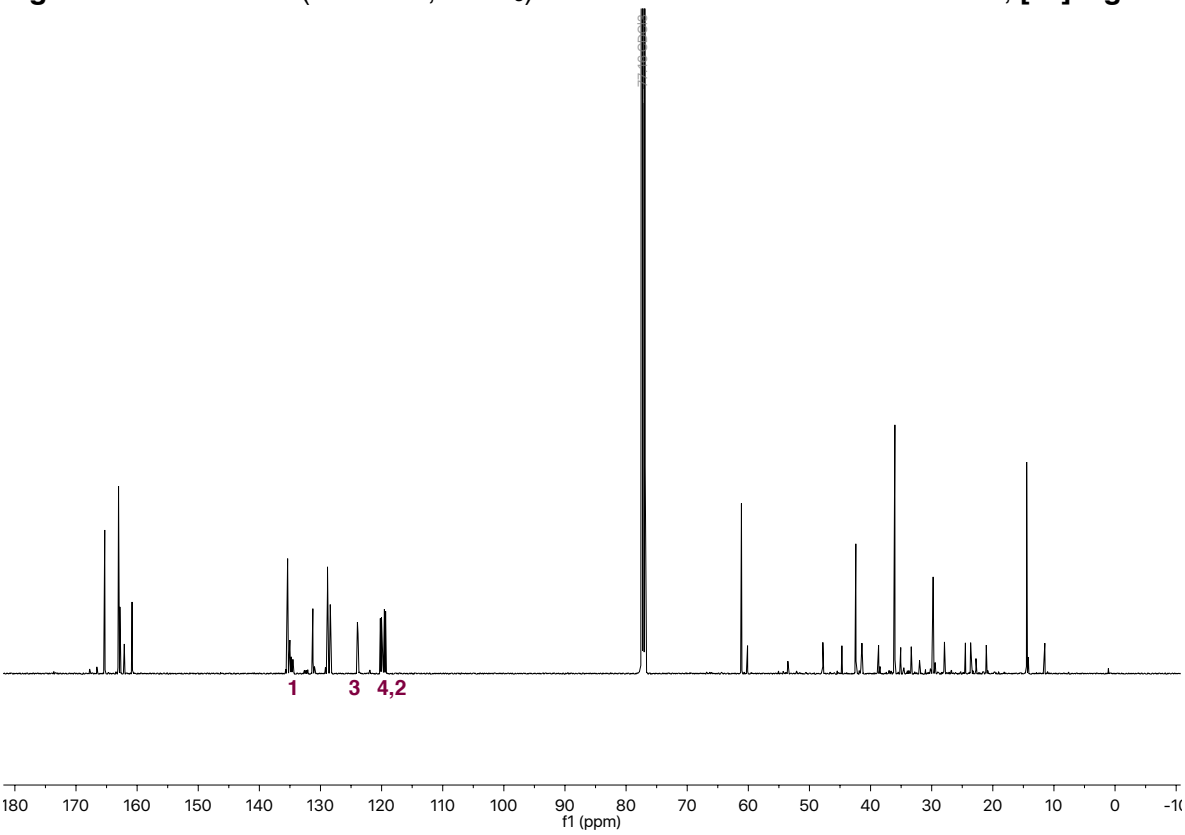

Figure S204. Quantitative ^{13}C{^{1}H} NMR (126 MHz, $CDCl_3$) of **[^{2}H]12g**.

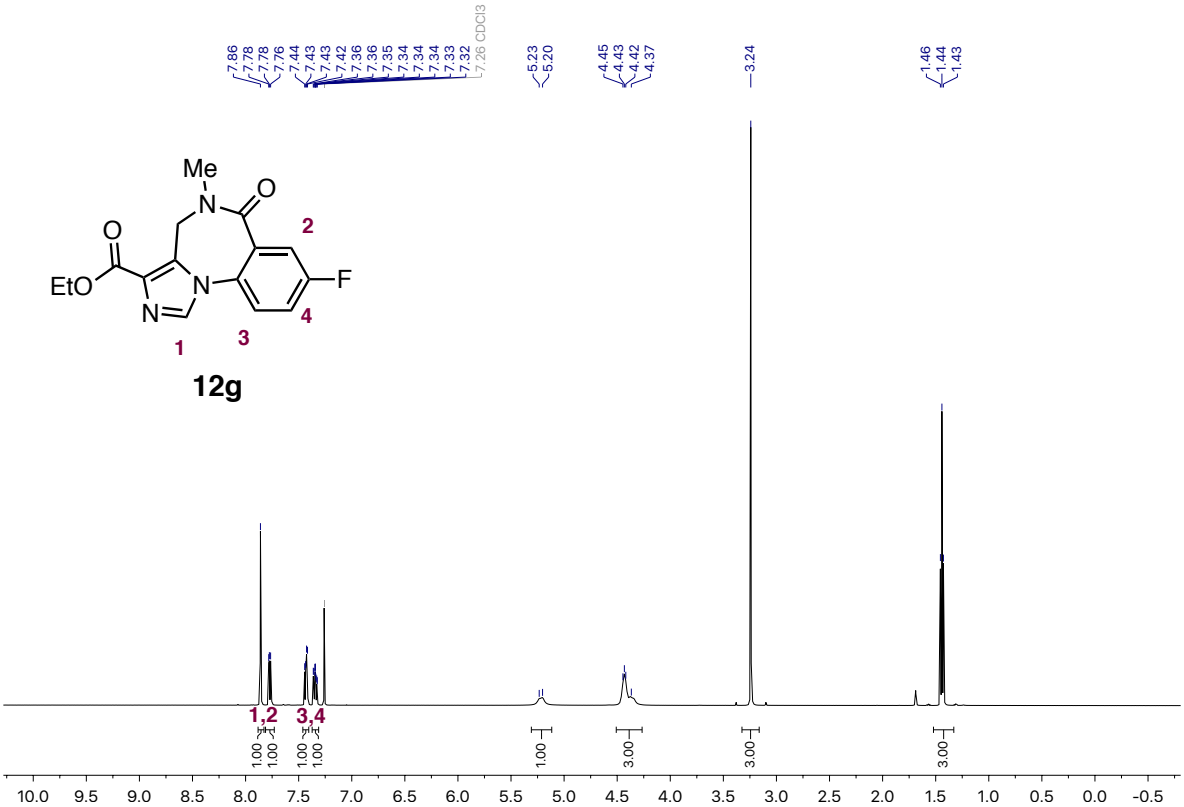

Figure S205. ^{1}H NMR (500 MHz, $CDCl_3$) of unlabeled flumazenil, **12g**.

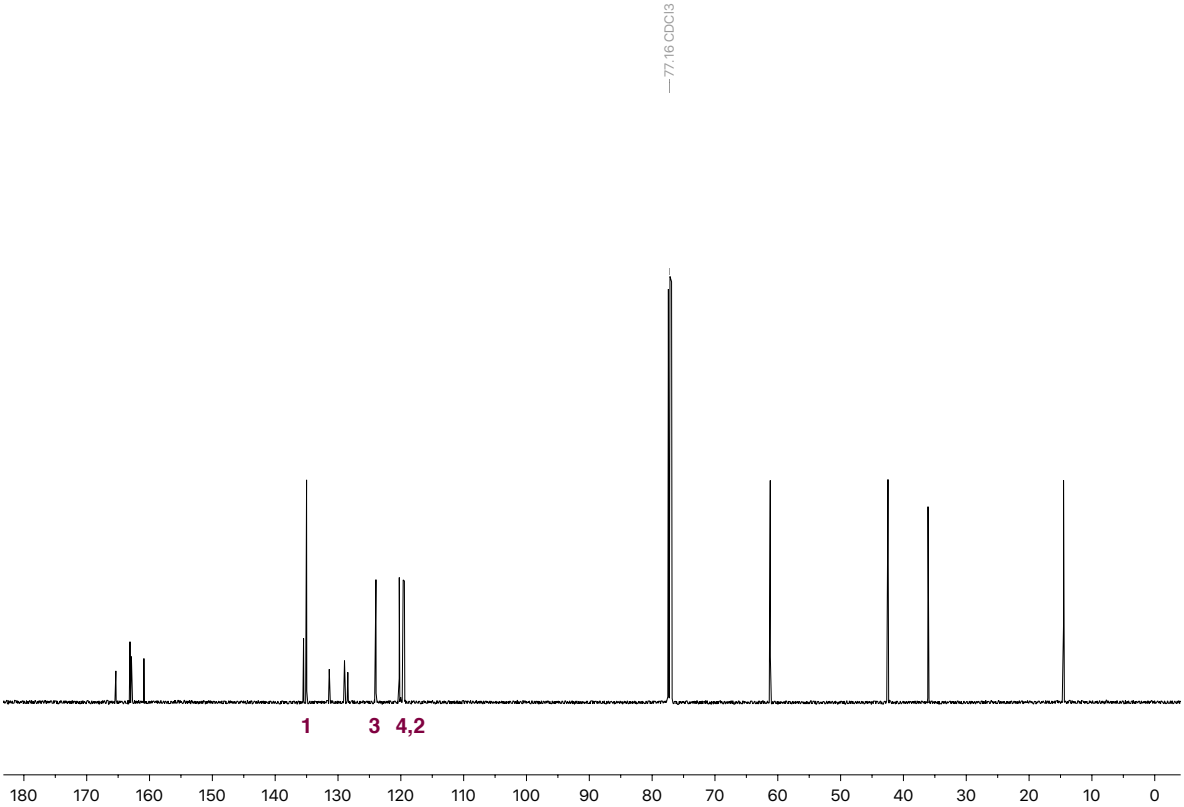

Figure S206. ^{13}C{^{1}H} NMR (126 MHz, $CDCl_3$) of **12g**.

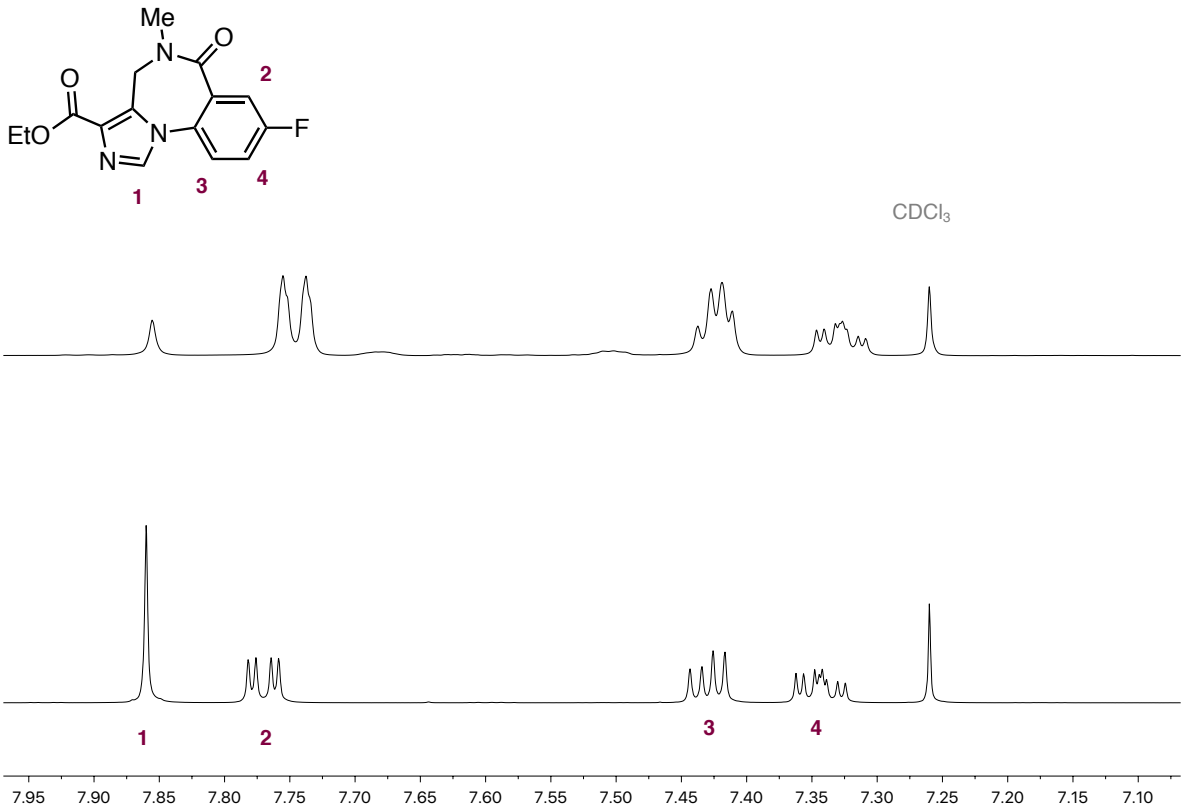

Figure S207. Stacked ^{1}H NMR spectra of flumazenil (aromatic region): labeled with Method A, **[^{2}H]12g** (first) and unlabeled, **12g** (second).

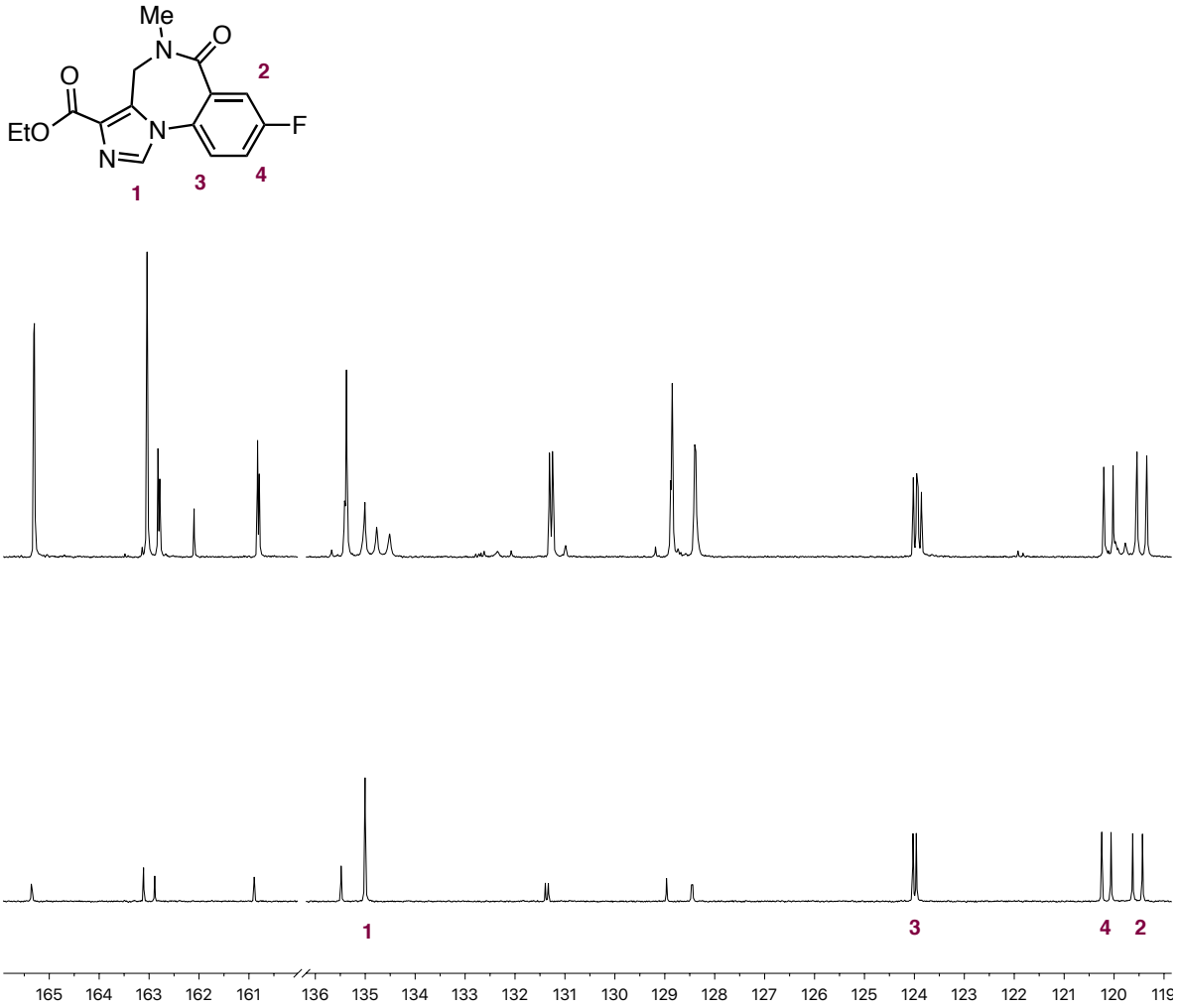

Figure S208. Stacked $^{13}C\{^{1}H\}$ NMR spectra of flumazenil (aromatic region): labeled with Method A, **[^{2}H]12g** (first, quantitative) and unlabeled, **12g** (second).

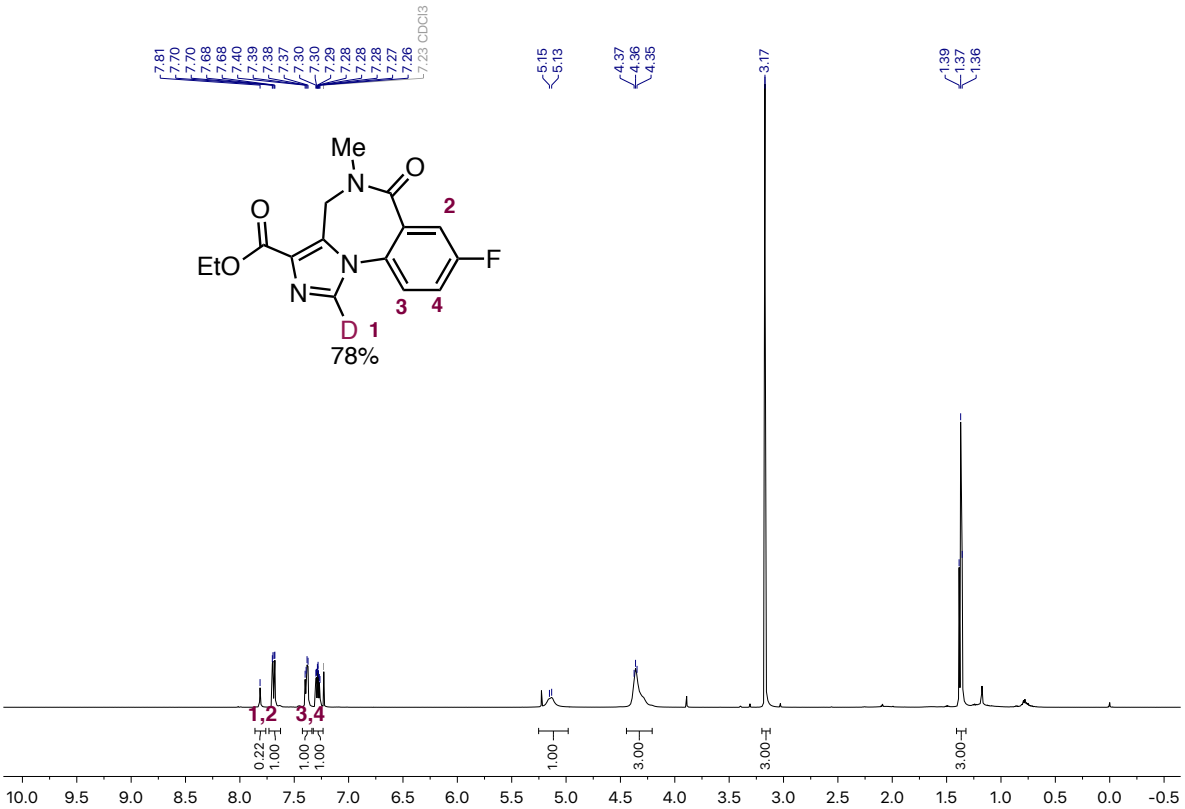

Figure S209. ^{1}H NMR (500 MHz, $CDCl_3$) of labeled flumazenil with $[(^{iPr}DI)Ni(\mu_2\text{-}H)]_2$.

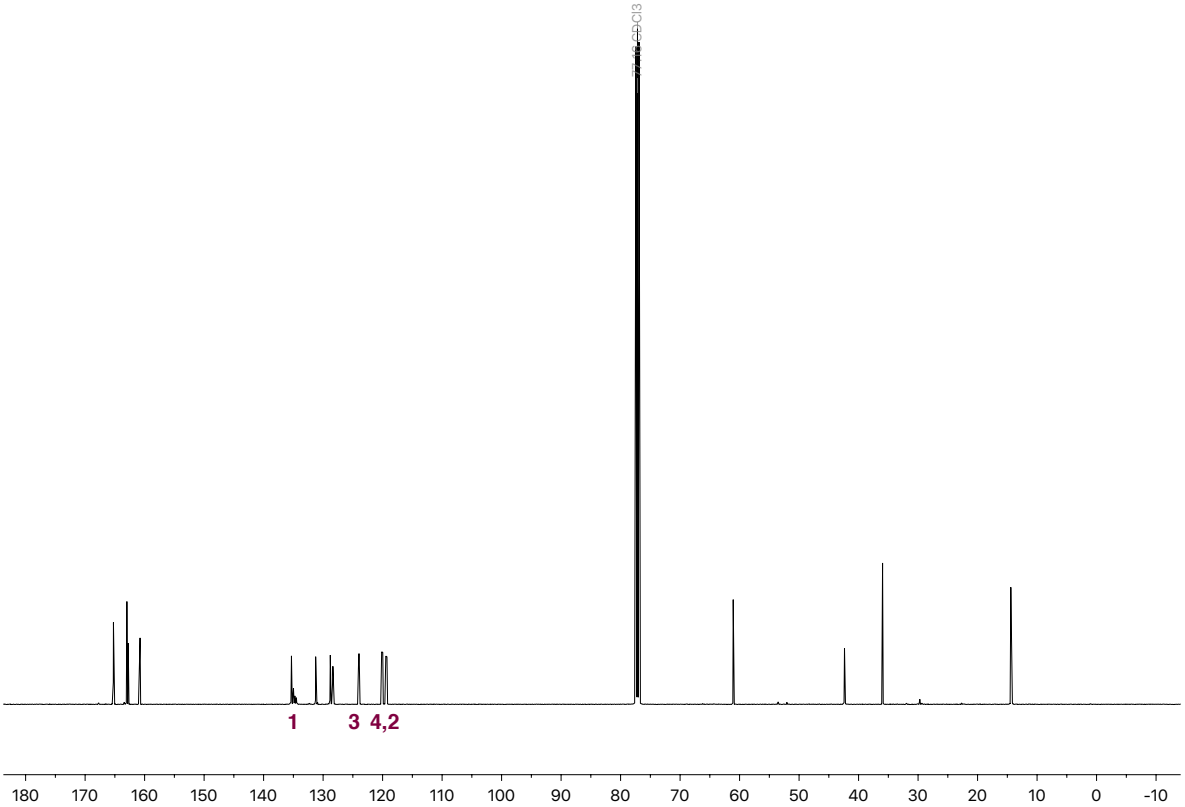

Figure S210. Quantitative $^{13}C\{^{1}H\}$ NMR (126 MHz, $CDCl_3$) of labeled flumazenil with $[(^{iPr}DI)Ni(\mu_2\text{-}H)]_2$.

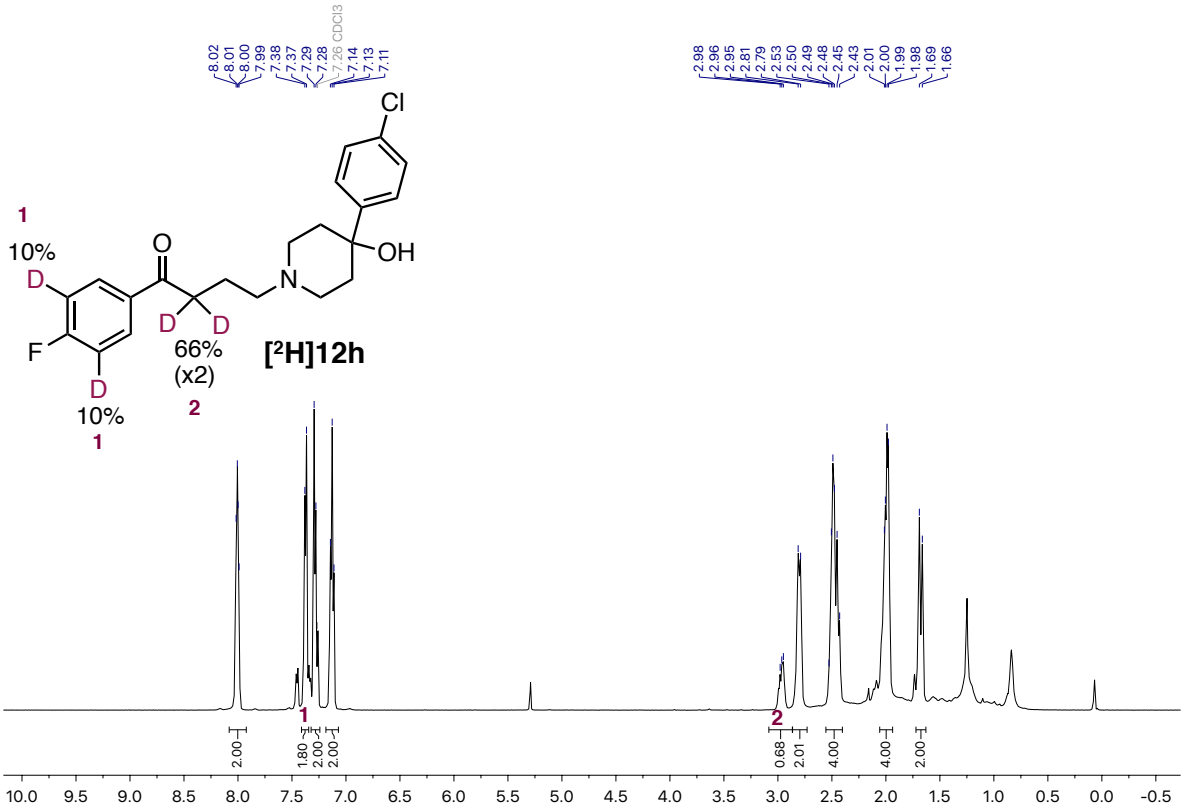

Figure S211. ^{1}H NMR (500 MHz, $CDCl_3$) of labeled haloperidol with Method A, **[^{2}H]12h**.

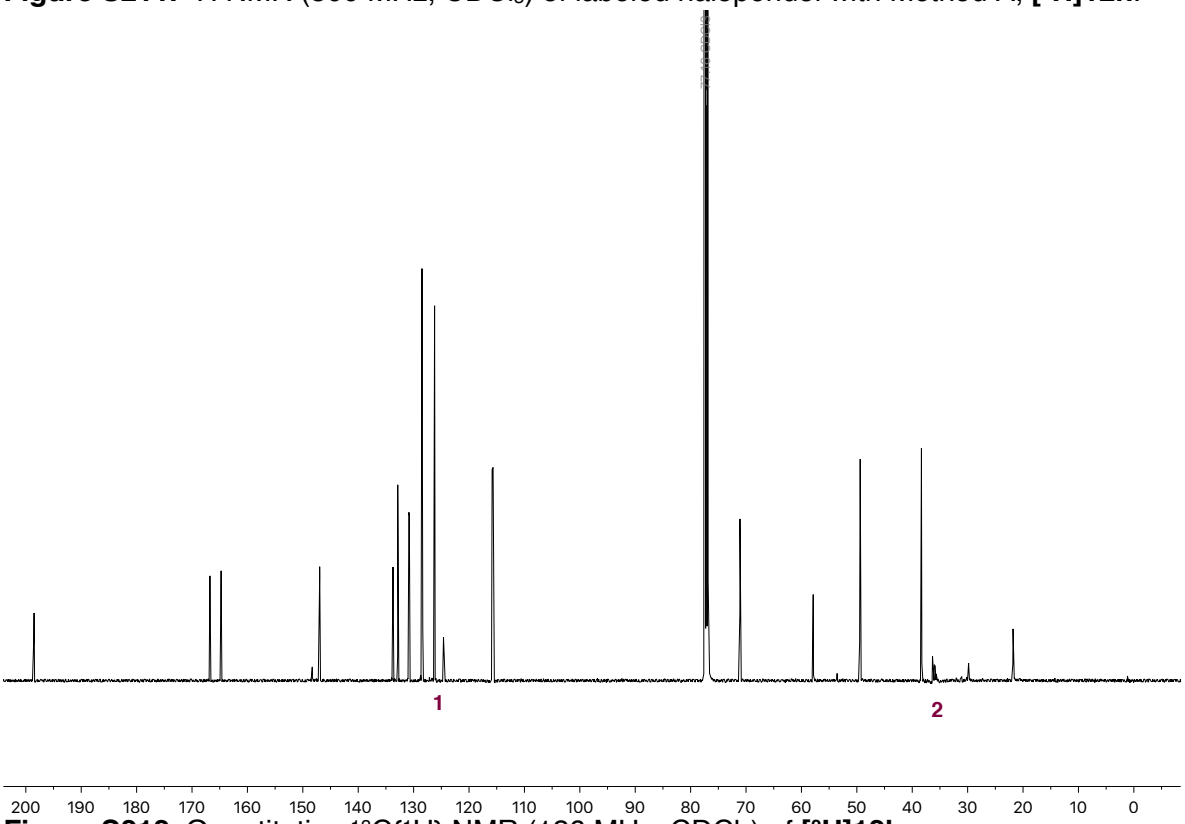

Figure S212. Quantitative ^{13}C{^{1}H} NMR (126 MHz, $CDCl_3$) of **[^{2}H]12h**.

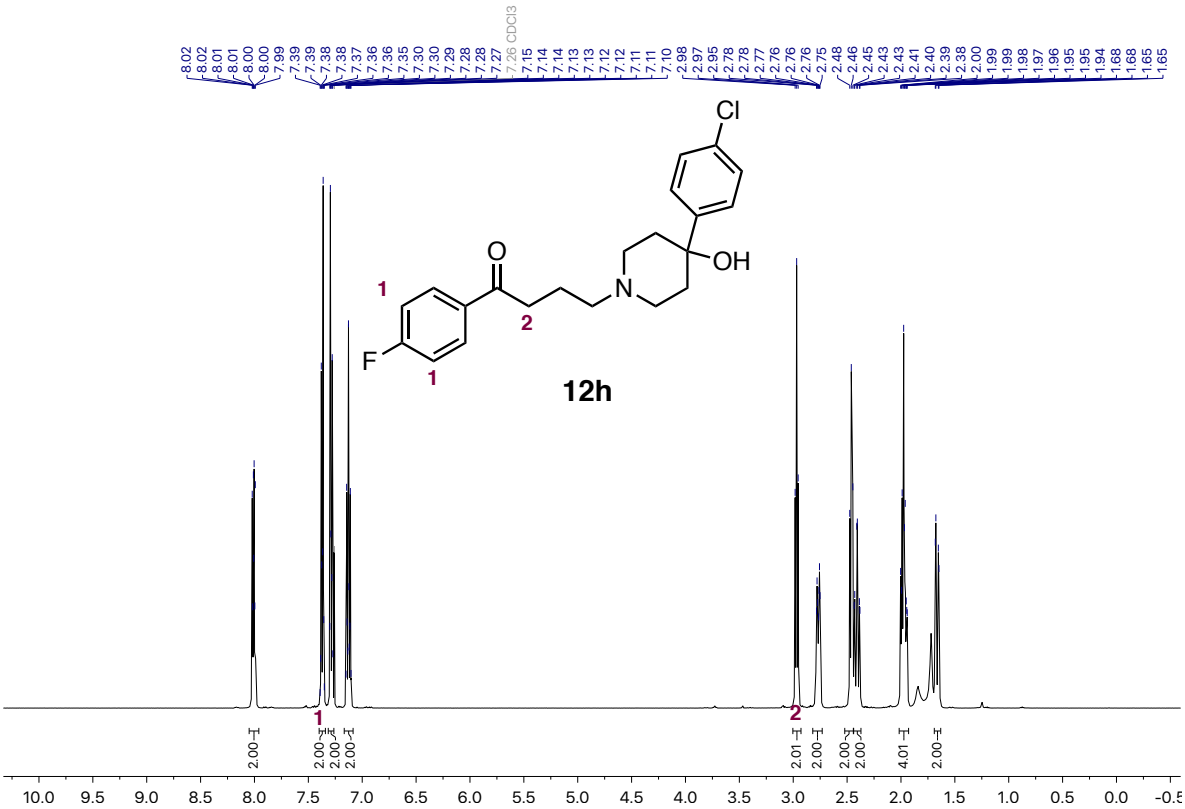

Figure S213. ^{1}H NMR (500 MHz, $CDCl_3$) of unlabeled haloperidol, **12h**.

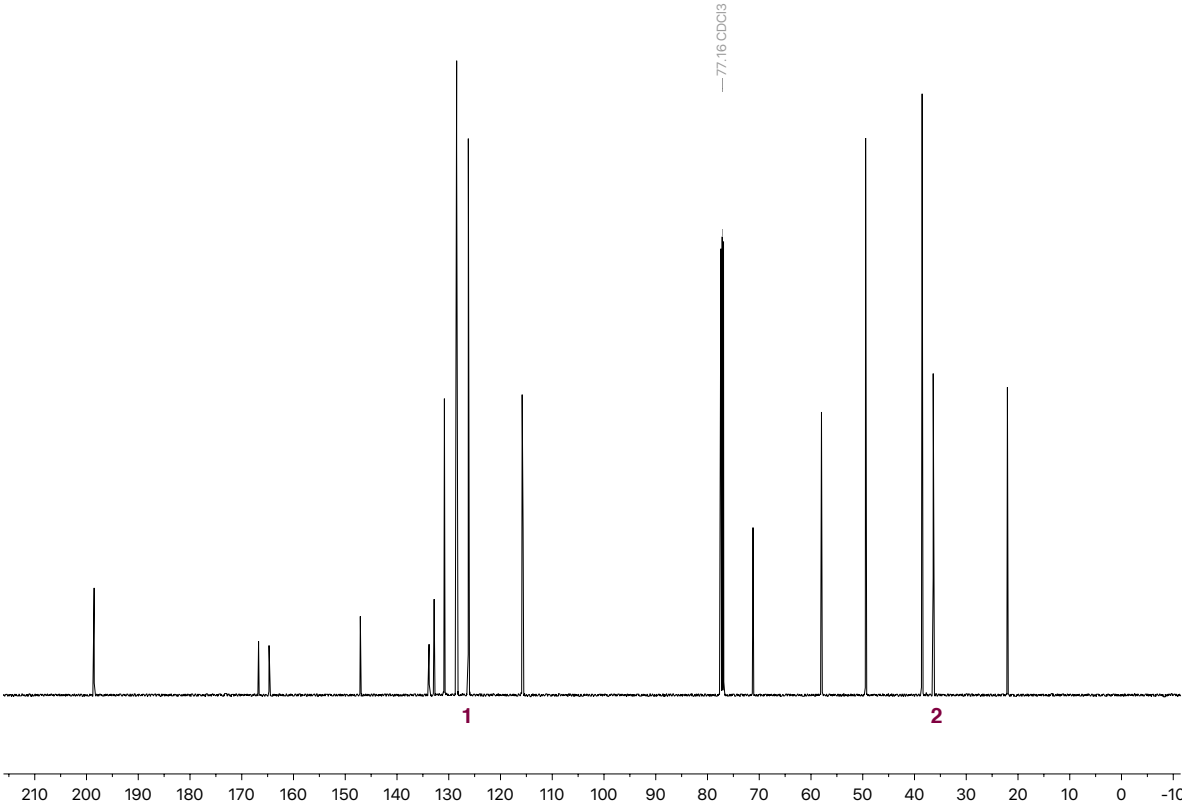

Figure S214. ^{13}C{^{1}H} NMR (126 MHz, $CDCl_3$) of **12h**.

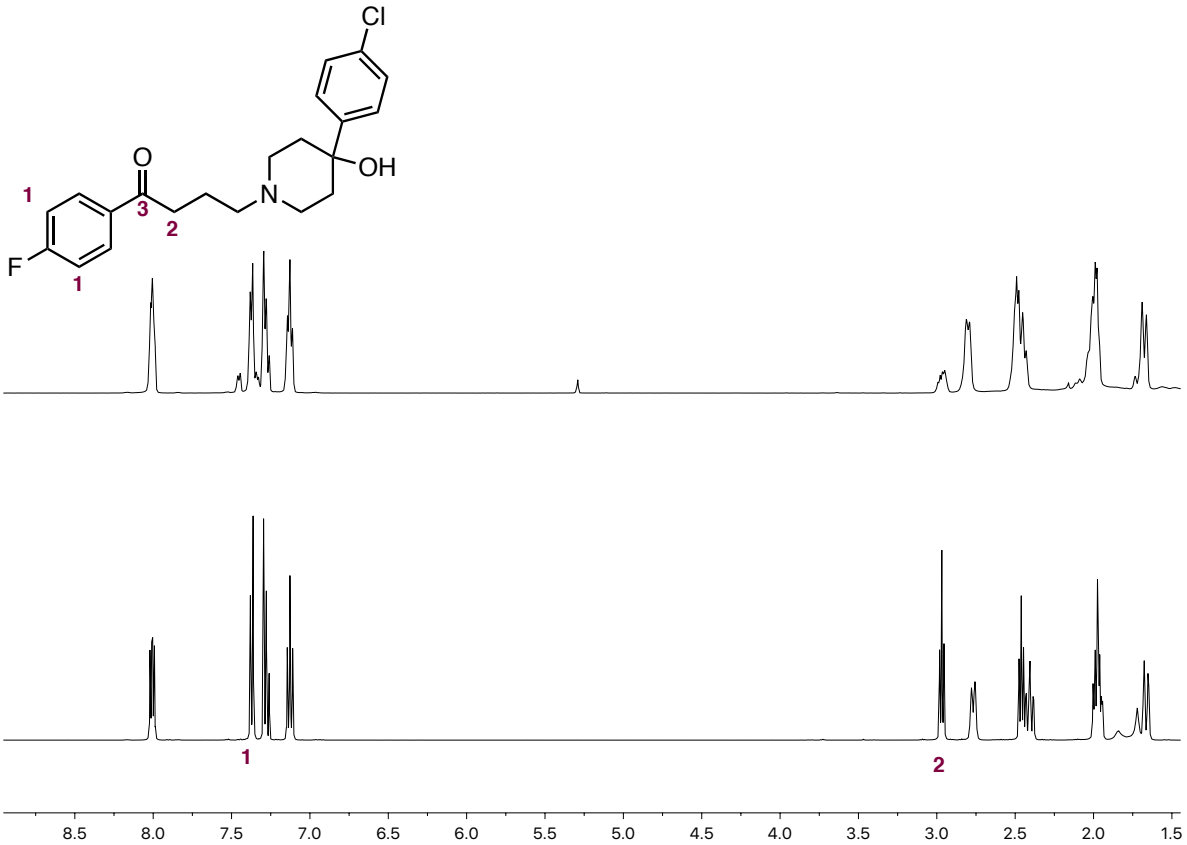

Figure S215. Stacked ^{1}H NMR spectra of haloperidol: labeled with Method A, **[^{2}H]12h** (first) and unlabeled, **12h** (second).

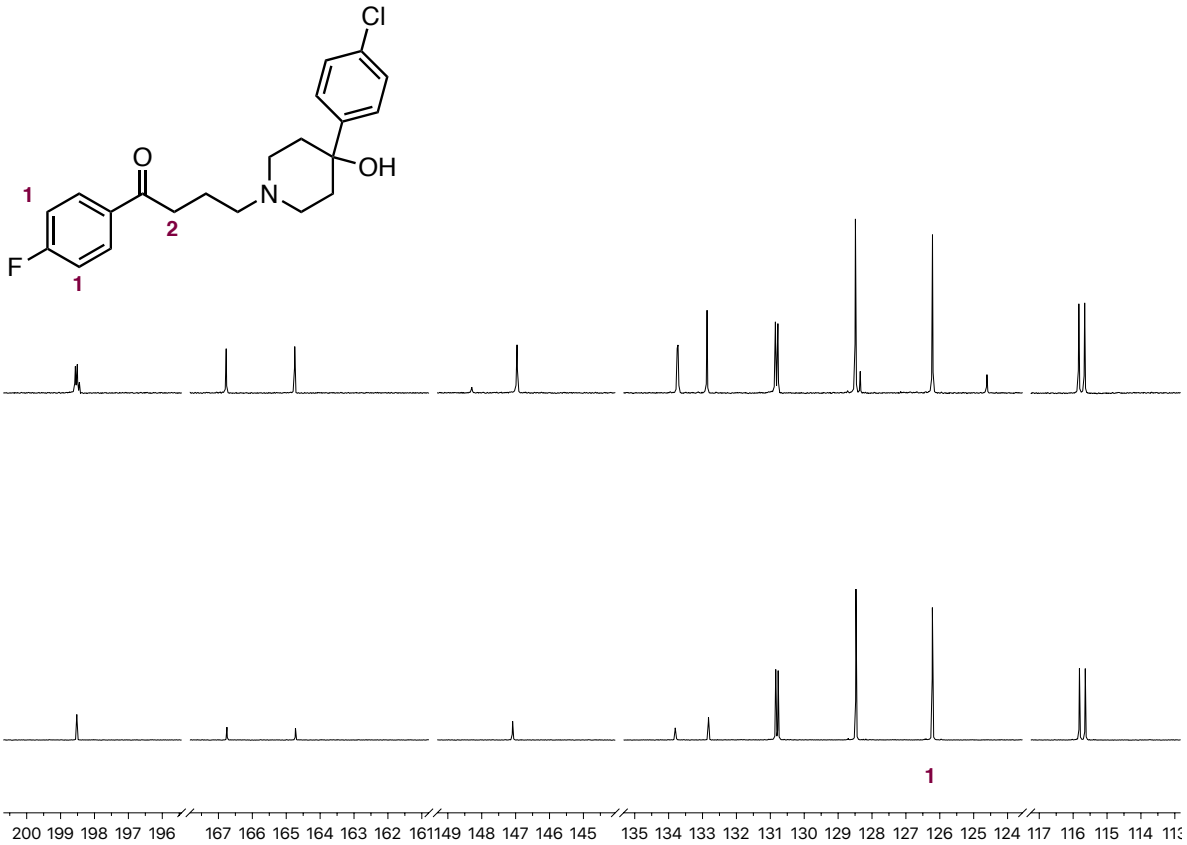

Figure S216. Stacked $^{13}C\{^{1}H\}$ NMR spectra of haloperidol (aromatic region): labeled with Method A, **[^{2}H]12h** (first, quantitative) and unlabeled, **12h** (second).

Figure S217. Stacked $^{13}C\{^{1}H\}$ NMR spectra of haloperidol (aliphatic region): labeled with Method A, **[^{2}H]12h** (first, quantitative) and unlabeled, **12h** (second).

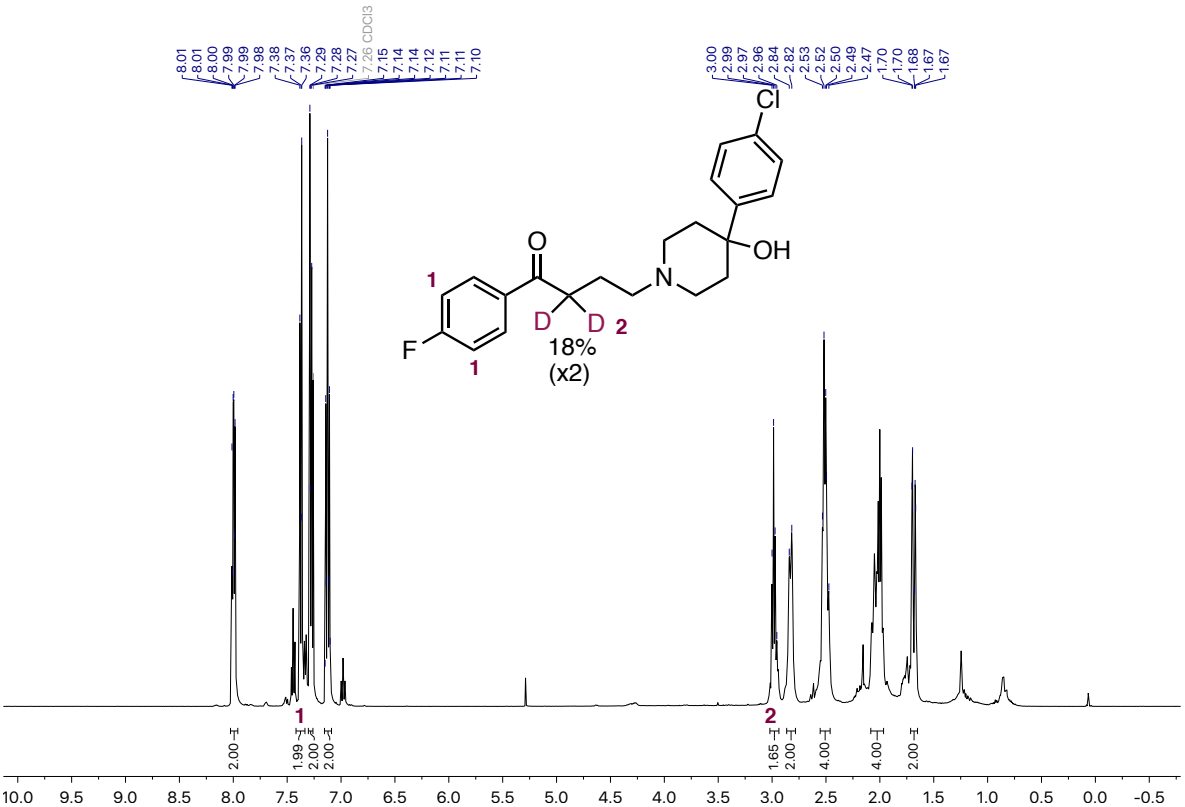

Figure S218. ^{1}H NMR (500 MHz, $CDCl_3$) of labeled haloperidol with $[(^{iPr}DI)Ni(\mu_2\text{-}H)]_2$.

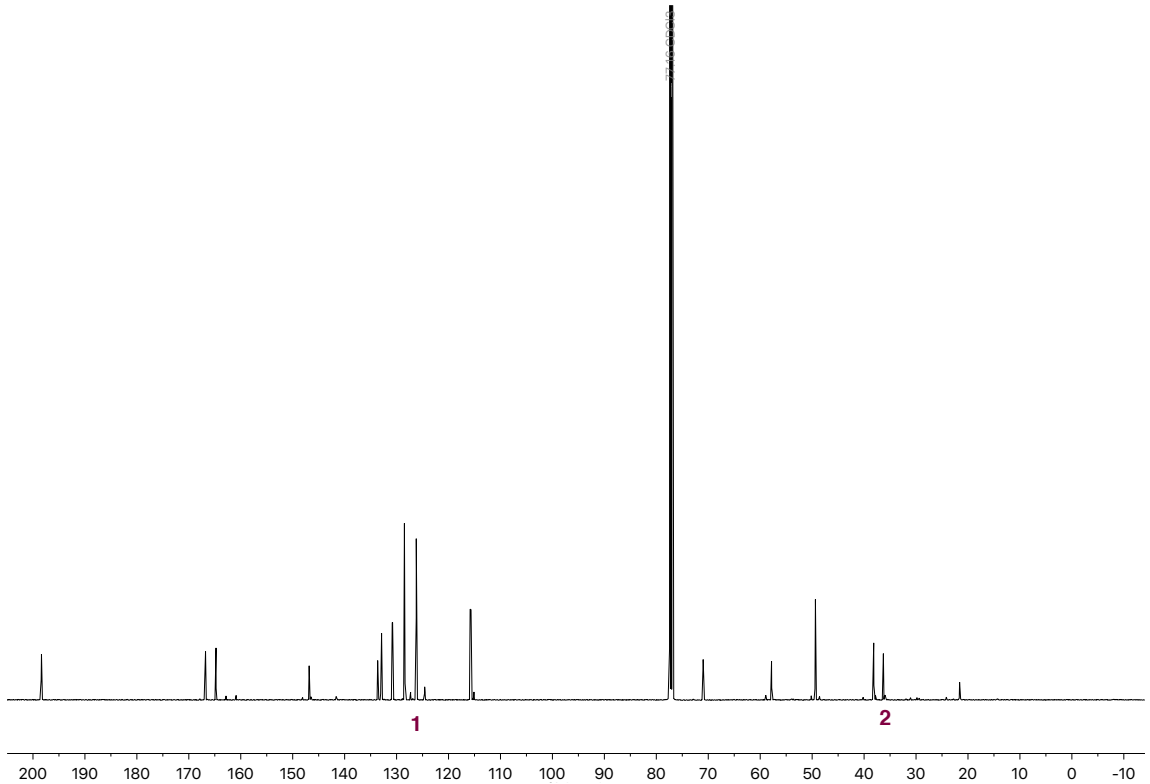

Figure S219. Quantitative $^{13}C\{^{1}H\}$ NMR (126 MHz, $CDCl_3$) of labeled haloperidol with $[(^{iPr}DI)Ni(\mu_2\text{-}H)]_2$.

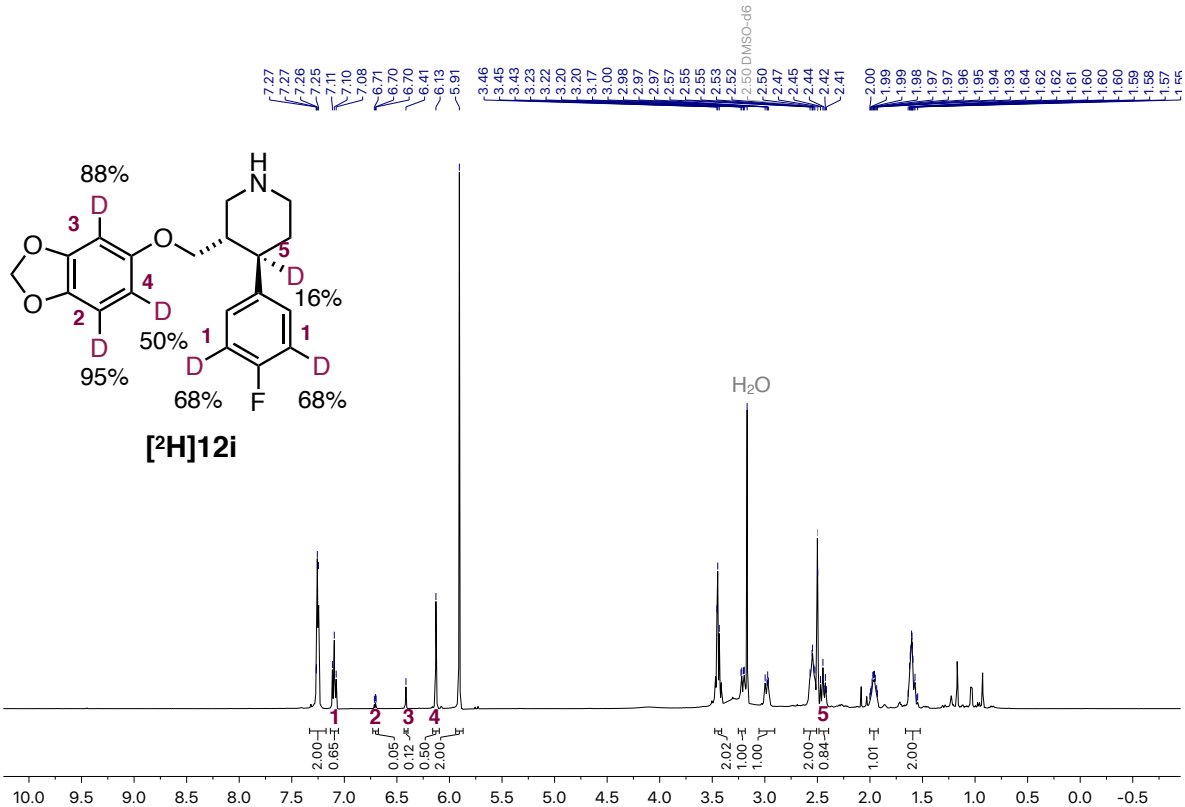

Figure S220. ^{1}H NMR (500 MHz, DMSO-d_6) of labeled paroxetine with Method A, **[^{2}H]12i**.

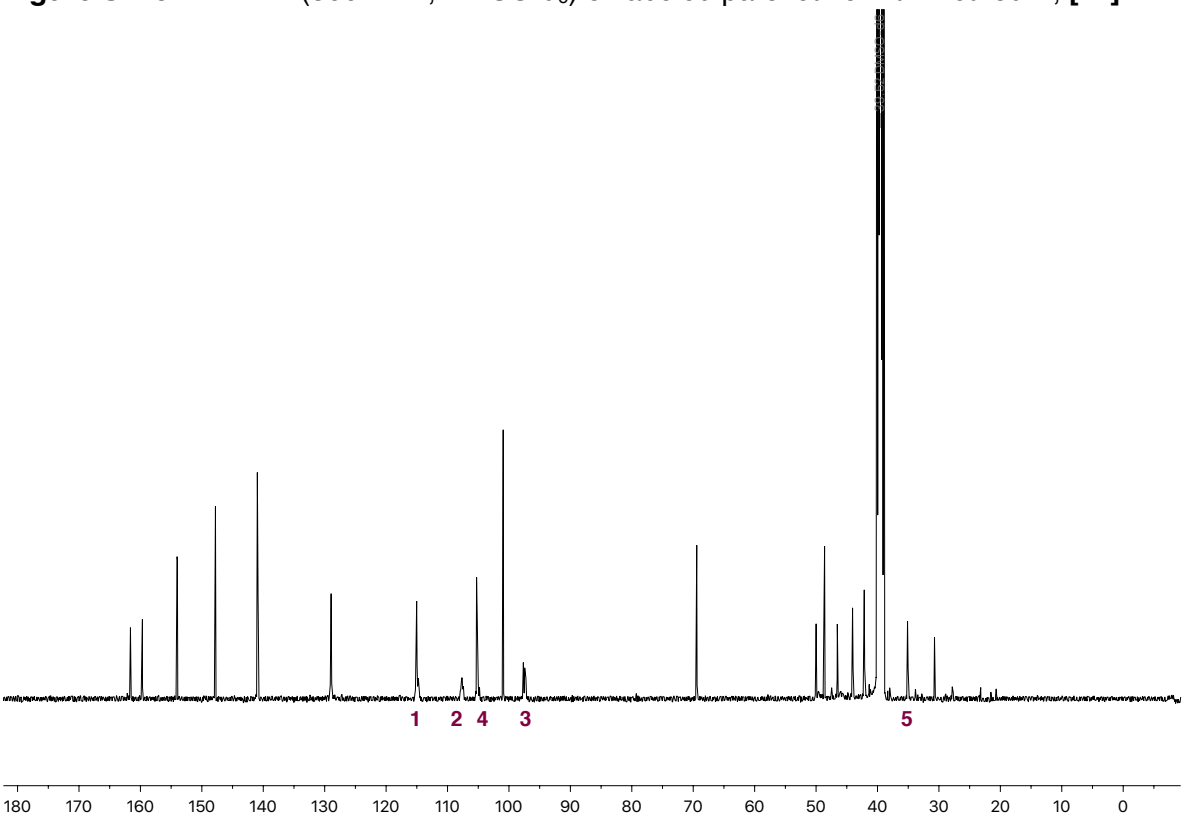

Figure S221. Quantitative ^{13}C{^{1}H} NMR (126 MHz, DMSO-d_6) of **[^{2}H]12i**.

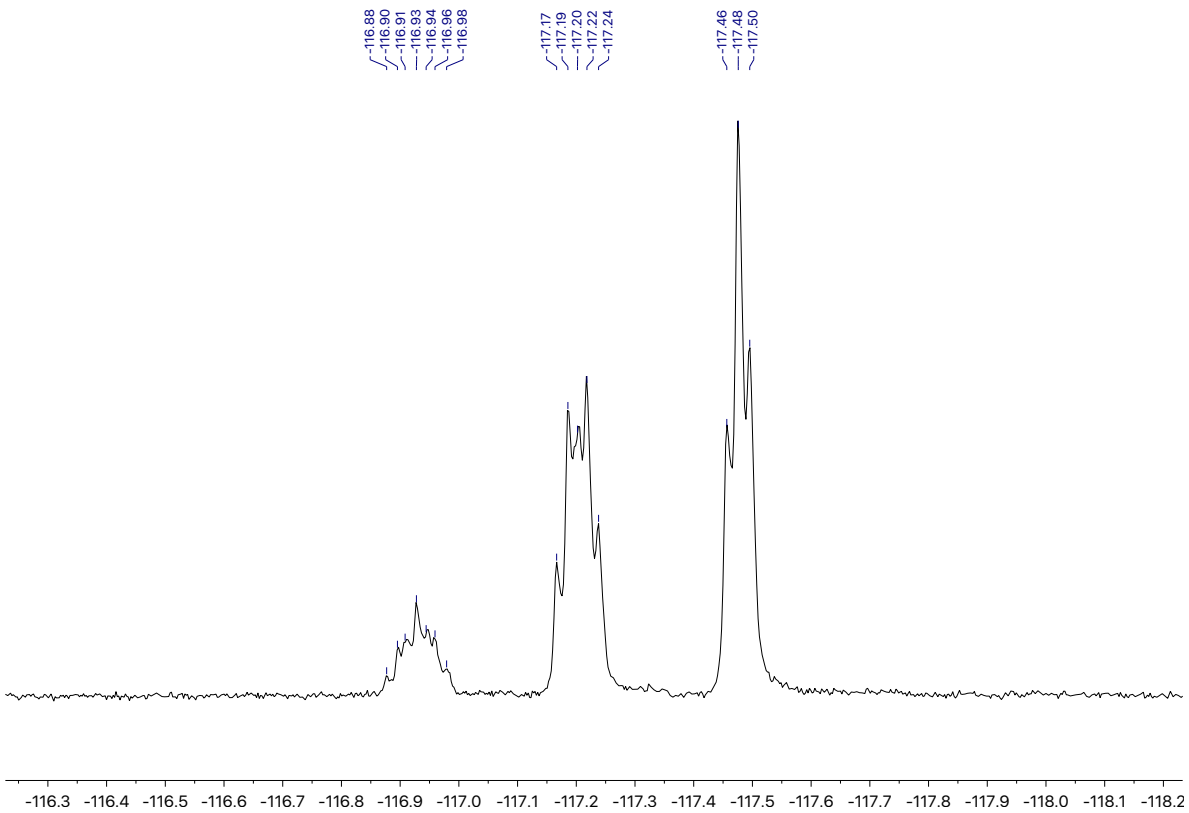

Figure S222. ^{19}F NMR (282 MHz, DMSO-d_6) of **[^{2}H]12i**.

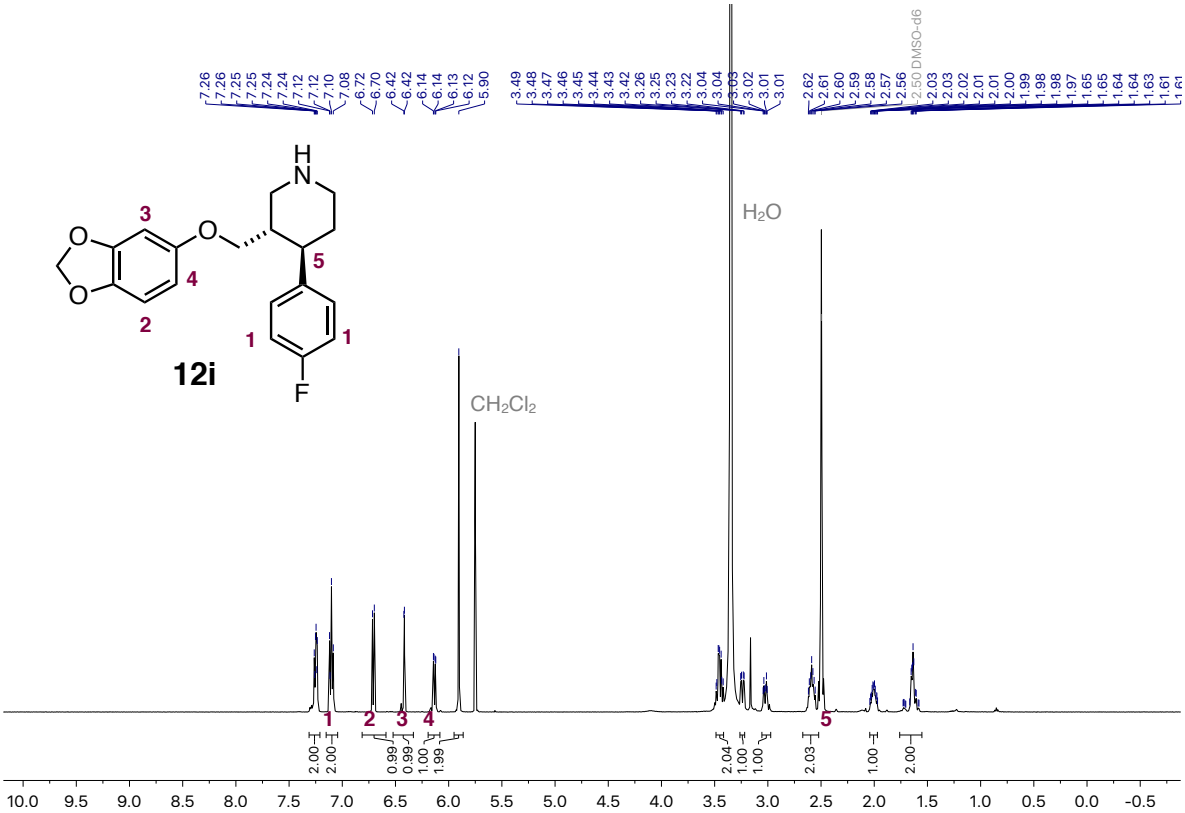

Figure S223. ^{1}H NMR (500 MHz, DMSO-d_6) of unlabeled paroxetine, **12i**.

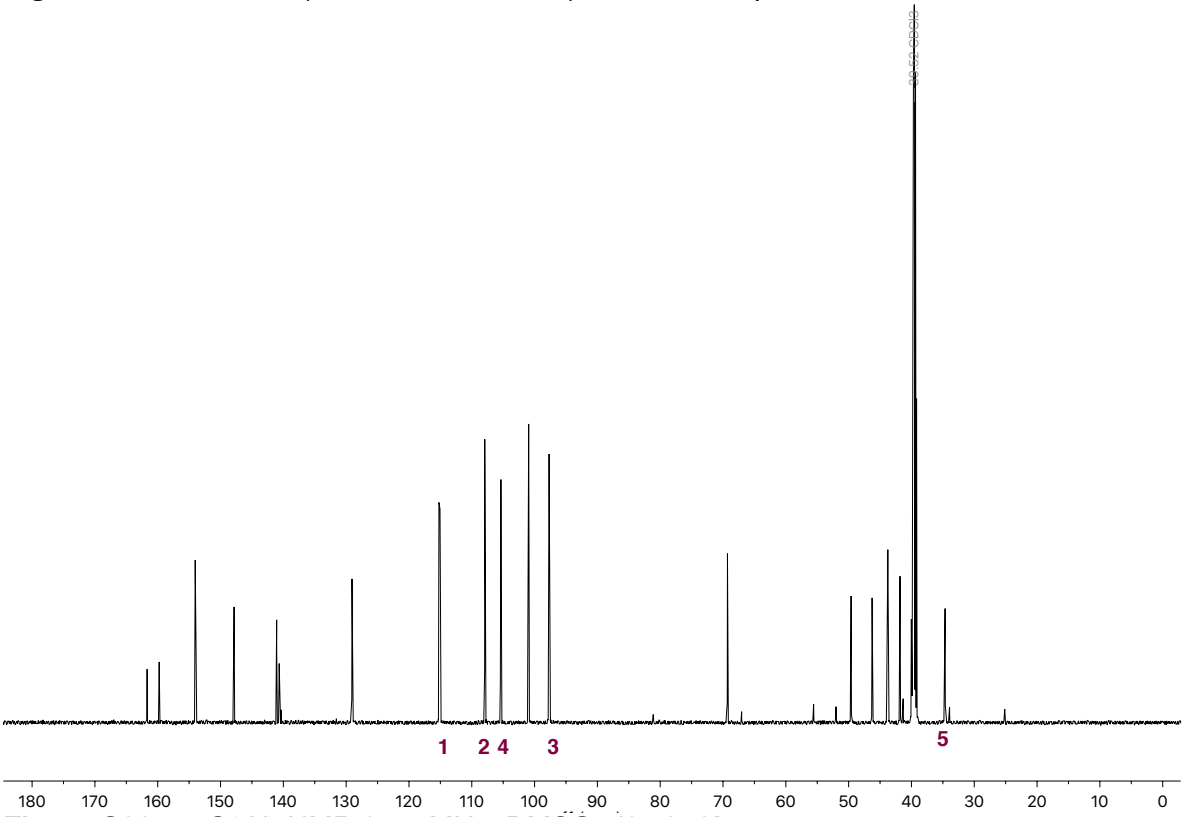

Figure S224. ^{13}C{^{1}H} NMR (126 MHz, DMSO-d_6) of **12i**.

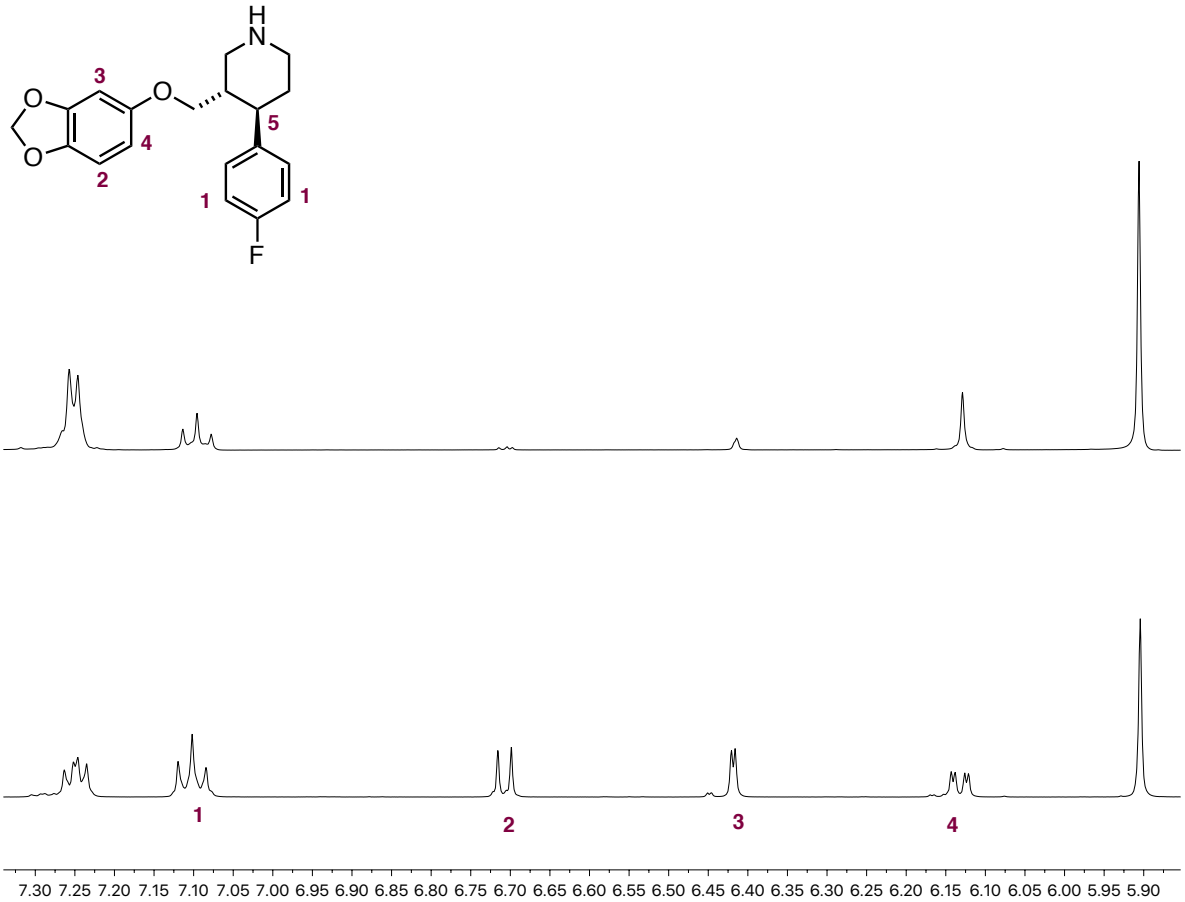

Figure S225. Stacked ^{1}H NMR spectra of paroxetine (aromatic region): labeled with Method A, **[^{2}H]12i** (first) and unlabeled, **12i** (second).

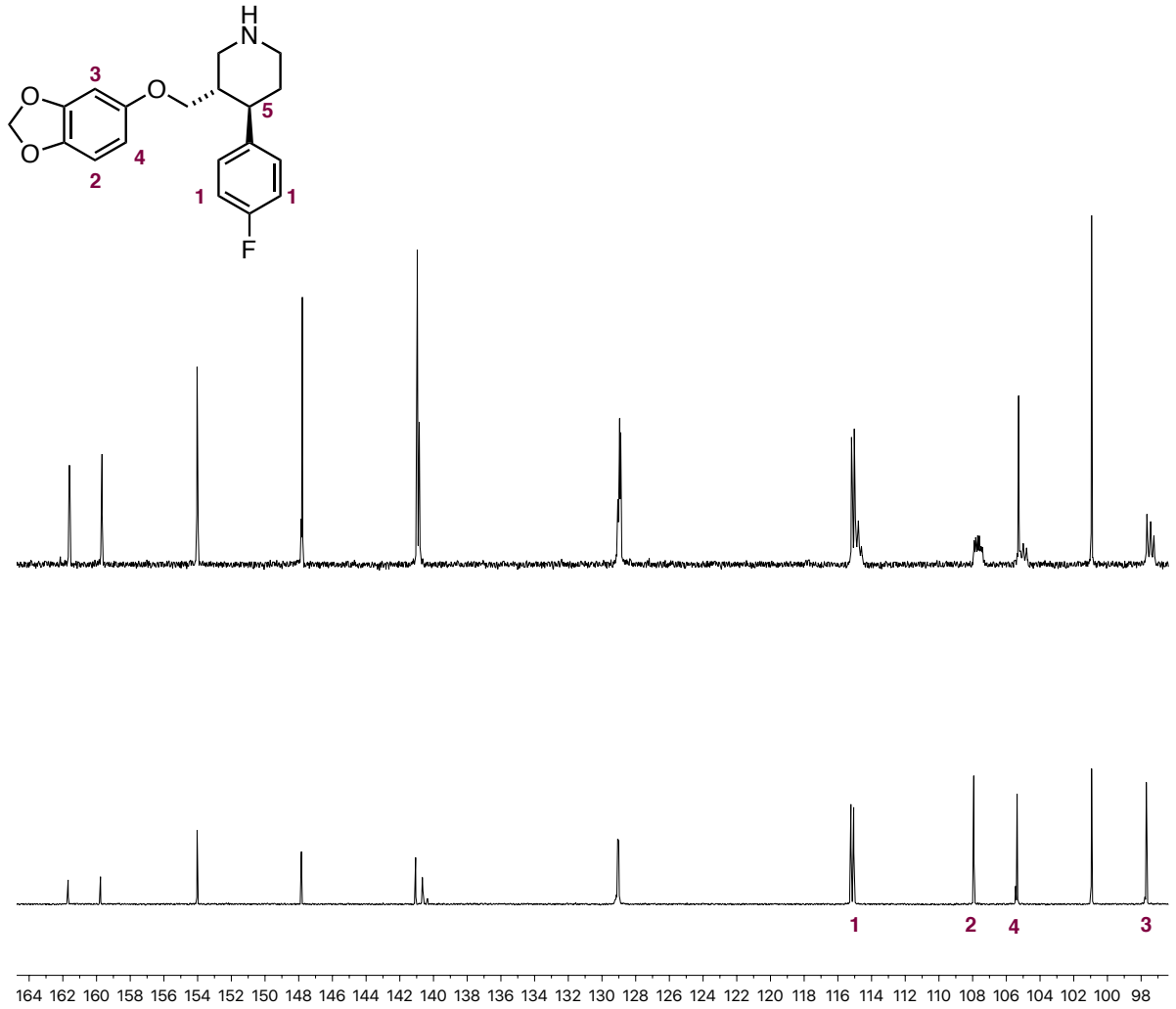

Figure S226. Stacked $^{13}C\{^{1}H\}$ NMR spectra of paroxetine (aromatic region): labeled with Method A, **[^{2}H]12i** (first, quantitative) and unlabeled, **12i** (second).

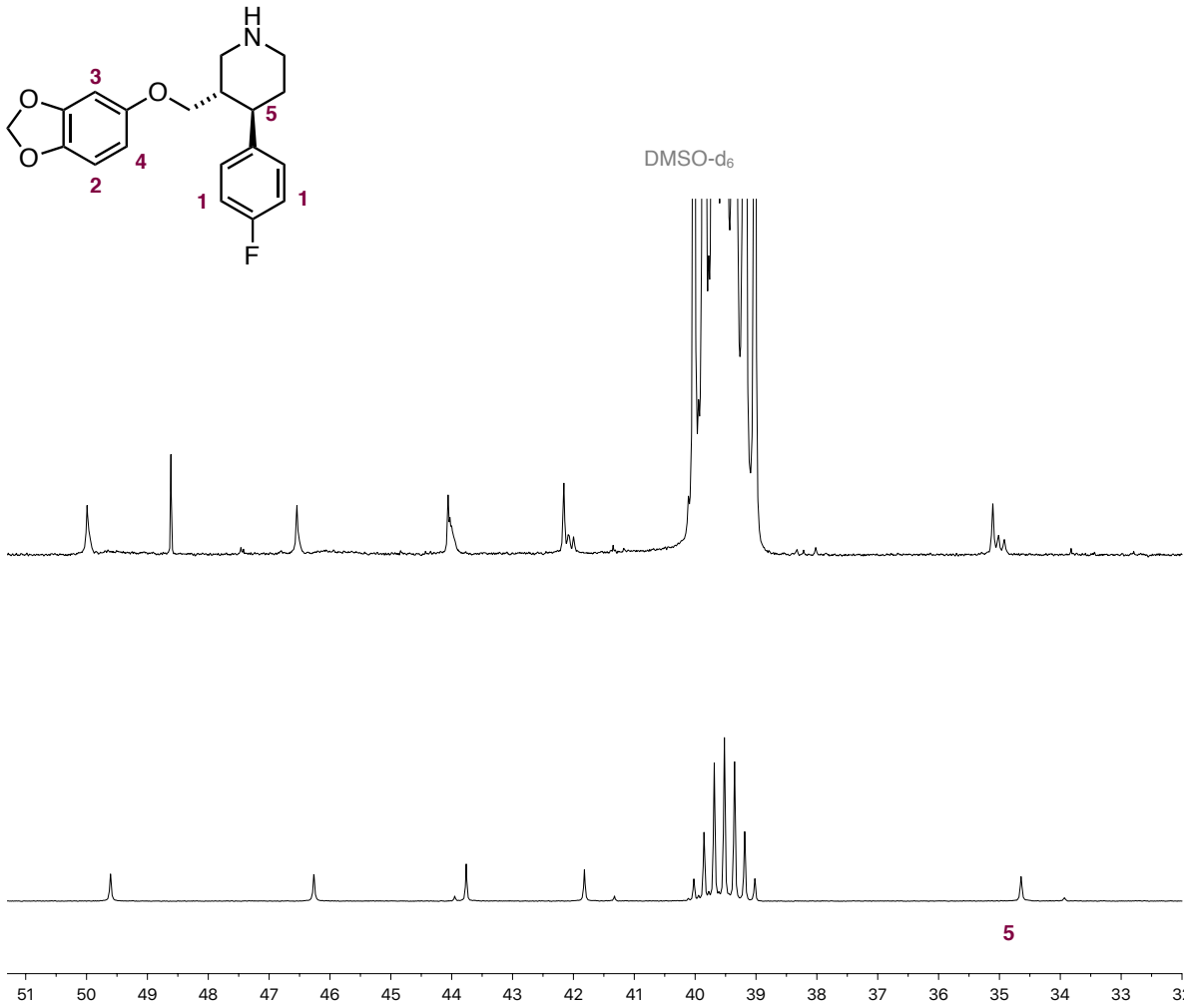

Figure S227. Stacked $^{13}C\{^{1}H\}$ NMR spectra of paroxetine (aliphatic region): labeled with Method A, **[^{2}H]12i** (first, quantitative) and unlabeled, **12i** (second).

XVI.C. NMR Spectra of Tritium Labeled Compounds

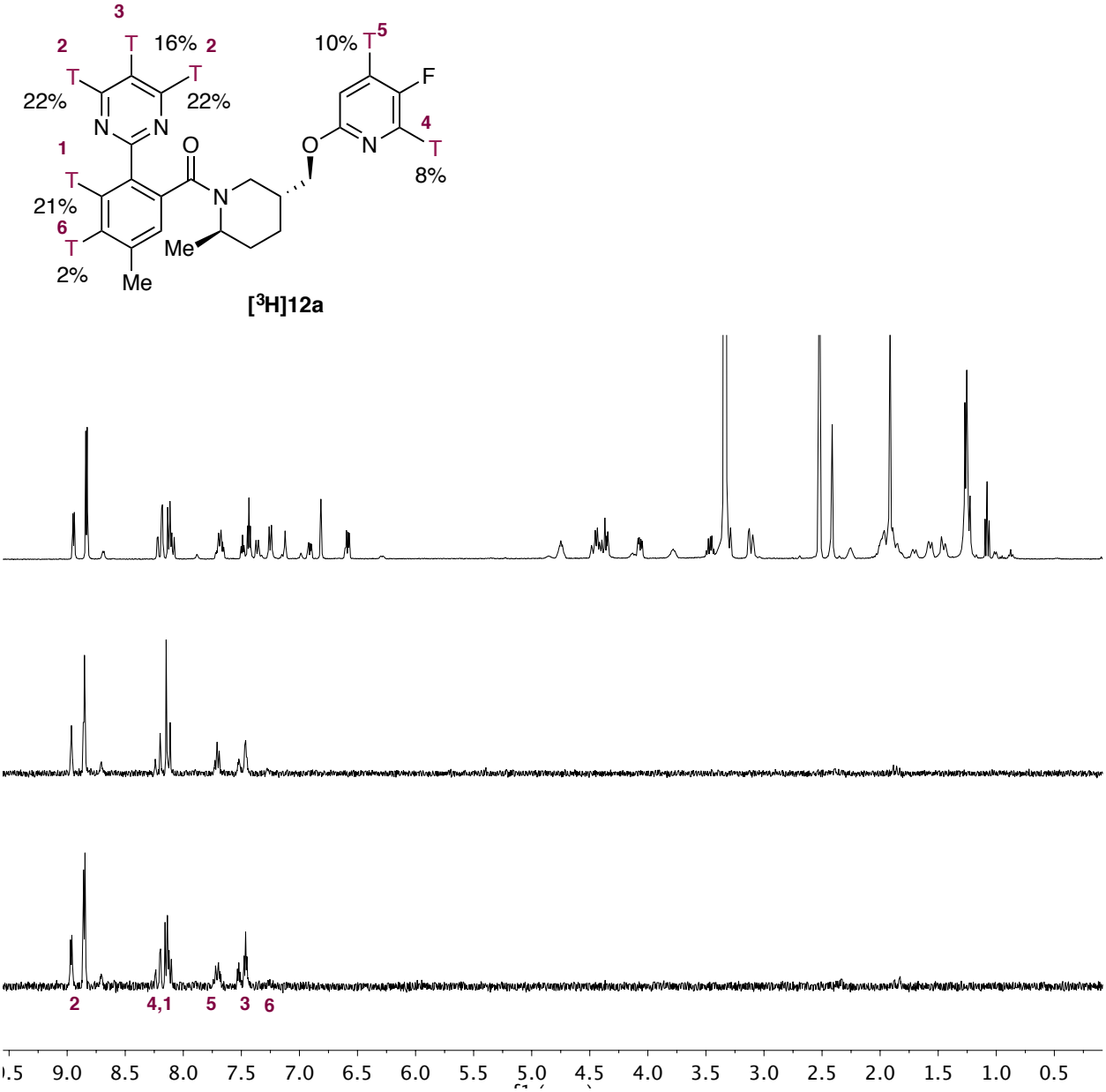

Figure S228. Stacked NMR spectra (DMSO-d_6) of labeled MK-6096, **[^{13}H]12a**, mixed with unlabeled MK-6096, **12a**: ^{1}H NMR (first), ^{3}H{^{1}H} NMR (second) and ^{3}H NMR (third).

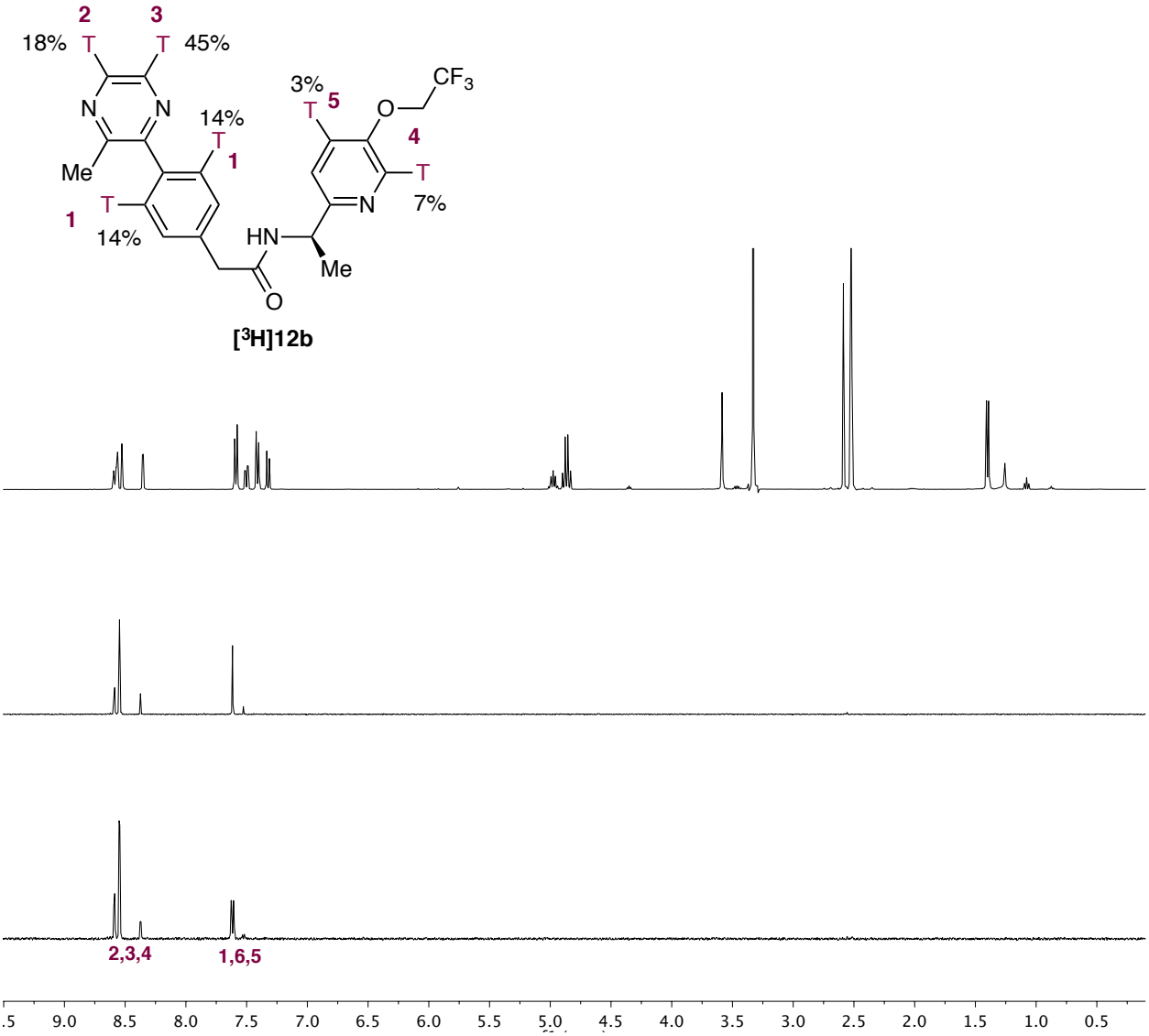

Figure S229. Stacked NMR spectra (DMSO-d_6) of labeled MK-5395, **[^{13}H]12b**, mixed with unlabeled MK-5395, **12b**: ^{1}H NMR (first), ^{3}H{^{1}H} NMR (second) and ^{3}H NMR (third).

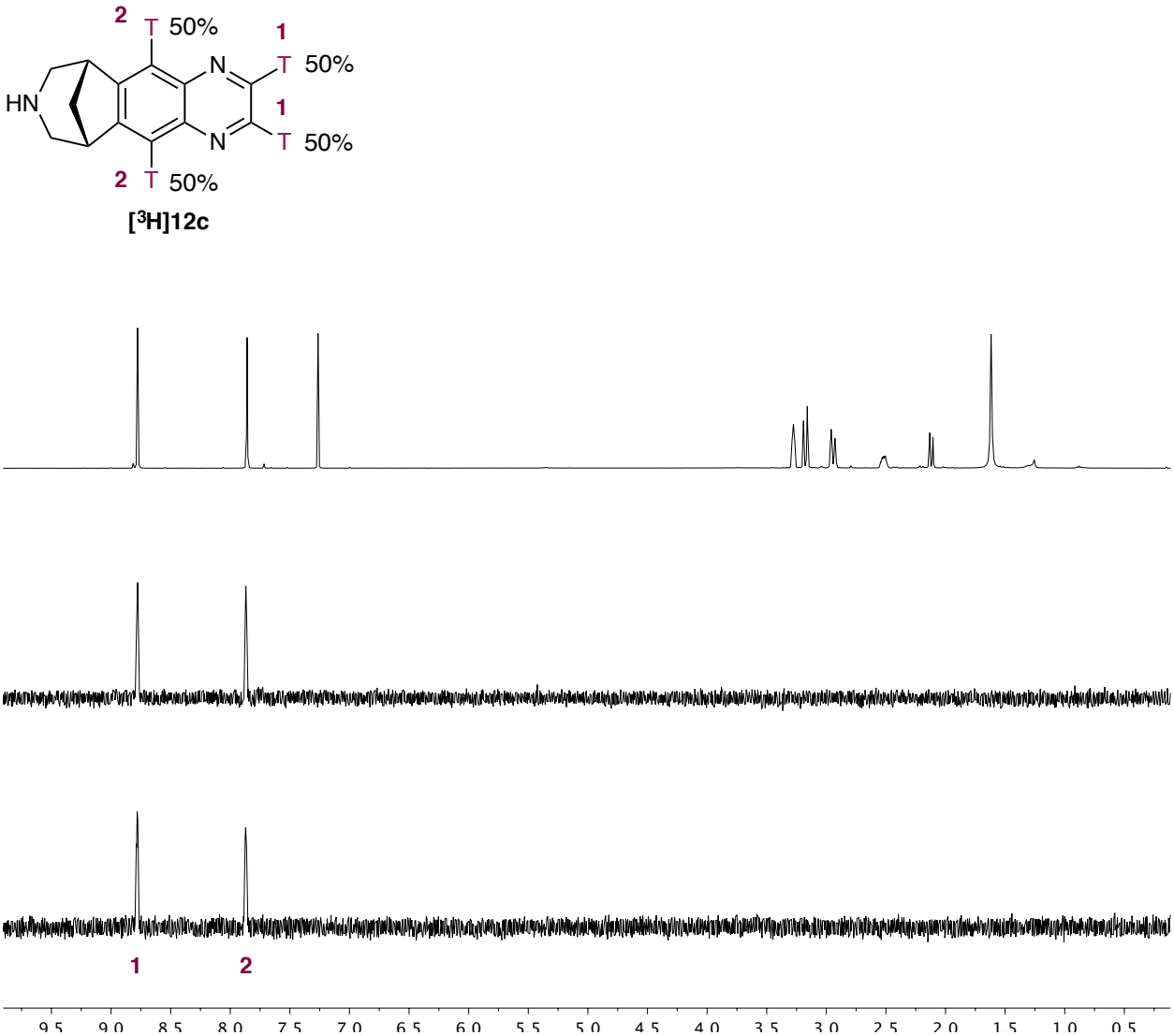

Figure S230. Stacked NMR spectra ($CDCl_3$) of labeled varenicline, **[^{13}H]12c**, mixed with unlabeled varenicline, **12c**: ^{1}H NMR (first), ^{3}H{^{1}H} NMR (second) and ^{3}H NMR (third).

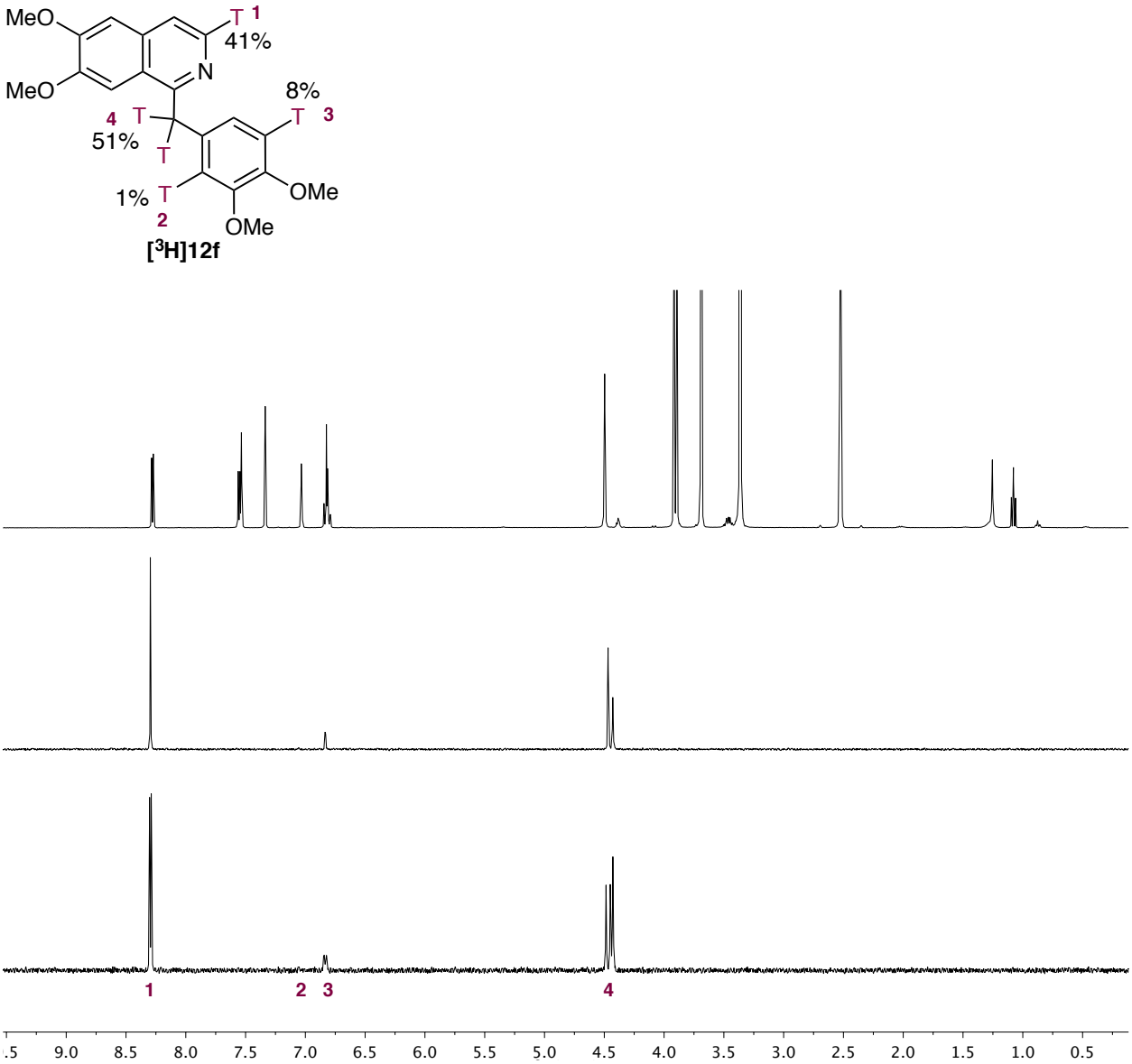

Figure S231. Stacked NMR spectra (DMSO-d_6) of labeled papaverine, **[^{13}H]12f**, mixed with unlabeled papaverine, **12f**: ^{1}H NMR (first), ^{3}H{^{1}H} NMR (second) and ^{3}H NMR (third).

XVII. References

1. Palmer, W. N.; Zarate, C.; Chirik, P. J. Benzyltriboronates: Building Blocks for Diastereoselective Carbon–Carbon Bond Formation. *J. Am. Chem. Soc.* **2017**, *139*, 2589–2592.

2. Pangborn, A. B.; Giardello, M. A.; Grubbs, R. H.; Rosen, R. K.; Timmers, F. J. Safe and Convenient Procedure for Solvent Purification. *Organometallics* **1996**, *15*, 1518–1520.

3. MestReNova Version 12.0.1-20560 © 2018 Mestrelab Research S.L.

4. Stoll, S.; Schweiger, A. EasySpin, A Comprehensive Software Package for Spectral Simulatioin and Analysis in EPR. *J. Magn. Reson.* **2006**, *178*, 42–55.

5. Neese, F. The ORCA Program System. *Wiley Interdiscip. Rev.: Comput. Mol. Sci.* **2012**, *2*, 73–78.

6. (a) Becke, A. D. Density Functional Calculations of Molecular Bond Energies. *J. Chem. Phys.* **1986**, *84*, 4524–4529. (b) Becke, A. D. Density-Functional Thermochemistry. III. The Role of Exact Exchange. *J. Chem. Phys.* **1993**, *98*, 5648–5652. (c) Lee, C. T.; Yang, W. T.; Parr, R. G. Development of the Colle-Salvetti Correlation-Energy Formula into a Functional of the Electron Density. *Phys. Rev. B.* **1998**, *37*, 785–789.

7. F. Neese, E. I. Solomon In Magnetism: From Molecules to Materials; J. S. Miller, M. Drillon, Eds.; Wiley: New York, 2002; Vol. 4, p 345.

8. (a) Schäfer, A.; Horn, H.; Ahlrichs, R. Fully Optimized contracted Gaussian Basis Sets for Atoms Li to Kr. *J. Chem. Phys.* **1992**, *97*, 2571–2577. (b) Schäfer, A.; Huber, C.; Ahlrichs, R. Fully Optimized Contracted Gaussian Basis Sets of Triple Zeta Valence Quality for Atoms Li to Kr. *J. Chem. Phys.* **1994**, *100*, 5829–5835. (c) Weigend, F.; Ahlrichs, R. Balanced Basis Sets of Split Valence, Triple Zeta Valence and Quadruple Zeta Valence Quality for H to Rn: Design and Assessment of Accuracy. *Phys. Chem. Chem. Phys.* **2005**, *7*, 3297–3305.

9. (a) Neese, F.; Wennmohs, F.; Hansen, A.; Becker, U. Efficient, Approximate and Parallel Hartree–Fock and Hybrid DFT Calculations. A 'Chain-of-Spheres' Algorithm for the Hartree–Fock Exchange. *Chem. Phys.* **2009**, *356*, 98–109. (b) Kossmann, S.; Neese, F. Comparison of Two Efficient Approximate Hartee–Fock Approaches. *Chem. Phys. Lett.* **2009**, *481*, 240–243. (c) Neese, F. An Improvement of the Resolution of the Identity Approximation for the Formation of the Coulomb Matrix. *J. Comput. Chem.* **2003**, *24*, 1740–1747.

10. (a) Eichkorn, K.; Weigend, F.; Treutler, O.; Ahlrichs, R. Auxiliary Basis Sets for Main Row Atoms and Transition Metals and their use to Approximate Coulomb

Potentials. *Theor. Chem. Acc.* **1997**, *97*, 119–124. (b) Eichkorn, K.; Treutler, O.; Öhm, H.; Häser, m.; Ahlrichs, R. Auxiliary Basis Sets to Approximate Coulomb Potentials. *Chem. Phys. Lett.* **1995**, *240*, 283–289. (c) Eichkorn, K.; Treutler, O.; Öhm, H.; Häser, M.; Ahlrichs, R. Auxiliary Basis Sets to Approximate Coulomb Potentials. *Chem. Phys. Lett.* **1995**, *242*, 652–660.

11. Kliegman, J. M.; Barnes, R. K. Glyoxal derivatives—I: Conjugated Aliphatic Diimines from Glyoxal and Aliphatic Primary Amines. *Tetrahedron* **1970**, *26*, 2555–2560.

12. Dong, Q.; Yang, X.-J.; Gong, S.; Luo, Q.; Li, Q.-S.; Su, J.-H.; Zhao, Y.; Wu, B. Distinct Stepwise Reduction of a Nickel–Nickel-Bonded Compound Containing an α-Diimine Ligand: From Perpendicular to Coaxial Structures. *Chem. Eur. J.* **2013**, *19*, 15240–15247.

13. Svoboda, M.; tom Dieck, H. Z. et al. Bis(diazadien)metall(0)-Komplexe, III [1] Nickel(0)-bis(chelate) mit aliphatischen N-Substituenten. *Naturforsch* **1981**, *36b*, 814–822.

14. Arduengo, A. J.; Dias, H. V. R.; Dixon, D. A.; Harlow, R. L.; Klooster, W. T.; Koetzle, T. F. Electron Distribution in a Stable Carbene. *J. Am. Chem. Soc.* **1994**, *116*, 6812–6822.

15. Eberhardt, N. A.; Guan, H. Nickel Hydride Complexes. *Chem. Rev.* **2016**, *116*, 8373−8426.

16. (a) Evans, D. F. The Determination of the Paramagnetic Susceptibility of Substances in Solution by Nuclear Magnetic Resonance. J. *Chem. Soc.* **1959**, 2003–2005. (b) Sur, S. K. Measurement of Magnetic Susceptibility and Magnetic Moment of Paramagnetic Molecules in Solution by High-Field Fourier Transform NMR Spectroscopy. *J. Magn. Reson.* **1989**, *82*, 169–173.

17. Gruber, C. C.; Oberdorfer, G.; Voss, C. V.; Kremsner, J. M.; Kappe, C. O.; Kroutil, W. An Algorithm for the Deconvolution of Mass Spectroscopic Patterns in Isotope Labeling Studies. Evaluation for the Hydrogen-Deuterium Exchange Reaction in Ketones. *J. Org. Chem.* **2007**, *72*, 5778–5783.

18. Formation of **2** was confirmed by ^{1}H NMR spectroscopy (300 MHz, benzene-d_6) of the reaction crude obtained upon treatment of **4** (0.10 mmol) with $NaHBEt_3$ (0.20 mmol) in THF (0.5 mL) and subsequent evaporation of THF solvent. Free ^{ipc}ADI ligand and presumed $Ni_n(^{ipc}ADI)_2$ (n = 1 or 2) were also detected in a **2**/ $Ni_n(^{ipc}ADI)_2$/^{ipc}ADI 12:6:1 ratio.

19. Yang, H.; Zarate, C.; Palmer, W. N.; Rivera, N.; Hesk, D.; Chirik, P. J. Site-Selective Nickel-Catalyzed Hydrogen Isotope Exchange in *N*-Heterocycles and Its

Application to the Tritiation of Pharmaceuticals. *ACS Catal.* **2018**, *8*, 10210−10218.

20. Similar behavior in $CDCl_3$: Coleman, P. J.; Schreier, J. D.; Cox, C. D.; Breslin, M. J.; Whitman, D. B.; Bogusky, M. J.; McGaughey, G. B.; Bednar, R. A.; Lemaire, W.; Doran, S. M.; Fox, S. V.; Garson, S. L.; Gotter, A. L.; Harrell, C. M.; Reissm D. R.; Cabalu, T. D.; Cui, D.; Prueksaritanont, T.; Stevens, J.; Tannenbaum, P. L.; Ball, R. G.; Stellabott, J.; Young, S. D.; Hartman, G. D.; Winrow, C. J.; Renger, J. J. Discovery of [(2R,5R)-5-{[(5-fluoropyridin-2-yl)oxy]-methyl}-2-methylpiperidin-1-yl][5-methyl-2-(pyrimidin-2-yl)phenyl]methanone (MK-6096): A Dual Orexin Receptor Antagonist with Potent Sleep-Promoting Properties. *ChemMedChem* **2012**, *7*, 415–424.

21. Assignment by comparison with electrochemical data of [(^{iPr}DAI)Ni(Mes)Br] (Mes = mesityl; iPrDAI = N,N'-diisopropyl-1,2-ethanediimine): Klein, A.; Kaiser, A.; Sarkar, B.; Wanner, M.; Fiedler, J. The Electrochemical Behaviour of Organonickel Complexes: Mono-, Di- and Trivalent Nickel. *Eur. J. Inorg. Chem.* **2007**, 965–976.